

# Landslides, Floods, and Marine Effects of the Storm of January 3-5, 1982, in the San Francisco Bay Region, California

---

U.S. GEOLOGICAL SURVEY PROFESSIONAL PAPER 1434





---

## AVAILABILITY OF BOOKS AND MAPS OF THE U.S. GEOLOGICAL SURVEY

---

Instructions on ordering publications of the U.S. Geological Survey, along with prices of the last offerings, are given in the current-year issues of the monthly catalog "New Publications of the U.S. Geological Survey." Prices of available U.S. Geological Survey publications released prior to the current year are listed in the most recent annual "Price and Availability List." Publications that are listed in various U.S. Geological Survey catalogs (see back inside cover) but not listed in the most recent annual "Price and Availability List" are no longer available.

Prices of reports released to the open files are given in the listing "U.S. Geological Survey Open-File Reports," updated monthly, which is for sale in microfiche from the U.S. Geological Survey, Books and Open-File Reports Section, Federal Center, Box 25425, Denver, CO 80225. Reports released through the NTIS may be obtained by writing to the National Technical Information Service, U.S. Department of Commerce, Springfield, VA 22161; please include NTIS report number with inquiry.

Order U.S. Geological Survey publications by mail or over the counter from the offices given below.

### BY MAIL

#### Books

Professional Papers, Bulletins, Water-Supply Papers, Techniques of Water-Resources Investigations, Circulars, publications of general interest (such as leaflets, pamphlets, booklets), single copies of Earthquakes & Volcanoes, Preliminary Determination of Epicenters, and some miscellaneous reports, including some of the foregoing series that have gone out of print at the Superintendent of Documents, are obtainable by mail from

U.S. Geological Survey, Books and Open-File Reports  
Federal Center, Box 25425  
Denver, CO 80225

Subscriptions to periodicals (Earthquakes & Volcanoes and Preliminary Determination of Epicenters) can be obtained ONLY from the

Superintendent of Documents  
Government Printing Office  
Washington, D.C. 20402

(Check or money order must be payable to Superintendent of Documents.)

#### Maps

For maps, address mail orders to

U.S. Geological Survey, Map Distribution  
Federal Center, Box 25286  
Denver, CO 80225

Residents of Alaska may order maps from

Alaska Distribution Section, U.S. Geological Survey,  
New Federal Building - Box 12  
101 Twelfth Ave., Fairbanks, AK 99701

### OVER THE COUNTER

#### Books

Books of the U.S. Geological Survey are available over the counter at the following Geological Survey Public Inquiries Offices, all of which are authorized agents of the Superintendent of Documents:

- WASHINGTON, D.C.--Main Interior Bldg., 2600 corridor, 18th and C Sts., NW.
- DENVER, Colorado--Federal Bldg., Rm. 169, 1961 Stout St.
- LOS ANGELES, California--Federal Bldg., Rm. 7638, 300 N. Los Angeles St.
- MENLO PARK, California--Bldg. 3 (Stop 533), Rm. 3128, 345 Middlefield Rd.
- RESTON, Virginia--503 National Center, Rm. 1C402, 12201 Sunrise Valley Dr.
- SALT LAKE CITY, Utah--Federal Bldg., Rm. 8105, 125 South State St.
- SAN FRANCISCO, California--Customhouse, Rm. 504, 555 Battery St.
- SPOKANE, Washington--U.S. Courthouse, Rm. 678, West 920 Riverside Ave..
- ANCHORAGE, Alaska--Rm. 101, 4230 University Dr.
- ANCHORAGE, Alaska--Federal Bldg, Rm. E-146, 701 C St.

#### Maps

Maps may be purchased over the counter at the U.S. Geological Survey offices where books are sold (all addresses in above list) and at the following Geological Survey offices:

- ROLLA, Missouri--1400 Independence Rd.
- DENVER, Colorado--Map Distribution, Bldg. 810, Federal Center
- FAIRBANKS, Alaska--New Federal Bldg., 101 Twelfth Ave.

# Landslides, Floods, and Marine Effects of the Storm of January 3-5, 1982, in the San Francisco Bay Region, California

STEPHEN D. ELLEN *and* GERALD F. WIECZOREK, *Editors*

---

U.S. GEOLOGICAL SURVEY PROFESSIONAL PAPER 1434



**DEPARTMENT OF THE INTERIOR**  
**DONALD PAUL HODEL, *Secretary***

**U.S. GEOLOGICAL SURVEY**  
**Dallas L. Peck, *Director***

**Library of Congress Cataloging-in-Publication Data**

Landslides, floods, and marine effects of the storm of January 3–5, 1982, in the San Francisco Bay region, California.

(U.S. Geological Survey professional paper ; 1434)

Bibliography: p.

Supt. of Docs. no. : I 19.16:1434

1. Rainstorms—California—San Francisco Bay Area. 2. Landslides—California—San Francisco Bay Area. 3. Flood—California—San Francisco Bay Area. I. Ellen, Stephen D. II. Wiczorek, Gerald F. III. California. Division of Mines and Geology. IV. Series.

QC925.1.U8C26 1988

363.3'492

88-600235

---

For sale by the Books and Open-File Reports Section,  
U.S. Geological Survey, Federal Center, Box 25425, Denver, CO 80225

# CONTENTS

[Numbers designate chapters]

	Page
Introduction	
Stephen D. Ellen, Gerald F. Wiczonek, William M. Brown III, and Darrell G. Herd, U.S. Geological Survey - - - - -	1
1. Historical setting of the storm: Perspectives on population, development, and damaging rainstorms in the San Francisco Bay region	
William M. Brown III, U.S. Geological Survey - - - - -	7
<i>Rainfall</i>	
2. Rainfall totals before and during the storm: Distribution and correlation with damaging landslides	
Robert K. Mark and Evelyn B. Newman, U.S. Geological Survey - - - - -	17
3. Rainfall that resulted in abundant debris-flow activity during the storm	
Susan H. Cannon and Stephen D. Ellen, U.S. Geological Survey - - - - -	27
4. Regional rainfall-threshold conditions for abundant debris-flow activity	
Susan H. Cannon, U.S. Geological Survey - - - - -	35
5. Rainfall, piezometric levels, and debris flows near La Honda, California, in storms between 1975 and 1983	
Gerald F. Wiczonek and John Sarmiento, U.S. Geological Survey - - - - -	43
<i>Debris flows and other landslides</i>	
6. Description and mechanics of soil slip/debris flows in the storm	
Stephen D. Ellen, U.S. Geological Survey; with contributions by Mitchell A. Albus, Susan H. Cannon, Robert W. Fleming, Philip C. Lahr, David M. Peterson, and Steven L. Reneau - - - - -	63
7. Distribution of debris flows in Marin County	
Stephen D. Ellen, Susan H. Cannon, and Steven L. Reneau, U.S. Geological Survey; with contributions by Bryan M. Langholz, Robert K. Mark, David M. Peterson, and Stephen W. Robinson - - - - -	113
8. Debris flows and other landslides in San Mateo, Santa Cruz, Contra Costa, Alameda, Napa, Solano, Sonoma, Lake, and Yolo Counties, and factors influencing debris-flow distribution	
Gerald F. Wiczonek, Edwin L. Harp, and Robert K. Mark, U.S. Geological Survey; and Arun K. Bhattacharyya, Jadavpur University, Calcutta - - - - -	133
9. Landslides in Pacifica, California, caused by the storm	
Terry R. Howard, Joel E. Baldwin II, and Howard F. Donley, Howard-Donley Associates - - - - -	163
10. A method for mapping relative susceptibility to debris flows, with an example from San Mateo County	
Theodore C. Smith, California Division of Mines and Geology - - - - -	185
11. Landslide damage: A costly outcome of the storm	
Carol L. Creasey, U.S. Geological Survey - - - - -	195
<i>Flooding</i>	
12. Impact of the January 1982 flood in Santa Cruz County	
Gary B. Griggs, University of California, Santa Cruz - - - - -	205
13. Peak discharge, volume, and frequency of the January 1982 flood in the Santa Cruz Mountains and vicinity	
James C. Blodgett and Karen R. Poeschel, U.S. Geological Survey - - - - -	229
14. Stream-channel response to the storm in the Santa Cruz Mountains	
K. Michael Nolan and Donna C. Marron, U.S. Geological Survey - - - - -	245
<i>Marine effects</i>	
15. Ephemeral delta development at the mouth of Aptos Creek, northern Monterey Bay	
Bruce M. Richmond, U.S. Geological Survey - - - - -	265
16. Sedimentologic consequences of the storm in Tomales Bay	
Roberto J. Anima, Jennifer L. Bick, and H. Edward Clifton, U.S. Geological Survey - - - - -	283

# ILLUSTRATIONS

[Plates are in pocket]

- PLATE 1. Map of the San Francisco Bay region, California, showing prestorm-rainfall contours (July 1, 1981, through January 2, 1982), rain-gage locations, and sites of damaging landslides
2. Map of the San Francisco Bay region, California, showing storm-rainfall contours, rain-gage locations, and sites of damaging landslides



- PLATE 3. Locations of debris flows in the La Honda, California, area, 1975-83
4. Maps and profiles of damaging soil slip/debris flows triggered by the storm of January 3-5, 1982, in the San Francisco Bay region, California
  5. Debris flows triggered by the storm of January 3-5, 1982, showing their habitats and relation to geologic and terrain units in Marin and part of Sonoma Counties, California
  6. Debris flows triggered by the storm of January 3-5, 1982, and their relation to slope and terrain units in the Hicks Mountain area, Marin County, California
  7. Field-checked areas, forest cover, and rainfall stations in San Mateo and Santa Cruz Counties, California
  8. Distribution and concentration of debris flows and other landslides in San Mateo County, California
  9. Distribution and concentration of debris flows and other landslides in Santa Cruz County, California
  10. Distribution and concentration of debris flows in Contra Costa County, California
  11. Distribution and concentration of debris flows in Alameda County, California
  12. Distribution and concentration of debris flows and other landslides in parts of Napa, Solano, Sonoma, Lake, and Yolo Counties, California
  13. *Development of a debris-flow-susceptibility map—an example from San Mateo County, California*
  14. Landslide-damage distribution in the San Francisco Bay region, California, for the January 3-5, 1982, storm

Any use of trade names and trademarks in this volume is for descriptive purposes only and does not constitute endorsement by the U.S. Geological Survey.

## UNITS

Metric (Système International [SI]) units are the main units of measurement in this volume. Rainfall is reported principally in millimeters, but conversion to inches is provided in the text as an aid to readers in the United States. Conversion of other units is facilitated by the table below.

### CONVERSION FACTORS

<i>To convert from</i>	<i>to</i>	<i>multiply by</i>
<b>LENGTH</b>		
millimeters (mm)	inches	0.039370
meters (m)	feet	3.2808
kilometers (km)	miles	0.62137
<b>AREA</b>		
square meters (m <sup>2</sup> )	square feet	10.764
hectares (ha)	acres	2.4710
square kilometers (km <sup>2</sup> )	square miles	0.38610
<b>VOLUME</b>		
cubic meters (m <sup>3</sup> )	cubic feet	35.315
cubic meters (m <sup>3</sup> )	cubic yards	1.3080
cubic meters (m <sup>3</sup> )	acre-feet	0.00081071
liters (L)	U.S. gallons	0.26417
<b>VELOCITY</b>		
meters per second (m/s)	feet per second	3.2808
kilometers per hour (km/h)	miles per hour	0.62137
<b>FLOW</b>		
cubic meters per second (m <sup>3</sup> /s)	cubic feet per second	35.315
<b>FLOW PER UNIT AREA</b>		
cubic meters per second per square kilometer [(m <sup>3</sup> /s)/km <sup>2</sup> ]	cubic feet per second per square mile	91.465
<b>MASS</b>		
megagrams (Mg)	tons (2,000 lb mass)	1.1023
<b>MASS PER UNIT AREA</b>		
megagrams per square kilometer (Mg/km <sup>2</sup> )	tons per square mile	2.8550
<b>DENSITY</b>		
kilograms per cubic meter (kg/m <sup>3</sup> )	pounds per cubic foot	0.062428
grams per cubic centimeter (g/cm <sup>3</sup> )	pounds per cubic inch	0.036127
<b>FORCE PER UNIT AREA</b>		
kilopascals (kPa)	pounds force per square inch (psi)	0.14504



# LANDSLIDES, FLOODS, AND MARINE EFFECTS OF THE STORM OF JANUARY 3-5, 1982, IN THE SAN FRANCISCO BAY REGION, CALIFORNIA

## INTRODUCTION

By STEPHEN D. ELLEN, GERALD F. WIECZOREK,  
WILLIAM M. BROWN III, and DARRELL G. HERD,  
U.S. GEOLOGICAL SURVEY

A catastrophic rainstorm in central California on January 3-5, 1982, dropped as much as half the mean annual precipitation within a period of about 32 hours, triggering landslides<sup>1</sup> and floods throughout 10 counties in the vicinity of the San Francisco Bay (fig. 1). More than 18,000 of the slides induced by the storm transformed into debris flows that swept down hillslopes or drainages with little warning. Debris flows damaged at least 100 homes, killed 14 residents, and carried a 15th victim into a creek. Shortly after rainfall ceased, more than 459,000 m<sup>3</sup> of earth and rock slid from a mountainside above the community of Love Creek in Santa Cruz County, burying 10 people in their homes (Cotton and Cochrane, 1982). Throughout the bay region, thousands of people vacated homes in hazardous areas, entire communities were isolated as roads were blocked, public water systems were destroyed, and power and telephone services were disrupted. Altogether, the storm damaged 6,300 homes, 1,500 businesses, and tens of kilometers of roads, bridges, and communication lines. Preliminary rough estimates of total storm damage, compiled for emergency purposes within 2 weeks of the storm, exceeded \$280 million (U.S. Federal Emergency Management Agency, 1982, p. 9-10). Carefully documented direct costs from landslides exceeded \$66 million (chap. 11); total costs from landslides certainly were greater and probably constituted a much larger proportion of the total storm damage than suggested by these disparate figures. Landslides accounted for 25 of the 33 deaths attributed to the storm (fig. 2).

The most abundant destructive landslides were debris flows,<sup>2</sup> which elsewhere have been called debris avalanches, mudflows, or mudslides. Before the storm, debris flows had been recognized locally in the San Francisco Bay region (Smith and Hart, 1982, p. 150), but their poten-

tial for widespread and devastating impact was not fully appreciated, partly because they had occurred only locally in the years since population spread into susceptible steep terrain. Evaluations of landslide hazard in the bay region had largely overlooked these relatively small, shallow landslides and focused, instead, on the larger, deeper, generally slower moving landslides that have produced distinctive features and perennial damage over much of the region (for example, Nilsen and others, 1979). Thus, the scientific and planning communities, as well as the general population, were not prepared for the sudden and devastating impact of debris flows during the storm.

As the magnitude of the disaster became apparent, geologists and engineers from consulting firms, local governments, colleges, universities, the U.S. Soil Conservation Service, the California Division of Mines and Geology, and the U.S. Geological Survey began examining evidence left by the storm. The region was reconnoitered by automobile, helicopter, and light airplane, aerial photographs were flown, eyewitnesses were interviewed, and the features left by landslides and floods were mapped and sampled. Documentation and analysis of the storm events benefitted from the large number of investigators and from public interest in the phenomena.

The contributions in this volume represent the fruit of these studies. The various chapters address most of the significant aspects of the storm and its effects. Excellent overviews of the storm are provided elsewhere (Griggs, 1982; Santa Cruz Sentinel, 1982; Smith and Hart, 1982; Brown and others, 1984).

The sequence of chapters begins with a historical setting of the storm by Brown, then proceeds through discussions of rainfall, debris flows, flooding, and marine effects. Rainfall is discussed in several chapters. Mark and Newman describe storm rainfall and prestorm seasonal rainfall on the basis of observations from as many as 750 stations throughout the region, and they determine the rainfall amounts that show significant correlation with damaging landslides. Cannon and Ellen use hourly records from recording gages and known times of nearby debris

<sup>1</sup>In this volume, "landslide" is used as a general term for various mass-movement processes, including debris flow. The principal classes of landslides caused by the storm were slides and flows, as these terms were defined by Varnes (1978).

<sup>2</sup>In almost all documented cases, debris flows caused by the storm began as shallow slides, so movement involved both sliding and flow. For simplicity, we generally use the term "debris flow" for this complex movement.



flows to define the hourly rainfall conditions that triggered debris flows. Cannon compares rainfall records from the storm with records from other major storms in the region to define threshold storm-rainfall conditions for abundant debris-flow activity. Wiecezorek and Sarmiento relate rainfall in a study area to the occurrence of debris flows and to measured ground-water levels over an 8-year period spanning the storm.

Debris flows resulting from the storm are described by Ellen, who examines the mechanics of shallow slides and analyzes the transformation from slide to flow. Distribution of debris flows is documented on inch-to-the-mile maps of most of the bay region, the areas shown in figure 2 as having an appreciable concentration of debris flows. Distribution in Marin County is analyzed by Ellen and others; distribution in the rest of the bay



FIGURE 1.—Shaded relief map showing the 10 counties in the San Francisco Bay region, Calif.

region is discussed by Wieczorek and others. Howard and others provide detailed descriptions of debris flows and other landslides that occurred in the city of Pacifica. Smith describes a method for mapping susceptibility to debris flows and checks his method against

the distribution of debris flows in a small part of San Mateo County. Costs of landslide damage from the storm are compiled by Creasey. The Love Creek landslide is described elsewhere (Cotton and Cochrane, 1982).

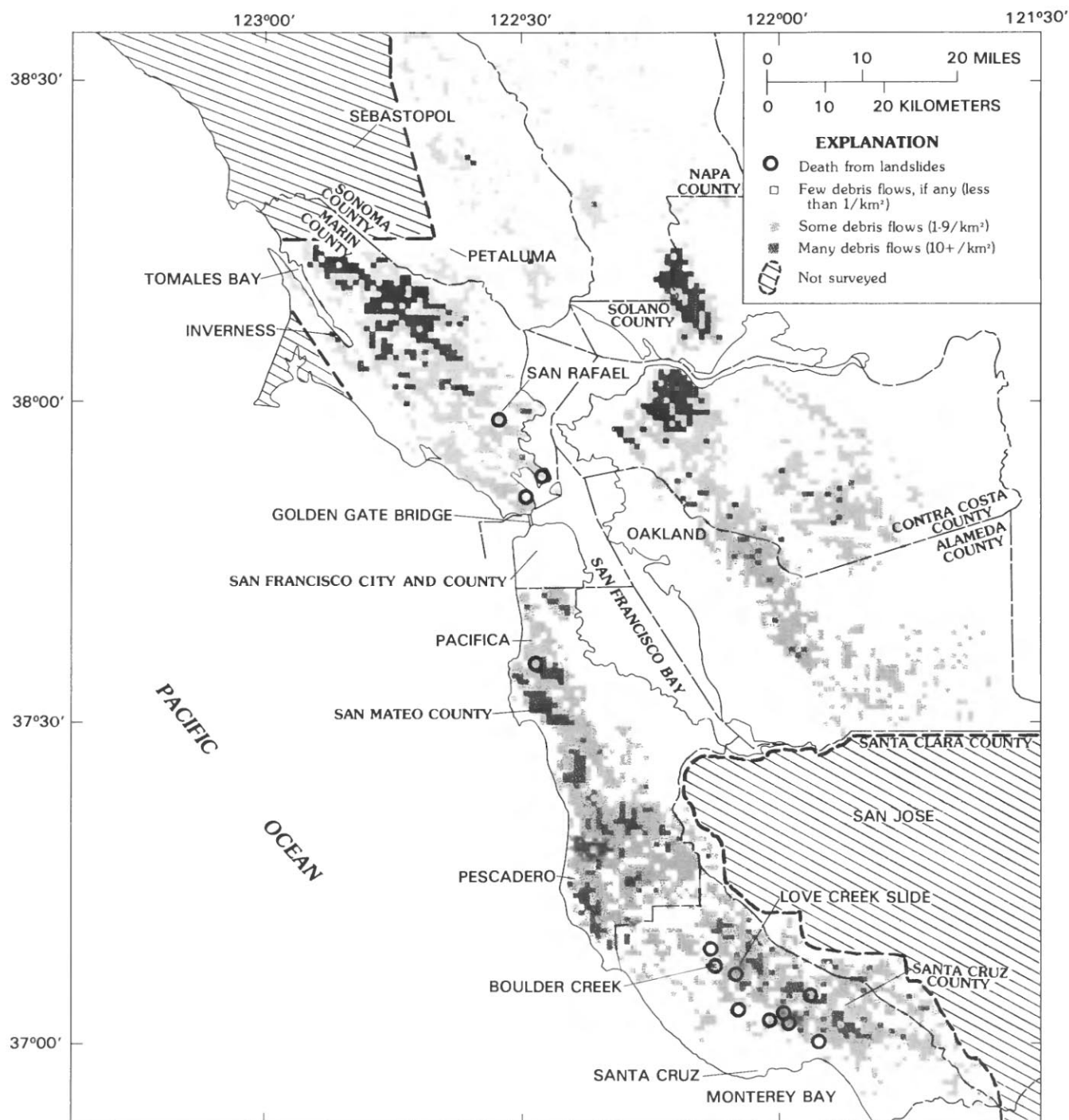


FIGURE 2.—San Francisco Bay region, showing distribution of mapped debris flows and locations of deaths caused by landslides in the January 3-5, 1982, storm.

Flooding is addressed by several studies in the Santa Cruz Mountains. Griggs describes the impacts of flooding on the San Lorenzo River, Soquel Creek, and Aptos Creek, and discusses the implications for flood-hazard mapping. Blodgett and Poeschel describe areal variations in rainfall, floodflow, and recurrence intervals, and they compare the flood with other historical floods, notably that of December 1955. Nolan and Marron describe sediment transport and the response of stream channels to the combination of floodflow and landslide processes.

Discussion of marine effects completes our portrayal of the storm. An ephemeral delta created by the storm at the mouth of Aptos Creek in Monterey Bay is described by Richmond. Anima and others describe the sediment generated by the storm in Tomales Bay and changes in this sediment during the months after the storm.

In summary, the authors of this volume document the effects of an exceptional rainstorm and analyze the physical processes involved. Their studies elucidate the processes of landsliding and flooding that operated during the storm, and thereby provide basic information toward predicting hazards from future storms. The chapters are technical, but interesting and useful information can be gleaned by the general reader or public official.

### TERMINOLOGY

In this volume, "landslide" is used as a general term encompassing various mass-movement processes, including debris flow. The principal classes of landslides caused by the storm were slides and flows, and these terms, as well as most specific landslide terms, are here used in the sense defined by Varnes (1978).

The principal landslides caused by the storm were rapid flows that developed from shallow slides. Such landslides have been called by various names, including debris avalanche (Sharpe, 1938), soil slip-debris flow (Campbell, 1975), flow slide (Hutchinson, 1968), soil avalanche (Wentworth, 1943; Keefer, 1984), and disintegrating soil slip (Kesseli, 1943). For convenience, in this volume these complex landslides generally are referred to simply as debris flows.

This broad usage of the term "debris flow" involves two simplifications. First, the landslides that involved both sliding and flow are called simply flows, even though both sliding and flow are critical to the process, sliding determining the timing and location of initiation, flow determining the path and rate of movement. A more complete term for the complex movement is soil slide/debris flow<sup>3</sup>

<sup>3</sup>Varnes (1978) used a hyphen or dash to join such compound terms, as in soil slip-debris flow, but in this volume we use a slant (or solidus) because use of the hyphen is confusing—it appears to join the middle two words of the four-word term, rather than separating the two elements of the complex landslide. The slant is appropriate for this function because it is an accepted punctuation mark for distinguishing separate elements of a compound term where a hyphen would lead to confusion.

or, as we prefer, soil slip/debris flow (Campbell, 1975), and these or similar combined terms are used where the distinction between slide and flow is useful, particularly in chapter 6.

The second simplification is that the flows designated "debris flows" include mudflows, debris avalanches, and debris torrents. Mudflows (Varnes, 1978) are included because many flows in the storm involved predominantly fine-grained soils rather than the predominantly coarse materials designated debris. Debris avalanches (Sharpe, 1938; Varnes, 1978) are included because the velocity of many, if not most, flows in the storm exceeded 3 m/s (10 km/h).<sup>4</sup> Debris torrents (Swanston and Swanson, 1976) are included because some flows during the storm involved abundant coarse organic debris and entrained much additional material from stream channels. Our inclusion of mudflows, debris avalanches, and debris torrents under the term "debris flow" is justified by the rheologic similarity of these processes (Costa, 1984; Johnson, 1984; Pierson and Costa, 1984).

"Soil" is used here in the engineering sense of unconsolidated earth material. A cover of soil, called soil cover, soil mantle, or regolith, blankets bedrock in hillside terrain of the region and was the source of most debris flows in the storm.

### REFERENCES CITED

- Brown, W.M., III, Sitar, Nicholas, Saarinen, T.F., and Blair, M.L., 1984, Debris flows, landslides, and floods in the San Francisco Bay region, January, 1982—overview and summary of a conference held at Stanford University, August 23–26, 1982: Washington, U.S. National Academy of Sciences, National Research Council and U.S. Geological Survey, 83 p.
- Campbell, R.H., 1975, Soil slips, debris flows, and rainstorms in the Santa Monica Mountains and vicinity, southern California: U.S. Geological Survey Professional Paper 851, 51 p.
- Costa, J.E., 1984, Physical geomorphology of debris flows, chap. 9 of Costa, J.E., and Fleisher, P.J., eds., *Developments and applications of geomorphology*: Berlin, Springer-Verlag, p. 268–317.
- Cotton, W.R., and Cochrane, D.A., 1982, Love Creek landslide disaster, January 5, 1982: *California Geology*, v. 35, no. 7, p. 153–157.
- Griggs, G.B., 1982, Flooding and slope failure during the January 1982 storm, Santa Cruz County, California: *California Geology*, v. 35, no. 7, p. 158–163.
- Hutchinson, J.N., 1968, Mass movement, in Fairbridge, R.W., ed., *Encyclopedia of geomorphology*: New York, Reinhold, p. 688–695.
- Johnson, A.M., 1984, Debris flow, chap. 8 of Brunsten, Denys, and Prior, D.B., eds., *Slope instability*: Chichester, U.K., John Wiley & Sons, p. 257–361.
- Keefer, D.K., 1984, Landslides caused by earthquakes: *Geological Society of America Bulletin*, v. 95, no. 4, p. 406–421.
- Kesseli, J.E., 1943, Disintegrating soil slips of the Coast Ranges of central California: *Journal of Geology*, v. 51, no. 5, p. 342–352.
- Nilsen, T.H., Wright, R.H., Vlasic, T.C., and Spangle, W.E., 1979,

<sup>4</sup>The velocity that distinguishes debris avalanche from debris flow, according to Varnes (1978).

- Relative slope stability and land-use planning in the San Francisco Bay region, California: U.S. Geological Survey Professional Paper 944, 96 p.
- Pierson, T.C., and Costa, J.E., 1984, A rheologic classification of subaerial sediment-water flows [abs.]: Geological Society of America Abstracts with Programs, v. 16, no. 6, p. 623.
- Santa Cruz Sentinel, 1982, The storm of '82: Santa Cruz, Calif., 98 p.
- Sharpe, C.S.F., 1938, Landslides and related phenomena, a study of mass movements of soil and rock: New York, Columbia University Press, 136 p.
- Smith, T.C., and Hart, E.W., 1982, Landslides and related storm damage, January 1982, San Francisco Bay region: California Geology, v. 35, no. 7, p. 139-152.
- Swanston, D.N., and Swanson, F.J., 1976, Timber harvesting, mass erosion, and steep-land forest geomorphology in the Pacific Northwest, in Coates, D.R., ed., Geomorphology and engineering: Stroudsburg, Pa., Dowden, Hutchinson & Ross, p. 199-221.
- U.S. Federal Emergency Management Agency, 1982, Interagency flood hazard mitigation report in response to the January 7, 1982, disaster declaration: report FEMA-651-DR-CA, 43 p.
- Varnes, D.J., 1978, Slope movement types and processes, chap. 2 of Schuster, R.L., and Krizek, R.S., eds., Landslides: Analysis and control: U.S. National Academy of Sciences, Transportation Research Board Special Report 176, p. 11-33.
- Wentworth, C.K., 1943, Soil avalanches on Oahu, Hawaii: Geological Society of America Bulletin, v. 54, no. 1, p. 53-64.





# 1. HISTORICAL SETTING OF THE STORM: PERSPECTIVES ON POPULATION, DEVELOPMENT, AND DAMAGING RAINSTORMS IN THE SAN FRANCISCO BAY REGION

By WILLIAM M. BROWN III,  
U.S. GEOLOGICAL SURVEY

## CONTENTS

	Page
Introduction - - - - -	7
Regional and localized storms - - - - -	7
Effects of regional and localized storms - - - - -	9
Population, development, and landslide damage - - - - -	11
Lessons of January 1982 - - - - -	12
References cited - - - - -	13

## INTRODUCTION

Many severe rainstorms and winter seasons of heavy rainfall have been observed in central coastal California (fig. 1.1) since the European colonization of the area in the late 1700's. Perceptions of the severity of these storms and seasons have varied greatly, depending on the numbers of people affected, the economic base for computing property losses, and the areal extent of reliable observations of the amount and intensity of precipitation and the flow of rivers. The most severe winter in terms of precipitation probably was that of 1861-62 (Waananen and others, 1977, p. 8). The storms of that season apparently were regional and pervasive, and flooding of great magnitude occurred in the San Francisco Bay region (fig. 1.2) and throughout the rest of California in response to frequent heavy rains in coastal areas and runoff from a massive snowpack in the Sierra Nevada. Frequent, major flood-producing seasons occurred in central coastal California between 1879 and 1915, a period that was followed by 22 years of less damaging or nondamaging precipitation seasons, except for the wet winter of 1926-27 (table 1.1). From 1937 to 1982, the bay region was struck by damaging rainstorms at a rate of about once every 3 years.

Table 1.1 lists the periods of heavy rain that have resulted in major flooding and other damage in coastal California since 1861. Table 1.1 also shows the approximate geographic extent of damage due to rainstorms, measured in those coastal counties where severe flooding or other major damage was reported during the indicated period. Since the early 1950's, when the Governor of California was given legislative authority to proclaim states of emergency or disaster and to request Federal disaster assistance, proclamations related to rainstorms and floods were entered on 40 occasions for coastal

California. During this period, part or all of the San Francisco Bay region was declared a State or Federal disaster area 18 times.

## REGIONAL AND LOCALIZED STORMS

The disastrous events listed in table 1.1 resulted primarily from two appreciably different and extreme rainfall patterns (Weaver, 1962, p. 1). One pattern is a series of regional storms wherein the terrain is saturated by persistent rainfall over periods of several weeks. The other pattern is a localized storm of high precipitation intensity, wherein rainfall lasts for a few hours to a few days and may or may not fall on presaturated ground. Both patterns may cause severe flooding. The regional storms tend to result in high volumes of flow on the main stems of major rivers as tributary inflow collects from many

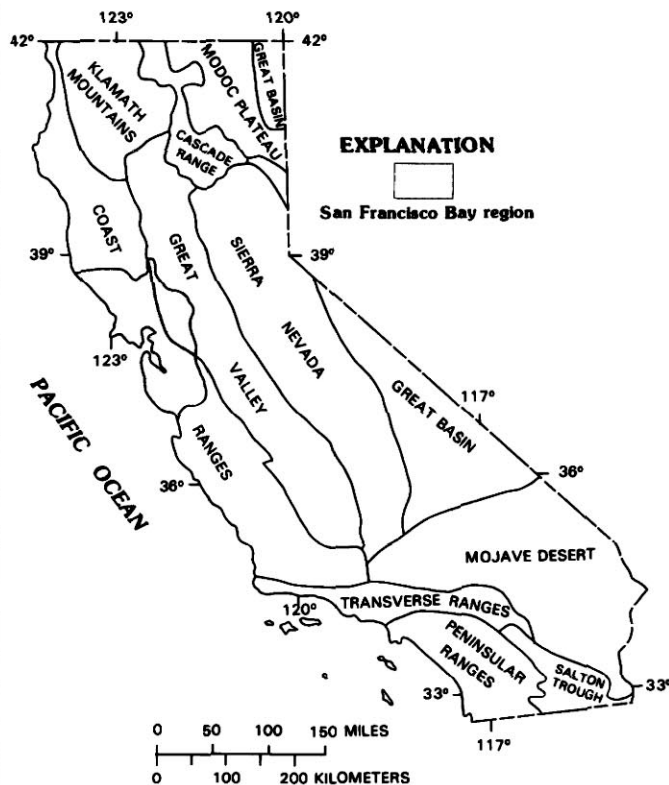


FIGURE 1.1.—California, showing location of the San Francisco Bay region and outlines of principal physiographic regions. Modified from Bailey (1966).

thousands of square kilometers of drainage area. Localized storms tend to generate floodflows on smaller streams but lack the areal extent and duration to cause flooding of major rivers. Generally, rainfall patterns between these two extremes lack combinations of precipitation intensity, duration, or areal extent sufficient to cause flooding of either large or small streams.

Regional storms characteristically move over the North Pacific Ocean onto about one-half to two-thirds of the Pacific coastline between British Columbia, Canada, and Baja California, Mexico. Examples of such storms are those that occur commonly during California's rainy season of October to May each year. When regional storms persist and follow one another along the same general path, heavy flooding may result throughout major river basins in Washington, Oregon, California, and adjacent States. Such flooding has occurred frequently in historical time, notably during the recent major flood seasons of 1955-56, 1964-65, 1968-69, 1977-78, and 1979-80. The storms of December 1955-January 1956 caused what were at the time record streamflows in the west third of Nevada, the north two-thirds of California, western Oregon, a third of western Idaho, and minor parts of Washington (Hofmann and Rantz, 1963, p. A1). Most of those streamflows were exceeded during the

December 1964-January 1965 floods that affected most of Oregon, southernmost Washington, northern California, western Idaho, and westernmost Nevada and Montana (Rantz and Moore, 1965, p. 3). The January-February 1969 storms caused record flooding throughout southern California (Waananen, 1969), and storm sequences during December 1977-March 1978 and January-February 1980 (Brooks, 1982a, b) hit central and southern California and carried heavy flooding eastward into southern Nevada and central and southern Arizona (Wahl and others, 1980; Aldridge, 1982).

The 1955-56 storms are significant in the context of this volume in that they affected the entire San Francisco Bay region, whereas the 1964-65 storms primarily hit areas to the north of San Francisco, and the 1979-80 storms flooded areas mostly to the south of there (fig. 1.2). Thus, the 1955-56 floodflows hold the distinction of being generally the greatest of the 20th century over the San Francisco Bay region, except in isolated places in Alameda County in 1962 and in Santa Clara County in 1911 (Waananen and others, 1977, p. 8). Hofmann and Rantz (1963, p. A1) described the 1955-56 storms as follows:

The floods were caused by a series of storms from December 15 to January 27; three occurring between December 15 and 27 and three more from January 2 to 27. In all but a few areas the storm of December 21-24 was the most severe. The storms all reflected the effect of the combination of a moist, unstable airmass, strong west-southwest winds, and mountain ranges oriented nearly at right angles to the flow of air. The unusual feature of the storms was the persistence of the strong flow of moist air. The major storm of December 21-24 was accompanied by high temperature and high wind velocities. As a result, a considerable amount of the snow which had accumulated at higher altitudes was melted. This snowmelt, added to the heavy precipitation at low altitudes, caused record-breaking runoff in the streams draining the Sierra Nevada, in Idaho, and in Washington. The coastal areas of northern California and southern Oregon had measurable rainfall on 39 of the 44-day period between December 15 and January 28. At several stations the recorded precipitation for the months of December and January exceeded 60 inches.

In contrast, localized storms impinge upon much smaller segments of the Pacific coastline and release continuous, very intense rains lasting for several hours to a maximum of about 4 days. Weaver (1962, p. 29-35), Rantz and Harris (1963), Brown (1984), and Monteverdi (1984) described five of the severest of such storms that affected the San Francisco Bay region between 1950 and 1982 and had similar rainfall intensities, duration, and areal extent. These storms occurred during November 16-20, 1950, October 11-13, 1962, January 29-February 1, 1963, January 20-21, 1967, and January 3-5, 1982. Each of these storms struck the Pacific coast in California between Monterey County on the south and Mendocino County on the north, and produced flooding and other damage mostly confined to the San Francisco Bay region but extending into central California and western Nevada as some of the storms

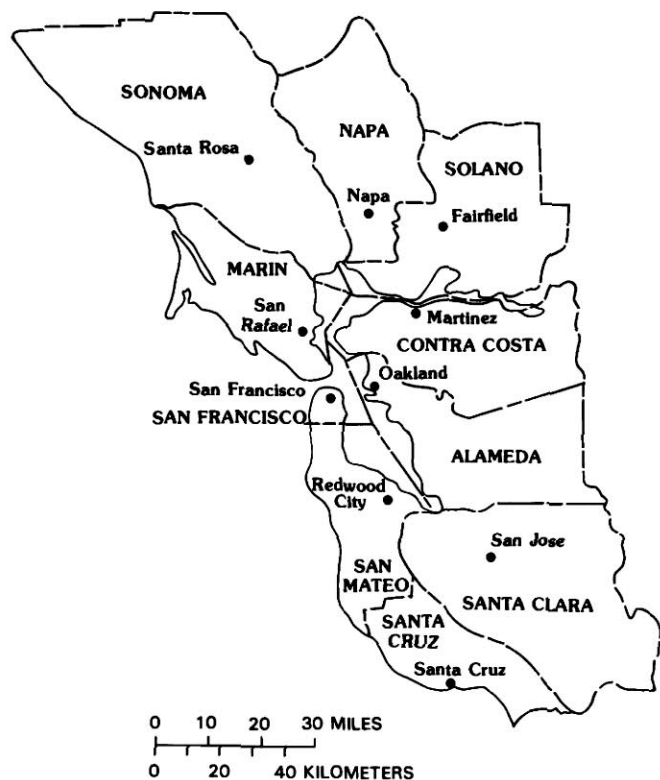


FIGURE 1.2.—San Francisco Bay region, showing locations of the 10 counties in the vicinity.

moved eastward. All of these storms were isolated events, in that they were not preceded or followed in close proximity by similar storms and so did not continue their effects over extended periods like the regional storms. For example, the November 1950 storm followed light rainfall on November 13–16 that was preceded by nearly 2 weeks of dry weather. The October 1962 storm was the first storm after California's normal, 6-month summer drought. The January–February 1963 storm produced the first major rain after that, terminating what at the time was one of the worst winter droughts for California and Nevada in 100 years (Rantz and Harris, 1963, p. 3). The January 1967 storm followed a month-long drought. Only the January 1982 storm among the five was preceded by substantial rainfall, most of which occurred during regional storms of moderate rainfall intensity during the previous 2 months (Smith and Hart, 1982, p. 139).

Each of these five storms had maximum rainfall intensities that exceeded 6.4 mm/h (0.25 in/h) continuously for at least 24 hours at some stations. The duration of such rainfall ranged from about 24 hours for the November 1950 storm to about 47 hours for the October 1962 storm. In contrast, the heaviest pulse of the December 1955–January 1956 regional storms during December 21–23, 1955, produced a more irregular sequence consisting of bursts of intense rainfall lasting for a few hours, followed by several hours of rainfall of much lesser intensity (Weaver, 1962, p. 24–28).

#### EFFECTS OF REGIONAL AND LOCALIZED STORMS

Whereas the flood effects of regional and localized storms historically have been readily noticed and documented, other specific effects, such as landslides, have been less clearly and comprehensively identified. Rainfall and streamflow have been monitored systematically in the San Francisco Bay region for more than 130 years, and inferences from early Spanish and Russian records provide a fairly thorough rainfall and flooding history for most of California, beginning in the late 1700's (Lynch, 1931; Waananen and others, 1977, p. 7; Goodridge, 1984). Coverage of landslides, however, has been spotty by comparison, and only in recent years have efforts been devoted to accounting for landslides on a regional scale. Nevertheless, detailed records of isolated events, as well as general observations (as in newspaper accounts), form a basis for suggesting the incidence of slope failures. For example, Smith and Hart (1982, p. 150) claimed:

Debris avalanches, debris flows, and associated storm-triggered landslides have caused most of the deaths and much of the structural damage attributed to landsliding in California. The landslides of January 3–5, 1982, were not at all unusual for California. Similar landslides have oc-

curred in southern California during the 1915–16, 1933–34, 1937–38, 1951–52, 1961–62, 1968–69, 1977–78, and 1979–80 rainfall seasons (Weber, 1979). In the San Francisco Bay region, similar landslides occurred during the winters of 1905–06, 1906–07, 1949–50, 1955–56, 1961–62, 1962–63, 1964–65, 1967–68, 1969–70, 1972–73, 1974–75, and 1977–78 (Lawson, 1908; Rice and others, 1976; Radbruch and Weiler, 1963; and T. C. Smith, unpublished data; Smith (oral commun., 1985) indicated that inclusion of the 1967–68 rainfall season for the San Francisco Bay region was an error, and that the 1966–67 season having the massive storm of January 1967 is the correct entry).

These references cite a general occurrence of landslides and distinguish among types in some instances, although none provides estimates of their numbers or areal extent. Nevertheless, all the regional and localized storms described in the previous section, as well as many earlier storms, caused damaging landslides in addition to flooding.

The landslides mostly consisted of two major types, described herein in general terms of depth to failure surface, velocity of downslope movement, and initiating mechanism. One type includes deep-seated, slow-moving failures, such as slumps and earth flows. These failures generally are initiated after extended periods of intermittent to continuous, moderately intense rainfall such as might be expected from a succession of regional storms. The failures generally occur in response to lengthy, gradual increases in ground saturation, and failure takes place after long periods of rainfall or during ground-water rise occurring weeks to months after the rain has ceased. The other type includes shallow, fast-moving slides and flows, such as debris flows, that occur during persistent, intense rainfall. These failures occur almost solely while the rain is falling and under certain specific conditions of antecedent ground saturation and rainfall intensity and duration (Wieczorek, 1982; see chaps. 3–6).

Both the patterns of rainfall from localized storms and intense bursts of rainfall within regional storms have been observed to generate debris flows. Localized storms are fully discussed in the other chapters of this volume, and regional storms are exemplified by at least two of the storms discussed above. Campbell (1975) noted for storms in southern California during January 18–26, 1969, that periods of debris-flow activity were confined to two intervals of sustained heavy rainfall, each lasting about 9 hours and separated by about 3 days. The activity persisted only during intense rainfall, and ceased when the amount of rainfall diminished. A similar situation apparently occurred, but was not so precisely documented, in the San Francisco Bay region during December 1955 and January 1956. During December 21–23, two 6- to 8-hour bursts of heavy rainfall separated by 12 hours followed a week of moderate to heavy rain. S.J. Rice (oral commun., 1982) observed debris flows in Marin County at these times, and again during a downpour on January 18 that was part of the regional storm sequence which began 35 days earlier.



TABLE 1.1.—Approximate areas of the Coast, Transverse, and Peninsular Ranges affected by damaging rainstorms, 1861-1982

[State proclamations of emergency or disaster, and Federal disaster declarations, are available only for the period 1954-82. State and Federal emergency and disaster proclamations and declarations typically describe the specific event by using such terms as "severe storms, heavy rains, flooding, mudslides, landslides," and combinations of these and other terms. Federal disaster declarations designate the type of event differently from the original State proclamations. Terminology in this table is extracted from a compilation by the California Office of Emergency Services and reflects the State Governor's original proclamation. Arrows denote approximate geographic extent of storm damage in coastal California during the indicated period; ?, no data available. Data compiled from Rantz (1964), Young and Cruft (1967), Waananen and others (1977), Kahrl (1978), California Office of Emergency Services (written commun., 1982), and Federal Emergency Management Agency (written commun., 1982)]

Approximate dates of severe rainstorms	Northern Coast Ranges (California-Oregon State line to Sonoma County)	Central Coast Ranges (Sonoma County to Santa Barbara County)	Transverse and Peninsular Ranges (Santa Barbara County to United States- Mexican border)	Type of disaster proclamation or declaration
December 1861-January 1862				
? 1879	← ? →	REGION		
January-February 1881	← ? →			
January-February 1890	← ? →	?	?	
February 1891				
? 1895	← ? →	BAY		
January 1907				
March 1911				
February 1914				
February 1915		SAN FRANCISCO		
January 1916				
February 1927				
December 1937-March 1938				
February 1940				
April 1941				
January 1943				
December 1951-January 1952				
January 1953				
February 1954				Federal: Fire, flooding, and erosion.
December 1955-January 1956				Federal: Flooding.
February 1958				State: Storm and flood damage.
April 1958				Federal: Storm and flood damage.
January 1959				State: Potential flood damage and landslides as result of fires.
February 1962				Federal: Flood and rainstorms.
October 1962				Federal: Flood and rainstorms.
January-February 1963				Federal: Flood and rainstorms.
February 1963				State: Abnormally heavy and continuous rainfall
February 1964				State: Abnormally heavy and continuous rainfall
April 1964				State: Excessively high winds; subsequent heavy rains and runoff of mud and silt.
December 1964-February 1965				Federal: Abnormally heavy and continuous rainfall and windstorm.
January 1965				State: Flooding and hill slide caused by heavy rains.
June 1965				State: Slide damage.
November-December 1965				Federal: Abnormally heavy and continuous rainfall.
January 1966		REGION		Federal: Abnormally heavy and continuous rainfall.
December 1966				State: Earth slides.
December 1966				Federal: Abnormally heavy and continuous rainfall.
January 1967				
January-March 1969				Federal: Storm, flooding, and other conditions.

TABLE 1.1.—Approximate areas of the Coast, Transverse, and Peninsular Ranges affected by damaging rainstorms, 1861–1982—Continued

December 1969–March 1970					Federal: Heavy winds, storms, and flooding.
February 1970			↔		State: Slide damage caused by heavy rains and storms.
March 1970			BAY	↔	State: Slide damage caused by heavy rains and storms.
April 1970			↔		State: Storms and flooding.
December 1971				↔	Federal: Heavy winds, flooding, and runoff of mud and silt.
January–March 1972	↔				Federal: Heavy rains, flooding, and mudslides.
October 1972			SAN FRANCISCO	↔	State: Heavy rains and mudslides.
January–February 1973		↔		↔	Federal: Heavy rains, winds, flooding, and tidal action.
February 1973		↔			State: Storms and flooding.
March 1973	↔				State: Storms and flooding.
April 1973			↔		State: Storms and flooding.
December 1973–January 1974	↔				Federal: Winds, storms, and flooding.
February 1974			↔		State: Severe storm conditions.
April 1974	↔				Federal: Winds, storms, and flooding.
September 1976				↔	Federal: High winds, heavy rains, and flooding.
August 1977				↔	State: Threat of flooding and mudslides from denuded watershed by major fires.
December 1977–March 1978	↔		↔		State: Heavy rains, winds, high tides, heavy seas, landslides, and flooding.
February–March 1978				↔	Federal: Heavy rains, winds, mudslides, heavy snow, and avalanches.
August 1979				↔	Federal: Flash floods.
February–March 1980			↔		Federal: Rain, winds, mudslides, and flooding.
January 1982	↔	↔			Federal: Heavy winds, rain, flooding, and mudslides.

Of particular interest are the data of Weaver (1962, p. 28), showing that during the December 21–23, 1955, storm, peak 6-hour rainfall bursts struck most of northern and central California simultaneously. These data suggest that rainfall and ground-moisture conditions sufficient for initiating rapid slope failures were probably widespread, although no comprehensive documentation is available of the number, type, and areal extent of slope failures associated with the 1955–56 storms.

#### POPULATION, DEVELOPMENT, AND LANDSLIDE DAMAGE

Population in the 10 San Francisco Bay region counties is listed in table 1.2 for 1940–80, with estimates for 1990. These dates are chosen to represent the period of the region's fastest growth and its coincidence with the onset of frequent storm-related disasters listed in table 1.1. Taking the Spanish discovery of the San Fran-

cisco Bay in 1769 as the beginning of European settlement of the region (Watkins, 1973, p. 35–40), the data show population growth from 1940–60 exceeding that of 1769–1940, and continued expansion at a slightly lesser rate from 1960 to 1980. By 1990, the projected population will exceed 6 million people, or about 300 people per square kilometer. Such growth implies attendant increases in the numbers of houses, transportation arteries, utilities, public buildings, and other construction. Between 1970 and 1980, for example, the net increase in housing units alone was 46,550 per year—almost half a million additional units for the decade (table 1.3). These units and associated construction typically are accommodated spatially in new, multiple-unit structures within existing built-up areas and by expansion onto lightly developed or undeveloped terrain.

Before the 1950's, most development took place on gently sloping lowlands, and nearly all the hillsides and uplands were undeveloped or used only for timber harvesting, orchards, and grazing (Brown and Kockelman,

TABLE 1.2.—*San Francisco Bay region population, by county, 1940-90*

[Data from Western Economic Research Co. (1982)]

County	1940	1950	1960	1970	1980	1990
Alameda-----	513,011	740,315	908,209	1,071,446	1,105,379	1,151,500
Contra Costa----	100,450	298,984	409,030	556,116	657,252	796,400
Marin-----	52,907	85,619	146,820	208,652	222,952	231,800
Napa-----	28,503	46,603	65,890	79,140	99,199	106,100
San Francisco----	634,536	775,357	740,316	715,674	678,974	660,600
San Mateo-----	111,782	235,659	444,387	557,361	588,164	629,800
Santa Clara-----	174,949	290,547	642,315	1,065,313	1,295,071	1,497,200
Santa Cruz-----	45,057	66,534	84,219	123,790	188,141	224,100
Solano-----	49,118	104,833	134,597	171,989	235,203	340,000
Sonoma-----	69,052	103,405	147,375	204,885	299,827	385,700
Total-----	1,779,365	2,747,856	3,723,158	4,754,366	5,370,162	6,023,200

TABLE 1.3.—*San Francisco Bay region housing units, by county, 1970-80*

[Data from U.S. Bureau of the Census (written commun., 1982)]

County	1970	1980	Difference
Alameda-----	378,833	444,607	+65,774
Contra Costa----	177,732	252,226	+74,494
Marin-----	72,000	92,903	+20,903
Napa-----	26,838	40,052	+13,214
San Francisco----	310,402	316,609	+6,207
San Mateo-----	191,077	233,494	+42,417
Santa Clara-----	336,873	473,817	+136,944
Santa Cruz-----	52,006	80,863	+28,857
Solano-----	53,762	84,270	+30,508
Sonoma-----	78,060	124,233	+46,173
Total-----	1,677,583	2,143,074	+465,491

1983, p. 3, 31). Since the 1950's, however, significant development on hillsides has created sprawling suburban landscapes susceptible to various natural and induced hillslope processes. Indeed, such development has been a prime force in creating or adding to problems of slope stability (Nilsen and Turner, 1975; Nilsen and others, 1976b). With that development came landslide disasters of sufficient frequency to call attention to a regional landslide problem, and to stimulate better record keeping of landslide occurrence. Nilsen and others (1976a, p. 6), for example, noted that although the oldest records of property damage by landslides in Alameda County date from 1940, most of the data are from the period 1958-71, when more accurate records were kept. The situation is similar throughout other San Francisco Bay region counties, and it was not until the 1970's that the regional scope of the landslide problem was widely recognized and attempts were made to document regional losses (Nilsen and others, 1979, p. 3-10, 16-19).

The late-appearing awareness of the landslide problem resulted in even later attempts to confront it, if, indeed, it was considered at all in new development. Whereas some communities and counties considered landslide hazards in revising building codes and grading ordinances, most of the San Francisco Bay region entered the 1980's with few or no considerations of slope stability mandated for hillside building. This situation is not surprising, considering the numerous financial, political, and other problems communities face in responding to geologic situations whose process and recurrence are difficult for them to understand. With respect to the specific hazard of debris flows, for example, little information of use for planning was available anywhere in the region before the storm of January 1982, and utilization of that information remains mostly in the research stage today.

### LESSONS OF JANUARY 1982

The preceding discussion briefly illustrates some of the complexities in understanding the January 1982 storm in comparison with previous storms and in the context of spreading hillside development. These complexities are summarized here in an attempt to focus on the need for reanalysis of past events and on the prospects for future studies.

1. Whereas some level of presaturation of the soil mantle is a necessary condition for debris-flow occurrence (see chap. 5), that level can be attained during the course of a single storm irrespective of soil mantle saturation conditions at the onset of the storm. Radbruch and Weiler (1963, p. 16-17) stated, for example, for Contra Costa County:

In October 1962, 13.82 inches of rainfall was recorded at Saint Mary's College during four days from October 10 through 14, with 8.40 inches recorded during the 24 hours ending at 5:00 P.M. on



October 13 (State Climatologist, U.S. Weather Bureau, oral communication, January 2, 1963). The rain was the first of the winter rainy season, and fell on ground that had dried during the summer. Most of the landslides that formed during the above four days of rain were mudflows, consisting of saturated soil that moved on the underlying bedrock surface. The soil did not move as a single mass, but flowed out of small pockets in a semi-liquid state, leaving a train of debris extending down the hillside for as much as several hundred feet. The debris consisted of thin mud containing pieces of turf and subangular to rounded pieces of soil. These landslides are the type described by Kesseli (1943) as "disintegrating soil slips."

Radbruch and Weiler made no further statements as to the abundance of these landslides, and it is unclear from their observations how the events of the 1962 storm compare with those of the 1982 storm. Cannon (see chap. 4) and Mark and Newman (see chap. 2) suggest that the abundance of debris flows is related to a level of soil mantle saturation determined by antecedent seasonal rainfall, measured from the beginning of the rainy season up to the beginning of a debris-flow producing storm. In the case of the 1981-82 rainfall sequence, soil-mantle saturation was high at the onset of the January 3-5 storm and thereby contributed to debris flows in apparently greater abundance and wider distribution than observed in 1962. Nevertheless, observations like those of Radbruch and Weiler, and the frequency of rainfall intensity, duration, and extent observed for storms discussed in this chapter, suggest that conditions for the local occurrence of debris flows are common. A dry soil mantle does not guarantee that debris flows will not occur during the next storm.

2. Whereas 2-day rainfall totals for specific parts of the San Francisco Bay region in January 1982 exceeded the "100 year" recurrence frequency, frequencies of 5 to 50 years were common for many areas where debris flows occurred (table 1.4). Recurrence intervals for floodflows of streams were generally in the range 4-40 years (see chap. 13). Furthermore, the rainfall intensity and duration at which debris-flow episodes began in 1982 fell far short of the "100 year" values eventually reached in some areas (see chap. 3). These factors suggest that significant local rainfall variations occur within a "100 year" storm and that storms of lesser frequency are also sufficient to cause significant debris-flow activity. The recurrence interval of a given storm parameter, such as 2-day rainfall, is an insufficient measure of debris-flow-generating capability. A better measure would be a combinatorial factor that includes a component of antecedent soil mantle saturation with individual storm factors (see chaps. 4, 5).
3. Great uncertainty exists about the effects of earlier storms because of the paucity of data on specific types

of landslides. The first documentation of the regional occurrence of debris flows as a unique process in the San Francisco Bay region came after the January 1982 storm. Thus, only limited opportunities exist for comparing the effects of that storm with those of others until the earlier storms are comparably analyzed (see chap. 4). A primary candidate for study is the December 1955-January 1956 storm sequence because of the availability of rainfall and photographic data, and many general and specific observations of debris flows then. Work in progress by C.M. Wentworth (written commun., 1984) suggests that abundant debris-flow scars on Montara Mountain, San Mateo County, resulted from the 1955-56 storms, but data from other areas are needed to determine the areal extent and relative abundance of debris flows during those events.

4. Confusion about storm effects results from ambiguities and inconsistencies in the terminology used to describe disasters. Table 1.1 lists the terminology applied to California storm disasters; it is apparent that no consistent distinctions among the types of landslides exist. Neither is the disaster declaration necessarily complete as to effects. For example, the Federal disaster declaration for 1955-56 specifies only floods and makes no mention of landslides as a disaster component. Whether landslides were not a problem or, more likely, were considered a part of the overall flooding is unclear in the disaster proclamation. Although floods and landslides are generally concurrent events, observers in the past have commonly emphasized only the flood aspects.
5. Population growth and development in the San Francisco Bay region have outpaced the recognition and accommodation of landslide hazards, and the development itself has created hazardous situations where none existed previously. The status of development today, and its trends for the near future, are such that the frequency of landslide problems will probably increase until sweeping changes in the regulations on hillside development are enacted on a regional basis. Such changes almost certainly will come, as they have for other heavily populated regions in unstable, hilly terrain (U.S. Geological Survey, 1982, p. 1). Meanwhile, the composite interactions of population growth, hillside development, and recurrence of damaging storms should be more thoroughly assessed.

## REFERENCES CITED

- Aldridge, B.N., 1982, Hydrology of the floods of March 1978 through February 1980 in the Phoenix area, Arizona, in Brooks, N.B., ed., Storms, floods, and debris flows in southern California and Arizona,

TABLE 1.4.—*Storm rainfall and estimated recurrence intervals at selected rainfall-measurement stations in the San Francisco Bay region*

[Water year is the 12-month period ending September 30 of the indicated year. Data from Goodridge (1982, p. 1)]

Rainfall-measurement station	Location	January 1982		Previous 2-day maximum	
		Maximum rainfall over 2 days (mm)	Estimated recurrence interval (yr)	Rainfall (mm)	Water year
Occidental-----	Southwestern Sonoma County.	231	5	302	1978
Graton-----	South-central Sonoma County.	187	5	240	1967
Sonoma-----	Southeastern Sonoma County.	201	25	194	1963
Alpine Dam-----	Southwestern Marin County.	345	100	293	1963
Kent Lake-----	do-----	380	40	339	1967
Lagunitas Lake----	do-----	313	50	292	1963
Pilarcitos-----	North-central San Mateo County.	207	5	451	1872
San Andreas Lake---	do-----	200	25	236	1963
San Francisco Airport.	Northeastern San Mateo County.	160	50	152	1967
Half Moon Bay-----	Western San Mateo County.	205	100+	197	1963
Ben Lomond-----	Central Santa Cruz County.	409	25	422	1963
Santa Cruz-----	South-central Santa Cruz County.	240	100+	202	1956

- 1978 and 1980—proceedings of a symposium, September 17-18, 1980: U.S. National Academy of Sciences, National Research Council Report CSS-CND-019A, p. 87-99.
- Bailey, E.H. ed., 1966, Geology of northern California: California Division of Mines and Geology Bulletin 190, 508 p.
- Brooks, N.D., ed., 1982a, Storms, floods, and debris flows in southern California and Arizona, 1978 and 1980—overview and summary of a symposium, September 17-18, 1980: U.S. National Academy of Sciences, National Research Council Report CSS-CND-019, 47 p.
- ed., 1982b, Storms, floods, and debris flows in southern California and Arizona, 1978 and 1980—proceedings of a symposium, September 17-18, 1980: U.S. National Academy of Sciences, National Research Council Report CSS-CND-019A, 487 p.
- Brown, R.D., Jr., and Kockelman, W.J., 1983, Geologic principles for prudent land use—a decisionmaker's guide for the San Francisco Bay region: U.S. Geological Survey Professional Paper 946, 97 p.
- Brown, W.M., III, 1984, Debris flows, landslides, and floods in the San Francisco Bay region, January 1982—overview and summary of a conference held at Stanford University, August 23-26, 1982: U.S. National Academy of Sciences, National Research Council Report CETS-CND-027, 83 p.
- Campbell, R.H., 1975, Soil slips, debris flows, and rainstorms in the Santa Monica Mountains and vicinity, southern California: U.S. Geological Survey Professional Paper 851, 51 p.
- Goodridge, J.D., 1982, Precipitation data supplement for the storm of San Francisco Bay area on January 2-5, 1982: California Department of Water Resources, 16 p.
- 1984, Climate records from California: Workshop on climate variability of the eastern North Pacific and western North America held at Pacific Grove, California, March 4-8, 1984: California Department of Water Resources, 8 p.
- Hofmann, Walter, and Rantz, S.E., 1963, Floods of December 1955-January 1956 in the Far Western States. Part 1. Description: U.S. Geological Survey Water-Supply Paper 1650-A, p. A1-A156.
- Kahl, W.L., ed., 1978, The California water atlas: Sacramento, California Governor's Office of Planning and Research, and California Department of Water Resources, 118 p.
- Kesseli, J.E., 1943, Disintegrating soil slips of the coast ranges of central California: Journal of Geology, v. 51, no. 5, p. 342-352.
- Lawson, A.C., chairman, 1908, The California earthquake of April 18, 1906: Report of the State Earthquake Investigation Commission: Carnegie Institution of Washington Publication 87, 2 v.

- Lynch, H.B., 1931, Rainfall and stream runoff in southern California since 1931: Los Angeles, Metropolitan Water District of Southern California, 30 p.
- Monteverdi, J.P., 1984, Similarities among three record rain-producing storms in north-central California, in Brown, W.M., III, Debris flows, landslides, and floods in the San Francisco Bay region, January 1982—overview and summary of a conference held at Stanford University, August 23–26, 1982: U.S. National Academy of Sciences, National Research Council Report CETS-CND-027, p. 59–63.
- Nilsen, T.H., Taylor, F.A., and Brabb, E.E., 1976a, Recent landslides in Alameda County, California (1940–71): An estimate of economic losses and correlations with slope, rainfall, and ancient landslide deposits: U.S. Geological Survey Bulletin 1398, 21 p.
- Nilsen, T.H., Taylor, F.A., and Dean, R.M., 1976b, Natural conditions that control landsliding in the San Francisco Bay region—an analysis based on data from the 1968–69 and 1972–73 rainy seasons: U.S. Geological Survey Bulletin 1424, 35 p.
- Nilsen, T.H., and Turner, B.L., 1975, Influence of rainfall and ancient landslide deposits on recent landslides (1950–71) in urban areas of Contra Costa County, California: U.S. Geological Survey Bulletin 1388, 18 p.
- Nilsen, T.H., Wright, R.H., Vlasic, T.C., and Spangle, W.E., 1979, Relative slope stability and land-use planning in the San Francisco Bay region, California: U.S. Geological Survey Professional Paper 944, 96 p.
- Radbruch, D.H., and Weiler, L.M., 1963, Preliminary report on landslides in a part of the Orinda Formation, Contra Costa County, California: U.S. Geological Survey open-file report, 49 p.
- Rantz, S.E., 1964, Surface-water hydrology of coastal basins of northern California: U.S. Geological Survey Water-Supply Paper 1758, 77 p.
- Rantz, S.E., and Harris, E.E., 1963, Floods of January–February 1963 in California and Nevada: U.S. Geological Survey open-file report, 74 p.
- Rantz, S.E., and Moore, A.M., 1965, Floods of December 1964 in the far western states: U.S. Geological Survey open-file report, 205 p.
- Rice, S.J., Smith, T.C., and Strand, R.G., 1976, Geology for planning, central and southeastern Marin County, California: California Division of Mines and Geology Open-File Report 76–2SF, 103 p.
- Smith, T.C., and Hart, E.W., 1982, Landslides and related storm damage, January 1982, San Francisco Bay region: California Geology, v. 35, no. 7, p. 139–152.
- U.S. Geological Survey, 1982, Goals and tasks of the landslide part of a ground-failure hazards reduction program: Circular 880, 49 p.
- Waananen, A.O., 1969, Floods of January and February 1969 in central and southern California: U.S. Geological Survey open-file report, 233 p.
- Waananen, A.O., Limerinos, J.T., Kockelman, W.J., Spangle, W.E., and Blair, M.L., 1977, Flood-prone areas and land-use planning—selected examples from the San Francisco Bay region, California: U.S. Geological Survey Professional Paper 942, 75 p.
- Watkins, T.H., 1973, California—an illustrated history: Palo Alto, Calif., American West Publishing Co., 543 p.
- Wahl, K.L., Crippen, J.R., and Knott, J.M., 1980, Floods of January and February 1980 in California: U.S. Geological Survey Open-File Report 80–1005, 56 p.
- Weaver, R.L., 1962, Meteorology of hydrologically critical storms in California: U.S. National Oceanic and Atmospheric Administration Hydrometeorological Report 37, 207 p.
- Weber, F.H., Jr., 1979, General features of landsliding and debris flooding in southern California, in Landslides in the Los Angeles region, California—effects of the February–March 1978 rains: California Division of Mines and Geology Open-File Report 79–4 LA, p. 15–47.
- Western Economic Research Co., 1982, Population trends in California: Sherman Oaks, Calif., 25 p.
- Wieczorek, G.F., 1982, Map showing recently active and dormant landslides near La Honda, central Santa Cruz Mountains, California: U.S. Geological Survey Miscellaneous Field Studies Map MF-1422, scale 1:4,800.
- Young, L.E., and Cruff, R.W., 1967, Magnitude and frequency of floods in the United States—part 11, Pacific slope basins in California—volume 1, Coastal basins south of the Klamath River basin and Central Valley drainage from the west: U.S. Geological Survey Water-Supply Paper 1685, 272 p.



## 2. RAINFALL TOTALS BEFORE AND DURING THE STORM: DISTRIBUTION AND CORRELATION WITH DAMAGING LANDSLIDES

By ROBERT K. MARK and EVELYN B. NEWMAN,  
U.S. GEOLOGICAL SURVEY

### CONTENTS

	Page
Abstract - - - - -	17
Introduction - - - - -	17
Previous work - - - - -	17
Data collection - - - - -	17
Computational methods - - - - -	18
Analysis - - - - -	18
Results - - - - -	19
Conclusions - - - - -	25
References cited - - - - -	26

### ABSTRACT

Analysis of the relation between rainfall totals and damaging landslides (predominantly debris flows) for the January 3-5, 1982, storm in the San Francisco Bay region indicates a significant relative increase in the density of damaging landslides in areas that had seasonal prestorm rainfall of at least 300 to 400 mm (12-16 in.) and storm rainfall of about 250 mm (10 in.), and that received 30 percent of mean annual precipitation during the storm.

### INTRODUCTION

The importance of collecting adequate rainfall and landslide data was recognized simultaneously with the realization of the magnitude of the January 3-5, 1982, storm. Research teams were assembled to collect data on rainfall, landslides (see "Introduction" to volume for landslide terminology), and economic losses due to landslides throughout the San Francisco Bay region.

The immediate goal was to understand the relation between rainfall totals and debris flows that occurred during this storm, and the long-term goal was to incorporate this relation into a multiparameter statistical model of susceptibility to debris flows in the bay region. Only the results of the rainfall/debris-flow study for the storm are reported here. Our approach to understanding the relation between rainfall and debris flows was to compare the rainfall at damaging-landslide localities with the regional storm and prestorm rainfall. From these data, we obtained a landslide-density ratio, which measures the relative increase or decrease in the areal density of damaging landslides from the storm average as a function of rainfall.

### PREVIOUS WORK

Other workers have also examined the relations between rainfall and debris flows or other landslides. Campbell's (1975) work on debris flows in the Santa Monica Mountains in southern California, and Nilsen and others' (1976) work on landslides during storms in the San Francisco Bay region, suggest that critical levels of rainfall intensity and prestorm rainfall must be reached before slopes fail. Preliminary intensity values of 6 mm (0.25 in.) of rain per hour with at least 250 mm (10 in.) of prestorm rainfall were noted for the Los Angeles area, whereas prestorm values of 250 to 380 mm (10-15 in.) and storm totals of 150 to 200 mm (6-8 in.) were recognized for the San Francisco Bay region (using data from Contra Costa County for the 1968-69 and 1972-73 rainy seasons).

A study of debris flows in northwestern Italy (Govi and Sorzana, 1980) indicated the importance of normalized rainfall (the ratio of storm rainfall to mean annual precipitation) in the triggering of debris flows. For dry antecedent conditions, a "catastrophic stage" was reported at normalized rainfall of 28 to 38 percent.

Wieczorek and Sarmiento (see chap. 5) analyze the triggering of debris flows in a small area near La Honda, Calif., as a function of rainfall intensity-duration and antecedent conditions, using data on 17 storms since 1977. Cannon and Ellen (1983; see chap. 3) relate the triggering of abundant debris flows during the January 3-5, 1982, storm to rainfall intensity and mean annual precipitation. Wieczorek and others (see chap. 8) relate the abundance of debris flows to normalized rainfall in the bay region.

*Acknowledgments.*—We are grateful to the hundreds of private citizens and public officials who shared their rainfall data and made our study possible. C.R. Northcut and B.R. Hamachi deserve special thanks for their major effort in assembling and plotting the rainfall data. Many other U.S. Geological Survey (USGS) colleagues assisted us in the inventory of damaging landslides and in collecting rainfall data.

### DATA COLLECTION

Because there are only about 50 U.S. National Weather Service (NWS) stations in the 10 bay-region counties, the USGS team launched an intensive effort to contact State and local agencies that might have rain gages. As a result,



data were collected from the Alameda County Flood Control and Water Conservation District; the California Departments of Forestry, Transportation, and Parks and Recreation; the East Bay Infiltration/Inflow Study and Municipal Utility District; the Marin County Flood Control and Water Conservation District, and Municipal Water District; the San Francisco Water Department; and the Santa Clara Valley Water District.

Immediately after the storm, the NWS launched a media appeal for data on storm totals from private rain-gage operators. The response, from more than 500 individuals, was impressive. The data made available by NWS officials were rechecked and carefully plotted. Data were deleted if the addresses could not be located. Anomalous values were checked by contacting rain-gage owners and requesting additional information on the location and surroundings of the gage; gages with obvious problems were deleted. After plotting the initial NWS, State, county, and local data, we sent teams into areas of sparse data to locate additional rain gages.

The final compilation (Mark and others, 1983) contains 759 entries for the January 3-5, 1982, storm and 434 entries of prestorm totals from July 1, 1981, through January 2, 1982. Even though the official rainfall year began July 1, measurable rain in most of the bay region did not occur until September 24-25, 1981. Significant rainfall accumulated from storms on October 7 and 27-29, November 11-17 and 21-18, and December 17-21. Rain fell almost every day in parts of central coastal California from December 27, 1981, through the January 3-5, 1982, storm.

Ideally, to assess the relation of storm and prestorm rainfall to debris-flow occurrence, a complete inventory of debris flows should be used. Because no such inventory was available, we used the damaging-landslide inventory (see chap. 11) as a representative sample (1,255 points). This inventory was largely of debris flows but included other landslide types—hence the use of the general term “landslide.” Use of the damaging-landslide inventory introduces some bias toward populated areas, and landslides in rural areas are underrepresented.

### COMPUTATIONAL METHODS

The prestorm- and storm-rainfall and damaging-landslide data sets were digitized to utilize computer techniques in contouring and analyzing the data. Because the density of these data varied greatly over the region (pls. 1, 2) and because rainfall information was needed but not generally available at each landslide site, the rainfall data had to be gridded. This procedure created generalized regional models of both prestorm and storm rainfall that were used in all subsequent analyses. These models

do not explicitly include topography, and so orographic rainfall may not be adequately modeled in areas with no data points.

The Surface Gridding Library (Dynamic Graphics, Inc., 1978; Mark and Newman, 1981) was used to generate the prestorm and storm grids with 2.5-km spacing. This spacing utilized 66 percent of the storm data points, with an average absolute deviation of all the original values from their grid-extrapolated values of 14 mm (0.6 in.), which is 2.6 percent of the total storm-rainfall range. The prestorm grid utilized 78 percent of the data points, with an average absolute deviation of all the data points from their grid-extrapolated values of 27 mm (1.1 in.), which is 2.1 percent of the prestorm-rainfall range. The grids were not extrapolated beyond the data points.

Mean-annual-precipitation contours from the isohyetal map of the San Francisco Bay region (Rantz, 1971a) were digitized and gridded. Normalized prestorm and storm grids were prepared by dividing the rainfall grids by the mean-annual-precipitation grid on a point-by-point basis. All the contour maps (pls. 1, 2; figs. 2.1-2.3) were generated by computer, using the Surface Display Library software (Dynamic Graphics, Inc., 1975; Mark and Newman, 1981). Generalized polygons bounding the regions with a slope of more than 5 percent were digitized (shaded areas, fig. 2.1). The area outside the polygons was omitted from the analysis so as to avoid biasing the regional rainfall distribution by including major flatland areas in which debris flows generally do not occur. The polygons include 70 percent of the land area and more than 95 percent of the digitized landslide points.

### ANALYSIS

The following analysis was performed for each of the four grids (prestorm rainfall, storm rainfall, normalized prestorm rainfall, and normalized storm rainfall):

1. Each set of grid points within the greater-than-5-percent-slope polygons was used as a sample of the rainfall distribution over the region.
2. Rainfall values at each landslide point were computed from the grid by interpolation to generate a sample of rainfall distribution at landslides.
3. The cumulative distribution of both regional rainfall and rainfall at damaging-landslide sites was calculated as a percentage of sample points exceeding some rainfall value, and the curves were plotted (fig. 2.4).
4. The corresponding distributions were compared by preparing histograms (fig. 2.5) and then taking histogram ratios, that is, the percentage of landslides in a given rainfall interval divided by the percentage of grid points in the same interval (fig. 2.6). These distributions were also compared in both dimensions (prestorm and storm) simultaneously (fig. 2.7).

## RESULTS

The pairs of cumulative curves (fig. 2.4) differ in the rainfall distributions at grid points and at landslides. In three of the four plots (figs. 2.4A, 2.4C, 2.4D), significant rightward shifts of the landslide-sample curves indicate

that for a given cumulative percentage of localities, heavier rainfall is associated with landslides. In the fourth plot (fig. 2.4B), near-identity of the curves indicates that the distribution of this variable does not differ between grid and landslide points. The curves can also be used to calculate the fraction of the region or of landslides that

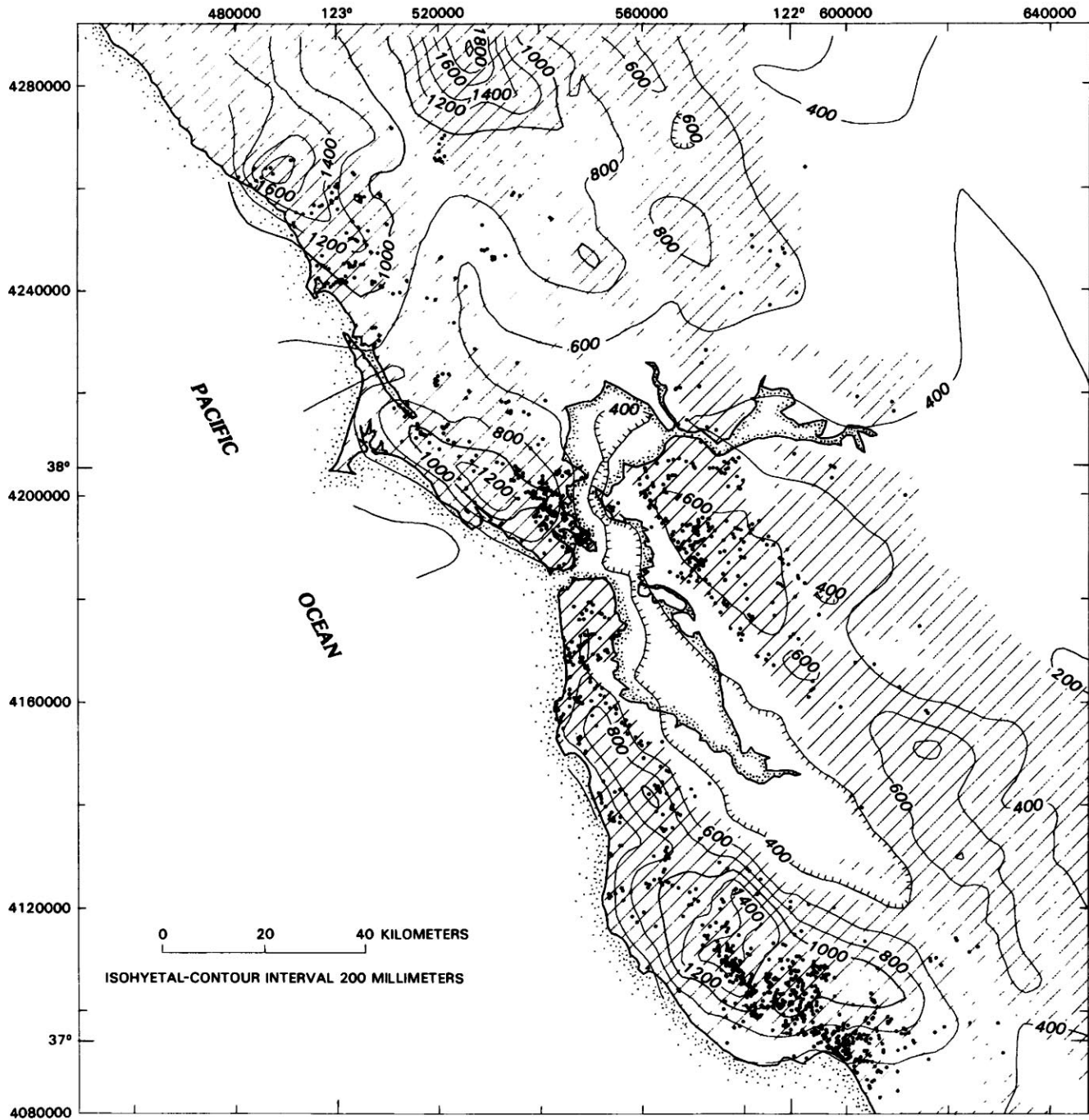


FIGURE 2.1.—Contour map of mean annual precipitation (in millimeters) in the San Francisco Bay region (Rantz, 1971a), showing sites of damaging landslides (dots) (see chap. 11). Line-patterned areas have slopes greater than 5 percent. Hachures indicate closed depressions in rainfall surface. Universal Transverse Mercator grid, zone 10, North American datum 1927, shown in meters.

received less (or more) than a given amount of rainfall. For example, in figure 2.4C, 50 percent of the damaging landslides occurred in localities receiving less than 250 mm (10 in.) of storm rainfall, whereas about 85 percent of the region received that much rainfall or less.

The probability of each total-rainfall interval (for example, 100–200 mm) at landslide points divided by the probability in that same interval at random points over the region measures the relative enhancement (with respect to the regional storm average) of landslides for that

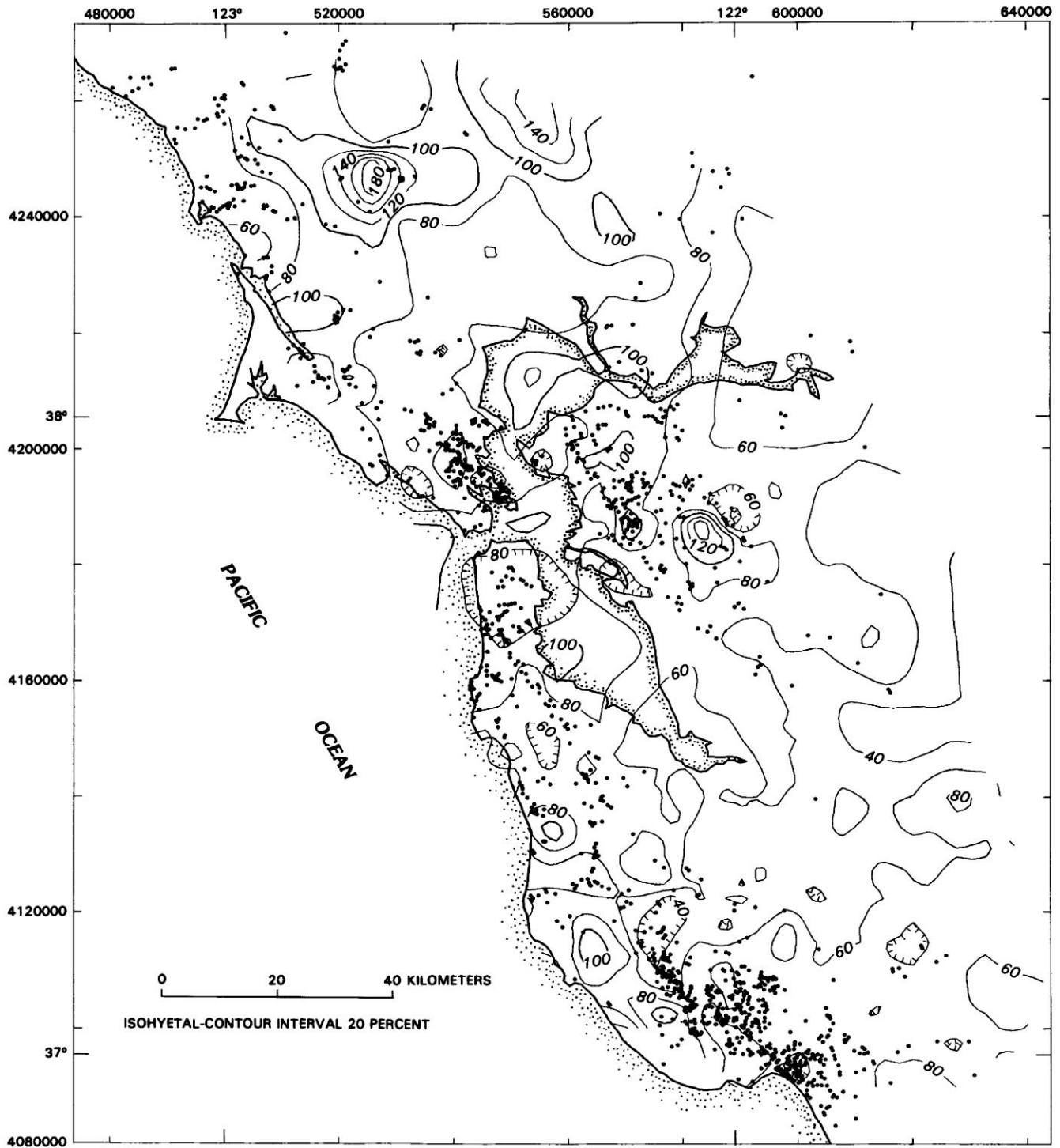


FIGURE 2.2.—Contour map of prestorm (July 1, 1981–Jan. 3, 1982) rainfall normalized with respect to mean annual precipitation in the San Francisco Bay region, showing sites of damaging landslides (dots) (see chap. 11). Hachures indicate closed depressions in rainfall surface. Universal Transverse Mercator grid, zone 10, North American datum 1927, shown in meters.

amount of rainfall. Prestorm and storm histograms (fig. 2.5) compare the rainfall sampled over the bay region with the rainfall sampled at damaging-landslide localities. The plots of storm rainfall versus landslide density (fig. 2.6) suggest that the density of landslides increased sharply where rainfall was more than about 250 mm

(10 in.) (fig. 2.6A) and where normalized storm rainfall (fig. 2.6B) was more than about 30 percent of mean annual precipitation. The plot of prestorm rainfall versus landslide density (fig. 2.6A) suggests that a minimum of 300 to 400 mm (12–16 in.) of prestorm rainfall was required before an appreciable number of damaging land-

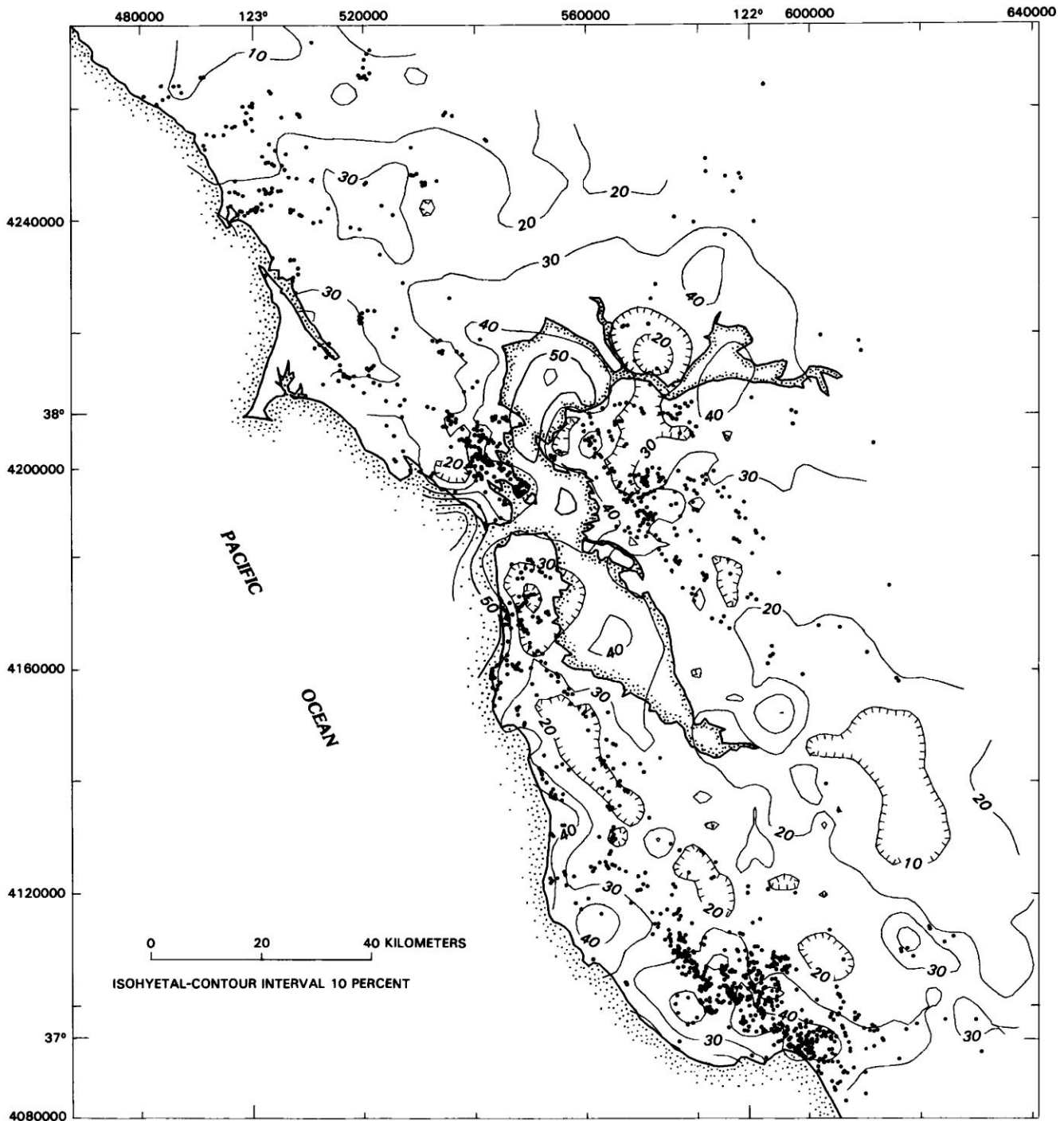


FIGURE 2.3.—Contour map of storm rainfall normalized with respect to mean annual precipitation in the San Francisco Bay region, showing sites of damaging landslides (dots) (see chap. 11). Hachures indicate closed depressions in rainfall surface. Universal Transverse Mercator grid, zone 10, North American datum 1927, shown in meters.

slides occurred; further increase had little apparent effect. However, the plot of normalized prestorm rainfall versus landslide density (fig. 2.6B) shows no discernible pattern.

The plots of storm versus prestorm rainfall (fig. 2.7) indicate additional complexity in the landslide/rainfall relation. Homogeneous regions on these plots are shown bounded by polygons that generally correspond to specific areas of the San Francisco Bay region (fig. 2.8). The area of polygon 1 has high prestorm and storm rainfall, and the highest landslide-density ratio of 5.9. This area encompasses some of the mountainous areas of Santa Cruz and Marin Counties. A total of 13.8 percent of the landslide sample had rainfall in this category, in contrast to 2.3 percent of the random sample.

The area of polygon 2 has midrange prestorm and storm rainfall, and a landslide-density ratio of 2.9. This area covers the remaining parts of Santa Cruz, southern Marin,

southern San Mateo, and southwestern Sonoma Counties. A total of 44.1 percent of the landslide sample had rainfall in this category, in contrast to 15.0 percent of the random sample.

The area of polygon 3 has lower midrange prestorm and low storm rainfall, and a landslide-density ratio of 1. Landslides with rainfall in this category occurred in southern Sonoma, southern Napa, southern Solano, San Francisco, northwestern San Mateo, western Contra Costa, Alameda, and Santa Clara Counties. Almost identical percentages of the landslide and random samples (31.9 and 32.0 percent, respectively) had rainfall in this category.

The area of polygon 4 has midrange to high prestorm rainfall and low to midrange storm rainfall, and a landslide-density ratio of 0.4. This area includes central Sonoma, central Napa, and small parts of Alameda, Contra Costa, Santa Clara, and San Mateo Counties. Only

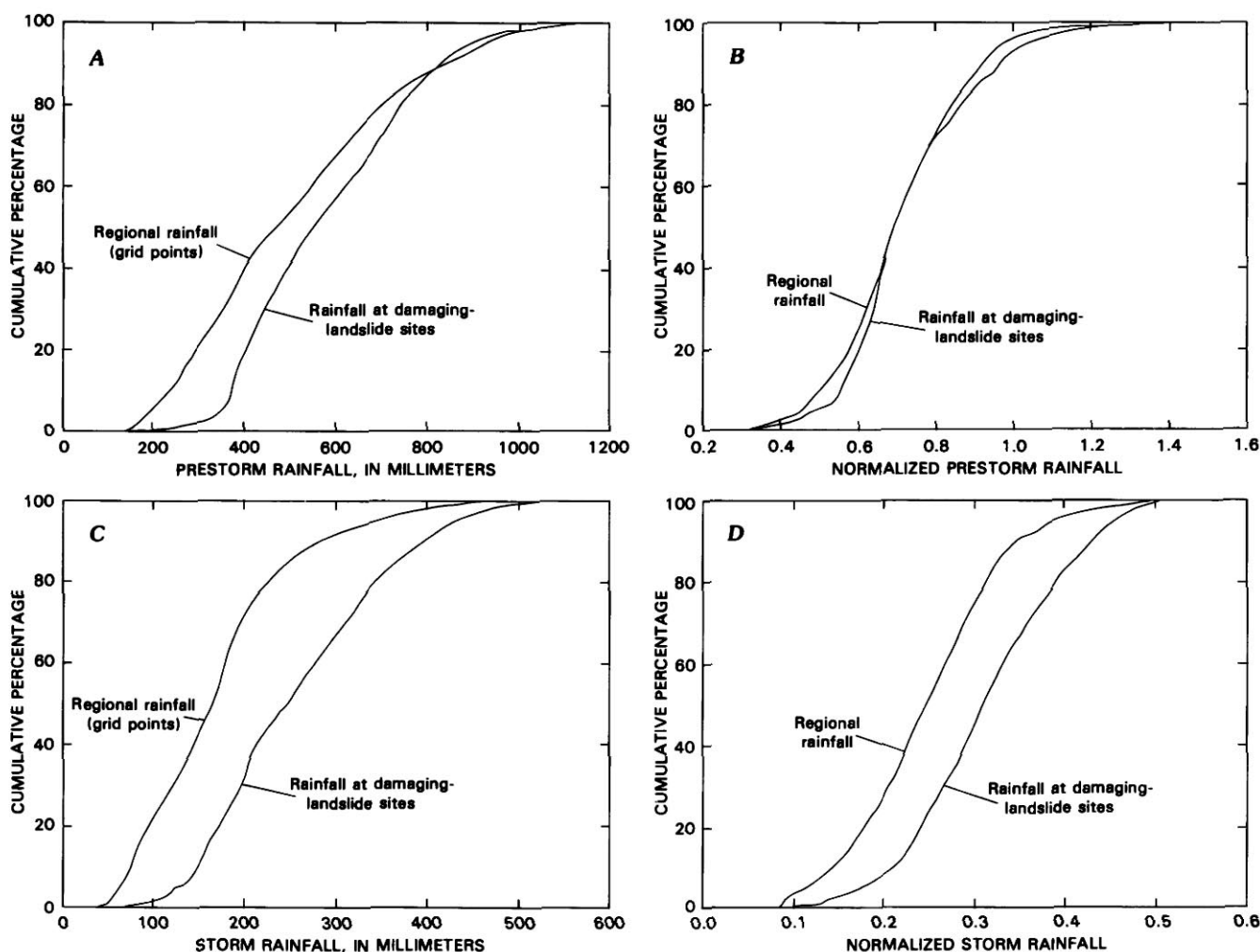


FIGURE 2.4.—Rainfall at sites of damaging landslides as a function of cumulative percentage of regional rainfall. A, Prestorm rainfall. B, Prestorm rainfall normalized with respect to mean annual precipitation. C, Storm rainfall. D, Storm rainfall normalized with respect to mean annual precipitation.



5.8 percent of the landslide sample had rainfall in this category, in contrast to 13.3 percent of the random sample.

The area of polygon 5 has the lowest values of both prestorm and storm rainfall, and the lowest landslide-density ratio of 0.1. This area encompasses the Diablo Range in southern Solano, eastern Contra Costa, eastern Alameda, and eastern Santa Clara Counties. A total of 4.5 percent of the landslide sample had rainfall in this category, in contrast to 37.3 percent of the random sample.

The main trend (polygons 1, 2, 3, 5) is consistent with the ratio plots. Polygon 4, however, represents an area

(largely on the north edge of the storm) that has midrange to high prestorm and low to midrange storm rainfall, and a lower landslide-density ratio (0.4) than polygon 3 (1.0), which has lowest prestorm but comparable storm rainfall. This result may reflect the bias introduced by using only damaging landslides in the sample. The northern bay region dominating polygon 4 is relatively sparsely populated, and so landslides that would have caused damage if these areas were more highly developed were not included in the sample.

Several points must be considered in evaluating these results.

1. Prestorm, storm, and mean annual precipitation are

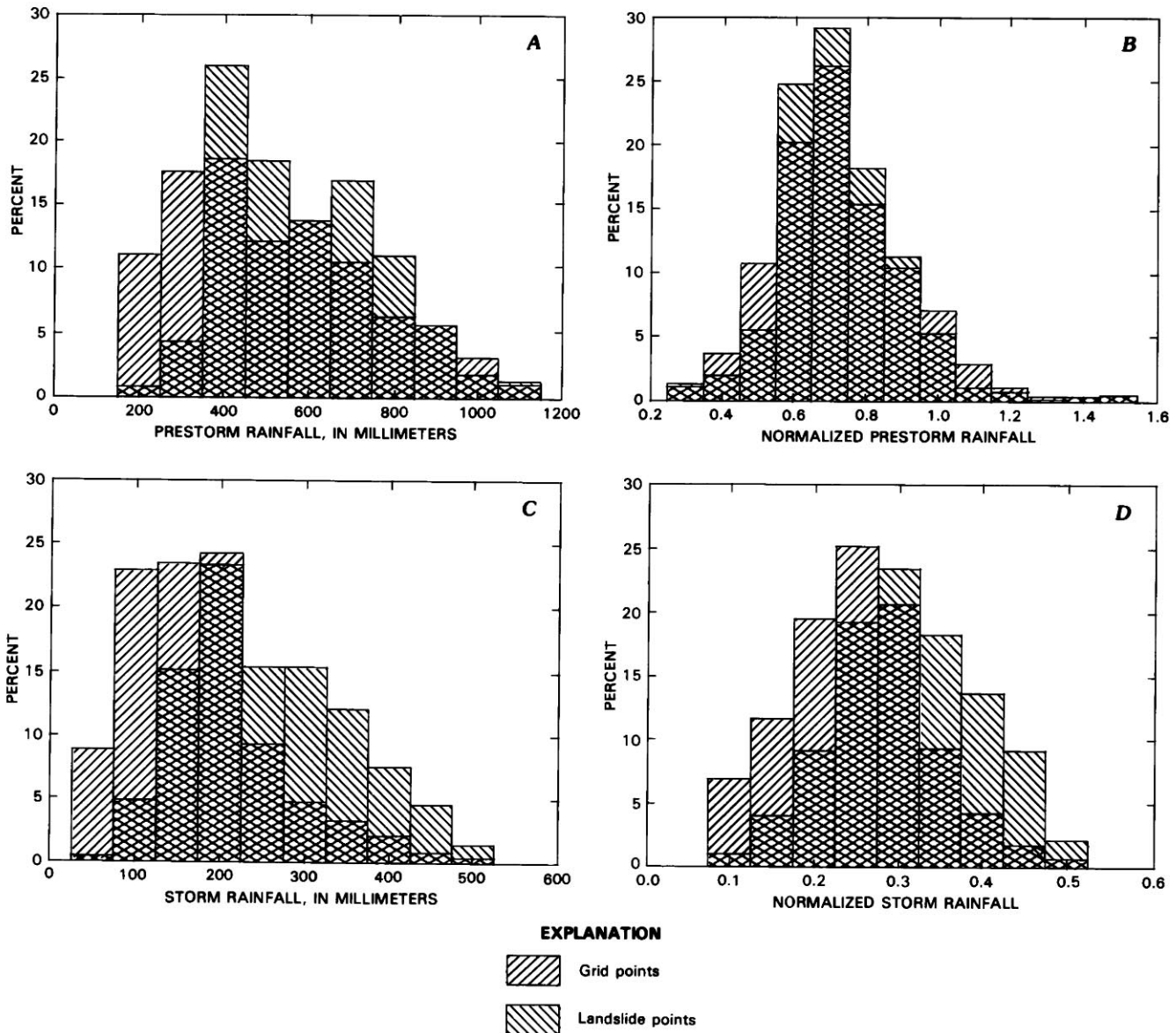


FIGURE 2.5.—Percentage of regional rainfall at grid points in comparison with prestorm rainfall or with storm rainfall at sites of damaging landslides. A, Prestorm rainfall. B, Normalized prestorm rainfall. C, Storm rainfall. D, Normalized storm rainfall.



positively correlated to varying degrees (prestorm with mean annual precipitation, 0.81; storm with mean annual precipitation, 0.52; storm with prestorm rainfall, 0.61).

2. The landslide sample is biased toward developed areas.
3. Landslides depend on many other factors besides rainfall; some of these factors, such as slope, may correlate with orographic rainfall.
4. In a particular storm, total storm rainfall may correlate with rainfall intensity (Rantz, 1971b), and so the relations between landslides and total rainfall could be due to variations in rainfall intensity (Cannon and Ellen, 1983). For a sample of 15 stations, the correla-

tion between peak 3-hour intensity and total storm rainfall was 0.7.

5. It cannot be determined, on the basis of one storm, whether some or all of the curves will be reproducible in other storms. Duration of the storm may also be an important factor. Additional data from other storms, whether or not they generate landslides, are needed.

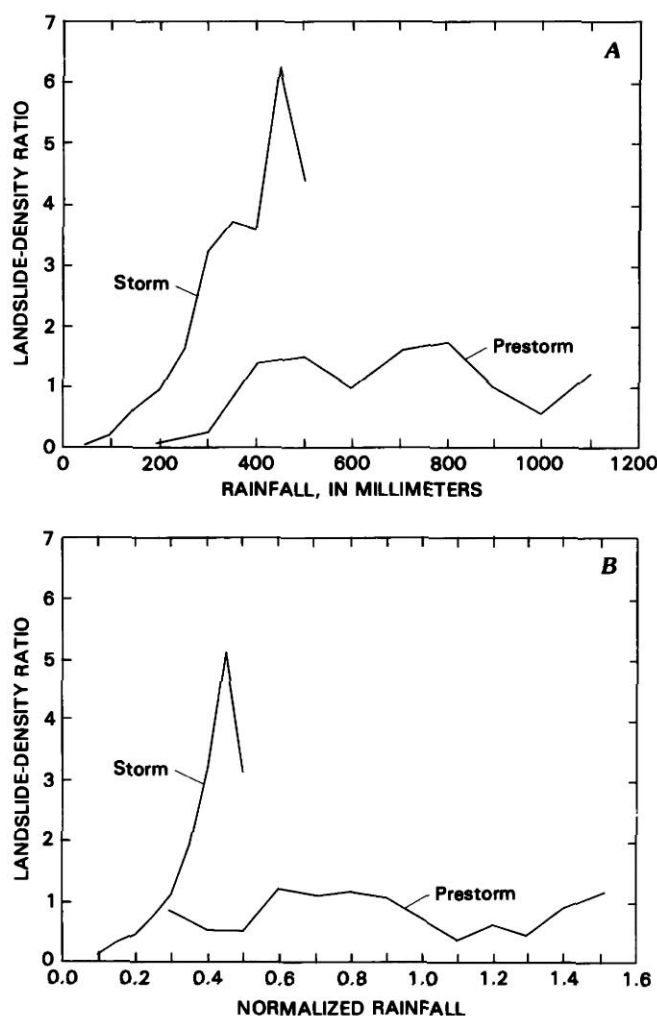


FIGURE 2.6.—Landslide-density-ratio plots showing relative density of damaging landslides as a function of rainfall, that is, ratios of histograms in figure 2.5. *A*, Ratios of prestorm and storm rainfall at sites of damaging landslides to prestorm and storm regional rainfall. *B*, Ratios of normalized prestorm and normalized storm rainfall at sites of damaging landslides to normalized prestorm and storm regional rainfall.

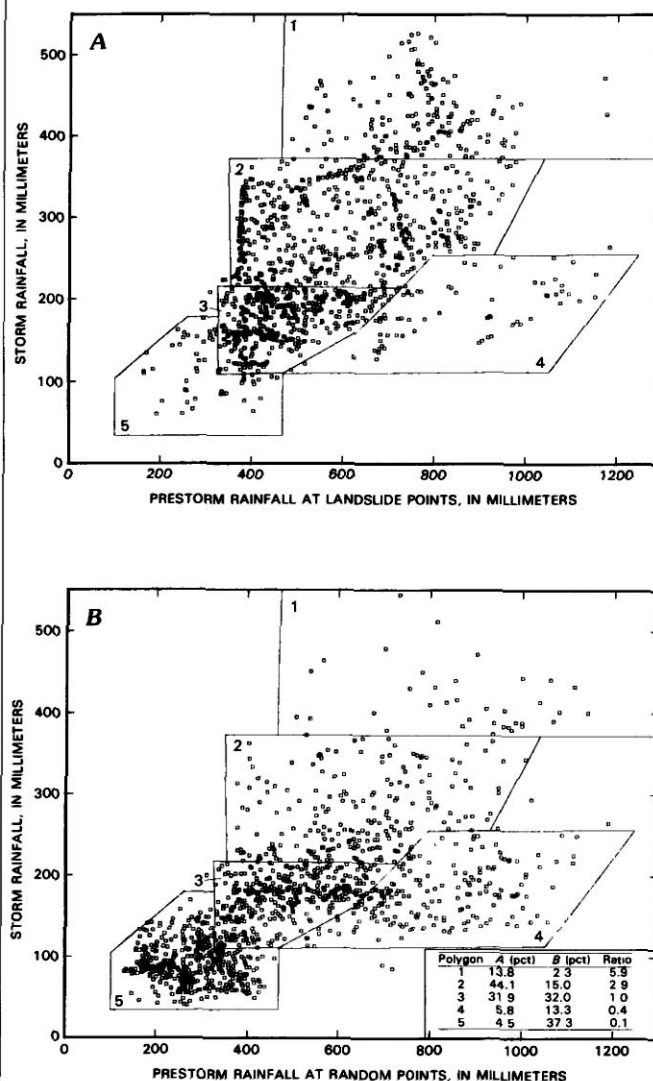


FIGURE 2.7.—Two-dimensional-ratio plots of prestorm and storm rainfall at sites of damaging landslides (*A*) and at an equal number of randomly selected points interpolated from rainfall grids (*B*). Polygons were arbitrarily drawn around areas of approximately homogeneous point density (see fig. 2.8 for areal distribution of polygons). Inset table in figure 2.7*B* lists percentages of landslide/rainfall and random-rainfall points that fall within comparable polygons, and their ratios (landslide-density ratios).

## CONCLUSIONS

Our analysis of rainfall and landslide data from the January 3-5, 1982, storm indicates a direct relation between damaging landslides and both storm and normalized storm rainfall. There appear to be thresholds with respect to landslide density at about 250 mm

(10 in.) of storm rainfall and at 30 percent of mean annual precipitation. Above these thresholds, the landslide probability increases significantly. The relation of landslides to prestorm seasonal rainfall displays a threshold at 300 to 400 mm (12-16 in.) but no significant increase in landslide probability above this value.

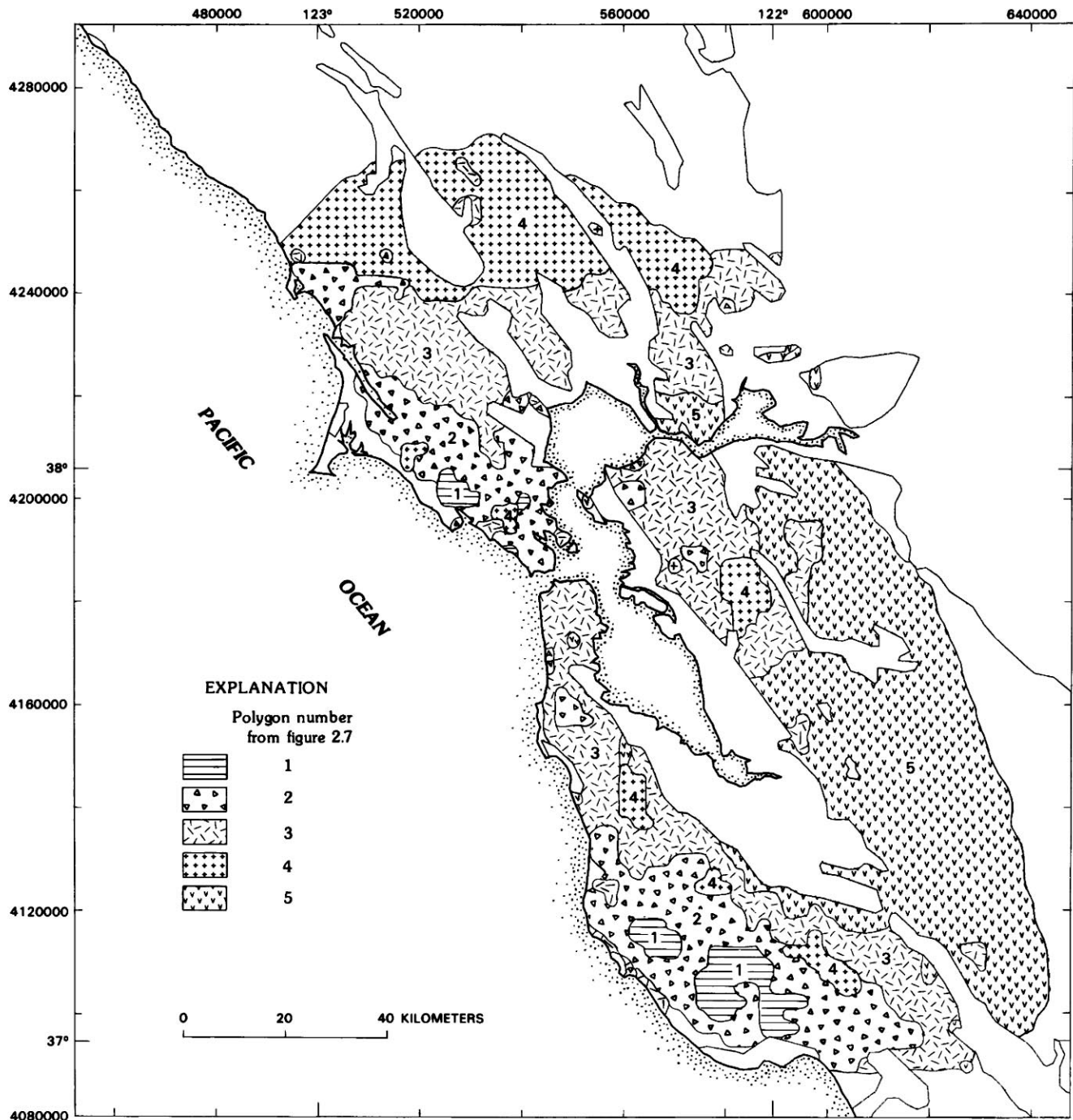


FIGURE 2.8.—San Francisco Bay region, showing areal distribution of polygonal fields in figure 2.7. Numbers correspond to polygon numbers. Areas with slopes of less than 5 percent and areas with no data are blank. Universal Transverse Mercator grid, zone 10, North America datum 1927, shown in meters.

## REFERENCES CITED

- Campbell, R.H., 1975, Soil slips, debris flows, and rainstorms in the Santa Monica Mountains and vicinity, southern California: U.S. Geological Survey Professional Paper 851, 51 p.
- Cannon, S.H., and Ellen, S.D., 1983, Rainfall that triggered abundant debris avalanches in the San Francisco Bay region, California, during the storm of January 3-5, 1982: U.S. Geological Survey Open-File Report 83-10, 4 p.
- Dynamic Graphics, Inc., 1975, User manual for the Surface Display Library: Berkeley, Calif., 238 p.
- 1978, User manual for the Surface Gridding Library: Berkeley, Calif., 129 p.
- Govi, Mario, and Sorzana, P.F., 1980, Landslide susceptibility as a function of critical rainfall amount in Piedmont basins (North-Western Italy): *Studia Geomorphologica Carpatho-Balcanica*, v. 14, p. 43-61.
- Mark, R.K., and Newman, E.B., 1981, User oriented, interactive Multics computer programs to create grid cell, contour, and perspective maps using Surface Display Library: U.S. Geological Survey Open-File Report 81-513, 49 p.
- Mark, R.K., Newman, E.B., Northcut, C.R., and Hamachi, B.R., 1983, Rainfall associated with the January 1982 rainstorm in the San Francisco Bay region, California: U.S. Geological Survey Open-File Report 83-16, scale 1:250,000, 2 sheets.
- Nilsen, T.H., Taylor, F.A., and Dean, R.M., 1976, Natural conditions that control landsliding in the San Francisco Bay region—an analysis based on data from the 1968-69 and 1972-73 rainy seasons: U.S. Geological Survey Bulletin 1424, 35 p.
- Rantz, S.E., 1971a, Mean annual precipitation and precipitation depth-duration-frequency data for the San Francisco Bay region: U.S. Geological Survey, San Francisco Bay Region Environment and Resources Planning Study Basic Data Contribution 32, 23 p.
- 1971b, Precipitation depth-duration-frequency relations for the San Francisco Bay region, California, in *Geological Survey research, 1971*: U.S. Geological Survey Professional Paper 750-C, p. C237-C241.

### 3. RAINFALL THAT RESULTED IN ABUNDANT DEBRIS-FLOW ACTIVITY DURING THE STORM

By SUSAN H. CANNON and STEPHEN D. ELLEN,  
U.S. GEOLOGICAL SURVEY

#### CONTENTS

	Page
Abstract	27
Introduction	27
Purpose and approach	27
Previous work	27
Acknowledgments	28
Methods	28
Data collection	28
Subdivision of the storm	28
Results	30
Storm rainfall and the onset of debris-flow activity	30
Prestorm seasonal rainfall	30
Recurrence of storm-rainfall conditions	30
Summary	32
References cited	33

#### ABSTRACT

We have determined the rainfall conditions that led to abundant debris-flow activity on natural hillslopes during the storm by comparing the known times of debris flows with the hourly records from nearby continuously recording rain gages. These rainfall conditions are described in terms of a prestorm seasonal-rainfall total and the duration of a range of rainfall intensities, for areas of different mean annual precipitation (MAP). In areas that receive more than 660 mm (26 in.) of MAP, abundant debris-flow activity followed 500 to 760 mm (20–30 in.) of prestorm seasonal rainfall and 8 hours of intense storm rainfall with intensities ranging from 10 to 20 mm/h (0.4–0.8 in/h). The onset of abundant debris-flow activity during the storm occurred after storm-rainfall totals had exceeded common values.

In areas that receive less than 660 mm (26 in.) of MAP, abundant debris-flow activity followed 381 to 483 mm (15–19 in.) of prestorm seasonal rainfall and 17 hours of intense storm rainfall with intensities ranging from 2.5 to 6.4 mm/h (0.1–0.25 in/h). The onset of abundant debris-flow activity during the storm occurred as storm-rainfall totals began to exceed common values.

#### INTRODUCTION

Intense and sustained rainfall during the January 3–5, 1982, storm triggered abundant fast-moving landslides throughout the San Francisco Bay region. The shallow empty scars left by these landslides marked the places from which material initially slid, and then flowed down slopes or channels as muddy slurries, generally at high velocities. We call these landslides debris flows (see "Introduction" to this volume for landslide terminology).

#### PURPOSE AND APPROACH

Our purpose is to document the rainfall conditions that triggered abundant debris flows during the storm.<sup>1</sup> We tabulate the hourly storm rainfall leading up to the onset of abundant debris-flow activity by comparing the known times of debris flows with the hourly storm-rainfall records from nearby continuously recording rain gages. The rainfall measured in this manner is that which actually contributed to the debris flow, in contrast to the storm total, which includes rain that fell after the debris flow mobilized. We then compare the frequency of recurrence of such rainfall with information on past debris-flow activity to check our findings.

#### PREVIOUS WORK

The role of rainfall in the initiation of debris flows has been studied in many parts of the world, using a variety of criteria. In Italy, Govi and Sorzana (1980) described the relation between widespread debris-flow activity and annual rainfall, 24-hour storm-rainfall totals, and prestorm moisture conditions. In New Zealand, Eyles (1979) correlated the occurrence of debris flows with 24-hour storm-rainfall totals and 4-month prestorm rainfall. Lumb (1975) described 24-hour maximum rainfall for the day of the event and cumulative rainfall over the previous 15 days as significant for debris-flow initiation in Hong Kong. Caine (1980) used a compilation of rainfall intensities associated with durations ranging from 1 minute to 90 days to derive a threshold equation for the rainfall conditions required for debris-flow activity.

Additional studies have been made in the San Francisco Bay region. Rice and others (1976, p. 46) concluded that 102 mm (4 in.) or more of rainfall in less than 10 hours is necessary to initiate debris-flow activity in Marin County. Nilsen and Turner (1975) suggested that 178 mm (7 in.) of storm rainfall, preceded by at least 254 mm (10 in.) of seasonal rainfall without an intervening dry period, describes a threshold for landslide activity in Contra Costa County; their work, however, does not distinguish debris flows from slower moving landslides.

More detailed information was used in southern California by Campbell (1975), who compared the times of

<sup>1</sup>The term "abundant" is used here to denote a wide areal distribution of large numbers of debris flows.

occurrence of debris flows with the rainfall records from continuously recording rain gages. His procedure, which we follow in this report, relates the occurrences of particular debris flows to the hourly intensities of rainfall leading up to failure.

#### ACKNOWLEDGMENTS

We appreciate the efforts of the individuals and agencies who provided rainfall records for this study, including Bill Baker of Ben Lomond, John Monteverdi of the San Francisco State University, the Alameda County Flood Control District, Camp Dresser and McKee, Inc., the U.S. National Weather Service, the East Bay Municipal Utilities District, the Marin County Flood Control District, the U.S. Geological Survey, the San Mateo County Department of Public Works, the Santa Clara Valley Water District, and the Santa Cruz County Department of Public Works.

Earl Hart of the California Division of Mines and Geology, Steve Singer of the U.S. Soil Conservation Service in Santa Cruz County, Joel Baldwin of Howard-Donley Associates, Gerald Weber of Cordex, Rick Holtz of Applied Earth Consultants, and Mark Foxx of the University of California, Santa Cruz, provided data on the times of debris-flow occurrence. Carol Creasey, Bette Hamachi, Darrell Herd, Robert Mark, Catherine McMasters, Evelyn Newman, Carol Northcut, Steven Reneau, Howard Wilshire, and Gerald Wiczorek also provided data for this study.

#### METHODS

##### DATA COLLECTION

To relate debris-flow activity to storm rainfall, we sought both continuous rainfall records and information on the times of debris flows throughout the San Francisco Bay region. Times of occurrence and locations of debris flows were documented through a search of newspaper accounts and through interviews of eyewitnesses and property owners by personnel of the U.S. Geological Survey, the California Division of Mines and Geology, the U.S. Soil Conservation Service in Santa Cruz County, and other agencies. A debris flow initially qualified for the study if its time of occurrence was known within 1 hour, if its location could be determined within 0.4 km, and if it was not reported to be associated with stream erosion or with manmade alterations of hillsides. The locations of debris flows that satisfied these criteria were then compared to the locations of continuously recording rain gages that operated during the storm. We considered rain-gage data to be representative of rainfall conditions at a particular debris-flow site if the gage was within approximately 5 km of the site and was within the same drainage

basin, or otherwise lacked major changes in intervening topography. Only those debris flows that satisfied all these criteria were included in this study. For these 27 debris flows, we know with some certainty the hourly storm rainfall that led to debris-flow activity from natural hillslopes. This information is shown in figure 3.1 by plots of cumulative storm rainfall on which are superimposed dots representing the times of nearby debris flows.

#### SUBDIVISION OF THE STORM

Very diverse storm rainfall triggered debris flows in different parts of the bay region (fig. 3.1). For example, debris flows near Ben Lomond, in Santa Cruz County, were triggered by a rainfall event very different in magnitude and pattern from that which triggered debris flows near San Bruno Mountain, in San Mateo County.

To characterize the varying storm-rainfall conditions that resulted in debris-flow activity in different parts of the bay region, we found it useful to divide the storm records. We divided the rain-gage records into two groups (shading, fig. 3.1) on the basis of storm-rainfall totals and the similarity of storm-rainfall patterns. The rain-gage records in the upper division show high storm-rainfall totals and rainfall at sustained high intensities. The rain-gage records in the lower division show lower storm-rainfall totals and a sustained period of rainfall at low intensities followed by a burst of high-intensity rainfall near the end of the storm.

By subdividing the storm in this manner, we can describe more precisely the rainfall conditions that led to debris-flow activity, and we can tentatively apply these conditions to different parts of the study area on the basis of the relation suggested by Rantz (1971) between MAP and the storm rainfall at a given site. Rantz reported that the rainfall total to be expected from a storm of given duration at a particular site in the San Francisco Bay region varies directly with the MAP at that site. According to Rantz, this relation applies to stations that receive more than 500 mm (20 in.) of MAP and for rainfall of more than 2 hours duration.

Work by Govi and Sorzana (1980) suggested that for some conditions, the storm-rainfall totals that accompany debris-flow activity also correlate with MAP. Our data show a linear relation between the storm rainfall up to the time of failure and MAP (fig. 3.2).

The work of Rantz (1971), combined with the relation suggested by Govi and Sorzana (1980) and plotted in figure 3.2, suggests that both storm-rainfall totals and the storm rainfall necessary to trigger debris flows might be expected to vary with MAP. Therefore, we associate the upper shaded part of the storm record in figure 3.1 with areas of high MAP (more than 660 mm/yr [26 in/yr]), and the lower shaded part with areas of low MAP (less than



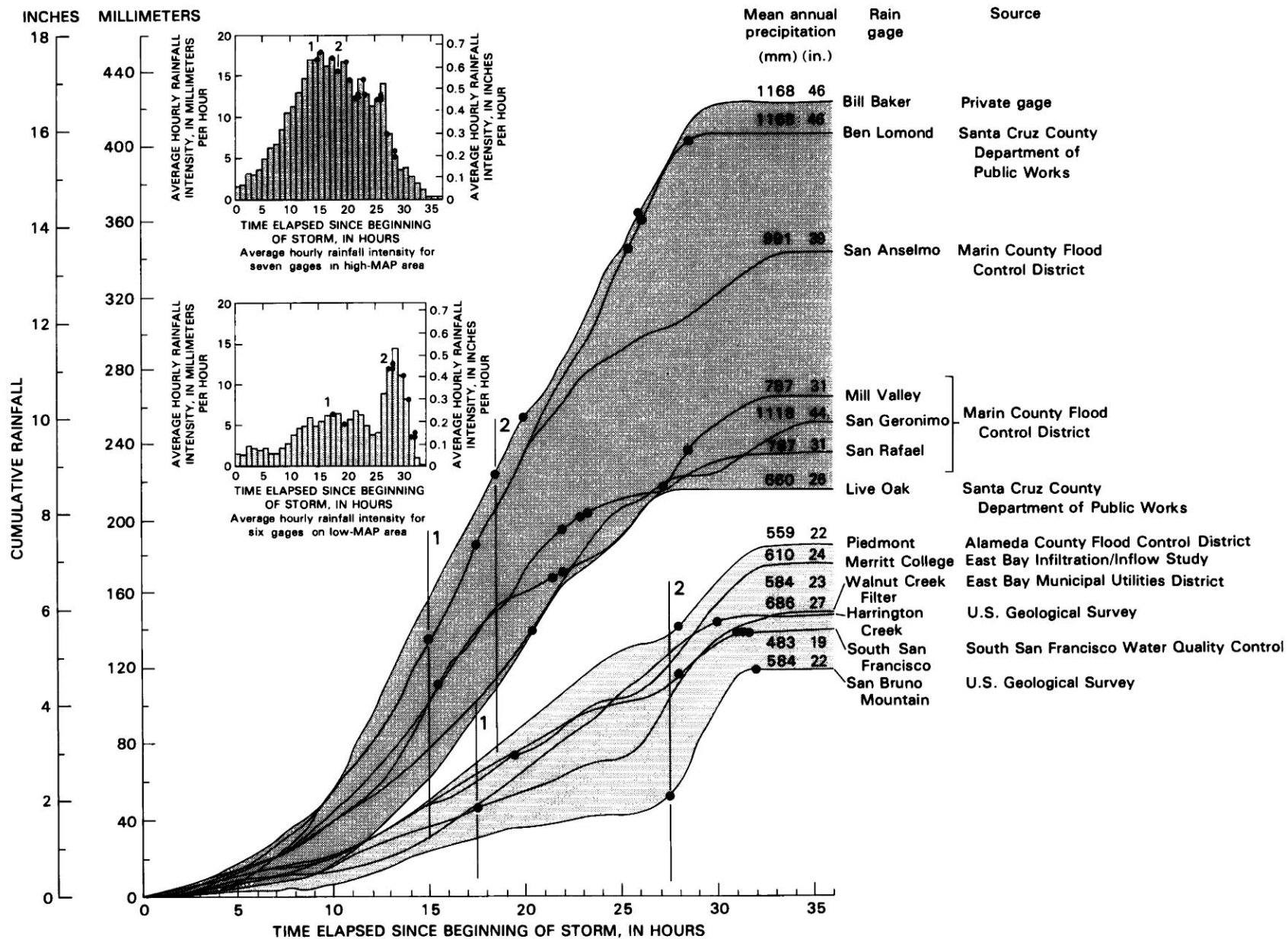


FIGURE 3.1.—Cumulative storm rainfall for 13 continuously recording rain gages used in this study, showing relations between storm rainfall and debris flows in the January 3–5, 1982, storm. Dots denote known times of debris flows near these gages; lines 1 and 2 denote onset of debris-flow activity and onset of abundant debris-flow activ-

ity, respectively. Mean annual precipitation (MAP) for each gage (in millimeters) is from Rantz (1971). Shading delineates grouping of storm records on the basis of the similarity of hourly rainfall-intensity patterns and of storm-rainfall totals. Bar graphs show average hourly intensities of storm rainfall for high- and low-MAP areas.



660 mm/yr [26 in/yr]).<sup>2</sup> Using the MAP map of Rantz (1971), we can tentatively apply these conditions to different parts of the study area. Figure 3.3 shows the areas of high and low MAP, generalized from Rantz (1971).

The rainfall necessary to trigger debris flows can be expected to vary with MAP because abundant debris-flow activity apparently occurs during extraordinary events, when rainfall at a particular site exceeds the commonly occurring conditions. Because commonly occurring rainfall conditions vary with MAP throughout the bay region (Rantz, 1971), the uncommonly heavy rainfall necessary to trigger abundant debris flows should be reflected by MAP as well.

## RESULTS

### STORM RAINFALL AND THE ONSET OF DEBRIS-FLOW ACTIVITY

The times of debris flows are plotted in figure 3.1 against the progression of storm rainfall at each of the continuously recording rain gages. The slopes of these plots indicate the intensity of rainfall at the gages; the slopes of the heavy lines that bound the shaded areas define the range in rainfall intensities for each MAP area. The bar graphs show the average hourly rainfall intensities of the storm for each of the two MAP areas.

The dots in figure 3.1 denote the times of occurrence of the debris flows that we included in this study. The line at 1 on the cumulative-rainfall plots indicates the first known time of debris-flow activity in each MAP area. The line at 2 represents what we define as the onset of abundant debris-flow activity; 80 percent of the debris flows included in this study within a given MAP area occurred after the time indicated by line 2.

All the storm records show debris flows occurring during or immediately after a period of increased rainfall intensity that started at about hour 10 of the storm. We distinguish this period of increased intensity as intense storm rainfall.

At the high-MAP rain gages, the onset of abundant debris-flow activity occurred after 18.5 hours of storm rainfall; of this period, the last 8 hours was intense storm rainfall with intensities of from 10 to 20 mm/h (0.4–0.8 in/h). At the low-MAP rain gages, the onset of abundant debris-flow activity occurred after 27.5 hours of storm rainfall; of this period, the last 17 hours was intense storm rainfall with intensities of from 2.5 to 6.4 mm/h (0.1–0.25 in/h). We note that the threshold described here applies specifically to an abundant, widespread distribution of debris flows; scattered occurrences of debris flows can certainly be expected before this threshold is reached.

<sup>2</sup>An exception to this generalization is the Harrington Creek rain gage. Although this gage was shown by Rantz (1971) as receiving an MAP of 686 mm/yr (27 in/yr), we included it in the low-MAP group because its storm record resembles that of the others in this group.

### PRESTORM SEASONAL RAINFALL

Although most researchers agree that prestorm seasonal rainfall is an important factor in the rainfall conditions that trigger debris flows, there is little agreement as to the time period significant for the buildup of antecedent soil-moisture conditions. Lumb (1975), Eyles (1979), and Govi and Sorzana (1980) reported rainfall totals for time periods ranging from 2 to 45 days before a storm as contributing to the soil-moisture conditions that lead to debris flows. Because of this uncertainty, we simply describe the prestorm seasonal-rainfall totals at the start of the January 1982 storm.

The prestorm seasonal rainfall for water year 1981–82 ranged from 508 to 813 mm (20–32 in.) in areas of high MAP and from 380 to 480 mm (15–19 in.) in areas of low MAP. Work by Campbell (1975) in southern California and by Wiczorek and Sarmiento (see chap. 5) suggests that 254 to 381 mm (10–15 in.) of seasonal rainfall is sufficient to establish the soil-moisture conditions conducive to debris-flow activity, should an intense storm occur.<sup>3</sup> Seasonal rainfall had exceeded these amounts by the beginning of the storm throughout the study area.

### RECURRENCE OF STORM-RAINFALL CONDITIONS

Some perspective can be gained on the events of the January 1982 storm by comparing the history of debris-flow activity in the bay region with the recurrence intervals for rainfall totals from the storm. Examination of historical records for the San Francisco Bay region

<sup>3</sup>Note that scattered distributions of debris flows can occur before these prestorm conditions are met (see chap. 4).

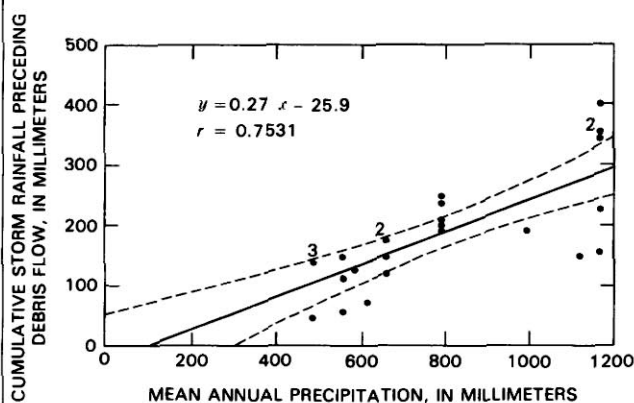


FIGURE 3.2.—Cumulative storm rainfall preceding debris flows as a function of mean annual precipitation (MAP). Numbers adjacent to dots indicate the number of values at that position. Regression equation: cumulative storm rainfall =  $(0.27 \times \text{MAP}) - 25.9$ . Dashed lines delineate the 95-percent-confidence interval. Significance testing of the correlation coefficient ( $r$ ) yields  $F = 31.4436$  and  $F_{0.05} = 4.24$ , with  $v = 25$ .

revealed no other storm that had resulted in debris flows of such abundance and broad areal extent (see chap. 4). Thus, the debris flows that occurred during the January 1982 storm must have been induced by aspects of the rainfall that are unique or, at least, uncommon during the last century in the bay region.

Rainfall-recurrence intervals can be used to indicate when, during the storm, rainfall totals became uncommon. Tables 3.1 and 3.2 list the recurrence intervals, calculated from the data of Rantz (1971), for rainfall totaled over several selected durations, starting at the beginning of the storm. We note that this use of rainfall recurrence

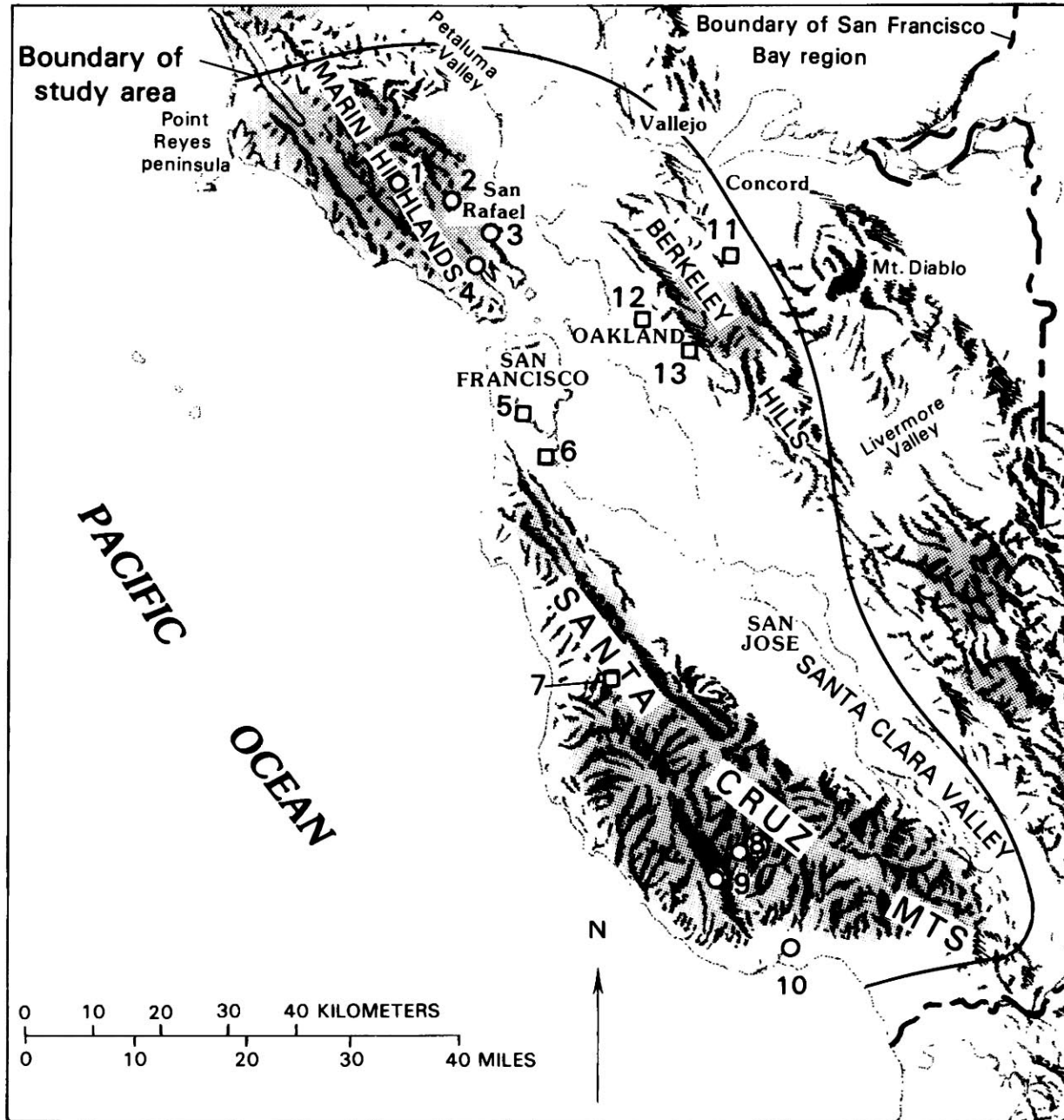


FIGURE 3.3.—San Francisco Bay region, showing boundary of study area. Shaded areas, high mean annual precipitation (MAP) (more than 660 mm/yr [26 in/yr]); unshaded areas, low MAP (less than 660 mm/yr [26 in/yr]). MAP data generalized from Rantz (1971). Squares, locations of rain gages used in low-MAP areas; circles, locations of rain

gages used in high-MAP areas. Rain gages: 1, San Geronimo; 2, San Anselmo; 3, San Rafael; 4, Mill Valley; 5, San Bruno Mountain; 6, South San Francisco; 7, Harrington Creek; 8, Ben Lomond; 9, Bill Baker; 10, Live Oak; 11, Walnut Creek Filter; 12, Piedmont; 13, Merritt College.

TABLE 3.1.—*Recurrence intervals for 12-, 18-, and 24-hour rainfall totals measured from the beginning of the January 3-5, 1982, storm in areas of high mean annual precipitation (MAP)*

Station	MAP (mm)	12-hour rainfall		18-hour rainfall		24-hour rainfall	
		Total (mm)	Recurrence interval (years)	Total (mm)	Recurrence interval (years)	Total (mm)	Recurrence interval (years)
Mill Valley----	787	53.3	1	109.2	10	166.4	49
San Geronimo---	1,118	32.3	1	104.6	2	191.0	20
San Rafael-----	787	66.0	2	149.9	100	201.9	>100
San Anselmo----	991	82.6	2	196.8	>100	283.2	>100
Live Oak-----	660	55.9	2	149.9	>100	184.1	>100
Ben Lomond-----	1,168	97.8	3	217.2	>100	327.8	>100
Bill Baker-----	1,168	102.9	4	220.2	>100	315.2	>100

TABLE 3.2.—*Recurrence intervals for 27-, 30-, and 36-hour rainfall totals measured from the beginning of the January 3-5, 1982, storm in areas of low mean annual precipitation (MAP)*

Station	MAP (mm)	27-hour rainfall		30-hour rainfall		36-hour rainfall	
		Total (mm)	Recurrence interval (years)	Total (mm)	Recurrence interval (years)	Total (mm)	Recurrence interval (years)
Walnut Creek-----	584	109.5	13	138.2	30	149.6	44
Harrington Creek----	686	126.7	14	146.6	21	149.1	18
San Bruno Mountain---	584	32.3	2	101.3	8	121.2	14
South San Francisco---	483	99.1	23	135.9	>100	141.0	>100
Piedmont-----	559	135.9	35	167.6	>100	187.5	>100
Merritt College-----	610	118.6	16	160.0	71	176.3	100

differs from that of Wieczorek and Sarmiento (see chap. 5), who report the recurrence intervals of maximum rainfall totals for selected durations.

For the high-MAP group of gages (table 3.1), the 1- to 4-year recurrence intervals for the first 12 hours of the storm indicate that storms with these rainfall totals within a 12-hour period pass through the bay region frequently. The 18- and 24-hour totals, however, occur less frequently; five of the seven rain-gage stations show recurrence intervals of 100 years or longer. Thus, between hours 12 and 18 of the storm, the amount of storm rainfall changed from common to rare. The onset of abundant debris-flow activity at hour 18.5 (fig. 3.1) occurred after the storm rainfall had exceeded common totals.

For the low-MAP group of gages (table 3.2), recurrence intervals are less consistent between stations, and changes in recurrence interval are not so abrupt as those for the high-MAP gages. For this low-MAP group, abundant debris-flow activity began at hour 27.5. The 27-hour January 3-5, 1982, storm totals show fairly short recurrence intervals (2-35 years) in comparison with the 30- and 36-hour totals (8-100 years). Although the onset of abundant debris-flow activity apparently occurred as the storm rainfall began to exceed common totals, the relation here is less clearly defined than for the high-MAP gages.

Long recurrence intervals of storm-rainfall totals throughout the bay region confirm that the broad areal extent of the storm was uncommon.

## SUMMARY

The abundance and broad areal extent of debris flows during the January 3-5, 1982, storm were an unusual occurrence in the San Francisco Bay region. In areas with more than 660 mm (26 in.) of MAP, comparison of the known times of debris flows on natural hillslopes with the hourly storm records of nearby continuously recording rain gages indicates that the onset of abundant debris-flow activity occurred at hour 18.5 of the storm. Rainfall-recurrence intervals indicate that storm-rainfall totals became uncommon between hours 12 and 18 of the storm, and so abundant debris-flow activity began after storm rainfall had exceeded common values. Abundant debris-flow activity followed 8 hours of intense storm rainfall with intensities ranging from 10 to 20 mm/h (0.4-0.8 in/h). In this MAP area, the prestorm seasonal rainfall had reached 508 to 813 mm (20-32 in.), well beyond the 254 to 381 mm (10-15 in.) considered sufficient to establish soil-moisture conditions that will lead to debris-flow activity, should an intense storm occur.

In areas with less than 660 mm (26 in.) of MAP, comparison of the known times of debris flows with the hourly storm records indicates that the onset of abundant debris-flow activity occurred after 27.5 hours of storm rainfall. Recurrence intervals indicate that the 27-hour rainfall totals occur frequently in comparison with the 30- and 36-hour totals, although the contrast is not so clearly defined as in the previous case. In these areas, the onset of abundant debris-flow activity followed 17 hours of intense storm rainfall with intensities ranging from 2.5 to 6.4 mm/h (0.1–0.25 in/h). The prestorm-seasonal rainfall had reached 380 to 480 mm (15–19 in.).

#### REFERENCES CITED

- Caine, Nel, 1980, The rainfall intensity-duration control of shallow landslides and debris flows: *Geografiska Annaler*, ser. A, v. 62, no. 1–2, p. 23–27.
- Campbell, R.H., 1975, Soil slips, debris flows, and rainstorms in the Santa Monica Mountains and vicinity, southern California: U.S. Geological Survey Professional Paper 851, 51 p.
- Eyles, R.J., 1979, Slip-triggering rainfalls in Wellington City, New Zealand: *New Zealand Journal of Science*, v. 22, no. 2, p. 117–121.
- Govi, Mario, and Sorzana, P.F., 1980, Landslide susceptibility as a function of critical rainfall amount in Piedmont basins (North-Western Italy): *Studia Geomorphologica Carpatho-Balcanica*, v. 14, p. 43–61.
- Lumb, Peter, 1975, Slope failures in Hong Kong: *Quarterly Journal of Engineering Geology*, v. 8, no. 1, p. 31–65.
- Nilsen, T.H., and Turner, B.L., 1975, Influence of rainfall and ancient landslide deposits on recent landslides (1950–71) in urban areas of Contra Costa County, California: U.S. Geological Survey Bulletin 1388, 18 p.
- Rantz, S.E., 1971, Precipitation depth-duration-frequency relations for the San Francisco Bay region, California: U.S. Geological Survey, San Francisco Bay Region Environment and Resources Planning Study Basic Data Contribution 25, 23 p.
- Rice, S.J., Smith, T.C., and Strand, R.G., 1976, Geology for planning, central and southeastern Marin County, California: California Division of Mines and Geology Open-File Report 76-2SF, 103 p.



## 4. REGIONAL RAINFALL-THRESHOLD CONDITIONS FOR ABUNDANT DEBRIS-FLOW ACTIVITY

By SUSAN H. CANNON,  
U.S. GEOLOGICAL SURVEY

### CONTENTS

	Page
Abstract - - - - -	35
Purpose - - - - -	35
Previous work - - - - -	35
Approach - - - - -	36
Prestorm seasonal rainfall - - - - -	36
Measures of storm rainfall - - - - -	36
Normalization of rainfall data - - - - -	36
Storms considered - - - - -	36
Rain-gage network - - - - -	38
Results - - - - -	38
Discussion - - - - -	38
Limitations - - - - -	40
References cited - - - - -	41

### ABSTRACT

Rainfall-threshold conditions that led to abundant debris-flow activity are determined by comparing the normalized intensities and durations of bursts of storm rainfall, segments of bursts, and within-storm averages from six storms in the San Francisco Bay region. Normalization is by the mean annual precipitation (MAP) at the rain-gage station from which the rainfall was measured. The threshold line is described by the equation  $D = 46.1 - 3.6 \times 10^3 I_n + 7.4 \times 10^4 I_n^2$ , where  $D$  is the duration (in hours) and  $I_n$  is the normalized intensity (per hour). A comparison of the threshold with the rainfall measured up to known times of debris flows generally supports the position of the threshold line but indicates that the threshold is less reliable when applied to areas of low MAP. This comparison also indicates that in storms consisting of a series of isolated bursts of high-intensity rainfall, the within-storm average is a better measure of the rainfall necessary to initiate debris-flow activity than is the isolated burst.

### PURPOSE

After the January 3-5, 1982, storm, concern arose regarding the conditions under which similar damage by debris flow could be expected in the future. In response to such concern, this study was designed to define the threshold storm-rainfall intensities and durations that have resulted in abundant<sup>1</sup> debris flows in the San Francisco Bay region. The threshold is defined by comparing the rainfall conditions during storms that triggered abundant debris flows with those during major storms that did not produce abundant debris flows. This comparison

defines the range of rainfall conditions that have accompanied abundant debris-flow activity in the historical past. Abundant debris-flow activity can be expected to accompany similar conditions in the future.

*Acknowledgments.*—Many individuals and agencies provided rainfall records for this study, including the East Bay Infiltration/Inflow Study, East Bay Municipal Utilities District, Marin County Flood Control District, Marin Municipal Water District, Santa Cruz Department of Public Works, and U.S. National Weather Service. I am indebted to S.D. Ellen for guidance and editorial advice on this project, and to R.K. Mark for computer expertise.

### PREVIOUS WORK

Rainfall thresholds for debris-flow activity in the San Francisco Bay region have been described by different workers in various ways. Smith and Hart (1982) suggested that 127 to 152 mm (5-6 in.) of rainfall within a 12- to 24-hour period is generally required for significant debris-flow activity in at least some parts of the bay region. Mark and Newman (see chap. 2) show that approximately 254 mm (10 in.) of storm rainfall correlated with a significant increase in the number of damaging landslides in the bay region during the January 1982 storm. Cannon and Ellen (see chap. 3) use hourly storm-rainfall records combined with known times of debris flows to determine rainfall conditions during the January 1982 storm that led to abundant debris-flow activity in areas of high and low mean annual precipitation (MAP). Cannon and Ellen (1985) compared hourly rainfall records of storms to calculate rainfall thresholds for abundant debris-flow activity in areas of high and low MAP in the bay region.

Other rainfall thresholds for debris-flow activity have been suggested for local areas in the bay region. Wiczorek and Sarmiento (see chap. 5) examined rainfall records from 22 storms to determine an intensity-duration threshold for scattered occurrences of debris flows in part of San Mateo County. Rice and others (1976) suggested that 102 mm (4 in.) of rainfall in less than 10 hours will lead to debris-flow activity in Marin County. Nilsen and Turner (1975) proposed that 178 mm (7 in.) of storm rainfall, preceded by 254 mm (10 in.) of seasonal rainfall without an intervening dry period, resulted in movement of various landslide types in Contra Costa County.

<sup>1</sup>The term "abundant" is used here to indicate an areal concentration of debris flows similar to that seen after the January 3-5, 1982, storm.



### APPROACH

Campbell (1975, p. 20) described two rainfall conditions that result in debris flows: "• • • an initial period of enough rainfall to bring the full thickness of the soil mantle to field capacity • • •, followed by rainfall intense enough to exceed the infiltration rate of the parent material underlying the soil mantle, and lasting long enough to establish a perched ground-water table of sufficient • • • thickness • • • to cause failure." To quantify such rainfall conditions, I measured prestorm-seasonal-rainfall totals and the intensity and duration of several storm-rainfall parameters from the hourly records of six storms in the San Francisco Bay region. Comparison of these parameters for different storms defines the rainfall conditions that have accompanied abundant debris-flow activity in this region.

#### PRESTORM SEASONAL RAINFALL

Prestorm seasonal rainfall, measured from the beginning of the water year (October 1) up to the day of a given storm, is used as a measure of the rainfall available to bring the soil mantle in Campbell's (1975) model to field capacity. Work by Campbell in southern California and by Wieczorek and Sarmiento (see chap. 5) in part of San Mateo County suggests that 254 to 381 mm (10-15 in.) of prestorm seasonal rainfall is sufficient to establish the soil-moisture conditions conducive to abundant debris-flow activity, should an intense storm occur. In a study of the various landslide types in Contra Costa County, Nilsen and others (1976) reached similar conclusions. Mark and Newman (see chap. 2) show a significant relative increase in the areal abundance of storm-generated damaging landslides, including debris flows, following the January 1982 storm in those parts of the bay region that received 305 to 406 mm (12-16 in.) of prestorm seasonal rainfall. On the basis of these studies, only storms preceded by at least 254 mm (10 in.) of seasonal rainfall were included in this analysis.

Timing of prestorm seasonal rainfall appears to influence the occurrence of various landslide types, as suggested by Nilsen and Turner (1975), who indicated that dry periods preceding storms had important effects on landslides in Contra Costa County. For example, the bay-region storm of January 20-21, 1967, which was preceded by a 40-day dry period, did not trigger abundant debris flows, although this storm had rainfall totals and storm duration similar to those of the January 1982 storm (J.P. Monteverdi, written commun., 1982). These two storms also had similar prestorm-seasonal-rainfall totals. The major difference between these storms thus appears to be the rainfall during the 40 days preceding each storm, and the absence of abundant debris flows during the 1967

storm may be attributed to its prestorm dry period. Therefore, this study includes only storms with measurable rainfall [2.5 mm (0.1 in.)] in the 40 days immediately preceding the storm.

#### MEASURES OF STORM RAINFALL

The intensity and duration of three storm-rainfall parameters (burst, segment, and within-storm average) were measured from the records of recording rain gages (fig. 4.1). Bursts and segments of bursts describe the periods of intense storm rainfall within a storm, as called for by Campbell's (1975) model. Segments distinguish periods of different rainfall rates within a burst. Within-storm averages, which include periods of both high- and low-intensity rainfall, quantify the occurrence of cycles of intense rainfall followed by periods of quiescence.

Because the particular aspects of storm rainfall that result in debris flows are not well understood, the intensity and duration of all three parameters were measured from hourly storm-rainfall records. Comparison of the values of these parameters for different storms, combined with documentation of debris flows in these storms, should define storm-rainfall conditions that have produced abundant debris flows throughout the bay region.

#### NORMALIZATION OF RAINFALL DATA

Because different rainfall conditions have triggered debris flows in different parts of the bay region, the rainfall intensities for the parameters measured were normalized by dividing by the MAP of the gages at which the intensities were measured. Normalization incorporates the relation between MAP and the amount of rain expected from a given storm at a specific site (see chap. 3; Rantz, 1971), and aids in characterizing the varied rainfall conditions that resulted in debris flows during the January 1982 storm.

#### STORMS CONSIDERED

Bursts, segments, and within-storm averages were measured from the hourly records of storms in the bay region that occurred during December 21-24 of 1955, December 21-23 of 1964, January 16 of 1973, January 13-14 of 1978, January 3-5 of 1982, and January 26-27 of 1983. Prestorm seasonal totals were measured from the records preceding these storms. These storms were selected because: (1) they satisfy the criteria for prestorm seasonal rainfall discussed above, (2) they are represented by the complete network of hourly rainfall records that covers the bay region, and (3) they either were declared emergencies or disasters at State or Federal levels or were mentioned in the U.S. National Oceanic and Atmo-

spheric Administration yearly summaries as causing damage by flooding or landsliding (see chap. 1). Although these reports do not distinguish debris flows from other kinds of landslides and do not mention the extent of landsliding or damage, they do indicate significant high-precipitation storms. Other major storms have occurred in the bay region, but absence of a complete rain-gage network that documents these storms requires the assumption that the six storms used in this study are representative of the range of possible high-intensity, long-duration storms that occur.

To distinguish storms that triggered abundant debris flows from those that resulted principally in flooding or other types of landslides, I used personal observations, newspaper accounts, and historical aerial photographs. W.M. Brown III, G.F. Wiczorek, and D.G. Herd of the U.S. Geological Survey, S.J. Rice and T.C. Smith of the California Division of Mines and Geology, Ed Barnes of the San Mateo Department of Public Works, personnel from the California Department of Transportation, and personnel from the Santa Cruz Department of Public Works provided information on the effects of storms in

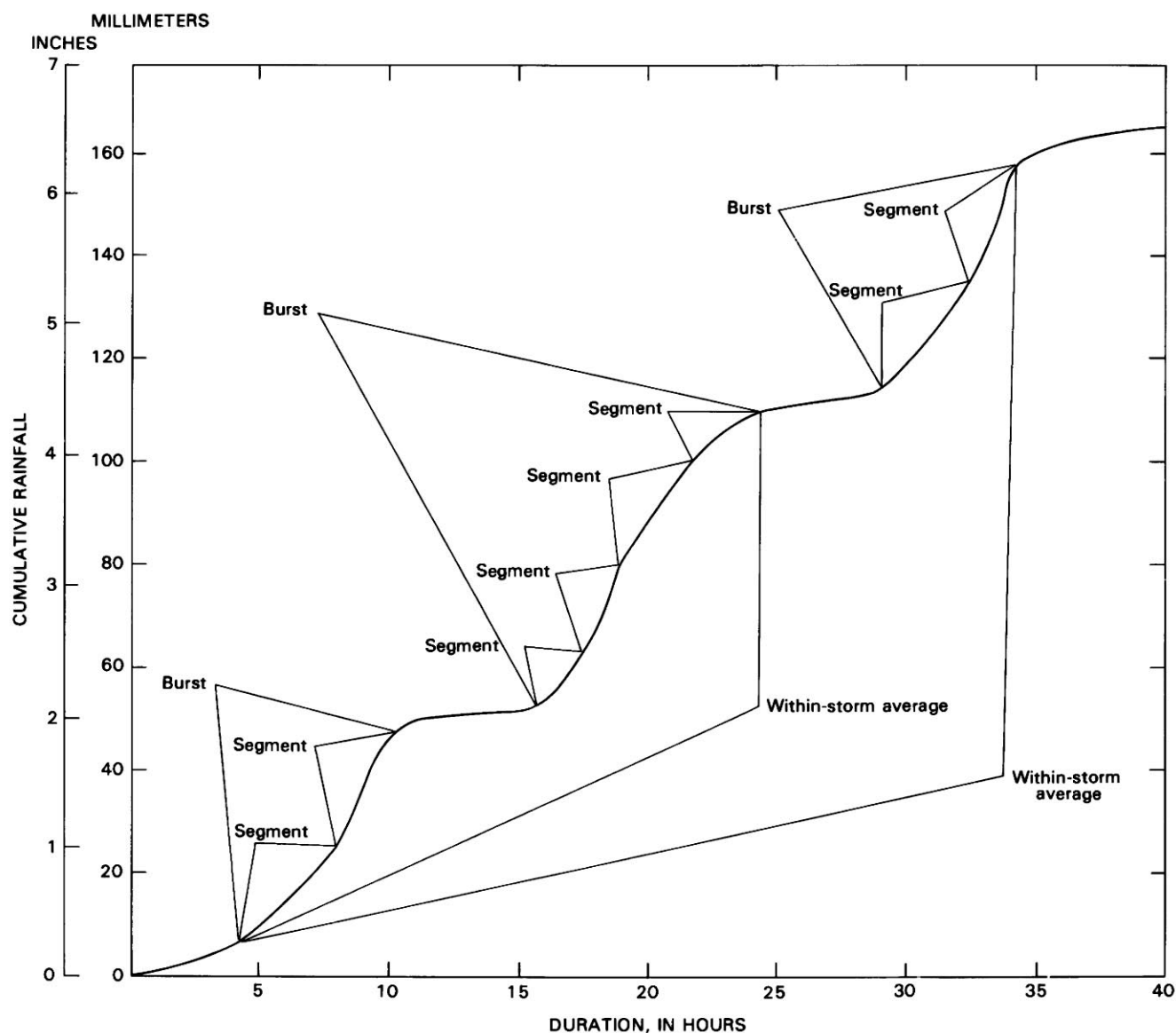


FIGURE 4.1.—Schematic example of an hourly cumulative rain-gage record, showing rainfall parameters measured for this study. Bursts are defined as periods of intense rainfall during the storm, and segments as periods of uniform intensity within bursts. Both bursts and segments are measured from changes in slope of rain-gage trace;

an initial rainfall rate of at least 2.5 mm/h (0.10 in/h) was required for an event to qualify as a burst. Within-storm averages are measured from the onset of intense storm rainfall to the end of each burst and thus include periods of low-intensity rainfall.

the bay region. For each of the storm periods considered, past issues of the *San Francisco Chronicle*, the *Mill Valley Record*, the *Independent Journal* (a Marin County newspaper), the *Half Moon Bay Review*, and the *Peninsula Times-Tribune*, where available, were reviewed for information. Sample aerial photographs of the bay region were examined for the effects of these storms. The scarcity of information documenting both the location and quantity of debris flows in each storm (see chap. 1) required reviewing the information from the various sources simply to determine whether debris flows had occurred in abundance.

Examination of these various historical records for the period 1955-83 indicated that, although some debris flows occurred in several of these storms, only the January 1982 storm is documented as triggering abundant debris flows throughout the bay region.<sup>2</sup> Thus, the storm-rainfall conditions unique to that storm include those conditions that led to regionwide abundant debris-flow activity.

#### RAIN-GAGE NETWORK

Rainfall conditions of the six storms are quantified by measuring intensity and duration for the storm-rainfall parameters from records from a network of continuously recording rain gages located throughout the study area (fig. 4.2). This network consists of 14 principal gages and 7 substitute gages. Where a record from a principal gage is missing or incomplete, a record from a nearby gage of similar elevation, slope aspect, and MAP was substituted where possible. The gages used for each storm are listed in table 4.1.

#### RESULTS

Comparison of the values of the normalized storm-rainfall parameters measured for the six storms defines the rainfall-threshold conditions that have accompanied abundant debris-flow activity in the bay region during the historical past for which sufficient records were available. Values of the normalized parameters and the position of the threshold line are shown in figure 4.3. This threshold was constructed by drawing a line that best separates the rainfall conditions unique to the January 1982 storm from more commonly occurring storm-rainfall conditions.

The threshold line is described by the equation

$$D = 46.1 - 3.6 \times 10^3 \ln + 7.4 \times 10^4 \ln^2,$$

where  $D$  is the duration (in hours) and  $\ln$  is the normal-

ized intensity (per hour). Values that plot to the right of and above the threshold line generally have accompanied abundant debris-flow activity in the past. Given sufficient prestorm seasonal rainfall, these values of storm rainfall can be expected to result in abundant debris-flow activity in the future.<sup>3</sup>

Note that some values from storms other than the January 1982 storm plot well above the threshold; these values were all measured from the records of gages operating during the December 1955 storm, and these values might well have accompanied debris-flow activity, although adequate documentation of such an occurrence has not been found (see chap. 1).

#### DISCUSSION

The rainfall conditions that led to known times of debris flow during the January 1982 storm (see chap. 3) provide a check on the position of the threshold line, because these rainfall values contributed directly to specific debris flows. For each of these debris flows, figure 4.3 shows values of rainfall measured up to the known time of failure. Most of these values represent both storm averages and bursts, which are the same in many cases for the January storm. However, the values that fall at 1- and 2-h duration are for bursts of rainfall that occurred late in the storm. Except for these low-duration values, most of the values of rainfall measured up to the time of failure fall above the threshold line, and this comparison generally supports the position of this line. Note that some of the values measured up to the known times of debris flows lie below the threshold line in figure 4.3. It is reasonable to expect some values to fall below the threshold line because it defines conditions for abundant debris-flow activity rather than for incipient debris-flow activity. The fact that six of the seven values, however, are from gages that receive less than 635 mm (25 in.) of MAP suggests that normalization introduces inconsistencies in areas of low MAP. This suggestion is consistent with Rantz's (1971) observation that the relation between MAP and storm rainfall is less well defined in areas of less than 508 mm (20 in.) of MAP. Therefore, the threshold line in figure 4.3 appears to be less reliable when applied to areas of low MAP.

The values that fall at 1- and 2-h duration and well below the threshold line are bursts of rainfall that occurred late in the storm (see chap. 3). The within-storm average measures of rainfall preceding failure that include these bursts, however, fall closer to the threshold line. This relation suggests that for this threshold line, the within-storm

<sup>2</sup>Brown (see chap. 1) mentions that although no comprehensive documentation of the occurrence of abundant debris flows was found for the December 21-24, 1955, storm, meteorologic conditions indicate that abundant debris-flow activity was possible.

<sup>3</sup>Some debris flows can be expected to occur before rainfall has attained the threshold calculated here for abundant debris-flow activity. A threshold for incipient debris-flow activity at a study area near La Honda is discussed by Wiecek and Sarmiento (see chap. 5).

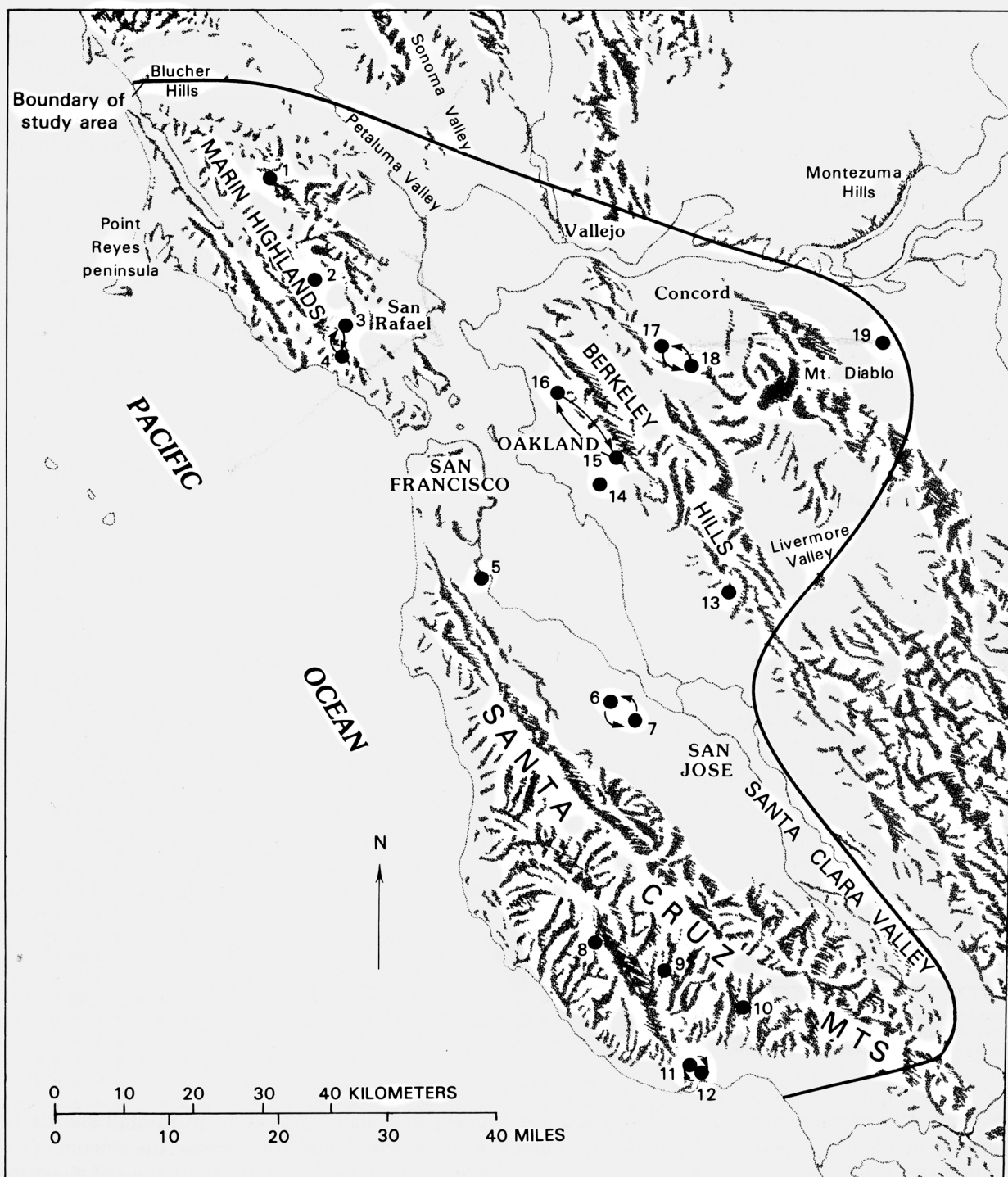


FIGURE 4.2.—San Francisco Bay region, showing boundary of study area and locations of rain gages used in this study (dots). Arrows between gages indicate that records from these gages were substituted for each other. Rain gages: 1, Novato; 2, San Geronimo and Woodacre; 3, Lake Lagunitas; 4, Mount Tamalpais; 5, San Francisco WSO AP and San Francisco WB AP;

6, Oak Grove; 7, Palo Alto; 8, Boulder Creek; 9, Ben Lomond; 10, Soquel; 11, Santa Cruz; 12, Live Oak; 13, Upper San Leandro Filter; 14, Hayward; 15, Merritt College; 16, Berkeley; 17, Walnut Creek East Bay Municipal Utilities District; 18, Walnut Creek National Weather Service; 19, Brentwood.



TABLE 4.1.—Recording rain gages at which rainfall parameters were measured for each storm

[Dash, no record available]

Storm-----	Location	Rain gage	Dec. 21-24, 1955	Dec. 21-23, 1964	Jan. 16, 1973	Jan. 13-14, 1978	Jan. 3-5, 1982	Jan. 26-27, 1983
Northern Marin County.	Novato <sup>1</sup>		X	X	X	X	X	X
Central Marin County.	San Geronimo <sup>1</sup> Woodacre <sup>1</sup>		--- ---	--- X	X ---	X ---	X ---	--- X
Southern Marin County.	Lake Lagunitas <sup>2</sup> Mount Tamalpais <sup>3</sup>		--- X	--- X	--- X	--- X	--- ---	X ---
San Francisco International Airport.	SF WSO Ap <sup>3</sup> SF WB AP <sup>3</sup>		X ---	--- X	X ---	X ---	X ---	--- X
Central Peninsula.	Oak Grove <sup>3</sup> Palo Alto <sup>3</sup>		--- X	--- X	--- X	X ---	X ---	X ---
Northern Santa Cruz County.	Boulder Creek <sup>3</sup>		X	X	X	X	X	X
Central Santa Cruz County.	Ben Lomond <sup>4</sup>		---	X	X	X	X	X
Eastern Santa Cruz County.	Soquel <sup>4</sup>		---	X	X	X	X	X
City of Santa Cruz.	Santa Cruz <sup>4</sup> Live Oak <sup>4</sup>		--- ---	X ---	X ---	--- X	--- X	--- X
East Bay South----	Upper San Leandro Filter <sup>3</sup> .		X	X	X	---	X	---
East Bay Central.	Hayward <sup>3</sup>		X	X	X	X	X	X
East Bay North----	Merritt College <sup>5</sup> Berkeley <sup>3</sup>		--- X	--- X	--- X	--- X	--- X	X ---
City of Walnut Creek.	Walnut Creek <sup>6</sup> Walnut Creek <sup>3</sup>		--- X	--- X	X ---	--- X	--- X	X ---
City of Brentwood.	Brentwood <sup>3</sup>		X	X	X	X	X	X

<sup>1</sup>Marin County Flood Control District.<sup>2</sup>Marin Municipal Water District.<sup>3</sup>U.S. National Weather Service.<sup>4</sup>Santa Cruz Department of Public Works.<sup>5</sup>East Bay Infiltration/Inflow Study.<sup>6</sup>East Bay Municipal Utilities District.

average is a better measure of the rainfall that will lead to the onset of debris-flow activity than is an isolated burst of high-intensity rainfall.

### LIMITATIONS

Although the rainfall threshold proposed here can be used as an approximate guide to abundant debris-flow activity, several uncertainties prevent its precise use. First, the exact role of prestorm rainfall in the initiation of debris flows is unclear. The model by Campbell (1975) sug-

gests that abundant prestorm rainfall shortly before a major storm could both decrease the amount of prestorm precipitation necessary to create the soil-moisture conditions conducive to debris-flow activity, and lower the storm-rainfall threshold for debris-flow activity; however, the threshold in this study does not account for such variation.

Second, the threshold developed here is based on a single storm that produced abundant debris flows, but debris flows might also be produced in abundance by storms with different characteristics, particularly storms of longer duration than those used in this study. Some



rainfall values from such storms would plot beyond the end of the threshold line in figure 4.3, and so this threshold cannot predict the consequences of such storms.

Third, records are insufficient to determine the specific aspects of storm rainfall that most strongly influence the initiation of debris flows. For this analysis, some likely factors were chosen—prestorm seasonal rainfall, and the intensity and duration of storm rainfall—but other aspects of storm rainfall may also have played significant roles. For example, the conceptual model by Campbell (1975) suggests that the occurrence of bursts of high-intensity rainfall late in the storm may favor the initiation of debris flows more than the occurrence of a similar burst early in the storm, but such variations are not adequately quantified in this study.

Most of these uncertainties arise because only a few storms have provided useful records of rainfall and abundant debris-flow activity. To reduce these uncertainties, we need records of more storms capable of triggering debris flows. Until future storms provide such records, the threshold developed here should be used only as an approximate guide for the onset of abundant debris-flow activity, rather than as a reliable predictor.

#### REFERENCES CITED

- Campbell, R.H., 1975, Soil slips, debris flows, and rainstorms in the Santa Monica Mountains and vicinity, southern California: U.S. Geological Survey Professional Paper 851, 51 p.  
Cannon, S.H., and Ellen, S.D., 1985, Rainfall conditions for abundant

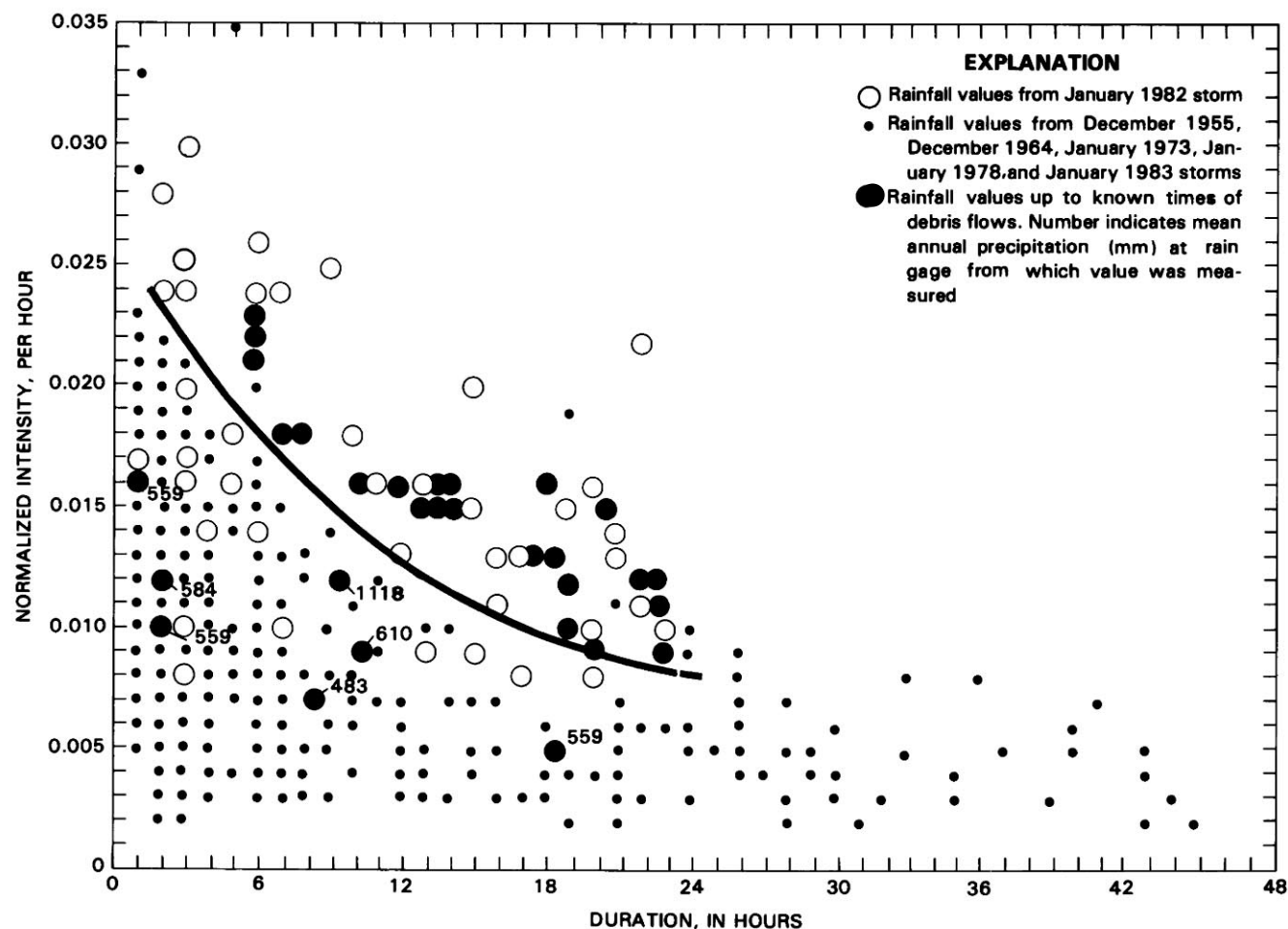


FIGURE 4.3.—Relations among normalized values of storm-rainfall parameters measured from hourly records of six storms in the San Francisco Bay region. Although more than one value may exist at a given point in the plot, only one symbol is shown at that point. Where values measured in the January 1982 storm are identical to those measured in other storms, the symbol for the other storm is shown

because the purpose is to show rainfall conditions unique to the January 1982 storm. Threshold line (dashed where uncertain) separates values measured from records of the January 1982 storm from those measured from records of other storms and thus delineates the storm-rainfall conditions that accompanied abundant debris-flow activity.

- debris avalanches in the San Francisco Bay region, California: *California Geology*, v. 38, no. 12, p. 267-272.
- Nilsen, T.H., Taylor, F.A., and Dean, R.M., 1976, Natural conditions that control landsliding in the San Francisco Bay region—an analysis based on data from the 1968-69 and 1972-73 rainy seasons: U.S. Geological Survey Bulletin 1424, 35 p.
- Nilsen, T.H., and Turner, B.L., 1975, Influence of rainfall and ancient landslide deposits on recent landslides (1950-1971) in urban areas of Contra Costa County, California: U.S. Geological Survey Bulletin 1388, 18 p.
- Rantz, S.E., 1971, Precipitation depth-duration-frequency relations for the San Francisco Bay region, California: U.S. Geological Survey, San Francisco Bay Region Environment and Resources Planning Study Basic Data Contribution 25, 23 p.
- Rice, S.J., Smith, T.C., and Strand, R.G., 1976, Geology for planning, central and southeastern Marin County, California: California Division of Mines and Geology Open-File Report 76-2SF, 103 p.
- Smith, T.C., and Hart, E.W., 1982, Landslides and related storm damage, January 1982, San Francisco Bay region: *California Geology*, v. 35, no. 7, p. 139-152.

# 5. RAINFALL, PIEZOMETRIC LEVELS, AND DEBRIS FLOWS NEAR LA HONDA, CALIFORNIA, IN STORMS BETWEEN 1975 AND 1983

By GERALD F. WIECZOREK and JOHN SARMIENTO,  
U.S. GEOLOGICAL SURVEY

## CONTENTS

	Page
Abstract - - - - -	43
Introduction - - - - -	43
Study area - - - - -	44
Methods and instrumentation - - - - -	45
Debris flows in the study area - - - - -	47
Description of debris flows: 1975-80 - - - - -	47
Description of debris flows: December 29, 1981 - - - - -	47
Description of debris flows: The January 3-5, 1982, storm - - - - -	47
Description of debris flows: December 1982-March 1983 - - - - -	48
Characteristics and properties of debris flows: 1975-83 - - - - -	48
Factors affecting the initiation of debris flows - - - - -	49
Effects of vegetation - - - - -	49
Effects of high piezometric levels - - - - -	51
Storms capable of triggering debris flows - - - - -	51
Effect of prestorm rainfall - - - - -	52
Effect of storm intensity-duration - - - - -	54
Significance of the January 3-5, 1982, storm - - - - -	57
Conclusions - - - - -	58
References cited - - - - -	59

## ABSTRACT

Debris flows are a significant geologic hazard in the San Francisco Bay region, as demonstrated by the January 3-5, 1982, storm. We measured rainfall and pore-water pressures and noted debris flows between 1975 and 1983 within a 10-km<sup>2</sup> area near La Honda, Calif., to examine the significance of prestorm seasonal rainfall, the duration of high-intensity rainfall, and the generation of high pore-water pressures for triggering debris flows. From a sample of 22 intense storms during this period, a threshold of 280 mm (11.0 in.) of prestorm rainfall was necessary for subsequent storms to trigger debris flows. For storms that occurred after this prestorm threshold had been achieved, the combination of storm intensity and duration controlled the triggering of debris flows.

To permit a more precise determination of the temporal distribution of high-intensity rainfall, we propose a new measure, intensity-duration (ID), which defines the duration that rainfall equals or exceeds a particular intensity. For example, ID<sub>5.0</sub> = 3 h signifies an intensity equaling or exceeding 5.0 mm/h (0.2 in/h) for 3 hours. For 22 intense storms, we determined ID<sub>2.5</sub>, ID<sub>5.0</sub>, ID<sub>6.5</sub>, ID<sub>7.5</sub>, and ID<sub>10.2</sub> values from records of continuously recording rain gages in the area. We identified a value of ID<sub>5.0</sub> equal to or greater than 3 h as the most significant single index of storm ID which characterized the 10 storms that triggered debris flows in the area. We also developed a general equation for a threshold of rainfall duration and intensity necessary to trigger debris flows.

We measured perched high piezometric levels in shallow regolith over highly weathered bedrock immediately after intense storms in proximity

to debris flows. The amount of piezometric rise after a storm depended on the prestorm rainfall as well as the intensity and duration of the storm.

Of the 10 storms that triggered debris flows, 8 storms caused less than 1 debris flow per square kilometer. On the basis of a recurrence analysis, a storm triggering less than one debris flow per square kilometer could be expected, on the average, at least every 2 years. Such storms as the January 3-5, 1982, storm, which triggered approximately seven debris flows per square kilometer and had a recurrence interval of 60 years in this area, indicate that although isolated debris flows can be expected regularly in the area, abundant debris flows will be much less frequent.

## INTRODUCTION

The association of high-intensity rainfall with debris flows (see "Introduction" to this volume for landslide terminology) has been documented in Japan (Fukuoka, 1980), New Zealand (Selby, 1976; Pierson, 1980) and Brazil (Jones, 1973), as well as in many other places worldwide (Caine, 1980). In the Santa Monica Mountains of southern California, Campbell (1975) found that prestorm seasonal rainfall exceeding 267 mm (10.5 in.), in combination with intensities exceeding 6.4 mm/h (0.25 in/h), were necessary to trigger debris flows.

Temporarily high pore-water pressures during intense storms have been measured and related to debris flows. Within small drainages of forested hillslopes in Oregon, Pierson (1977, 1980) measured piezometric response to storms in very permeable shallow regolith over bedrock and found that the height and timing of the piezometric rise are controlled by a combination of antecedent soil moisture and rainfall intensity. In thin till regolith of coastal Alaska, Sidle and Swanston (1982) measured high piezometric levels near a debris slide during and shortly after several intense storms.

We have measured rainfall and piezometric levels and observed debris flows in a small study area to determine the importance of prestorm rainfall, the duration of high-intensity rainfall, and temporary piezometric levels in triggering debris flows. We compared the characteristics of the January 3-5, 1982, storm and other storms in the San Francisco Bay region between 1975 and 1983 that resulted in debris flows. From these comparisons, we have developed minimum thresholds for triggering debris flows, based on prestorm rainfall and storm intensity and duration, for this study area in northern California.

**Acknowledgments.**—Michael Bennett, Philip McLaughlin, and Randall Jibson performed the various laboratory tests and aided with the field observations cited in this study. Access to the study area was graciously provided by the landowner, Rudy Driscoll, his agent, George M. Shawback, and the farmers of the property, Fred and Henry Cunha. In particular, the many worthwhile discussions with Fred and his son Bill provided a valuable historical perspective and a keen insight concerning the slope processes active in this area.

### STUDY AREA

Our study was conducted within a 10-km<sup>2</sup> area in the La Honda and Harrington Creek watersheds northwest of the town of La Honda in the Santa Cruz Mountains, San Mateo County, Calif. (fig. 5.1). The study area ranges in elevation from 60 to 360 m and contains both gently sloping areas (less than 30 percent slope), where grasses, chaparral, and oaks predominate, and steep canyons (greater than 50 percent slope), where various conifers and redwoods are concentrated. The study area was

logged for redwood between 1868 and 1906 (Stanger, 1967). It has also been subject to wildfires, grazing by cattle, and periodic removal of brush for pasture areas since at least the turn of the 20th century. Thus, the distribution of vegetation, as well as the species present in the area, may have changed during historical time. However, the effects of these historical changes in land use on the slope stability have not yet been evaluated in this area.

The study area receives an average of 762 mm/yr (30 in/yr) of seasonal rainfall (Rantz, 1971), measured between July 1 and June 30, mostly between October and May. We supplemented daily-precipitation records for La Honda from the U.S. National Oceanic and Atmospheric Administration (NOAA) with continuous hourly records for La Honda available from the San Mateo County Department of Public Works and with continuous onsite monitoring begun in 1975.

Bedrock geology, weathering characteristics of bedrock, and thickness and characteristics of soils derived from bedrock all influence slope stability in this area (Wieczorek, 1982). The bedrock geology of the area (pl. 3) consists of three Tertiary bedrock units, from oldest to youngest: (1) the Lambert Shale and San Lorenzo Formation, undivided; (2) the Mindego Basalt and other volcanic rocks; and (3) the Tahana Member of the Purisima Formation (Brabb, 1980). Residual soils developed on all three bedrock units consist of moderately plastic clayey silt; however, they differ in their characteristic thicknesses (Wieczorek, 1982).

The Mindego Basalt consists mainly of basaltic volcanic rock. This unit weathers shallowly; slightly weathered or fresh rock<sup>1</sup> is common beneath the residual soil at depths of 1.5 to 5 m. Both debris slides and debris flows are common within the shallow regolith on steep slopes underlain by Mindego Basalt, whereas deeper types of slope movement are less common. The regular, well-defined drainage system developed on Mindego Basalt (fig. 5.2) provides abundant channels for debris flows. Large fan-shaped deposits below many short gullies (Wieczorek, 1982) suggest that debris flows have been a significant geomorphic process. Because the volume of such deposits far exceeds that of any individual debris flow observed during this study, such deposits probably accumulated from successive debris-flow episodes.

The undivided Lambert Shale and San Lorenzo Formation consists primarily of mudstone, siltstone, and shale; the Tahana Member of the Purisima Formation consists of very fine grained sandstone and siltstone (Brabb, 1980).

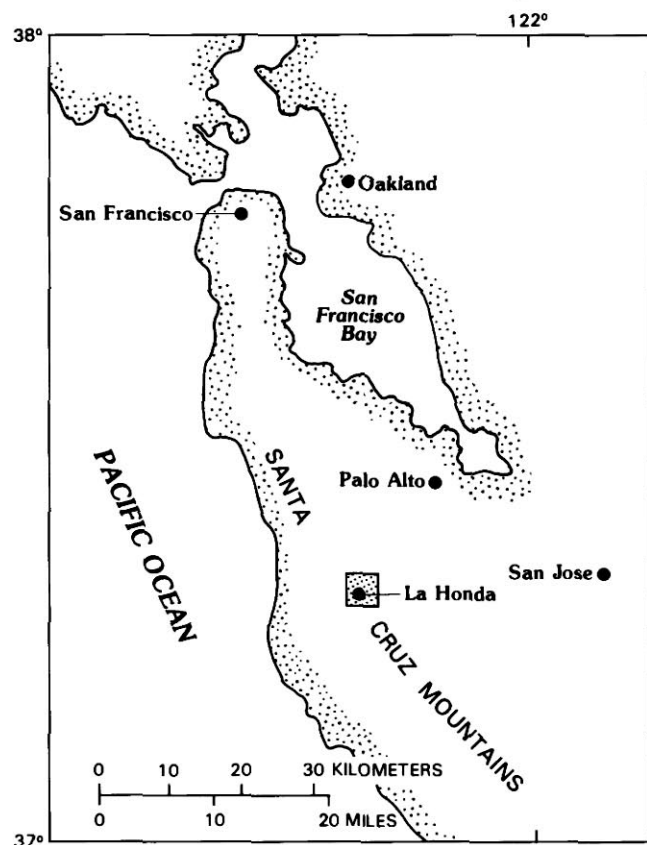


FIGURE 5.1.—Sketch map of the San Francisco Bay region, showing approximate location of study area (shaded) in the Santa Cruz Mountains.

<sup>1</sup>The degree of bedrock weathering has been classified by the terms "fresh," "slightly weathered," "moderately weathered," "highly weathered," "completely weathered," or "residual soil," according to the system adopted by the Geological Society Engineering Group Working Party (1972).

Bedrock of all these units weathers deeply; moderately weathered rock occurs to depths of 10 m beneath residual soils. Within the moderately weathered bedrock of these units, deep-seated slumps and earth flows are common. Shallow debris slides and debris flows are less common and are limited to slopes oversteepened by previous deep-seated failure (scarps) or by streambank erosion (Wieczorek, 1982).

### METHODS AND INSTRUMENTATION

We measured rainfall and piezometric levels<sup>2</sup> and observed debris flows within the study area beginning in 1975. These measurements and observations provide

<sup>2</sup>Measurements of water levels in a plastic tube connected to the porous stone piezometer are referenced to the depth of water in the tube below the ground surface. These measurements are termed "piezometric levels" rather than "ground-water levels." During periods of nonsteady flow and in places where the flow does not parallel the ground surface, the piezometric level from a piezometer sealed at a particular depth may not equal the water level in an open or perforated well.

climatologic and hydrologic data for comparing storms and their effects.

A tipping-bucket, continuously recording rain gage was installed in October 1975 near Harrington Creek (1, fig. 5.3). This gage recorded rainfall continuously to the nearest 0.25 mm (0.01 in.) with an accuracy of 1 percent for intensities as great as 76 mm/h (3.0 in/h). The chart from this gage can be read to determine rainfall totals or intensities for periods as short as 5 minutes. When the Harrington Creek gage malfunctioned, we used data from either the continuous gage at Weeks Creek (3, fig. 5.3) or the gage at the San Mateo County Yard in La Honda (2, fig. 5.3). The La Honda gage, however, is less precise because it records only to the nearest 2.5 mm (0.1 in.) at hourly increments. During one storm (Jan. 13–14, 1978), none of these gages was operating, and so hourly intensity was estimated from continuous records from other stations having comparable storm totals. In addition to these continuous gages, two Forestry rain buckets and a fencepost gage (1, 4, 5, fig. 5.3) were used to measure

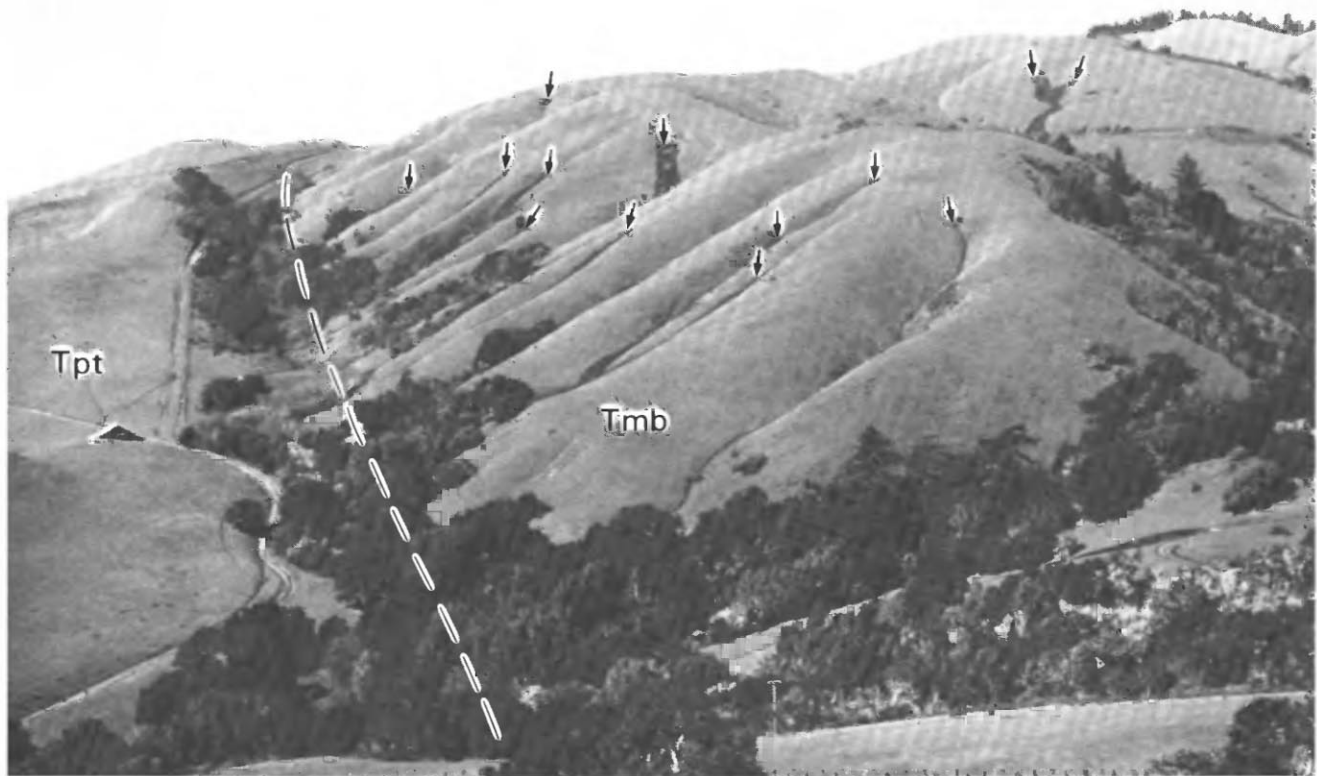


FIGURE 5.2.—Regular, dissected drainage pattern developed on steep slopes underlain by the Mindego Basalt (Tmb) provides pathways for debris flows. Arrows denote scars from debris flows triggered by the January 3–5, 1982, storm. Irregular drainage pattern to left is developed on slopes underlain by the Tahana Member of the Purisima Formation (Tpt).



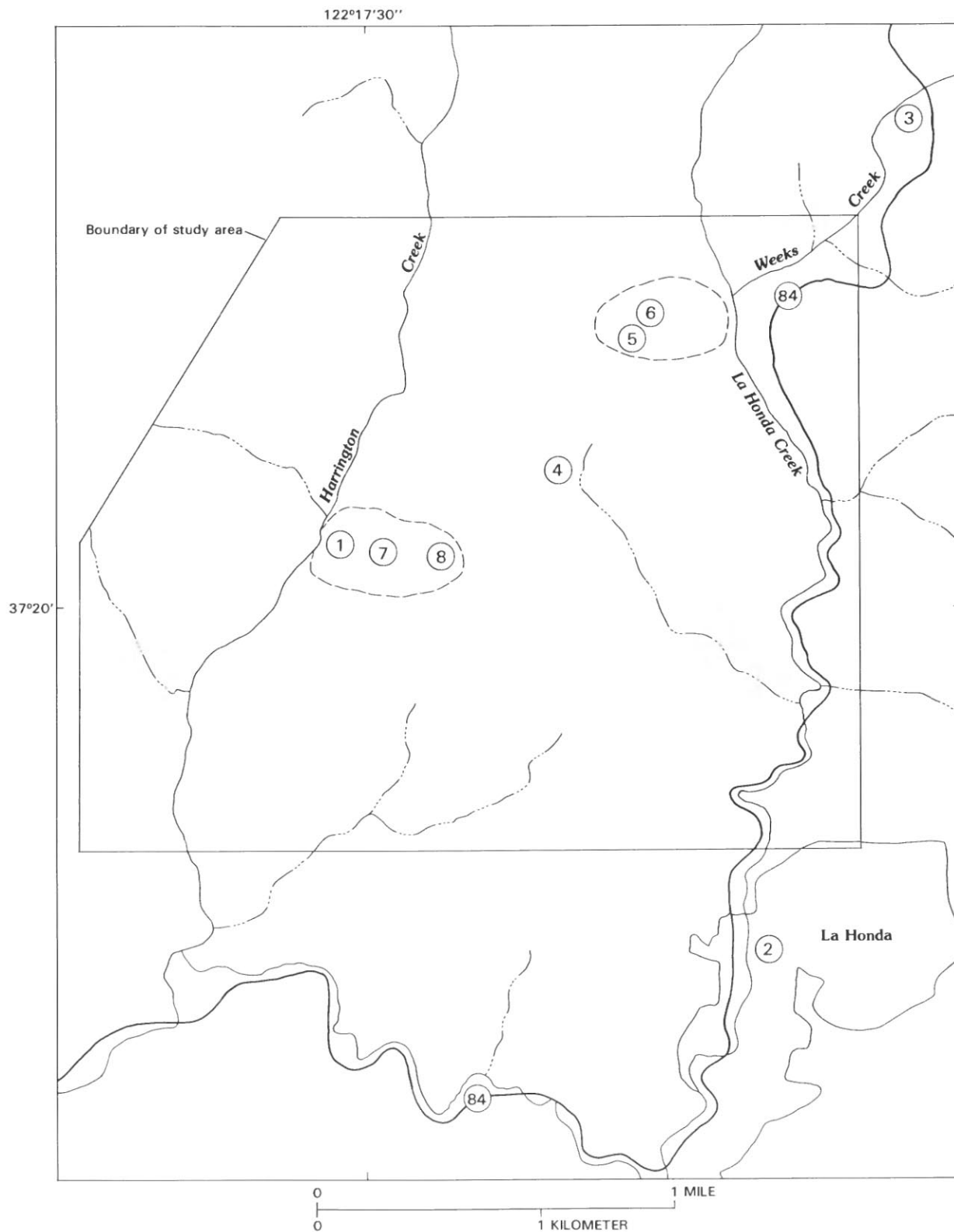


FIGURE 5.3.—Study area, showing locations of rain gages, piezometers, and instrumented slopes. 1, continuously recording rain gage (also a Forestry bucket rain gage) at Harrington Creek; 2, continuously recording rain gage at San Mateo County Yard, La Honda; 3, continuously recording rain gage at Weeks Creek; 4,

fencepost rain gage; 5, Forestry bucket rain gage; 6-8, Casagrande porous-stone piezometers. Dashed ovals enclose hillslopes instrumented with piezometers; solid line denotes boundary of study area (approx 10 km<sup>2</sup>). Planimetric base from La Honda 1:24,000-scale quadrangle.

local variation in storm totals, which was found to be minimal within the study area. This close distribution of three continuous rain gages and three storm-total gages within and near the 10-km<sup>2</sup> study area was sufficient to accurately represent storm totals and intensities for the purposes of comparison with debris flows within the study area.

Several piezometers (6–8, fig. 5.3) were installed at depths of less than 5 m to measure temporary piezometric levels that develop during and immediately after intense storms. These piezometers remained dry during most of the year but showed rapid piezometric rise after intense storms. We observed these levels to drop rapidly within hours to days after each storm; for example, two measurements taken within hours of each other 1 day after the December 20–22, 1982, storm showed the piezometric level to be dropping at a rate of 4.8 cm/h. Because these piezometers record neither peak nor continuous readings, we do not know the peak levels attained or their precise times. Our measurements were taken as soon as possible after each storm to document as well as possible the high piezometric levels attained. Therefore, these spot piezometric measurements should be used only as general indicators of high pore-water pressures and would be inadequate for a detailed stability analysis of the slope at the time of failure.

Instrumentation was inadequate in the study area to determine the delay between peak intensity during a storm and peak piezometric level. Because of the low relative permeability of the clayey-silt regolith in the study area, the delay time required for peak piezometric response of shallow aquifers after a storm is probably longer than the 4- to 18-hour delay observed in more permeable soils in Oregon (Pierson, 1977). Improvements in continuous monitoring of shallow ground-water levels and for recording peak levels have recently been developed by Pierson (1980) and Sidle and Swanston (1982); these procedures should provide more precise information on the temporal relation between high-intensity rainfall and peak piezometric levels.

## DEBRIS FLOWS IN THE STUDY AREA

### DESCRIPTION OF DEBRIS FLOWS: 1975–80

Five debris flows (1–5, pl. 3) were observed in the study area after high-intensity storms between 1975 and 1980. These flows initiated as shallow (max 1.5 m deep) slides, either rotational or translational, that involved only regolith or a combination of regolith and completely weathered bedrock. The translational slides involved slabs of regolith and incorporated rock fragments sliding over a planar surface of intact weathered rock inclined at an angle of at least 26° (fig. 5.4). The rotational slides occurred on concave hillslopes steeper than 20° (fig. 5.5) that commonly had more deeply developed soil profiles.

Characteristics and properties of these flows are listed in tables 5.1 and 5.2.

### DESCRIPTION OF DEBRIS FLOWS: DECEMBER 29, 1981

The storm of December 29, 1981, triggered five debris flows in the study area, all of which were small in volume (less than 10 m<sup>3</sup>) and had relatively short runout distances (less than 20 m). Only the largest of these debris flows (6) is identified on plate 3; the others are omitted because of their diminutive size and because they occurred in areas where other larger flows were subsequently mapped.

Soil moisture was probably high immediately before this storm because of heavy rainfall during the preceding months, particularly during November and December 1981 (fig. 5.6). The prestorm seasonal rainfall (July 1–Dec. 28, 1981) at Harrington Creek was 396 mm (15.60 in.), significantly above the to-date seasonal average (1954–81) for La Honda of 278 mm (10.94 in.). Rainfall of 80 mm (3.13 in.) during the 15 days preceding this storm probably put the regolith in a nearly saturated condition by the beginning of the storm.

Although 24-hour rainfall total of 55 mm (2.15 in.) for the December 29, 1981, storm was not unusually high in comparison with other storms (table 5.2), the steady, moderately intense rainfall equal to or exceeding 5.0 mm/h (0.20 in/h) for a 6-hour period (fig. 5.7A) was unusual.

### DESCRIPTION OF DEBRIS FLOWS: THE JANUARY 3–5, 1982, STORM

Rain began falling in the La Honda area at approximately 6 p.m. P.s.t. January 3, 1982, and continued for 38 hours until 8 a.m. January 5, by which time 153 mm (6.04 in.) had fallen. The continuous record of this storm from the Harrington Creek gage (fig. 5.7B) illustrates that the intensity was relatively steady during the 11-hour period between 5 a.m. and 4 p.m. January 4, when intensities consistently ranged from 5.1 to 8.1 mm/h (0.20–0.32 in/h). During the later part of the storm, between 4 and 10 p.m. January 4, intensities increased slightly to between 5.8 and 10.7 mm/h (0.23–0.42 in/h). The few documented times of debris flows in the La Honda vicinity occurred during this 6-hour period, the most intense part of the storm.

Numerous (74) debris flows (fig. 5.8) and less numerous (15) other landslides—slumps and block slides—were mapped (see pl. 3) in the field 1 day after the storm and from aerial photographs taken during the week after the storm. The volumes of these flows were generally large and were estimated to range as large as several hundred cubic meters. Runouts of some flows exceeded 100 m. Commonly, the thickness of material involved in the initial failure at the debris-flow scar ranged from 0.5 m to slightly more than 1 m.

**DESCRIPTION OF DEBRIS FLOWS:  
DECEMBER 1982-MARCH 1983**

Five storms during the unusually wet 1982-83 rainfall season triggered 26 debris flows in the study area (see pl. 3). Most of these debris flows occurred during the storms of January 22-23 and January 26, 1983. Seasonal rainfall before the January 22-23 storm of 495 mm (19.48 in.) was above average and, in combination with rainfall of 41 mm (1.60 in.) during the week before this storm, created ideal soil-moisture conditions for triggering debris flows.

Debris flows occurring during the 1982-83 season initiated similarly to those described previously for the other storms, that is, as shallow slides involving thin slabs of regolith. Volumes of individual flows ranged from 2 to 30 m<sup>3</sup>, with runout distances of from 6.5 to 64 m.

**CHARACTERISTICS AND PROPERTIES OF  
DEBRIS FLOWS: 1975-83**

From field examination and sampling of the debris-flow-source areas (scarps and base, fig. 5.9) and deposits, we

characterized the debris flows that occurred in this area near La Honda between 1975 and 1983. Descriptions and measurements of the source and runout areas for selected debris flows are listed in table 5.1, and geotechnical properties of selected debris flows, including grain-size distribution, Atterberg limits, and field water contents, are listed in table 5.2. Profiles of two typical debris flows illustrating the terms utilized in tables 5.1 and 5.2, in relation to measurements and sampling locations on debris flows, are shown in figure 5.9. In general, most debris flows initiated as slabs of regolith sliding along planar bedrock surfaces inclined at 26°-45°. After translational movements of as little as 1 m, these slabs mobilized into flows that commonly left lateral levees bounding a well-defined central channel (fig. 5.10A). Deposition typically occurred on slopes of 9°-22°, where the flow front was typically from 0.1 to 0.3 m thick.

Measurements of natural water content from the deposits of four debris flows sampled within the day after a particular storm indicate that the material in these deposits was within  $\pm 6$  percent water content of the liquid



FIGURE 5.4.—Debris flow from the January 26, 1983, storm (13, table 5.1) that originated as a translational slide of soil over a planar bedrock surface. Debris-flow scar is approximately 4 m wide, 8 m long, and from 23 to 40 cm deep on a uniform slope of between 35° and 38°.

limit (table 5.2). Natural water content of the intact material from the scarps and base of three of these debris flows was approximately 11 percent less than the liquid limit, a value suggesting that water was absorbed during the process of debris-flow mobilization and (or) transport (see section entitled "Mobilization," chap. 6). Mobilization of intact sliding slabs of regolith into flows by the incorporation of water has been postulated (Johnson and Rahn, 1970; Rodine, 1975) to be a significant mechanism of debris-flow generation on hillsides. Mobilization of an intact slab into a flow while undergoing small displacement was described by Rogers and Selby (1980).

We observed cracks adjacent to and upslope of many of the debris-flow scars in the study area, similar to those shown in figure 5.10B, after the January 3-5, 1982, storm. These cracks provide a route by which water from overland surface flow can enter the slope materials, further saturate the slope, reduce material strength, and contribute to the initiation of debris flows. During the January 3-5, 1982, storm in another part of the Santa Cruz Mountains, an eyewitness (Gary Greene, written

commun., 1982) reported narrow cracks developing on a chaparral-covered slope on which overland surface flow was occurring. For as long as 2 minutes, the cracks continued to open with water flowing in, until the slope mobilized suddenly as a rapid debris flow.

### FACTORS AFFECTING THE INITIATION OF DEBRIS FLOWS

#### EFFECTS OF VEGETATION

We observed in the field and from aerial photographs that more debris flows began on grass-covered slopes than in brush-covered and forested areas. Because slopes in the study area are estimated to be covered approximately as much by grass as by brush and trees, these grass-covered slopes appear to have been more susceptible to debris flow. Root strength may contribute to this apparent difference in debris-flow susceptibility. In several different laboratory soil profiles, roots of grasses have been found to provide most strength to the surficial soil mass above 0.3 m but only negligible strength below 0.45 m, whereas



FIGURE 5.5.—Debris flow of February 13, 1979 (4, table 5.1), that originated as a rotational slide within a topographic depression. Note scars of previous debris flows.



TABLE 5.1.—*Characteristics of selected debris flows*

Debris flow (pl. 3)	Description of initial failure and source of debris flow	Date of storm	Volume of initial slide (m <sup>3</sup> )	Maximum thickness (m)		Slope angle		Runout distance (m)
				Initial slide	Flow deposits	Initial failure	Flow termination	
1	Translational sliding of topsoil along planar siltstone bedrock surface below planar grassy slope.	1/13-14/78	4.0	0.61	---	26°-28°	---	30
2	Three coalescing slumps in black topsoil below concave grassy slope (no bedrock observed).	1/13-14/78	16.0	.50	---	24°-28°	---	70
3	Slump in saturated uniform black topsoil below concave grassy slope (no bedrock observed).	1/13-14/78	6.6	.91	.21	25°	22°	45
4	Slump through black topsoil into gray siltstone below large concave grassy slope.	2/13/79	200.0	1.50	.61	20°	---	75
5	Translational sliding of black topsoil along planar surface within area of brush and trees.	2/18/80	18.0	.91	---	38°	---	90
6	Translational sliding of black clayey silt along planar yellow siltstone bedrock surface below planar grassy slope.	12/29/81	4.2	.52	.15	32°	17°	8
7	do-----	1/3-5/82	9.1	.64	.40	29°	18°	21
8	do-----	1/3-5/82	6.3	.50	.09	29°	10°	45
9	Translational sliding of black topsoil and weathered pebbly siltstone over planar siltstone bedrock surface below planar grassy slope.	12/20-22/82	1.5	.33	.30	---	---	7
10	Translational sliding of brown soil over planar surface of completely weathered shale below concave grassy slope.	12/20-22/82	4.2	.70	.24	45°	9°	6
11	Slump in black topsoil below planar grassy slope (no bedrock observed).	1/22-23/83	10.5	.50	.37	26°	11°	8
12	Slump in uniform black topsoil below planar grassy slope (no bedrock observed).	1/22-23/83	5.2	.61	.37	40°	14°	9
13	Three translational slides of brown soil over surface of weathered gray sandstone below planar grassy slope, merging within channel into a single debris flow path.	1/26/83	30.0	.50	.09	35°-47°	17°	64
14	Large translational slide of black topsoil that generated debris flow along one lateral margin of slide below planar grassy slope (no bedrock observed).	2/25-3/2/83	37.0	.61	.21	28°	---	37

roots of brush and trees develop maximum strengths at deeper levels, generally below 0.3 m (Waldron, 1977; Waldron and Dakessian, 1981). Especially in coarse soils, the cohesion provided by roots may contribute most resistance against shallow sliding because of the small contribution of frictional strength, owing to low confining pressures at shallow depths. Because the depth of most observed failures ranged from 0.5 to 1.0 m, as indicated

by the initial slab thickness in table 5.1, grass-covered slopes with generally shallower roots could be expected to provide far less resistance to failure than slopes covered with brush and trees with generally deeper root systems. In fact, in the debris-flow scars we examined in grass-covered areas, the fact that the roots did not extend below the failure plane confirmed that roots contribute negligible strength at the depths significant to the initial failure



TABLE 5.2.—Physical properties of debris-flow materials

Debris flow	Particle-size distribution (percent)			Plasticity index	Liquid limit	Field water content (pct)
	Sand and gravel	Silt	Clay			
6						
Deposit---	5	64	31	26	58	---
Base-----	15	70	15	---	---	---
Scar-----	7	62	31	---	---	---
7						
Deposit---	5	67	28	19	51	---
Base-----	7	65	28	---	---	---
Scar-----	7	65	28	---	---	---
8						
Deposit---	7	63	30	28	58	---
Scar-----	8	60	32	---	---	---
Base-----	5	53	42	---	---	---
9						
Deposit---	6	72	22	25	57	52
Scar-----	3	63	34	---	---	46
10						
Deposit---	11	56	33	21-30	60-69	58
Scar-----	17	59	24	---	---	---
11						
Deposit---	18	59	23	29	61	55
Scar-----	10	49	41	---	---	50
12						
Deposit---	14	64	22	15	43	50
Base-----	14	63	23	---	---	39
13						
Deposit---	27	52	21	20	46	---
Scar-----	63	28	9	---	---	---

of debris flows. Thus, the root strength and depth of various vegetation may contribute to the differences in susceptibility of hillsides to debris flows.

#### EFFECTS OF HIGH PIEZOMETRIC LEVELS

We measured piezometric levels in shallow piezometers after many of these intense storms. Fortunately, we were able to measure piezometric levels near several debris flows (6-8, pl. 3) that occurred on December 29, 1981, and January 3-5, 1982. Piezometric levels were within 0.36 m of the ground surface on December 30 (approx 18 hours after the storm ended) and within 0.25 m on January 6 (approx 26 hours after the storm ended). The locations of the piezometers and the depths to the piezometric surface in relation to the debris flows are shown in figure 5.9.

Although neither continuous nor maximum-stage measurements were obtained, these data document that relatively high piezometric levels developed with respect to the thickness of the initial slab that failed. If ground-water flow remained strictly parallel to the slope surface, these piezometric levels would have extended about halfway between the failure surface and the top of the

slab, significantly reducing the resistance of the slab to sliding. However, because we do not know the actual ground-water-flow configuration between the piezometer and the debris flows, pore-water pressures may have been either greater or less than those estimated by assuming ground-water flow parallel to the slope surface.

After the intense storm of January 13-14, 1978, an artesian pore-water pressure of +0.38 m above the ground surface was measured at a piezometer installed in a swale (6, fig. 5.3). Convergence of three-dimensional subsurface flow from steep upslope concave depressions into flatter areas can be expected to cause nonparallel ground-water flow and upward flow gradients that result in artesian conditions. We measured artesian pore-water pressures of 0.41 m at a piezometer on a more nearly planar slope (7, fig. 5.3) after the storm of March 12-13, 1983; these measurements indicate that exceptionally high pore-water pressures can also develop in topography other than concave depressions.

#### STORMS CAPABLE OF TRIGGERING DEBRIS FLOWS

To determine the storm characteristics significant for triggering debris flows in the study area, we compiled meteorologic data (table 5.3) for those storms between 1975 and 1983 that triggered debris flows. For comparison, we compiled similar data on other storms during this same period that did not result in debris flows. We used several measures of both prestorm and storm rainfall for all these storms, and then compared the effect of each of these measures on the triggering of debris flows.

During this examination, we developed a new measure, intensity-duration (ID), which defines the duration (in hours) that rainfall intensity (in millimeters per hour) equals or exceeds a particular value. For example, an ID<sub>5.0</sub> of 3 h signifies that an intensity of at least 5.0 mm/h (0.20 in/h) lasted 3 hours. This measure permits a more precise determination of the effect of the time distribution of rainfall on the triggering of debris flows.

The ID values listed in table 5.3 were compiled from data from the continuously recording rain gages at Harrington Creek and La Honda County Yard, with exceptions as noted. Although both gages measured similar rainfall totals in the storms, we selected the data from Harrington Creek when both sets of data were available, because of its proximity to the observed debris flows as well as the greater precision of that gage. For periods when the Harrington Creek gage malfunctioned, data from La Honda were used.

Values of ID<sub>2.5</sub>, ID<sub>5.0</sub>, ID<sub>6.5</sub>, ID<sub>7.5</sub>, and ID<sub>10.2</sub> for 22 intense storms between 1975 and 1983 are listed in table 5.3. As noted, rainfall intensity during this period seldom exceeded 12.7 mm/h (0.50 in/h), and intensities ex-

ceeding 10.2 mm/h (0.40 in/h) seldom lasted longer than 2 hours. In other parts of the Santa Cruz Mountains, particularly farther south in Santa Cruz County, intensities typically exceed 25 mm/h (1.0 in/h) several times seasonally, and such intensities occasionally last several hours. Because of such contrasts in rainfall intensity within various parts of the Santa Cruz Mountains, our discussion of threshold prestorm rainfall and storm intensity and duration significant for the triggering of debris flows applies only to the study area.

#### EFFECT OF PRESTORM RAINFALL

The data listed in table 5.3 also show the importance of prestorm seasonal rainfall in generating debris flows. We divided the storms into three groups, based on the prestorm seasonal rainfall and the ability of the storms to trigger debris flows. The storms in group 1 (1-10), which occurred after a seasonal rainfall of 280 mm (11.0 in.), triggered debris flows; the storms in group 2 (11-17), which occurred before 280 mm (11.0 in.) of seasonal rain-

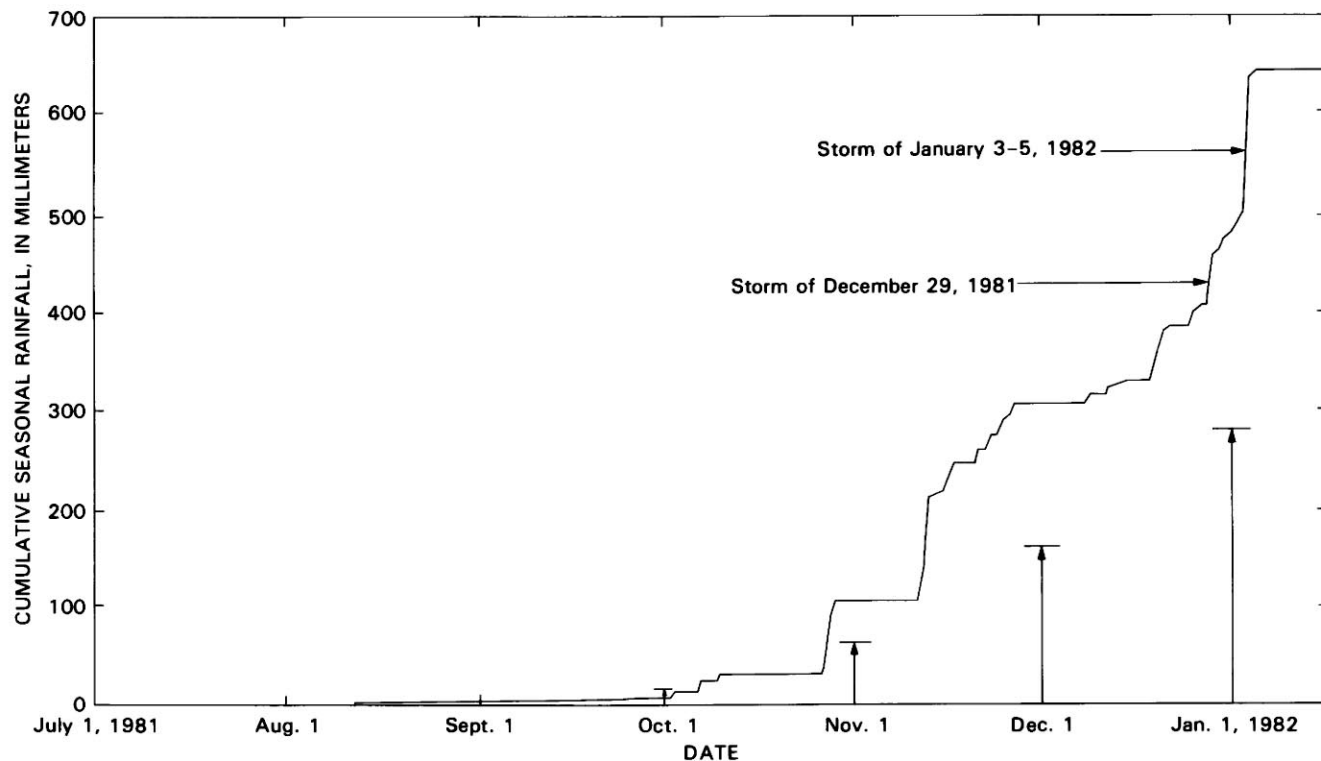


FIGURE 5.6.—Daily cumulative rainfall from July 1, 1981, to January 15, 1982, at Harrington Creek, in comparison with averages of monthly cumulative rainfall (arrows) for La Honda for 1954-81.

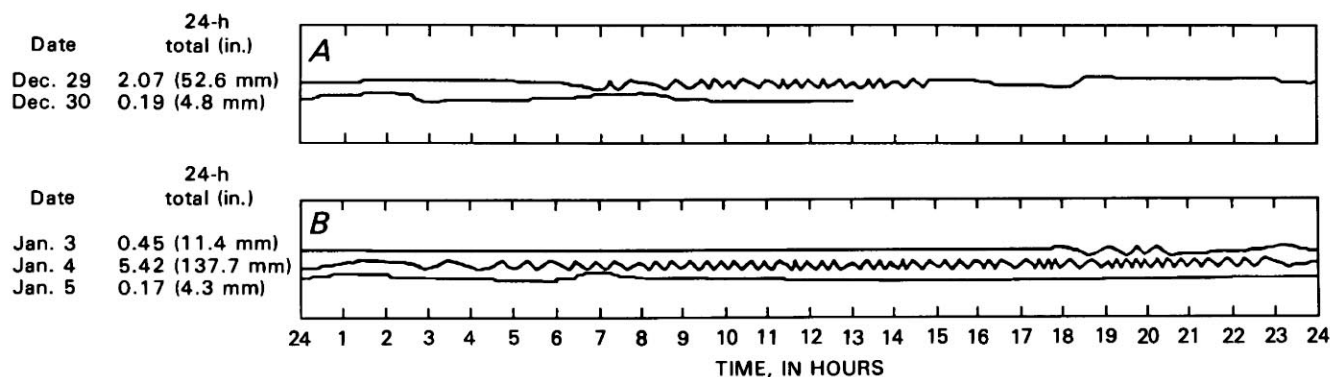


FIGURE 5.7.—Rainfall hydrographs from Harrington Creek gage. A, December 29-30, 1981. B, January 3-5, 1982. Each peak represents 2.5 mm (0.1 in.), and each individual step 0.25 mm (0.01 in.), of rainfall; each horizontal trace represents 1 d (24 h). ID values listed in table 5.3 were calculated from these hydrographs.

fall, triggered no debris flows; and the storms in group 3 (18–22), which occurred after a seasonal rainfall of 280 mm (11.0 in.), triggered no debris flows. The importance of prestorm seasonal rainfall can be seen by comparing the rainfall characteristics and effects between groups 1 and 2. Even though the storms in group 2 had storm totals, 24-hour maximums, 1-hour intensities, and ID values exceeding those for most of the storms in group 1 (1–4, 6–10), the storms in group 2 did not trigger debris flows, apparently because of insufficient prestorm seasonal rainfall. Prestorm seasonal rainfall of 280 mm (11.0 in.) was identified as a threshold.

Rainfall during the 2-, 7-, 15-, and 30-day periods preceding each storm is compiled in table 5.4. These values were not so distinctive as prestorm seasonal rainfall for distinguishing storms capable of triggering debris flows. At least 12.7 mm (0.50 in.), generally from 38 to 152 mm (1.5–6.0 in.), of rain fell during the 15-day periods before storms that triggered debris flows. Rainfall during the 7- and 15-day periods before storms 1, 5, and 8,

which caused the greatest number of debris flows, was significantly higher than for other storms, an observation suggesting that rainfall during the 1- or 2-week period preceding an intense storm may be significant in addition to the prestorm seasonal rainfall.

The average of the values listed in table 5.4 for groups 1, 2, and 3 indicates that rainfall during the 15- and 30-day periods preceding a storm for group 1 doubled that for group 2, yet was below that for group 3, a result suggesting insignificance for these periods of antecedent rainfall. A comparison of the average rainfall for the 2- and 7-day periods preceding a storm shows that the average for group 1 exceeds the averages for groups 2 and 3, a result suggesting possible significance for rainfall during the week preceding a storm. Nonetheless, conclusions based on these averages for such a small number of samples should be preliminary and subject to further verification. Additional data are needed to further establish the amount of prestorm rainfall that is significant during these periods before storms and to establish the effect



FIGURE 5.8.—Numerous debris flows triggered near La Honda by the January 3–5, 1982, storm. Arrows indicate debris-flow scars. Same hillslope as in figure 5.5.

of week-long dry periods on soil-moisture conditions and the ability of storms to trigger debris flows.

By the time of the January 3-5, 1982, storm, seasonal rainfall of 460 mm (18.9 in.) had far exceeded the prestorm threshold of 280 mm (11.0 in.) (see fig. 5.6). In addition, rainfall within 7- and 15-day periods preceding the storm was extremely heavy—86 mm (3.4 in.) and 155 mm (6.1 in.), respectively. That soils were nearly or completely saturated early in this storm in the La Honda area is also suggested by calculations from the U.S. National Weather Service's Sacramento Streamflow Model, which determined complete saturation of the mountainous San Lorenzo River drainage of Santa Cruz County by 9:00 a.m. P.s.t. January 4, 1982 (R.J.C. Burnash, oral commun., 1982).

The rise in piezometric level after intense storms was also observed to depend on whether the prestorm seasonal-rainfall threshold had been achieved; the data listed in table 5.5 show that piezometric levels after the storms in group 2 (11-17) remained generally below those after the storms in group 1 (1-10) and group 3 (18-22) (except for storm 8, for which there is a possible error in piezometric measurement). These data further show that storms 18 through 22, which occurred after the

prestorm threshold had been reached, resulted in relatively high piezometric levels, even though ID values, particularly  $ID_{5.0}$ , were not so high as those for storms 1 through 10, a relation indicating the importance of soil-moisture storage and downslope flow, even within a shallow hydrologic regime.

#### EFFECT OF STORM INTENSITY-DURATION

By comparing the ID values for the different storms in groups 1 and 3 (table 5.3), an intensity-duration threshold was identified for storms that triggered at least one debris flow within the study area. On a plot of values of continuous duration at different levels of intensity for the storms in groups 1 and 3, this threshold is evident in figure 5.11A, separating the storms that triggered debris flows (circles) from those that did not (dots). Each storm is represented by a family of circles, with a value corresponding to a duration of each particular intensity. The two circles that lie to the left of the threshold are minimums, and the error in measurement associated with these values spans the threshold and confirms the trend.

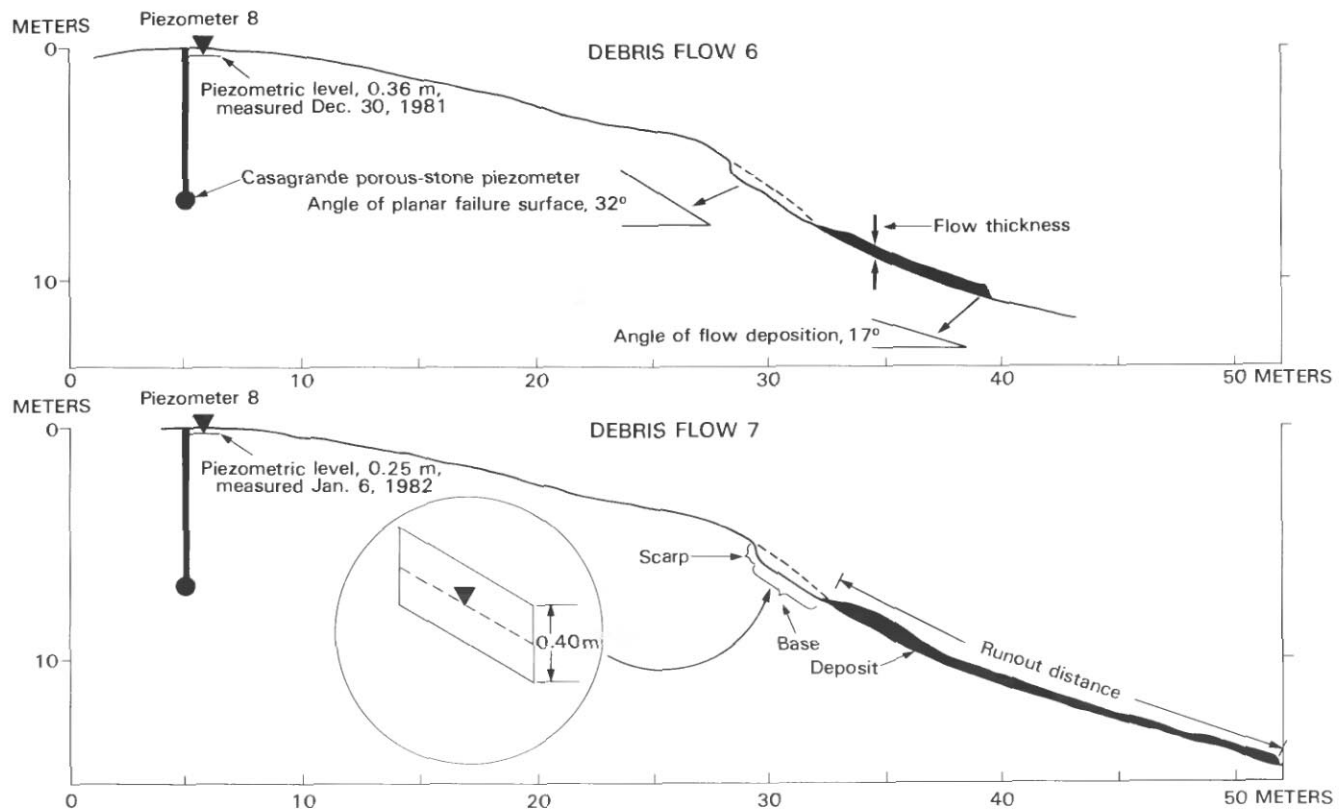


FIGURE 5.9.—Profiles of debris flows 6 and 7 (pl. 3), showing location of piezometer (8, fig. 5.3). Inset shows level of ground water within failure slab equivalent to piezometric level measured nearby on January 6, 1982; actual maximum level in slab is unknown.





FIGURE 5.10.—Debris flow 3 (pl. 3) triggered January 13–14, 1978, by slumping in regolith within a topographic depression. *A*, Lateral levees bounding channel about midway along debris flow. *B*, Slump and scar at head of debris flow. *C*, Entire debris flow, showing locations of closeups in figures 5.10A and 5.10B.



Below an intensity of approximately 2.5 mm/h (0.10 in/h), the threshold in figure 5.11A is not particularly well constrained. Physically, the independence of duration and intensity on triggering debris flows below this low intensity may correspond to the ability of soils on steep slopes to drain under low rates of rainfall infiltration without appreciable buildup of pore-water pressure. For higher intensities, the data are not sufficiently accurate to extend the threshold for durations of less than 1 hour. High-intensity rainfall of short duration may not be so significant for triggering debris flows in the low-permeability, cohesive soils of this area as in other areas of more highly permeable, cohesionless soils, where pore pressures can rapidly respond to high-intensity rainfall (Sidle and Swanston, 1982).

The intensity-duration threshold is best defined within the range of intensities from 5.0 to 10 mm/h (0.20-0.40 in/h). If this threshold is considered as asymptotic at its extremes, then the relation between duration and inten-

sity to trigger debris flows can be expressed by the equation

$$D = 9.0/(I - 1.7),$$

where  $D$  is the continuous duration of rainfall (in hours) equal to or exceeding an intensity  $I$  (in millimeters per hour) (R.C. Wilson, written commun., 1985).

The effect of antecedent rainfall is again demonstrated in figure 5.11B, where duration and intensity for storms with less than 280 mm (11.0 in.) of prestorm seasonal rainfall (group 2, table 5.3) are plotted. The triangles (representing storms in group 2 of table 5.3) are distributed on both sides of the intensity-duration threshold line. Significantly higher intensities and longer durations, above the threshold in some of these storms that nonetheless did not trigger debris flows, confirm the strong influence of antecedent rainfall on the ability to trigger debris flows within the range of storm intensity and duration observed.



FIGURE 5.10.—Continued

### SIGNIFICANCE OF THE JANUARY 3-5, 1982, STORM

The rainfall characteristics of the January 3-5, 1982, storm, in comparison with those of other storms that resulted in debris flows, indicate that this storm was exceptional from a recurrence standpoint. All the ID values for the January 3-5, 1982, storm generally exceeded those for the other storms listed in table 5.3.

We evaluated the January 3-5, 1982, storm, using the depth-duration-frequency analysis developed by Rantz (1971) for areas within the San Francisco Bay region. Using depth-frequency curves for the 760-mm (30 in.) average seasonal rainfall of the La Honda study area, storm-recurrence intervals  $R_c$  (in years) were evaluated for the maximum 1-, 2-, 3-, 6-, 12-, 18-, and 24-hour rainfall totals measured at Harrington Creek. As listed in table 5.6, the unusual aspect of the rainfall during the January 3-5, 1982, storm was the total rainfall for the 18-hour period, which had a recurrence interval of

60 years. Interestingly, the January 26, 1983, storm, which was responsible for the second highest number of debris flows, had an  $R_c$  of 7 years for the maximum 6-hour-period rainfall total. Tabulation of the recurrence intervals for the other storms indicates that isolated, less abundant debris flows could be expected to occur at least every 2 years.

This threshold is notably less than that identified for abundant debris flows in the San Francisco Bay region (see chap. 4) and that proposed by Caine (1980) for debris flows reported worldwide. However, because the threshold for the study area is based on storms that caused as few as one debris flow in the 10-km<sup>2</sup> area, this difference is not too surprising. We characterized isolated debris flows as less than 1 per square kilometer, and abundant as greater than 1 per square kilometer, following the general procedure of Govi and Sorzana (1980) for calibrating the intensity of debris-flow effects. Within the study area, the number of debris flows generally increased with increasing ID values. We have developed preliminary

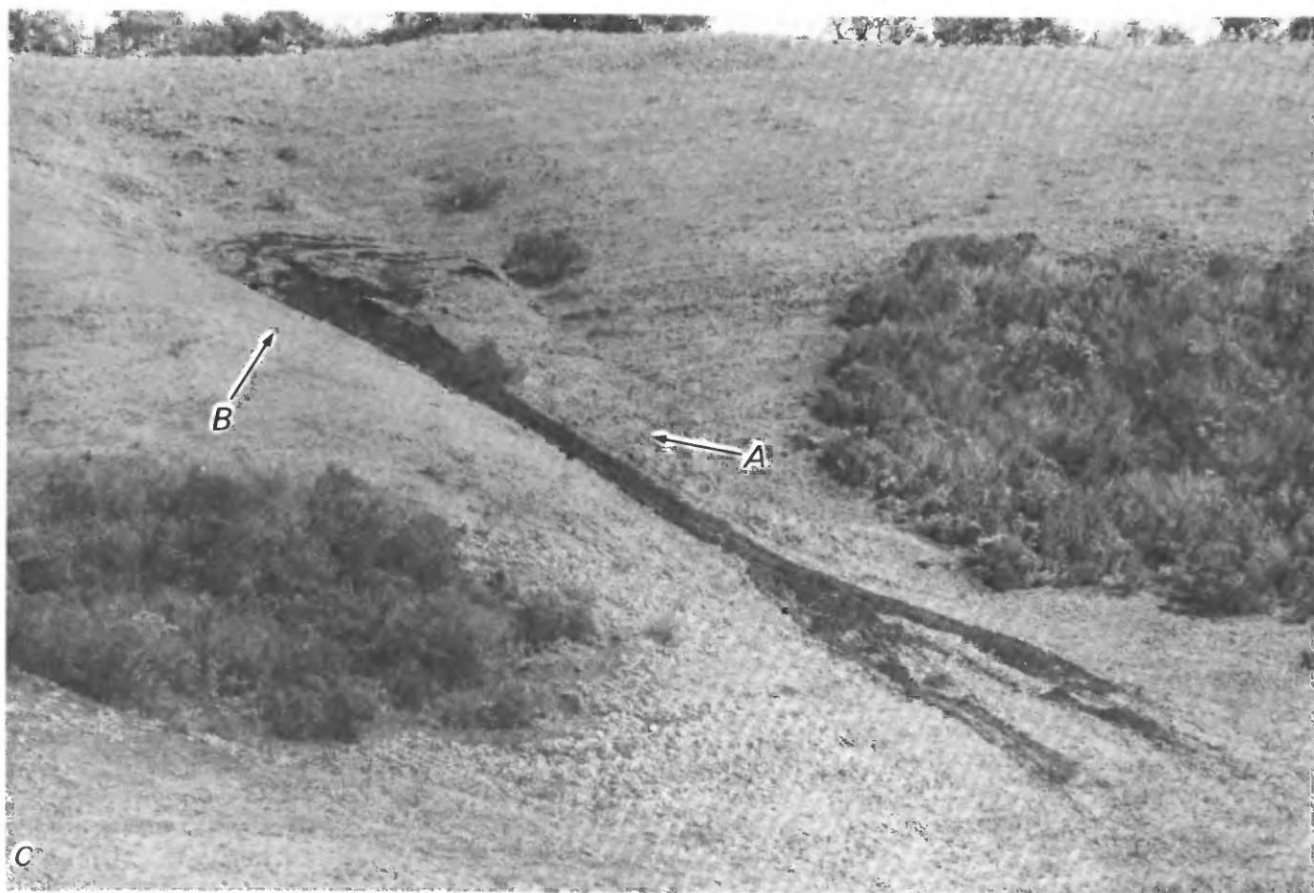


FIGURE 5.10.—Continued

TABLE 5.3.—Storm-rainfall characteristics related to debris flows in the study area, 1975-83

[Data for storm 1 averaged from U.S. National Oceanic and Atmospheric Administration continuously recording rain gages at Berkeley and San Francisco Weather Station offices. Data for storms 2, 3, and 14 from continuously recording rain gage at La Honda-San Mateo County Yard (2.5-mm [0.1 in.] hourly readings). Data for storm 10 from continuously recording rain gage at Weeks Creek (2.5-mm [0.1 in.] hourly readings). Data for all other storms from continuously recording rain gage at Harrington Creek (0.25-mm [0.01 in.] continuous readings)]

Storm	Date	Prestorm seasonal rainfall (mm)	Storm total (mm)	Max 24 h (mm)	Max 1 h (mm)	ID <sub>2.5</sub> (h)	ID <sub>5.0</sub> (h)	ID <sub>6.5</sub> (h)	ID <sub>7.5</sub> (h)	ID <sub>10.2</sub> (h)	Number of debris flows
Group 1											
1	1/13-14/78	388	70.1	61.0	8.1	4	3	2	2	0	3
2	2/13/79	282	55.9	55.9	10.2	9	3	1-2	1	1	1
3	2/18/80	492	45.7	45.7	10.2	7	3	2-3	2	1	1
4	12/29/81	396	57.4	54.6	8.1	6.7	6.3	5.5	2.4	0	5
5	1/3-5/82	480	153.4	137.7	10.7	19.2	16.5	13.8	4.3	1.7	74
6	12/20-22/82	351	104.1	64.8	10.9	3.8	3.3	3.2	2.8	1.3	2
7	1/22-23/83	495	98.3	58.7	14.2	6.4	3.1	2.2	2.1	1.3	8
8	1/26/83	601	77.5	76.2	24.4	6.1	5.0	4.8	4.5	2.0	13
9	2/25-3/2/83	873	154.9	62.2	10.9	3.5	3.1	2.3	2.1	1.2	1
10	3/12-13/83	1,059	55.9	55.9	10.2	6	5	3-4	3	1	2
Group 2											
11	3/15-16/77	264	51.6	51.6	6.4	8.7	3.1	1.0	0	0	0
12	1/7-11/79	90	103.9	47.0	15.2	5.5	2.0	1.6	1.6	1.6	0
13	1/14-15/79	197	68.8	68.8	14.0	5.5	3.4	1.6	1.6	1.3	0
14	12/23-24/79	231	127.0	116.8	20.3	10	4	3	3	2	0
15	1/26-29/81	165	122.7	71.4	10.9	5.2	3.5	2.5	1.2	1.0	0
16	11/18/82	168	81.3	81.3	10.2	9.3	7.4	5.5	5.3	1.0	0
17	11/27-30/82	256	81.5	35.6	12.7	4.9	2.4	2.3	2.1	1.4	0
Group 3											
18	3/12-13/81	376	60.4	60.4	11.9	7.9	2.2	2.0	1.7	1.0	0
19	2/13-17/82	724	127.8	72.9	8.9	8.1	2.7	1.5	1.0	0	0
20	3/28-4/3/82	949	139.9	63.2	8.9	7.0	2.4	1.7	1.5	0	0
21	4/10-11/82	1,096	59.7	50.8	6.9	3.8	1.7	1.2	0	0	0
22	2/5-8/83	708	100.8	50.5	8.9	2.4	1.7	1.6	1.2	0	0

criteria (table 5.7) for storms that would induce isolated as well as abundant debris flows.

## CONCLUSIONS

For the La Honda study area, both prestorm rainfall and the duration of high-intensity rainfall determine whether a storm will trigger debris flows. Once a prestorm seasonal threshold of 280 mm (11.0 in.) is exceeded, high-intensity storms are capable of generating debris flows. We quantified the duration of high-intensity rainfall, using a measure termed ID, the duration over which rainfall equals or exceeds a particular intensity. We determined a general equation for a threshold for triggering at least one debris flow within the area that is best defined for ID<sub>5.0</sub> to ID<sub>10.0</sub>. An ID<sub>5.0</sub> value of 3 hours or more represents the most significant single index of those

storms that caused debris flows in contrast to those that did not.

High piezometric levels in shallow regolith and highly weathered bedrock, generated during and immediately after intense storms, triggered translational and rotational slides that mobilized into debris flows. The piezometric rise after a storm depended on prestorm rainfall as well as ID value. These observations compared well with the limited previous piezometric measurements obtained near debris flows (Sidle and Swanston, 1982), as well as with previously witnessed initiations of debris flows (Rogers and Selby, 1980).

The significance of the January 3-5, 1982, storm from a mass-wasting perspective is conveyed by the large number of debris flows within this area in comparison with the number of flows observed after other storms. From a meteorologic viewpoint, the significance of this storm was indicated by a 60-year recurrence of the 18-hour max-

TABLE 5.4.—Rainfall during the 2-, 7-, 15-, and 30-d periods preceding storms

Storm	Date	Prestorm rainfall (mm)				Prestorm seasonal rainfall (mm)
		2 d	7 d	15 d	30 d	
Group 1						
1	1/13-14/78	1.8	53.6	120.9	246.9	388
2	2/13/79	.0	.0	12.9	88.9	282
3	2/18/80	22.9	71.1	71.1	71.1	492
4	12/29/81	2.8	18.3	79.5	95.8	396
5	1/3-5/82	15.2	86.4	154.7	179.3	480
6	12/20-22/82	.0	10.2	13.5	98.0	351
7	1/22-23/83	.5	41.1	41.1	86.1	495
8	1/26/83	7.6	106.4	147.1	147.1	601
9	2/25-3/2/83	5.0	32.2	63.5	272.0	873
10	3/12-13/83	.0	20.6	185.4	248.9	1,059
Average-----		5.6±7.7	44.0±34.9	89.0±60.4	153.4±77.8	---
Group 2						
11	3/15-16/77	2.8	9.1	9.4	43.7	264
12	1/7-11/79	2.3	2.8	2.8	16.3	90
13	1/14-15/79	1.8	103.9	106.9	120.4	197
14	12/23-24/79	.0	19.3	19.3	25.1	231
15	1/26-29/81	.0	55.4	58.9	86.9	165
16	11/18/82	.0	20.3	25.4	118.1	168
17	11/27-30/82	.0	3.0	84.3	132.6	256
Average-----		1.0±1.3	30.5±37.0	43.9±40.1	77.6±48.7	---
Group 3						
18	3/12-13/81	0.0	0.0	43.4	65.8	376
19	2/13-17/82	.0	.0	.0	90.7	724
20	3/28-4/3/82	3.0	10.4	53.3	97.8	949
21	4/10-11/82	.0	19.1	150.1	201.7	1,096
22	2/5-8/83	22.9	43.4	213.9	254.5	708
Average-----		5.2±10.0	14.6±18.0	92.1±87.4	142.1±81.6	---

imum rainfall, whereas the other storms that caused debris flows generally had a less than 2-year recurrence. Therefore, although a few isolated debris flows can be expected on a more or less regular yearly basis, most slope modification from widespread and abundant debris flows appears to occur far less frequently—only during such long-duration, high-intensity storms as that of January 3-5, 1982.

#### REFERENCES CITED

- Brabb, E.E., 1980, Preliminary geologic map of the La Honda and San Gregorio quadrangles, San Mateo County, California: U.S. Geological Survey Open-File Report 80-245, scale 1:24,000.
- Caine, Nel, 1980, The rainfall intensity-duration control of shallow landslides and debris flows: *Geografiska Annaler*, v. 62, ser. A, no. 1-2, p. 23-27.
- Campbell, R.H., 1975, Soil slips, debris flows, and rainstorms in the Santa Monica Mountains and vicinity, southern California: U.S. Geological Survey Professional Paper 851, 51 p.
- Fukuoka, Masami, 1980, Landslides associated with rainfall: *Geotechnical Engineering*, v. 11, no. 1, p. 1-29.
- Geological Society Engineering Group Working Party, 1972, The preparation of maps and plans in terms of engineering geology: *Quarterly Journal of Engineering Geology*, v. 5, no. 4, p. 295-382.
- Govi, Mario, and Sorzana, P.F., 1980, Landslide susceptibility as a function of critical rainfall amount in Piedmont basins (North-Western Italy): *Studia Geomorphologica Carpatho-Balcanica*, v. 14, p. 43-61.
- Johnson, A.M., and Rahn, P.H., 1970, Mobilization of debris flows, in Macar, Paul, New contributions to slope evolution: *Zeitschrift für Geomorphologie*, supp. v. 9, p. 168-186.
- Jones, F.O., 1973, Landslides of Rio de Janeiro and the Serra das Araras Escarpment, Brazil: U.S. Geological Survey Professional Paper 697, 42 p.
- Pierson, T.C., 1977, Factors controlling debris flow initiation on forested

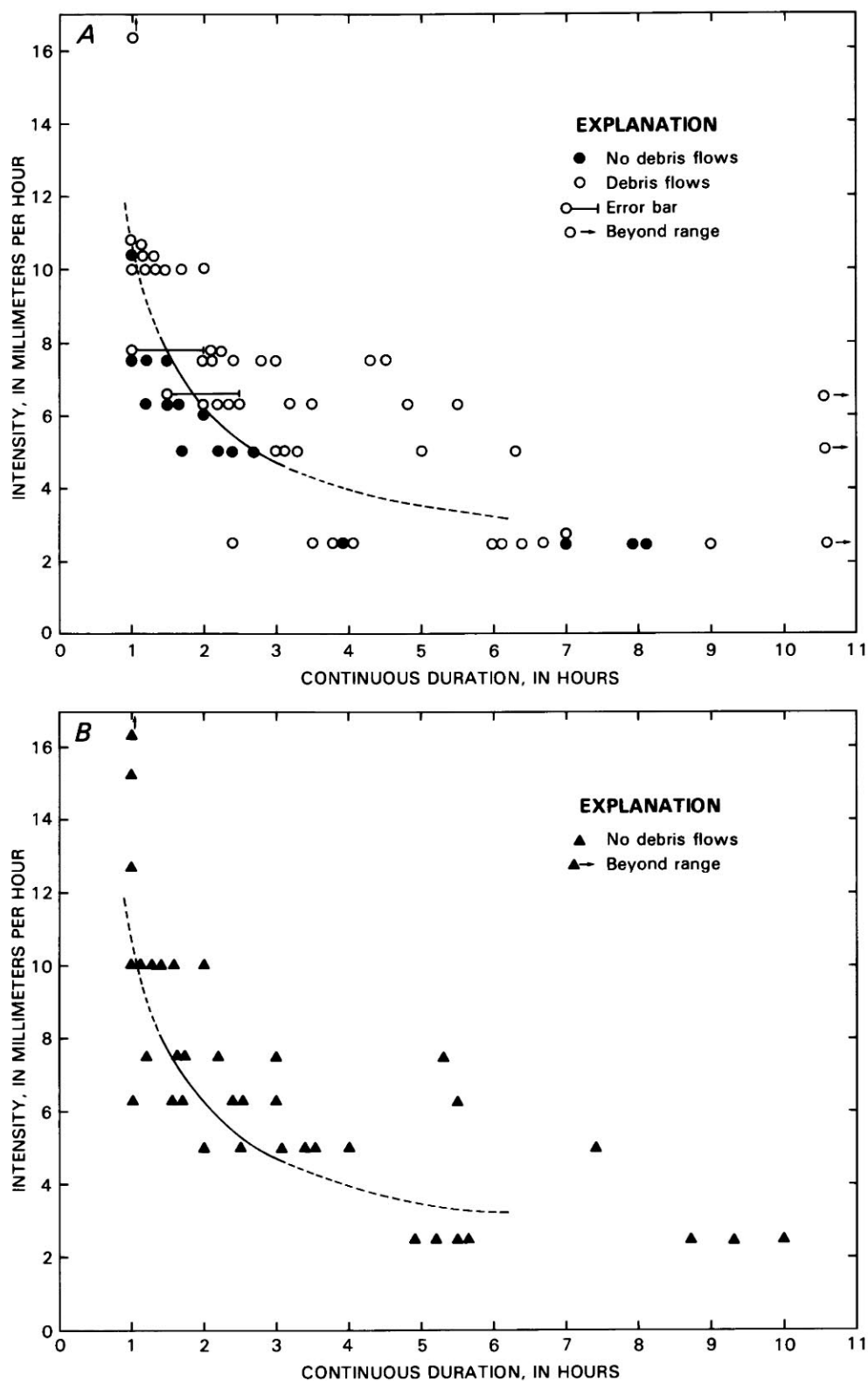


FIGURE 5.11.—Relations among rainfall intensity-duration from records of 22 storms in the study area from data listed in table 5.3. *A*, Values from storms that occurred after a prestorm seasonal threshold of 280 mm (11 in.). Solid line represents intensity-duration threshold that delineates storm-rainfall conditions which resulted in debris flows; line is dashed where threshold is less certain. *B*, Values from storms that occurred before a prestorm rainfall of 280 mm (11 in.) had been reached. Threshold line from figure 5.11A is shown for comparison.



TABLE 5.5.—Piezometric levels measured after storms

[Plus sign indicates pore-water pressure above ground surface, commonly referred to as artesian. All other piezometric levels indicate depth beneath ground surface]

Storm	Date	Prestorm seasonal rainfall (mm)	ID <sub>5.0</sub> (h)	Depth to piezometric level (m)		Time of measure- ment after storm (d)
				(8, fig. 5.3)	(7, fig. 5.3)	
Group 1						
1	1/13-14/78	388	3	0.94	0.42	5
2	2/13/79	382	3	.51	.10	10
3	2/18/80	492	3	---	---	---
4	12/29/81	396	6.3	.36	.51	1
5	1/3-5/82	480	16.5	.25	.43	1.5
6	12/20-22/82	351	3.3	2.03	.03	1
7	1/22-23/83	495	3.1	.86	.03	1.5
8	1/26/83	601	5.0	4.38(?)	.38	2
9	2/25-3/2/83	873	3.1	.53	+.10	1
10	3/12-13/83	1,059	5	2.36	+.41	2
Group 2						
11	3/15-16/77	264	3.1	dry	4.43	5
12	1/7-11/79	90	2.0	2.76	.88	1
13	1/14-15/79	197	3.4	5.82	.84	7
14	12/23-24/79	231	4	5.08	1.78	5
15	1/26-29/81	165	3.5	5.79	1.42	5
16	11/18/82	168	7.4	4.67	---	1
17	11/27-30/82	256	2.4	4.85	---	3
Group 3						
18	3/12-13/81	376	2.2	---	---	---
19	2/13-17/82	724	2.7	.38	.15	1
20	3/28-4/3/82	949	2.4	.59	.19	4
21	4/10-11/82	1,096	1.7	.76	.33	9
22	2/5-8/83	708	1.7	2.76	.03	2

hillslopes in the Oregon Coast Range: Seattle, University of Washington, Ph.D. thesis, 166 p.

- 1980, Piezometric response to rainstorms in forested hillslope drainage depressions: *Journal of Hydrology*, v. 19, no. 1, p. 1-10.
- Rantz, S.E., 1971, Mean annual precipitation and precipitation depth-duration-frequency data for the San Francisco Bay region: U.S. Geological Survey open-file report, 23 p.
- Rodine, J.D., 1975, Analysis of the mobilization of debris flows: Stanford, Calif., Stanford University, Ph.D. thesis, 226 p.
- Rogers, N.W., and Selby, M.J., 1980, Mechanism of shallow translational landsliding during summer rainstorms: North Island, New Zealand: *Geografiska Annaler*, v. 62, ser. A, no. 1-2, p. 11-21.
- Selby, M.J., 1976, Slope erosion due to extreme rainfall: A case study from New Zealand: *Geografiska Annaler*, v. 58, ser. A, no. 2, p. 131-138.
- Sidle, R.C., and Swanston, D.N., 1982, Analysis of a small debris slide in coastal Alaska: *Canadian Geotechnical Journal*, v. 19, no. 2, p. 167-174.
- Stanger, F.M., 1967, Sawmills in the redwoods: San Mateo, Calif., San Mateo County Historical Association, 160 p.
- Waldron, L.J., 1977, The shear resistance of root-permeated homogeneous and stratified soil: *Soil Science Society of America Journal*, v. 41, no. 5, p. 843-849.
- Waldron, L.J., and Dakessian, Suren, 1981, Soil reinforcement by roots: Calculation of increased soil shear resistance from root properties: *Soil Science*, v. 132, no. 6, p. 427-435.
- Wieczorek, G.F., 1982, Map showing recently active and dormant landslides near La Honda, central Santa Cruz Mountains, California: U.S. Geological Survey Miscellaneous Field Studies Map MF-1422, scale 1:4,800.

TABLE 5.6.—Recurrence intervals of maximum rainfall during 6-, 18-, and 24-h periods for storms that caused debris flows in the study area

[For each storm, recurrence intervals ( $R_c$ ) are for maximum rainfall during each period, as determined by the method of Rantz (1971). Those  $R_c$  values listed as 2 may actually be somewhat less than 2]

Period-----		6 h		18 h		24 h	
Storm	Date	Maximum rainfall (mm)	$R_c$ (yr)	Maximum rainfall (mm)	$R_c$ (yr)	Maximum rainfall (mm)	$R_c$ (yr)
1	1/13-14/78	26.2	2	36.8	2	61.0	2
2	2/13/79	25.4	2	50.8	2	55.9	2
3	2/18/80	38.1	2	45.7	2	45.7	2
4	12/29/81	40.6	2	52.1	2	54.6	2
5	1/3-5/82	51.3	3.4	129.5	60	137.7	18
6	12/20-22/82	30.5	2	52.1	2	64.8	2
7	1/22-23/83	39.4	2	58.7	2	58.7	2
8	1/26/83	59.4	7.0	63.5	2	76.2	2
9	2/25-3/2/83	26.7	2	48.8	2	62.2	2
10	3/12-13/83	38.1	2	48.3	2	55.9	2

TABLE 5.7.—*Intensity-duration and prestorm seasonal rainfall thresholds for storms that triggered isolated and abundant debris flows near La Honda, Calif.*

[The size of individual debris flows falls within a fairly narrow range (10-100 m<sup>2</sup>). Because individual debris-flow areas are small in relation to the monitored field area, the magnitude of the effects from individual storms is expressed in terms of the number of flows per square kilometer, according to the procedure of Govi and Sorzana (1980)]

	Minimum prestorm seasonal rainfall (mm)	ID <sub>5.0</sub> (h)	ID <sub>7.5</sub> (h)	R <sub>c</sub> (yr)
Isolated debris flows (less than 1/km <sup>2</sup> ), storms 1-4, 6, 7, 9, 10.	280	3-6	2	2
Abundant debris flows (more than 1/km <sup>2</sup> ), storms 5, 8.	381	5-16	4-14	7-60

## 6. DESCRIPTION AND MECHANICS OF SOIL SLIP/DEBRIS FLOWS IN THE STORM

By STEPHEN D. ELLEN,  
U.S. GEOLOGICAL SURVEY;  
with contributions by

MITCHELL A. ALGUS, SUSAN H. CANNON, ROBERT W. FLEMING,  
PHILIP C. LAHR, DAVID M. PETERSON, and STEVEN L. RENEAU

### CONTENTS

	Page
Abstract - - - - -	64
Introduction - - - - -	64
Terminology - - - - -	64
Acknowledgments - - - - -	66
Description of soil slip/debris flows in the storm - - - - -	66
Case studies - - - - -	66
Three Peaks, by Stephen D. Ellen and David M. Peterson - - - - -	66
Murray Park - - - - -	68
Homestead Valley - - - - -	68
Tiburon Ridge - - - - -	69
Inverness area, by Steven L. Reneau - - - - -	70
First Valley - - - - -	77
Single soil slip/debris flows - - - - -	79
Size and form - - - - -	80
Slopes of failure and flow - - - - -	80
Soils involved - - - - -	82
Degree of mobilization - - - - -	83
Complexes of soil slip/debris flows - - - - -	83
Summary - - - - -	83
Mechanics of soil slip/debris flow - - - - -	84
Movement of water to sites of failure - - - - -	84
Rainfall and dynamic balance - - - - -	84
Concentration of water - - - - -	85
Surface flow and throughflow - - - - -	85
Bedrock contacts - - - - -	87
Bedrock seepage - - - - -	87
Breaks in slope and contrasts in soils - - - - -	88
Hillslope modifications - - - - -	88
Elevated pore pressure - - - - -	89
Summary - - - - -	89
Initial failure - - - - -	89
Infinite-slab model - - - - -	90
Slopes of failure - - - - -	91
Location of the failure surface - - - - -	92
Mobilization, by Stephen D. Ellen and Robert W. Fleming - - - - -	92
Contrasts in mobilization - - - - -	92
Theory of mobilization - - - - -	93
Soil texture - - - - -	93
Transition from slide to flow - - - - -	94
Mobility index - - - - -	94
Approximate mobility index - - - - -	94
The steady state and liquefaction - - - - -	95
Possible means of mobilization - - - - -	97
Contractive case - - - - -	97
Dilative case - - - - -	99
Mobilization during the storm - - - - -	99
Reed, by Stephen D. Ellen, Philip C. Lahr, and Susan H. Cannon - - - - -	100
Salmon Creek, by Stephen D. Ellen, Robert W. Fleming, and Mitchell A. Algus - - - - -	101

Mechanics of soil slip/debris flow—Continued	
Mobilization, by Stephen D. Ellen and Robert W. Fleming—Continued	
Predicting mobilization	105
Summary	105
Travel	105
Effect of channels	106
Effect of vegetation in the path	106
Deposition	107
Triggering mechanisms within complexes	108
Conclusions	109
References cited	111

#### ABSTRACT

Almost all documented debris flows triggered by the storm of January 3-5, 1982, in the San Francisco Bay region developed from shallow slides (soil slips). These soil slip/debris flows ranged from small events that traveled about 10 m, to soil slip/debris torrents that traveled down major canyons for more than a kilometer. Elements common to these phenomena were their typical occurrence during intense storm rainfall, flow as slurry, generally rapid movement, and sudden impact.

Typical soil slips originated in the soil mantle on steep (26°–40°) hillslopes and left empty scars, 1 to 3 m deep and 5 to 15 m across. Leading downslope from these scars were debris-flow trails marked by flattened or stripped vegetation and by remnants of the flow material, particularly along the trail margins. Soil that mobilized as debris flows ranged from nonplastic sandy soil (SM of the Unified Soil Classification [USC] system) to moderately plastic soil (MH and CL of the USC system) containing as much as 35 percent clay-size (less than 2  $\mu$ m) particles. Most soil slips mobilized completely as debris flows, leaving scars empty of failed material, but some mobilized only partially. Many soil slips and debris flows, especially in areas of brush and woodland, were interrelated as parts of complexes that included numerous scars.

The development of soil slip/debris flows consisted of several phases: movement of water to sites of failure, initial failure by sliding, mobilization of the sliding mass as a flowing slurry, and flow of the slurry. Failure at susceptible sites generally required both concurrent intense rainfall and concentration of water in the landscape. Mobilization occurred by both contractive and dilative means, and these can be predicted by using steady-state soil testing or the ratio of saturated water content to liquid limit. The resulting debris flows were facilitated by channels and affected by vegetation in the path, which influenced their capacity to augment themselves by triggering auxiliary soil slips.

#### INTRODUCTION

The rainstorm of January 3-5, 1982, in the San Francisco Bay region triggered thousands of shallow landslides that flowed rapidly downslope as debris flows (see "Introduction" to this volume for landslide terminology). This storm left abundant evidence of the mechanics of these landslides and provided an incentive to understand them, so that damage can be anticipated and avoided in the future.

This chapter describes these landslides and analyzes the mechanics of their development. Descriptions are based on field observations and limited soil testing during 1982. The analysis uses simple, approximate models intended

to clarify the process, rather than sophisticated models designed for precise prediction.

#### TERMINOLOGY

Use of terms in this chapter generally follows the usage described in the "Introduction" to this volume. Debris flows of the storm typically originated in *soil*, a term used here in the engineering sense of unconsolidated earth material. Soil is called *granular* where it consists dominantly of sand and silt and thus is noncohesive to slightly cohesive. A thin cover of soil, here called *soil mantle*, blankets bedrock in hillside terrain of the region. The soil mantle typically ranges in thickness from about 0.3 to 3 m, thickening toward draws; it includes both residual and transported (colluvial) soil and typically consists of both debris (soil containing a significant proportion of coarse fragments) and earth (soil lacking any significant proportion of coarse fragments). Both earth and debris were significant components of debris flows in the storm. In addition, *organic debris*, such as logs and bushes, was a common component and, in places, constituted much of the transported material.

The debris flows typically originated as *soil slips*, shallow slides in the soil mantle that left empty scars on hillslopes (fig. 6.1). Leading downslope from the scars were trails of soil, organic debris, and stripped or flattened vegetation left by the process of *debris flow* (Johnson, 1970; Varnes, 1978). Scars and trails thus marked the sources from which material slid and the paths along which it flowed down hillslopes or channels as muddy slurries, commonly at high velocities. In this chapter, such complex landslides are designated by combined terms, such as *soil slip/debris flow* (after Campbell, 1975), because such terms distinguish the principal parts of the process by which debris flows develop from slides of the soil mantle. Thus, the term "debris flow" in this chapter designates only the flow part of the complex process. "Debris flow" includes mudflow, debris avalanche, and debris torrent, as discussed in the "Introduction" to this volume, because these processes are considered mechanically similar (Johnson, 1984, p. 257; Pierson and Costa, 1984).

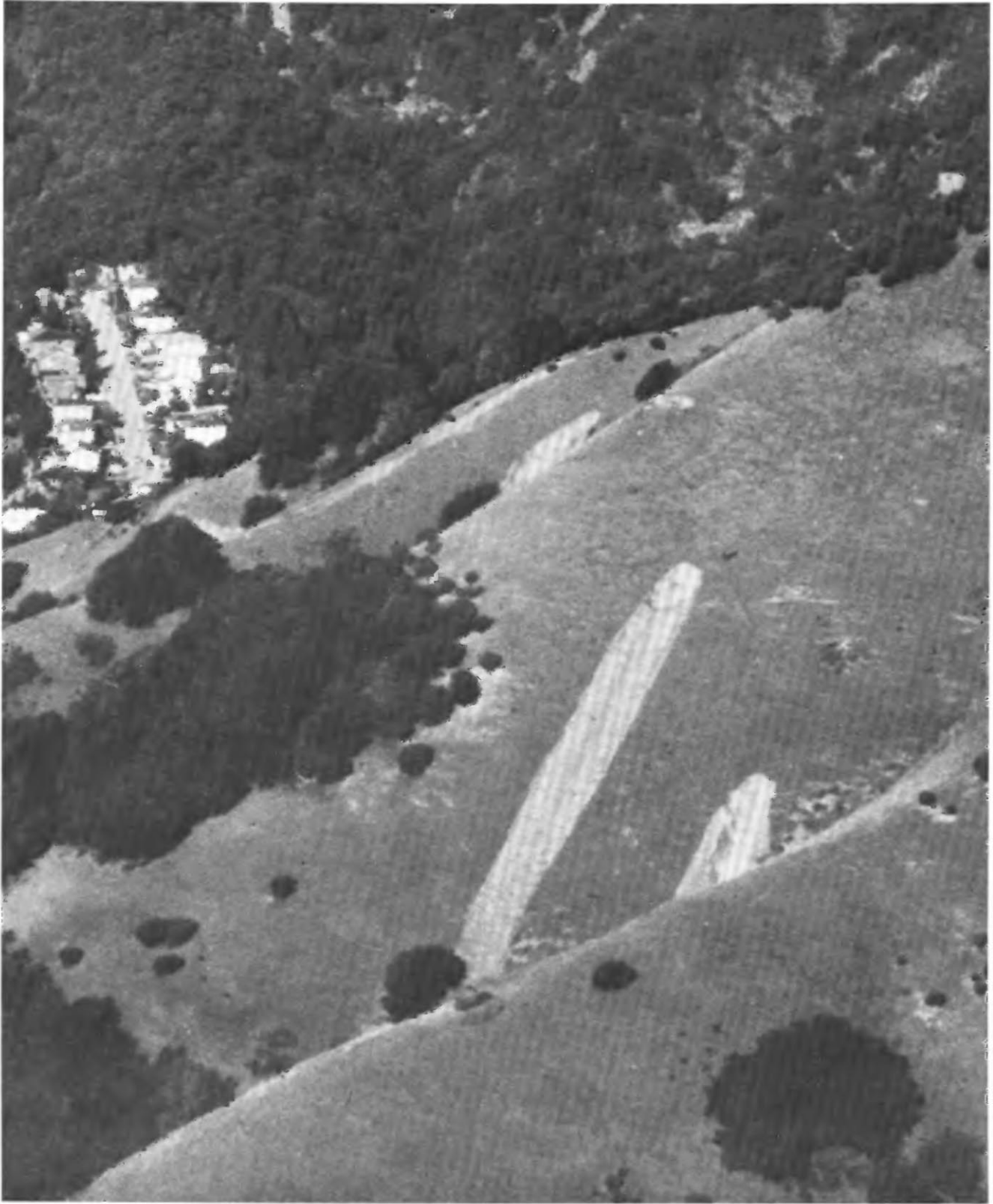


FIGURE 6.1.—Typical scars and trails of soil slip/debris flows on a hillslope near San Rafael, Marin County. Soil-slip scar near center is about 5 m wide.



### ACKNOWLEDGMENTS

During the storm, soil slip/debris flows caught the attention of many observers, almost all laypeople. Careful descriptions provided by eyewitnesses were important to the analysis that follows.

The discussion here is based on the observations and ideas provided by the team of earth scientists who studied features left by the storm. Significant contributions came from personnel of the California Division of Mines and Geology, particularly C.W. Davenport, E.W. Hart, S.J. Rice, and T.C. Smith; from J.E. Baldwin II of Howard-Donley Associates, Inc.; from P.C. Lahr of the California Polytechnic State University, San Luis Obispo; and from C.S. Alger, M.A. Albus, S.H. Cannon, R.W. Fleming, E.L. Harp, D.G. Herd, D.K. Keefer, D.M. Peterson, S.L. Reneau, C.M. Wentworth, G.F. Wiczorek, H.G. Wilshire, and R.C. Wilson of the U.S. Geological Survey. In addition to authoring sections of this chapter, Reneau and Cannon mapped the landslide features shown on plate 4, and Cannon assisted in the case studies not attributed to other authors. H.J. Lee clarified theoretical relations concerning mobilization of debris flows.

### DESCRIPTION OF SOIL SLIP/DEBRIS FLOWS IN THE STORM

Nearly all documented debris flows that resulted from the storm were soil slip/debris flows.<sup>1</sup> Typical configurations of soil-slip scars and debris-flow trails are shown on plates 4 and 6 and in figure 6.1. Some trails extended only several meters downslope, some down sidehill channels to gentle ground, and some down major canyons for considerable distances. Figure 6.2 shows the range in scale of these phenomena.

### CASE STUDIES

The variety of soil slip/debris flows is illustrated by case studies of five events in Marin County. These studies show the range in scale and complexity of the phenomena, document their impact on society, and describe other noteworthy aspects of their behavior. Locations of the case studies are shown by number on plate 5; detailed maps and profiles of most of the case studies are shown on plate 4. Additional case studies are reported in chapters 8 and 9.

<sup>1</sup>The sole documented exception resulted from failure of a road embankment crossing Fall Creek in San Mateo County (see chap. 8). A plugged culvert at the base of the embankment ponded water, which led to the failure and resulting debris flow.

### THREE PEAKS (CASE STUDY 1, PLS. 5, 6)

By STEPHEN D. ELLEN and DAVID M. PETERSON

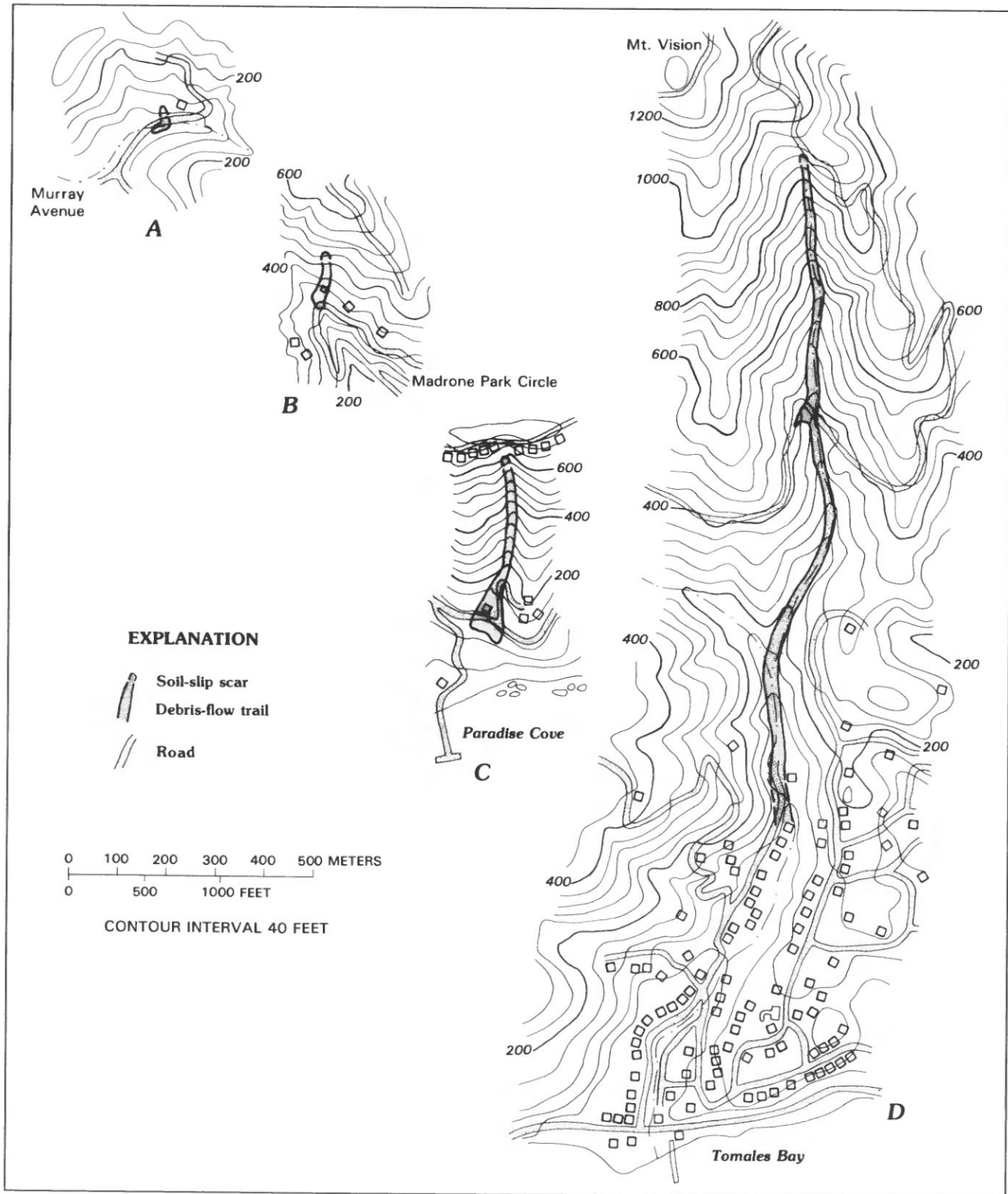
At about noon on January 4, a soil slip/debris flow near Three Peaks moved approximately 120 m down a steep brush-covered hillslope and across a dirt road, then turned sharply (approx 90°) and traveled about 300 m farther down a canyon of gentle gradient. The soil-slip scar developed in granular soil mantle overlying sandstone of the Franciscan assemblage.

The movement of the debris flow from its inception near the top of the steep hillslope to its sharp turn at the foot was witnessed by Dan Adams (oral commun., 1982), whose view of the event was similar to that shown in figure 6.3. He heard a roar (above the sound of the motorcycle he was riding) and saw a single pulse of soil and organic debris, including abundant pieces of brush, move at about 40 km/h down the hillslope and across the road. No soil-slip scars or debris-flow trails were evident on the hillslope before the pulse, and nothing followed except a trickle of water. The debris flow left no mud on the road. Adams estimated the height of the front to be about 3 m when it reached the road; he estimated the length of the slug of flowing material to be about one-fourth the combined length of the scar and trail above the road. The front showed a rolling or tumbling motion as material high in the front advanced faster than material near the ground surface. The front was higher than the rest of the flow and appeared to impede the progress of the flow somewhat. He likened the rest of the flow to a rushing creek.

The major soil-slip scar (near top, fig. 6.3) bottoms at a depth of about 1 m in a light-colored lower layer of the soil mantle. A large auxiliary scar, which extends from this major scar down the right half of the flow trail (as viewed), bottoms within a dark upper layer of the soil mantle at a depth of about 0.5 m. Comparison of these scar depths to the 3-m thickness observed at the front of the flow indicates that the flow thickened considerably in its course down to the road. In contrast, a cross section of the debris-flow trail well down canyon (beyond view in fig. 6.3) measured only one-fifth the estimated cross section at the road, a relation indicating that the flow had strung out in its passage down the gently sloping canyon.

The principal significance of this event is that all the scars (major scar, large auxiliary scar, and scars from uprooted trees) were observed to form during a single pulse of short duration. Thus, the soil slips within the trail apparently were triggered instantaneously by passage of the debris flow from the major scar.

Adams also witnessed another debris flow advancing at about walking speed down a gently sloping channel near the site described above.



## MURRAY PARK (CASE STUDY 2, PL. 5)

On the afternoon of January 4, a soil slip/debris flow originating only several meters away broke through a 25-cm-thick reinforced-concrete wall that formed both the rear foundation of a small house and the rear wall of its basement garage (fig. 6.4; Leary, 1982; S.J. Rice, oral commun., 1982). Most of the house, which was unoccupied at the time, was pushed about 10 m to a position across Murray Avenue (pl. 4; fig. 6.2). The house was subsequently moved by another debris flow traveling down the valley parallel to Murray Avenue.

This soil slip/debris flow is noteworthy because it exhibited considerable power, yet had almost no space for acceleration before impact. At house level, a walkway about 1 m wide had separated the steep cut slope from the rear wall of the house; below floor level, the concrete wall of the basement garage had been flush against the hill. The sliding or flowing mass thus had 1 m or less of free space to accelerate before reaching the house and breaking the wall. This behavior suggests that at least

some soil slip/debris flows lost strength abruptly at the very start of downslope travel.

The soil-slip scar developed on a wooded 31° hillslope that lacked detectable channels. The base of this hillslope had been steepened to make room for the house. The soil slip involved granular colluvium and an underlying highly permeable rubble, in turn overlying sandstone of the Franciscan assemblage. There is evidence of piping near this permeable rubble at the head of the scar. The position of the landslide on what appears to be a uniform hillslope may have resulted from colluvial fill in a bedrock depression without surface expression (Dietrich and Dunne, 1978), or from the presence of the house, either through damming of ground water by the concrete wall (which appears to truncate the permeable rubble zone) or through decreased stability caused by the cut slope.

## HOMESTEAD VALLEY (CASE STUDY 3, PL. 5)

At about 9:15 p.m. P.s.t. January 4, a soil slip/debris flow originated approximately 60 m upslope from a house



FIGURE 6.3.—Scars and upper part of trail of soil slip/debris flow near Three Peaks; rest of trail extends a short distance downslope below road, then turns abruptly to right down a canyon. Major light-colored soil-slip scar extends from crown downward to break in slope (upper third of view). Trail within view consists of two parts. On right side

of photograph, a shallow (0.5 m) scar extends from major scar to road and from edge of trail to about midway across trail; muddy deposit coats brush along lower edge of trail. On left side, most vegetation has been stripped, trees have been plucked (leaving small scars, such as at left center), and a small tree at edge of trail has been bent over.

on Madrone Park Circle in Homestead Valley (pl. 4; fig. 6.2; Kearney, 1982; S.J. Rice, oral commun., 1982). The house, occupied since 1962, was built on stilts and was served by a small tramway because of the steep ( $37^\circ$ ) slope. The debris flow moved toward the house down a shallow draw in the wooded hillslope, incorporating vegetation and soil and leaving mud plastered as high as 2 m on trees within the path (fig. 6.5). "A waterfall of mud," as the occupants described it, struck the house and sent it tumbling or flying down the hillslope (fig. 6.6). Pieces of the house sheared the top from a power pole and broke overhanging limbs of trees (fig. 6.6). The house came to rest in the canyon bottom at the base of the hillslope, about 45 m from its foundation. Two women were trapped in the wreckage until rescued; both sustained nonfatal injuries. The shattered house, along with other material carried by the debris flow, dammed the canyon bottom and thus blocked further progress of the debris flow, which might otherwise have damaged at least several other houses immediately downcanyon.

The soil slip/debris flow originated on a  $30^\circ$  slope and traveled down slopes of  $25^\circ$  to greater than  $35^\circ$ , incorporating much material from its path. The soil-slip scar is in granular colluvium that overlies sandstone of the

Franciscan assemblage; soil-test data are listed in table 6.1. Vegetated subdued soil-slip scars are present near the head of the subtle draw that channeled the debris flow to the housesite. This event is described in more detail by Reneau and Dietrich (1987b).

#### TIBURON RIDGE (CASE STUDY 4, PL. 5)

At about 2:00 p.m. P.s.t. January 4, a soil slip/debris flow developed on a  $36^\circ$  slope at the head of a canyon on the forested east side of Tiburon Ridge above Paradise Cove (pl. 4; fig. 6.2; S.J. Rice, oral commun., 1982; Smith and Hart, 1982, p. 146). The material traveled 300 m down the steep canyon, incorporating trees, forest-floor vegetation, and soil from much of its path. The debris flow leaped from a small waterfall (approx 1.5 m high) in the canyon bottom, leaving delicate ferns on the vertical face undisturbed. Trees along the debris-flow path show mud-splash marks as high as 4 m above the margin of the path, which lies approximately 6 m above the present canyon bottom.

Following closely behind a pulse of muddy water, the debris flow emerged from the canyon mouth. A young man who narrowly escaped the flow estimated its veloc-



FIGURE 6.4.—Soil-slip scar behind site of destroyed house in Murray Park. Broken concrete wall of basement garage is at left center.



ity at 80 km/h, but this estimate is probably exaggerated. The debris flow struck a house in its path, moved it 20 m from its foundation, and killed its owner. The debris flow then continued across Paradise Drive and through the parking lot of Paradise Cove County Park. Most of the material appears to have stopped while descending a 26° slope in the park, but some, possibly waterborne, reached the San Francisco Bay.

Almost all the material involved was granular soil overlying metasandstone of the Franciscan assemblage; soil-test data are listed in table 6.1. Subdued soil-slip scars from previous events are present near the head of the canyon, and probable deposits from previous debris flows are present near the mouth of the canyon (pl. 4).

The path of the debris flow includes several discrete scars, in addition to large areas where soil was removed from the canyon bottom (pl. 4). Relations between these scars and lateral deposits suggest that the major scars

developed in a sequence that progressed downcanyon. The time interval between these failures is unknown; they may all have contributed to a single event triggered by the major flow, as at Three Peaks, or they could have produced a sequence of discrete debris-flow events. The apparent downcanyon progression suggests that most scars contributed to a single major event (see subsection below entitled "Triggering Mechanisms Within Complexes").

The pulse of muddy water that immediately preceded the debris flow may have resulted from a discrete failure early in the sequence of events, but more likely it was a wave of water pushed ahead of the debris flow. A similar pulse of water apparently occurred at Slide Mountain, Nev., immediately before the debris flow or hyperconcentrated flood of May 30, 1983 (P.A. Glancy, oral commun., 1983).

#### INVERNESS AREA (CASE STUDY 5, PL. 5)

By STEVEN L. RENEAU

Much of the storm damage in the steep and heavily forested area near Inverness resulted from brief high-energy surges of logs and sediment, or debris torrents, that traveled down many of the main canyons on January 4 (fig. 6.7). Debris torrents are a type of debris flow, probably grading to hyperconcentrated streamflow, that consists of slurries and near-slurries of soil and coarse organic debris that can travel as far as several kilometers down canyons, commonly entraining much additional material from the streambed and streambanks (Swanston and Swanson, 1976; Swanson and Lienkaemper, 1978). A debris torrent that emerged from the narrow canyon above Dream Farm was described by a witness as a wall of logs as high as a building, dropping in height rapidly as the valley floor widened, and passing by within seconds. Another debris torrent destroyed two houses at Redwood Avenue and knocked a third off its pilings, carrying it 30 m to the edge of Tomales Bay. Buildings were also destroyed by debris torrents at Dream Farm and in First and Second Valleys.

All the canyons known to have been affected by debris torrents retained distinctive features absent in the other canyons; these features are illustrated on the detailed map of First Valley (pl. 4). The most conspicuous feature is erosion of the soil mantle and removal of nearly all the vegetation from a swath commonly 15 to 20 m wide (fig. 6.8); small scarps in the soil are abundant, and bedrock is commonly exposed. The few trees that remain are plastered with mud to a height of 1 to 2 m on the upstream side. In many places, the canyon bottoms are freshly scoured to bedrock; at one locality above Redwood Avenue, an estimated 6 m of material was eroded.

These canyons are also marked by persistent, commonly narrow belts outside of the heavily eroded swaths, in which the vegetation has been flattened, oriented down-



FIGURE 6.5.—View down debris-flow trail in Homestead Valley toward destroyed house (center). Note debris plastered 2 m high against tree at right (top of debris indicated by arrow) and loose branch hanging from tree at center.



canyon. The forest litter has been removed here, or the vegetation has been plastered with mud. Piles of organic debris and muddy deposits are present locally.

Debris torrents have several possible origins. In the Pacific Northwest, landslides from adjacent hillslopes dominate as a triggering mechanism, although some originate by mobilization of organic debris in channels (Swanson and Lienkaemper, 1978). Failure of temporary landslide dams is another possible mechanism. On Inverness Ridge, all the debris-torrent paths observed in this study originated from shallow landslide scars, commonly in the headwater regions of drainage basins, and so these debris torrents could be called soil slip/debris torrents. Beginning as soil slip/debris flows, the slurries were apparently diluted by floodwater, and their organic-debris content was increased manyfold by stripping of vegetation during travel of a kilometer or more down the canyons.

Few debris torrents reached the base of Inverness Ridge and Tomales Bay. The debris torrent at Redwood Avenue continued across Sir Francis Drake Boulevard and into the bay because the canyon remains narrow to the base of the ridge. At Dream Farm, a pulse continued across the highway as a wave 0.3 m high, but most of the

logs were left against thick groves of alders upstream from the highway. In First, Second, and Third Valleys, stripping of vegetation and erosion of the soil mantle decreased well upstream from the bay, where the valley floors widen and the stream gradients drop. Many of the fresh logjams that remained in the canyons after the storm are terminal deposits of debris torrents that stopped either where the logs themselves blocked the channel or where the logs were held behind groves of trees.

Most of the debris torrents occurred within a brief timespan (fig. 6.7), according to the times provided by eyewitnesses (J. Bauer, E. Clerico, M. Coronado, D. Engler, T. Haney, G. Kohler, K. Kohler, T. Moses, and B. O'Neil, oral commun., 1982). The general concurrence in timing suggests that the debris torrents were triggered by a period of exceptionally intense rainfall. One resident of Second Valley reported that the surge there occurred 10 to 15 minutes after an exceptionally heavy 15-minute downpour. A rain gage at the Nicasio Dam, 9 km to the east, recorded the most intense rainfall between 11:00 a.m. and noon; this record provides supporting evidence that the debris torrents accompanied a period of unusually intense rainfall.



FIGURE 6.6.—Remains of Homestead Valley house resting in canyon bottom, about 45 m from its foundation (at right). Debris-flow trail in foreground. Note impact marks on tree trunk and branches (arrows).

TABLE 6.1.—Engineering test data on soils related to soil slip/debris flows of the storm

[Soils that flowed are noted in descriptions. All percentages by weight. C, cohesion;  $\phi$ , angle of internal friction; LL, liquid limit; PI, plasticity index; USC, Unified Soil Classification system. Sources of data: DK, D.K. Keefer and R.W. Jibson; EH, E.L. Harp; GW, G.F. Wieczorek; JB, J.E. Baldwin II of Howard-Donley and Associates; PL, Lahr (1982); RF, R.W. Fleming and M.A. Albus; SE, S.D. Ellen; SR, S.L. Reneau and Alan Kropp and Associates. Do., ditto]

Location	Sample	Source	Description	Bedrock unit	Grain size (percent)					Strength		Dry density (g/cm <sup>3</sup> )	Saturated water content (percent)	Natural water content (percent)	Atterberg limits (percent water)		USC designation
					Gravel	Sand	Silt	Clay (<2µm)	Silt and clay	C (kPa)	φ (°)				LL	PI	
Alameda County																	
Davilla Hill earth-flow complex, Eden Canyon.	DK-DHS 82 flow	DK	Deposit of debris flow from margin of active earth-flow complex.	Orinda Formation-----	5	9	61	25	--	--	--	--	--	--	--	--	--
Do-----	DK-DHS 82 scarp	DK	Soil from soil-slip scar of same debris flow, flowed.	do-----	2	14	57	27	--	--	--	--	--	--	--	--	--
Marin County																	
Homestead Valley (case study, this chap.).	SR-1	SR	Dark top layer of soil in soil-slip scar of Homestead Valley debris flow, from 0.5-m depth, flowed.	Franciscan sandstone.	2	44	--	--	54	--	--	1.30	40	--	24	4	CL-ML or OL
Do-----	SR-2	SR	Lower layer of soil in soil-slip scar of same debris flow, from 1.1-m depth, flowed.	do-----	2	48	--	--	50	--	--	1.75	20	--	20	2	ML
Tiburon Ridge (case study, this chap.).	DK-292	DK	Deposit of debris flow upslope from destroyed house.	Franciscan meta-sandstone.	2	40	49	9	--	--	--	--	--	--	--	--	--
Do-----	DK-293	DK	do-----	do-----	7	40	45	8	--	--	--	--	--	--	--	--	--
Do-----	DK-294	DK	do-----	do-----	5	39	38	18	--	--	--	--	--	--	--	--	--
Do-----	DK-295	DK	do-----	do-----	9	42	39	10	--	--	--	--	--	--	--	--	SM or SC
Reed (case study, this chap.).	1DS	PL	Dark topsoil in soil-slip scar of debris flow 1, from 0.6-m depth, flowed.	do-----	4	42	42	12	--	--	--	--	--	--	27	2	ML or OL
Do-----	1LS	PL	Tan subsoil in soil-slip scar of debris flow 1, from 1.2-m depth, flowed.	do-----	17	43	30	10	--	--	--	1.57	26	--	21	--	SM
Do-----	1LD	PL	Tan soil in deposit of debris flow 1.	do-----	17	43	30	10	--	--	--	1.72	21	--	--	--	SM
Do-----	2DS	PL	Dark topsoil in soil-slip scar of debris flow 2, from 0.6-m depth, flowed.	do-----	2	36	45	17	--	--	--	1.22	45	--	27	6	CL-ML or OL
Do-----	2DD	PL	Dark soil in deposit of debris flow 2.	do-----	2	36	45	17	--	--	--	1.61	25	--	--	--	CL-ML or OL
Do-----	2LS	PL	Tan subsoil in soil-slip scar of debris flow 2, from 1.8-m depth, flowed.	do-----	3	47	35	15	--	--	--	1.70	22	--	18	1	SM
Do-----	2LD	PL	Tan soil in deposit of debris flow 2.	do-----	3	47	35	15	--	--	--	1.69	22	--	--	--	SM

Do-----	3DS	PL	Dark topsoil in soil-slip scar of debris flow 3, from 0.6-m depth, flowed.	do-----	24	31	33	12	--	--	--	1.47	31	--	26	1	SM
Do-----	3DD	PL	Dark soil in deposit of debris flow 3.	do-----	24	31	33	12	--	--	--	1.41	34	--	--	--	SM
Do-----	3LS	PL	Tan subsoil in soil-slip scar of debris flow 3, from 1.0-m depth, flowed.	do-----	20	24	48	8	--	--	--	2.00	13	--	24	2	ML
Do-----	3LD	PL	Tan soil in deposit of debris flow 3.	do-----	20	24	48	8	--	--	--	1.63	24	--	--	--	ML
Do-----	4DS	PL	Dark topsoil in soil-slip scar of debris flow 4, from 0.5-m depth, flowed.	do-----	4	44	41	11	--	--	--	1.52	28	--	25	3	ML or OL
Do-----	5	PL	Clayey soil in earth slide (landslide 5); small parts flowed slowly.	Franciscan sheared rock.	2	22	50	26	--	--	--	--	--	--	44	21	CL
Do-----	SQ-15A	SE	Dark surficial soil in soil-slip scar of landslide 6, flowed.	Franciscan sandstone or meta-sandstone within melange.	0	35	51	14	--	--	--	--	--	--	--	--	--
Do-----	SQ-15B	SE	Brown subsoil from base of soil-slip scar in landslide 6, did not flow.	do-----	1	33	47	19	--	--	--	--	--	--	20	5	CL-ML
Immediately NE. of Reed case study (this chap.).	SQ-9	SE	Deposit from debris flow down 33° cut slope.	Franciscan sheared rock.	7	23	35	35	--	--	--	--	--	--	--	--	--
Salmon Creek (case study, this chap.).	SP-1,4	RF	Dark top layer of soil in scar of Salmon Creek landslide, from ground surface to 0.6-m depth, flowed.	Franciscan sandstone.	0	52	32	16	--	--	--	1.40	34	--	20	3	SM or SC
Do-----	SP-2,5	RF	Brown subsoil in scar of Salmon Creek landslide, from 0.6- to 0.9-m depth, flowed.	do-----	0	57	29	14	--	--	--	1.87	16	--	--	--	SM or SC
Do-----	SP-3,6	RF	Tan lower layer of soil in scar of Salmon Creek landslide, from 0.9- to 2.5-m depth, flowed.	do-----	0	56	32	12	--	132	132	1.77	19	--	23	4	SM-SC
Along Salmon Creek, E. of case study (this chap.).	WLS-1	RF	Dark top layer of soil from soil-slip scar in forest, flowed.	do-----	--	--	--	--	--	--	--	1.24	43	--	--	--	--
Do-----	WLS-2	RF	do-----	do-----	--	--	--	--	--	--	--	1.03	60	--	--	--	--
Shell Beach, Tomales Bay State Park.	DK-Shell Beach 1A	DK	Soil at base of soil-slip scar above debris-flow complex, flowed.	Granitic rock or overlying terrace deposits.	2	60	25	13	--	--	--	--	--	--	--	--	SM or SC
Hicks Valley Road, 600 m E. of dam.	SG-9A	SE	Dark surficial soil, flowed from nose of active earth slide.	Franciscan meta-greenstone.	35	41	14	10	--	--	--	--	--	--	--	--	SM or SC
Do-----	SG-9B	SE	Orange-red subsoil, flowed from nose of same active earth slide.	do-----	43	41	7	9	--	--	--	--	--	--	--	--	GM or GC
Near Hicks Mountain, S. of Cheese Factory.	P-16A	SE	Dark surficial soil in soil-slip scar, flowed.	Franciscan sandstone.	0	48	36	16	--	--	--	--	--	--	28	--	--

TABLE 6.1.—Engineering test data on soils related to soil slip/debris flows of the storm—Continued

Location	Sample	Source	Description	Bedrock unit	Grain size (percent)					Strength		Dry density (g/cm <sup>3</sup> )	Saturated water content (percent)	Natural water content (percent)	Atterberg limits (percent water)		USC designation
					Gravel	Sand	Silt	Clay ( $<2\mu\text{m}$ )	Silt and clay	C (kPa)	$\phi$ ( $^{\circ}$ )				LL	PI	
Marin County--Continued																	
Do-----	P-16B	SE	Red-brown subsoil in same scar, did not flow.	do-----	2	52	29	17	--	--	--	--	--	--	--	--	SM or SC
Barnabe Mountain.	B-86A	SE	Brown surficial soil, flowed from slump/earth flow that mobilized downslope as slow-moving debris flow.	Franciscan greenstone.	5	14	56	25	--	--	--	--	--	--	45	20	CL
Do-----	B-86B	SE	Red subsoil, flowed as slow-moving debris flow, from about 1.3-m depth in scar of same slump/earth flow.	do-----	17	23	<sup>2</sup> 35	<sup>2</sup> 25	--	--	--	--	--	--	--	--	--
Do-----	B-86C	SE	Slow-moving debris-flow deposit from same landslide, plastered on tree.	do-----	11	18	<sup>2</sup> 41	<sup>2</sup> 30	--	--	--	--	--	--	42	10	ML
Do-----	B-88	SE	Dark surficial soil from soil-slip scar, flowed.	do-----	15	10	42	33	--	--	--	--	--	--	45	13	ML
San Mateo County																	
La Honda test area (see chap. 5).	S-1	GW	Deposit of debris flow 6----	Tahana Member of the Purisima Formation.	--	<sup>3</sup> 5	64	31	--	--	--	--	--	--	58	26	MH
Do-----	S-3	GW	Soil in soil-slip scar of debris flow 6.	do-----	--	<sup>3</sup> 7	62	31	--	--	--	--	--	--	--	--	--
Do-----	S-4	GW	Deposit of debris flow 7----	do-----	--	<sup>3</sup> 5	67	28	--	--	--	--	--	--	51	19	MH
Do-----	S-6	GW	Soil in soil-slip scar of debris flow 7.	do-----	--	<sup>3</sup> 7	65	28	--	--	--	--	--	--	--	--	--
Do-----	S-7	GW	Deposit of debris flow 8----	do-----	--	<sup>3</sup> 7	63	30	--	--	--	--	--	--	58	28	CH-MH
Do-----	S-8	GW	Soil in soil-slip scar of debris flow 8.	do-----	--	<sup>3</sup> 8	60	32	--	--	--	--	--	--	--	--	--
Do-----	df9-flow	GW	Deposit of debris flow 9----	do-----	--	<sup>3</sup> 6	72	22	--	--	--	--	--	52	57	25	MH
Do-----	df9-scar	GW	Soil in soil-slip scar of debris flow 9.	do-----	--	<sup>3</sup> 3	63	34	--	--	--	--	--	46	--	--	--
Do-----	df10-flow	GW	Deposit of debris flow 10---	Lambert Shale and San Lorenzo Formation, undivided.	--	<sup>3</sup> 11	56	33	--	--	--	--	--	58	60-69	21-30	MH
Do-----	df10-scar	GW	Soil in soil-slip scar of debris flow 10.	do-----	--	<sup>3</sup> 17	59	24	--	--	--	--	--	--	--	--	--
Pacifica (see chap. 9).	EE-2	JB	Soil from soil-slip scar of debris flow at Big Bend site, from 0.9-m depth.	Franciscan greenstone.	10	41	--	--	49	<sup>4</sup> 9.7	<sup>4</sup> 28	1.76	19	20	42	20	SC
Do-----	FF-1	JB	Soil from soil-slip scar of debris flow at Woodlawn site, from 3.1-m depth.	do-----	7	53	--	--	40	<sup>4</sup> 12.0	<sup>4</sup> 37	1.63	24	19	35	16	SC



Do-----	JJ-2	JB	Soil from soil-slip scar of debris flow at Yosemite site, from 0.9-m depth.	Franciscan greenstone and sandstone(?).	1	58	--	--	41	<sup>4</sup> 3.4	<sup>4</sup> 47	1.54	28	27	33	14	SC
Do-----	JJ-3	JB	Soil from soil-slip scar of debris flow at Yosemite site, from 1.5-m depth.	do-----	2	55	25	18	--	<sup>4</sup> 12.5	<sup>4</sup> 36	1.94	14	10	18	3	SM
Do-----	AA-1	JB	Deposit of debris flow at Oddstad site, from 1.2-m depth.	Franciscan sandstone.	--	--	--	--	--	<sup>4</sup> 9.6	<sup>4</sup> 37	1.62	24	24	--	--	--
Do-----	AA-2A	JB	Slip surface of soil slip at Oddstad site, from 4.6-m depth.	do-----	3	57	25	15	--	<sup>4</sup> 23.9	<sup>4</sup> 39	1.65	23	22	36	16	SC
Do-----	AA-5A	JB	Soil in soil-slip scar of debris flow at Oddstad site, from 2.4-m depth.	do-----	4	39	29	28	--	<sup>4</sup> 18.2	<sup>4</sup> 26	1.57	26	24	30	5	ML
Do-----	AA-9	JB	Soil in soil-slip scar of debris flow at Oddstad site, from 1.2-m depth.	do-----	0	42	--	--	58	--	--	--	--	--	39	20	CL
Oddstad Boulevard, Pacifica (case study, chap. 9).	Oddstad	EH	Deposit of debris flow-----	Franciscan sandstone, probably with greenstone or limestone.	8	25	42	25	--	--	--	--	--	--	--	--	--
Valdez Way, Pacifica (see chap. 9).	Valdez	EH	do-----	Unnamed sandstone, shale, and conglomerate of Paleocene age near Point San Pedro.	0	18	66	16	--	--	--	--	--	--	--	--	--
Thornton Beach State Park, near Daly City.	DK-Tb1	DK	Very slightly cemented, well-sorted, well-rounded sand forming sea cliff, flowed.	Merced Formation-----	1	93	3	3	--	--	--	--	--	--	--	--	SP-SM or SP-SC
Butano Road, near Gazos Creek.	DK-131	DK	Surficial dark-gray soil in debris-flow deposit, flowed.	Purisima Formation.	0	16	60	24	--	--	--	--	--	--	--	--	--
Do-----	DK-132	DK	Light-gray subsoil in same debris-flow deposit, generally did not flow.	do-----	0	13	55	32	--	--	--	--	--	--	--	--	--
Elkus 4-H Ranch, Purisima Canyon (case study, chap. 8).	DK-4H colluvium	DK	Deposit of slow-moving, plastic debris flow.	do-----	2	46	38	14	--	--	--	--	--	--	--	--	--
Do-----	4H1	EH	Deposit near toe of same slow-moving, plastic debris flow.	do-----	0	14	72	14	--	--	--	--	--	--	--	--	--
Do-----	4H2	EH	do-----	do-----	0	5	76	19	--	--	--	--	--	--	--	--	--
Do-----	4H3	EH	do-----	do-----	32	38	22	8	--	--	--	--	--	--	--	--	SM or SC
Santa Cruz County																	
Old San Jose Road, near Sugarloaf Mountain.	S-1	EH	Deposit of debris flow-----	Purisima Formation and Butano Sandstone.	0	83	--	--	17	--	--	--	--	--	--	--	SM or SC
Hubbard Gulch-----	HUB	EH	do-----	Monterey Formation.	5	25	46	24	--	--	--	--	--	--	--	--	--
Mount Cross Camp.	Mount Cross	EH	do-----	do-----	4	34	43	19	--	--	--	--	--	--	--	--	--

<sup>1</sup>Best estimate of peak strength from several drained triaxial tests.<sup>2</sup>Estimated.<sup>3</sup>Sand plus gravel.<sup>4</sup>Determined by direct shear.



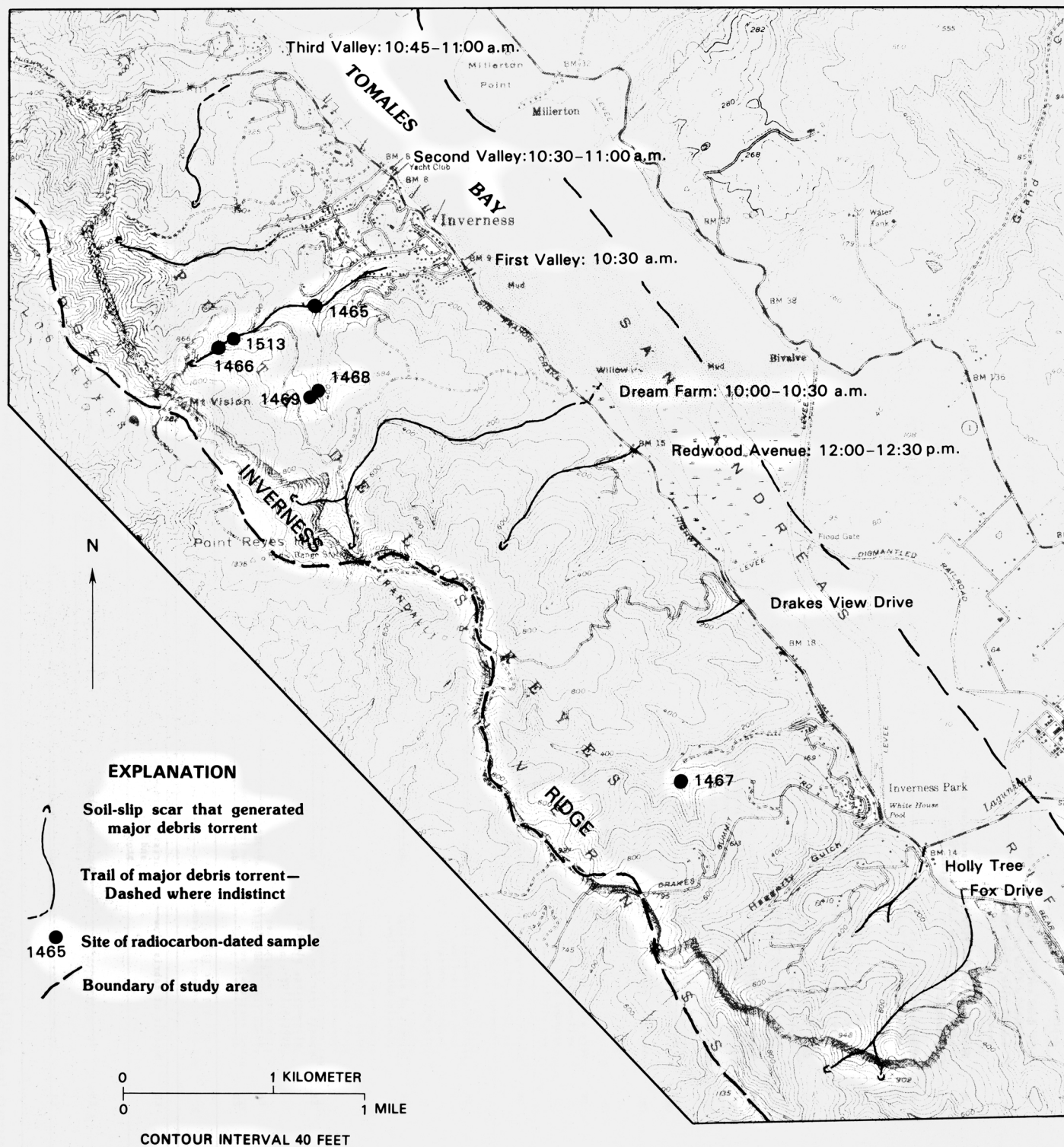


FIGURE 6.7.—Index map of Inverness, Calif., area, showing locations of soil slip/debris torrents and other major soil slip/debris flows located in the field, times of debris torrents during morning and early afternoon of January 4, and locations of radiocarbon-dated samples (see subsection entitled "Radiocarbon Sites near Inverness" in chap. 7).

Upper parts of many canyons were not checked in the field, and mapping is probably incomplete. Base from U.S. Geological Survey, scale 1:24,000, Drakes Bay, 1953 (photorevised 1971), and Inverness, 1954 (photorevised 1971).

## FIRST VALLEY

The soil slip/debris torrent in the north fork of First Valley was chosen for more detailed study. The general topographic setting is shown in figures 6.2 and 6.7, and a detailed map and longitudinal profile of the debris-torrent path are shown in plate 4. The principal soil-slip scar is at about 300-m elevation, near the top of the drainage basin, in a thick Bishop-pine forest (fig. 6.9). From there, the debris flow/debris torrent traveled about 1.3 km, dropping more than 280 m, before it reached the uppermost houses in the canyon. Shortly above the confluence with the southern branch of First Valley, 0.2 km upstream from houses, the valley floor widens, and the stream gradient drops from 6° to 4°. Here, the energy of the flow decreased, and trees were effective in deflecting the force of the debris torrent away from most buildings (fig. 6.10). Where a dirt road crosses the canyon 0.56 km downstream from the head scar, the flow ran up the road for 65 m and left a large deposit of sediment and organic debris; with this exception, no significant subaerial deposits were produced by this flow.

Scarps in the soil mantle are common along the path. In many places, these scarps are small and arcuate, apparently owing to the uprooting of trees; in places, the scarps are accompanied by partially toppled trees or by large broken roots. In other places, the scarps mark the boundary of areas where thin soils were completely eroded to bedrock (fig. 6.11). Upstream from a 10-m-high waterfall, gullies as deep as 3.5 m are incised into colluvium in the path. Collectively, these erosional features represent a substantial increase in the volume of sediment carried by the flow. On the basis of scarp-height measurements and the detailed planform map (pl. 4), the total volume of eroded soil is estimated to be about 5,000 m<sup>3</sup>, an order of magnitude greater than the 300 m<sup>3</sup> soil-slip scar at the head.

Along the lower reaches of the path, short soil-slip scarps on adjacent slopes are common; no consistency in timing in relation to the debris torrent could be found. A debris flow from one of these soil slips crossed the main debris-torrent path and ran directly up the opposite slope, rising 10 m in elevation. The maximum velocity of this flow can



FIGURE 6.8.—Path of debris torrent upstream from Redwood Avenue in Inverness. Path is smooth surface stripped of vegetation; flow traveled from right to left. Note scarp in left foreground truncating soil mantle. Deep gully has been cut by a small tributary. View southward. Photograph by D.G. Herd.

be calculated from a conservation of momentum equation,

$$u = (2gh)^{1/2},$$

where  $u$  is the velocity,  $h$  is the rise in elevation, and  $g$  is the acceleration due to gravity. This equation is derived by relating the kinetic energy of the flow to its potential energy, and provides a maximum velocity of 14 m/s for the flow.

Details of the soil-slip scar at the head of the path (fig. 6.9) are of particular interest. The scar is 2.0 to 2.5 m deep, 11 m wide, and 20 m long. The failure plane is within colluvial soil derived from granitic bedrock, near the boundary between an upper red soil horizon and a lower yellow gravel-rich colluvium. Water was observed flowing from coarse gravel at the southeast base of the scarp. The headwall scarp encroaches 0.5 m into the surface of a dirt road at a point where a culvert collecting runoff from the road drained onto a broad swale. The roadcut here shows that the swale is underlain by a thick colluvial deposit in a bedrock depression (Dietrich and Dunne, 1978).

Immediately below the headscarp, three distinct deposits from the storm were identified, all from soil slips that mobilized as debris flows (pl. 4). The outermost deposit (A) is red and matches the upper soil horizon; a younger deposit (B) is orange and includes abundant roadfill; the youngest deposit (C) is yellow and is probably composed entirely of roadfill. Deposit C apparently was less fluid than the others and stayed within the center of the path; it probably resulted from failure of the west edge of the headscarp.

Key relations are displayed between deposits A and B. At one place near the edge of the path, a tree was clearly toppled by the debris flow represented by deposit A; farther downcanyon, a scarp near the path's edge is plastered by deposit B. This and other evidence indicate that the debris flow that cleared the path of trees, created the scarps, and generated the log surge is represented by deposit A; this event involved primarily the natural soil and not the roadfill. A second debris flow, represented by deposit B, did involve roadfill but was not responsible



FIGURE 6.9.—Soil-slip scar and head of debris-flow trail in thick Bishop-pine forest, north fork of First Valley, Inverness Ridge. Scar, which is as much as 2.5 m deep, occupies most of lower half of view; dirt road into which scar encroached is in immediate foreground, and debris-flow trail lies in upper half of view. Scar occupies axis of a subtle colluvium-filled swale. View downslope. Photograph by C.M. Wentworth.



for the log surge. Thus, the primary slope failure probably resulted not from the presence of the roadfill but from the concentration of water provided by the culvert.

### SINGLE SOIL SLIP/DEBRIS FLOWS

Typical features of single soil slip/debris flows are shown in figure 6.12. Most of the material that flowed, corresponding to most of the volume missing from the scar, typically traveled far from the scar and ended up as deposits along the debris-flow trail or as fan deposits, stream deposits, or deposits on the floors of bays or the ocean.

The typical configuration of scar and trail (fig. 6.12) gives a sense of the behavior of the typical soil slip as it moved from the scar. The lateral deposits, which consisted largely of remolded soil that had behaved as a slurry, typically led from the scar near its widest point, where it initially narrows downslope (figs. 6.1, 6.13). This relation indicates that at least some material (that remaining as lateral deposits) was fluid as it left the scar, but

that during initial movement the mass had enough strength to force its widest parts up onto the ground surface, rather than contracting laterally to flow from the narrower lip of the scar.

Debris-flow trails commonly led down swales or channels and typically were elevated on the outside of bends in the channels, a relation suggesting considerable velocity (figs. 6.11, 6.14). Trails differed, depending on the vegetative cover. Grass-covered hillslopes typically displayed trails of flattened grass, with varyingly abundant patches of deposit, between continuous or discontinuous lateral deposits, or levees, of remolded soil and clumps of sod (figs. 6.13, 6.15). The flattened blades of grass pointed downslope parallel to the trail, recording the direction of movement. Debris-flow trails on wooded and brush-covered hillslopes, as in the preceding case studies, typically were cleared of forest duff and were partly bounded by lateral deposits (fig. 6.8); bushes and clumps of ferns in some places were removed from the path but in other places remained stretched downslope under a plaster of muddy deposit. Within some trails, such trees



FIGURE 6.10.—Pile of debris at north edge of debris-torrent path in First Valley, Inverness. Single Douglas-fir (1.3 m diam) immediately upstream of house blocked the logs and deflected the debris torrent, so that only the house's deck was destroyed. Immediately upstream, a filter house of the Inverness Water Co., located in center of path, was destroyed. Downstream, large trees were abundant enough to deflect the logs and prevent major damage to buildings. Photograph by S.L. Reneau.

as oak and madrone remained in place; other trails contained partly uprooted trees lying downslope, or small subsidiary scars with broken roots remaining from trees torn away (fig. 6.3). Trees that remained within debris-flow trails were plastered with muddy deposits to observed heights of as much as 2 m above the ground (pl. 4; fig. 6.5), and splashed with muddy deposits to observed heights of as much as 4 m above the path margin. Many trees showed abrasions higher up resulting from the impact of trees that moved with the debris flow. Particularly in woodland and brush-covered areas, many debris-flow trails contained elongate scars where soil had been removed (pl. 4).

#### SIZE AND FORM

Soil-slip scars ranged in width from 1 to as much as 60 m; most were from 5 to 15 m across. Scars ranged in depth from about 0.5 to 3 m or more, measured normal to the hillslope; most were 1 to 2 m deep. Thus, the typical soil slip had a breadth-to-thickness ratio of from 3 to 15.

Some soil slips left broad sheetlike scars (fig. 6.13), and others narrow pockets (fig. 6.15). Reneau and Dietrich (1987a) have described and analyzed the sizes of scars left by the storm in a study area in Marin County.

#### SLOPES OF FAILURE AND FLOW

Slopes at soil-slip scars that developed in the storm are compared in figure 6.16 with those of pre-1982 soil-slip scars in the bay region, as well as with slopes at soil slips described from other places. The approximate slopes at soil-slip scars in Marin County are shown in figures 7.3 and 7.6. Almost all soil slip/debris flows in the storm originated on slopes steeper than 20°, most on slopes steeper than 26°, but one originated on a slope of 14° (C.M. Wentworth, oral commun., 1982; see section entitled "Grant Road" in chap. 8).

Debris flows moved down slopes ranging from nearly horizontal to steeper than slopes of failure. In places, debris flows moved upslope for short distances (see Inverness area case study above).



FIGURE 6.11.—Path of debris torrent in north fork of First Valley, Inverness Ridge, showing removal of vegetation and soil mantle. Note that path margin is much higher on right side, owing to banking around a sharp curve. Kneeling man in center for scale. Photograph by C.M. Wentworth.



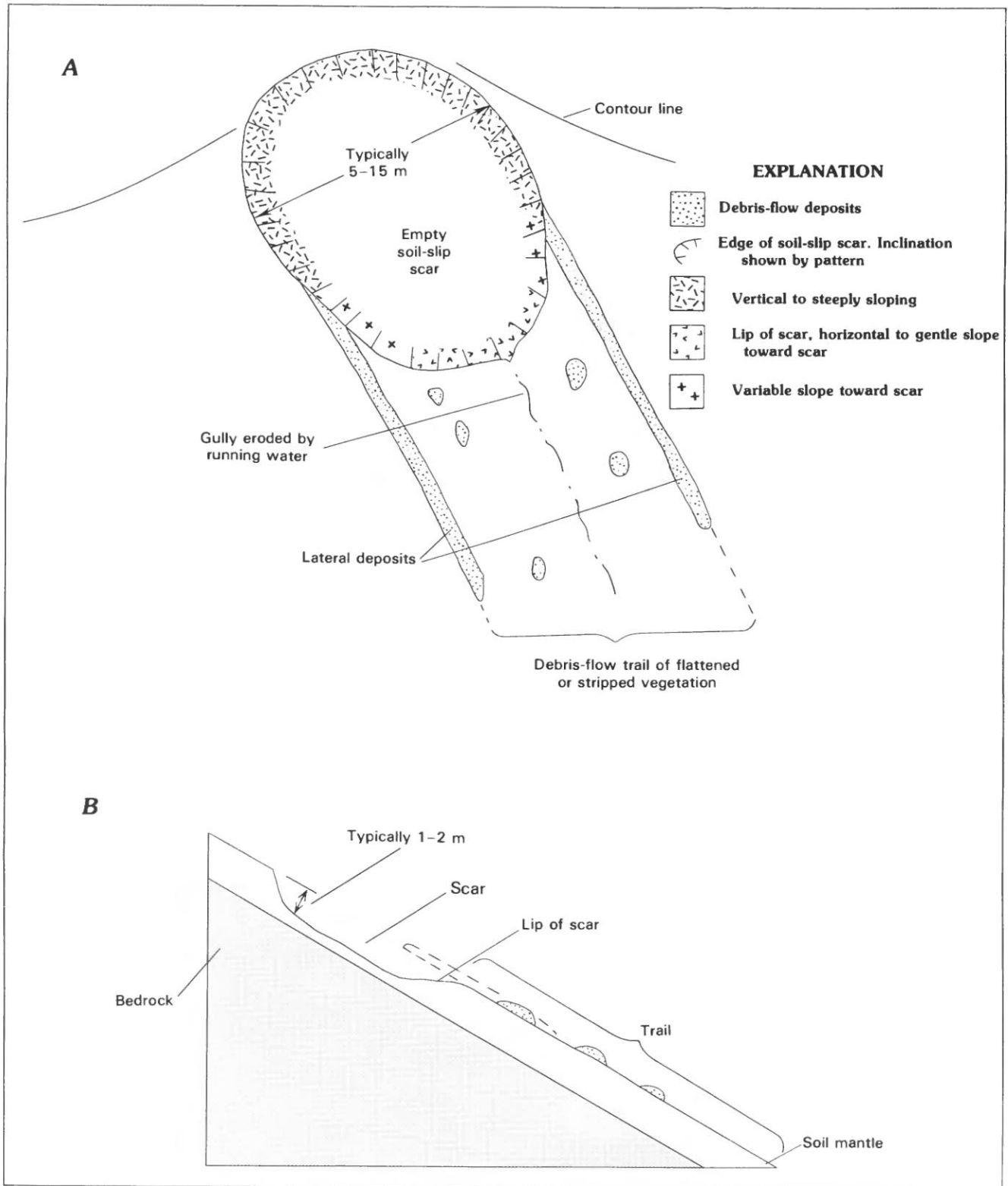


FIGURE 6.12.—Schematic map (A) and downslope cross section (B) showing typical features remaining from a single soil slip/debris flow. In figure 6.12B, dashed lines show position of lateral deposits projected into plane of cross section at center of scar and trail. Slope of ground surface is shown as 30°, a typical value.

## SOILS INVOLVED

Soils involved in soil slip/debris flows varied broadly in texture and plasticity, as described in table 6.1. Most of the samples in table 6.1 are fine-grained soils. About 90 percent of the samples are classified as earth rather than debris, according to Varnes (1978, p. 24).

Soil textures ranged from nearly clean sand to clayey silt, as indicated by size analyses of 50 samples from table 6.1 that flowed as debris flows during the storm (fig. 6.17). Content of clay-size particles (less than  $2\ \mu\text{m}$ ) ranges upward from 3 percent, but 98 percent of the samples have clay contents of 8 percent or more. The upper limit of clay content in these samples is 35 percent; an upper limit of 45 percent clay (of undefined size) is reported in chapter 9.

The upper limit of clay content is reduced if we consider only fast-moving debris flows originating from hillslopes in long-term equilibrium. This restricted sample is obtained by excluding debris flows that were anomalously slow moving (velocities of meters per minute rather than meters per second; see section entitled "Elkus Ranch" in chap. 8) and debris flows from cut slopes, from scarps

of deep-seated landslides, and from the margins of active slow-moving shallow slides, all of which are distinguished in figure 6.17. The upper bound of clay content for 93 percent of this restricted sample is 25 percent.

Data on soil plasticity are less abundant than those on soil texture, in part because many soils had such a low plasticity that the Atterberg tests which describe plasticity were not considered worthwhile. Figure 6.18 shows fine-grained soils from table 6.1 that flowed in the storm plotted on the plasticity chart of the Unified Soil Classification (USC) system. Most samples plot as ML or OL (inorganic silty soils and organic soils of low liquid limit), but some plot as MH or OH (inorganic silty soils and organic soils of high liquid limit), and three plot as CL (inorganic clay of low liquid limit). Two of these three CL soils showed evidence of uncommonly slow flow, a reasonable consequence of their plasticity. Thus, debris flows involved soils with a broad range in plasticity, from nonplastic and slightly plastic granular soils to silts and clays of moderate plasticity. The only common type of soil mantle not significantly involved was highly plastic clay (CH of the USC system).



FIGURE 6.13.—Soil slip/debris flow on the Tiburon Peninsula, Marin County. Broad tabular soil-slip scar at left (upslope from dashed line) leads downslope to debris-flow trail of flattened grass that includes scattered remnants of muddy deposit and clumps of sod. Slide mass climbed over steep downslope corner of scar (shadowed, at right center) and left lateral deposits leading from widest part of scar.

#### DEGREE OF MOBILIZATION

Most soil slip/debris flows mobilized entirely and left scars empty of failed material. Others mobilized from only the flanks or toe of a slide, resulting in empty scars on parts of a larger slab that shifted only slightly (figs. 6.19, 6.35). Degree of mobilization varied in another respect: Some soils became extremely fluid and flowed far, leaving little deposit; others became barely fluid, flowed only short distances, and left abundant thick deposits in and near the scar (see figs. 6.32–6.35; see Reed and Salmon Creek case studies below).

#### COMPLEXES OF SOIL SLIP/DEBRIS FLOWS

Many debris-flow trails, especially in woodland or brush, involved more than one soil-slip scar (pl. 4). Each such soil slip was related to others as part of a complex. If the soil slips coincided in time, the major debris flow from such a complex could be considerably larger than from a single scar. Complexes ranged in scale from small features like those in figure 6.20 to major complexes, as at First Valley in Inverness.

In most of the complexes shown in plate 4, almost all scars lie within the path of the major pulse. In complexes like the one at Tiburon Ridge, extensive parts of the lowermost canyon walls were stripped of soil, resulting in abundant elongate scars along the drainage channel.

#### SUMMARY

Soil slip/debris flows triggered by the storm ranged from small isolated events on hillsides, as at Murray Park, to major complexes, as at First Valley, that affected entire canyons as flood phenomena. In virtually all cases, these events originated as soil slips, flowed largely as slurries, and impacted the landscape and its occupants as pulses or surges that generally moved rapidly and arrived suddenly.

Individual soil slips varied in size, form, and degree of mobilization as debris flows; most occurred on slopes steeper than  $26^\circ$ . The soils that flowed ranged broadly in texture and plasticity but did not include clayey soils of high plasticity. Debris torrents and many of the larger debris flows resulted from complexes involving numerous soil-slip scars that typically lay within the path of the major pulse.



FIGURE 6.14.—View downslope along soil slip/debris flow near Barnabe Mountain, Marin County. Debris-flow trail leading downslope from empty scar climbs right side of its path in making a turn. Knapsack in foreground for scale.

## MECHANICS OF SOIL SLIP/DEBRIS FLOW

The development of soil slip/debris flows is analyzed here as a sequence of phases: (1) movement of water to the site of failure, (2) failure of the soil mantle by sliding, (3) mobilization of the soil slip as a debris flow, and (4) travel of the debris flow.

### MOVEMENT OF WATER TO SITES OF FAILURE

Previous investigations have documented that slope failure is commonly the consequence of high water levels

(and resulting high pore-water pressures) in slope-forming materials (for example, Terzaghi, 1950). Thus, the means by which water moves to various parts of the landscape are principal controls on the distribution and timing of soil slip/debris flows. Movement of water in and on hillslopes was measured only locally during the storm (see chap. 5), and so the discussion here is limited to aspects of the movement and concentration of water that are reflected in the distribution and timing of soil slip/debris flows.

### RAINFALL AND DYNAMIC BALANCE

Accumulations of water in the soil mantle of hillsides are generally perched above less permeable bedrock or soil, and the level of soil saturation is determined by a dynamic balance between the rate of infiltration and the rate of seepage from the soil mantle (Campbell, 1975). For water level to rise, the rate of addition of water to the perched water table must exceed the rate of exit. In places where direct rainfall is the principal source of water, the rainfall intensity must exceed some critical value. Under these circumstances, the soil slip leading to a debris flow would have to occur during or shortly after intense rainfall.

Observations in the bay region during the storm document the association between soil slip/debris flows and concurrent intense rainfall. Almost all the soil slip/debris flows plotted in figure 3.1 occurred during reasonably intense rainfall; the several exceptions, plotted on records from the San Bruno and SSF-WQC gages, occurred within about an hour of the end of storm rainfall. A more noteworthy exception was the event at Hurricane Gulch near Sausalito (Smith and Hart, 1982, p. 148-149), which occurred 22 hours after rainfall had ended.

Local differences in the intensity of rainfall appear to have influenced the distribution of soil slips. Evidence of this comes particularly from the Montara Mountain area of San Mateo County, where detailed mapping of soil-slip scars shows significant differences between the January 1982 storm and the storm of December 1955 (Wentworth, 1986). South of Montara Mountain, an elongate patch about 0.5 by 2 km, which was indistinguishable in the 1955 pattern of abundant soil slips throughout the steep granitic terrain, emerged in 1982 as an island devoid of soil slips in an otherwise similar pattern of abundant soil slips. Similarly, the Franciscan terrane in the nearby Pacifica area, which was almost completely spared in 1955, produced many soil slips in 1982. Such comparison between storms, especially in areas of uniform materials and topography like Montara Mountain, is essential for determining the influence of local variations in rainfall, which in most places may be masked by the heterogeneity of materials and terrain.



FIGURE 6.15.—Trail of debris flow over grassland, leading from pocket-shaped scar, on the Tiburon Peninsula, Marin County. Note lateral deposit bounding trail, flattened old grass marking trail, and deposits within trail. Young grass standing upright in trail has grown since the event.



## CONCENTRATION OF WATER

Water levels capable of triggering soil slips in the storm generally were not attained by direct rainfall alone, as evidenced by the fact that the great majority of susceptible hillslopes did not fail when subjected to heavy rainfall. The areal distribution of soil-slip scars shows patterns suggesting that local concentration of water, both from the storm and from prestorm rainfall, played a major role in triggering failures (see chap. 7, especially section entitled "Local Topographic Setting").

Water can be concentrated in the landscape by several means, some of which are illustrated in figure 6.21. Surface flow is concentrated by the topography. Flow within the soil mantle is concentrated by the form of the bedrock surface, as well as by the topography, by breaks in slope, and by differences in soil mantle. Water can enter bed-

rock, concentrate, and reemerge into the soil mantle. Finally, flow can be affected by manmade modifications. Evidence for these various water-concentration mechanisms is discussed further in chapter 7.

## SURFACE FLOW AND THROUGHFLOW

Water on the ground surface in hillside terrain concentrates in the concave parts of hillslopes (see chaps. 9, 10). Because surface flow of water is rapid, concentration in the subsurface by such means may be delayed only by the time required for seepage of water into the soil at the site of concentration. For the granular soils typically involved in soil slips during the storm, saturation of the soil mantle by this means could occur within a matter of hours (on the basis of a thickness of 1-2 m and an estimated permeability of  $10^{-3}$  to  $10^{-2}$  cm/s).

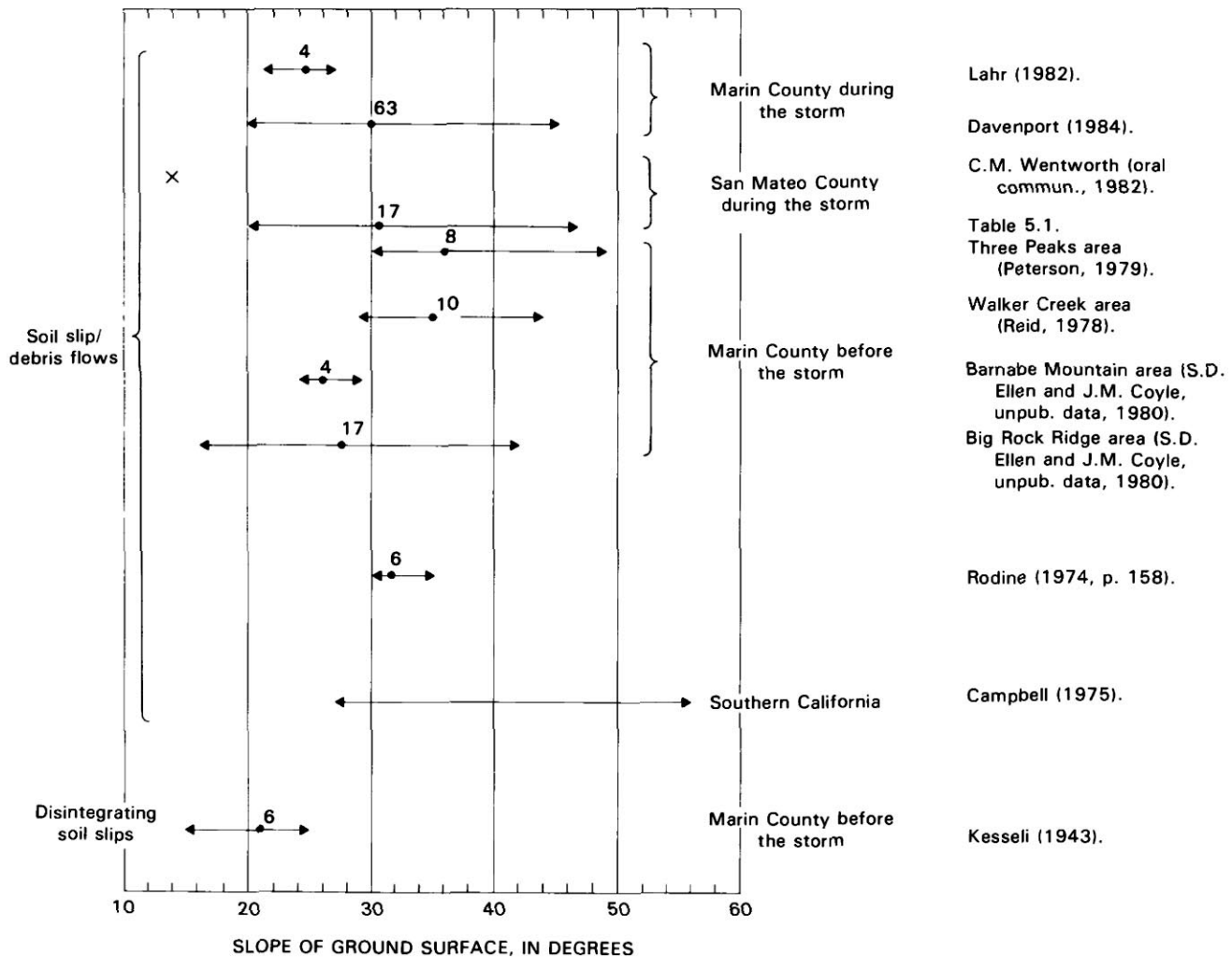


FIGURE 6.16.—Slopes of ground surface at soil-slip sources of debris flows resulting from the storm, in comparison with those at other soil-slip sources of debris flows. Slopes were measured in the field. Arrows show range of slopes; dots denote average of measured slope angles. Numbers above dots indicate number of measurements averaged; x, single observation.



Water can also concentrate by downslope seepage within the soil mantle, called throughflow or interflow (fig. 6.21B). Throughflow is governed largely by the form of the bedrock surface below the soil mantle. Because the bedrock surface generally approximately parallels the ground surface, throughflow, like surface flow, is com-

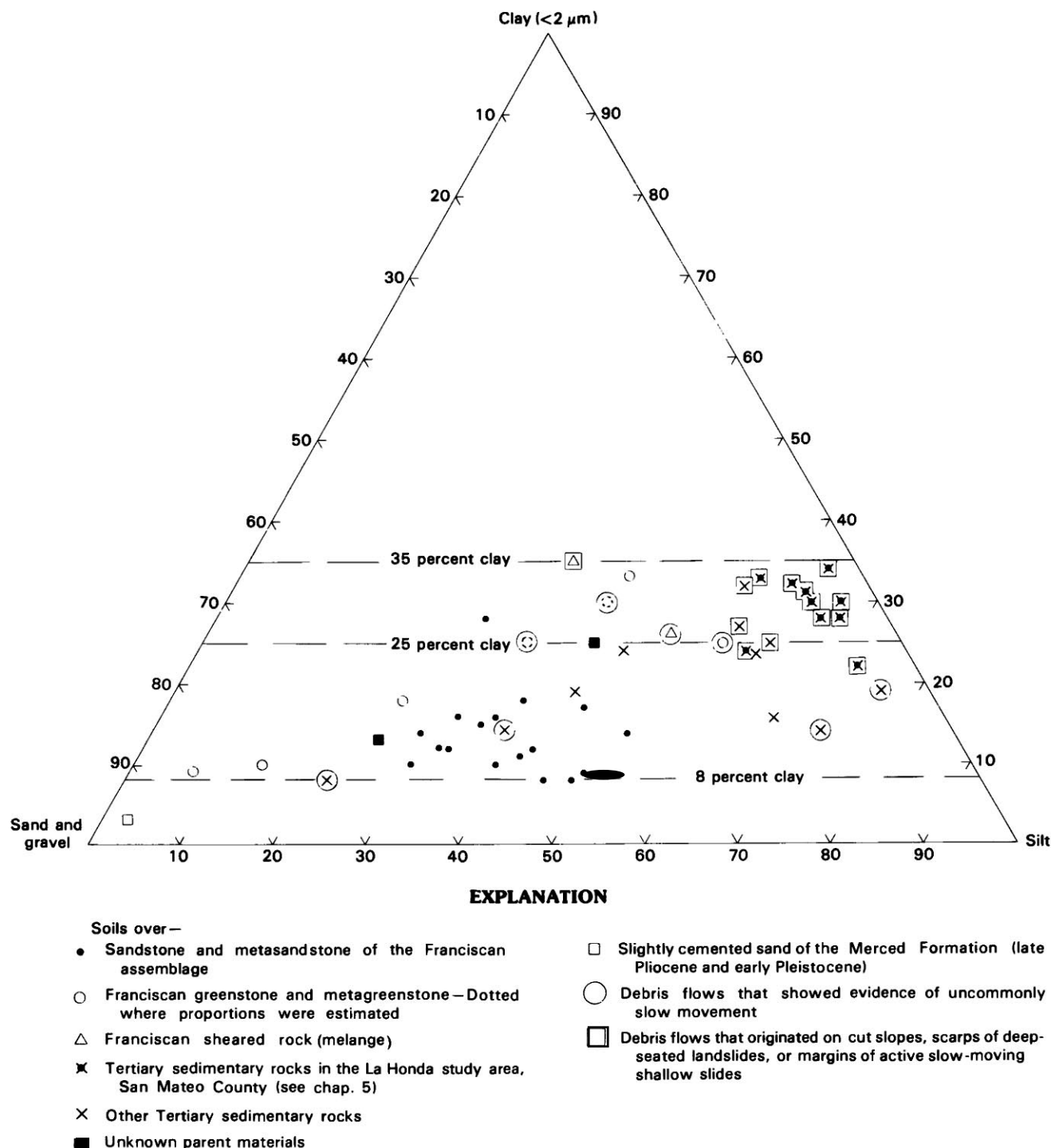


FIGURE 6.17.—Size-fraction diagram showing soils that flowed as debris flows in the storm. Dashed lines show significant boundaries of clay content discussed in text. Data from table 6.1.

monly concentrated in concave areas. Some concavities in the bedrock surface, however, may be entirely filled by accumulations of soil (Dietrich and Dunne, 1978), and so areas of water concentration by throughflow may be concealed. In some soils, throughflow may contribute to water levels in the soil mantle almost as rapidly as surface flow (Sidle, 1984).

Occurrence of soil slips in concave parts of the landscape during the storm suggests that throughflow, surface flow, or both contributed significantly to water levels that led to these soil slips. For a study area in Marin County, Reneau and Dietrich (1987a) found that 62 percent of the debris flows triggered by the storm occurred in concavities. In the Hicks Mountain area of Marin County, 49 percent of the scars that produced debris flows occupy conspicuously concave parts of hillslopes; and in selected smaller areas of Marin County, more than 70 percent of the scars occupy conspicuous concavities (see chap. 7); even higher percentages would result if less conspicuous concavities were included. Thus, water concentration by surface flow and throughflow appears to have contributed significantly to a large proportion of the soil slips in the storm.

#### BEDROCK CONTACTS

Several conditions that concentrate ground water commonly occur along bedrock contacts. Water can concen-

trate along bedrock contacts by seepage through bedrock, by changes in slope that typically accompany contacts, and by contrasts in soil mantle that accompany the contrasts in bedrock. Many breaks in slope in the bay region coincide with contrasts in both bedrock and soil materials, and so it is difficult to distinguish the effects of these several conditions.

These conditions apparently exerted a significant influence on soil slips during the storm because many soil-slip scars lie conspicuously along bedrock contacts (fig. 6.22). The tendency for soil slips to occur at bedrock contacts and over bedrock units with abundant strong permeability contrasts is discussed in chapter 7.

#### BEDROCK SEEPAGE

Water that infiltrates bedrock can be concentrated by permeability contrasts in bedrock (fig. 6.21B). Seepage of water from bedrock out into the soil mantle would be favored where the bedrock has strong permeability contrasts that dip out of slope, particularly where permeable bedrock that has a broad areal contact with the ground surface overlies impermeable material. Seepage through bedrock can take months or years, but at least some of the bedrock seepage that influenced soil slips in the storm appears to have been fed by storm rainfall that emerged into the soil mantle while rain was still falling. Seepage from bedrock in the storm was suggested by sustained

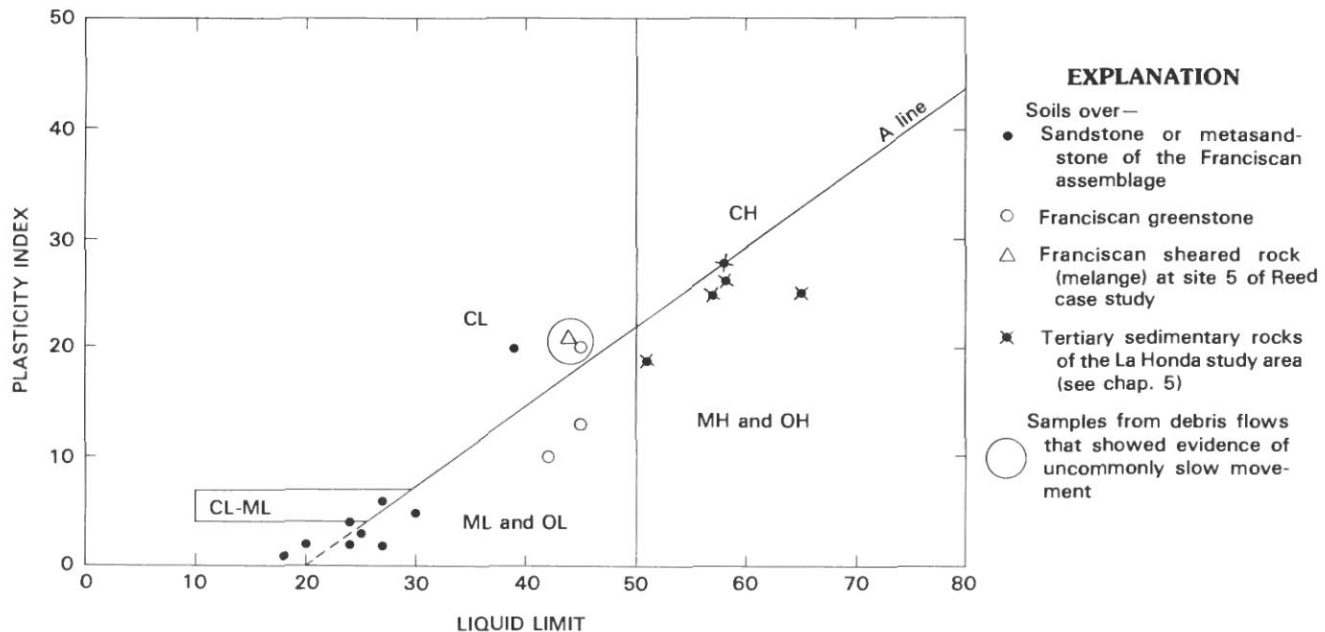


FIGURE 6.18.—Plasticity chart (U.S. Army Corps of Engineers, 1953, pl. 2) showing fine-grained soils involved in soil slip/debris flows resulting from the storm. Letters designate soil groups of the Unified Soil Classification system, which, along with the A line, are described in most texts on soil engineering (for example, Lambe and Whitman,

1969, p. 34–38). Coarse-grained soils are not plotted. Also not plotted are soils that lack sufficient plasticity for the Atterberg tests that define the plasticity chart; if slightly more plastic, such soils would plot near points in lower left. Data from table 6.1.

flow of large volumes of water from some soil-slip scars, as reported by E.W. Hart and S.J. Rice (oral commun., 1982; see chap. 10), and by other eyewitnesses.

#### BREAKS IN SLOPE AND CONTRASTS IN SOILS

Throughflow can be concentrated at places along the downslope profile of a hillslope by decreases in slope and changes in soils. Throughflow is impeded wherever its gradient of flow, which commonly approximates the slope of the ground surface, decreases. Water levels must rise near such points unless the soil mantle increases in permeability or thickness. In fact, the permeability of soil mantle in the bay region commonly decreases below such breaks in slope because the soil derived from bedrock below such slope breaks is typically more clayey. At many such places, the less permeable soil probably combines with decreased gradient to impede throughflow, and so water levels in the soil mantle rise near the break in slope.

Although water concentration by these means generally was indistinguishable from bedrock seepage, in places soil-

slip scars are concentrated where hillsides abut alluviated surfaces (see chap. 7). Water concentration at these scars probably resulted largely from these breaks in slope.

#### HILLSLOPE MODIFICATIONS

Where hillslopes have been modified by even such small features as animal trails, water may collect from large parts of the landscape and then be transported along roads, gutters, or trails to induce failure at a distant site. Many soil slips in the storm occurred where water was concentrated by such means; the debris torrent at First Valley in Inverness, for example, originated from a soil slip immediately downslope from a road culvert.

In at least one case related to the storm, modification of hillslopes significantly affected the transit time of ground water to a soil-slip site. At Hurricane Gulch in Sausalito, a soil slip/debris flow originated from highway fill about 22 hours after rainfall had ceased (see Smith and Hart, 1982, p. 148-149). The delay can be attributed, at



FIGURE 6.19.—Three small debris flows near San Geronimo, Marin County, issue from flank and toe of larger shallow slide. Larger slide, defined by dark cracks at crown and toe, is about 35 m wide.

least in part, to the gravelly-clay highway fill of low permeability that dammed throughflow down a colluvium-filled draw (D.G. Heyes, oral commun., 1983). Seepage through bedrock may also have contributed to the delay, as suggested by the abundance of water that seeped from the scar after failure (more than 2,000 m<sup>3</sup>/d) and by the proximity of the scar to an old tunnel excavated either for water collection or for manganese mining—in either case, suggesting strong permeability contrast in the bedrock.

#### ELEVATED PORE PRESSURE

Concentration of water can result in pore pressures greater than those possible from throughflow parallel to the ground surface, and such elevated pore pressures permit failure on relatively gentle slopes. Elevated pore pressures can develop from seepage in an out-of-slope direction and from artesian conditions. Out-of-slope seepage may accompany several of the water-concentration mechanisms discussed above, namely, bedrock seepage, breaks in slope, and contrasts in soil.

Artesian conditions, which can generate greater pore pressures than can unconfined aquifers, are possible where sloping permeable materials are confined between less permeable materials. During the storm, artesian pressures may have developed in bedrock with such contrasts in permeability, as where more and less permeable sedimentary beds are interlayered or where zones of permeable shattered rock pass through an impermeable sheared rock mass. Artesian pressures may also have developed within the soil mantle and underlying shallow weathered bedrock (see chap. 5; Wilson and Dietrich, 1985). In the bay region, such shallow confined aquifers can occur where the soil mantle includes impermeable clayey soil overlying permeable sandy soil (Hayes, 1985), where colluvial accumulations include highly permeable layers of rock fragments (see Murray Park and Inverness area case studies above), where fractured weathered bedrock is more permeable than the overlying soil mantle (Nicholas Sitar and K.A. Johnson, oral commun., 1986), or where animal burrows or other passageways in the soil mantle terminate downslope (Pierson, 1983; see section entitled "Grant Road" in chap. 8).

#### SUMMARY

Movement of water to sites of failure occurred by several means that are reflected in the timing and distribution of soil slip/debris flows in the storm. Timing of debris flows indicates that intense rainfall was almost always involved, and the common occurrence of soil-slip scars at such features as concavities, breaks in slope, soil and bedrock contacts, or manmade modifications suggests that concentration of water in the landscape was almost

always required for failure. Because features suggesting concentration of water so commonly accompany scars, those places where scars occur in the absence of such features, such as on smooth planar or convex hillslopes, are suspect for concealed colluvial fill or bedrock seepage. Several of the likely water-concentration mechanisms are capable of generating pore pressures in excess of those attainable by unconfined slope-parallel seepage.

#### INITIAL FAILURE

Once water has arrived at a site, it interacts with the materials there to determine the occurrence of ground failure, the geometry of the failed mass, and the type of movement. Initial failure is discussed in this section; the type of movement after initial failure is discussed below in the subsection entitled "Mobilization."

Failure of hillslopes generally results from shear along a basal slip zone, as modeled by the Coulomb criterion for failure. In any place where the upward force of ground-water seepage equals or exceeds the weight of the soil, however, failure may occur by static liquefaction, or quick conditions (Iverson and Major, 1986). Such quick conditions might have been responsible for the "water blow-outs" described by Hack and Goodlett (1960, p. 45), but they were probably not a common trigger for debris flows



FIGURE 6.20.—Small soil-slip/debris-flow complex near Barnabe Mountain, Marin County. Complex consists of two scars along a debris-flow trail, 3 to 4 m wide. Between scars, trail is defined by lateral deposits.

in the storm, judging from the steep slopes occupied by virtually all soil slips in the storm (fig. 6.16). Thus, the following analysis focuses on Coulomb failure.

Hillslope failure is best analyzed quantitatively by using detailed information from specific sites. The results of such analyses are discussed in chapter 9 for landslides that occurred in Pacifica. The present discussion lacks suitable site studies, and so initial failure is discussed only briefly, using a simplified model for the materials and geometry of failure.

#### INFINITE-SLAB MODEL

Most soil-slip scars left by the storm define slide masses that resemble planar slabs, and so soil slips are modeled here as slab failures. For further simplicity, soil slips are modeled as infinitely long and wide slabs of homogeneous soil, for which edge effects are absent; such infinite-slope analysis has been applied to similar landslides by other investigators (see chap. 9; Campbell, 1975; Moser and Hohensinn, 1983). For the general case in which soil has

cohesive as well as frictional strength, and seepage is parallel to the hillslope, stability of the infinite slab is described by

$$FS = \frac{c'}{\gamma_t h \sin \beta} + \left( \frac{\gamma_t - m \gamma_w}{\gamma_t} \right) \left( \frac{\tan \phi'}{\tan \beta} \right), \quad (1)$$

where FS is the factor of safety,  $c'$  is the apparent cohesion,  $h$  is the thickness of the slab measured normal to the slope,  $\gamma_t$  is the saturated unit weight of soil,  $\gamma_w$  is the unit weight of water,  $\phi'$  is the effective angle of internal friction of the soil at peak strength,  $\beta$  is the inclination of the hillslope, and  $m$  is the proportion of the slab thickness that lies below the piezometric surface (for example, Campbell, 1975, p. 19). Failure occurs when  $FS \leq 1$ .

Equation 1 provides a general model for the initial failure of hillslopes during the storm. At a given site, where slope ( $\beta$ ), soil thickness ( $h$ ), and soil properties ( $c'$ ,  $\gamma_t$ ,  $\phi'$ ) were fixed, rising water level during the storm

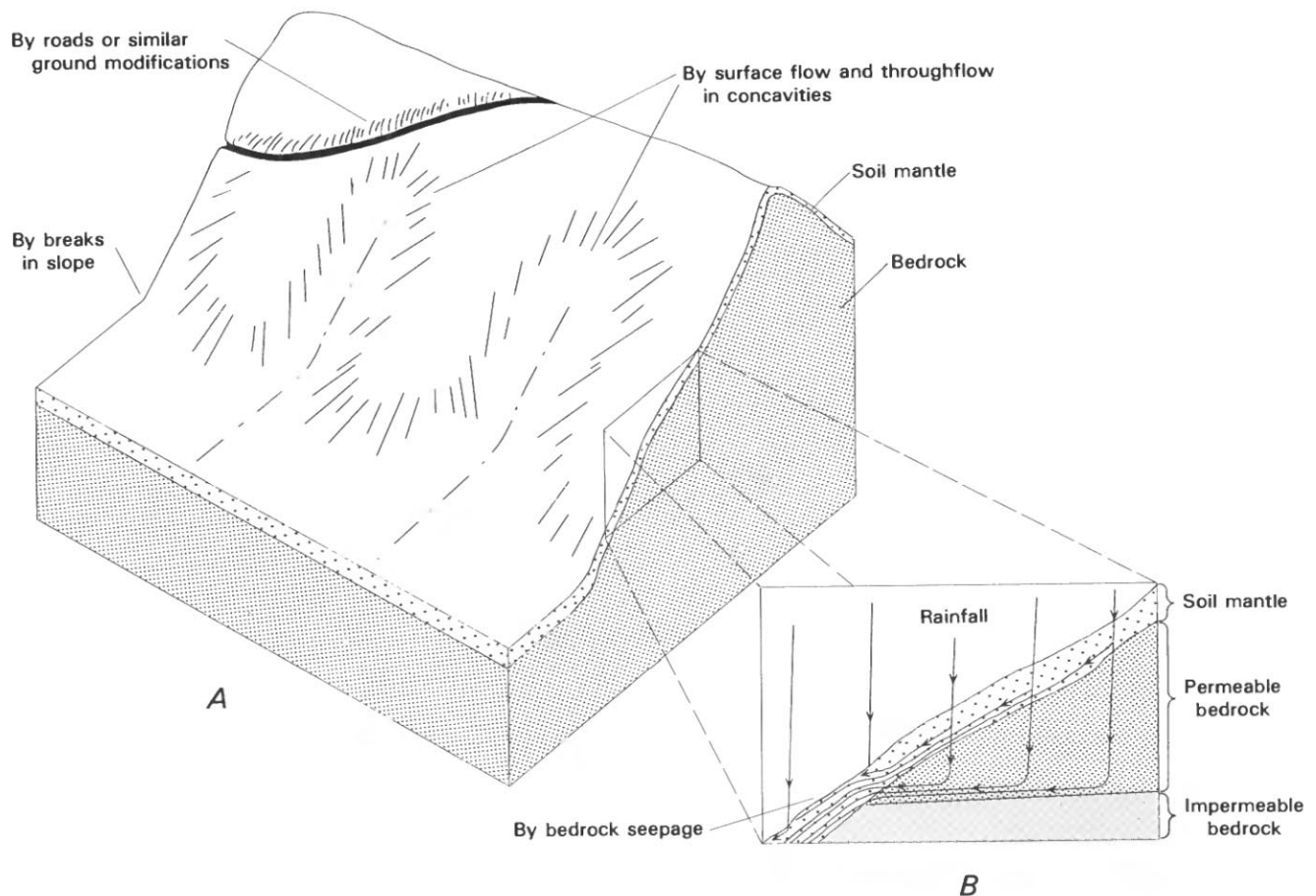


FIGURE 6.21.—Schematic block diagram (A) and cross section (B) showing some means of water concentration in the landscape. Schematic water paths in cross section illustrate throughflow (within soil mantle) and bedrock seepage.



(expressed by increasing  $m$ ) decreased the FS until failure occurred. This theoretical relation is supported by studies in the bay region that correlate soil slips during the storm with high measured ground-water levels (see chap. 5). Similar work has confirmed this relation elsewhere (for example, Swanston, 1970; Sidle and Swanston, 1982).

The dimensions of soils slips appear to be determined by edge effects, which are not included in the infinite-slab model. Reneau and Dietrich (1987a) have discussed the influence of edge effects on the dimensions of soil slips triggered by the storm in a study area in Marin County.

#### SLOPES OF FAILURE

According to the infinite-slab model, failure on relatively gentle slopes is favored where soils have relatively low internal friction (as in clayey soils), where relatively high water levels are necessary to trigger failure, and where cohesive strength, commonly provided by roots, is low.

Failure on relatively steep slopes is favored where soil has high frictional strength, where roots provide high cohesive strength, and where relatively low water levels are sufficient to trigger failure. Differences in slope at soil-slip scars in Marin County appear to reflect some of these controls (see chap. 7).

Measured slopes of failure in the storm (fig. 6.16) lie within a broad range that appears to be reasonable for the soil properties listed in table 6.1, when these are substituted into equation 1 with values of  $m$  between 0 and 1. A more specific discussion of stability analyses in chapter 9 implies that total saturation of infinite slabs, with seepage parallel to the ground surface, generally was sufficient to account for the observed slopes of failure at 9 sites in Pacifica. In some cases, however, hillslopes failed at slopes gentler than calculated for infinite slabs of the tested soils under these ground-water conditions. In those cases, pore pressures greater than attainable by slope-parallel seepage may have contributed to failure.



FIGURE 6.22.—Landslides on the Tiburon Peninsula, Marin County, localized along a prominent break in slope that coincides with a contact between permeable bedrock and soil mantle above and impermeable clayey bedrock and soil mantle below. Contact extends about horizon-

tally across center of view, at foot of broad rounded hill. Complex scars from soil slip/debris flows are at center and left above contact; shallow slide at right above contact (arrow) did not mobilize as a debris flow, although distinct boundaries suggest movement during the storm.

## LOCATION OF THE FAILURE SURFACE

An infinite slab of homogeneous cohesionless soil, represented by the second term in equation 1, should fail near the permeability boundary that perches the water table; as the water table rises, this surface will reach the critical value of  $m$  before shallower hypothetical slabs. The effect of cohesion on failure, represented by the first term in equation 1, is similar in favoring failure of thick slabs. However, variations in soil properties can favor failure well above the bedrock surface (Moser and Hohensinn, 1983, p. 209; Reneau and Dietrich, 1987a).

Many soil-slip scars resulting from the storm bottomed in soil close above the bedrock surface, which generally forms the chief permeability boundary. In many places, however, soil slips bottomed near low-permeability horizons within the soil mantle (Davenport, 1984; see Inverness area case study above and Reed case study below).

## MOBILIZATION

By STEPHEN D. ELLEN and ROBERT W. FLEMING

Once failure has begun, the soil slip must mobilize as a slurry if debris flow is to take place. This process of transformation is the critical step between localized sliding of soil and its rapid flowage to distant parts of the landscape. Our discussion focuses on the means by which mobilization is accomplished and the factors that control these means. Mobilization is also discussed elsewhere (Ellen and Fleming, 1987; Fleming and others, in press).

Johnson and Hampton (1969) distinguished four general means by which debris flows can mobilize: (1) saturation of soils in place; (2) incorporation of water by sliding; (3) erosion, particularly by strong gushes of water; and (4) incorporation of coarse debris into clayey slurries. Because almost all the debris flows during the storm mobilized from soil slips, they did not involve the last two of these processes to any significant degree. Thus, soil slips apparently gained the water content necessary for debris flow either by saturation of in-place soil or by incorporation of water during sliding.

## CONTRASTS IN MOBILIZATION

Accounts from the world literature, as cited by Rodine (1974), confirm that debris flows can mobilize from slides in different ways. In some places, mobilization has resulted from slow sliding; in other places, hillslopes have mobilized as masses of flowing debris without preceding macroscopic movement.

Eyewitness reports from the storm suggest a similar contrast in speed of mobilization. Most eyewitnesses reported signs of movement preceding rapid flow, in some cases by many hours (table 6.2; see subsections entitled "Alba Road" and "Creekwood Drive" in chap. 8); these

TABLE 6.2.—*Eyewitness accounts of mobilization in the storm*

Source person and location	Indications of movement	Time interval between indication of movement and rapid movement
Susan Melvin, Woodacre, Marin County.	Intermittent waterfall in small drainage changed from white to brown in an instant, then disappeared downslope in a fast-moving debris flow.	3 seconds.
Dave McCleery, Mill Valley, Marin County.	Scotch-broom (a tall brushy plant) leaned downhill across driveway in area that later mobilized as liquid mud; other areas of Scotch-broom did not lean.	8 hours.
Dustin Leer, San Rafael, Marin County.	Water from horizontal drainpipes changed from clear to muddy (always clear before, even during heavy storms). Sound like tree cracking, then hillside turned to liquid; looked like wave breaking on beach.	At least half an hour. 3-5 seconds.
Barbara Denton, Crockett, Contra Costa County.	Cracks opened across hillslope, then stream of water from hillside, then slide in surficial soil (moved approx 0.3-1.5 m/s).	Several hours between cracks and rapid movement.
Thomas Lewis, San Rafael, Marin County.	Hollow rumbling sound like thunder, close by (no other major slides in area), then varying rapid movement, generally progressing upslope.	45 minutes.
Leonard Davis, Sausalito, Marin County.	Brush and trees lean downslope. Numerous small (less than 1 m <sup>3</sup> volume) failures from the same place. Heavy runoff of viscous water and earth.	24 hours. Several hours. Immediately before major pulse.
Gary Greene, near Branciforte Creek, Santa Cruz County.	Noticed pullaway cracks on brush-covered hillslope; mass left the scar as a slab, rapidly became fluid, then turned and flowed down canyon at about 6 m/s.	Less than 2 minutes.

debris flows were mobilizing from slow-moving slides. Instantaneous movement was also witnessed: At one site, within a span of several seconds an observer saw a small waterfall in an intermittent drainage change in color from white to brown and then disappear as the hillside collapsed downslope as part of a debris flow (table 6.2). Such reports of instantaneous mobilization are inconclusive, however, because eyewitnesses might not have detected movements preceding mobilization, especially during storm conditions.

Another prominent contrast was degree of mobilization. Most shallow slides that mobilized during the storm mobilized completely, leaving scars empty of failed material (figs. 6.1, 6.3, 6.4, 6.14, 6.15, 6.20). Other slides mobilized partially, leaving dislocated slide masses as well as scars from which soil had flowed (figs. 6.19, 6.35); debris flows in such cases characteristically issued from the flanks or toes of slides. Many other shallow slides moved during the storm but did not mobilize at all as debris flows (figs. 6.22, 6.23).

Deposits of debris flows differed in several respects that may have reflected contrasts in the style of mobilization. Differences in the thickness and lumpiness of deposits particularly caught our attention (see case studies below).



These various contrasts raise such questions as: Why was mobilization faster in some cases than in others? Why did some slides mobilize and not others? Why did only parts of some slides mobilize? To pursue such questions, we discuss the influence of soil texture and the relation between slide and flow, and then consider possible means of debris-flow mobilization.

### THEORY OF MOBILIZATION

#### SOIL TEXTURE

Soil texture, particularly clay content, influences the susceptibility of soils to debris flow. Debris flows generally occur in poorly sorted soil that contains a small proportion of clay-size material (Rodine, 1974, p. 69). The lower limit of clay content is important because sustained flow requires at least a small proportion of clay (Rodine, 1974),

presumably because clay content permits a clay-water pore fluid that helps to maintain the pore pressures which facilitate flow (Pierson, 1981). At the other extreme, large proportions of clay may prevent mobilization by providing cohesion that inhibits remolding. In soils that must take on water to flow, abundant clay also increases the amount of water needed to reach states capable of flow, and it limits the permeability needed for incorporation of water. Slow-moving slides called earth flows, rather than debris flows, are typically found in such clay-rich soils (Keefer and Johnson, 1978).

The influence of clay content on mobilization of debris flows is illustrated in figure 6.17, which shows textures of 50 soils that flowed in the storm. Minimum 2  $\mu$ m-clay content is 3 percent, and 8 percent clay forms the lower bound for 98 percent of the samples. The highest clay content is 35 percent, which suggests that clay content higher than about 35 percent was sufficient to prohibit mobiliza-



FIGURE 6.23.—Mobilized and nonmobilized shallow landslides induced by the storm on a hillslope near Tomales Bay. Soil slip/debris flows have left trails at A, B, and C, extending downslope from scars; at least one fresh scar (D) developed from a subdued old soil-slip scar. Slide at E has not mobilized; movement is evidenced by fresh cracks at head and bulge at toe. Subtle break in slope that crosses hillside

horizontally immediately above the slide at E probably follows a bedrock contact. Contrast in materials across this contact probably accounts for difference in style of movement, and concentration of water along this contact probably contributed to soil slips that left debris-flow trails at A and C.

tion of debris flows during the storm. Most fast-moving debris flows that originated from hillslopes in long-term equilibrium had clay contents less than 25 percent, as discussed above in the subsection entitled "Soils Involved." Thus, susceptibility to mobilization was limited to soils with clay contents of 3 to 35 percent, more commonly 8 to 25 percent. These ranges are so broad, however, that clay content, by itself, has only a limited use in determining the potential for debris flow.

#### TRANSITION FROM SLIDE TO FLOW

The conditions under which a debris flow can develop from a soil slip may be evaluated by using the concept of plug flow, in which flowing debris is modeled as a relatively rigid plug or slab rafted on a zone of laminar flow (fig. 6.24). Johnson (1970) called the thickness of the plug the critical thickness for flow, because as a debris flow thins to this point the plug bottoms out and becomes a deposit. Thus, critical thickness is reflected, at least approximately, in the thickness of the lateral deposits or the lobe at the distal end of the flow. For a broad sheet of Bingham material, which is representative of the flow as it leaves the soil-slip scar (figs. 6.1, 6.13), the critical thickness ( $T$ ) measured normal to the slope is given by the relation

$$T = \frac{k_f}{\gamma_f \sin \beta}, \quad (2)$$

where  $k_f$  and  $\gamma_f$  are the shear strength and saturated unit weight of the flow, respectively, and  $\beta$  is the slope (Johnson, 1970, p. 488, 503). Thus, the thickness of the plug is proportional to the strength of the debris-flow material.

For the process of soil slip/debris flow, inherent relations exist between critical thickness for flow and thickness of the sliding slab. For a sliding slab of soil to

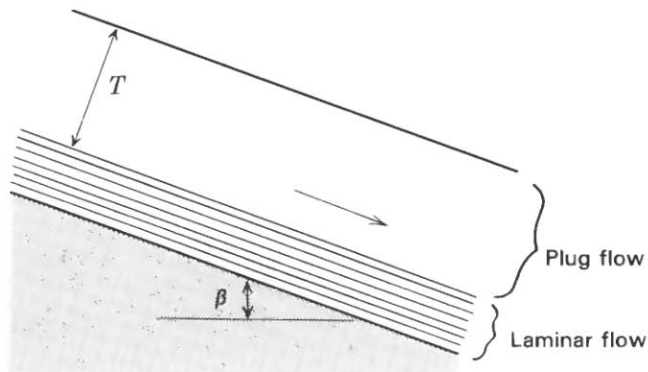


FIGURE 6.24.—Schematic cross section of a debris flow on a hillside of slope  $\beta$ .  $T$ , critical thickness for debris flow; arrow indicates downslope movement. Modified from Johnson (1970, p. 488).

transform directly into a debris flow, its critical thickness when remolded must not exceed the thickness of the sliding slab; otherwise, the slab must thicken for flow to begin, which is unlikely (fig. 6.25). Thus, the theoretical limiting case for flow from the scar is described by equation 2 when  $T$  equals the slide thickness. In actuality, the critical thickness probably must be somewhat less than the slide thickness if much of the slab is to be remolded during sliding. As a result, mobilization apparently requires development of slurry strengths low enough that the critical thickness is somewhat less than the slide thickness.

#### MOBILITY INDEX

Rodine (1974) and Johnson (1984) considered water content to be the key to the low slurry strengths needed for mobilization. They devised a mobility index (M.I.), defined by Johnson (1984) as the ratio of saturated water content of the in-place soil to the water content needed for flow of that soil down the available channel. They assumed the soil to be saturated, as we do in the following analysis, because high water levels typically accompany failure and mobilization. They determined the water content needed for flow through innovative strength testing and measurement of channel form. Mobilization was considered likely where the saturated water content of in-place soil was sufficient for debris flow down the available channel, and less likely where soil must take on additional water to flow. They found that the soils involved in debris flow had  $M.I. > 0.85$ .

#### APPROXIMATE MOBILITY INDEX

An approximation of the M.I. can be obtained by using the Atterberg liquid limit to approximate the water content needed for flow.<sup>2</sup> Thus, this approximate mobility index (A.M.I.) is the ratio of the saturated water content of in-place or undisturbed soil to its liquid limit. Qualitatively, the liquid limit seems suitable for this use because it represents the water content at which soil behavior is marginally fluid under shallow conditions. Quantitatively, the liquid limit represents a shear strength of about 2 kPa (Seed and others, 1964, p. 77), which can be translated to a critical thickness of 20 cm by using equation 2 with typical values for the debris flows under discussion ( $\beta = 30^\circ$ ; saturated unit weight of flow material,  $20 \text{ kN/m}^3$ ). This critical thickness is substantially less than the typical thickness of soil slips induced by the storm (approx 1 m), and it lies near the upper end of the typical

<sup>2</sup>We use liquid limit to represent the water content at which soil would flow as a slurry because it is a simple, reproducible test. Unfortunately, however, the liquid limit is measured on only the fine fraction of the soil (fraction smaller than the No. 40 sieve size—fine sand and smaller). For soils that contain an abundant coarse fraction, the liquid limit is probably significantly larger than the water content needed for flow.

range of thicknesses of lateral deposits left by debris flows during the storm. For these reasons, the liquid limit seems well suited to approximate the water content needed for debris flow during the storm.

The A.M.I. is plotted in figure 6.26 for the soils listed in table 6.1 that mobilized as debris flows during the storm. Soils that plot above the solid line (case A,  $A.M.I. > 1$ ), had an initial capacity to hold more water than their liquid limit. When remolded, these soils would flow readily because they would have low shear strengths and critical thicknesses well below typical slide thickness.

Soils that plot below the solid line ( $A.M.I. < 1$ ) must have taken on water in order to flow. These soils correspond to a low potential for flow according to the M.I., yet figure 6.26 demonstrates that many such soils flowed during the storm. We subdivide this area of the plot into two zones. For soils of case B ( $0.45 < A.M.I. < 1$ ), incorporation of water was sufficient for flow, at least in parts of slide masses. Soils of case C ( $A.M.I. < 0.45$ ) apparently could not incorporate enough water for flow.

#### THE STEADY STATE AND LIQUEFACTION

The M.I. approach can be elaborated by considering the initial sliding of a slab of soil. As significant deformation begins at failure, soil in the basal shear zone will approach a critical, or steady, state (Castro, 1969; Casagrande, 1976). Critical-state soil mechanics indicates that a saturated soil, if continuously distorted until it flows as a frictional fluid, will come into a well-defined state characterized by a water content and corresponding strength, both of which are related to effective confining stress (Schofield and Wroth, 1968). A similar concept was described by Poulos (1981) as the steady state of deformation.

The significance of the steady state is summarized in figure 6.27. Figure 6.27A shows that the void ratio (or water content) of a drained saturated sand undergoing shear approaches a single value regardless of its initial density; loose sand contracts (contractive behavior), whereas dense sand dilates (dilative behavior). Where deformation occurs in undrained conditions, loose soil behaves very differently from dense soil. This contrast is illustrated in figure 6.27B, which shows the variations in both axial load and pore pressure in undrained, load-controlled, monotonic triaxial tests on sand (Castro, 1969; Casagrande, 1976). As strain begins, both loose and dense sands behave similarly; but at strains of about 1 percent, sudden decrease in the resistance to shear in the loose material permits rapid acceleration of strain, even at reduced load. This decrease in strength results from increased pore pressure, generated by a tendency for contraction of the loose material; the approach of this pore pressure to the confining load of the test indicates that most of the load is borne by the pore fluid and little by grain-to-grain contact that provides frictional strength. Such behavior is called actual liquefaction (Casagrande, 1976). Dense undrained sand does not show this weakening but initially strengthens with strain as a tendency for dilation reduces pore pressure. Figure 6.27C shows that the steady-state void ratio, or critical void ratio (Terzaghi and Peck, 1967, p. 108; Casagrande, 1976), depends on the effective confining stress under which deformation occurs.

Repeated tests like those in figure 6.27B have shown that liquefaction occurs only in soil that is contractive, that is, soil for which the combination of void ratio and effective confining stress plots above its steady-state line (Casagrande, 1976; fig. 6.27C). Loose soil that is not

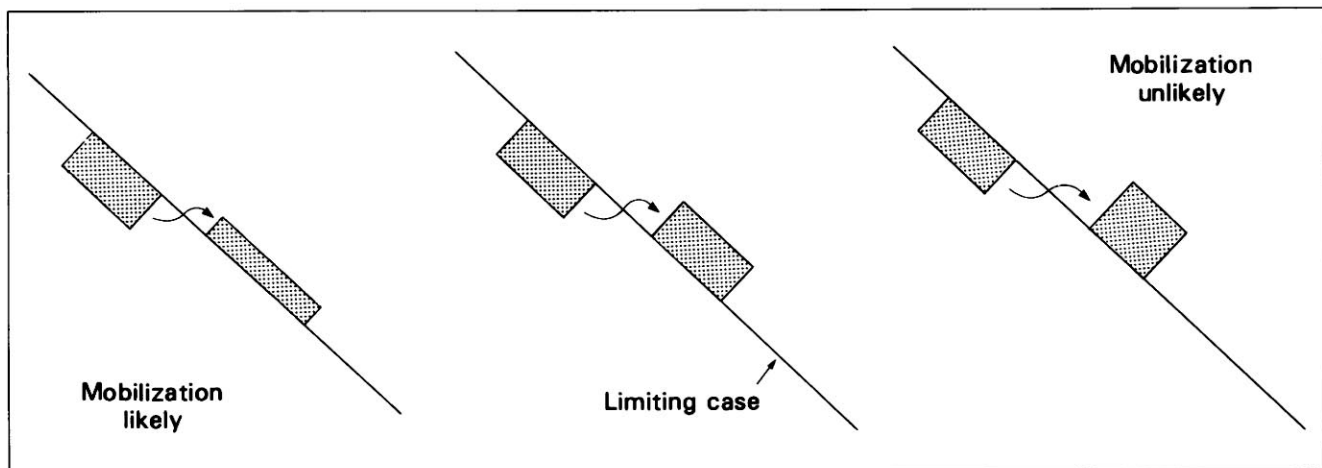


FIGURE 6.25.—Schematic cross sections of soil slip/debris flows, showing hypothetical relations between slide depth (upslope rectangle) and critical thickness (downslope rectangle) for debris flow. Transformation to flow is likely where critical thickness is less than slide depth, and unlikely where slide mass must thicken for flow to begin.



highly contractive (fig. 6.27B, test B) may not undergo significant loss of strength or may liquefy only temporarily ("limited liquefaction" of Casagrande, 1976).

The transition of soil in the basal shear zone from an initial void ratio at critical equilibrium just before failure to a steady-state void ratio can be described by using "state diagrams" (fig. 6.28), in which the soil's void ratio ( $e$ ) is plotted against effective confining stress ( $\bar{\sigma}_3$ ). For loose (contractive) soil at an initial state represented by point A in fig. 6.28A, shear deformation during failure moves the soil state toward the steady-state line. If defor-

mation is undrained, the increased pore pressures result in a horizontal path to point B, at which steady-state flow conditions would be attained. This path is the common result of strongly contractive behavior in soils without high permeability, and so it is emphasized by shading in figure 6.28A. Any contraction permitted by drainage during shear reduces  $e$  and thus shifts the state downward to a point such as C. The unlikely circumstance of drained conditions, in which there is no increase in pore pressure, would permit a vertical path to point D on the steady-state line.

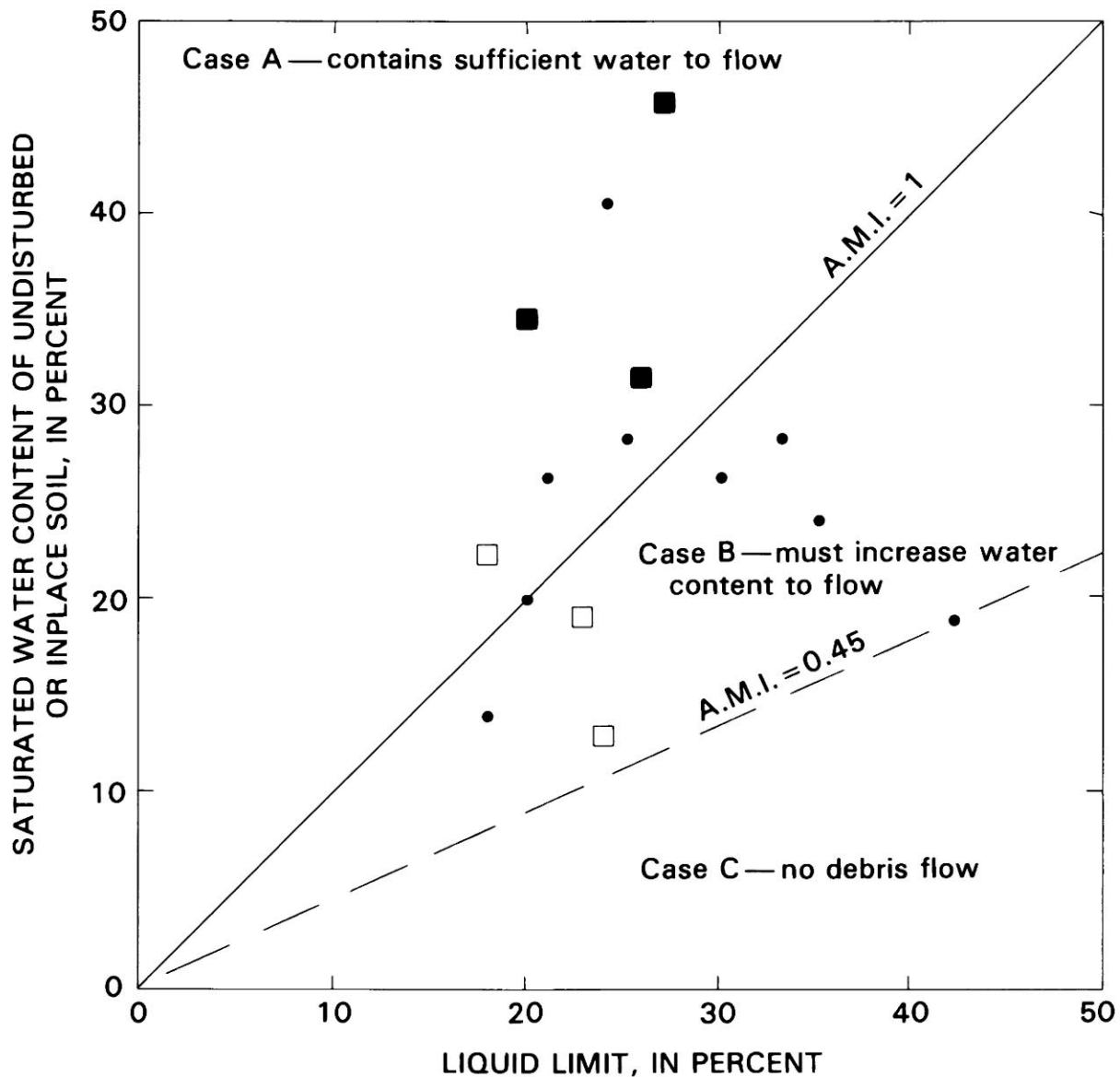


FIGURE 6.26.—Relation between saturated water content and liquid limit for soils in table 6.1 that mobilized as debris flows during the storm. Approximate mobility index (A.M.I.) is ratio of saturated water content to liquid limit. Dashed line, lower limit of A.M.I. for soils that flowed in the storm; upper limit is 1.70. Squares represent soils in two-layer soil slip/debris flows at three sites in Marin County: solid squares, dark surficial soils; open squares, tan subsoils.

Dense (dilative) soils, in contrast, must draw water to the dilating zone for deformation to continue, and so dilation, and the mobilization that may result, requires time, particularly in soil of low permeability. On the state diagram in figure 6.28B, shear deformation shifts the state upward (increases  $e$ ) from a prefailure, critical-equilibrium state (point E) that lies below the steady-state line. Drained conditions with no change in effective stress would permit a vertical path to point F. Partially drained and undrained conditions would result in paths toward the right in figure 6.28B, such as to points G and H. However, paths that veer far to the right are unlikely in rainfall-triggered landslides, particularly where soil is noncohesive, because movement and the resulting deformation in the basal shear zone are brought about by low effective confining stress; in such landslides the basal shear strain is probably held to a rate that permits enough drainage for movement. Paths that veer somewhat to the left from point E could occur, for example, if continuing rainfall during drained deformation increased pore pressures sufficiently to reduce the effective confining stress below the value at point E. In general, however, state paths in dilative soils in basal shear zones of rainfall-induced landslides probably are constrained to a nearly vertical zone, as shown by shading in figure 6.28B.

#### POSSIBLE MEANS OF MOBILIZATION

When the steady-state concept is combined with the M.I. approach, means of mobilization can be portrayed on state diagrams through relations among three factors: the initial state, the steady-state line, and the minimum void ratio needed for flow from the scar ( $e_f$ ), which corresponds uniquely to the strength  $k_f$  defined by equation 2 when  $T$  equals the slide thickness. Figure 6.29 portrays these factors for examples of both contractive and dilative soils, with the likely paths of contractive and dilative behavior shown by shading.

If these three factors were independent, there would be six relations logically possible among the factors, defining six possible cases of mobilization or absence of mobilization. The value of  $e_f$ , however, is not independent of the other factors. To define the position of  $e_f$  along the steady-state line in figure 6.29, particular hypothetical examples of dilative and contractive soils are plotted. These particular soils are noncohesive, have similar steady-state behavior as represented by the single steady-state line, and have similar unit weight; each soil lies under a slope of inclination  $\beta$  in a potential failure zone at depth  $h$  that is at critical equilibrium under slope-parallel seepage with saturation to the ground surface. These soils thus have similar effective confining stress before deformation, in each case resulting from the normal component of buoyant weight of the soil (fig. 6.29; see Lambe and Whit-

man, 1969, p. 354). The position of  $e_f$  on this plot can be determined by noting that the driving shear stress at failure of an infinite slab of thickness  $h$ , under conditions of slope-parallel seepage with saturation to the ground surface, equals the driving shear stress for the limiting case of flow at the same thickness ( $T=h$  in eq. 2), namely, the downslope component of saturated weight of the soil per unit area (see Lambe and Whitman, 1969, p. 354; Johnson, 1970, p. 488). Thus, the frictional strengths mobilized in resistance, and their corresponding effective confining stresses, must also be equal, and the limiting-case steady-state void ratio  $e_f$  must correspond to point C in figure 6.29.

Mobilization probably requires void ratios somewhat greater than  $e_f$ , as mentioned previously, and so the void ratio at liquid limit is shown in figure 6.29 to approximate the lower limit of void ratios likely to mobilize. The plotted position of liquid limit represents a strength severalfold lower than  $k_f$ . Plotting the position of the liquid limit also clarifies the relation of the A.M.I. to the state diagram. Where A.M.I. $>1$ , initial conditions fall above the void ratio at the liquid limit, in the upper part of figure 6.29. Where A.M.I. $<1$ , initial conditions fall below the void ratio at the liquid limit. Thus, the A.M.I. serves as a guide to contractive or dilative soil behavior in shallow landslides.

With the basic relations among these factors defined as in figure 6.29, two principal cases of mobilization emerge, the contractive and the dilative. These results confirm the impressions of many investigators, as reported by Costa (1984, p. 270), that liquefaction and dilation constitute the principal processes of debris-flow mobilization.

#### CONTRACTIVE CASE

For strongly contractive soils, shear deformation at the base of the slide results in paths like path 1 from point A (fig. 6.29). Such paths result in steady-state void ratios that are much greater than  $e_f$ , and so flow from the scar can occur readily by liquefaction (as defined by Poulos and others, 1985). Mobilization is essentially instantaneous because strains of only about 1 percent are sufficient to initiate liquefaction (Casagrande, 1976). Mobilization is typically complete because strength is so greatly reduced upon small strain. Deposits that reflect critical thickness are much thinner than the parent scar because slurry strength is much less than  $k_f$ ; thus, travel distance may be great because little material tends to be left along the path (Cannon, 1985, 1986). Deposits are of smooth consistency because excess water was present initially throughout the saturated portion of the soil. This means of mobilization corresponds approximately to case A of figure 6.26 (A.M.I. $>1$ ).

For soils that are weakly contractive or that have sufficient permeability to permit significant drainage, state

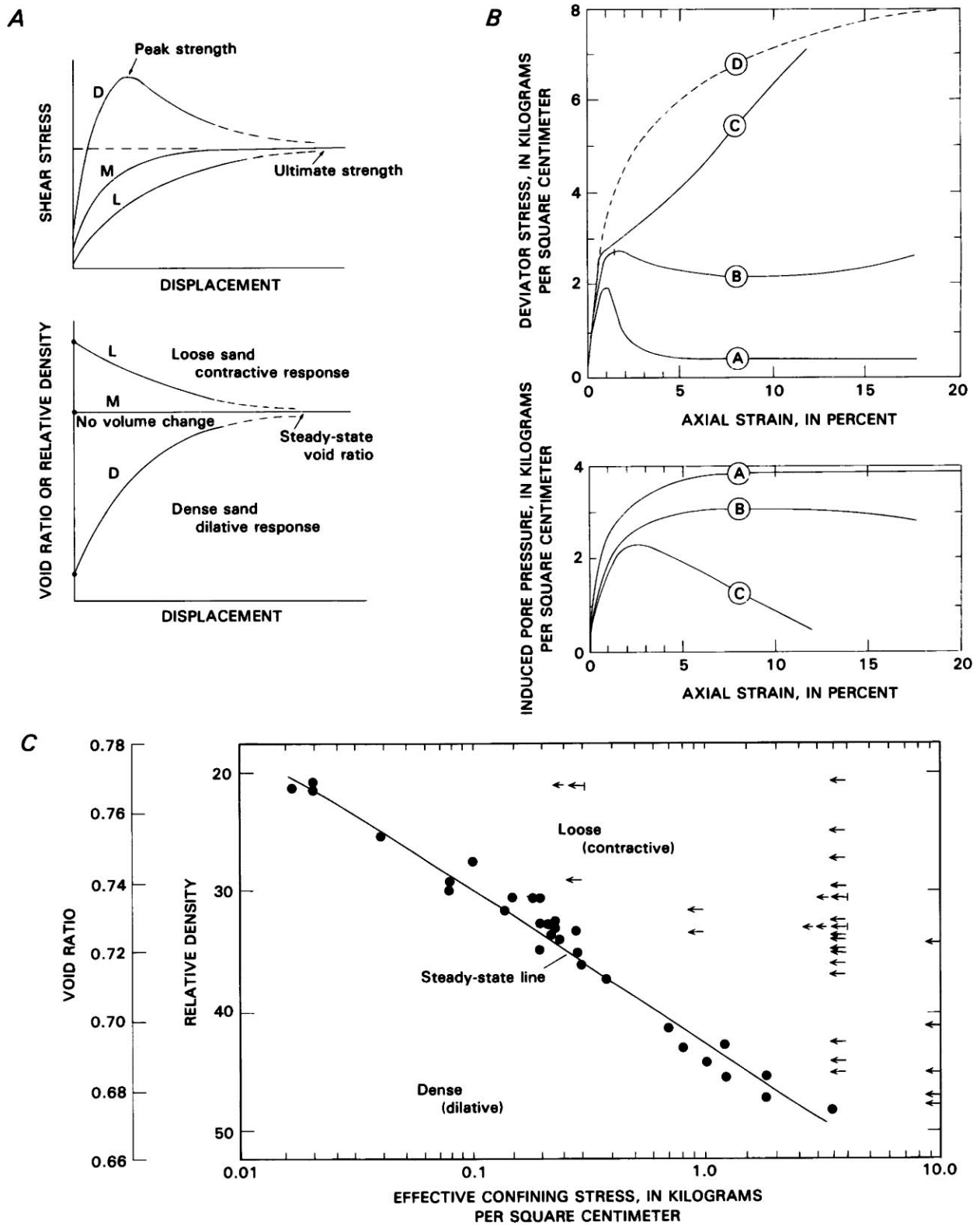


FIGURE 6.27.—The steady state of sands (modified from Casagrande, 1976, figs. 1, 3, 6). A, Shear stress (upper plot) and void ratio (lower plot) as functions of displacement, from drained direct shear tests

on sand at different initial densities. D, dense sand; L, loose sand; M, sand initially at steady-state void ratio. A steady-state void ratio is approached during shear from either a dense or a loose initial

paths will intersect the steady-state line lower down (such as path 2, fig. 6.29). Here, the steady-state void ratio is closer to  $e_f$  and the resulting flows are stronger. Where drainage is complete or where soil is barely contractive (initial condition A', figure 6.29), the soil may not mobilize because the steady-state void ratio may be less than the void ratio at the liquid limit.

#### DILATIVE CASE

Dilative soils in the basal shear zone start from states such as B, below the steady-state line (fig. 6.29). Dilation by basal shear deformation during failure results in paths like path 3, which reach the steady-state line with void ratios near  $e_f$ , marginally capable of flow from the scar. Such paths may originate somewhat to the right or left of point B, and then follow more or less vertical paths to the steady-state line. Paths to the right of path 3 would occur in cases where failure is triggered by pore pressures lower than those resulting from slope-parallel seepage with saturation to the ground surface. Under the conditions illustrated in figure 6.29, such paths could not attain mobilization through steady-state behavior in the basal shear zone. Paths to the left of path 3 would occur in cases where failure is triggered by pore pressures greater than those represented by path 3.<sup>3</sup> Such high pore pressures promote mobilization by steady-state deformation in the basal shear zone, and mobilization by this means can be complete because the entire basal shear zone can undergo sufficient dilation.

In many cases, dilative soils probably cannot mobilize solely by steady-state deformation of the basal shear zone. Slide movement may not be sustained enough to reach the steady state, in part because cracks opened by movement tend to lower water levels in the slide mass, and steady-state void ratios, if achieved, may not be quite sufficient for flow. Parts of the sliding mass, however, may be mobilized by local dilations that result from deformation outside of the basal shear zone. Such partial mobilization may occur along the flanks of the slide, where shear may be accompanied by extension and by abundant water channeled along pullaway cracks, and at the toe of the slide, where dilation may be accompanied by abundant

water and oversteepened slopes. Dilation from such sources is reflected in the pattern of flows shown in figure 6.19. Major deformation also occurs where the slab passes over the lip of the scar (fig. 6.30). Bending here causes successive dilations and contractions that, with sufficient water, would promote mobilization.

Mobilization by dilation is slower than by liquefaction because the water content must increase. Deposits that reflect critical thickness are thinner than the scar depth, but they are typically thicker with respect to scar depth than are deposits mobilized by liquefaction; thus, travel distance is generally less. Deposits are lumpy because water content has increased in some parts of the mass more than others, as when milk is added to oatmeal. Dilative mobilization is documented in the Salmon Creek case study below and by Fleming and others (in press). This means of mobilization corresponds approximately to case B in figure 6.26.

The foregoing analysis of mobilization has focused largely on behavior in the basal shear zone. Mobilization of a slide mass is also facilitated by other deformations incurred as it moves from the scar, some of which are illustrated in figure 6.30. The results of these deformations are influenced by soil state in the general manner discussed above. In homogeneous soil, deformation in the body of the slide mimics that in the basal shear zone and thus results in the features described above for each case. Where soil is heterogeneous at a site, means of mobilization and the resulting features may be mixed.

#### MOBILIZATION DURING THE STORM

Although we lack the steady-state test data needed to identify the specific means of mobilization that occurred in the storm, the wide range in A.M.I. (fig. 6.26) suggests that mobilization occurred by both contractive and dilative means. The debris flows that eyewitnesses observed to follow from slow sliding probably occurred in dilative soils, whereas apparently instantaneous debris flows probably resulted from liquefaction of contractive soils. Empty scars, as shown in figures 6.1 and 6.3, probably resulted from contractive behavior, although complete mobilization is possible also in dilative soils. The partial mobilization shown in figure 6.19 is typical of dilative behavior. Nonmobilized slides, such as those shown in figures 6.22 and 6.23, probably occurred in dilative soils. The following case studies illustrate these means of mobilization.

<sup>3</sup>Regardless of loose or dense soil behavior, initial conditions well to the left of line AB approach the quick conditions ( $\bar{\sigma}_3 = 0$ ) described by Iverson and Major (1986).

state. B, Deviatoric stress (upper plot) and induced pore pressure (lower plot) as functions of axial strain ( $\epsilon$ ), from undrained triaxial tests on sand at different initial relative densities after consolidation ( $D_{rc}$ ). Curves: A,  $D_{rc} = 30$  percent, 0.2 s from peak to  $\epsilon = 18$  percent; B,  $D_{rc} = 44$  percent, 0.4 s from peak to  $\epsilon = 18$  percent; C,

$D_{rc} = 47$  percent, 37 minutes to  $\epsilon = 12$  percent; D, drained test for comparison,  $D_{rc} = 30$  percent. C, Steady-state void ratio as a function of effective confining stress. Arrows, start of test (after consolidation); dots, liquefaction. Actual liquefaction occurred only in loose (contractive) soil.



REED (CASE STUDY 7, PL. 5)

By STEPHEN D. ELLEN, PHILIP C. LAHR, and SUSAN H. CANNON

Several soil slip/debris flows and other landslides occurred during the storm on a hill near Reed, in the southern part of Marin County (fig. 6.31). Residents witnessed four debris-flow events from the wooded northwest side of the ridge between 1:00 and 9:00 p.m. P.s.t. January 4 (E.W. Hart, written commun., 1983); these events probably correspond to the four scars in the northwestern part of figure 6.31. Sounds of snapping trees accompanied the afternoon events. One house, approximately 275 to 300 m from the soil-slip scars and 180 m from the nearest point of the debris-flow trail, shook noticeably during at least one of these events (Harry North, Jr., oral commun., 1982).

Lahr (1982) tested materials from five of the landslides shown in figure 6.31. Most of these landslides were soil

slip/debris flows, both in woodland (site 1, fig. 6.31) and in grassland (sites 2-4). For comparison, he also sampled clayey soil from a complex of earth slides, small parts of which had mobilized as a slow-moving debris flow (site 5). The results of his field and laboratory tests are listed in table 6.1 and plotted in figures 6.16 through 6.18 and figure 6.26.

Scars of the soil slips studied by Lahr are underlain by Franciscan metasandstone; similar bedrock underlies the entire area, according to mapping by Rice and others (1976). The scars occur in granular soil mantle derived from metasandstone, similar to the soil mantle over Franciscan sandstone in the bay region. Permeability contrasts are present in bedrock near each of these soil-slip scars, as evidenced by springs emanating from scars (sites 1, 2, fig. 6.31) and by clayey materials immediately downslope of scars (sites 1, 3, 4). Proximity of these scars to permeability contrasts suggests the influence of water-concentration mechanisms that operate along bedrock contacts. Slopes at these scars range from  $21^\circ$  to  $27^\circ$ ; these relatively gentle slopes of failure (see fig. 6.16) suggest elevated pore pressures that can accompany these water-concentration mechanisms.

Sites 2 and 3 show evidence of two distinct flows from each scar (fig. 6.32). At each site, one flow developed from dark surficial soil, and one from underlying tan colluvial soil; a zone of clay enrichment separated these two soils. In each case, the first material to flow from the scar was the dark, organic-rich surface layer. This material left a broad trail, largely of flattened grass, bounded by low (approx 10 cm) lateral deposits that were smooth textured except for lumps of sod, suggesting a broad thin sheet of fluid, fast-moving slurry (figs. 6.33, 6.34). The second flow in each case involved the tan inorganic lower part of the soil mantle; at site 3, where relations were clear, this second flow resulted from partial mobilization. This flow left a narrower trail lined by generally thicker (approx 30 cm) and lumpier lateral deposits and including more abundant patches and lumps of deposit within the trail (figs. 6.33, 6.34), suggesting a stronger, less fluid slurry that moved as a thicker sheet. The single scar suggests that both flows began mobilization at the same instant from a sliding failure that extended down into the tan colluvial soil; otherwise, the precise superposition of scars would be fortuitous. Thus, the time interval between the two flows apparently resulted solely from different rates of mobilization.

The behavior of these two-layer soil slip/debris flows is clarified through the test results plotted in figure 6.26, which include data for a third site that shows similar relations (see Salmon Creek case study below). At all three sites, dark surficial soil has A.M.I.  $>1$ , suggesting contractive behavior. The underlying tan soil at site 3 and at Salmon Creek had A.M.I.  $<1$ , suggesting dilative behavior;

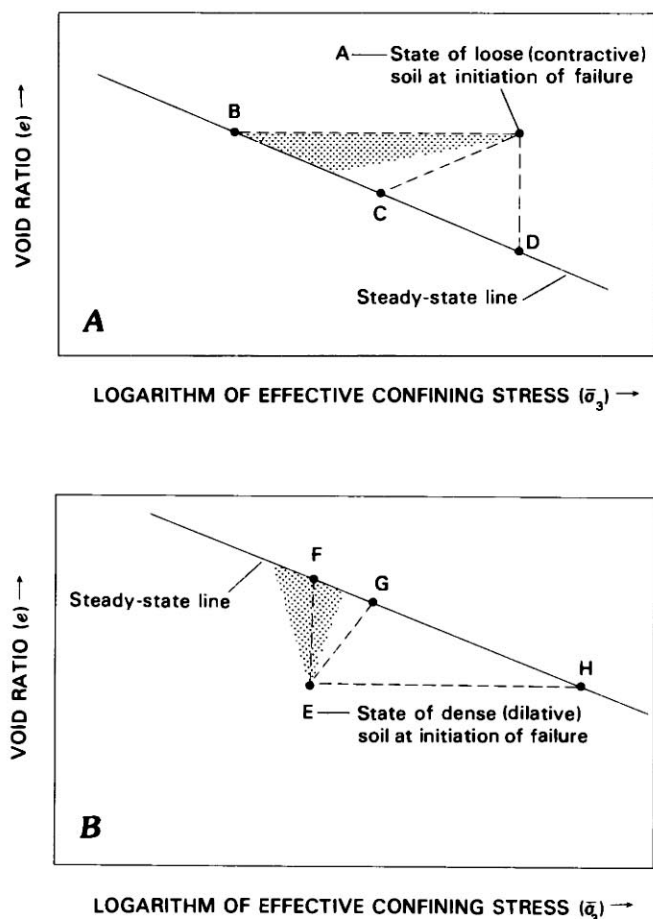


FIGURE 6.28.—“State diagrams” illustrating changes in state during deformation of contractive soil (A) and dilative soil (B). Shading shows state paths likely in rainfall-induced landslides. Letters identify state paths discussed in text.



at site 2, the A.M.I. of tan soil was slightly greater than 1, and so this soil appears to be slightly contractive. Thus, these results are consistent with the observed relations between rapidly mobilized, thin, smooth deposits derived from the dark soil, and more slowly mobilized, thicker, lumpy deposits derived from the tan soil.

Some features of the deposits at these sites may have been influenced by other factors. Water held by the grass before passage of the flows probably was incorporated into the flows and contributed to thinning and smoothing of the first flow episode at each site. Geometry of the landslide failure surface probably also affected the results. Because rotational slides tend to stabilize themselves by movement, they are less likely than slab slides to mobilize completely, particularly for soils that must dilate to flow. Partial mobilization at these sites may have resulted in part because sliding in the tan soil involved considerable rotation.

Similar modes of failure and mobilization occurred at other sites. Failure of dark surficial soil without failure of underlying tan soil was common during the storm (Davenport, 1984; see subsection entitled "Brookhaven Site" in chap. 9). At Canham Road (see chap. 8), a rapid debris flow of black soil, followed by less-fluid debris flows, suggests a two-layer soil slip/debris flow.

#### SALMON CREEK (CASE STUDY 8, PLS. 5, 6)

By STEPHEN D. ELLEN, ROBERT W. FLEMING, and MITCHELL A. ALGUS

The features shown in figure 6.35 resulted from a complex landslide in which some parts mobilized as debris flows and another part slid approximately 1 m and rotated slightly but did not mobilize. The site is described more fully by Fleming and others (in press). R.W. Nichols and S.H. Cannon assisted in sampling and testing. We appreciate access to the site granted by Alvin and Robert Gambonini.

The landslide developed in a broad subtle swale near the base of a nearly planar hillslope adjacent to an alluvial terrace along Salmon Creek. Franciscan sandstone is exposed in the scar, and the hillslope was mapped as Franciscan sandstone by Blake and others (1974). The dominantly colluvial soil in which the landslide occurred is granular and slightly cohesive (SM or SC of the USC system), similar to soil over Franciscan sandstone elsewhere in the bay region. The soil mantle consists of a dark layer (dry density,  $1.40 \text{ g/cm}^3$ ) extending from the ground surface to 0.6-m depth, a clay-rich zone (dry density,  $1.88 \text{ g/cm}^3$ ) from 0.6- to 0.9-m depth, and a homogeneous tan colluvium (dry density,  $1.75 \text{ g/cm}^3$ ) from 0.9 m to bedrock at about 2- to 2.5-m depth. Features in a large concavity

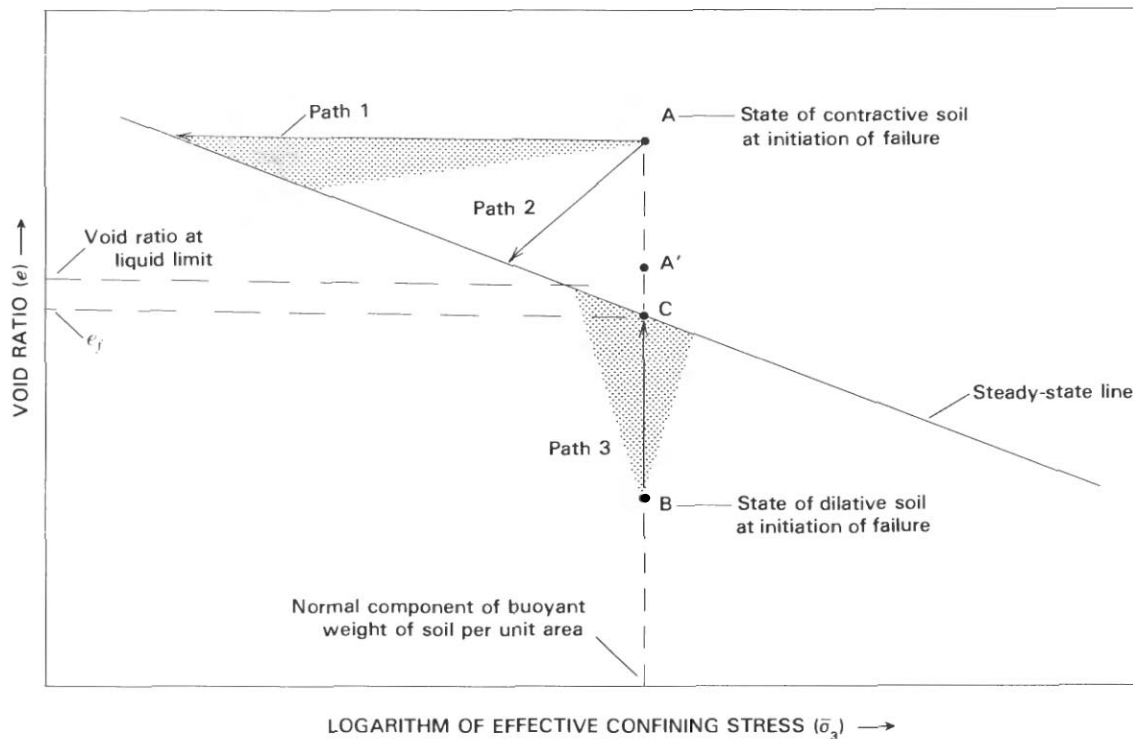


FIGURE 6.29.—“State diagram” showing contractive and dilative means of mobilization. Shading shows state paths likely in rainfall-induced landslides from initial conditions A and B; points A' and C are discussed in text. Steady-state void ratio greater than  $e_f$  is necessary for debris flow from soil-slip scar. Initial conditions that plot above void ratio at liquid limit have A.M.I.>1.

upslope from the site suggest past soil-slip activity; the soil mantle at the site probably consists of, or is derived from, deposits of these past events.

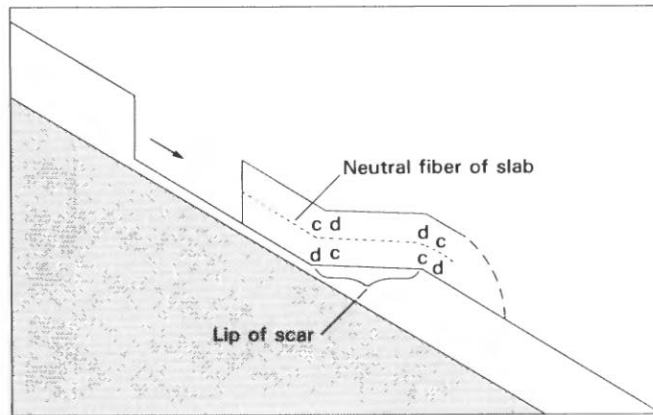


FIGURE 6.30.—Schematic downslope cross section of soil slip/debris flow as it leaves scar, showing zones of dilation (d) and contraction (c) in slab as it passes over lip. Position of neutral fiber depends on behavior of soil.

Seepage, which occurred for at least several months after the storm from a broad zone directly below the scar (fig. 6.35), suggests the presence of permeability contrasts that during the storm may have resulted in out-of-slope seepage. The uncommonly gentle ( $22^\circ$ ) slope of failure in typical materials suggests elevated pore pressures, which could result from out-of-slope seepage.

Principal landslide features (fig. 6.35) are the large arcuate scar from which materials mobilized; the slab remaining within the arc of the scar; and the debris-flow deposits that lead downslope from both ends of the scar, then turn on the very gently sloping terrace surface to extend beyond the left side of figure 6.35.

Both the deposits and scar showed evidence of two-layer soil slip/debris flows. In trails leading from both ends of the scar, lateral deposits of tan soil, which were lumpy and commonly at least 60 cm thick, lay nested within thin (max 10 cm thick) lateral deposits, consisting largely of grass clods, mobilized from the dark upper layer. This nested relation indicates that the dark soil flowed first. At both ends of the arcuate scar, paired dark lateral deposits led from the very edges of remnants of shallow scars in the dark surface layer. Several lateral deposits

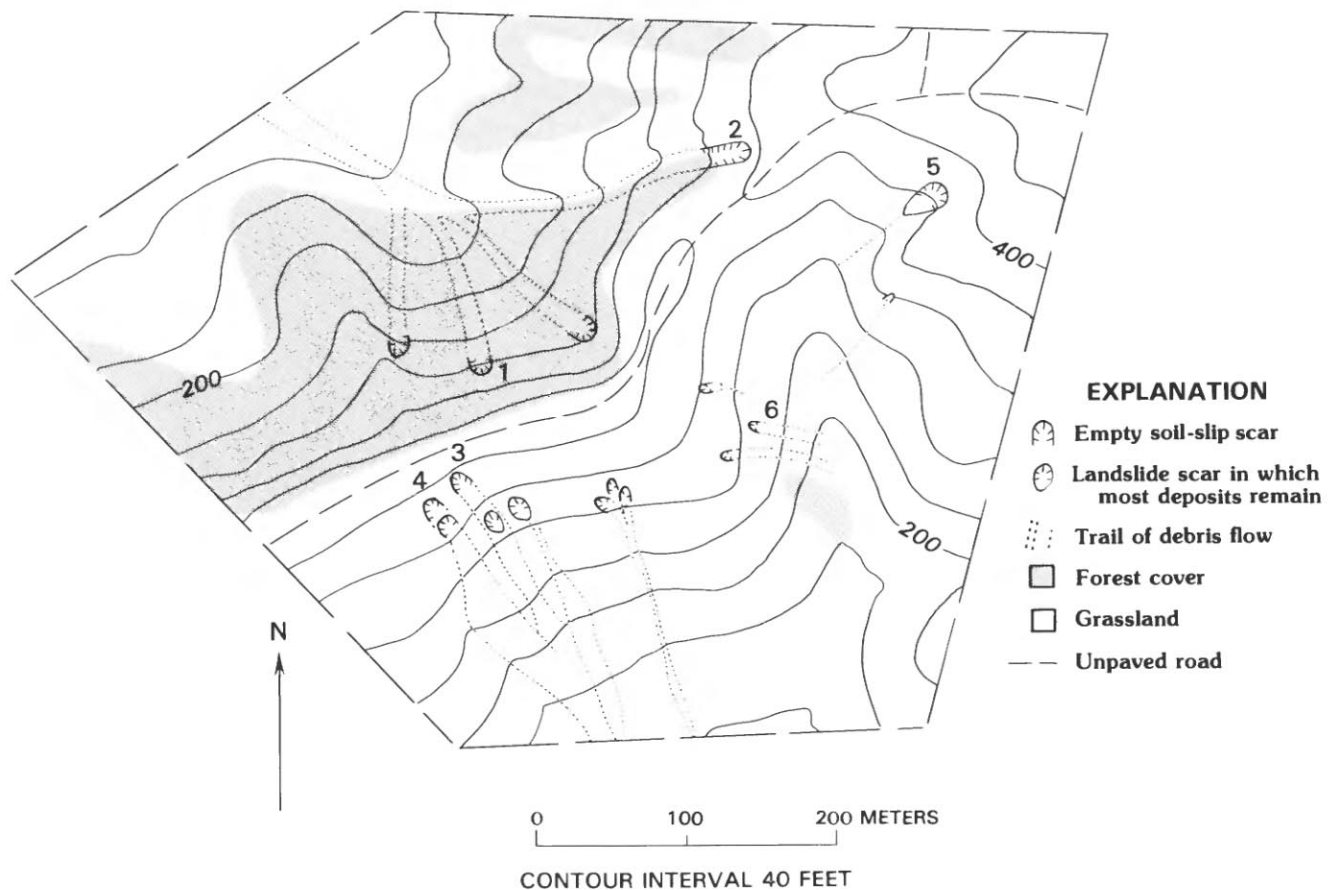


FIGURE 6.31.—Storm-generated landslides near Reed, Marin County. Sites 1 through 5 denote landslides studied by Lahr (1982); site 6 is a landslide from which samples SQ-15A and SQ-15B (table 6.1) were taken. Base enlarged from U.S. Geological Survey San Rafael (1954) and San Quentin (1959) 7.5-minute quadrangles.

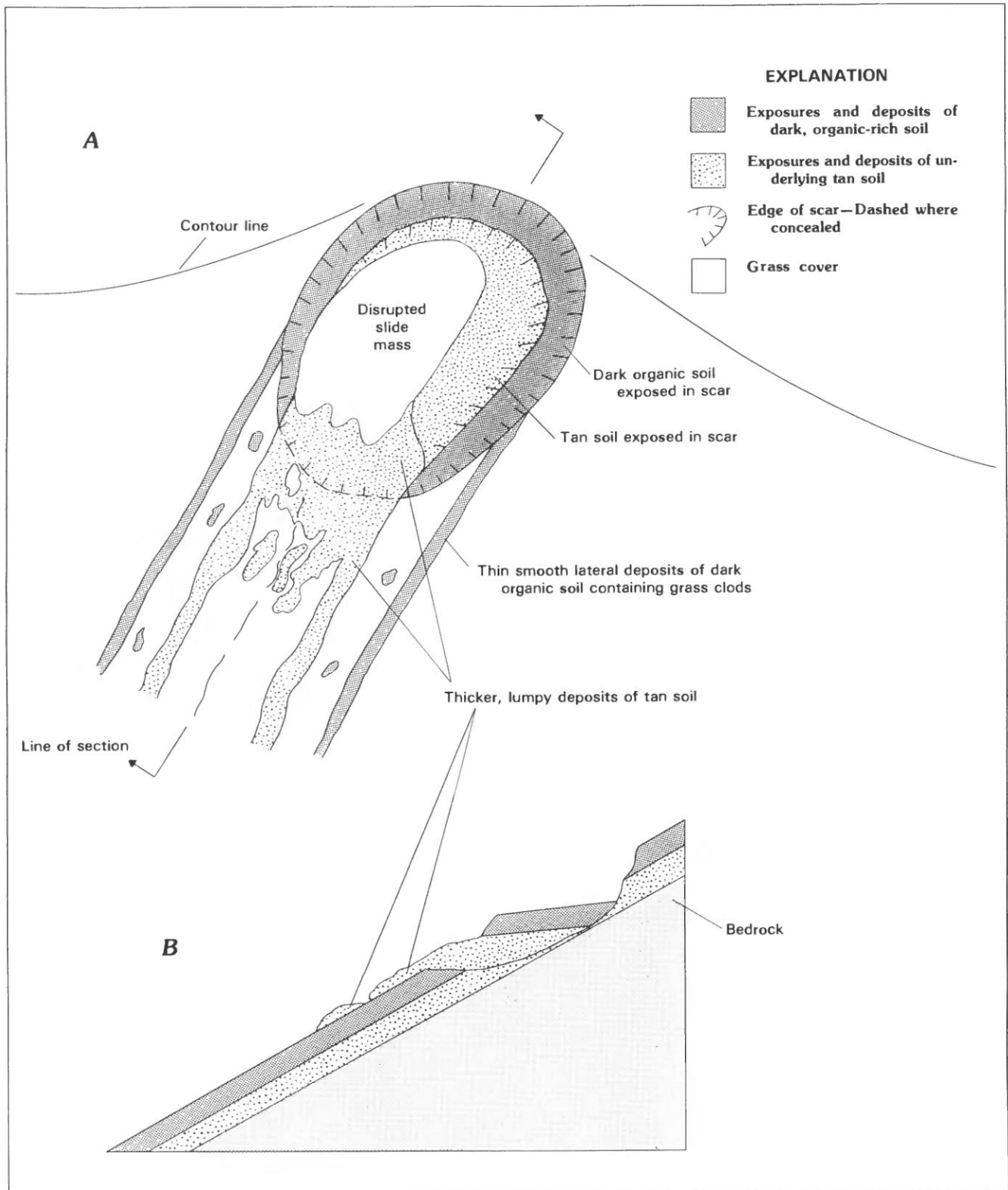


FIGURE 6.32.—Schematic map (A) and downslope cross section (B) showing features typical of two-layer soil slip/debris flows. Figure 6.32B shows only those deposits in plane of cross section. Grass cover not shown in cross section.

of tan soil extended from the lips of the scar, at least on the end of the scar at the right side of figure 6.35, but identification of matching pairs is complicated by the partially mobilized slump (including nonmobilized dark surficial soil) that occupied most of the right half of this trail, upslope from the calf.

Laboratory testing described representative samples (table 6.1) and concentrated on factors affecting mobilization. The dark soil had A.M.I. = 1.70, suggesting contractive behavior; the tan soil had A.M.I. = 0.83, suggesting dilative behavior. Typical samples of the tan soil, which was studied in more detail, had liquid limits 3 to 4 percent higher than saturated water contents, and slurries that would pour from a beaker could be mixed with as little as 2 percent water beyond the liquid limit. An undisturbed sample of the tan soil, collected just above the basal shear zone, showed dilation in simple shear under confining pressure appropriate for the depth of the basal shear zone (approx 1.5 m). The measured dilation corresponded to a 3.4-percent increase in saturated water

content, and the sample may not have reached its steady-state void ratio. Thus, shear dilation near the slip surface was apparently sufficient or nearly sufficient to increase water content to the liquid limit, and thus barely sufficient to mobilize debris flows from the tan soil.

The landslide features and measured soil properties suggest the following sequence of events.

1. Failure occurred in the shear zone that defines the base of the slab, near the base of the tan soil. The sliding mass occupied most of the volume of the present empty scar plus the slab remaining. Sliding of the large mass was slow and probably sporadic because the soil at the slip surface was dilative; if this soil had been contractive, small displacements of the mass would probably have resulted in liquefaction and consequent rapid movement of the entire mass.
2. Movement of the slide mass affected the hillslope in two principal ways: (i) By opening a pullaway crack at the crown, it interrupted throughflow and surface flow to the slide mass, tending to arrest its movement,



FIGURE 6.33.—Deposits from two-layer soil slip/debris flow near Reed, Marin County. Dark surficial soil forms thin deposit of relatively smooth consistency near auger; underlying tan colluvial soil forms thicker lumpy deposits at bottom center of view.

- and channeled this flow toward the flanks of the slide, promoting further movement there; and (ii) it dilated soil in the basal shear zone and in other parts of the landslide, particularly near the flanks, head, and toe, where dilation could result from extension and shear.
3. Near the flanks of the slide mass, elevated water levels induced failures in the weakened materials. First, the contractive dark surface soil mobilized rapidly by liquefaction to produce a fluid flow that left thin lateral deposits. Then, the tan soil, dilated by extension and shear, mobilized slowly as a more viscous slurry that left thick lumpy deposits, reflecting dilation to a water content barely sufficient for debris flow down the hillslope. The remaining slab did not mobilize because either it was stabilized by slight rotation, access of water was insufficient for continued failure, or dilation from basal shear alone was insufficient to mobilize the soil.
  4. Failure and mobilization occurred in the crown area of the slide (to complete the arc of the scar), in the slump near the right side of figure 6.35, and at the subsidiary scars that cut back into the main scar. Erosion by seeping and running water modified the scar throughout the sequence.

#### PREDICTING MOBILIZATION

The foregoing analysis provides three principal methods for predicting mobilization of debris flows from soil slips: clay content, A.M.I., and steady-state soil testing. Clay content provides a crude first cut at predicting susceptibility to debris flow at sites subject to shallow slope failure. Soils with clay contents between 3 and 35 percent were capable of debris flow in the storm, and a more limited sample of fast-moving debris flows from hillslopes in long-term equilibrium showed clay contents generally between 8 and 25 percent (fig. 6.17). The breadth of these ranges, however, makes this measure, by itself, of limited use.

The ratio of saturated water content to liquid limit, the A.M.I. (fig. 6.26), distinguishes in approximate manner soils capable of rapid mobilization by liquefaction ( $A.M.I. > 1$ ) from soils that must dilate to flow ( $A.M.I. < 1$ ). This index also provides an empirical limit for soils susceptible to soil slip/debris flow (boundary between cases B and C, fig. 6.26;  $A.M.I. = 0.45$ ), and the simplicity of this index encourages additional testing that can define this boundary more precisely. Clay content or plasticity of soils may be a useful supplement to the A.M.I. for evaluating the susceptibility of dilative soils. At sites where failure is likely, the A.M.I. provides a simple and inexpensive means of predicting the likelihood of debris flow and the nature of its initiation.

The most precise site-specific method of prediction permitted by this analysis uses the liquefaction-evaluation

procedures of Poulos and others (1985) to determine the steady-state parameters of critical soils at sites of potential failure. These procedures permit determination of the initial state and the steady-state line, and thus the soil's contractive or dilative behavior, the magnitude of divergence from steady-state conditions, and the steady-state strengths that can be expected. When combined with liquid limit or a more precise measure of conditions needed for flow, these measures provide as precise a description as possible of the aspects of soil behavior critical to mobilization. Testing required by the steady-state method may be complicated by heterogeneity of materials, coarse particles in the soil, and the low confining stresses that characterize shallow landslides.

#### SUMMARY

Almost all the debris flows induced by the storm mobilized directly from soil slips. Theoretical analysis and limited test data indicate that the rapid and complete mobilization that produced thin lateral deposits resulted from liquefaction of contractive soils, whereas mobilization that was slow and partial, or slide movement that did not produce debris flow, resulted from dilative soil behavior. The means of mobilization may be evaluated in approximate or precise fashion by soil testing. Such evaluation will help in predicting: (1) the potential for mobilization—whether debris flow is likely from a given slide or potential slide; (2) the completeness of mobilization—the proportion of a slide or potential slide that may be expected to transform into debris flow; (3) the speed of mobilization—the lag time between initial failure and flow; (4) the velocity and thickness of flow from the scar, based on likely strength of the slurry; and (5) the travel distance of the debris flow.

#### TRAVEL

Debris flow, as modeled by either simple plastic or Coulomb viscous (Bingham) material, consists of a relatively rigid plug riding on a zone of slurry that is undergoing flow (fig. 6.24; Johnson and Hampton, 1969; Johnson, 1970, 1984; Rodine, 1974). Travel of debris flows can be analyzed by using the concept of critical thickness, the thickness of the rigid plug, as discussed above in the subsection entitled "Transition from Slide to Flow." For a debris flow to travel, its thickness must remain greater than its critical thickness; deposition occurs where the plug bottoms out, as the flow's thickness decreases to its critical thickness. The critical thickness of a simple plastic or Bingham material in a broad channel is described by equation 2, in which the critical thickness  $T$  varies directly with the strength of a slurry. According to Johnson and Hampton (1969, fig. 3.3), the strength of a slurry is determined chiefly by its water content and the proportions



of various grain sizes. Pierson (1981) showed that slurry strength also depends on pore pressures within the slurry, which dissipate after deformation ceases.

Equation 2 shows the effect of change in slope on travel of debris flows. Where slope steepens along the path, decrease in the critical thickness promotes flow. Where slope decreases along the path, a greater critical thickness must be maintained for flow to continue.

#### EFFECT OF CHANNELS

Because debris flow requires a critical thickness of slurry, a channel greatly facilitates sustained flow. As expressed by Rodine (1974, p. 69), " \* \* \* flow containment appears to be a necessary condition for continued flow of debris flows." Drainage channels may further promote flow by providing additional water to weaken the slurry.

During initial flow from soil-slip scars, debris flows in the storm typically moved without preexisting channels;

in some places, such flows traversed considerable distances (fig. 6.36). During this initial phase of debris flow, lateral deposits left by the leading part of a flow probably channelized the rest of the flow. Once preexisting channels were entered by a debris flow, its chances for sustained flow were greatly enhanced. Those debris flows that traveled farthest moved down channels, and some channels sustained debris flows on gradients as gentle as several degrees (pl. 6).

#### EFFECT OF VEGETATION IN THE PATH

Debris flows in grassland typically left only lateral deposits lining a swath of flattened grass that included bits of muddy deposit (figs. 6.13, 6.15, 6.20). Some of these trails showed evidence of subsequent running water, but most appeared to be as they were left by the debris flow. Movement of slurry over grassland appears to have been accomplished by sliding as well as flow (fig. 6.36). Sliding seems to be reasonable, considering the water-laden con-



FIGURE 6.34.—Two-layer soil slip/debris flow at site 3 near Reed, Marin County. A, Different debris-flow deposits lead from single soil-slip scar. B, Lateral deposit to left of flagged stake in foreground of figure 6.34A consists of soil from organic upper layer of soil mantle. This deposit

is thinner and smoother than light-colored lumpy deposits to right of flagged stake, which derive from lower horizons of soil mantle. Much light-colored lumpy material remains in and near scar as a disaggregated slump that only partially mobilized.

dition of the standing grass and the rapid movement of the debris flows, which would flatten the grass and release water to form a near-frictionless blanket at its base. During movement over grass, incorporation of some of the water released from the grass into the debris flow probably permitted progressive thinning of the deposits.

Brush and trees did not provide such slick paths for debris flows. Such vegetation either caught and held bits of the flow, or was torn from the hillslope to become part of the flow (figs. 6.3, 6.5, 6.8). Brush and trees thus served to transfer some of the downslope force of the debris flow to the path and thereby facilitated additional failures that probably added directly to the volume of the major pulse (see Three Peaks case study above). This effect helps explain the abundance of soil-slip/debris-flow complexes on forested and brush-covered hillslopes, and why such hillslopes appeared to be capable of larger debris-flow events than grassland hillslopes.

The interaction that brush and trees provide between debris flow and path also increases frictional drag on the base of the debris flow. By slowing the front and base of debris flows, frictional drag appears to encourage tall flow fronts by permitting materials from the top and rear of

the flow to overtake materials at the front and base. Such effects help explain observed flow heights greater than scar depth and the tumbling or rolling motion observed at flow fronts (see Three Peaks case study above).

#### DEPOSITION

Debris flows may cease their movement and form deposits for various reasons, most of which can be explained through the concept of critical thickness. Broadening of the channel may decrease flow thickness to the critical thickness. Decrease in channel slope or dewatering of the flow may increase critical thickness to the point of stoppage. Deposits left along the path, described by the lag rate (Cannon, 1985, 1986), may diminish the volume of the flow to the extent that a critical thickness cannot be maintained. And the tendency for concentration of coarse particles at the front and lateral margins of debris flows may lead to strong marginal rims that cause deposition of weaker flow material within (Pierson, 1984).

The most conspicuous deposits left by the storm were lateral deposits, or levees, lining flow paths (figs. 6.15,



FIGURE 6.34.—Continued

6.33-6.36). These lateral deposits generally represented the edges of broad tabular flows, where their thickness decreased toward zero. Except where coarse clasts were concentrated or velocities were great, the thickness of lateral deposits recorded the critical thickness of debris flows.

#### TRIGGERING MECHANISMS WITHIN COMPLEXES

Within complexes of soil slip/debris flows (pl. 4), the spatial association between auxiliary scars and the major path suggests that the auxiliary slope failures were triggered by other failures in the complex, either by loss of support due to movement of adjacent ground or by debris flows passing over the ground surface. The likely influence of different triggering mechanisms can be explored through time relations among scars in a complex and through the likely role of vegetation in the path.

Most of the complexes examined in this study showed evidence of complex sequences of events, suggesting that different parts of a given complex failed at different times during the storm. Within this complexity, however, some consistent time relations emerged. Where one scar was contiguous to the downslope side of another, time relations commonly suggested that the debris flow from the

upslope scar followed a debris flow from the downslope scar; in such places, failure at the upslope scar appeared to have been triggered by removal of support from below. In contrast, where scars lay separated within the path of a debris flow, evidence commonly suggested that these scars were absent when the debris-flow front passed. In such places, auxiliary scars were probably triggered by passage of the major debris flow; otherwise, the strong spatial association between auxiliary scars and the major path would make little sense.

Triggering of auxiliary soil slips by the passage of debris flows could result from three possible mechanisms. Shaking accompanying passage would add dynamic loads to soil in the path. The suddenly imposed weight on soil underlying the path would constitute an undrained loading (Hutchinson and Bhandari, 1971). And the downslope force of the moving debris, where coupled to the path by vegetation, would add directly to the forces facilitating failure. The greater abundance of complexes in forested and brush-covered areas provides a clue to the relative significance of these mechanisms. Whereas shaking and undrained loading would probably not be significantly affected by type of vegetation, the downslope pull of a debris flow would be decidedly more effective in forest or brush than in grassland. Thus, the downslope pull of debris flows

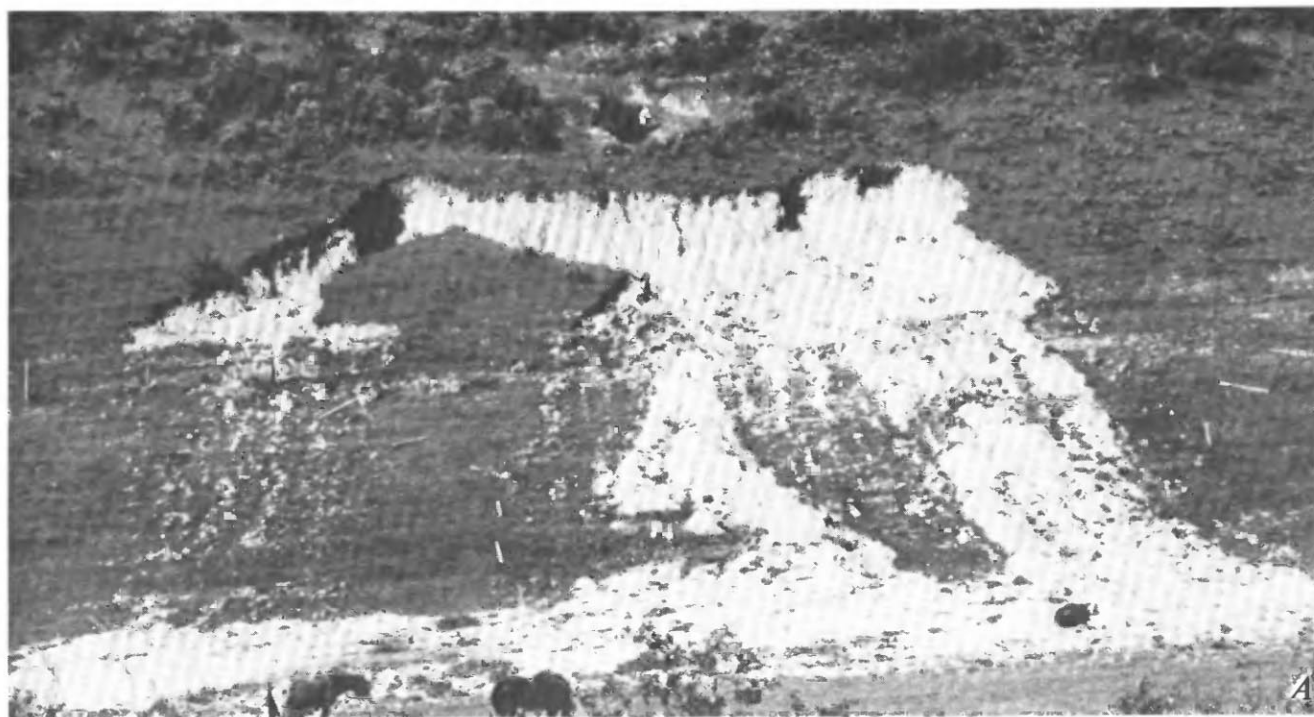


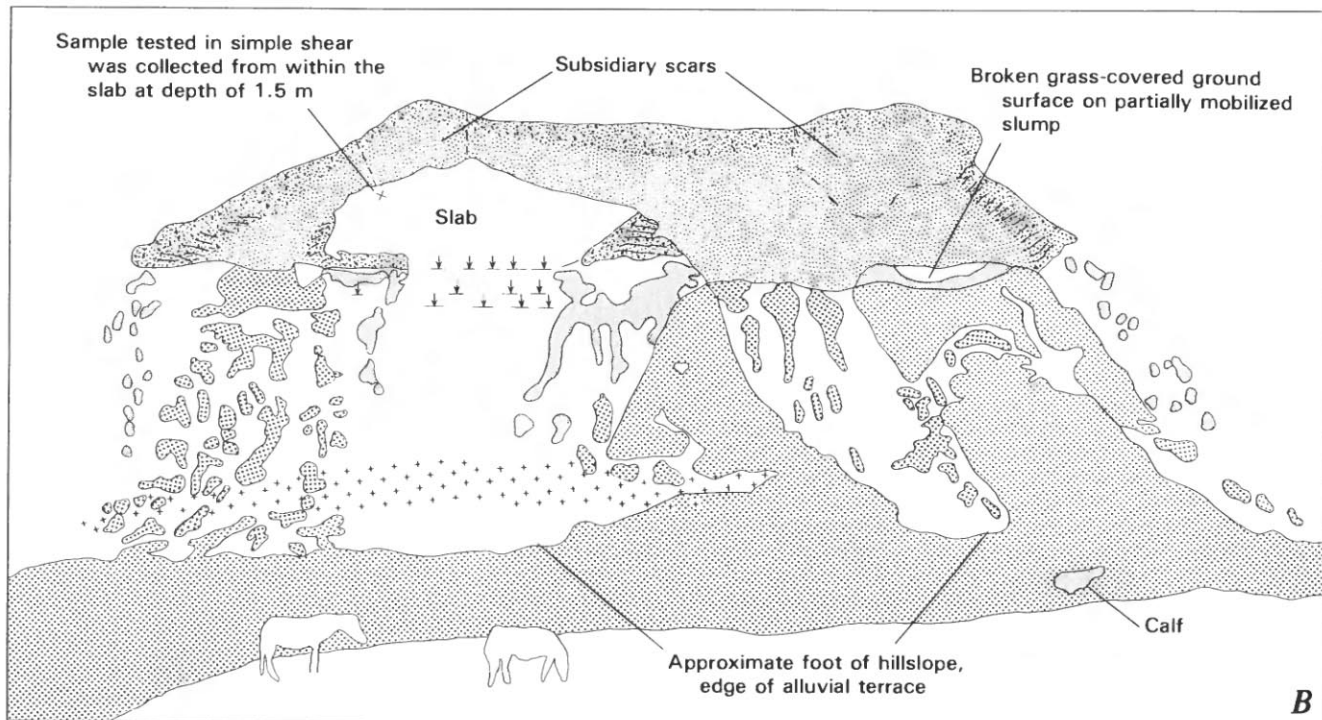
FIGURE 6.35.—Shallow landslide along Salmon Creek, Marin County, of which both margins have mobilized as debris flows. A, Hillside slopes 22° toward observer; alluvial terrace in foreground is approximately horizontal. Slab remaining within arcuate scar (above horses) has slid downslope about 1 m; its toe is near fenceline that formerly crossed hillside horizontally near center. B, Sketch identifying features discussed in text.

on their paths appears to be the most effective triggering mechanism for auxiliary soil slips.

### CONCLUSIONS

Debris flows in the San Francisco Bay region during the storm originated from shallow slides of the soil mantle on steep hillslopes. These soil slip/debris flows varied widely in scale and complexity, from small single events to large complexes in which numerous soil slips apparently were triggered by passage of a major debris flow and thus contributed to its volume.

The distribution and features of soil slip/debris flows triggered by the storm make sense mechanically when the overall process is viewed as a sequence of steps. The perched water tables that triggered failure of the soil mantle generally resulted from a combination of current intense rainfall and concentration of water in the landscape. Failure in most cases can probably be explained by saturation to the ground surface, with seepage parallel to the hillslope, but in some cases failure may have required elevated pore pressures. Soil slips mobilized into debris flows by two principal processes that are reflected in basic features of scars, trails, and timing of events. The



0 5 METERS  
APPROXIMATE SCALE AT SCAR

### EXPLANATION





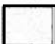




	Ground surface covered by grass or brush		Deposits largely from light-colored soil
	Dark soil exposed in scar		Remnants of slip surface at base of dark soil
	Light-colored soil and bedrock exposed in scar, and lesser light-colored deposits on floor of scar		Area of seepage
	Deposits from dark soil		Slip surface at toe of slab
			Boundary of subsidiary scars

FIGURE 6.35.—Continued



resulting debris flows were sustained by channels and affected by vegetation in their paths.

The following points summarize the practical information gained or confirmed through this analysis.

*Timing with respect to rainfall.*—Soil slip/debris flows generally occurred during intense rainfall or within several hours after intense rainfall. In uncommon cases, where water concentration was delayed by passage through bedrock or by hillslope modifications, debris flows occurred as much as 22 hours after rainfall ceased.

*Susceptible hillslopes.*—Although most soil slip/debris flows originated on slopes of at least  $26^\circ$ , they were commonly reported on slopes as gentle as  $20^\circ$ , and one occurred on a slope of  $14^\circ$ . Most soil slips occupied areas where concavity, break in slope, or geologic contacts could account for a concentration of water, but some occurred in areas without such recognizable features.

*Susceptible soils.*—Soil slip/debris flows occurred in a broad range of soils, from noncohesive sandy soils to moderately plastic soils containing as much as 35 percent

clay-size particles, but none was documented in highly plastic clayey soils. At sites where shallow sliding is likely, susceptibility to debris flow can be determined by steady-state soil testing or estimated from the approximate mobility index (A.M.I.), the ratio of saturated water content to liquid limit. The same index indicates whether mobilization is likely to be partial or complete.

*Movement preceding mobilization.*—Although many debris flows were preceded by detectable sliding movement at the source area, many others probably mobilized without preceding macroscopic movement. The likelihood of detectable antecedent movement at a site can be determined by using the A.M.I. or steady-state soil testing.

*Effect of channels.*—Sustained debris flow generally required a channel, and channels sustained debris flows on gradients as gentle as several degrees.

*Effect of vegetative cover.*—Although abundant soil slip/debris flows occurred in grassland as well as in forest and brushland, large debris flows resulting from complexes generally occurred in forest or brushland.



FIGURE 6.36.—Trail of unchannelized debris flow in grassland near Nicasio, Marin County. Upright clump of sod resting on flattened grass suggests that debris flow slid over ground surface; delicate stems of tall dry grass remain undisturbed by their ride tens of meters downslope. Photograph by S.L. Reneau.



## REFERENCES CITED

- Blake, M.C., Jr., Bartow, J.A., Frizzell, V.A., Jr., Schlocker, Julius, Sorg, D.H., Wentworth, C.M., and Wright, R.H., 1974, Preliminary geologic map of Marin and San Francisco Counties and parts of Alameda, Contra Costa, and Sonoma Counties, California: U.S. Geological Survey Miscellaneous Field Studies Map MF-574, scale 1:62,500, 2 sheets.
- Campbell, R.H., 1975, Soil slips, debris flows, and rainstorms in the Santa Monica Mountains and vicinity, southern California: U.S. Geological Survey Professional Paper 851, 51 p.
- Cannon, S.H., 1985, The lag rate and the travel-distance potential of debris flows: M.S. thesis, University of Colorado, Boulder, Colorado, 141 p.
- 1986, The lag rate and the travel-distance potential of debris flows [abs.]: Geological Society of America Abstracts with Programs, v. 18, no. 2, p. 93.
- Casagrande, Arthur, 1976, Liquefaction and cyclic deformation of sands, a critical review: Cambridge, Mass., Harvard University Soil Mechanics Series, no. 88, 27 p.
- Castro, Gonzalo, 1969, Liquefaction of sands: Cambridge, Mass., Harvard University Soil Mechanics Series, no. 81, 112 p.
- Costa, J.E., 1984, Physical geomorphology of debris flows, chap. 9 of Costa, J.E., and Fleisher, P.J., eds., Developments and applications of geomorphology: Berlin, Springer-Verlag, p. 268-317.
- Davenport, C.W., 1984, An analysis of slope failures in eastern Marin County, California, resulting from the January 3rd and 4th, 1982, storm: California Division of Mines and Geology Open-File Report 84-22SF, 38 p.
- Dietrich, W.E., and Dunne, Thomas, 1978, Sediment budget for a small catchment in mountainous terrain, in Slaymaker, H.O., Rapp, Anders, and Dunne, Thomas, eds., Field instrumentation and geomorphological problems: Zeitschrift für Geomorphologie, supp. 29, p. 191-206.
- Ellen, S.D., and Fleming, R.W., 1987, Mobilization of debris flows from soil slips, San Francisco Bay region, California, January, 1982, in Costa, J.E., and Wiczeorek, G.F., eds., Debris flows/avalanches: Process, recognition, and mitigation: Geological Society of America Reviews in Engineering Geology, v. 7, p. 31-40.
- Fleming, R.W., Ellen, S.D., and Albus, M.A., in press, Transformation of dilative and contractive landslide debris into debris flows, an example from Marin County, California, in Johnson, A.M., ed., Memorial volume dedicated to R.H. Jahns: Amsterdam, Elsevier.
- Hack, J.T., and Goodlett, J.C., 1960, Geomorphology and forest ecology of a mountain region in the central Appalachians: U.S. Geological Survey Professional Paper 347, 66 p.
- Hayes, Joseph, 1985, Hydrologic behavior of a colluvium-filled bedrock hollow [abs.]: Eos (American Geophysical Union Transactions), v. 66, no. 46, p. 897.
- Hutchinson, J.N., and Bhandari, R.K., 1971, Undrained loading, a fundamental mechanism of mudflows and other mass movements: Geotechnique, v. 21, no. 4, p. 353-358.
- Iverson, R.M., and Major, J.J., 1986, Groundwater seepage vectors and the potential for hillslope failure and debris flow mobilization: Water Resources Research, v. 22, no. 11, p. 1543-1548.
- Johnson, A.M., 1970, Physical processes in geology: San Francisco, Freeman, Cooper & Co., 577 p.
- 1984, Debris flow, chap. 8 of Brunsten, Denys, and Prior, D.B., eds., Slope instability: New York, John Wiley & Sons, p. 257-361.
- Johnson, A.M., and Hampton, M.A., 1969, Subaerial and subaqueous flow of slurries: Stanford, Calif., Stanford University, School of Earth Sciences, 137 p.
- Kearney, J.O., 1982, On the long road to recovery; a family's nightmare: Mill Valley, Calif., Record, v. 82, no. 2 (Jan. 13), p. A1.
- Keefer, D.K., and Johnson, A.M., 1978, Mobilization and movement mechanics of earth flows, in Sierakowski, R.L., ed., Recent advances in engineering science: Society of Engineering Science Annual Meeting, 15th, Gainesville, Fla., 1978, Proceedings, p. 223-226.
- Kesseli, J.E., 1943, Disintegrating soil slips of the Coast Ranges of central California: Journal of Geology, v. 51, no. 5, p. 342-352.
- Lahr, P.C., 1982, A study of debris flows and investigation of debris flow theories: San Luis Obispo, California Polytechnic State University, B.S. senior project report, 64 p.
- Lambe, T.W., and Whitman, R.V., 1969, Soil mechanics: New York, John Wiley and Sons, 553 p.
- Leary, Kevin, 1982, Marin residents start wiping up: San Francisco Chronicle, v. 117, no. 304 (Jan. 6), p. 6.
- Moser, Manfred, and Hohensinn, F., 1983, Geotechnical aspects of soil slips in Alpine regions: Engineering Geology, v. 19, no. 3, p. 185-211.
- Peterson, D.M., 1979, Hillslope erosional processes related to bedrock, soils, and topography of the Three Peaks area, Marin County, California: San Jose, Calif., San Jose State University, M.S. thesis, 94 p.
- Pierson, T.C., 1981, Dominant particle support mechanisms in debris flows at Mt. Thomas, New Zealand, and implications for flow mobility: Sedimentology, v. 28, no. 1, p. 49-60.
- 1983, Soil pipes and slope stability: Quarterly Journal of Engineering Geology, v. 16, no. 1, p. 1-11.
- 1984, Why debris flows stop [abs.]: Geological Society of America Abstracts with Programs, v. 16, no. 6, p. 623.
- Pierson, T.C., and Costa, J.E., 1984, A rheologic classification of subaerial sediment-water flows [abs.]: Geological Society of America Abstracts with Programs, v. 16, no. 6, p. 623.
- Poulos, S.J., 1981, The steady state of deformation: American Society of Civil Engineers Proceedings, Geotechnical Engineering Division Journal, v. 107, no. GT5, p. 553-562.
- Poulos, S.J., Castro, Gonzalo, and France, J.W., 1985, Liquefaction evaluation procedure: Journal of Geotechnical Engineering, v. 111, no. 6, p. 772-791.
- Reid, G.O., 1978, The relationships among slope processes, soils, bedrock, and topography in an area of Franciscan terrane in Marin County, California: San Jose, Calif., San Jose State University, M.S. thesis, 90 p.
- Reneau, S.L., and Dietrich, W.E., 1987a, Size and location of colluvial landslides in a steep forested landscape, in Beschta, R.L., Blinn, T., Grant, G.E., Ice, G.G., and Swanson, F.J., eds., Erosion and sedimentation in the Pacific rim: International Association of Hydrological Sciences Publication 165, p. 39-48.
- 1987b, The importance of hollows in debris flow studies: Examples from Marin County, California, in Costa, J.E., and Wiczeorek, G.F., eds., Debris flows/avalanches: Process, recognition, and mitigation: Geological Society of America Reviews in Engineering Geology, v. 7, p. 165-180.
- Rice, S.J., Smith, T.C., and Strand, R.G., 1976, Geology for planning in central and southeastern Marin County, California: California Division of Mines and Geology Open-File Report 76-2SF, 103 p.
- Rodine, J.D., 1974, Analysis of the mobilization of debris flows: Stanford, Calif., Stanford University, Ph.D. thesis, 226 p.
- Schofield, A.N., and Wroth, C.P., 1968, Critical state soil mechanics: London, McGraw-Hill, 310 p.
- Seed, H.B., Woodward, R.S., and Lundgren, Raymond, 1964, Fundamental aspects of the Atterberg limits: American Society of Civil Engineers Proceedings, Soil Mechanics and Foundations Division Journal, v. 90, no. SM6, p. 75-105.
- Side, R.C., 1984, Shallow ground water fluctuations in unstable hillslopes of coastal Alaska: Zeitschrift für Gletscherkunde und Glazialgeologie, v. 20, p. 79-95.
- Side, R.C., and Swanson, D.N., 1982, Analysis of a small debris slide in coastal Alaska: Canadian Geotechnical Journal, v. 19, no. 2, p. 167-174.

- Smith, T.C., and Hart, E.W., 1982, Landslides and related storm damage, January 1982, San Francisco Bay region: *California Geology*, v. 35, no. 7, p. 139-152.
- Swanson, F.J., and Lienkaemper, G.W., 1978, Physical consequences of large organic debris in Pacific Northwest streams: U.S. Department of Agriculture, Forest Service General Technical Report PNW-69, 12 p.
- Swanston, D.N., 1970, Mechanics of debris avalanching in shallow till soils of southeast Alaska: U.S. Department of Agriculture, Forest Service, Pacific Northwest Range and Experiment Station Research Paper PNW-103, 17 p.
- Swanston, D.N., and Swanson, F.J., 1976, Timber harvesting, mass erosion, and steep-land forest geomorphology in the Pacific Northwest, in Coates, D.R., ed., *Geomorphology and engineering*: Stroudsburg, Pa., Dowden, Hutchinson & Ross, p. 199-221.
- Terzaghi, Karl, 1950, Mechanism of landslides, in Paige, Sidney, chairman, *Application of geology to engineering practice* (Berkey volume): New York, Geological Society of America, p. 83-123.
- Terzaghi, Karl, and Peck, R.B., 1967, *Soil mechanics in engineering practice*: New York, John Wiley and Sons, 729 p.
- U.S. Army Corps of Engineers, 1953, Unified soil classification system: Vicksburg, Miss., Waterways Experiment Station Technical Memorandum 3-357, 3 v.
- Varnes, D.J., 1978, Slope movement types and processes, chap. 2 of *Landslides: Analysis and control*: Washington, U.S. National Academy of Sciences, Transportation Research Board Special Report 176, p. 11-33.
- Wentworth, C.M., 1986, Maps of debris-flow features evident after the storms of December 1955 and January 1982, Montara Mountain area, California: U.S. Geological Survey Open-File Map 86-363, scale 1:24,000.
- Wilson, C.J., and Dietrich, W.E., 1985, Lag in the saturated zone and pore pressure development after peak runoff in hollows [abs.]: *Eos* (American Geophysical Union Transactions), v. 66, no. 46, p. 898.

## 7. DISTRIBUTION OF DEBRIS FLOWS IN MARIN COUNTY

By STEPHEN D. ELLEN, SUSAN H. CANNON, and STEVEN L. RENEAU,  
U.S. GEOLOGICAL SURVEY;  
with contributions by  
BRYAN M. LANGHOLZ, ROBERT K. MARK, DAVID M. PETERSON,  
and STEPHEN W. ROBINSON

### CONTENTS

	Page
Abstract	113
Introduction	113
Previous work	114
Acknowledgments	114
Areal distribution of debris flows	114
Methods of inventory	114
Controls on areal distribution	116
Rainfall, by Robert K. Mark	116
Ground modification	116
Slope	117
Materials, slope, and water concentration, as described by terrain mapping	117
Terrain units	117
Distribution of scars among terrain units	120
Distribution of scars within terrain units	120
Slope at scars in different terrain units	121
Local topographic setting	122
Distribution of scars among habitats	122
Scars and individual habitats of previous soil slips, by Susan H. Cannon and Bryan M. Langholz	123
Statistical method	124
Results	124
Discussion	125
Conclusions concerning areal distribution	125
Distribution of debris flows over time	125
Radiocarbon site near Three Peaks, by Stephen D. Ellen, David M. Peterson, and Stephen W. Robinson	126
Radiocarbon sites near Inverness, by Steven L. Reneau and Stephen W. Robinson	129
Conclusions concerning distribution over time	130
References cited	130

### ABSTRACT

Debris flows, generally soil slip/debris flows but including soil slip/debris torrents, were abundant and widespread in Marin County during the January 3-5, 1982, storm. We mapped about 4,600 debris flows; the areal density of soil-slip sources for debris flows was generally less than 5 per square kilometer but ranged as high as 55 per square kilometer. Most of the debris flows developed in the natural landscape and were not affected by geologically recent ground modifications. Regional distribution of soil-slip sources for debris flows was not strongly associated with the amount of rainfall, but it was associated with steep slopes (80 percent occurred on slopes steeper than 27.5°, as measured from contour maps); with granular soil mantle, as mapped using terrain analysis; and with both bedrock contacts and materials that have strong contrasts in permeability. Within the local landscape, debris flows

were closely associated with drainages; about half of the debris flows originated in amphitheaters at the heads of first-order drainages, and most debris-flow trails of significant extent followed drainages. In selected areas of steep, regular terrain, statistical analysis shows that debris flows originated preferentially in amphitheaters that contained scars from previous soil slips, and this preference is explained by the 26 percent of new scars that developed contiguous to preexisting scars.

Temporal distribution of debris flows in the county is associated with intense rainstorms. Rainfall equivalent to that of the January 1982 storm, along with a corresponding level of debris-flow activity, can be expected to recur every 20 to 100+ years in the county. Radiocarbon dating suggests that the recurrence interval of debris flows at sites may range from less than 33 to more than 1,950 years and that debris flows have occurred in the county for more than 46,500 years.

### INTRODUCTION

Intense and sustained rainfall on January 3-5, 1982, triggered abundant landslides in Marin County, as well as in other parts of the San Francisco Bay region. Landslides occurred in the county both on natural hillslopes and on hillslopes modified by grading, and they ranged from slow-moving earth slides and earth flows to fast-moving debris flows (see "Introduction" to this volume for landslide terminology). These debris flows caused the three landslide-related fatalities and most of the \$18,464,000 in landslide damage in the county that resulted from the storm (see chap. 11). Thus, the discussion here is limited to debris flows.

Debris flows triggered by the storm were dominantly soil slip/debris flows, in which debris flows mobilized from shallow landslides of the soil mantle. Soil slip/debris flows ranged from small, isolated events, in which damage occurred within several meters of the soil-slip scar, to large complexes that involved numerous soil slips along debris-flow trails hundreds of meters long. Soil slip/debris torrents, recognized near Inverness, formed the end member of this spectrum of phenomena; originating as soil slips, they flowed more than a kilometer down major canyons and impacted populated areas as flood phenomena, far from landslide sources. These various types and scales of debris flows are described through case studies in chapter 6. Terms used here to denote earth materials and landslide processes are defined in the "Introduction" to this volume.

Our primary purpose is to document the areal distribution of debris flows that occurred in Marin County during

the storm and to analyze this distribution by comparing it with maps of likely causal factors. We also discuss the temporal distribution, or recurrence, of debris flows in the county, using case studies that involve radiocarbon dating.

#### PREVIOUS WORK

Landslide features throughout most of Marin County were mapped from aerial photographs at 1:24,000-scale by Wentworth and Frizzell (1975). This mapping, however, did not recognize debris flows because it emphasized the generally slow moving landslides that are large enough to leave recognizable disruptive patterns in the topography. These maps were incorporated into landslide maps of the entire San Francisco Bay region at 1:125,000-scale by Nilsen and others (1979).

Phenomena similar to soil slip/debris flows, called disintegrating soil slips, were previously recognized in the county by Kesseli (1943). Rice and others (1976) described several kinds of landslides, including debris flows, during 1:12,000-scale field mapping in the central and southeastern parts of the county; the text that accompanies their map discusses the nature, timing, and distribution of debris flows.

Detailed mapping at scales of 1:6,000 to 1:8,000 has documented debris flows within small areas in the northern and western parts of the county (Trautmann, 1976; J.M. Coyle, unpub. data, 1978; Reid, 1978; Peterson, 1979; Savina, 1982). That work was directed toward determining the relations of different types of shallow landslides to types of bedrock, to types of soil mantle, and to the topographic form of hillsides as viewed in high-altitude aerial photographs (Ellen and others, 1979). This detailed mapping was later used to calibrate a 1:62,500-scale map that distinguishes areas in the county susceptible to different kinds of shallow landslides, including debris flows (Ellen and others, 1982).

#### ACKNOWLEDGMENTS

Information on landslides in the storm was efficiently supplied by personnel of the California Division of Mines and Geology, particularly S.J. Rice, E.W. Hart, D.L. Wagner, and C.W. Davenport. The observations obtained from their quick response provided essential basic information on the nature of debris flows in the storm. C.M. Wentworth of the U.S. Geological Survey originated the terrain-mapping approach, including the concept of landslide habitats, on which much of our analysis is based.

Ellen supervised this study and is responsible for the discussion of the regional and temporal distribution of debris flows. Cannon and Reneau gathered most of the map information on the distribution and features of debris flows (pls. 5, 6). R.K. Mark prepared figures 7.1 and 7.2. In addition, several sections have separate authorship.

#### AREAL DISTRIBUTION OF DEBRIS FLOWS

Although debris flows were numerous and highly disruptive during the storm, they directly affected only a small fraction of the land area in Marin County. As shown in figure 7.1, most of the county had less than 5 mapped soil-slip sources for debris flows per square kilometer; however, much of the county had more than 10 soil slips per square kilometer, and locally the concentration exceeded 50 soil slips per square kilometer.

The countywide inventory map on plate 5 (1:62,500 scale) and the quadrangle inventory map of the Hicks Mountain area on plate 6 (1:24,000 scale) record our knowledge of the regional distribution of debris flows in the county that resulted from the storm; plate 5 shows more than 4,600 debris flows, plate 6 about 1,800. Damaging debris flows are documented in chapter 11. We first discuss preparation of the inventory maps and then examine controls on the distribution they document.

#### METHODS OF INVENTORY

The inventories in plates 5 and 6 were compiled largely by mapping on stereoscopic pairs of vertical aerial photographs taken about midday on January 6 and 7, 1982, several days after the storm. Most of the county was inventoried by using 1:20,000-scale photographs, but the Hicks Mountain area (see pl. 6) was inventoried by using 1:12,000-scale photographs. Mapping from aerial photographs was supplemented by field observations along roads in parts of the county, by field observations in the eastern part of the county by personnel of the California Division of Mines and Geology, and by field observations near Inverness; however, most areas in the county were surveyed solely by means of the aerial photographs.

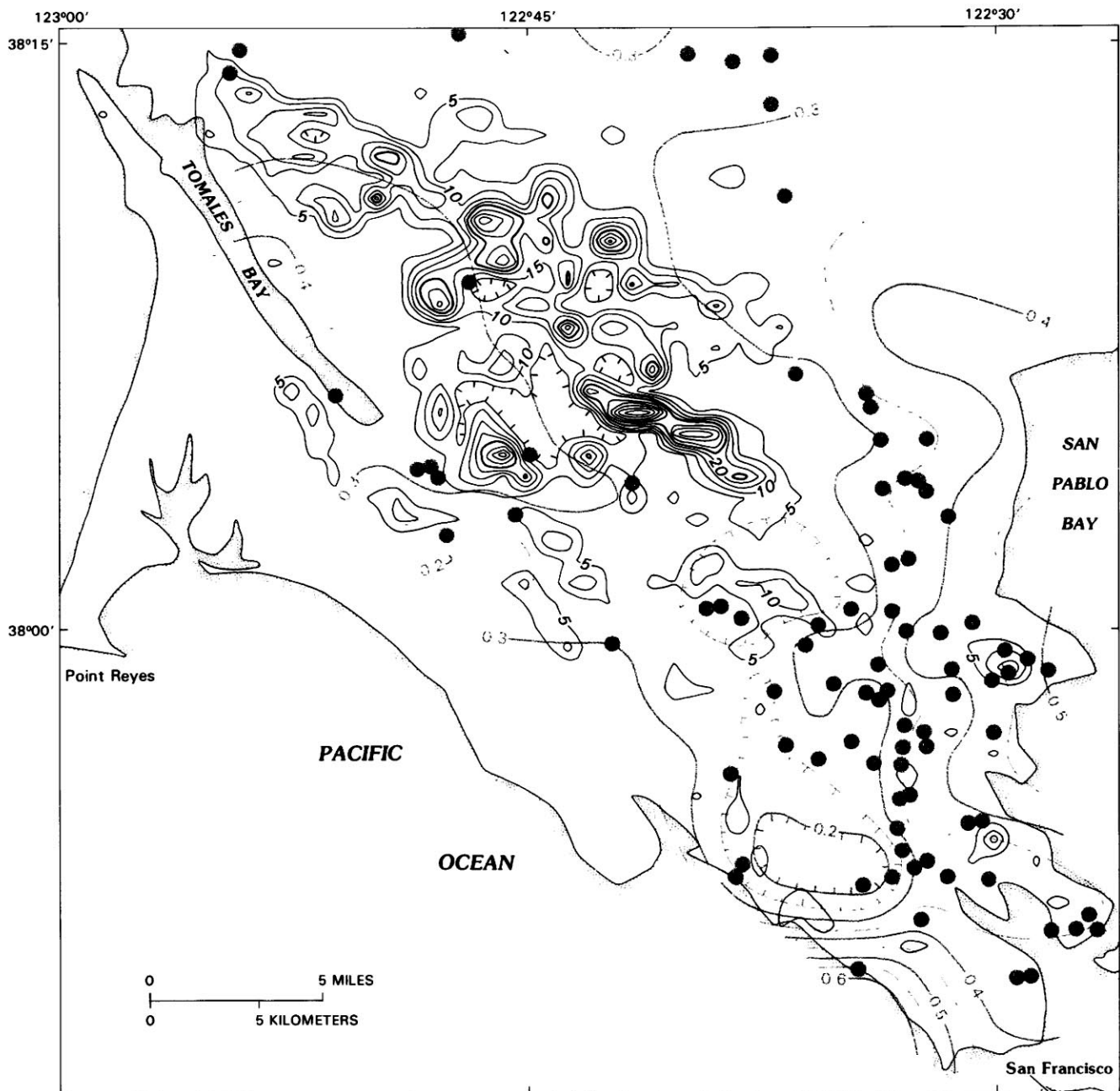
Only landslides that appeared fresh in the photographs and that mobilized as debris flows are shown in the inventories. These landslides exhibited empty soil-slip scars, commonly with debris-flow trails leading downslope. Fresh movement was also evident in many shallow landslides that had not mobilized as debris flows, but these landslides are not shown in the inventories.

Although use of aerial photographs permitted economical areal coverage, it has two principal limitations: Forest cover, where present, conceals most debris-flow features; and shadows present at the time of photography almost completely conceal debris-flow features. Shadows were particularly extensive in the photographs because of the low sun angle in early January; they obscured steep north-facing hillslopes, and near such hillslopes they concealed valley bottoms, which hold evidence for debris-flow trails. Thus, the inventories on plates 5 and 6 are incomplete in areas of forest cover and shadow. To facilitate proper use of these maps, areas of woodland cover compiled from



7.5-minute quadrangle maps are superimposed on the inventories. Because almost all the areas concealed by shadow are wooded as well, the woodland cover shown

on plates 5 and 6 includes almost all areas where the inventories are incomplete. The most likely exception is that shadows may locally have concealed steep north-facing



## EXPLANATION


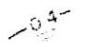

-  Contours showing areal density of mapped soil-slip sources for debris flows. Contour interval 5 soil slips per square kilometer; bold contour at 25 soil slips per square kilometer. Hachures indicate closed depressions in contour portrayal
-  Contours showing normalized storm rainfall. Hachures indicate closed depressions in contour portrayal
-  Data points for storm rainfall

FIGURE 7.1.—Areal density of soil-slip sources for debris flows in comparison with normalized storm rainfall in Marin County.



slopes and adjacent valley bottoms shown on the maps as lacking woodland cover.

The inventories on plates 5 and 6 show two principal kinds of features left by soil slip/debris flows—the scars of soil-slip sources for the flows and the trails left by debris flows; plate 6 in places shows deposits as well. Trails are shown only where they are long enough to portray at the map scale. In places, trails are shown without accompanying soil-slip scars because these scars are concealed in the photographs; likewise, scars shown as lacking trails may be accompanied by trails that are concealed in the photographs.

#### CONTROLS ON AREAL DISTRIBUTION

The development of debris flows from soil slips requires several conditions that serve as likely controls on debris-flow distribution. These conditions have been explored by studies in Marin County (Kesseli, 1943; Rice and others, 1976; Trautmann, 1976; Reid, 1978; Ellen and others, 1979; Peterson, 1979) and elsewhere (for example, Campbell, 1975; Hollingsworth and Kovacs, 1981; Smith and Hart, 1982). The principal requirements at source areas appear to be steep hillslopes, granular soil,<sup>1</sup> and the presence of perched ground-water levels in the soil mantle. The low cohesion in granular soil permits the initially sliding mass to mobilize and flow as a slurry; steep slopes are necessary for failure of granular soil; and high ground-water levels in the soil mantle, generally perched on less permeable bedrock or soil, typically trigger the soil slips that mobilize as debris flows.

In the analysis that follows, the effect of slope is discussed directly, but the other two conditions—granular soil and perched water table—are evaluated indirectly through terrain form, rainfall, and topographic setting. Also evaluated is the affinity of soil slips for scars from previous soil slips, as well as the role of recent natural and manmade ground modifications. The analysis primarily addresses the distribution of soil-slip scars; the resulting debris-flow trails extend more or less predictably down hillslopes and channels.

Other likely controls on the distribution of soil slips are not evaluated here. Local variation in rainfall, resulting from passage of high-intensity rainfall cells, is not discussed, although it probably affected the distribution of soil slips in the storm (C.M. Wentworth, written and oral commun., 1982). The roles of vegetation and slope aspect are not examined because the inventories in plates 5 and 6 are biased by forest cover and shadow.

#### RAINFALL

By ROBERT K. MARK

Although the debris flows in Marin County were triggered by rainfall, their distribution in the county shows little correlation with amounts of rainfall. Several measures of rainfall were tested against map distribution, and none showed a good correlation. For example, figure 7.1 illustrates in map form the relation between areal density of soil slips and normalized storm rainfall, which is the ratio of total storm rainfall to mean annual precipitation. Normalized storm rainfall should be a useful measure because it reflects divergence from typical rainfall conditions (see chap. 3; Govi and Sorzana, 1980). Figure 7.1, however, shows little correlation between soil slips and normalized storm rainfall; and similar apparent absence of map correlation is evident for total storm rainfall, total prestorm rainfall, and normalized prestorm rainfall.

Poor correlation is also evident from graphs of these data (fig. 7.2). Figure 7.2A compares the areal density of soil slips, expressed as landslide-density ratio (see chap. 2), with storm-rainfall and prestorm-rainfall totals. Both curves show peaks in landslide density, and for rainfall values exceeding those peaks the decrease in landslide density indicates that amount of rainfall in itself does not explain the areal density of soil slips. Similar conclusions hold for plots of normalized storm and prestorm rainfall (fig. 7.2B). Thus, Marin County contrasts with the bay region as a whole (see chaps. 2, 8) by showing a poor correlation with all these measures of rainfall.

Bias in the inventories may explain much of this poor correlation. Areal density of soil slips is low in areas concealed by forest cover and shadow, and high in the Hicks Mountain area, where more detailed photographs were used (pl. 6). If areal densities in unconcealed areas are compared, however, it is evident that factors in addition to aggregate amount of rainfall controlled the distribution of soil slips.

#### GROUND MODIFICATION

At several places in the inventories, soil-slip scars are concentrated in parts of the landscape where the ground configuration has been modified in geologically recent time by natural processes or human activity. Oversteepened bluffs resulting from coastal erosion appear to be responsible for the concentration of scars at Tomales Point (area B-3/4, pl. 5). Abundant scars in area G/H-3 on plate 5 occupy canyon walls steepened by downcutting of Walker Creek; similarly, stream impingement on canyon walls appears to be largely responsible for the groups of scars in area O-15 on plate 5 and in area D-11 on plate 6. Clusters of scars in area I-2/3 on plate 6 and in area W-27 on plate 5 occupy scarps or deposits of large preexisting landslides, places where deep-seated move-

<sup>1</sup>The term "granular soil," as used here, means noncohesive to slightly cohesive soil composed dominantly of sand, silt, and rock fragments.

ment could be expected to leave oversteepened hillslopes. Finally, cuts, fills, and resulting water concentration along roads appear to be responsible for groupings of scars, as in area T/U-25 on plate 5. In most of the landscape, however, soil slips developed in the absence of such natural and manmade modifications, under relatively longterm, steady-state conditions of landscape evolution.

#### SLOPE

The inventory on plate 6 is combined with a slope map, for which the areas of each slope interval were generated by photomechanical means from the contours on 7.5-minute topographic maps. Examination of this plate indicates that almost all the soil-slip scars lie in areas mapped as steep slopes. The scars, however, by no means occupy all steep hillslopes; and in many places scars occupy other than the steepest parts of an area, as in areas E-6, I-5, G-3, and B/C-6. Thus, the relations shown on plate 6 indicate that steep slope was generally necessary to initiate debris flows but that other factors must have influenced debris-flow distribution as well.

Examination of plate 6 shows that most soil-slip scars lie on slopes shown as steeper than  $27^\circ$  but that many lie in areas shown as having gentler slopes (to less than  $22^\circ$ ). Figure 7.3A, a plot of slopes at 202 of the scars shown on this plate, shows that the debris flows typical of this sample originated on slopes shown by contour spacing to lie between  $27.5^\circ$  and  $37.5^\circ$ . The cumulative plot in figure 7.3B shows that 80 percent of the scars lie in areas shown by contour spacing to be steeper than  $27.5^\circ$  and that nearly 94 percent lie in areas shown to be steeper than  $22.5^\circ$ .

Slope values determined from contour spacing, as used in this analysis, should be regarded only as approximations to the true slopes. These approximations may be useful, but work elsewhere suggests that the correlation can be poor (E.E. Brabb, oral commun., 1983). Measurement of slope from contour spacing has several major limitations. First, as illustrated on figure 7.4, slopes determined from contour spacing are, at best, average slopes over elevation differences equal to the contour interval, in this case 40 ft. Thus, small steep parts of irregular hillslopes, as shown on figure 7.4B, are not revealed by the contours, and soil-slip scars at such places will appear to occupy the gentler slope shown by the contour spacing. Second, slope information generated from contours on the 7.5-minute quadrangle maps used in this study retains inaccuracies present in these contours—inaccuracies that are inevitable both because of forest cover and because these maps were prepared for less precise uses. Third, when used to prepare slope maps, the method produces false slope information where contours double back on themselves, as in many of the draws and at some of the ridge crests shown on plate 6.

#### MATERIALS, SLOPE, AND WATER CONCENTRATION, AS DESCRIBED BY TERRAIN MAPPING

A terrain map predicting the regional distribution of debris flows in most of Marin County had been prepared before the January 1982 storm (Ellen and others, 1982). This map formed a major basis for our analysis of areal distribution, largely because it shows the distributions of bedrock materials, soil materials, and topographic configurations, all of which probably controlled the distribution of soil-slip scars. We first describe the terrain map and its units, and then we examine the relation of soil-slip scars developed in the storm to these units.

#### TERRAIN UNITS

The terrain map was prepared by systematically mapping differences in the forms of hillsides as viewed stereoscopically in small-scale (1:80,000) aerial photographs. The

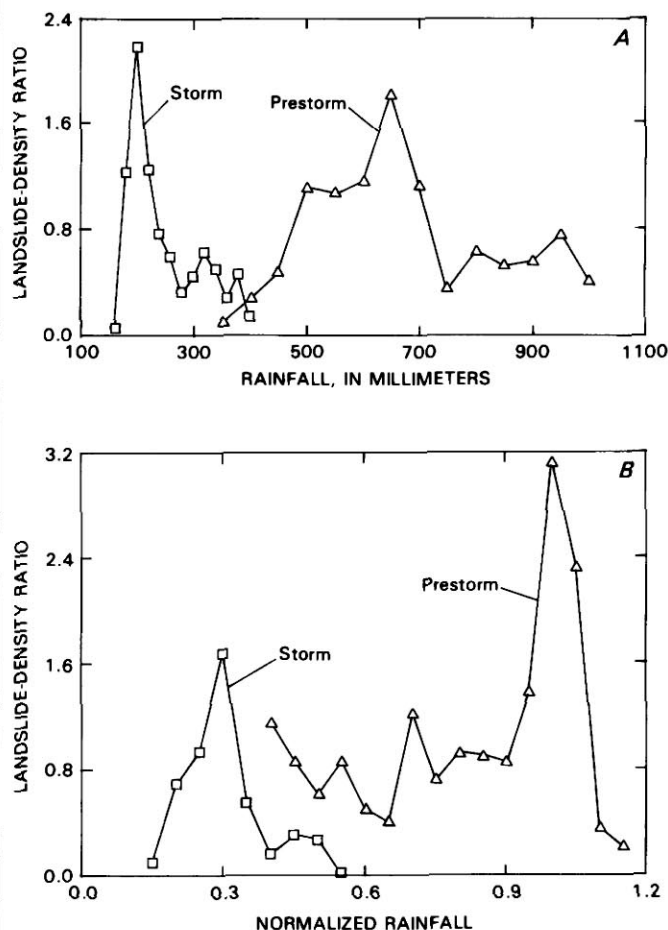


FIGURE 7.2.—Relations between areal density of soil-slip sources for debris flows, expressed as landslide-density ratio, and measures of rainfall. A, Relations for storm-rainfall and prestorm-rainfall totals. B, Relations for normalized storm and prestorm rainfall.

topographic forms so distinguished, called terrain units, were calibrated by detailed (1:8,000-scale) field studies of bedrock, soil, and landslides (Trautmann, 1976; Reid, 1978; Ellen and others, 1979; Peterson, 1979; Savina, 1982). These studies showed spatial associations between the various terrain units and types of bedrock, types of soil mantle, and types of shallow landslides—associations that were sufficiently consistent to justify extrapolation of these relations to the entire terrain-map area. The terrain mapping is shown on plates 5 and 6; the terrain units are listed in table 7.1 and described on plate 5.

Terrain mapping and field calibration were applied only in that part of Marin County, east of the San Andreas fault, that is underlain by the highly disrupted and hetero-

geneous bedrock of the Franciscan assemblage. In parts of the county underlain by bedrock other than the Franciscan assemblage, bedrock and soil mantle are described on plate 5 by means of the geologic units mapped by Blake and others (1974).

The terrain units form a continuum that ranges from steep, sharp-crested, regularly incised (fluted) topography (see block diagram, pl. 5) to gently sloping, rounded topography (table 7.1). The relation between slope and terrain units is shown on plate 6, where strong associations are evident in many places, particularly where contrasting terrain units are juxtaposed, as in area A-4. The range in topographic form corresponds to a range in composition and structural condition of the Franciscan bedrock materials, from highly sheared and mixed rock (melange) that includes masses of relatively resistant and intact rock, through varyingly disrupted and sheared rock, to essentially intact rock masses (fig. 7.5; see Bailey and others, 1964).

The several terrain units that consist of steep, fluted topography, called collectively *hard terrains*, are under-

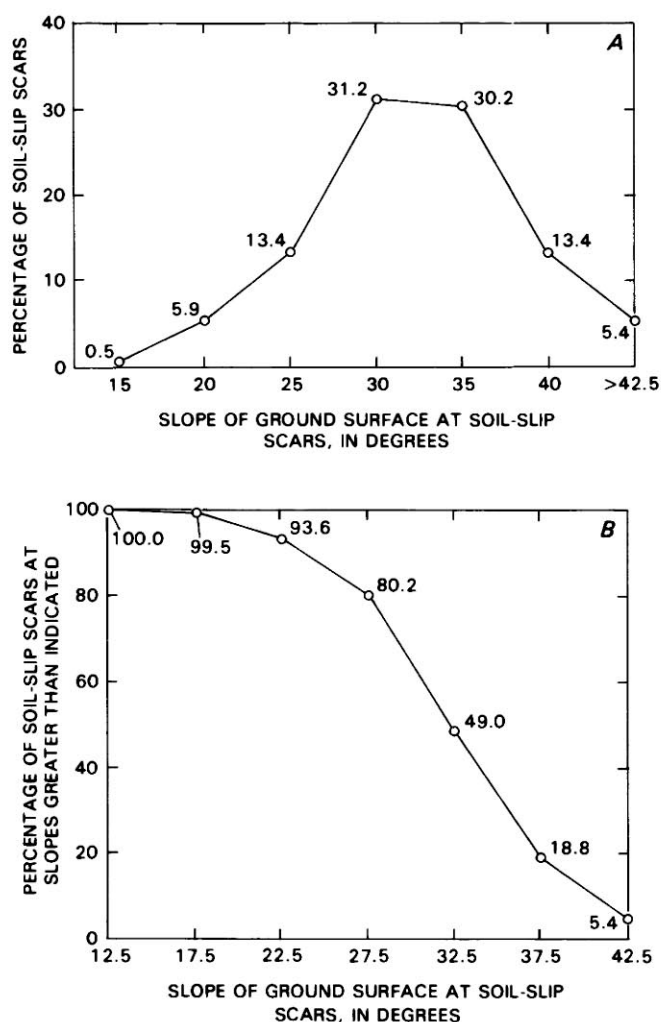


FIGURE 7.3.—Slope of ground surface at 202 soil-slip sources for debris flows formed during the storm in the Hicks Mountain area of western Marin County (pl. 6). Slope is measured to nearest 5° from spacing of 40-ft contours on 1:24,000-scale topographic map. A, Percentage of soil-slip scars in each slope interval. B, Cumulative percentage of scars at slopes greater than indicated values.

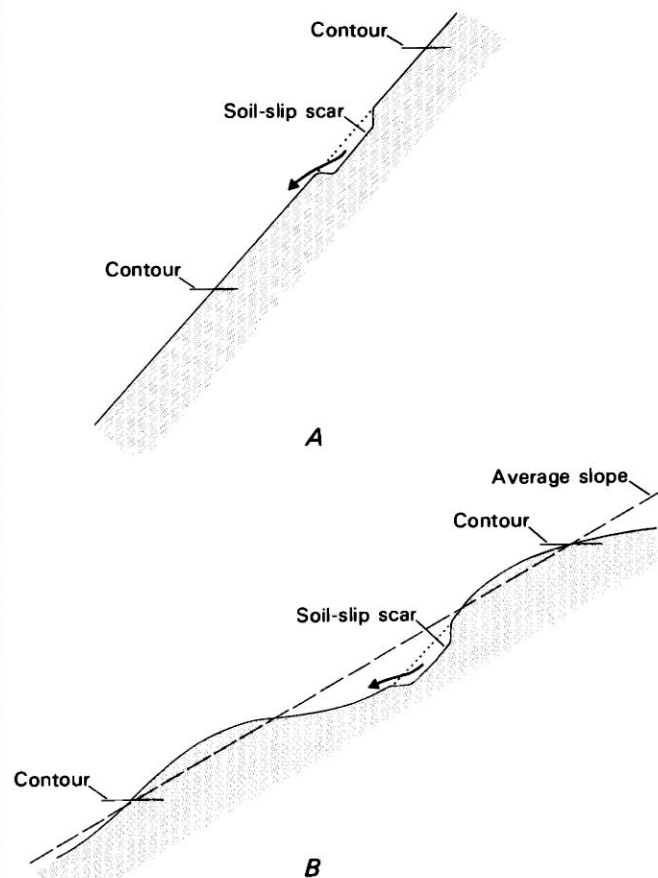


FIGURE 7.4.—Schematic downslope cross sections of uniform (A) and irregular (B) hillslopes, showing relation of actual slopes to average slope described by contour spacing.

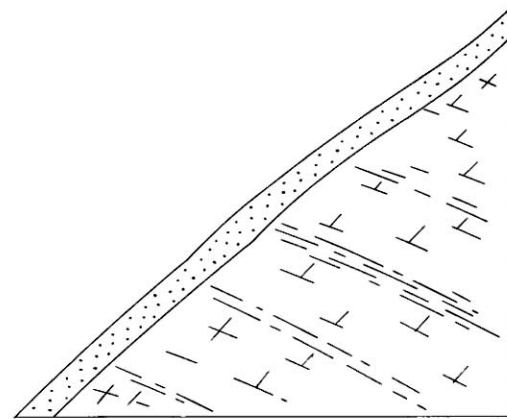
TABLE 7.1.—Principal terrain units mapped in Marin County

Unit	Description
Hard terrains:	Steep, sharp-crested,
Very hard terrain	angular terrain with
Rounded, very hard terrain	regular, sharply
Hard terrain	incised fluting.
Intermediate terrains:	Irregular terrain of
Fluted intermediate terrain	intermediate form.
Intermediate terrain	
Smooth intermediate terrain	
Soft terrain-----	Gently sloping, rounded terrain.

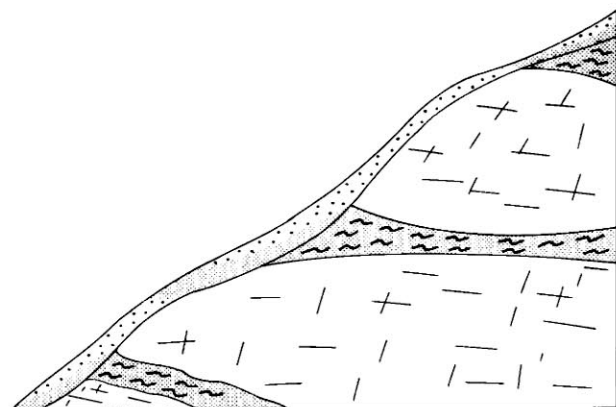
lain by intact bedrock (largely sandstone and interbedded shale) that is mantled by granular soil which fails principally as debris flows (fig. 7.5A). The gently sloping, rounded topography, called *soft terrain*, is underlain by highly sheared and mixed bedrock materials, including abundant impermeable clayey sheared rock (fig. 7.5C). Soft terrain is mantled principally by clayey soil that fails by slow-moving earth flows and earth slides, although granular soil exists in many places where blocks of relatively intact rock are too small to distinguish at the scale of the terrain mapping (smaller than about 400 m in maximum dimension).

Topography intermediate between the hard terrains and soft terrain is mapped as several units that are called collectively *intermediate terrains*. Bedrock of intermediate terrains is disrupted but contains less abundant clayey sheared rock than does soft terrain; thus, it probably consists dominantly of masses of sandstone or other resistant rock types, separated by zones of sheared rock that include impermeable clayey sheared rock (fig. 7.5B). Soil mantle in intermediate terrains includes granular soil, clayey soil, and soil of intermediate texture, and this variety results in various kinds of shallow landslides.

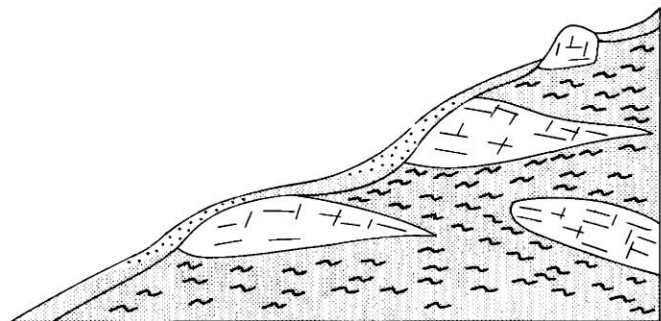
Terrain units are useful to an analysis of the distribution of debris flows because each such unit represents a combination of materials and topographic form, which includes steepness of slope. If we consider the simple combination of steep slope and granular soil as the principal controls on the distribution of soil-slip scars, then we would expect most soil slips to occur in hard terrains, which consist almost entirely of steep slopes with granular soil. Intermediate terrains should show soil-slip scars, but scars there should be less abundant than in hard terrains because steep slopes and granular soils constitute only parts of intermediate terrains. By similar reasoning, soft terrain, which is dominated by gentle slopes and clayey soil, should lack scars except where masses of relatively intact rock with steep slopes and granular soil are included because of the map scale. The distribution of debris flows



A



B



C

## EXPLANATION




-  Permeable granular soil mantle
-  Clayey sheared bedrock; orientation indicates direction of shear foliation
-  Relatively permeable, fractured, resistant rock, typically sandstone or greenstone

FIGURE 7.5.—Schematic downslope cross sections of hillsides in hard (A), intermediate (B), and soft (C) terrains.



predicted by Ellen and others (1982), which is described on plate 5, is based on such reasoning, supported by the mapped distribution of landslide features in the calibration studies.

#### DISTRIBUTION OF SCARS AMONG TERRAIN UNITS

Plates 5 and 6 show that scars of the soil slips triggered by the storm generally occupy intermediate and hard terrains, but the relations are far from simple. Soil-slip scars in such areas as A-4, C-3, D-3, and I-6 on plate 6 are strongly concentrated in hard terrains. In contrast, broad forested areas of hard and intermediate terrains, including much of the southern part of the county (pl. 5), show few debris flows. This small areal concentration generally could be explained by gaps in the inventory that resulted from forest cover or shadow, but it cannot be determined whether forest cover simply concealed features or whether forested areas actually had fewer debris flows. Field mapping by Davenport (1984) in forested hard terrains near San Rafael (areas BB/CC-18/19, pl. 5) shows abundant scars and trails not detected in our photographic inventory. In contrast, some areas of hard terrains that are not concealed, as in areas F/G-6 and D-7/8 on plate 6, show few scars. Thus, soil-slip scars generally coincide with intermediate and hard terrains, but the distribution of scars within hard terrains is nonuniform, and so it must have been influenced by factors other than steep slope and granular soil.

In many places, the inventories reveal unexpected patterns of distribution. Scars in some places are particularly abundant in intermediate terrains, as in areas H-8, D-2, and I-9 on plate 6; in such areas as BB/CC-19, J-5, I-6, T-22, and R/S-11 on plate 5, intermediate terrains show more scars than nearby unconcealed hard terrains. Similarly, soft terrain shows abundant scars in places, as in areas H-3, I-9, and G/H-10/11 on plate 6. In several places, as in areas H-11, H-3, H/I-2/3, F-6, G-7, E-2, and E/F-5 on plate 6 and areas DD-26, EE-26, and X-16/17 on plate 5, scars are conspicuously concentrated along contacts between terrain units.

These unexpected patterns of distribution have a common element: They suggest that debris flows during the storm originated preferentially in places where materials have strong permeability contrast, which is where ground water can be concentrated by several means (see chap. 6). This affinity for permeability contrast is explicit where scars are concentrated along terrain-unit contacts, reflecting contacts between contrasting soil and bedrock materials. Preferential occurrence of scars in intermediate rather than hard terrains can likewise be explained by the material contrasts that characterize intermediate terrains. Local abundance in soft terrain may arise from similar material contrasts. This suggestion is supported by the

inventory on plate 5, which distinguishes scars that lie along distinct breaks in slope at which gentle slope (reflecting impermeable material) lies downslope from steeper slope (reflecting relatively permeable material); such scars are especially abundant in soft terrain, as in areas L/M-9, O-10, and P-11 on plate 5.

In summary, the distribution of soil-slip scars among terrain units is consistent with the hypothesis that granular soil and steep slope are principal controls on the distribution of scars. Some conspicuous aspects of this distribution, however, suggest that concentration of ground water related to contrast in materials favored development of debris flows in the storm.

#### DISTRIBUTION OF SCARS WITHIN TERRAIN UNITS

At a local scale, commonly within a terrain unit, the soil-slip scars shown in plate 6 show several patterns of distribution. In such areas as I-6, scars are distributed more or less evenly on a hillside. In other areas, such as B/C-6 and F/G-7/8, scars are grouped in clusters; and in such areas as F/G-4, scars are grouped in linear patterns. In many places, groupings of scars are related to local steep slopes in otherwise gently sloping ground, but in other places, such as areas G-3 and I-5, clusters show little relation to steep slope.

Contrast in local patterns of distribution is well illustrated in area B-9 on plate 6, where hard terrain along the south side of an east-west-trending canyon shows scars regularly distributed near each sidehill drainage. On the north side of the canyon, scars occur in a linear group, which is apparently related to the boundary between a relict erosional surface (unit e) and smooth intermediate terrain (unit si).

Inspection of plate 6 shows that these different patterns of distribution, which reflect different controls on soil-slip failure, are generally related to terrain units. Soft and intermediate terrains typically show the strongest groupings, probably because the susceptible soils and slopes, as well as permeability contrasts, are distributed as irregular masses and crudely planar zones within these units. Some clusters in soft terrain appear to be related to mapped or unmapped masses of resistant rock, as in areas C-6, H-3, and G/H-10/11; however, other clusters, as in areas G-3, I-5, and E-4, show little obvious relation to discernible factors. In hard terrains, scars typically occur singly in a pattern related to hillside drainages, as discussed below in the subsection entitled "Local Topographic Setting." This distribution reflects the relatively uniform materials and slopes of hard terrains, in that soil slips appear to be controlled largely by topographic effects on water concentration rather than by variations in slope or materials. Locally, however, as in area F/G-4, hard terrains show a strong linear grouping of scars.

Scars related to relict erosional surfaces (unit e) typically lie along the unit margins because unstable conditions are generally confined to the edges of such surfaces.

Some scars are grouped at the bases of hillslopes that abut alluvium (whether mapped or unmapped), such as in areas G/H-3, F/G-3, I-3/4, and I-6 on plate 6. These clusters probably result largely from ground-water concentration at breaks in slope (see chap. 6).

#### SLOPE AT SCARS IN DIFFERENT TERRAIN UNITS

Slopes at soil-slip scars, as measured from the contours on plate 6, are systematically related to terrain units (fig. 7.6). Scars in hard terrains show the steepest slopes,

scars in soft terrain show gentler slopes, and scars in intermediate terrains show a bimodal distribution of slopes.

These relations between terrain units and slope at soil-slip scars could result from differences in true slope at the scars, or they could arise simply from measurement of slope by means of contours. Even if actual slopes at scars were uniform, relations similar to those plotted in figure 7.6 would result from the averaging effect of the contours from which these slopes were measured. Thus, the relatively uniform slopes that accompany the relatively uniform materials of hard terrains would be accurately reflected in the contours (fig. 7.44). In contrast, the

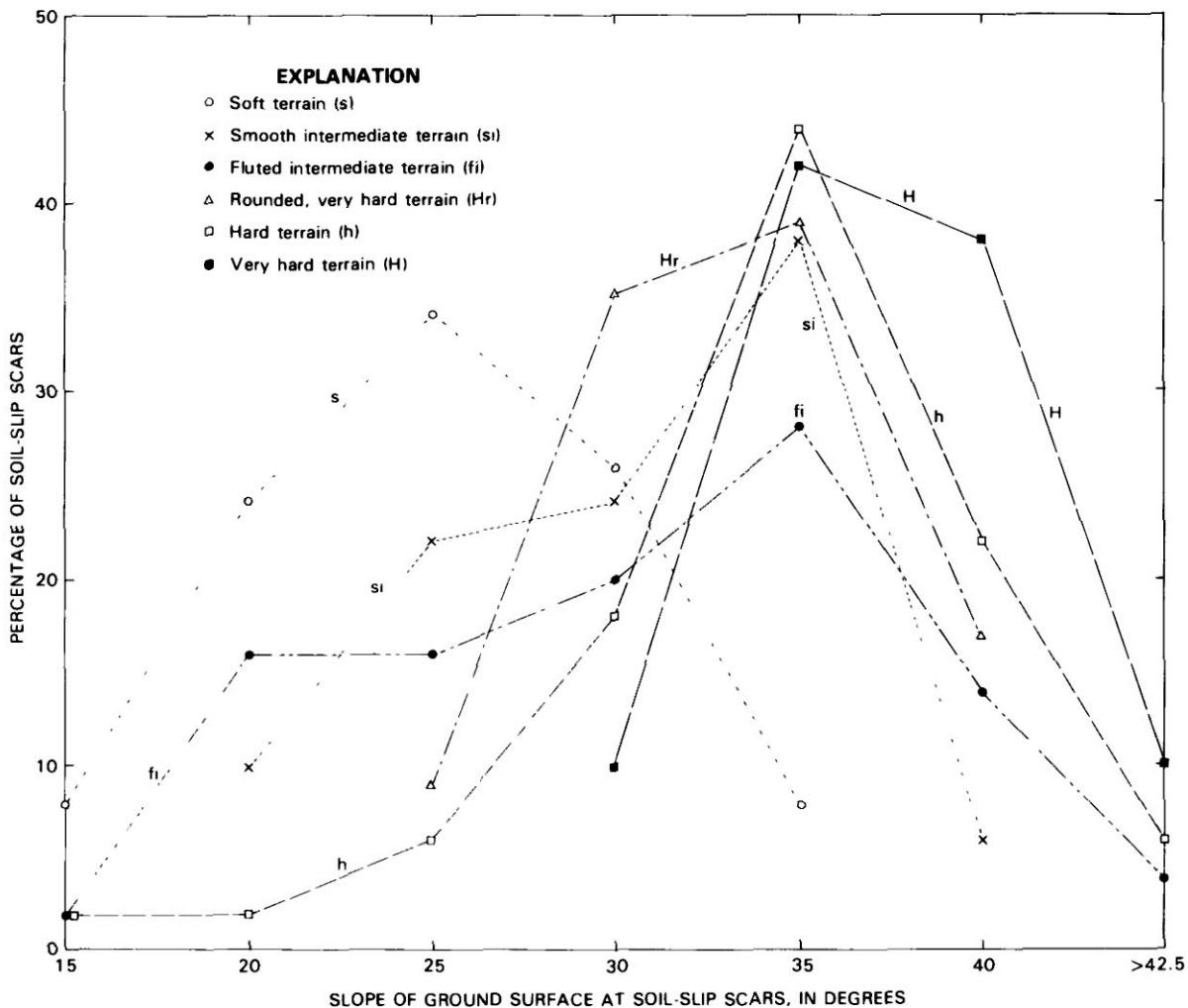


FIGURE 7.6.—Slope of ground surface at soil-slip sources for debris flows formed during the storm in the Hicks Mountain area of western Marin County (pl. 6), plotted by terrain units containing the soil-slip scars. Slope is measured to nearest 5° from spacing of 40-ft contours on 1:24,000-scale topographic map. Slopes are shown for samples of 50 scars in each terrain unit except the rounded, very hard terrain unit, for which only 23 scars are included.

irregular slopes that accompany the mixed materials of soft and intermediate terrains would tend to dilute the local steep slopes at which failure occurred, and so the slopes measured in these terrain units would appear to be gentler than the actual slopes at the scars (fig. 7.4B).

Differences in the true slope of failure can be expected theoretically from differences in the materials that constitute the terrain units. Relatively gentle slopes of soil-slip failure can generally be expected either where granular soil mantle is somewhat clayey, as would be expected in soft and intermediate terrains, or where concentration of water and resulting high pore pressures are favored by contrasts in permeability or by breaks in slope, as would be expected in the mixed materials of soft and intermediate terrains (see chap. 6). Even the small differences evident in figure 7.6 between the several hard terrains are consistent with these explanations. The relatively gentle slopes of failure in rounded, very hard terrain are consistent with the relatively clayey soil mantle of this terrain unit, and the relation shown between hard and very hard terrain is consistent with the relatively uniform and clay-free materials of very hard terrain.

The relations plotted in figure 7.6 probably result from both true slopes of failure and contour representation of slope, and the relations between true slopes of failure and terrain units can be resolved only with a large number of field-measured or photogrammetrically measured slopes at soil-slip scars. Without such resolution, however, the relations in figure 7.6 may still be useful; in comparison with the slopes shown in figure 7.3, figure 7.6 provides a detailed breakdown of the contour-generated slopes at which debris flows originated in the storm.

#### LOCAL TOPOGRAPHIC SETTING

Debris flows in the storm typically originated in, then flowed through, particular topographic settings, or *habitats*, within hillside areas. The affinity of debris flows for certain habitats is shown on plate 6 and figure 7.7 by the mapped positions of scars and trails on the contour base. Examination of these maps indicates two principal associations between local topographic setting and the features left by debris flows: A large proportion of the scars lie near the heads of sidehill drainages, and most trails follow sidehill drainages or canyon bottoms. Local topographic setting probably influences initial failure of soil slips principally by concentration of water (see chap. 6).

#### DISTRIBUTION OF SCARS AMONG HABITATS

To quantify the spatial association between debris flows in the storm and topographic settings, we distinguished several principal habitats and subunits; then, using aerial

photographs, we tallied the habitats occupied by 1,816 soil-slip scars in and about the Hicks Mountain area shown on plate 6. The habitats distinguished are illustrated in the "Explanation" to plate 5, and the principal habitats are mapped in figure 7.7. Habitats of scars throughout most of Marin County are shown by symbol on plate 5.

Habitat 1 consists of amphitheaters at the heads of sidehill draws and first-order drainages, as well as bottoms of drainages except where drainages occupy alluviated valleys (fig. 7.7). Habitat 1A designates the amphitheaters; habitat 1B designates zones along the drainages. A total of 47 percent of the scars tallied lie in the amphitheaters that constitute habitat 1A. Only 2 percent of the scars tallied lie along drainages (habitat 1B), but this habitat is occupied by most trails and by almost all trails longer than 100 m (pl. 6). Thus, the small part of the landscape represented by habitat 1 includes almost half of the scars tallied and most of the trails.

Habitat 2 consists of hillsides that lack well-defined draws and that slope down toward nonalluviated drainages (fig. 7.7). Habitat 2B designates the lowermost edges of these hillsides, where failure could be affected by undercutting along the draw; habitat 2A designates the rest of such hillsides. A total of 33 percent of the scars tallied lie in habitat 2A, and 4 percent lie adjacent to drainages in habitat 2B. Thus, 37 percent of the scars tallied lie on sideslopes from which material would tend to flow into nonalluviated drainages.

Habitat 3 consists of hillsides that abut alluviated surfaces and that lack well-defined draws (fig. 7.7). These hillsides may be planar, somewhat concave, or convex. A total of 13 percent of the scars tallied lie in this habitat. Debris flows originating in this habitat flowed downslope toward alluviated surfaces, so they could impact flatland directly from the hillside; the remaining 87 percent of the debris flows could impact flatland only from the mouths of canyons or hillside draws.

All scars tallied could reasonably be assigned to one of these three habitats. No scars occupied ridge crests, which constitute the rest of hillside terrain (fig. 7.7), but many scars lie contiguous to ridge crests.

A separate tally of 107 scars in several selected areas of hard terrains in the county shows a stronger influence of habitat 1. A total of 71 percent of these scars lie in habitat 1, 28 percent in habitat 2, and 1 percent in habitat 3. This tally, in combination with the previous tally, suggests that the affinity of soil-slip scars for habitat 1 was strongest in hard terrains and that habitat 3 was most commonly occupied by scars in soft and intermediate terrains. The dominance of habitat 1 makes this tally similar to several others: Chapter 10 reports that about two-thirds of the debris flows studied there originated in habitat 1; chapter 9 reports that a preponderance of debris flows originated near the heads of first-order drainages;

and Reneau and Dietrich (1987, p. 42) reported that 62 percent of the debris flows in an area of hard terrains near San Rafael in Marin County originated in hollows.

We note that the several habitats are distinguished for different reasons. We distinguished habitat 1, particularly habitat 1A, because of its propensity for generating debris flows. In contrast, habitat 3 was distinguished because debris flows originating there would not intersect draws that could channelize, and thus sustain, the flow. In propensity for debris flow, habitat 2 may differ little from habitat 3; both habitats may contain the surface and sub-surface concavities that serve to concentrate water and promote soil-slip failure (see chap. 6). One such concavity in habitat 3 is shown in figure 7.7 on the triangular hillslope between points A and B, although the degree of concavity here is exaggerated by the contours.

#### SCARS AND INDIVIDUAL HABITATS OF PREVIOUS SOIL SLIPS

By SUSAN H. CANNON and BRYAN M. LANGHOLZ

Many debris flows in the storm originated near the scars left by soil slips of past years. In some places, scars that formed during the storm lie within old scars or contiguous to old scars; in other places, new scars lie apart from old scars but within the same individual habitat occupied by old scars (fig. 7.7). By *individual habitat* we mean a particular area on a hillside, in contrast to the group of similar areas designated as a habitat, such as habitat 1.

To determine whether the presence of old scars in an individual habitat indicated an increased susceptibility to debris flows in the storm, we statistically tested for spatial association between new and old scars within three small

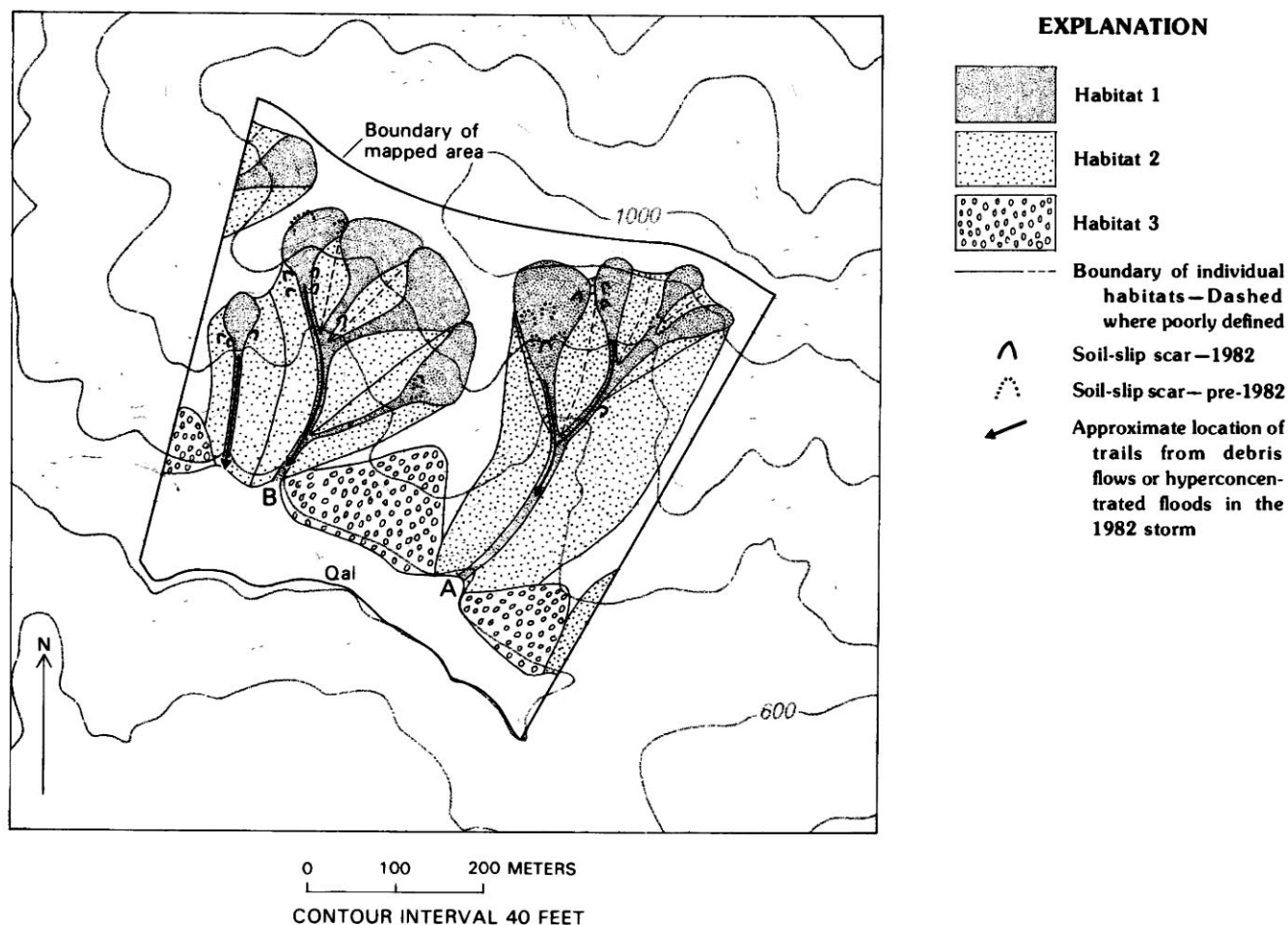


FIGURE 7.7.—Contour map of hillslopes and an alluvial flat in hard terrain near Three Peaks, showing habitats, soil-slip scars, and trails from debris flows or hyperconcentrated floods in 1982 storm. Ridge crests and alluvium (Qal) lack shading and pattern. Soil-slip scars from 1982 storm mapped from aerial photographs by D.M. Peterson and S.H.

Cannon; pre-1982 scars are from Peterson (1979). Points A and B are discussed in text in subsection entitled "Radiocarbon Site near Three Peaks." Base from U.S. Geological Survey, 1:24,000 scale, Point Reyes NE, 1954 (photorevised 1971).



areas in the western part of the county. These areas consist of hard terrains where soil slips and debris flows had been mapped at a scale of 1:8,000 before the January 1982 storm and where previous work had shown the bedrock and soil mantle to be uniform (S.D. Ellen and J.M. Coyle, unpub. data, 1978; Reid, 1978; Peterson, 1979). Analysis is restricted to hard terrains because individual habitats are most clearly defined there and because the uniformity of materials and topographic configuration in hard terrains reduces variables other than the presence of old scars that could influence the initiation of debris flows.

To test for spatial association, we superimposed maps of the soil-slip scars generated in the January 1982 storm on maps of old scars and of habitats (fig. 7.7). Maps of old scars included all scars recognized in the field or on photographs during previous work; some of these scars had been dated by using sequential aerial photographs (Reid, 1978; Peterson, 1979), but most had formed at unknown times before 1978. New scars, as well as habitats, were mapped from aerial photographs taken several days after the storm. The resulting composite maps, as in figure 7.7, show the spatial association between new scars, old scars, and individual habitats; each individual habitat shows either only new scars, only old scars, new scars with old scars, or no scars. These associations were tallied on  $2 \times 2$  contingency tables for each study area (table 7.2); analysis is restricted to habitat 1.

#### STATISTICAL METHOD

To determine whether a statistical association exists between the occurrence of new soil slips in the January 1982 storm and the existence of old soil-slip scars, a stratified analysis of the odds ratio was used. The odds ratio, a measure of association between two factors, has become the measure of choice for analysis of  $2 \times 2$  contingency tables; its advantages were described by Fleiss (1973, p. 43-49). For the present purposes, the odds ratio gives the proportional increase (or decrease) in the odds of occurrence of new scars, given the existence of old scars, to the odds that new scars will occur in the absence of old scars. The odds, probabilities, and odds ratios for each study area are listed in table 7.2.<sup>2</sup>

Conditional-maximum-likelihood methods were used for inference and hypothesis testing based on the odds ratio, as described by Gart (1971) and Zelen (1971). The procedure begins with testing of the hypothesis of homogeneity of the odds ratio, which indicates whether the proportional relations of new and old scars are similar for the three study areas. The test consists of determining whether the odds ratios for each of the three study

TABLE 7.2.—Statistical data for recurrence from individual habitats in three areas

[Numbers in contingency tables are numbers of individual habitats. Expressions in parentheses are given as examples of how the various values were calculated]

Study area-----	. Barnabe	Walker Creek	Three Peaks
	New scars		
	• -	+ -	• -
Old scars	+	+	+
	11 16	9 21	7 4
	-	-	-
	19 54	3 27	17 21
Individual habitats with new scars and no old scars			
Probability-----	0.26 [19/(19+54)]	0.10	0.45
Odds-----	.35 (19/54)	.11	.77
Individual habitats with new and old scars			
Probability-----	0.41 [11/(11+16)]	0.30	0.64
Odds-----	.69 (11/16)	.43	1.75
Odds ratio-----	1.95 (0.69/0.35)	3.86	2.16

areas are statistically close enough to be considered equal. If the hypothesis of homogeneity of the odds ratio is not rejected, then it may be tested whether an association exists between the two factors. This further test indicates whether the presence of old scars is predictive of the occurrence of new scars. To reject the null hypothesis of no association, or to conclude that an association does, in fact, exist, we test to see whether the odds ratios in the three study areas, taken together, are greater than one. If the hypothesis of no association is rejected, then we conclude that a relation exists between old and new scars. The estimate of the common odds ratio then gives a measure of that association.

#### RESULTS

The test of the hypothesis that the odds ratios for the three study areas are equal yields a  $p$ -value of 0.81; the hypothesis of homogeneity of the odds ratio is clearly not rejected. The test of association yields a  $p$ -value of 0.009, indicating that within habitat 1 the existence of old scars is associated with the presence of new scars.

The estimate of the common odds ratio is a measure of the association of old and new scars within habitat 1. For this analysis, the common odds ratio is 2.3, which indicates that during the January 1982 storm the odds were 2.3 times greater that a new scar would occur in an individual habitat 1 where an old scar was present than that a new scar would occur in an empty individual habitat 1.

<sup>2</sup>We note that the odds and probabilities of new scars, given no old scars, vary substantially among the study areas. Thus, combining the tables into one by adding across the study areas would be inappropriate (Feinburg, 1977, p. 48-51; Breslow and Day, 1980, p. 93-108).

## DISCUSSION

This analysis indicates that an association clearly exists between old and new scars, but the nature of this association is not immediately obvious. If the association resulted from inherent differences in the susceptibility of individual habitats, the long-term product would appear to be an irregular topography with marked contrasts in the size of flutes and ribs, the result of selective erosion by debris flows in the susceptible individual habitats. Such is not the case in the regular and uniform hard terrains to which this analysis was restricted.

The results of this analysis may indicate short-term disequilibrium at sites of soil-slip scars, rather than long-term differences in the susceptibility of individual habitats. From this point of view, the association of old and new scars might result from increased susceptibility to failure along the headwalls or sidewalls of preexisting scars. This possibility is investigated by calculating the excess number of individual habitats with both old and new scars, over and above the number predicted (or expected) on the basis of the probabilities of new landslides in individual habitats with no old scars (table 7.2). This calculation (table 7.3) suggests that the excess number of individual habitats with both old and new scars can be more than accounted for by individual habitats which contain contiguous old and new scars. Contiguity was determined by comparison of aerial photographs taken before and after the storm. In terms of numbers of scars, 26 percent of the scars that produced debris flows during the storm in these study areas formed contiguous to preexisting scars; this proportion holds for the scars in habitat 1, as well as for the areas as a whole.

Short-term disequilibrium at sites of soil-slip scars suggests that, to some extent, individual habitats may undergo cycles consisting of a discrete period of colluviation followed by a period of debris-flow activity. Within such a cycle, colluviation would occur until a critical thickness of material accumulated and a storm sufficient to trigger debris flows occurred. Once debris-flow activity had been initiated during a cycle, it would continue at times of extreme rainfall until the accumulated material was removed; then, a new period of colluviation would begin. Such cycles, repeated over a long time period and in a number of individual habitats, could result in the uniform, regular topography that characterizes hard terrains.

## CONCLUSIONS CONCERNING AREAL DISTRIBUTION

Except where influenced by recent ground modification, the distribution of soil-slip sources for debris flows resulting from the storm generally coincides with the mapped distributions of steep slope and granular soil mantle, but neither of these factors alone nor their combination as represented by hard terrains explains some significant

aspects of the distribution of soil-slip scars. Variation in the abundance of scars in hard terrains, concentration of scars along contacts and in intermediate terrains, local groupings of scars in clusters and linear patterns, and concentration of scars in certain local topographic settings (habitats) all suggest that concentration of water was the principal control on distribution of scars within areas with susceptible slope and soil. Distribution of scars suggests that water was significantly concentrated both by configuration of the local topography, as described by habitats, and by conditions resulting from contrasts in soil and (or) bedrock; variation in rainfall had little detectable effect. Distribution of scars was also influenced significantly by preexisting scars; statistical analysis shows that new scars in hard terrains were more than twice as likely in amphitheaters containing recognizable old scars than in those lacking old scars, and this bias is explained by the 26 percent of new scars that developed contiguous to preexisting scars.

DISTRIBUTION OF DEBRIS FLOWS  
OVER TIME

In Marin County and elsewhere in the bay region, almost all the debris flows related to the January 1982 storm occurred during or immediately after intense storm rainfall (see chap. 3; Smith and Hart, 1982, p. 148). The principal exception is the event at Hurricane Gulch in Sausalito, which occurred about 22 hours after rainfall had ceased (see chap. 6 and case study by Smith and Hart, 1982, p. 148-149). The concurrence of debris torrents near Inverness suggests that at least some debris flows were triggered at times of exceptionally intense rainfall during the storm (see Inverness area case study, chap. 6).

Rainstorms capable of triggering at least some debris flows in the county have occurred about every 5 years (E.W. Hart, oral commun., 1983); in the San Francisco Bay region as a whole, debris flows have occurred during at least 12 winters between 1905 and 1978, and during 8 winters between 1961 and 1981 (Smith and Hart, 1982, p. 150). Debris flows as abundant as those in the 1982 storm have occurred less frequently. Before 1982, the most recent occurrence of abundant debris flows in the county was in January 1973 (S.J. Rice, oral commun., 1982), and these debris flows occurred largely in the southern part of the county. Rainfall-recurrence intervals for the January 1982 storm at gages in the county (see table 3.1) suggest that debris flows of the abundance seen in the January 1982 storm can be expected in the county every 20 to 100+ years. Rainfall criteria for storms capable of triggering abundant debris flows in the bay region are defined in chapter 4, and criteria for abundant debris flows in Marin County were discussed by Rice and others (1976).

TABLE 7.3.—*Comparison of excess number of individual habitats that have both old and new scars with the number of individual habitats that have contiguous old and new scars*

[Expected number is given by probability of new scars, given no old scars, times total number of individual habitats with old scars. Excess number is observed number minus expected number]

Study area	Expected number of individual habitats with both old and new scars if old scars have no influence	Observed number of individual habitats with both old and new scars	Excess number of individual habitats with both old and new scars	Number of individual habitats with contiguous old and new scars
Barnabe-----	7.0	11	4.0	7
Walker Creek----	3.0	9	6.0	7
Three Peaks-----	4.9	7	2.1	5

Long-term frequency of recurrence is addressed by the following case studies.

#### RADIOCARBON SITE NEAR THREE PEAKS (CASE STUDY 6, PLS. 5, 6)

By STEPHEN D. ELLEN, DAVID M. PETERSON, and STEPHEN W. ROBINSON

A hillside and adjacent alluviated valley near Three Peaks, in the northwestern part of the county, show evidence of a succession of debris flows. Soil-slip scars and debris-flow trails were formed during the January 1982 storm, older scars and trails were present when the area was mapped by Peterson (1979), and a series of deposits, which we dated by radiocarbon methods, were left at a canyon mouth by pre-1978 debris flows. Bedrock underlying the hillside is thin-bedded sandstone and shale of the Franciscan assemblage; soil mantle is approximately uniform in texture and is classified as ML-CL in the Unified Soil Classification System. Figure 7.7 shows the area and features related to this succession of events.

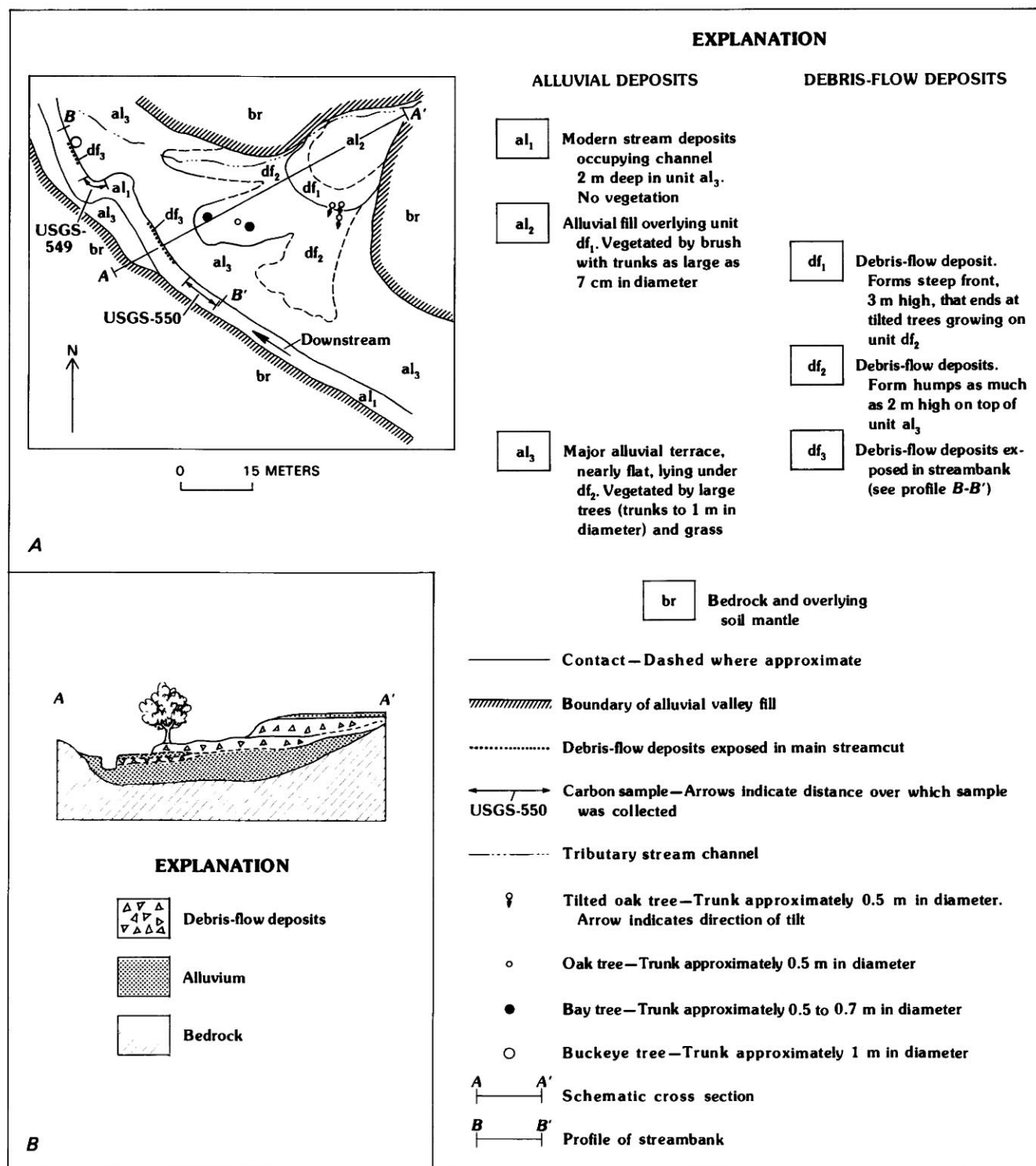
At point A in figure 7.7, deposits from pre-1982 debris flows lie on a somewhat irregular alluvial terrace; other deposits from debris flows are exposed in the bank of the modern stream channel, which is incised into the terrace deposits (fig. 7.8). A shallow bulldozed jeep trail crosses the area between trees tilted by debris-flow deposits unit  $df_1$  and trees growing on debris-flow deposits unit  $df_2$ , but this trail does not appear to have significantly affected the features observed. Units  $df_1$  and  $df_2$  in figures 7.8A and 7.8B clearly postdate the terrace surface on alluvial deposits unit  $al_3$ , and unit  $df_3$  appears to postdate most of the section of unit  $al_3$  exposed in the bank of the stream channel.

Samples of charcoal fragments from fluvial lenses and discontinuous beds of medium to coarse sand along two horizons in deposits of unit  $al_3$  (figs. 7.8A, 7.8C) were

dated. Sample USGS-549 yielded an age of less than 100 years B.P., and sample USGS-550 an age of  $230 \pm 55$  years B.P. Using the precise calibration between radiocarbon ages and calendar dates by Stuiver (1982), the date for sample USGS-550 falls in the range A.D. 1610–1810 (140–340 years B.P.), with a most likely date of A.D. 1680 (270 years B.P.). We note that radiocarbon ages on charcoal in alluvial deposits tend to be older than the age of deposition (for example, Blong and Gillespie, 1978).

Interpretation of the ages of debris-flow deposits from these dates is made somewhat uncertain by the discontinuity of fluvial bedding exposed in the streambank, in combination with the complexity of deposits that can result from migration of streams across alluviated surfaces (Clyde Wahrhaftig, oral commun., 1978). These relations appear to indicate that all three debris-flow episodes have occurred since sample USGS-549 was deposited, within the past 100 years. However, this sample may have occupied the fill of an undetected channel that, like the present stream channel, had incised into unit  $al_3$ . Given this possibility, sample USGS-550 provides a more reliable maximum age for the debris-flow episodes because it was collected lower in the deposits, although this sample, like sample USGS-549, might be younger than those parts of the terrace occupied by debris-flow deposits. The evidence thus suggests an average recurrence interval for debris flows at this canyon mouth of less than 33 years, more certainly less than 90 years.

During the January 1982 storm, debris flows occurred in the canyons above points A and B in figure 7.7, but there is no evidence that debris flows issued from either canyon mouth. Features typical of fresh debris-flow trails were absent in the lowermost reaches of these canyons at the time of our inspection shortly after the storm. Also absent near these canyon mouths were fresh deposits that were poorly sorted like those identified as debris-flow deposits in figure 7.8; fresh deposits near these canyon





mouths consisted of sorted and bedded fluvial deposits, including much cobble gravel with a matrix of clean to silty sand. Thus, the debris flows in 1982 must either have stopped in the upper parts of these canyons or have been diluted in passage downcanyon. The fact that so major

an event as the January 1982 storm was not represented by debris-flow deposits at these canyon mouths demonstrates that debris flows have reached these canyon mouths less frequently than rainfall events capable of triggering abundant debris flows.

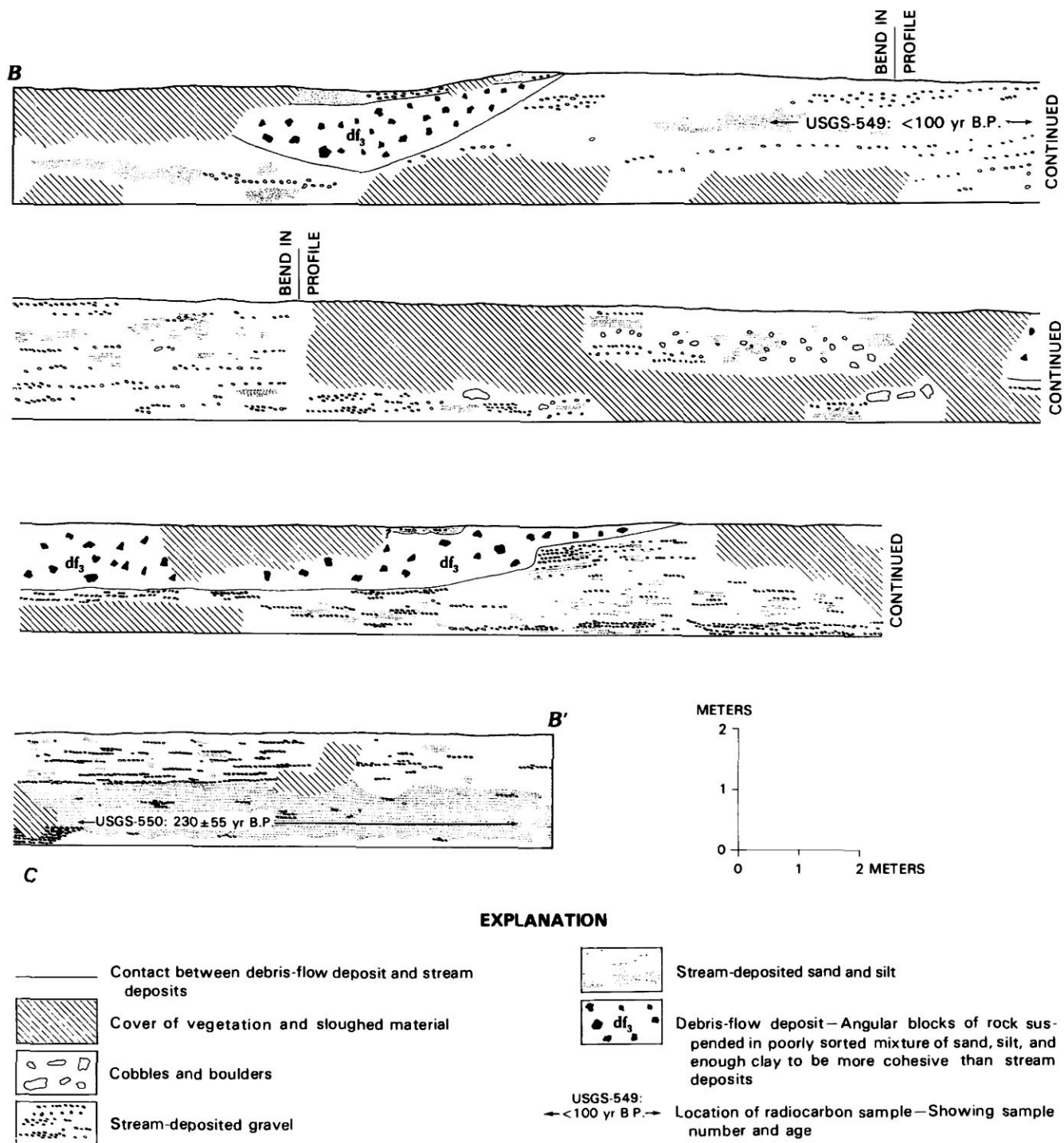


FIGURE 7.8.—Continued

# **RADIOCARBON SITES NEAR INVERNESS (CASE STUDY 5, PL. 5)**

By STEVEN L. RENEAU and STEPHEN W. ROBINSON

During the January 1982 storm, debris torrents and other debris flows in canyons on the east side of Inverness Ridge (see Inverness area case study, chap. 6) eroded large volumes of material from stream channels and exposed many surficial deposits that contained charcoal and wood debris. Six samples were chosen from these exposures for radiocarbon dating to explore the timing of past depositional events along the channels and to evaluate the usefulness of these deposits for estimating recurrence intervals for debris flows. The radiocarbon ages and calendar dates of samples are listed in table 7.4, and sample locations are shown in figure 6.7.

In small, forested drainage basins, scour by debris flows can be the dominant erosional process, as discussed by Swanston and Swanson (1976) and Dietrich and Dunne (1978). This condition existed in 1982 on Inverness Ridge, where extensive erosion occurred along the debris-flow paths, commonly scouring colluvium and sediment to bedrock. In contrast, comparable channels unaffected by debris flows showed little erosion. Significant deposition during the storm occurred behind logjams left at the termini of debris flows and on flood plains where debris flows upstream were a source of sediment. The apparent relation between major erosion and deposition in these canyons and debris-flow events provides a means to infer the timing of particular events by dating these deposits. The age of discrete depositional units can be used to date events directly, and the age of material immediately overlying bedrock provides a minimum age for a preceding period of scour at that point.

Three of the dated samples were collected from the north fork of First Valley (pl. 4). An age of  $1,950 \pm 35$  years B.P. (sample USGS-1466) was obtained in the upper drainage basin from charcoal in an organic-rich layer directly overlying granitic bedrock. This layer was buried beneath 3 m of fairly uniform granitic sand, possibly colluvial in origin, that was deeply eroded during the January 1982 storm. The drainage channel there appears to have been a smooth swale before passage of the debris flow. An age of  $1,215 \pm 40$  years B.P. (sample USGS-1465) was obtained from charcoal in a similar organic-rich layer beneath the eroded flood plain of the lower valley. The sampled layer was overlain by 1 m of granitic sand and was separated from bedrock by a sand and gravel unit that pinched out 10 m upstream. An age of  $110 \pm 50$  years B.P. (sample USGS-1513) was obtained from a large wood fragment within a buried layer of woody debris in the intermediate part of the canyon. This layer, which was exposed immediately below the surface of an eroded flood plain, was similar in appearance to logjams left by the

TABLE 7.4.—Radiocarbon ages from the Inverness area

[Calibrated dates from Stuiver (1982, p. 1)]

Sample	Locality	Material	Radiocarbon age (yr)	Calibrated date
USGS-1465	North fork of First Valley.	Charcoal---	$1,215 \pm 40$	A.D. 670-920
USGS-1466	do-----	do-----	$1,950 \pm 35$	110 B.C.-A.D. 110
USGS-1467	Vallejo Street Canyon.	Wood-----	$14,720 \pm 50$	---
USGS-1468	South fork of First Valley.	do-----	$675 \pm 40$	A.D. 1260-1380
USGS-1469	do-----	do-----	$>46,500$	---
USGS-1513	North fork of First Valley.	do-----	$110 \pm 50$	After A.D. 1650

1982 debris flows. The layer exceeded 1 m in thickness, with the base unexposed.

Two dated samples were collected from the southern basin of First Valley (see fig. 6.7), along a small tributary to the main stream. The lower 150 m of this tributary was scoured in 1982 by a debris flow originating immediately below a dirt road, apparently related to road drainage. For 90 m upstream from its confluence with the main stream, the tributary flows through a sequence of partially cemented granitic gravel that has an estimated exposed thickness of 15 to 20 m. This sequence contains layers of sand, woody debris, and buried soils, and includes a probable debris-flow deposit that consists of clayey sand containing randomly oriented pieces of wood. A sample of wood from near the top of the sequence yielded an age older than 46,500 years B.P. (sample USGS-1469). An age of  $675 \pm 40$  years B.P. (sample USGS-1468) was obtained from wood in a 0.5-m-thick layer containing decomposed vegetation and many small sticks, situated 15 m upstream from the confluence and immediately below a 3- to 4-m-high waterfall over the gravel sequence. The sampled layer was deposited unconformably against the gravel, with the base unexposed, and was overlain by 0.25 m of granitic sand. These latter units were almost completely eroded during the January 1982 storm.

The sixth sample was collected from the basin above Vallejo Street in Inverness Park, a short distance up a narrow tributary canyon. An age of  $14,720 \pm 50$  years B.P. (sample USGS-1467) was obtained from a large piece of wood within a blue-gray sandy clay overlying granitic bedrock. This deposit was exposed by approximately 1 m of local incision.

The dated samples record various events. Two samples (USGS-1467, USGS-1469) are Pleistocene in age and probably cannot be used to evaluate the frequency of modern processes, although this fact was not obvious in the field.

The youngest dated event is a probable debris flow, represented by a buried debris layer on the north fork of First Valley (sample USGS-1513). Because the correlation between radiocarbon ages and calendar dates is imprecise, a post-A.D. 1650 date is all that can be obtained for the wood in this deposit. Possible subsequent debris flows could have passed by without leaving a record, as in January 1982, and so this date is inferred to represent a maximum age for the latest debris flow there.

The next youngest sample (sample USGS-1468) is from a loose deposit of sticks in the southern basin of First Valley. Because a major debris flow down that tributary should have eroded this material, the latest major event there is inferred to predate A.D. 1260-1380. The overlying sand may record a landslide event upstream that did not send a debris flow past this point.

The sampled layer from the lower flood plain of First Valley (sample USGS-1645) overlies bedrock and places a minimum date of latest erosion to bedrock at this point of A.D. 670-920. Deposition of the overlying sand may have been related to debris flows from a later storm.

The sample from the upper north fork of First Valley (sample USGS-1466) places a minimum date on the latest major erosion there at 110 B.C.-A.D. 110. The drainage basin above this site is relatively small, and the only debris flow produced in January 1982 was related to road drainage. These observations suggest that the natural frequency of erosional events in this basin is low and that the date may indirectly record the latest major debris-flow event passing this site.

The individual debris flows that were triggered during the January 1982 storm left varying records of their passage. Each flow scoured material from its path, but the efficiency of this process varied greatly along each debris-flow path and in different drainages, and no debris flow was completely effective in this erosion. Deposition by each flow was also sporadic, and the effects of earlier debris flows probably were equally irregular. The varying dates obtained show that the material mantling each canyon bottom should be viewed as a mosaic of different-age deposits, recording many separate events. The youngest dated deposit in any canyon places an approximate maximum limit on the timing of the most recent previous debris flow. To calculate an average recurrence interval for debris-flow events in a single canyon or a given area, a large-enough sample set is needed to include most events; some events will probably be missed, and so this method provides, at best, a maximum average recurrence interval. If the dates cluster around particular times, this clustering would provide evidence for discrete erosional periods.

The dated samples from Inverness Ridge do not have concurrent ages. The disparity in the ages indicates that the deposits do not record a common storm event and that

the record is complex. Although a minimum of four events in the past 2,000 years is shown, the data set is too small to calculate a meaningful recurrence interval. These four dates suggest, however, that the mean residence time of material along these channels is less than 2,000 years. The two older samples demonstrate local preservation of Pleistocene deposits, which complicates interpretation of all the deposits there in relation to the frequency of modern processes.

#### CONCLUSIONS CONCERNING DISTRIBUTION OVER TIME

Almost all the debris flows induced in Marin County by the January 1982 storm probably occurred during intense storm rainfall, and concurrence of the debris torrents near Inverness suggests that at least some events were triggered by periods of exceptionally intense rainfall during the storm. Rainstorms capable of triggering some debris flows in the county have occurred about every 5 years or so. However, rainfall capable of abundant debris flows, as in the January 1982 storm, has occurred less frequently; rainfall-recurrence intervals for this storm suggest that similar rainfall and, thus, similar levels of debris-flow activity can be expected every 20 to 100+ years in the county.

Radiocarbon dating suggests that the recurrence intervals of debris flows at different sites in the county may range from less than 33 to more than 1,950 years. Dates from many more sites would be needed to determine a recurrence interval for abundant debris flows. The earliest date from Inverness suggests that debris flows have occurred in the county for more than 46,500 years.

#### REFERENCES CITED

- Bailey, E.H., Irwin, W.P., and Jones, D.L., 1964, Franciscan and related rocks, and their significance to the geology of western California: California Division of Mines and Geology Bulletin 183, 177 p.
- Blake, M.C., Jr., Bartow, J.A., Frizzell, V.A., Schlocker, Julius, Sorg, D.H., Wentworth, C.M., and Wright, R.H., 1974, Preliminary geologic map of Marin and San Francisco Counties and parts of Alameda, Contra Costa, and Sonoma Counties, California: U.S. Geological Survey Miscellaneous Field Studies Map MF-574, scale 1:62,500, 2 sheets.
- Blong, R.J., and Gillespie, R., 1978, Fluvially transported charcoal gives erroneous  $^{14}\text{C}$  ages for recent deposits: *Nature*, v. 271, no. 5647, p. 739-741.
- Breslow, N.E., and Day, N.E., 1980, Statistical methods in cancer research: Lyon, International Agency for the Research of Cancer, 338 p.
- Campbell, R.H., 1975, Soil slips, debris flows, and rainstorms in the Santa Monica Mountains and vicinity, southern California: U.S. Geological Survey Professional Paper 851, 51 p.
- Dietrich, W.E., and Dunne, Thomas, 1978, Sediment budget for a small catchment in mountainous terrain, in Slaymaker, Olav, Rapp, Anders, and Dunne, Thomas, eds., *Field instrumentation and*

- geomorphological problems: *Zeitschrift für Geomorphologie*, supp. v. 29, p. 191-206.
- Davenport, C.W., 1984, An analysis of slope failures in eastern Marin County, California, resulting from the January 3rd and 4th, 1982, storm: California Division of Mines and Geology Open-File Report 84-22SF, 38 p. and appendix.
- Ellen, S.D., Peterson, D.M., Reid, G.O., and Savina, M.E., 1979, Hillslope forms and landslide processes in erosional terrain on Franciscan rocks of the Marin Peninsula, California [abs.]: Geological Society of America Abstracts with Program, v. 11, no. 3, p. 77.
- Ellen, S.D., Peterson, D.M., and Reid, G.O., 1982, Map showing areas susceptible to different hazards from shallow landsliding, Marin County and adjacent parts of Sonoma County, California: U.S. Geological Survey Miscellaneous Field Studies Map MF-1406, 8 p., scale 1:62,500.
- Feinburg, S.E., 1977, The analysis of cross-classified data: Cambridge, Mass., MIT Press, 151 p.
- Fleiss, J.L., 1973, Statistical methods for rates and proportions: New York, John Wiley and Sons, 223 p.
- Gart, J.J., 1971, The comparison of proportions: A review of significance tests, confidence intervals, and adjustments for stratification: *International Statistical Institute Review*, v. 39, no. 2, p. 148-168.
- Govi, Mario, and Sorzana, P.F., 1980, Landslide susceptibility as a function of critical rainfall amount in Piedmont basins (North-Western Italy): *Studia Geomorphologica Carpatho-Balcanica*, v. 14, p. 43-61.
- Hollingsworth, Robert, and Kovacs, G.S., 1981, Soil slumps and debris flows: Prediction and protection: *Association of Engineering Geologists Bulletin*, v. 18, no. 1, p. 17-28.
- Kesseli, J.E., 1943, Disintegrating soil slips of the Coast Ranges of central California: *Journal of Geology*, v. 51, no. 5, p. 342-352.
- Nilsen, T.H., Wright, R.H., Vlastic, T.H., and Spangle, W.E., 1979, Relative slope stability and land-use planning in the San Francisco Bay region, California: U.S. Geological Survey Professional Paper 944, 96 p.
- Peterson, D.M., 1979, Hillslope erosional processes related to bedrock, soils, and topography of the Three Peaks area, Marin County, California: San Jose, Calif., San Jose State University, M.S. thesis, 94 p.
- Reid, G.O., 1978, The relationships among slope processes, soils, bedrock, and topography in an area of Franciscan terrane in Marin County, California: San Jose, Calif., San Jose State University, M.S. thesis, 90 p.
- Reneau, S.L., and Dietrich, W.E., 1987, Size and location of colluvial landslides in a steep forested landscape, in Beschta, R.L., Blinn, T., Grant, G.E., Ice, G.G., and Swanson, F.J., eds., *Erosion and sedimentation in the Pacific rim*: International Association of Hydrological Sciences Publication 165, p. 39-48.
- Rice, S.J., Smith, T.C., and Strand, R.G., 1976, Geology for planning, central and southeastern Marin County, California: California Division of Mines and Geology Open-File Report 76-2SF, 103 p.
- Savina, M.E., 1982, Studies in bedrock lithology and the nature of downslope movement: Berkeley, University of California, Ph.D. thesis, 298 p.
- Smith, T.C., and Hart, E.W., 1982, Landslides and related storm damage, January 1982, San Francisco Bay region: *California Geology*, v. 35, no. 7, p. 139-152.
- Stuiver, Minze, 1982, A high-precision calibration of the AD radiocarbon time scale: *Radiocarbon*, v. 24, no. 1, p. 1-26.
- Swanston, D.N., and Swanson, F.J., 1976, Timber harvesting, mass erosion, and steep-land forest geomorphology in the Pacific Northwest, in Coates, D.R., ed., *Geomorphology and engineering*: Stroudsburg, Pa., Dowden, Hutchinson and Ross, p. 199-221.
- Trautmann, C.H., 1976, Engineering geology in Franciscan melange terrane in the Red Hill area, Petaluma, California: Stanford, Calif., Stanford University, M.S. thesis, 74 p.
- Wentworth, C.M., and Frizzell, V.A., Jr., 1975, Reconnaissance landslide map of parts of Marin and Sonoma Counties, California: U.S. Geological Survey Open-File Report 75-281, scale 1:24,000.
- Zelen, M., 1971, The analysis of several 2x2 contingency tables: *Biometrika*, v. 58, no. 1, p. 129-137.





# 8. DEBRIS FLOWS AND OTHER LANDSLIDES IN SAN MATEO, SANTA CRUZ, CONTRA COSTA, ALAMEDA, NAPA, SOLANO, SONOMA, LAKE, AND YOLO COUNTIES, AND FACTORS INFLUENCING DEBRIS-FLOW DISTRIBUTION

By GERALD F. WIECZOREK, EDWIN L. HARP, and ROBERT K. MARK,  
U.S. GEOLOGICAL SURVEY;

and

ARUN K. BHATTACHARYYA,  
JADAVPUR UNIVERSITY, CALCUTTA

## CONTENTS

	Page
Abstract - - - - -	133
Introduction - - - - -	134
Acknowledgments and responsibility - - - - -	134
Distribution of debris flows - - - - -	134
Procedure for describing distribution - - - - -	134
Airphoto coverage - - - - -	134
Field checking - - - - -	135
Map representation - - - - -	136
Contouring the concentration of debris flows - - - - -	137
Factors affecting the distribution of debris flows in San Mateo County - - - - -	137
Rainfall - - - - -	137
Bedrock geology - - - - -	138
Ranking of debris-flow incidence - - - - -	138
Comparison with previous landslide-susceptibility evaluation - - - - -	138
Correlation with mapped colluvial deposits - - - - -	140
Slope steepness - - - - -	140
Vegetation - - - - -	141
Debris-flow abundance on Butano Ridge - - - - -	141
Distribution of debris flows elsewhere in the San Francisco Bay region - - - - -	142
Discussion of debris-flow concentration - - - - -	144
Description of large landslides - - - - -	144
Elkus Ranch - - - - -	145
Grant Road - - - - -	147
Fall Creek - - - - -	147
Whitehouse Creek - - - - -	149
Canham Road - - - - -	152
Alba Road - - - - -	153
Creekwood Drive - - - - -	155
Other large landslides - - - - -	156
Conclusions - - - - -	158
References cited - - - - -	158

### ABSTRACT

Debris flows and other landslides resulting from the January 3-5, 1982, storm were mapped throughout the San Francisco Bay region from aerial photographs, with limited field checking. The concentration of debris flows (number per square kilometer) was measured and contoured. Maximum concentrations reached 63 debris flows per square kilometer, which, though high, is lower than observed from some intense rainstorms in other parts of the world.

In San Mateo County, we examined factors affecting the distribution of debris flows, including rainfall, bedrock geology, slope steepness, and vegetation. Normalized storm rainfall (total storm rainfall divided by

mean annual precipitation) influenced debris-flow distribution more strongly than did total storm rainfall; areas of high debris-flow concentration showed normalized storm rainfall greater than 0.30. The influence of bedrock geology on debris-flow incidence was evaluated by a comparison of debris flows with bedrock geology, using digitized data bases; this evaluation correlated with a suggestive geologic indicator of long-term geomorphic slope-forming processes. Slope steepness determined from a digital elevation model (DEM) showed that debris flows most commonly occurred on DEM-derived slopes of 19-22°, below typical field-measured values. However, when normalized by taking into account the availability of slopes of different steepness, the DEM slope interval most densely populated by debris flows was 25° to 29°, more in accord with

experience elsewhere. Vegetation showed no distinct influence on regional distribution of debris flows, but in one area logging correlated with an increase in debris-flow concentration. In Santa Cruz, Contra Costa, Alameda, Napa, Solano, Sonoma, Lake, and Yolo Counties, we noted areas of dense debris-flow concentration and related those areas to high values of normalized storm rainfall.

In addition to describing the regional distribution and factors affecting debris-flow concentration, in this chapter we describe several of the largest landslides in San Mateo and Santa Cruz Counties to illustrate the complexity of the landslides that occurred in the storm.

## INTRODUCTION

The January 3-5, 1982, storm triggered thousands of landslides in the San Francisco Bay region (see "Introduction" to this volume for landslide terminology). Field reconnaissance after this storm revealed that many slides transformed into flows, and we use the term "debris flow" for these complex landslides. The distribution of debris flows within the bay region was irregular; some areas had dense concentrations (more than 60 debris flows per square kilometer), whereas other areas were virtually devoid of debris flows (less than 1 per square kilometer). We document here the distribution of debris flows and discuss factors that significantly affected this distribution.

Few studies have inventoried the debris-flow distribution resulting from a single storm over a large area, or quantified debris-flow distribution on a regional basis, and then assessed the factors that affected this distribution. In northwestern Italy, Govi and Sorzana (1980) quantified debris-flow distribution and examined this distribution with respect to several parameters, including slope, bedrock lithology, soil type and thickness, and measures of storm rainfall. In the Kinki District of Japan, Okuda and others (1979) examined the relations of debris-flow distribution to geology, geomorphology, and rainfall. In the Shizuoko Prefecture of Japan, Omura and Nakamura (1983) related debris-flow distribution to bedrock lithology, vegetative land use, and rainfall.

We describe the method, difficulties of preparation, and limitations of the debris-flow inventory, and describe the procedure for quantifying the distribution of debris flows. For areas with a high concentration of debris flows, we examine the factors that contributed to that concentration.

We also present case studies of seven large landslides in San Mateo and Santa Cruz Counties for which site investigation revealed details, such as initial failure conditions or characteristics of movement, that illustrate slope processes during the storm. For comparative purposes, the characteristics of large landslides in the storm, including volume, degree of slope, and distance of travel, are tabulated.

## ACKNOWLEDGMENTS

Numerous individuals contributed information or assisted with field checking or other aspects of this study. Carl M. Wentworth assisted with mapping debris flows in the Montara quadrangle of San Mateo County and pointed out differences in the freshness of debris-flow scars. Vincent Chavez assisted with photointerpretative mapping in San Mateo and Solano Counties. Raymond C. Wilson, Randall W. Jibson, David K. Keefer, Christopher S. Alger, and Vincent Chavez assisted with field checking in San Mateo County. Jeffrey H. Peters of Western Ecological Services Co. and Stephen R. Staub of Big Creek Lumber Co. supplied information on the chronology of logging practices in the vicinity of Butano Ridge, San Mateo County. Hans P. Nielson and Mark Foxx of Rogers Johnson and Associates, Laurel M. Collins of the East Bay Regional Park District, and David K. Keefer and Randall W. Jibson assisted by bringing interesting debris-flow sites to our attention and providing us with detailed information for these sites.

Debris flows in Contra Costa County were mapped by Wiecezorek and Bhattacharyya, a visiting United Nations Educational, Scientific, and Cultural Organization (UNESCO) Fellow from the Department of Geological Sciences at Jadavpur University in Calcutta, India. Debris flows and other landslides in Santa Cruz and San Mateo Counties were mapped and partially field checked by Harp and Wiecezorek. Debris flows and other landslides in Alameda and parts of Napa, Solano, Sonoma, Yolo, and Lake Counties were mapped by Wiecezorek. Mark provided computer-generated maps of normalized storm rainfall and performed computer correlation between slope, geologic units, and debris-flow distribution.

## DISTRIBUTION OF DEBRIS FLOWS

### PROCEDURE FOR DESCRIBING DISTRIBUTION

#### AIRPHOTO COVERAGE

The distribution of debris flows was compiled from interpretation of aerial photographs, in some areas coupled with aerial and ground-based reconnaissance. Aerial reconnaissance from fixed-wing aircraft immediately after the storm identified the areas most affected by debris flows. On the basis of this preliminary evaluation, the U.S. Geological Survey contracted for black-and-white aerial stereophotography at 1:20,000 scale for the areas most affected—Marin, San Mateo, and Santa Cruz Counties. Independently, the U.S. National Aeronautics and Space Administration (NASA) took false-color infrared photography at 1:24,000 scale for selected parts of the San Francisco Bay region, including parts of Contra

Costa County. Both sets of photographs were taken within a 7-day rain-free period after the storm in early January, and so none of the fresh-appearing debris flows can be attributed to rainfall after the storm. However, field observations in San Mateo County during the weeks before the storm revealed that a few debris flows had been triggered by storms during late December (see chap. 5; R.C. Wilson, written commun., 1982). In the La Honda study area (see chap. 5), 5 debris flows were triggered in December, in comparison with 74 triggered by the January 1982 storm—a difference suggesting that about 6 percent of the fresh debris flows identified from the January photographs are attributable to previous storms.

Because airphoto coverage was incomplete for some parts of the bay region, a subsequent series of 1:24,000-scale infrared photographs was commissioned from NASA and flown during summer 1982. We used these photographs to map areas not previously covered in Contra Costa, Alameda, Napa, Solano, Sonoma, Yolo, and Lake Counties, and to remap areas obscured by shadow in the January 1982 photography. In steep, heavily forested canyons, as much as 30 percent of the inventoried debris flows were detected by using the summer photography.

Although some landslides and debris flows may have occurred between the times of the January and summer 1982 photography, our field observations and photointerpretation in areas covered by both sets of photographs indicate that they were few. For example, field observations after the February 14–15, 1982, storm revealed no additional debris flows in either the Pleasant Valley area of Santa Cruz County or the La Honda area of San Mateo County, both of which had been examined extensively after abundant debris flows in the January 1982 storm. This February 1982 storm was the most intense to occur in the San Francisco Bay region between January 5 and the time of the summer photography. In the Montara Mountain area of San Mateo County, only 1 percent of the debris flows mapped in areas visible in both sets of photographs are attributable to the period after the January 1982 storm (C.M. Wentworth, oral commun., 1985). Considering the small percentages of debris flows in sample areas shortly before (6 percent) and after (1 percent) the January 1982 storm, the debris flows detected by photointerpretation represent a generally accurate distribution from the storm in unforested areas.

In forested areas, however, photointerpretation has underestimated the abundance of debris flows, as discussed below. In some aerial photographs, recent debris-flow deposits could be identified at the mouth of a canyon, but the scar and (or) track could not be identified because of tree cover on the hillside. In other photographs, because of obscuration by trees, the tracks and deposits of debris flows may extend farther downslope than mapped.

In addition to the numerous debris flows, we noticed in the field less common falls, slumps, and translational slides. These other types of landslides, if small, were difficult to detect in aerial photographs; thus, some of these landslides may have been missed, and others may have been identified as debris flows. However, because relatively few of these other types of landslides occurred during the storm, the inventory of debris flows is essentially accurate. Landslides other than debris flows are shown to scale and distinguished from debris flows in the inventory, but they are not subdivided further by type of movement. Several such landslides, numbered on plates 8 and 9, are tabulated and described further below.

We noted several large, slow-moving landslides, specifically earth flows and earth block slides, that began to move between mid-January and summer 1982. These subsequent large landslides were not included in the inventory.

#### FIELD CHECKING

Fieldwork during 1982 provided a check on the accuracy of photointerpretative mapping, allowed detection of landslides not visible on the airphotos, and permitted investigation of individual sites. Because of the size of the study area and the total number of debris flows, field observations were limited largely to areas with high concentrations of debris flows and to areas easily accessible by roadway.

After reconnaissance of debris flows<sup>1</sup> from roads, more thorough examination was undertaken. Officials of parks and public lands were contacted to determine the extent of debris flows in the areas under their jurisdiction. Some of these officials provided rainfall measurements or information on the times of debris flows or on previous debris flows. In San Mateo County, field examinations were conducted in Huddart and Pescadero County Parks, Butano and Portola State Parks, and on the extensive public lands administered by the San Francisco Water Department, in addition to detailed studies that were carried out in the La Honda study area (see chap. 5). In Santa Cruz County, field examination was conducted in Big Basin State Park and in the area of Pleasant Valley. No field checking was done in the other counties. The extent of the areas field checked is shown in plate 7.

Field examination generally confirmed the locations of the debris flows mapped from aerial photographs; however, we recognized that not all debris flows had been identified in thickly forested areas. Particularly in parts

<sup>1</sup>In this section, we omit further discussion of other types of slope movement, except where complex movement involved debris flow.



of northern Santa Cruz County, the number of debris flows that occurred was greater than identified from aerial photographs because many of the smaller debris flows did not disrupt the tree canopy. In Big Basin State Park, for example, a debris flow 7 to 10 m wide traveled 45 m and destroyed the park's water-treatment plant (figs. 8.1, 8.2), but it did not disrupt any trees and was not recognized in the photographs. In the heavily forested areas of San Mateo and Santa Cruz Counties (identified on pl. 7), the distribution shown on plates 8 and 9 represents a lower bound to the number of debris flows that actually occurred.

#### MAP REPRESENTATION

The scar of a typical debris flow is represented schematically on the 1:62,500-scale maps (pls. 8-12) by arcuate

lines drawn upslope of the more accurately plotted location of the track of the debris flow. The widths of the arcuate scar and the track are not necessarily drawn to scale; small features are shown at the minimum size distinguishable on the maps. Thus, the larger debris flows are shown at approximately true scale; for a smaller flow, only the location of the track is shown accurately. Large debris-flow deposits are shown with a dotted pattern for emphasis, but they do not differ significantly from smaller debris-flow deposits, except, possibly, in thickness.

Because of their regional scale, the maps on plates 8 through 12 are insufficient to evaluate debris-flow hazards at individual sites, for which detailed engineering-geologic mapping at a scale of 1:1,000 or larger is generally necessary. These maps are sufficient, however, for the purpose of documenting the regional distribution of debris flows and evaluating the factors that affected this distribution.



FIGURE 8.1.—View upslope to a small (less than 75 m<sup>3</sup> volume) debris-flow scar in black organic soil and tan weathered sandstone from which a slump mobilized into a debris flow. This flow traveled 45 m before hitting the water-treatment plant at Sempervirens Creek in Big Basin State Park, Santa Cruz County. Scar is about 1 m deep. Note organic debris against base of trees in path at left.

## CONTOURING THE CONCENTRATION OF DEBRIS FLOWS

The inventory of debris flows was quantified by digitizing the number of debris flows and contouring this distribution per square kilometer. Isopleth mapping of landslide deposits was used by Campbell (1973) and Wright and Nilsen (1974); Okuda and others (1979) and Govi and Sorzana (1980) applied this technique to depict abundance of debris flows.

Contours were drawn in increments of 5 debris flows per square kilometer to represent different debris-flow concentrations. Areas of less than 5 debris flows per square kilometer were assigned a sparse concentration rating, areas of 5 to 20 debris flows per square kilometer a moderate rating, areas of 20 to 30 debris flows per square kilometer a dense rating, and areas of more than 30 debris flows per square kilometer a very dense rating.

## FACTORS AFFECTING THE DISTRIBUTION OF DEBRIS FLOWS IN SAN MATEO COUNTY

## RAINFALL

About 50 storm-rainfall measurements were available from stations in the hilly and mountainous parts of San Mateo County where debris flows were most abundant (pl. 7; Mark and others, 1983). Using the measurements from these stations, we compared rainfall totals with the concentrations of debris flows. Many areas of moderate and dense debris-flow concentration lacked nearby measurements; however, in a few places, measurements were recorded within such areas or nearby (within 0.8 km in the same drainage).

When mean storm rainfall was compared for areas with different debris-flow concentrations, no clear relation was apparent (table 8.1). Mean storm rainfall was even slightly



FIGURE 8.2.—Water-treatment plant in Big Basin State Park after impact of debris flow shown in figure 8.1. Plant was moved nearly 7 m from its foundation by debris flow, which was only about 0.6 m thick.

TABLE 8.1.—Mean storm rainfall, mean normalized storm rainfall, and standard deviations for areas of varying debris-flow concentrations in San Mateo County

[Sample locations: sparse--rainfall-measurement stations were more than 0.8 km from areas of dense debris-flow concentration; moderate--rainfall-measurement stations were within areas; dense--rainfall-measurement stations were less than 0.8 km from areas; very dense--rainfall-measurement station was less than 0.25 km from area.  $R_s$ , mean storm rainfall;  $N_s$ , mean normalized storm rainfall, defined by  $N_s = R_s/R_a$ , where  $R_a$  is the mean annual precipitation. All measurements from 53 rainfall stations shown on plate 7]

Debris-flow concentration	$R_s$ (mm)	Sample size	$N_s$
Sparse-----	214.3±53.2	36	0.280±0.069
Moderate-----	224.2±47.0	22	.302±0.077
Dense-----	209.5±42.6	14	.316±0.079
Very dense-----	223	1	.338

higher for areas of moderate concentration than for areas of dense concentration.

Normalized storm rainfall, which is defined as the storm total divided by the mean annual precipitation, was also compared with debris-flow concentration. This measure might better reflect a storm's effect on slope stability because hillslopes must adjust over time to average rainfall, and the magnitude of departures from average rainfall can best be compared through normalized storm rainfall. Using the isohyetal map of Rantz (1971), we computed the normalized storm rainfall at each measurement station. The group mean of values within and near areas of different debris-flow concentration revealed the positive relation between normalized storm rainfall and debris-flow concentration evident in table 8.1. Though not obvious on plate 8, this statistical analysis indicated that areas with normalized storm rainfall above 0.30 showed moderate concentrations of debris flows, and those above 0.32 showed dense concentrations. Although only one measurement was near an area of very dense debris-flow concentration, its 0.34 value is consistent with this statistical trend. This result is consistent with that of Mark and Newman (see chap. 2), who found that parts of the San Francisco Bay region with greater than 0.30 normalized storm rainfall had a significant increase in the propensity for damaging landsliding.

#### BEDROCK GEOLOGY

Bedrock geology (from Brabb and Pampeyan, 1983) appeared to influence the distribution of debris flows in San Mateo County. Although almost all the debris flows observed in the field involved only shallow residual or

colluvial soils overlying bedrock, the material properties of these soils, as well as their thicknesses, were influenced by bedrock geology.

#### RANKING OF DEBRIS-FLOW INCIDENCE

The effect of bedrock geology was evaluated by comparing the abundance of debris flows in different geologic units. The percentage of debris flows that occurred within each geologic unit was divided by the percentage of the county occupied by that geologic unit to give a ratio called incidence. The incidence was evaluated by using a computer to compare the digitized locations of the 4,571 debris flows that occurred in the storm in San Mateo County with the 53 geologic units. On the basis of their incidence to debris flow, the units were ranked and divided into groups of high-, medium-, and low-incidence, as listed in table 8.2.

The group of 10 geologic units of high incidence accounted for more than 50 percent of the debris flows in the county within less than 20 percent of the area (table 8.2). Within this group, the debris-flow concentration averaged 10.4 debris flows per square kilometer, well below the peak values shown on plate 8. The group of units with medium incidence had more nearly equal percentages of debris flows (20.6) and area (16). The remaining group of units of low debris-flow incidence constitute 64 percent of the county area but accounted for only 27 percent of the debris flows; concentration averaged less than 1.6 debris flows per square kilometer. The fact that most debris flows occurred within a group of geologic units composing less than 20 percent of the area of the county indicates that bedrock geology strongly influenced debris-flow distribution.

#### COMPARISON WITH PREVIOUS LANDSLIDE-SUSCEPTIBILITY EVALUATION

The ranking of geologic units by debris-flow incidence shows differences from the ranking of susceptibility to landsliding in San Mateo County determined by Brabb and others (1972). Several geologic units of high debris-flow incidence, notably the unnamed volcanic rocks (KJv), the granitic rocks of Montara Mountain (Kgr), the Pigeon Point Formation (Kpp), and the unnamed sandstone unit of Jurassic or Cretaceous age (KJs), had relatively low susceptibility to landsliding according to Brabb and others (1972). This difference arose because ranking of landslide susceptibility by Brabb and others (1972) was based on the areal proportions of geologic units that had failed by landsliding. The areal predominance of large, deep-seated landslides in San Mateo County (Brabb and Pampeyan, 1972) weighted the assessment toward susceptibility to large, deep-seated landslides. Areas with many small landslides noted by Brabb and Pampeyan (1972) did not strongly affect their evaluation of landslide susceptibility because of the small areas involved.

TABLE 8.2.—*Debris-flow incidence in bedrock geologic units of San Mateo County during the January 1982 storm, in decreasing order*

[Unit names and map symbols follow nomenclature of Brabb and Pampeyan (1983). Asterisks denote bedrock units with associated colluvial deposits shown by Brabb (1980) or Brabb and Pampeyan (1983). Incidence for a unit is ratio of its percentage of debris flows to its percentage of areal extent]

Bedrock geologic unit	Symbol	Areal extent in county (pct)	Debris flows (pct)	Incidence
High debris-flow incidence				
Unnamed volcanic rocks-----	KJv	0.01	0.11	11.00
Pomponio Mudstone Member of the Purisima Formation-----	Tpp*	2.50	7.46	2.98
Granitic rocks of Montara Mountain-----	Kgr*	5.18	15.10	2.91
Purisima Formation, undivided-----	TP*	5.09	14.29	2.81
San Gregorio Sandstone Member of the Purisima Formation-----	Tpsg	.56	1.53	2.73
Pigeon Point Formation-----	Kpp*	1.32	3.41	2.58
Unnamed sandstone of Jurassic or Cretaceous age-----	KJs*	1.07	2.71	2.53
San Lorenzo Formation, undivided-----	Tsl	.12	.26	2.17
Unnamed sandstone, shale, and conglomerate of Paleocene age-----	Tss*	.91	1.95	2.14
Mindego Basalt and related volcanic rocks-----	Tmb	2.80	5.51	1.97
Total-----		19.56	52.33	---
Medium debris-flow incidence				
Lambert Shale and San Lorenzo Formation, undivided-----	Tls	1.47	2.89	1.96
Lompico Sandstone-----	Tlo	.09	.17	1.88
Lobitos Mudstone Member of the Purisima Formation-----	Tpl*	.92	1.64	1.78
Limestone of the Franciscan assemblage-----	fl	.09	.13	1.44
Twobar Shale Member of the San Lorenzo Formation-----	Tst	.19	.24	1.26
Tahana Member of the Purisima Formation-----	Tpt*	7.71	9.52	1.23
Tunitas Sandstone Member of the Purisima Formation-----	Tptu	.60	.70	1.17
Sandstone of the Franciscan assemblage-----	fs*	4.89	5.32	1.09
Total-----		15.96	20.61	---
Low debris-flow incidence				
Greenstone of the Franciscan assemblage-----	fg	2.50	2.23	0.89
Vaqueros Sandstone-----	Tvq	1.75	1.51	.86
Lambert Shale-----	Tla	4.85	4.16	.86
Colluvium-----	Qcl	2.26	1.79	.79
Butano Sandstone-----	Tb	10.61	8.09	.76
Santa Cruz Mudstone-----	Tsc	4.40	3.33	.76
Monterey Formation-----	Tm	1.16	.81	.70
Shale in the Butano Sandstone-----	Tbs	.03	.02	.67
Santa Margarita Sandstone-----	Tsm	.25	.15	.60
Merced Formation-----	Qtm	1.95	1.03	.53
Marine-terrace deposits-----	Qmt	3.21	1.47	.46
Franciscan assemblage, undivided-----	KJf	.46	.15	.33
Sand-dune and beach deposits-----	Qs	.54	.18	.33
Sheared rock of the Franciscan assemblage-----	fsr	2.42	.35	<.15
Rices Mudstone Member of the San Lorenzo Formation-----	Tsr	.32	.04	<.15
Serpentine-----	sp	1.15	.15	<.15
Coarse-grained alluvial-fan deposits-----	Qyf	2.86	.33	<.15
Coarse-grained older alluvial-fan and stream-terrace deposits-----	Qof	4.10	.46	<.15
Butano(?) Sandstone-----	Tb(?)	2.02	.20	<.15
Colma Formation-----	Qc	2.50	.22	<.15
Santa Clara Formation-----	Qts	2.14	.18	<.15
Fine-grained younger alluvial-fan deposits-----	Qyfo	2.49	.17	<.15
Artificial fill-----	Qaf	6.19	.04	<.15
Unnamed sedimentary and volcanic rocks-----	Tuv	.01	.00	.0
Marble and hornfels-----	m	.01	.00	.0
Basin deposits-----	Qb	1.03	.00	.0
Conglomerate of the Franciscan assemblage-----	fsg	.01	.00	.0
Metamorphic rocks of the Franciscan assemblage-----	fm	.01	.00	.0
Bay mud-----	Qm	2.11	.00	.0
Chert of the Franciscan assemblage-----	fc	.34	.00	.0
Unnamed shale-----	Ksh	.01	.00	.0
Fine-grained older basin and alluvial-fan deposits-----	Qob	.13	.00	.0
Page Mill basalt-----	Tpm	.01	.00	.0
Unnamed sandstone-----	Tus	.45	.00	.0
Alluvium-----	Qal	.20	.00	.0
Total-----		64.48	27.06	---



In contrast, the evaluation of debris-flow incidence in the storm reflects principally the number of debris flows per square kilometer rather than the area occupied. Thus, in a geologic unit with a high debris-flow incidence, with about 10 debris flows per square kilometer, probably less than 5 percent of the area was occupied by debris flows. Thus, the evaluation by Brabb and others (1972) reflects primarily susceptibility of bedrock to large, deep-seated landsliding, whereas the evaluation here reflects debris-flow incidence in shallow soils developed over bedrock.

#### CORRELATION WITH MAPPED COLLUVIAL DEPOSITS

Colluvial deposits along valley bottoms or below steep slopes, as shown on geologic maps (Brabb and Pampeyan, 1983; Brabb, 1980), correlate with many bedrock units with a medium or high debris-flow incidence in the storm (table 8.2), whereas mapped colluvial deposits are generally absent over bedrock units with a low debris-flow incidence. This association suggests that the colluvium is derived from previous debris flows and that the geologic units with mapped colluvium have been producing debris flows over a long period.

#### SLOPE STEEPNESS

The effect of steepness on slope stability has long been recognized. In particular, the importance of slope steepness for the initiation of debris flows has been documented in southern California (Campbell, 1975), where debris flows most commonly originate on slopes of  $26^{\circ}$  to  $45^{\circ}$ . In San Mateo County, onsite measurements of slopes at which debris flows originated in the January 1982 storm ranged from  $14^{\circ}$  to  $45^{\circ}$  (see chaps. 5, 6, 9).

A digital elevation model (DEM) of San Mateo County with a 30-m grid spacing was used to determine the effect of slope steepness on debris-flow distribution. A quadratic surface was fitted to each set of nine points from the model, and its steepness assigned to the centerpoint of the set. By repeating this process for all sets, a file of digitized slope-steepness values at 30-m spacing was generated that could then be compared with the digitized data base of debris-flow-scar locations. The slopes derived from the DEM are representative of terrain areas with dimensions of approximately 100 m. They cannot be directly compared with values measured in the field at debris-flow scars. Experience shows that generally the DEM slopes are substantially lower than field-measured slopes.

The population of slopes within the county, represented by the first histogram in figure 8.3, shows that gentle slopes ( $0^{\circ}$ – $3^{\circ}$ ) predominate, moderate slopes ( $3^{\circ}$ – $17^{\circ}$ ) are common, steep slopes ( $17^{\circ}$ – $42^{\circ}$ ) are progressively less common, and very steep slopes ( $42^{\circ}$ +) are rare. The frequency of debris-flow-scar locations with slope steepness

is shown by the second histogram in figure 8.3. The peak of this second histogram lies at  $19^{\circ}$ – $22^{\circ}$ , the DEM-derived slope steepness where debris flows most frequently initiated. As expected, this range is well below the  $26^{\circ}$ – $45^{\circ}$  range where debris-flow sources are most common in southern California (Campbell, 1975), well below the typical values shown in figure 7.3 for part of Marin County during this storm, and well below typical field-measured values (fig. 6.16).

The means by which we determined slope steepness must account for most of the discrepancy. Although determination of slope from either DEM or topographic contours tends to give lower values than field measurements (see fig. 7.4), the values cited above for Marin County, which were determined from topographic contours, are considerably higher than those reported here for San Mateo County and more in line with field-measured values. Thus, the DEM method of slope determination appears largely responsible for the low San Mateo County values.

To explore this apparent discrepancy, we normalized the histogram of the frequency of debris flows in San Mateo County with respect to the slope population, dividing by the area of available slopes with different degrees of steepness. This ratio, shown as a curve in figure 8.3, indicates that for an equal area of slopes of different steepness the peak of the debris-flow distribution shifts to  $25^{\circ}$ – $29^{\circ}$ , more in agreement with experience elsewhere. This shift results from the fact that the tendency to fail increases as the slope increases, but fewer steep slopes are available to fail. Above the peak range of  $25^{\circ}$ – $29^{\circ}$ , the abundance of debris flows as well as the ratio decreases, possibly reflecting the inability of debris to form and remain on steeper slopes.

The correlation of debris flows with slope is affected by interaction of the geology with geomorphic processes shaping the terrain. As indicated in our analysis of San Mateo County, the relatively gentle ( $19^{\circ}$ – $22^{\circ}$ ) DEM-derived slopes that favored debris flows reflect the paucity of steep slopes. In Marin County, the peaks of debris-flow frequency with slope varied between different terrain units, from a peak of  $25^{\circ}$  in soft terrain to a peak of  $35^{\circ}$  in hard terrains (see fig. 7.6). Inasmuch as geologic units correlate with terrain units (Ellen and others, 1982), the range of slope frequency for debris flows within a county reflects the composite of geologic units in that area. Therefore, the frequency of debris flows with slope could vary from area to area, depending on differences in slope population and geologic units, but the normalized distribution of debris flows with slope should show a more consistent range of slope values from area to area by eliminating the effects of differences in slope population. Remaining differences in slope could reflect differences in the strength of soil materials or vegetative root mats.

## VEGETATION

The influence of vegetation on the regional distribution of debris flows in San Mateo County is difficult to assess, at least in part because geology, rainfall, and slope steepness all influence vegetation, as well as the distribution of debris flows.

In general, heavily forested areas in southernmost San Mateo County and along California Highway 35 (Skyline Boulevard) (pl. 7) generally show sparse debris-flow concentration, whereas many grass- and brush-covered hillslopes, as at San Bruno Mountain, Montara Mountain, and many areas west of California Highway 35, show moderate, dense, or very dense debris-flow concentrations. However, this apparent relation may be biased because debris flows were difficult to detect beneath thick forest cover.

## DEBRIS-FLOW ABUNDANCE ON BUTANO RIDGE

In the southern part of San Mateo County near Butano Ridge, timber harvesting appears to have affected debris-flow abundance in the storm. Debris flows were very densely concentrated in parts of the upper watershed of Butano Creek. This area had been clearcut between 1953 and 1967, and a small part of the clearcut area subsequently was selectively logged between 1979 and 1981. In adjacent parts of the Pescadero Creek watershed, which had been either tractor clearcut between 1925 and 1953 or selectively logged between 1968 and 1971, notably fewer debris flows occurred. Similar topography and bedrock geology in these areas suggest that the difference in abundance of debris flows could be associated with the method and age of timber harvest, although differences in the direction and degree of bedding dip, as well as other factors, could also account for the observed distribution.

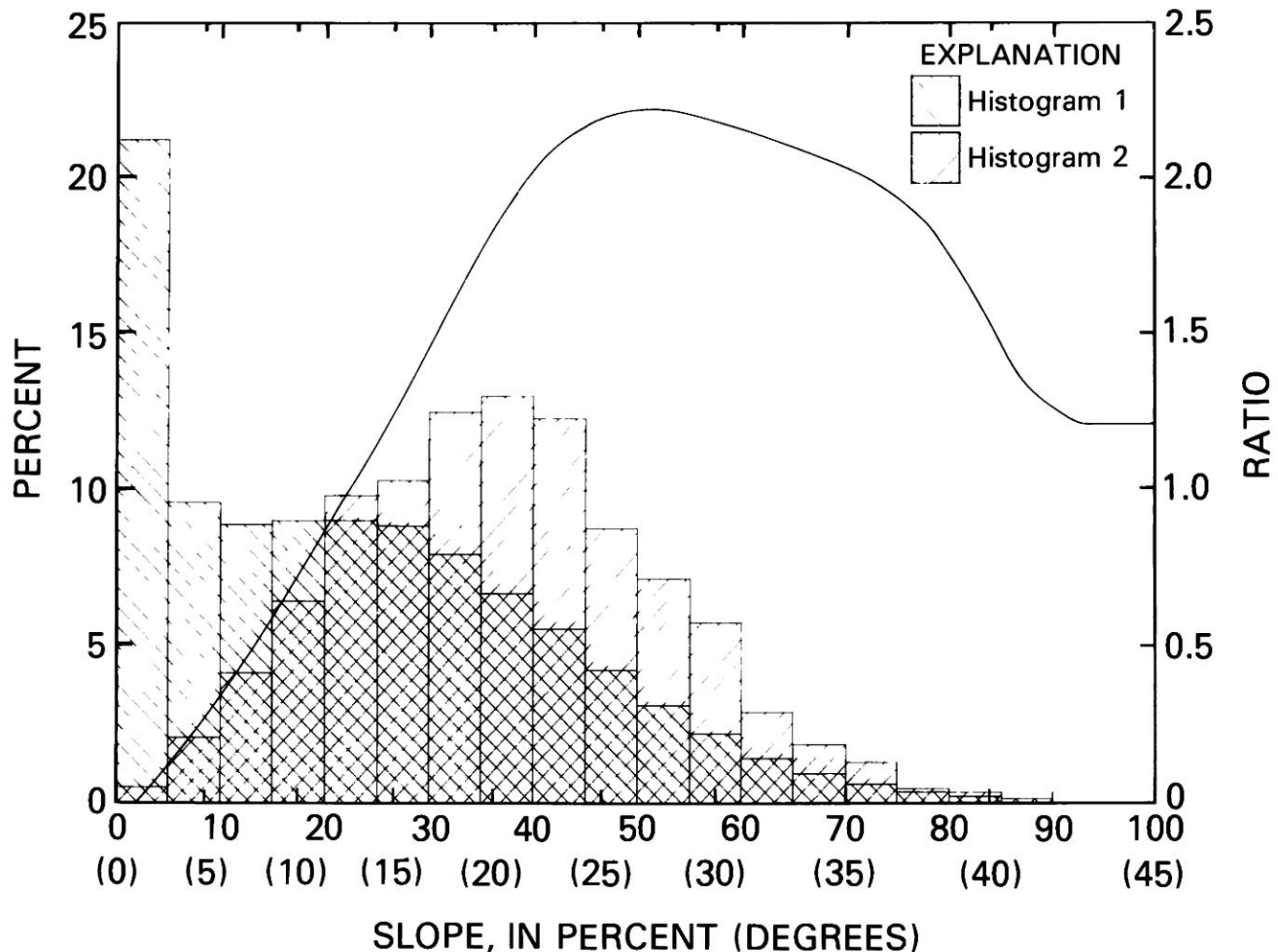


FIGURE 8.3.—Slope steepness at debris-flow sources in San Mateo County, derived from digital elevation model. Histogram 1 shows steepness of all slopes, whereas histogram 2 shows steepness at debris-flow source areas. Normalized curve of steepness distribution of debris flows is ratio of histogram 2 to histogram 1.

Although data from San Mateo County or other areas of central California are unavailable, data from forest lands in the Pacific Northwest indicate a severalfold increase in the abundance of debris flows in clearcut areas over that in forested areas, and even greater increases are associated with roads in these areas (Swanson and others, 1981). Thus, available data suggest that timber harvest can affect the abundance of debris flows.

According to studies in the Pacific Northwest, the shear strength of decaying roots generally begins to decrease markedly within 3 years after cutting and reaches a minimum some 15 years after cutting (Swanson and Swanson, 1976). Correspondingly, shallow landsliding and debris-flow activity noticeably increase beginning after 2 years and continuing as long as 20 years after deforestation (Wu and Swanson, 1980; Swanson and others, 1981; Selby, 1982, p. 142). Loss of root strength is not so likely in San Mateo County, however, because in the Santa Cruz Mountains of California, part of the native vegetation (redwood, tanoak, and madrone) resprouts after cutting and thus tends to maintain root strength. No detailed studies have been conducted in this part of California to document the temporal relation of deforestation to slope stability.

Approximately two-thirds of the abundant debris flows triggered by the storm in the clearcut parts of the Butano Creek watershed originated outside of areas selectively logged in 1979-81. The very dense concentrations of debris flows in this area may be due largely to the clear-cutting and road construction some 15 to 29 years earlier. In the Pescadero Creek watershed, the debris-flow concentration was sparse to moderate, possibly because resprouting and reforestation had strengthened soils within the 3 to 5 decades after clearcutting. Any inferences concerning the effects of logging on debris-flow abundance near Butano Ridge are tentative because detailed site-specific studies are necessary to evaluate the importance of the many factors affecting debris-flow initiation.

#### DISTRIBUTION OF DEBRIS FLOWS ELSEWHERE IN THE SAN FRANCISCO BAY REGION

We determined debris-flow concentrations from the digitized inventory of debris flows in Santa Cruz, Contra Costa, Alameda, Napa, and parts of Solano, Sonoma, Lake, and Yolo Counties (pls. 9-12). Inspection of aerial photographs indicated that the concentration dropped off noticeably to the north into Lake County, to the east toward the Sacramento Valley in Alameda, Contra Costa, Solano, and Yolo Counties, and to the south into Santa Clara and Monterey Counties. Debris flows were observed but not mapped in the western part of Sonoma County west of Santa Rosa. These trends in concentration are also evident in figure 2 (see "Introduction" to this volume);

TABLE 8.3.—Mean storm rainfall, normalized storm rainfall, and maximum debris-flow concentration for areas of dense to very dense debris-flow concentration

[ $R_s$ , mean storm rainfall;  $N_s$ , normalized storm rainfall;  $C_{max}$ , maximum debris-flow concentration.  $R_s$  values are the mean and standard deviation of closest measurements, generally within 3 km of the area under consideration; where there is only a single nearby measurement, the value is given without a standard deviation. N/A, no nearby measurement available]

Area	$R_s$ (mm)	$N_s$	$C_{max}$ ( $km^{-2}$ )
San Mateo County			
Montara Mountain-----	218	0.358	51.0
San Bruno Mountain-----	118	.212	23.0
Santa Cruz County			
Lompico Creek-Zayante Creek-----	455.2±89.3	0.390	32.0
Bean Hill-Pleasant Valley-----	243.3±53.7	.342	63.0
Soquel-Branciforte Creek-----	313.5±58.7	.386	28.0
Contra Costa County			
San Pablo Ridge-Wildcat Creek----	225.5±43.6	0.386	25.9
Franklin Ridge-Pinole Creek-----	173.7±23.2	.311	60.0
Solano County			
Sulphur Springs Mountain-----	N/A	N/A	43.2
American Canyon-Jameson Canyon---	201.3±8.5	.360	37.0

the areas of highest debris-flow concentration are listed in table 8.3.

In Santa Cruz County, debris-flow concentrations show maximums in the central part of the county. The drainage of the San Lorenzo River and its tributaries, particularly the upper watersheds of Newell, Lompico, Bean, Carbonera, and Zayante Creeks, had concentrations, as did the drainages of Soquel and Branciforte Creeks. The Aptos Creek and Valencia Creek drainages between Bean Hill and Pleasant Valley had the highest concentrations, as shown in figure 8.4. The concentration of debris flows drops off sharply to the southeast toward Freedom and Chittenden, to the west of Ben Lomond Mountain, and to the northeast over the crest of the Santa Cruz Mountains.

A detailed study by Coats and others (1982), in a heavily forested small part of Santa Cruz County, addressed landslide distribution and sediment transport after the January 1982 storm. In an inventory of 242 landslides along roads and streams in the Zayante Creek basin, they collected data on the volume, steepness, material, and type of slope movement for comparison with bedrock lithology and other factors that might have affected landslide distribution. They quantified the sediment contribution



of landslides within each channel and, dividing by the length of channel underlain by each bedrock unit, quantified the landslide sediment contributed by each unit. They examined only the channels of the main subwatershed streams (Zayante, Bean, Lompico, Mackenzie, and Ruins Creeks, and Lockhart and Mount Charlie Gulches); because sediment contributions from tributaries and hillsides high in the drainages were not accounted for, the sediment volumes were minimum estimates. They found that differences in bedrock alone could not explain the differences in landslide distribution.

In Contra Costa County (pl. 10), debris flows were most heavily concentrated in the northwestern part of the county, between San Pablo Ridge and Wildcat Creek, and between Franklin Ridge and Pinole Creek. In this last area, concentrations were very dense, reaching a maximum of 60 debris flows per square kilometer (table 8.3). Areas of moderate concentration were in the Berkeley Hills near Moraga and Lafayette, and in the area on the south side of Mount Diablo near the Black Hills.

In Alameda County (pl. 11), debris-flow concentration was sparse to moderate. Only two areas of any appreciable



FIGURE 8.4.—Numerous debris-flow scars and tracks on brush-covered hillslopes above Pleasant Valley, Santa Cruz County. These flows coalesced into a single flow track that extended through buildings at bottom of view and 0.3 km beyond. Photograph taken March 25, 1983, after revegetation and grading along valley bottom had obscured main debris-flow track (dashed lines).



size had a moderate concentration of debris flows. The area of the San Leandro, Cull, and Crow Creek drainages to the northeast of Castro Valley, and the area between Walpert Ridge and Sunol Ridge north of Niles Canyon, reached comparable maximums in the range of 13-16 debris flows per square kilometer.

In the North Bay area of Napa, Solano, Sonoma, Lake, and Yolo Counties (pl. 12), debris-flow concentration was dense in only two localities, in the vicinity of Vallejo—along Sulphur Springs Mountain and in the American Canyon—Jameson Canyon area. In other parts of these counties, debris-flow concentration was sparse to moderate, with no sizable areas of dense concentration.

Although rainfall totals during the storm (see chap. 2; Mark and others, 1983) varied greatly between the areas of highest debris-flow concentration, normalized storm rainfall presented a somewhat more consistent pattern. As listed in table 8.3, debris flows were generally concentrated where normalized rainfall exceeded 0.30. This result is similar to that reported in chapter 2 for an independent analysis of normalized rainfall versus the locations of damaging landslides in the storm. The contours of normalized storm rainfall shown on plates 9 through 12 generally indicate that the areas of densest debris-flow concentration had values of normalized storm rainfall exceeding 0.30.

#### DISCUSSION OF DEBRIS-FLOW CONCENTRATION

The concentrations of debris flows observed in the January 1982 storm throughout the San Francisco Bay region were not nearly so high as those resulting from some intense storms elsewhere throughout the world. In San Mateo, Santa Cruz, Contra Costa, Alameda, Napa, Solano, Sonoma, Lake, and Yolo Counties, maximum concentrations ranged from 25 to 63 debris flows per square kilometer (table 8.3); and in Marin County, concentrations locally reached 55 debris flows per square kilometer (see chap. 7). In contrast, Okuda and others (1979) reported more than 100 debris flows per square kilometer in parts of the Minamiyamashiro region of Japan on August 15, 1953; Omura and Nakamura (1983) reported concentrations as high as 90 debris flows per square kilometer near Shizuoka, Japan, on September 12, 1982; and Govi and Sorzana (1980) reported maximum concentrations that generally ranged from 20 to 50 debris flows per square kilometer for many storms in northwestern Italy.

Concentration of debris flows—that is, the number of debris flows per unit area—is not necessarily the best indicator of debris-flow hazard. The cumulative area of debris flows per unit area (areal ratio) or the volume (in cubic meters) of debris flows within a unit area may be a more accurate measure of debris-flow hazard, but these values are difficult to compile on a regional basis. If the

size of individual debris flows falls within a narrow range and if the areal ratio is relatively small (possibly less than 5 percent), then the concentration of debris flows is a good comparative measure of debris-flow hazard. Investigators that have evaluated the size distribution of debris flows in storm events (Govi and Sorzana, 1980; Omura and Nakamura, 1983; Okuda and others, 1979) found that most debris flows fall within a fairly narrow range of sizes, and so these investigators used concentration to compare storm effects. However, in places where entire slopes have been denuded by coalescing debris flows (Jones, 1973, p. 25-26), counting individual debris flows may be impossible, and so the areal ratio would be a better indicator of debris-flow effects. The relatively small areal ratio depicted on plates 8 through 12 confirms that concentration is an appropriate measure for comparing the debris-flow effects of the January 1982 storm in the San Francisco Bay region.

Although bedrock lithology, in part through its influence on soil type and thickness, affected the concentration of debris flows in San Mateo County, worldwide evidence of lithologic control on debris flows is far from conclusive. For example, Govi and Sorzana (1980) found no direct control by bedrock lithology on debris flows, whereas Pomeroy (1980) found soils derived from certain clay-rich stratigraphic units to be more susceptible than soils from other units. Although the reason for this apparent disparity is unknown, differences in the characteristics of soils derived from bedrock are likely to be central to the solution (see section entitled "Soils Involved," chap. 6).

A major difficulty in evaluating the factors that influence the concentration of debris flows in San Mateo County and elsewhere is the probable interaction among these factors. Ideally, a multivariate analysis should be used to detect the individual and combined effects of important variables. Such analysis for debris flows should include the following factors: rainfall (prestorm, storm total, normalized storm total, hourly intensity, and duration and timing of intense bursts within storms), bedrock lithology, properties and thickness of soils, vegetation (root strength and depth of penetration), and slope steepness and configuration. With new digital techniques for manipulating spatial information (for example, Sailor and Berry, 1980), such regional analyses should soon become more common.

#### DESCRIPTION OF LARGE LANDSLIDES

Site investigations of particular landslides revealed details that illustrate slope processes during the storm in San Mateo and Santa Cruz Counties. The following descriptions illustrate the complexity and variety of many of the landslides. This section concludes with a brief men-

tion of other large landslides in these two counties that either are described elsewhere or were only briefly observed during reconnaissance. Information on all these large landslides is compiled in tables 8.4 and 8.5; locations are numbered on plates 8 and 9.

#### ELKUS RANCH

About 240 m upslope of the Elkus 4-H Ranch house in Purisima Canyon, San Mateo County (site 1, pl. 8), a slump mobilized into a relatively slow moving debris flow. This debris flow reached the house during the evening of January 4, piled against it, and flowed around both sides but did not move the house from its foundation (fig. 8.5). Two vehicles in the driveway were pushed against the garage and partly through the walls.

The hillside where the slump occurred was irregular in profile, with a pronounced bench immediately upslope from the slump and a distinct break in slope just downslope. The slope of the hillside averaged 20°, but above and below the bench, slopes were steeper, averaging 30° to 40° (as measured on a 1:24,000-scale topographic map). The scarp of the slump exposed colluvium over weathered silty sandstone of the Purisima Formation. Ground water issued from the scarp for at least several days after the failure (fig. 8.6).

On the basis of measurements on 1:20,000-scale aerial photographs and field reconnaissance, the slump was approximately 61 m long by 34 m wide, with a maximum thickness of 15 m. The volume of the slump was about 15,000 m<sup>3</sup>. About half of the material from the slump mobilized into the debris flow.

TABLE 8.4.—Large landslides in San Mateo County triggered by the storm

[Average slope is slope at site of initial failure, measured in the field from adjacent slopes or from maps of prefailure topography. Travel distance is measured along slope and so does not necessarily agree with distance measured on plate 8. n.a., not available]

Site (pl. 8)	Locality	Landslide material	Dominant type(s) of movement	Estimated volume (10 <sup>3</sup> m <sup>3</sup> )	Average slope	Travel distance (km)	Remarks/references
1	Elkus Ranch, Purisima Canyon.	Colluvium and weathered silty sandstone of the Purisima Formation, undivided.	Slump/debris flow-----	15	20°	0.27	Near Elkus Ranch house; rate of movement was observed to be only about a meter per minute, slow for a debris flow. Flow carried and pushed two vehicles into walls of house. Flow split and moved around both sides of house but did not move house from foundation.
2	Grant Road, Moss Beach.	Angular gravelly-sand colluvium derived from the granitic rocks of Montara Mountain.	Translational slides coalescing into a single debris-flow track.	8.6	14°	.76	Gentlest measured slope to generate a debris flow in the storm. Piping probably influenced failure; subsequent erosion incised source and track of debris flow. Average slope measured by C.M. Wentworth (oral commun., 1985).
3	Fall Creek, Pescadero County Park.	Clayey-sand colluvium on steep hillsides; large boulders, gravel, sand, and logs scoured from channel. Deposit at mouth of Pescadero Creek consisted of silty sand containing abundant logs and other organic debris.	Translational debris slides, at least nine of which coalesced into two debris-flow tracks in upper tributaries of Fall Creek. Hyperconcentrated streamflow occurred in middle of drainage; in lower part, a debris flow traveled to near mouth of Pescadero Creek.	n.a.	34°-40°	n.a.	Channel exhibited evidence of debris flows and hyperconcentrated streamflow in different reaches over 3.5-km length. Blocking of culvert embankment where Old Haul Road crosses Fall Creek created small pond before embankment failed. Area where debris slides initiated in upper part of drainage had been tractor clearcut logged in 1968-69 (Jeffrey Peters, written commun., 1982).
4	Oddstad Boulevard, Pacifica.	Colluvium of dark-brown clayey-silty sand and gravel, overlain by very dark gray to grayish-brown clayey-sand topsoil; bedrock not exposed in scarp.	Translational slide(s)/debris avalanche.	2.3	26°	.20	Evidence indicates possibly three separate events, but time between events could have been so short as to appear as one continuous event. Maximum rate of movement probably exceeded 10 m/s. The fast-moving flow destroyed two houses and killed three children at approximately 11:10 p.m. P.s.t. January 4, 1982 (see chap. 9).
5	Mindego Creek, near La Honda.	Bedrock mapped as the Tahana Member of the Purisima Formation; very fine sandstone and siltstone, and some silty mudstone (Brabb and Pampeyan, 1983).	Translational soil, debris, and rock(?) slides/debris flow.	50-135	19°	.47	Site was observed only from light airplane, and so these are only approximate estimates from low-altitude aerial photographs and measurements from 1:20,000-scale aerial photographs and 1:24,000-scale topographic maps.

TABLE 8.5.—Large landslides in Santa Cruz County triggered by the storm

[Average slope is slope at site of initial failure, measured in the field from adjacent slopes or from maps of prefailure topography. Travel distance is measured along slope and so does not necessarily agree with distance measured on plate 9. n.a., not available]

Site (pl. 9)	Locality	Landslide material	Dominant type(s) of movement	Estimated volume ( $10^3 \text{ m}^3$ )	Average slope	Travel distance (km)	Remarks/references
6	Whitehouse Creek, north flank of Chalk Mountain.	Colluvium and fractured bedrock of the Santa Cruz Mudstone exposed in main scarp.	Slump/debris flow-----	120-175	29°-31°	0.69	One of the largest debris flows in the storm. Debris flow mobilized where slumps slid over springs. Near terminus of flow, several cabins were destroyed by toppled trees or inundation by debris (D.K. Keefer, written commun., 1985).
7	Canham Road and Carbonera Creek, Scotts Valley.	Colluvium, weathered Santa Cruz Mudstone, and Santa Margarita Sandstone.	Soil and rock slumps coalescing into a single debris-flow track.	<sup>1</sup> 16.8, 9.2; 28.1	27°-36°	2.45	Nine landslides at this site generated four nearly simultaneous debris-flow pulses that traveled down Bethany Drive between 7:00 and 7:15 p.m. P.s.t. January 4, 1982. Two boys walking on Bethany Drive were swept into the flow; one was later thrown clear of the flow, and the other drowned in Carbonera Creek (Nielson, 1984).
8	Alba Road and California Highway 9, Ben Lomond.	Colluvium and weathered silty sandstone and siltstone of the Monterey Formation.	Slump/debris flow-----	6.8	30°-31°	.20	Very rapid movement took place between 7:30 and 8:00 p.m. P.s.t. January 4, 1982, preceded for several hours by development and enlargement of cracks. The landslide destroyed five structures and damaged six; no one was injured (Mark Foxx, written commun., 1982).
9	Creekwood Drive, Lompico.	Colluvium containing weathered shale and siltstone fragments derived from the Monterey Formation.	Translational slide/debris avalanche.	.6	35°-47°	2.20	Slide on very steep slopes generated a very rapidly moving debris flow. (Mark Foxx, written commun., 1982).
10	Love Creek, near Ben Lomond.	Mixture of colluvium and rock debris derived from sandstone and shale of the Monterey Formation. Bedrock exposed along basal surface.	Block slide, which triggered several smaller debris flows.	460	25°-32°	<sup>3</sup> 0.06-0.15	Largest and most disastrous landslide in the storm. Catastrophic failure of the dip slope occurred at approximately 1 a.m. P.s.t. January 5, 1982, and was extremely rapid. Landslide buried 9 homes and killed 10 people. Information from Cotton and Cochran (1982).
11	Newell Creek, near Ben Lomond.	Similar to Love Creek (see site 10).	Block slide-----	72-268	33°	.05	Landslide caused no damage to structures. Information from Cotton and Cochran (1982) and D.G. Herd (written commun., 1982).
12	Año Nuevo Creek, south flank of Chalk Mountain.	Bedrock, mapped as the Santa Cruz Mudstone (Brabb, 1970).	Slump/debris flow-----	150-190	26°-30°	.78	One of the largest debris flows in the storm. Site was observed only from light airplane, and so estimates here are crude, based on low-altitude photographs, 1:20,000-scale aerial photographs, and 1:24,000-scale topographic maps.

<sup>1</sup>Volume of two largest individual slumps and total volume of nine slumps, respectively.

<sup>2</sup>Because debris-flow runout into major streams was not traced, this travel distance is a minimum.

<sup>3</sup>Range of distances from scarp to landslide mass, suggesting that different parts of slide moved different distances.

Beyond the toe of the slump, the flow traveled a sinuous path for about 200 m on a slope of about 13° until it reached the house. A steep debris-flow front, as much as 2.4 m high, alerted the occupants by slowly pushing against the garage door. The debris piled up against the house to the level of the eaves without pushing the house from its foundation, as this debris-flow front came to rest. Near the house, the rate of movement was observed to be only about 1 m/min—a slow rate for a debris flow. The flow then split and flowed around the house as two lobes that traveled a short distance and formed distinct toes.

The distance from the scarp of the slump to the toes of the lobes was about 0.27 km.

A sample of the material in the flow from near the toe of the slump is a silty sand composed of 14 weight percent clay finer than 2  $\mu\text{m}$ . Two samples from near the terminus of the flow were of silt containing 14 to 19 weight percent clay. One other sample from the terminus was a silty-gravelly sand containing only 8 weight percent clay (see table 6.1 for results of grain-size analyses). On the basis of these four samples, the material in the flow appeared to be heterogeneous, including both fine



and coarse materials. Steep, high flow fronts, which indicate significant cohesive strength in a flow, suggest a predominately fine grained material.

#### GRANT ROAD

About 300 m upcanyon from Grant Road, north of Moss Beach in San Mateo County (site 2, pl. 8), two debris flows from translational slides coalesced into a single debris-flow track that extended about 0.76 km. For much of this distance the track followed a street and an existing gully. The flow left a broad, thin deposit on nearly flat slopes.

The principal slide initiated in a swale on brush-covered slopes of about  $14^\circ$ ; thus, this was the gentlest measured slope to generate a debris flow in the storm (fig. 8.7). The material from both slides mobilized entirely. The combined volume of the empty scars was crudely estimated at about  $8,600 \text{ m}^3$ . The scarp and the base of the slide exposed crumbly, angular, gravelly-sand colluvium. Where subsequent erosion incised the slide scar, creating a badlands

topography, weathered granitic rocks of Montara Mountain were exposed. Pipes were observed in association with the scar, and closed pipes could locally have increased pore-water pressures and permitted failure on such a gentle slope.

#### FALL CREEK

Debris slides, debris flows, and hyperconcentrated streamflows disrupted the Fall Creek drainage in Pescadero Creek County Park, San Mateo County (site 3, pl. 8). The steep upper part of the  $1.3\text{-km}^2$ -area Fall Creek drainage was tractor clearcut logged during 1968–69; the middle and lower parts were logged during 1940 and 1941 (Jeffrey Peters, written commun., 1982). Major features of this site are illustrated in figure 8.8.

Nine debris slides that initiated near skid tracks, roads, or pads left from logging were noted in aerial photographs in the steep upper part of the drainage. Slopes in this area averaged  $34^\circ$  to  $40^\circ$ , as measured on a 1:24,000-scale



FIGURE 8.5.—Debris flow against house at the Elkus 4-H Ranch, San Mateo County. Near the house, occupants observed the debris flow moving about 1 m/min.



topographic map. These debris slides, as well as slumps noted in the channel banks during field examination, contributed large amounts of sediment to two major debris-flow tracks in the two main tributaries of the drainage. These debris-flow tracks joined at point A in figure 8.8. The flows continued downstream (fig. 8.9) until stopped in a massive blockage of logs, boulders, and finer sediment where the stream gradient flattened.

Below this blockage, in the middle of the drainage, debris-flow effects were noticeably absent, although high-water-line marks and extensive removal of loose material from the channel attest to high floodflows (or hyper-concentrated streamflows). Deposition of sediment in this section of the drainage was minimal, except for a few large boulders that evidently could no longer be carried along by the streamflow.

In the lower part of the drainage, where Old Haul Road crosses Fall Creek, a small lake formed during the storm, apparently because a 0.91-m-diameter steel culvert was

plugged with debris. High strandlines from the lake, marked by leaves and twigs, indicated that the lake was approximately 225 m<sup>2</sup> in area and as much as 1.2 m deep. The 275-m<sup>3</sup>-volume embankment gave way, mixed with the water behind it, and flowed rapidly as a debris flow down the narrow gorge in the lower part of Fall Creek. A thin veneer of deposit on the channel sides indicated that, at one downstream location, the debris flow was 3 to 5 m deep and 11 to 12 m wide. Much debris, including large redwoods, previously cut and discarded logs, and loose sediment and colluvium from the channel sides and bottom, was scoured and incorporated into the flow. Bedrock was exposed in many places, and the appearance of Tip-Toe Falls was changed appreciably by this scouring, according to park personnel.

This debris flow in the lower part of the drainage came to rest behind a massive logjam where Fall Creek emerges from its narrow gorge onto a wide, flat plain near the confluence with Pescadero Creek. Logs backed up against



FIGURE 8.6.—Slump at source of debris flow at Elkus 4-H Ranch several days after failure. Abundant subsurface water was issuing from this scarp. Note man (circled) in left center for scale.

a stand of redwoods in the center of the plain. The logjam was 18 m wide and blocked about 3,000 m<sup>3</sup> of sediment, 0.5 to 0.85 m thick.

Though not examined in detail, several other small drainages in Pescadero Creek County Park had debris flows and (or) hyperconcentrated floods that were comparable in scale and caused similar effects. Because of the absence of development and the remote location of Fall Creek and these other tributaries of Pescadero Creek, there was no known damage to structures and only minor damage to secondary roads.

#### WHITEHOUSE CREEK

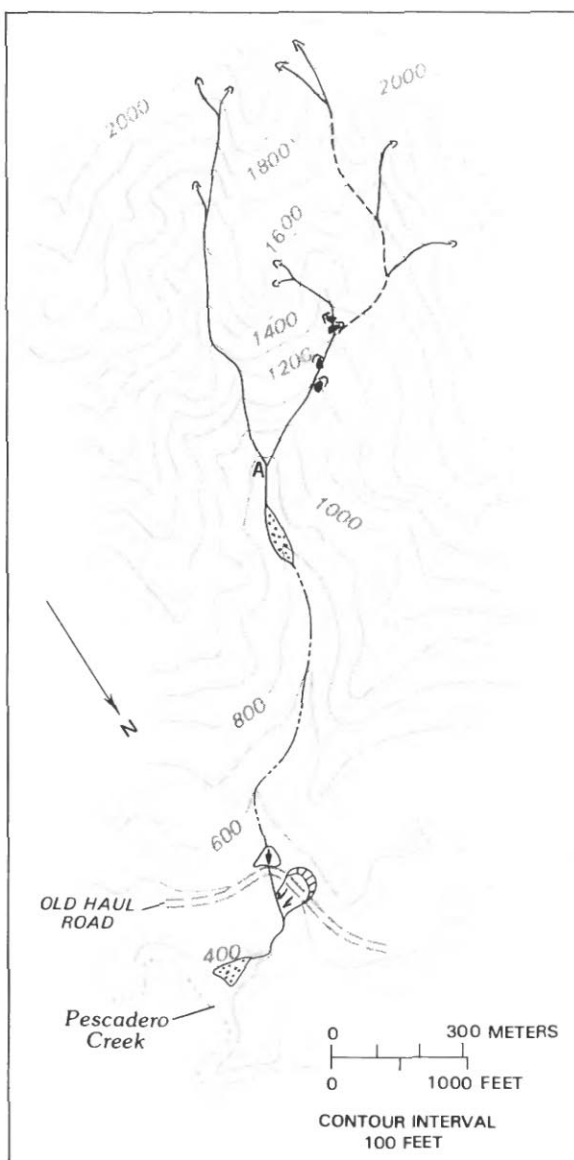
The complex landslide in Whitehouse Creek, Santa Cruz County, initiated as several slumps near the crest of the north flank of Chalk Mountain (site 6, pl. 9) and mobilized into a debris flow that traveled northward down an existing draw to near the confluence with Whitehouse

Creek. Pertinent features of this landslide are shown in the sketch map in figure 8.10. The distance from the crown of the uppermost slump to the end of the debris-flow deposit is nearly 0.70 km. The main scarp, which is inclined at 45°, about 50 m high, and 50 to 60 m wide, exposes colluvium and bedrock composed of Santa Cruz Mudstone. Depending on assumptions of landslide geometry, the volume of material involved in slumping ranged from 120,000 to 175,000 m<sup>3</sup> (fig. 8.11).

Within the area of slumping, several springs were observed; below these springs, the slide material mobilized into a debris flow. For about 250 m below the springs, the debris flow scoured a channel, exposing bedrock in places. The width of the flow here was about 20 m, and the height of flow indicated by lateral levees generally ranged from 5 to 7 m, with a maximum height of 10 m. The presence of at least three pairs of levees in this scoured section below the springs indicates several pulses of debris flow.



FIGURE 8.7.—Source area and beginning of track of debris flow near Grant Road, Moss Beach, San Mateo County. Light-colored sandy debris (arrows) above walls of gully incised into debris-flow track indicates original level of flow.



#### EXPLANATION

- Scar and track of debris flow—  
Dashed where concealed
- Slumps into channel—Arrows  
show direction of movement
- Reach of channel affected by  
flooding and (or) hypercon-  
centrated streamflow
- Debris-flow deposit associated  
with blockage by logs
- Lake formed by blockage of culvert  
beneath Old Haul Road at Fall  
Creek crossing

FIGURE 8.8.—Features related to slides, flows, and hyper-concentrated floods in Fall Creek drainage, San Mateo County. Two major debris-flow tracks joined at point A. Topographic base modified from map of Pescadero Creek by San Mateo County Department of Public Works.

Below this scoured section, the debris flow widened to about 60 m and continued for 180 m on slopes of  $14^\circ$  to  $16^\circ$ . About 80 m past a distinct break in slope, a blockage formed, some 50 m wide, as the fallen timber carried by the flow became lodged against a stand of redwoods. Behind this blockage, subsequent flow was deflected to the east, where it continued another 200 m on slopes of  $10^\circ$ . The flow traveled a total distance of about 0.6 km from the springs before terminating short of Whitehouse Creek.

Several houses were destroyed, mainly by trees toppled by the debris flow. One house was inundated with debris-flow material (fig. 8.12), and a tree fell through its roof. Only one house near the flow was occupied at the time; the people escaped when they saw their neighbor's house being carried along by the flow.

The description of this site is based primarily on descriptions and field notes by David K. Keefer (written commun., 1985).



FIGURE 8.9.—Debris-flow track lined with fallen trees, boulders, and sediment in channel along upper part of Fall Creek, San Mateo County. Slump with rotated trees is visible in lower left. Standing trees along the track are about 15 m high. Photograph by Jeffrey Peters.

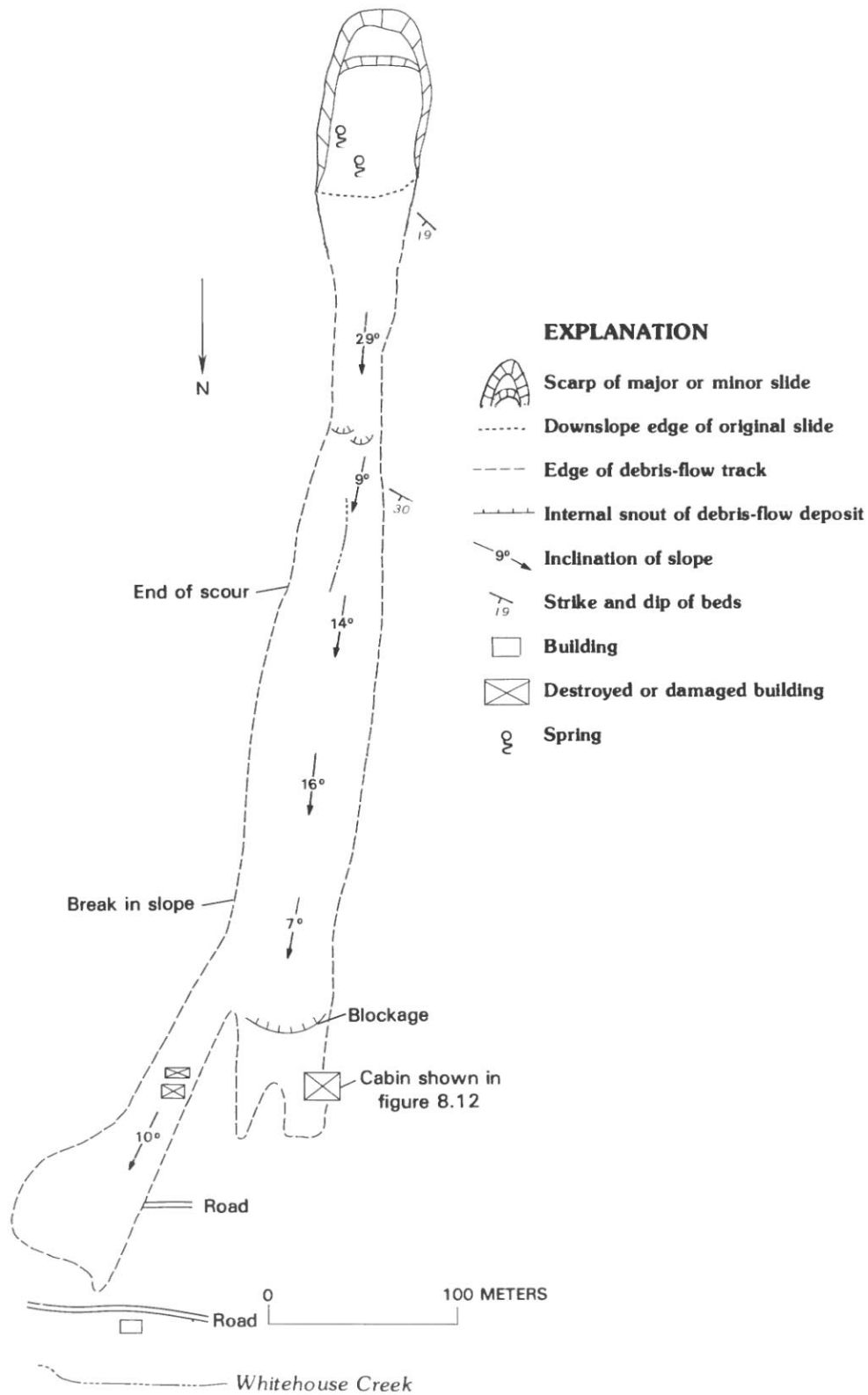


FIGURE 8.10.—Features of slump/debris flow from north flank of Chalk Mountain toward Whitehouse Creek. Modified from D.K. Keefer (written commun., 1985).



## CANHAM ROAD

In northeastern Scotts Valley, Santa Cruz County (site 7, pl. 9), several slides on steep slopes above a small valley mobilized as debris flows that crossed an old apple orchard and coalesced in a narrow canyon. Two boys walking along a road in the canyon were picked up by a flow; one boy was thrown clear of the flow and survived, but the other was carried away and eventually drowned in Carbonera Creek.

An eyewitness observed the series of events between 7:00 and 7:15 p.m. P.s.t. January 4 at Bethany Drive, part-way down the canyon. The first of four debris-flow pulses traveled down the canyon shortly before 7:00 p.m. This first pulse was mostly of black, highly fluid mud. Shortly thereafter, a massive wall of rock, mud, and water, about 2.1 m high, flowed by very rapidly, carrying blocks of rock "half as big as a car." Two smaller pulses of rock and mud followed this main flow mass.

The debris flows continued to the confluence with Carbonera Creek; beyond that point, the flows were not

traced. However, if the flows entered Carbonera Creek during the storm, it is unlikely that they traveled far before being significantly diluted by floodwaters. The distance from the source area of the flows to the confluence with Carbonera Creek is about 0.45 km.

Nine landslide scars were found in the source area, where the brush-covered slopes ranged from 27° to 36° in steepness. A site map of this area is shown in figure 8.13. The two largest landslides were both about 7.7 m deep and mobilized 9,200 and 16,800 m<sup>3</sup> of material, mostly bedrock composed of Santa Cruz Mudstone and a minor amount of colluvium. Six other shallow landslides of soil, less than 2.5 m deep, contributed another 2,150 m<sup>3</sup> to the flows (fig. 8.14). At the south end of the valley, a shallow sand flow from outcrops of Santa Margarita Sandstone added to the total volume of flow.

These debris flows occurred during an intense part of the storm, as indicated by average intensity values of 24.9 mm/h (0.98 in/h) measured between 4:00 and 8:00 p.m. January 4 about 120 m east of the source area along Canham Road (fig. 8.15). This was the highest average



FIGURE 8.11.—Slump/debris flow from north flank of Chalk Mountain toward Whitehouse Creek. This was one of the largest debris flows in the storm; it traveled nearly 0.7 km. Cabins at lower left show scale.

intensity measured at this site during the storm. The timing of the debris flows and the prolonged high average rainfall intensities can be compared with those at the other sites where continuous rainfall measurements are available (see chap. 3).

The description of this site is based on field examination and documentation by Nielsen (1984).

#### ALBA ROAD

Between 7:30 and 8:00 p.m. P.s.t. January 4, a slump from above Alba Road, near Ben Lomond, Santa Cruz County (site 8, pl. 9), mobilized as a debris flow that traveled nearly 0.20 km to California Highway 9. This debris flow totally destroyed one house and four cabins, and substantially damaged another house, two other cabins, a preschool, and two utility buildings. A site map of this area is shown in figure 8.16.

At about 3:00 p.m., a crack was noticed on Alba Road; by 4:30 p.m., this crack had developed a 0.15- to 0.25-m

vertical offset, making vehicular crossing difficult. A plugged culvert drop inlet directed water into a ditch alongside the road; this ditch overflowed across Alba Road in the vicinity of the slide (fig. 8.16). Approximately 10 minutes before the debris flow initiated, a loud crack was heard that sounded like a tree crashing to the ground. The debris flow moved rapidly and with considerable force, crushing several structures, tearing sections from structures on the edge of the flow path, and carrying structures as far as 30 m. However, there was little turbulence in the flow; most of the pieces of pavement from Alba Road stayed on the surface during transport of more than 100 m. Where these pieces came to rest, their distribution was arcuate, reflecting a displacement profile that was smallest along the edges of flow and largest in the center.

The hillslope that failed was almost planar, without major gullies; it was vegetated with redwood, pine, tan oak, and madrone. Slopes in the vicinity of the slump measured 30° to 31°. During previous storms, the hillside



FIGURE 8.12.—Cabin inundated by debris flow near Whitehouse Creek (fig. 8.11) to a depth of 1.2 to 2.4 m (see fig. 8.10 for location). Note track of debris flow and blockage by fallen timber in background.

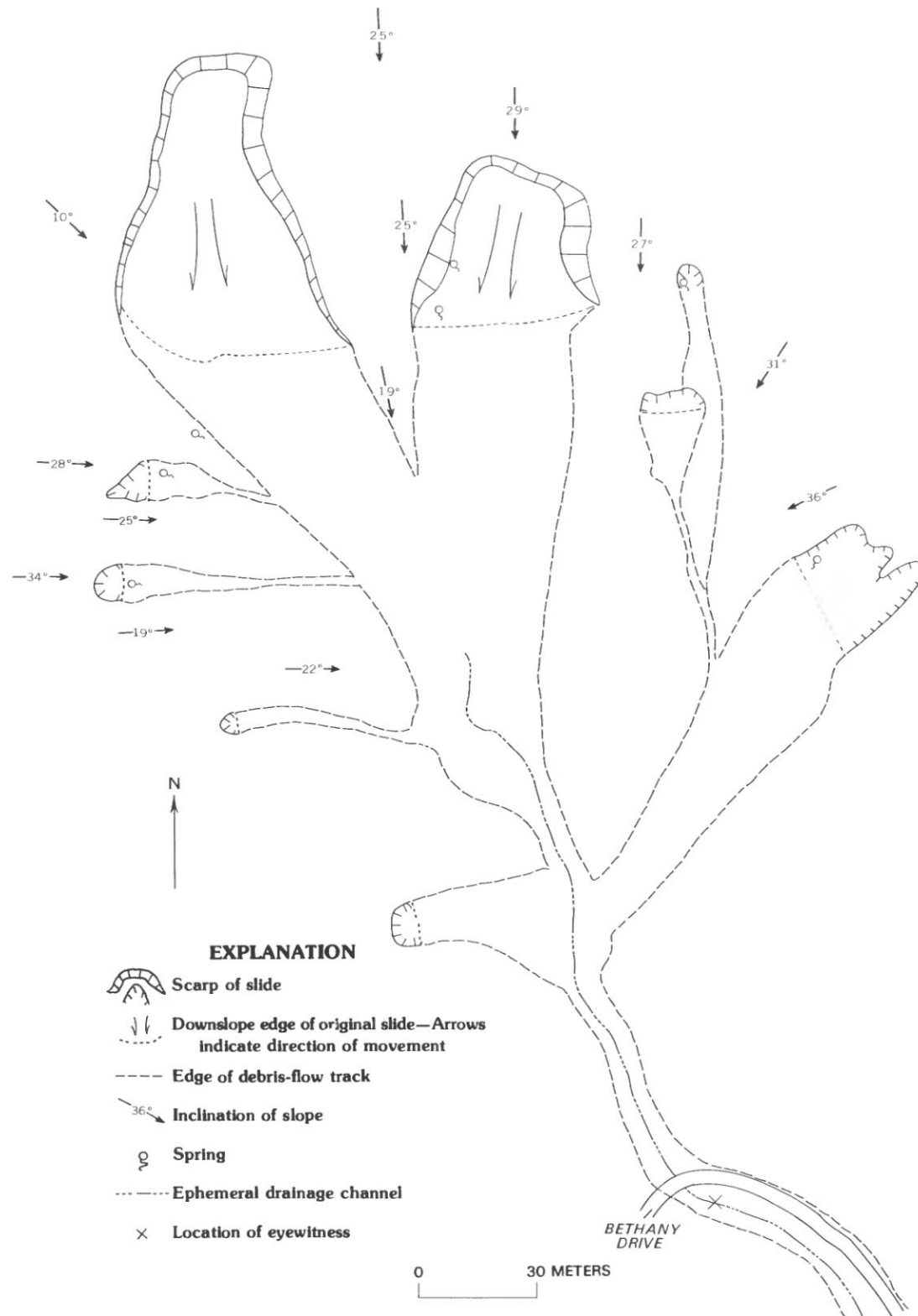


FIGURE 8.13.—Source area of debris flows at Canham Road, Santa Cruz County. Modified from Nielsen (1984, fig. 4).

was reported to produce little runoff. This particularly intense storm, however, in combination with the preceding rainfall, generated overland flow.

The slump above Alba Road measured about 30 m wide by 55 m long and had a maximum thickness of 6.4 m. The slump involved a total of about 6,800 m<sup>3</sup> of material, most of which mobilized into the debris flow. Rotational movement was indicated by fallen trees oriented with their tops in an uphill direction.

Massive silty sandstone of the Monterey Formation was exposed in the slickensided basal shear surface of the slump. Bedding in siltstone exposed in the scar was somewhat irregular, varying in dip from 26° to 45° in a generally eastward direction. The downslope component of dip was at some localities less than the slope gradient, providing a dip slope conducive to sliding (fig. 8.16). A thin layer of highly plastic clay was found in places immediately over bedrock. The main scarp and flanks of the slump exposed colluvium, as much as 4.5 m thick, of saturated and moderately plastic, clayey soil containing

weathered siltstone fragments as large as 45 cm in maximum dimension. A silty-clay-loam topsoil, 20 to 25 cm thick, mantled the colluvium.

Intense rainfall measured in nearby Ben Lomond was continuous through the afternoon and into the evening before the debris flow (fig. 8.17). Hourly measurements indicate intensities of 15.2 to 22.4 mm/h (0.60–0.88 in/h) between 4:00 and 8:00 p.m. This prolonged intense rainfall, which resulted in saturated ground conditions, in combination with crack opening, provided access for water that facilitated further failure and the resulting debris flow.

The description of this site is based on field examination and documentation by Mark Foxx (written commun., 1982).

#### CREEKWOOD DRIVE

At about 1:10 p.m. P.s.t. on January 4, a debris flow mobilized from a slide below Lake Boulevard, near the



FIGURE 8.14.—Slides at Canham Road that generated debris flows which coalesced into a single debris-flow track in a narrow canyon (out of view) and eventually flowed into Carbonera Creek, Santa Cruz County. Houses at far right show scale.



town of Lompico, Santa Cruz County (site 9, pl. 9). This debris flow traveled rapidly down a long, narrow drainage, crossed Creekwood Drive, and flowed into Lompico Creek, a distance of about 0.2 km. The flow destroyed or damaged several houses in its path by toppling trees onto them, battering them with fast-moving debris, or piling debris against them until they collapsed. A site map of this area is shown in figure 8.18.

The landslide initiated just below Lake Boulevard on a slope ranging in steepness from  $35^{\circ}$  to  $47^{\circ}$ , forested with secondary-growth redwood, oak, and madrone, as well as brush. A gentle swale, gullied before the January 1982 storm, is in the vicinity of the slide. During the storm, surface runoff from Lake Boulevard was flowing over the slide area.

Eyewitness reports indicate that for 1 or 2 hours before the slope failed, rocks as large as 15 cm had been rolling down the slope. Failure was rapidly followed by a debris flow. The scar left by the slide measured approximately 10 m wide, 35 m long, and as much as 4.3 m deep; its volume of approximately  $625 \text{ m}^3$  almost entirely mobilized as a debris flow. Siltstone of the Monterey Formation is exposed at the base of the slide scar; colluvium

containing fragments of weathered shale and siltstone, as large as 30 cm, is exposed in its flanks and main scarp. A 10- to 20-cm-thick topsoil of silty-clayey loam mantles the colluvium.

Between the initial slide and Creekwood Drive, the debris flow widened to as much as 21 m. An eyewitness described the flow as initially moving as fast as a frightened man can run at full speed downhill (possibly about 7.6 m/s) and therefore could be called a debris avalanche on the basis of its velocity. The material in the flow had a consistency of stiff, wet concrete, and surface waves were visible on the flow as it moved downslope. Below Creekwood Drive, the flow widened and bifurcated on slopes ranging from  $10^{\circ}$  to  $15^{\circ}$ . Both flow lobes reached Lompico Creek, adding debris to the creek, which was in flood stage.

The description of this site is based on field examination and documentation by Mark Foxx (written commun., 1982).

#### OTHER LARGE LANDSLIDES

Several other large landslides were investigated by others and are reported elsewhere, or were observed only in reconnaissance. Tables 8.4 and 8.5 list data on large landslides, including those described above, triggered by the storm in San Mateo and Santa Cruz Counties.

Primary among the other large landslides was the block slide at Love Creek (fig. 8.19) near Ben Lomond in Santa Cruz County (site 10, pl. 9), which was described by Cotton and Cochrane (1982). Another large block slide, shown in figure 8.20, occurred at nearby Newell Creek (site 11, pl. 9); this slide was similar in several aspects to the Love Creek landslide (Cotton and Cochrane, 1982). The debris flow at Oddstad Boulevard (fig. 8.21; site 4, pl. 8) and several other landslides in Pacifica, San Mateo County, are described in chapter 9.

A complex landslide from the south flank of Chalk Mountain (site 12, pl. 9) began as a slump that mobilized into a debris flow and traveled approximately 0.8 km into the headwaters of Año Nuevo Creek. We viewed this landslide only from the air and estimated its volume at 150,000 to 190,000  $\text{m}^3$ , on the basis of measurements from 1:20,000-scale aerial photographs and 1:24,000-scale topographic maps. This landslide and the Whitehouse Creek landslide from Chalk Mountain were two of the largest debris flows in the storm.

A large debris flow was observed during aerial reconnaissance near Mindogo Creek in the vicinity of La Honda, San Mateo County (site 5, pl. 8). Because this site was observed only from light airplane, the data listed in table 8.4 are approximate estimates from low-altitude aerial photographs and measurements from 1:20,000-scale aerial photographs and 1:24,000-scale topographic maps.

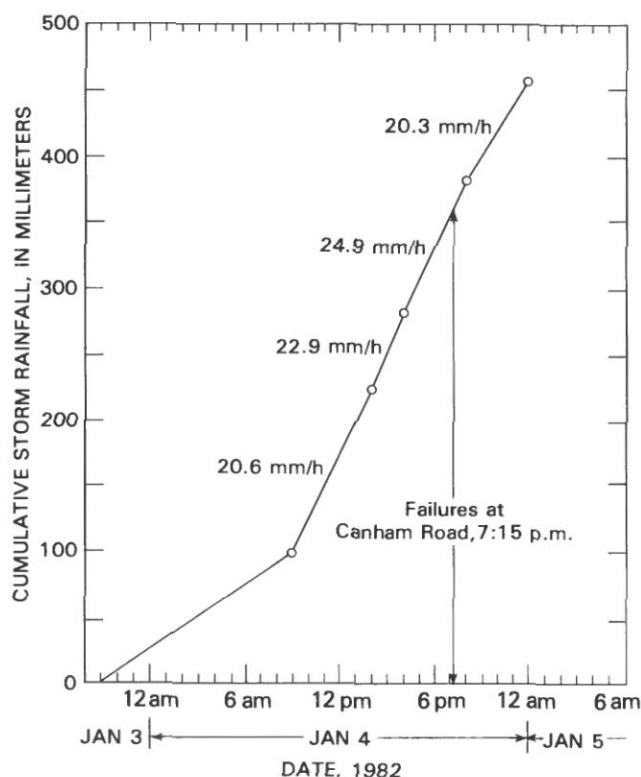
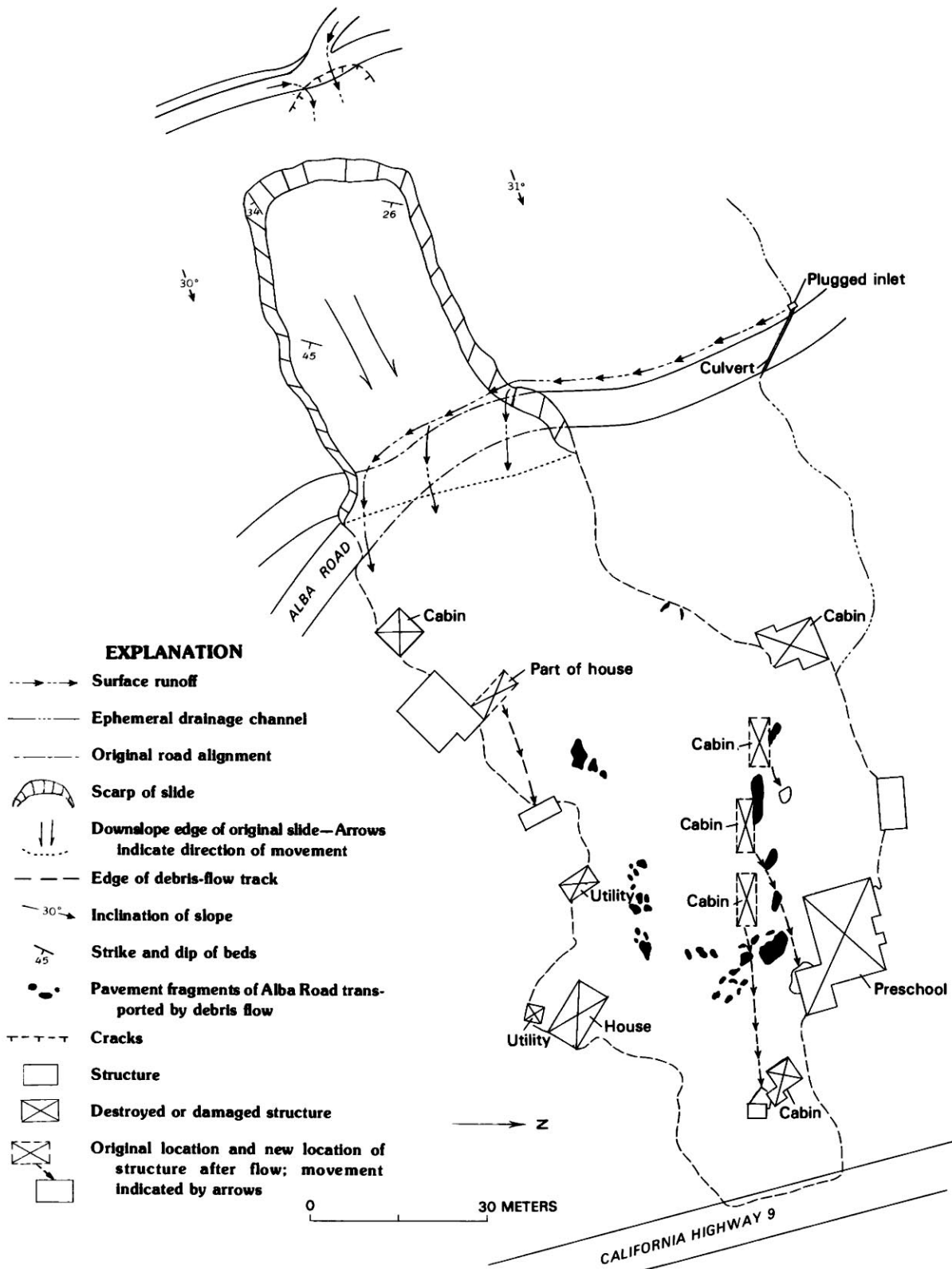


FIGURE 8.15.—Rainfall during the storm measured at 709 Canham Road, about 120 m east of debris-flow source area. Time of failures coincides with period of most intense rainfall. Modified from Nielsen (1984, fig. 5).



## CONCLUSIONS

1. Normalized storm rainfall appears to have been more significant than total storm rainfall in determining the concentration of debris flows in the San Francisco Bay region. Debris-flow concentration (number of debris flows per square kilometer) increased with increasing amounts of normalized storm rainfall, a result consistent with those of Govi and Sorzana (1980) and chapter 2. Dense and greater debris-flow concentration (20 or more per square kilometer) occurred where normalized storm rainfall exceeded 0.30. This threshold agrees with the results of an independent analysis of rainfall that caused damaging landslides in the San Francisco Bay region during the storm (see chap. 2).
2. Bedrock geologic units influenced the distribution of debris flows in San Mateo County. The quantitative measure of debris-flow incidence showed a wide range of values for different geologic units, indicating that some units are highly susceptible to debris flows, whereas others are only slightly so. Colluvial deposits mapped over many geologic units with a medium or high incidence suggest that the colluvium is derived from previous debris flows and that these geologic

units have been producing debris flows over a long period.

3. In San Mateo County, debris flows initiated most commonly on slopes with DEM-derived steepness of  $19^{\circ}$  to  $22^{\circ}$ . This range is well below the  $26^{\circ}$ – $45^{\circ}$  range where debris-flow sources were most common in southern California, and well below typical field-measured values in Marin and San Mateo Counties during this storm. When the frequency of debris flows with DEM-derived steepness was normalized by taking into account the population of slopes with different steepnesses, the peak of debris-flow frequency shifted to  $25^{\circ}$ – $29^{\circ}$ , more in accord with experience elsewhere.
4. The effect of vegetation on the regional distribution of debris flows in San Mateo County was not clarified by our analysis. In one area, however, the strong influence of removal of vegetation by logging on the concentration of debris flows indicates the control of vegetation on the susceptibility to debris flows.
5. Few, if any, generalizations can be drawn from the wide range of characteristics exhibited by the few documented large landslides in San Mateo and Santa Cruz Counties. Most landslides involved either colluvium or a combination of colluvium and weathered bedrock, initial average slopes covered a wide range of values, and rates of movement varied.

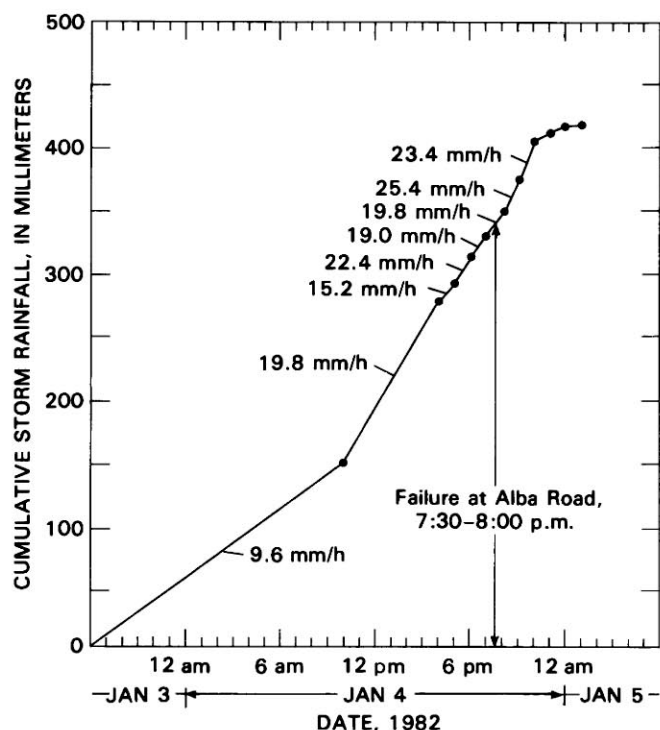


FIGURE 8.17.—Rainfall during the storm measured at 205 Willowbrook, Ben Lomond, about 2.7 km from the Alba Road landslide. From 3 p.m. P.s.t. on January 4, 1982, when cracks were first noticed, until failure at 7:30-8:00 p.m., rainfall intensity averaged 19.8 mm/h.

## REFERENCES CITED

- Brabb, E.E., 1970, Preliminary geologic map of the central Santa Cruz Mountains, California: U.S. Geological Survey, San Francisco Bay Region Environment and Resources Planning Study Basic Data Contribution 6, scale 1:62,500, 3 sheets.
- 1980, Preliminary geologic map of the La Honda and San Gregorio quadrangles, San Mateo County, California: U.S. Geological Survey Open-File Report 80-245, scale 1:24,000.
- Brabb, E.E., and Pampeyan, E.H., 1972, Preliminary map of landslide deposits in San Mateo County, California: U.S. Geological Survey Miscellaneous Field Studies Map MF-344, scale 1:62,500.
- 1983, Geologic map of San Mateo County, California: U.S. Geological Survey Miscellaneous Investigations Map I-1257-A, scale 1:62,500.
- Brabb, E.E., Pampeyan, E.H., and Bonilla, M.G., 1972, Landslide susceptibility in San Mateo County, California: U.S. Geological Survey Miscellaneous Field Studies Map MF-360, scale 1:62,500.
- Campbell, R.H., 1973, Isopleth map of landslide deposits, Point Dume quadrangle, Los Angeles County, California; an experiment in generalizing and quantifying areal distribution of landslides: U.S. Geological Survey Miscellaneous Field Studies Map MF-535, scale 1:62,500.
- 1975, Soil slips, debris flows, and rainstorms in the Santa Monica Mountains and vicinity, southern California: U.S. Geological Survey Professional Paper 851, 51 p.
- Coats, Robert, Collins, Laurel, Florsheim, Joan, and Kaufman, Darrell, 1982, Landsliding, channel change, and sediment transport in Zayante Creek and the lower San Lorenzo River, 1982 water year, and implications for management of the stream resource: Berkeley,

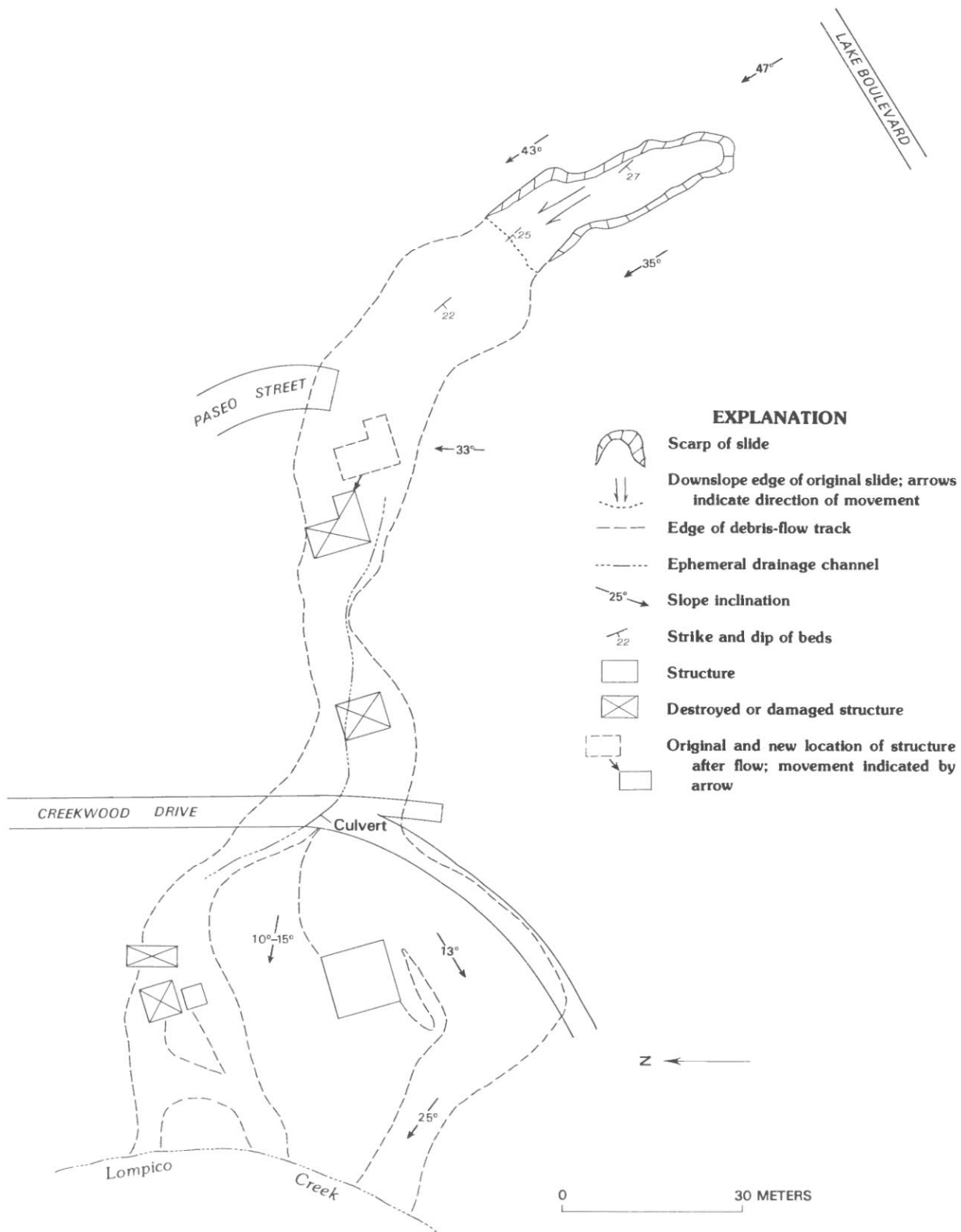


FIGURE 8.18.—Features of Creekwood Drive landslide, Santa Cruz County. Modified from Mark Foxx (written commun., 1982).



- Calif., Center for Natural Studies report to California Water Resources Control Board, 70 p.
- Cotton, W.R., and Cochrane, D.A., 1982, Love Creek landslide disaster, January 5, 1982: *California Geology*, v. 35, no. 7, p. 153-157.
- Ellen, S.D., Peterson, D.M., and Reid, G.O., 1982, Map showing areas susceptible to different hazards from shallow landsliding, Marin County and adjacent parts of Sonoma County, California: U.S. Geological Survey Miscellaneous Field Studies Map MF-1406, scale 1:62,500.
- Govi, Mario, and Sorzana, P.F., 1980, Landslide susceptibility as a function of critical rainfall amount in Piedmont Basin (North-Western Italy): *Studia Geomorphologica Carpatho-Balcanica*, v. 14, p. 43-61.
- Jones, F.O., 1973, Landslides of Rio de Janeiro and the Serra das Araras escarpment, Brazil: U.S. Geological Survey Professional Paper 697, 42 p.
- Mark, R.K., Newman, E.B., Northcut, C.R., and Hamachi, B.R., 1983, The January 1982 rainstorm in the San Francisco Bay region, California: U.S. Geological Survey Open-File Report 83-16, scale 1:250,000.
- Nielsen, H.P., 1984, Geology, rainfall, and groundwater associated with several debris flows in Santa Cruz County, California: Santa Cruz, University of California, M.S. thesis, 104 p.
- Okuda, Setsuo, Ashida, Kazuo, Gocho, Yukio, Okunishi, Kazuo, Sawada, Toyooki, and Yokoyama, Koji, 1979, Characteristics of heavy rainfall and debris hazard: *National Disaster Science*, v. 1, no. 2, p. 41-55.
- Omura, Hiroshi, and Nakamura, Fumio, 1983, Some features of landslide caused by Typhoon 18, 1982 at different land use in Fujieda: Society of Mudflow Prevention Symposium, Kyoto, Japan, 1983, Proceedings, p. 20-21.
- Pomeroy, J.S., 1980, Storm-induced debris avalanching and related phenomena in the Johnstown area, Pennsylvania, with references to other studies in the Appalachians: U.S. Geological Survey Professional Paper 1191, 24 p.
- Rantz, S.E., 1971, Mean annual precipitation and precipitation depth-duration-frequency data for the San Francisco Bay region: U.S. Geological Survey open-file report, 23 p.



FIGURE 8.19.—Block slide at Love Creek near Ben Lomond, Santa Cruz County, which failed at approximately 1 a.m. P.s.t. on January 5, 1982, killing 10 people and burying 9 homes. This was the largest landslide in the storm, with an estimated volume of 460,000 m<sup>3</sup>. Slide extends about 610 m from crown to toe (in shadows at bottom). The slide triggered several debris flows, the largest of which (indicated by dashed lines on left) flowed rapidly down the margin of the main landslide mass and into the channel of Love Creek (Cotton and Cochrane, 1982). Note bulldozer (indicated by circle) in lower center for scale (site 10, pl. 9).



FIGURE 8.20.—Newell Creek block slide (site 11, pl. 9) below and Love Creek block slide above, near Ben Lomond, Santa Cruz County. Movement was toward left. Both slides moved initially along bedding in Monterey Formation on flank of the Scotts Valley syncline (Cotton and Cochrane, 1982). Note house (circled) in left center for scale.

- Sailor, J.K., and Berry, J.K., 1980, The use of a geographic information system in storm runoff prediction: Cambridge, Mass., Harvard University, Harvard Library of Computer Graphics, v. 14, p. 73-79.
- Selby, M.J., 1982, Hillslope materials and processes: Oxford, U.K., University Press, 264 p.
- Swanson, F.J., Swanson, M.M., and Woods, Chris, 1981, Analysis of debris-avalanche erosion in steep forest lands: An example from Mapleton, Oregon, USA, *in* Erosion and sedimentation in Pacific Rim steeplands: International Association of Hydrological Sciences Publication 132, p. 67-75.
- Swanston, D.N., and Swanson, F.J., 1976, Timber harvesting, mass erosion, and steepland forest geomorphology in the Pacific Northwest, *in* Coates, D.R., ed., *Geomorphology and engineering*: Stroudsburg, Pa., Dowden, Hutchinson & Ross, p. 199-221.
- Varnes, D.J., 1978, Slope movement types and processes, chap. 2 of Schuster, R.L., and Krizek, R.S., eds., *Landslides: Analysis and control*: U.S. National Academy of Sciences, National Research Council, Transportation Research Board Special Report 176, p. 12-33.
- Wright, R.H., and Nilsen, T.H., 1974, Isopleth map of landslide deposits, southern San Francisco Bay region, California: U.S. Geological Survey Miscellaneous Field Studies Map MF-550, scale 1:125,000.
- Wu, T.H., and Swanston, D.N., 1980, Risk of landslides in shallow soils and its relation to clearcutting in southeastern Alaska: *Forest Science*, v. 26, no. 3, p. 495-510.



FIGURE 8.21.—Debris flow from brush-covered, concave hillside above Oddstad Boulevard in Pacifica, San Mateo County, where three children were killed and two houses destroyed at about 11:10 p.m. P.s.t. January 4, 1982. Debris and remains of two houses had been removed (lower left) by the time of this photograph (site 4, pl. 8).



## 9. LANDSLIDES IN PACIFICA, CALIFORNIA, CAUSED BY THE STORM

By TERRY R. HOWARD,<sup>1</sup>

HOWARD-DONLEY ASSOCIATES, INC., and THE UNIVERSITY OF IDAHO;  
and

JOEL E. BALDWIN II<sup>2</sup> and HOWARD F. DONLEY,<sup>3</sup>

HOWARD-DONLEY ASSOCIATES, INC.

### CONTENTS

	Page
Abstract - - - - -	163
Introduction - - - - -	163
Purpose - - - - -	163
Scope - - - - -	164
Setting - - - - -	164
Geography - - - - -	164
Climate - - - - -	164
Geology - - - - -	164
Study methods - - - - -	167
Landslide classification - - - - -	167
Regional study - - - - -	167
Detailed studies - - - - -	167
Brookhaven site - - - - -	167
Big Bend site - - - - -	169
Oddstad site - - - - -	171
Yosemite site - - - - -	175
Discussion - - - - -	178
Landslide distribution and type - - - - -	178
Topomorphology - - - - -	178
Soil characteristics - - - - -	178
Landslide geometry - - - - -	178
Slope-stability analyses - - - - -	179
Mechanics and mode of failure - - - - -	180
Conclusions - - - - -	182
References cited - - - - -	183

### ABSTRACT

The January 3-5, 1982, storm caused 475 landslides in Pacifica, Calif. A total of 85 percent of the landslides mapped involved both sliding and flow. Most of these landslides occurred in soils with common engineering properties, near the head of first-order drainages, on slopes of 26°-45°. Each landslide was probably preceded by a near-vertical tension crack extending to bedrock. The rupture surfaces occurred in soil near or on the soil-bedrock contact.

### INTRODUCTION

The city of Pacifica, located in northwestern San Mateo County (fig. 9.1), received exceptionally heavy rainfall during the January 3-5, 1982, storm in the San Francisco Bay region. The heavy rains triggered hundreds of land-

slides. These landslides caused 3 deaths, the destruction of 4 homes, damage to tens of other homes, and perceived life-threatening situations for at least 500 families living at the foot of steep hillsides. Never before had the potential danger of landsliding been so widely experienced in Pacifica. Damage to municipal facilities and city cleanup costs alone exceeded \$1.5 million.

### PURPOSE

The purpose of this chapter is to report on the distribution and types of landslides that were triggered by the storm, to evaluate the geologic conditions and mechanics

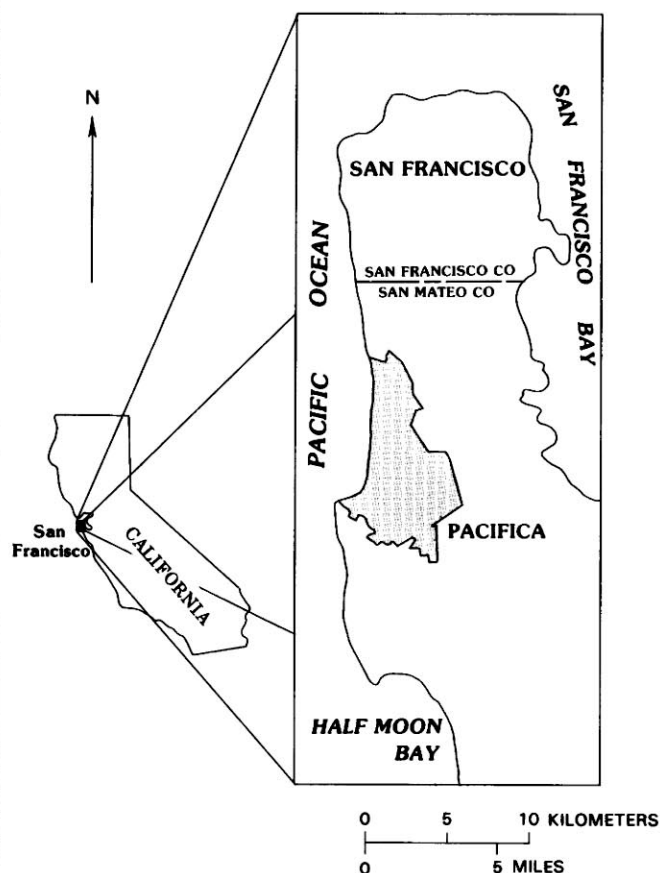


FIGURE 9.1.—Sketch map of the San Francisco peninsula, showing location of the city of Pacifica.

<sup>1</sup>Current affiliation: Howard Consultants, Inc., and the University of Idaho, Moscow, ID 83843.

<sup>2</sup>Current affiliation: Baldwin-Wright, Inc., Pacifica, CA 94044.

<sup>3</sup>Current affiliation: Howard F. Donley Associates, Inc., Redwood City, CA 94063.



of failure for four representative landslides, and to present soil-property and shear-strength data for the materials involved in the landslides.

### SCOPE

We mapped landslides occurring as a result of the storm (1) to locate all the landslides; (2) to correlate the locations of landslides with such slope features as degree of slope, aspect, vegetation, and drainages; and (3) from this correlation, to identify slopes with a high potential for failure, given the prediction of more rainfall to come. These data were then used by city officials to warn the citizens of Pacifica of immediate danger and, if necessary, to require them to move temporarily (see subsection below entitled "Regional Study").

After this preliminary work, we began a more detailed investigation of nine landslides, selected for further study by their location, classification, and potential for future hazard. This detailed investigation included geology, geometry, ground water, and laboratory shear-strength and moisture-density relations. Four of these nine landslides are discussed here.

### SETTING

#### GEOGRAPHY

The city of Pacifica is located within the northern Santa Cruz Mountains. The south half of the city includes interior valleys and highlands that are influenced by Montara Mountain, situated slightly south of the city (fig. 9.2). Montara Mountain exhibits deeply entrenched stream valleys. The drainage divides that separate the valleys are characteristically flat topped. Their moderately dissected margins contain numerous subtle linear swales and well-developed first-order drainages. Elevations in the south half of the city range from sea level to approximately 365 m.

North of Sharp Park, the highland terrain consists of subdued, isolated hills with a crude north-northwestward grain. The drainage divides are much broader here than to the south, and relief is generally less than 180 m. Numerous first-order drainages occupy the hillsides.

The coastal margin, like the interior highlands, varies in topographic expression from south to north. South of Sharp Park, the coastal margin is characterized by broad, low alluvial plains and intermittent, west-northwest-trending bedrock promontories, with an average relief of 60 m. The coastal margin north of Sharp Park is characterized by hillsides into which has been cut a nearly linear, slightly dissected seacliff with a relief of approximately 30 m. Shelter Cove, in the southwest extremity of the city, is steeper and expresses higher relief.

### CLIMATE

The climate of Pacifica is characterized by dry, mild summers and moist, cool winters (Wagner and Nelson, 1961). Mean annual precipitation is 635 mm (25 in.), most of which occurs during the months of December through March. Since 1940, mean annual precipitation has been exceeded in 18 of these years. During the rainy season from October 1981 through April 1982, the total rainfall measured at the Half Moon Bay Weather Station near Pacifica was 1221 mm (48.07 in.), of which 150 to 200 mm (6-8 in.) fell on January 4, 1982 (J.P. Monteverdi, written commun., 1982). This rainfall occurred over a period of less than 30 hours, giving an average intensity of 5.0 to 6.6 mm/h (0.20-0.26 in/h)—certainly above average for Pacifica.

### GEOLOGY

Published information on the geology of Pacifica is generally on a regional scale. Lawson (1914) was the first to map the areal geology. Darrow (1951) published a geologic map of the Montara Mountain quadrangle, which was later revised by Pampeyan (1981). Bonilla (1960) mapped landslides and briefly described the geology of the San Francisco South quadrangle. Brabb and Pampeyan (1972) compiled geologic data on a 1:62,000-scale map of San Mateo County; figure 9.3 shows their mapping in the city of Pacifica.

Most of the study area is underlain by alternating, northwest-trending bodies of sheared greenstone and sandstone of the Jurassic and Cretaceous Franciscan assemblage, containing local inclusions of diabase, basalt, serpentinite, chert, and limestone. Near the ground surface, these rocks are commonly weathered and are mantled by residual soil and colluvium. Weathering is pronounced in the more highly altered rocks.

The valleys contain unconsolidated deposits of Quaternary alluvium. Artificial fill is present in many of the larger valleys occupied by residential developments. Remnants of marine-terrace deposits occur along the western part of the study area. Other Quaternary surficial deposits include slope wash, windblown sand, and beach deposits.

A northwest-trending structural grain, influenced by deformation along the San Andreas and related faults, dominates the geology of Pacifica (fig. 9.3). The San Andreas fault passes through the north end of the city. The Pilarcitos fault, a generally northwest-trending structure that enters the Pacific Ocean near Point San Pedro, is mapped through the southern part of the city. Paleocene rocks adjacent to this fault have been deformed into tight northwest-trending folds. Several unnamed mapped faults transect the Franciscan assemblage between the Pilarcitos and San Andreas faults.

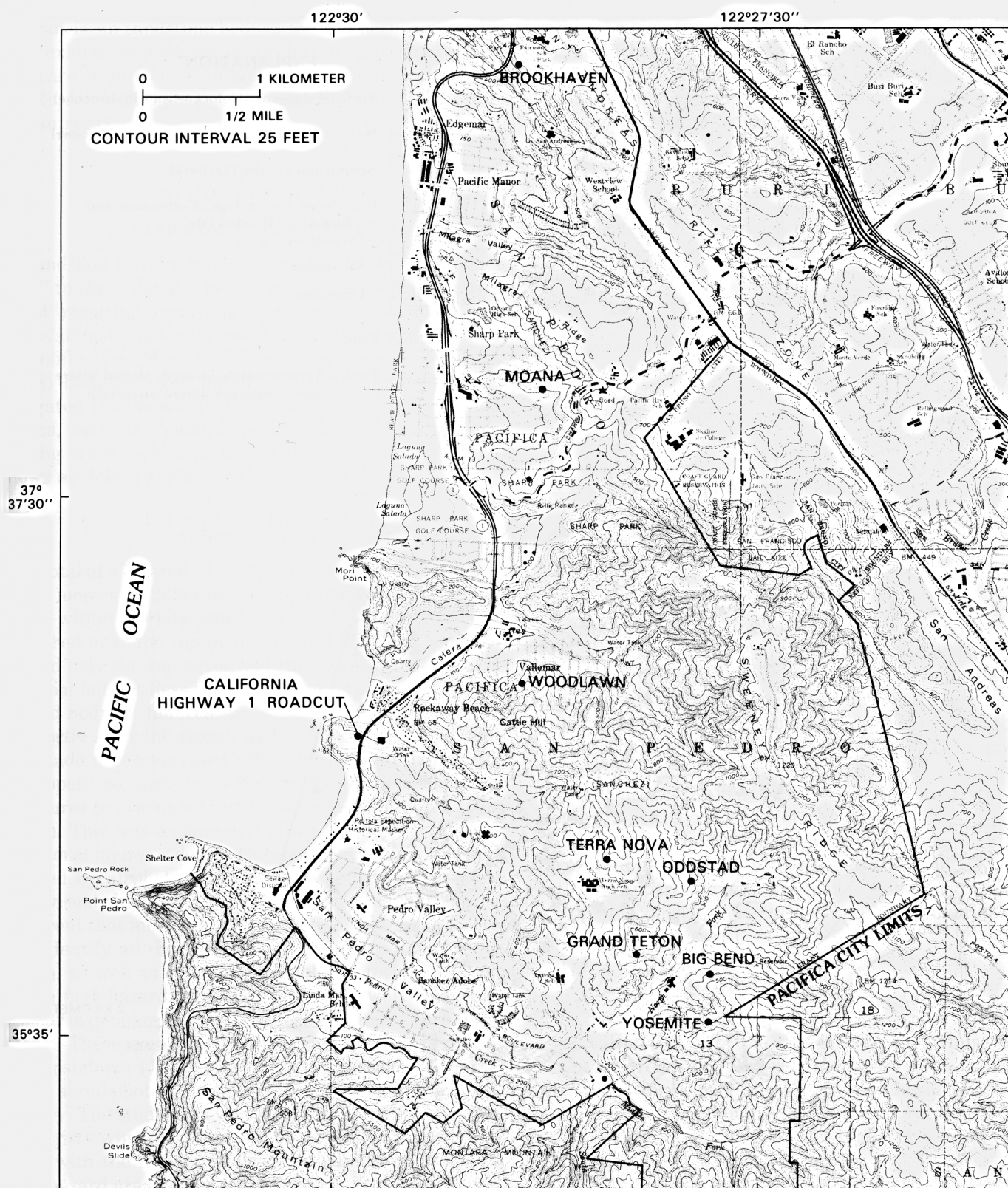


FIGURE 9.2.—Pacifica, Calif., area, showing locations of the nine landslides (dots) analyzed in detail. Base from U.S. Geological Survey, 1:24,000 scale, Montara Mountain and San Francisco South, 1980.

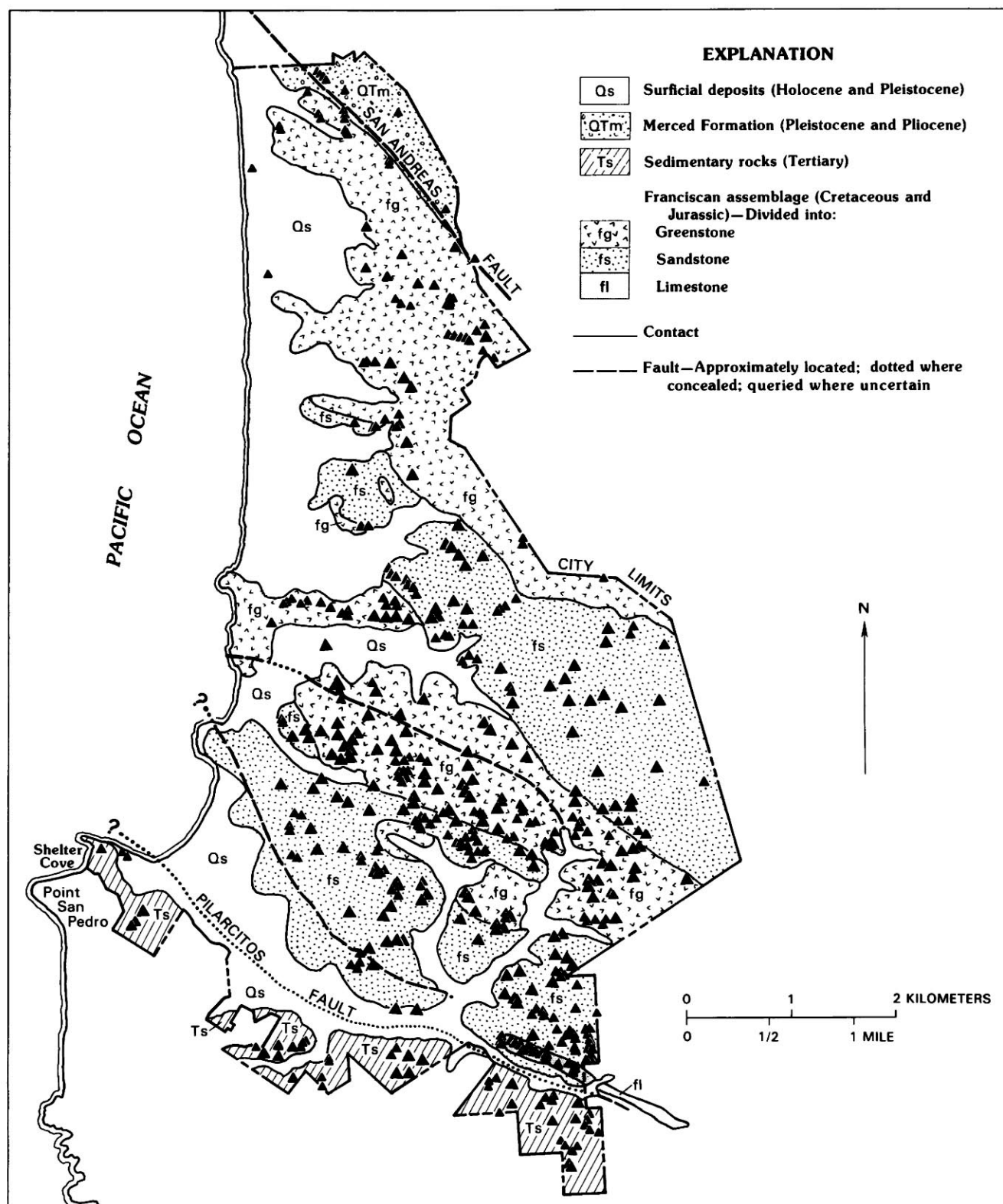


FIGURE 9.3.—Geologic sketch map of Pacifica, Calif., area (modified from Brabb and Pampeyan, 1972), showing locations of landslides (triangles) mapped in the inventory.



Franciscan sandstone beds in the southern part of the city exhibit no systematic, preferred structural trend; beds are oriented in all directions (Brabb and Pampeyan, 1972). Joints and shear zones are common in the Franciscan rocks.

## STUDY METHODS

### LANDSLIDE CLASSIFICATION

Landslide terminology is described in the "Introduction" to this volume. The major types of landslide movement resulting from the storm were rotational and translational slides and flows. One landslide was classified as solifluction. Most landslides were complex (Varnes, 1978) because after initial sliding the masses disaggregated into flows. In this chapter we use combined terms, such as "slump/debris flow," that distinguish sliding from flow, and we identify fast-moving debris flows as debris avalanches.

### REGIONAL STUDY

A total of 475 landslides, ranging in volume from a few cubic meters to 2,290 m<sup>3</sup> of earth material, were identified within the city limits of Pacifica. Most landslides occurred near the top of the natural hills, and most involved only the soil cover and thus were categorized as surficial failures (less than 3 m deep), as opposed to deep-seated bedrock failures.

Shortly after the storm, with a forecast of more rain, we made a concentrated effort to delineate hazardous hillslopes, so that the affected residents could take measures to evacuate their homes when additional rains began. This was a concerted effort by the city to avert additional injury or death. The emergency effort was performed by airphoto interpretation and reconnaissance field visual observation only. However, it quickly became apparent that more thorough study was needed to locate and identify all the landslides that occurred during the storm, as well as to obtain valuable geotechnical data.

The high-hazard areas we delineated were hillslopes similar in geomorphic form to those that failed during the storm. These areas were initially delineated by examining poststorm (Jan. 8, 1982) 1:20,000-scale black-and-white aerial photographs provided by the U.S. Geological Survey. The study area was then overflowed by a team of geologists who compared the photogeologic interpretations with the results of direct visual observation. The high-hazard areas were plotted onto existing San Mateo County 1:4,800-scale orthophotographs and submitted to the city, who, in turn, distributed evacuation advisories to homeowners in high-hazard areas on January 16, 1982. This advisory list was later revised by careful ground

checking, which resulted in a corrected and official list of affected homesites. An updated evacuation advisory was distributed on January 28, 1982. Cataloging of landslide distribution and analysis of nine representative landslides were performed during and after the emergency measures.

### DETAILED STUDIES

We selected four landslides from the nine analyzed in detail (fig. 9.2) for discussion here. We mapped each landslide on 1:120-scale base maps generated photogrammetrically from poststorm aerial photographs. We paid particular attention to the landslide-source areas, where failure geometry was well exposed. We also studied the soils along the failure surfaces.

During geologic mapping, we collected samples from representative soil horizons adjacent to the failure surfaces at each landslide site for testing in our laboratory. Tests included moisture content, dry density, Atterberg limits, gradation, and direct shear.

## BROOKHAVEN SITE

### GEOGRAPHIC SETTING

At the Brookhaven site, located on the north side of Pacifica (fig. 9.2) in the Fairmont No. 2A subdivision, a series of failures occurred on a natural slope immediately above a cut slope. Additional grading had been done at the top of this slope. Grading and development in the area preceded 1970. Tract homes built since 1970 have apparently been affected only slightly by recurring shallow failures of the hillside, which are evidenced by two older scars at the southeast end of the site.

The hillside at the site (fig. 9.4) is 46 m high, slightly convex, and inclined at a slope of approximately 34°. A gentle and apparently natural break in slope occurs midway up this hillside. Vegetation consists primarily of sagebrush and grass.

### GEOTECHNICAL SETTING

The inferred active trace of the San Andreas fault passes within 300 m of the Brookhaven site. Thus, the Franciscan greenstone that underlies most of the hillside is strongly deformed and sheared, as revealed in adjacent roadcuts and in hand-dug holes. Sheared rock that includes other Franciscan rock types is also present at the site (fig. 9.4).

Greenstone observed in the test pits and headscarp within the failure area was highly weathered and sheared, in contrast to more competent, less weathered greenstone encountered elsewhere. The bedrock is overlain by a light-colored lower layer of colluvium, as much as 1.2 m thick,



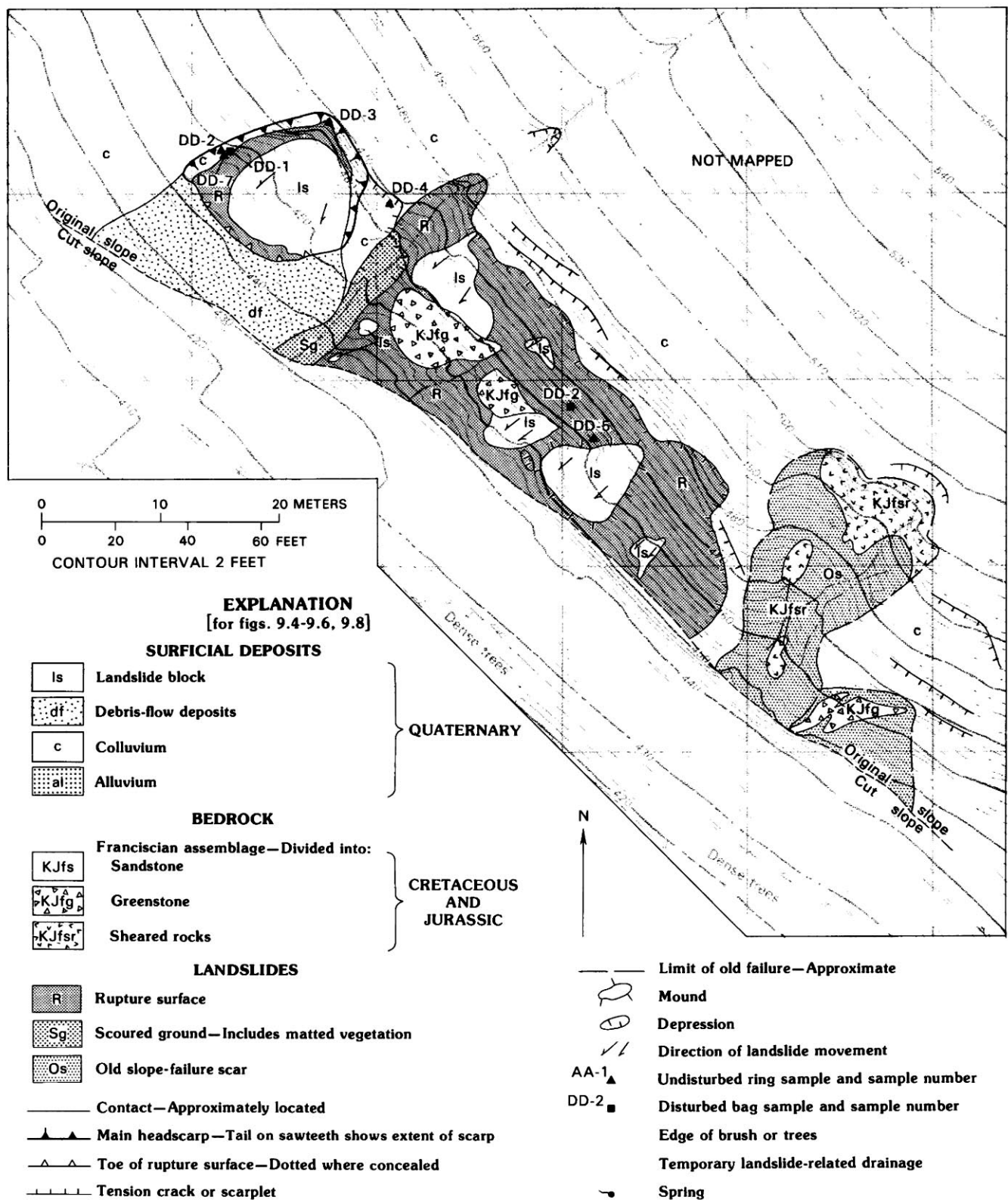


FIGURE 9.4.—Brookhaven site, showing series of failures on a natural slope immediately above a cut slope. Original topographic base prepared for the city of Pacifica by Hammon-Jensen-Wallen & Associates, Oakland, Calif., 1982.

which consists of moist, yellowish-brown, sandy to silty clay containing rock fragments. This material, in turn, is overlain by about 0.6 m of dark colluvium, consisting of moist, dark-grayish-brown, friable, coarse-sandy clay to clayey sand containing rock fragments.

#### LANDSLIDE CHARACTERISTICS

A slump/debris flow (northwesternmost landslide, fig. 9.4) dominated the slope failure at the Brookhaven site. It was 15 m wide, 9 m long, and about 2.1 m deep, and was characterized by a nearly square crown and a hummocky, cracked ground surface. The other landslides were shallow translational slides/debris flows that removed soil from the slope to a depth of 0.6 m. The resulting scars were characterized by 0.6-m-high, jagged headscarps and by slip surfaces that were continuously exposed except where concealed by a few rafted clumps of topsoil and vegetation.

Scarplets, generally less than 0.3 m high, and cracks indicating incipient failure bounded the slope areas between the failed areas (fig. 9.4); similar scarplets (not shown in fig. 9.4) extended nearly to the top of the slope.

The affected area included about 1,600 m<sup>2</sup>, and the total volume of the landslides was approximately 765 m<sup>3</sup>. An estimated 380 m<sup>3</sup> of additional material exhibited cracking that indicated incipient failure. Areas bounded by fresh cracks upslope of the landslides are omitted from these estimates.

#### MODE OF FAILURE

The Brookhaven site includes debris flows that resulted from both translational and rotational slides. Translational sliding occurred at depths of about 0.6 m, near the boundary between the dark top layer of colluvium and the underlying light-colored colluvium. After initial sliding, most of these masses disaggregated into viscous slurries of soil and water. However, numerous clumps of dark soil, held together by shallow roots, slid without disaggregation. At the time of our investigation, these clumps formed unstable masses that rested on the sloping rupture surface.

The dominant failure, in terms of both volume and disruption to an adjacent residential site, began as a rotational slide. The rupture surface was concave upward and extended to a maximum depth of about 2 m. Like the shallow translational failures, the mass disaggregated during failure into a viscous flow. Occupants of a residence downslope and across a road said that the mass moved slowly enough for them to move safely from its path. It had enough momentum, however, to flow downslope, topple an embedded basketball goal, and slightly damage their house.

### BIG BEND SITE

#### GEOGRAPHIC SETTING

Big Bend Drive, located near the southeast point of Pacifica (fig. 9.2), occupies a 1-km<sup>2</sup> drainage basin in the Park Pacifica No. 2 subdivision. The area is characterized by dense residential development at the foot of a steep, east-west-trending ridgeline. Development of the area began during the late 1960's. Debris-flow hazards in the drainage basin were discussed by Fowler (1984).

The Big Bend failure (fig. 9.5) originated near the head of a broad first-order drainage swale on a north-facing natural slope. The drainage channel broadens upslope and is widest near the ridgetop. Review of historical aerial photographs indicates that the broadest part of the channel is the site of past slope failures.

Vegetation on the slope consists of dense scrub brush and grasses, with local stands of trees in the drainage channel. Vegetation within the drainage appears stunted in comparison with the vegetation in adjacent drainages and on divides, an appearance possibly reflecting paths of past debris flows. The average slope gradient is about 30°; over short reaches of the channel, gradients range from 20° to 45°.

#### GEOTECHNICAL SETTING

Bedrock exposed on the hillslope is Franciscan greenstone (fig. 9.5). Where observed in place, the greenstone is moderately fractured. Where orientations of fractures were measured, they dipped obliquely out of slope. The greenstone in most exposures is deeply weathered to a soft, cohesive, green clayey soil. Seepage was discharging from the greenstone exposure at the base of the headscarp. Sandstone float in the headscarp area suggests that Franciscan sandstone occurs upslope, but dense vegetation prevented mapping bedrock.

Overlying the bedrock was about 5 cm of moist, very plastic, dense, brown gravelly-sandy clay. This material had a massive structure and resembled a greenstone saprolite or residual soil.

Above the clay was about 1 m of light-colored colluvium, consisting of loose, brownish-yellow silty and clayey sand containing rock fragments, that might be old debris-flow material. The material was moist, massive, and friable. Where damp or wet, it displayed a slightly plastic consistency.

About 35 cm of dark colluvium rested on the light-colored colluvium. This material was damp, loose, and porous and consisted of very dark grayish brown silty coarse sand containing clay and rock fragments. The structure was granular and very friable.

Gaping tension cracks and scarps, as much as 0.6 m high, were initially observed upslope from the source area just off the map. Subsequently, scarplike features as much

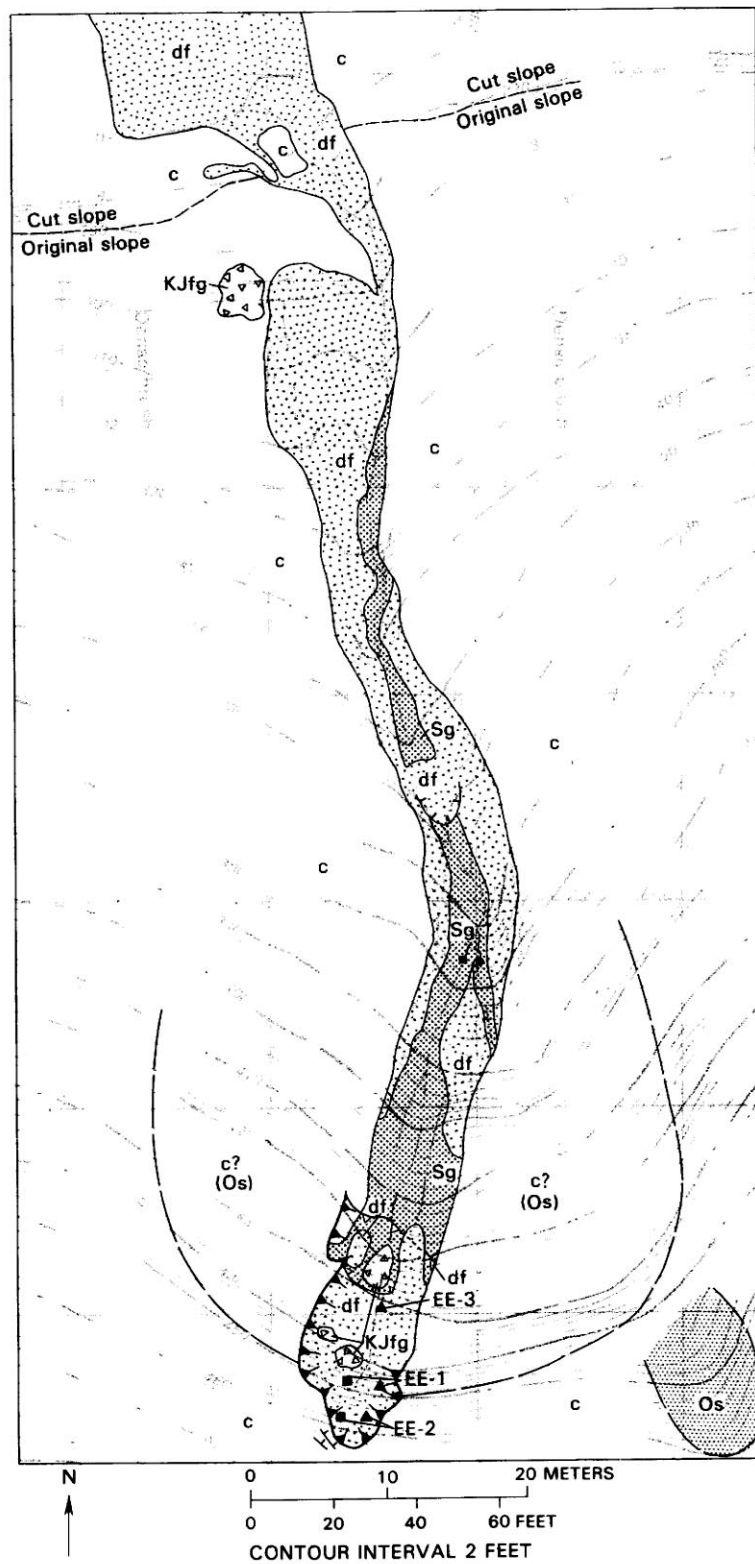


FIGURE 9.5.—Big Bend site, showing landslide in a first-order drainage swale. See figure 9.4 for explanation of symbols. Original topographic base prepared for the city of Pacifica by Hammon-Jensen-Wallen & Associates, Oakland, Calif., 1982.

as 2 m high were observed. Although the depth of penetration of these tension cracks is unknown, they are evidence of incipient failure. Their areal extent suggests a potential slope failure much larger than that in January 1982.

There is evidence on 1941 aerial photographs of a past, larger slope failure at this site. Its scar morphology is identical to that of the failure in January 1982. This older landslide appears in the 1941 photographs as an arcuate scar area, partly denuded of vegetation, that extends nearly to the ridgetop (beyond edge of fig. 9.5). This older failure must have occurred at least a few years before 1941 because much of the scar had been revegetated.

This older failure suggests the time required to mask the scar by vegetation and to degrade the scarps. By 1970 the scar was completely revegetated, and the scar slopes were reduced to the angle of the adjacent hillslopes. In 1970, however, the secondary growth of vegetation was recognizably lighter toned and shorter than in adjacent undisturbed areas. This is the sole evidence in the 1970 photographs that a failure had occurred on this hillslope.

#### LANDSLIDE CHARACTERISTICS

The landslide occurred on January 4, 1982, behind the residence at 831 Big Bend Drive. Its volume was estimated at 660 m<sup>3</sup>. The landslide occurred in two time-separated surges. The smaller, first surge occurred during the day; it moved slowly downslope, overtopped a low retaining wall, and oozed into the backyard. The larger, second surge occurred that evening and probably moved as did the first; it had enough momentum and volume to overtop the retaining wall, fill a 1.2-m-deep swimming pool, and cover much of the yard with mud.

The Big Bend landslide exhibited the long, shallow, narrow and sinuous path typical of debris flows (fig. 9.5). It exhibits the classic debris-flow morphology, consisting of three distinct sections: source area, main track, and depositional area.

The source area of the Big Bend flow was 23 m long, measured along slope, and averaged 7.6 m in width. It was defined by a 0.3- to 1.2-m-high headwall and flanks that exposed primarily colluvial material. Exposed in the irregular basal failure surface was weathered Franciscan greenstone and associated materials. Downslope, within the source area, a minor scarp was partly covered by material that had flowed from upslope.

Downslope from the source area, the main track was characterized by a relatively narrow, deep gully, flanked on both sides by thin lateral deposits that overlay matted grass and brush. The main track was about 70 m long and 4.5 to 6.0 m wide.

The main track extended downslope to an area where it appeared that the decreasing slope angle and a debris dam of small trees and brush had caused deposition on

the hillslope above the affected residence. This damming of the flow resulted in a fan-shaped, two-lobed deposit, at least 1.2 m thick. Much of the depositional area, however, was the backyard and swimming pool.

#### MODE OF FAILURE

The presence of an irregular rupture surface and a minor scarp below the headscarp suggests that initial failure was by two translational sliding events. Sliding was probably retrogressive; it started with failure at the lower scarp. This movement, in turn, removed lateral support and triggered subsequent sliding of the source area adjacent to the headscarp.

As each slide mass moved downslope, it disaggregated into a flow. The flows, following the drainage course, made a turn of approximately 30° before reaching the bottom of the slope. Obstructions in the path and an incised drainage channel along this lower course probably retarded movement and limited acceleration of the flows.

The combination of translational sliding and probable low velocity of flow classify this complex landslide as a translational slide/debris flow.

#### ODDSTAD SITE

##### GEOGRAPHIC SETTING

The slope failure at the Oddstad site occurred on a natural east-facing hillslope above the 1200 block of Oddstad Boulevard in the Park Pacifica subdivision (fig. 9.2). This failure, which was the largest and most destructive of the landslides studied, occurred at about 11:00 p.m. P.s.t. January 4. A translational slide/debris avalanche with an estimated volume of 2,290 m<sup>3</sup> destroyed two homes and killed three children in one of the homes; two other homes were slightly damaged. Features of this landslide were discussed by Shlemon and others (1987).

Failure occurred near the head of a broad first-order drainage on a hillslope about 85 m high and generally inclined 26° (fig. 9.6). Vegetation on the slope consists of dense coyote brush, poison oak, and scrub oak; the ridge is covered by low perennial grass.

Drainage was controlled by the broad swale. Scouring of the topsoil and vegetation by the passing debris avalanche removed much of the erosion-retardant vegetation, to the extent that subsequent runoff established gullies in the lower part of the slope. Gullying also took place where the runoff crossed landslide deposits.

##### GEOTECHNICAL SETTING

Franciscan sandstone with a fracture spacing closer than 10 cm was exposed downslope of the source area, where soil had been stripped by the passing debris ava-



lanche. The scar locally exposed a minimum of 3.3 m of a lower layer of colluvium, which consisted of dark-brown clayey-silty sand containing rock fragments, overlain by an upper, darker colluvial layer about 0.6 m thick, which consisted of very dark gray to grayish-brown clayey sand (fig. 9.7). Bedrock was not exposed in the landslide scar.

The lower layer of colluvium was dense and moist and had a moderately developed, vertically oriented prismatic structure. The hard, slightly friable soil had thin clay films lining pores and soil-structure faces.

The upper layer of colluvium was moist to damp and had a moderately developed, medium-size granular struc-

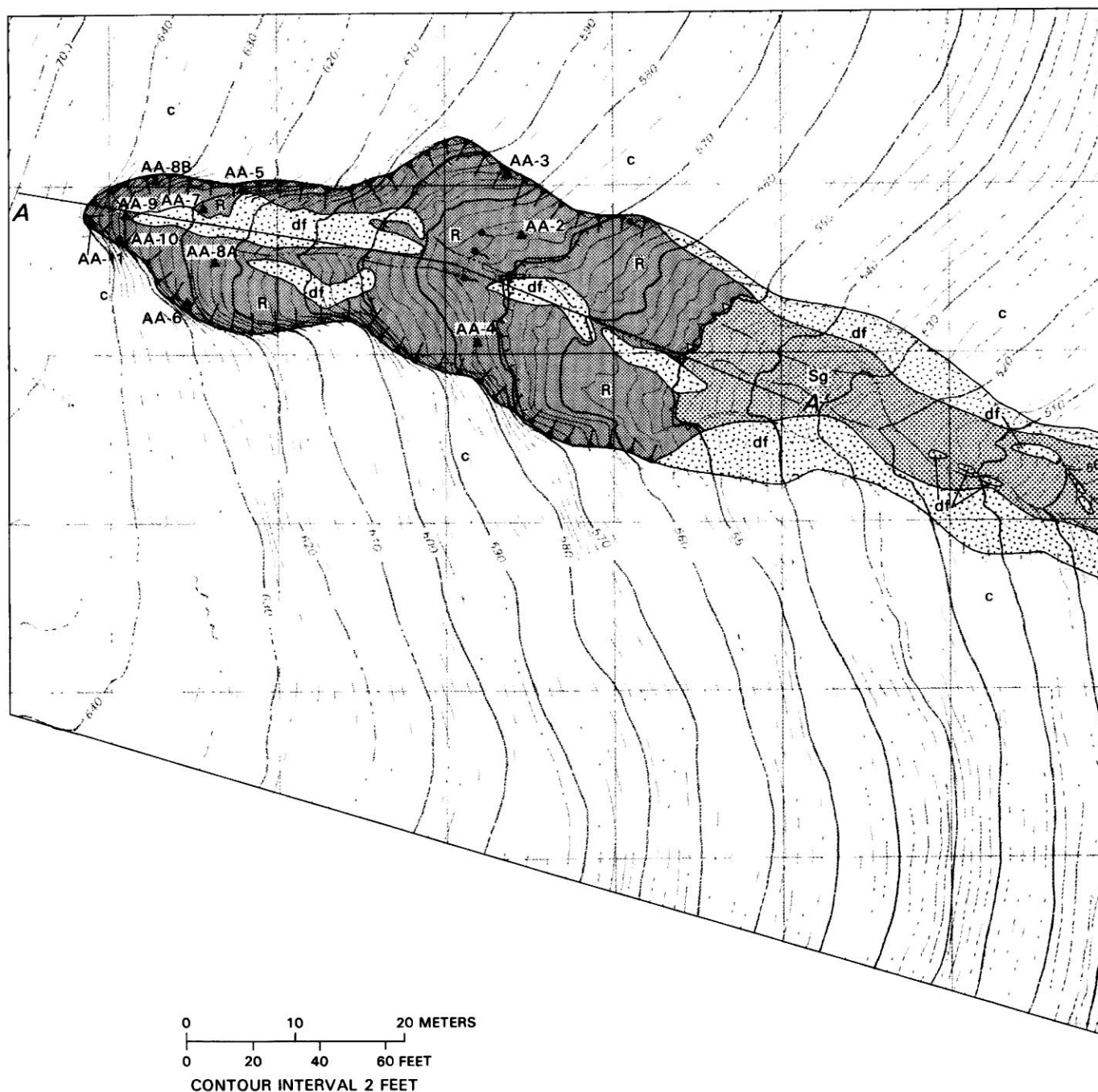


FIGURE 9.6.—Oddstad site, showing landslide on a natural east-facing slope and location of cross section A-A' in figure 9.7. See figure 9.4 for explanation of symbols. Original topographic base prepared for the city of Pacifica by Hammon-Jensen-Wallen & Associates, Oakland, Calif., 1982.

ture. The soil was loose and friable. Dense root growth occupied this porous horizon. High-angle tension cracks and fissures were oriented perpendicular to the flanks of the slope-failure surface exposed in the colluvium.

Ground water was seeping from the colluvium midway up the source-area scar. Seepage issued from a linear zone of nearly equal elevation across the scar. Enough ground water was discharging at the time of our site investiga-

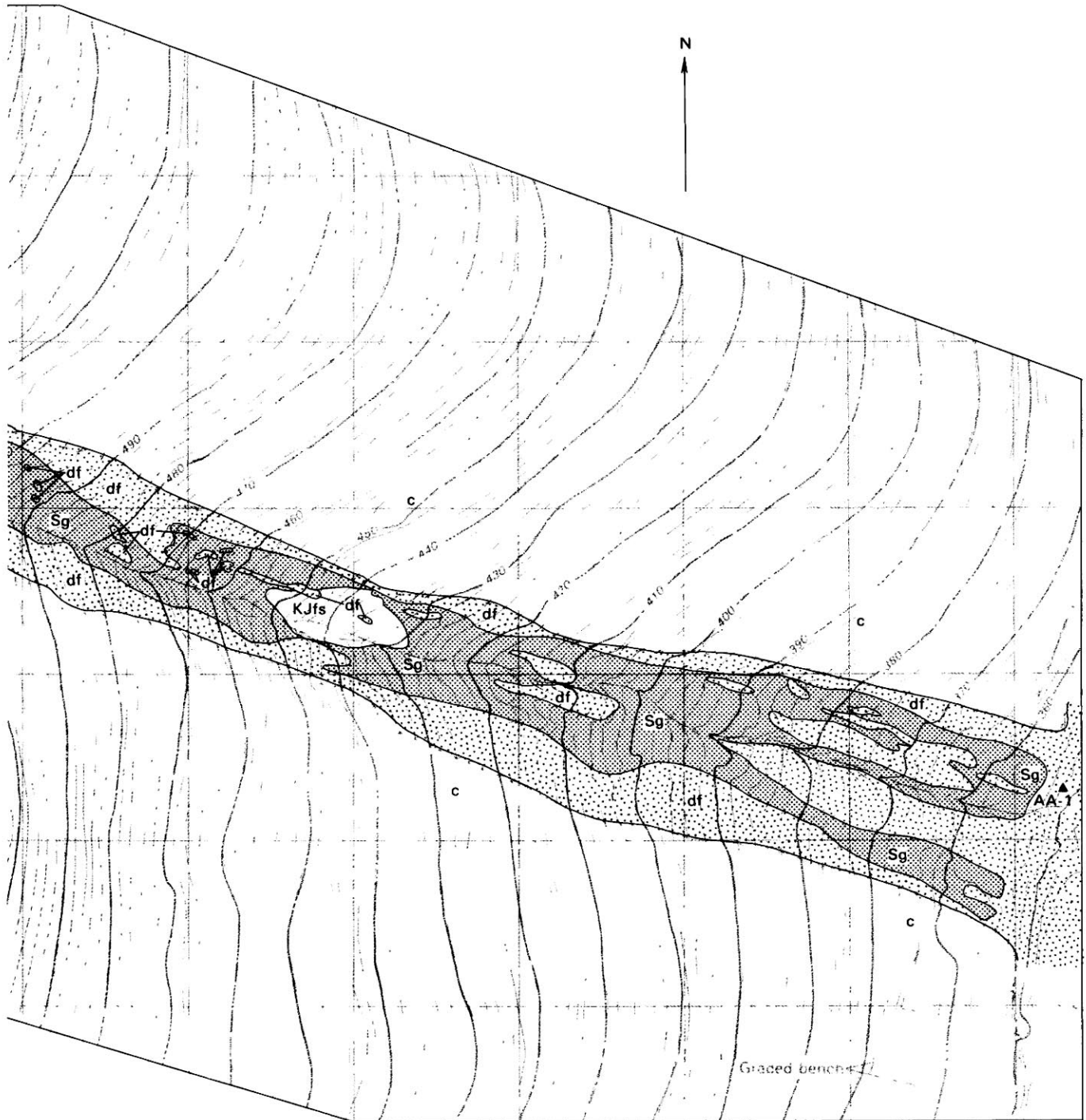


FIGURE 9.6.—Continued

tion (Jan. 25, 1982) to form a steady erosive flow that extended to the bottom of the slope.

#### LANDSLIDE CHARACTERISTICS

The landslide source area was characterized by an irregular, 58-m-long, U-shaped scarp that ranged in height from about 2.5 m at the crown to more than 3.4 m near the toe (figs. 9.6, 9.7). The source area exposes an irregular rupture surface of approximately 840 m<sup>2</sup>, with scattered patches of landslide debris.

The main track extended 140 m from the toe of the source area to the edge of the residential development located at the foot of the slope. The width ranged from about 11 m in the midpart to approximately 18 m at the upper and lower ends.

Vegetation in the track was stripped to the roots by the passing debris avalanche, and some larger roots were sheared off. Where vegetation remained in the track, it characteristically lay flat, pointing in the direction the debris traveled.

Scattered, 0.3- to 0.6-m-thick deposits of debris-avalanche material, commonly striated and pushed into mounds by subsequent surges of debris, occupied the central part of the main track. The margins of the main track

contained a nearly continuous, 0.3-m-thick mantle of debris (lateral deposits) resting on the original vegetated ground surface. The depositional area was the housing tract at the base of the slope. The debris crashed through and between two houses, crossed Oddstad Boulevard, and slightly damaged another two homes.

#### MODE OF FAILURE

Slope failure at this site was complex. The geometry of the rupture surface and of the onsite soil structure indicated that the failure was initiated by translational sliding near the lower third of the source area. After an unknown amount of movement and time, the landslide mass mobilized as a debris flow, which gained debris-avalanche speeds (probably greater than 9 m/s) by the time it reached homes at the foot of the slope.

The initial failure caused loss of support and, probably, simultaneous sliding of the remaining two-thirds of the source area. These subsequent failures began as translational slides that transformed, first, into debris flows and, then, high-velocity debris avalanches as they moved downslope.

Although witnesses claim to have seen only one surge of debris, the presence of two distinct scarplets in the rup-

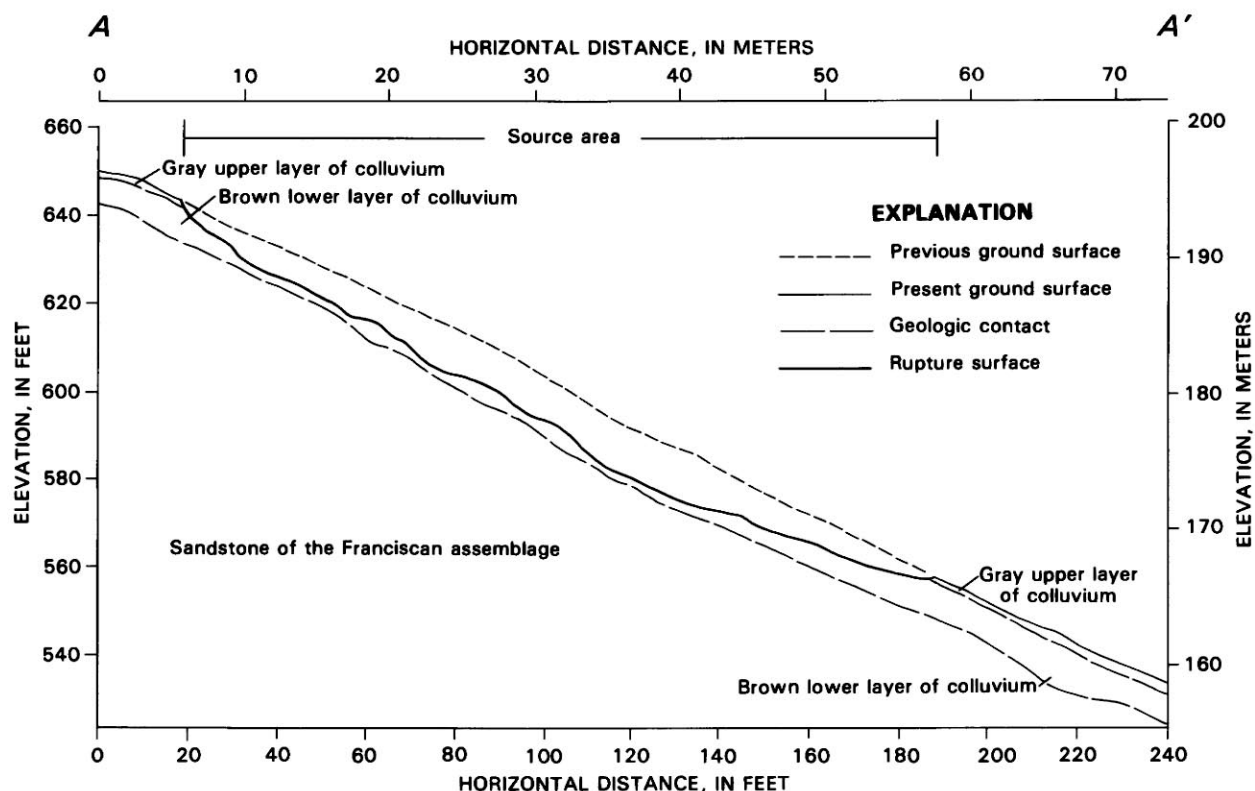


FIGURE 9.7.—Cross section A-A' through source area of debris flow at the Oddstad site. See figure 9.6 for location of cross section.

ture surface (fig. 9.6) and the occurrence of several sets of striated levees of debris in the source area and main track suggest a minimum of three time-separated events. However, the timespan could have been so short that the failures appeared to be one continuous event.

## YOSEMITE SITE

### GEOGRAPHIC SETTING

Several landslides occurred on a natural north-facing hillside above Frontierland Park, located at the end of Yosemite Drive (fig. 9.2). The main slope failure (fig. 9.8), consisting of about 280 m<sup>3</sup> of material, and two other failures that occurred on adjacent slopes created a total material volume estimated at 610 m<sup>3</sup>.

These landslides damaged landscaping and recreational facilities in the southeastern part of the park. The main debris flow originated in a moderately well developed first-order drainage, then traveled along a V-shaped channel that extended downslope to the park. Stairs leading to a nature trail near the source area were badly damaged by impact from the debris flow. The site details and geology are shown in figure 9.8.

The source area of the main debris flow had a natural slope of about 26°. The channel extended downslope to the park at a gradient ranging from 18° to 26°. Arcuate, locally steepened segments of the slope to the southwest of the affected slope were photogeologically interpreted as old landslide scars.

Dense vegetation occupied the entire slope except for the stair area. The dominant vegetation types are coyote brush, poison oak, scrub oak, and grass. Several small trees occupied the central part of the drainage channel.

### GEOTECHNICAL SETTING

The affected slope is underlain by Franciscan rocks consisting of greenstone and some sandstone. The greenstone is highly sheared and includes hard blocks of massive greenstone. Foliation in the greenstone dips steeply in various directions. A contact between greenstone and sandstone was inferred near the head of the source area. The sandstone is highly weathered and has no distinct structure.

Approximately 1 m of colluvium overlay the bedrock. This colluvium consisted of a 30-cm-thick upper layer of moist, loose, very dark grayish brown to black silty-clayey sand that had a well-developed granular structure, grading to a lower layer with a weak blocky structure. The upper layer of colluvium was porous, containing fine and coarse roots, and was friable and slightly plastic.

Curvilinear tension fissures were aligned subparallel to the headscarp adjacent to the flanks and above the source area. Numerous rodent burrows were observed in the

scarp exposures and in the undisturbed ground surface. Surface manifestation of these features, however, was commonly masked by organic debris.

Seepage was observed in the source area, discharging from the contact between colluvium and bedrock. Piping by ground water had resulted in development of a 20-cm-diameter hole in the headscarp.

### LANDSLIDE CHARACTERISTICS

The landslide was defined by a straight, steep-sided source area, a long, narrow, sinuous main track, and remnants of a depositional area at the foot of the slope. The source area was approximately 26 m long and 8 m wide, characterized by a U-shaped main scarp diminishing in height from 2.1 to 1.2 m at the headscarp to 0 m at the toe, and ranging in inclination from about 26° to vertical. The basal rupture surface followed the bedrock-colluvium contact and was highly irregular. Subsequent runoff caused local gullying of the basal rupture surface.

The main track was approximately 70 m long and 8 m wide in the upper reach, and increased in width to about 14 m below the point where a 30° change of course occurred. Preexisting vegetation within the main track was either stripped down to the ground surface or laid flat to the ground in the direction of movement. Immature trees in the main track were impacted by the debris flow but not toppled. Mud from the advancing debris flow splashed onto tree trunks as high as 3 m above the original ground surface.

Part of the debris flow was deposited approximately 30 m from the foot of the slope and was less than 0.3 m thick. Most of the debris flow, however, made a 60° change in course and continued nearly 610 m downslope to Oddstad Boulevard, depositing soil along the way. This deposit was generally less than 0.3 m thick and discontinuous.

### MODE OF FAILURE

The presence of an irregular rupture surface coincident with the colluvium-bedrock contact and of three scarplets below the main scarp suggests that the main failure occurred as four separate translational slides, which were probably simultaneous or nearly so. Disaggregation of the slide blocks into a debris flow probably occurred instantaneously. The long confining drainage course and the distance of travel from the foot of the slope suggest that high speeds were attained; thus, this complex landslide could be called a translational slide/debris avalanche. The length and composition of the deposit suggest that the debris avalanche had a relatively low viscosity. Impact by the debris avalanche on obstacles along the path probably dissipated some of the kinetic energy and lowered the peak velocity.



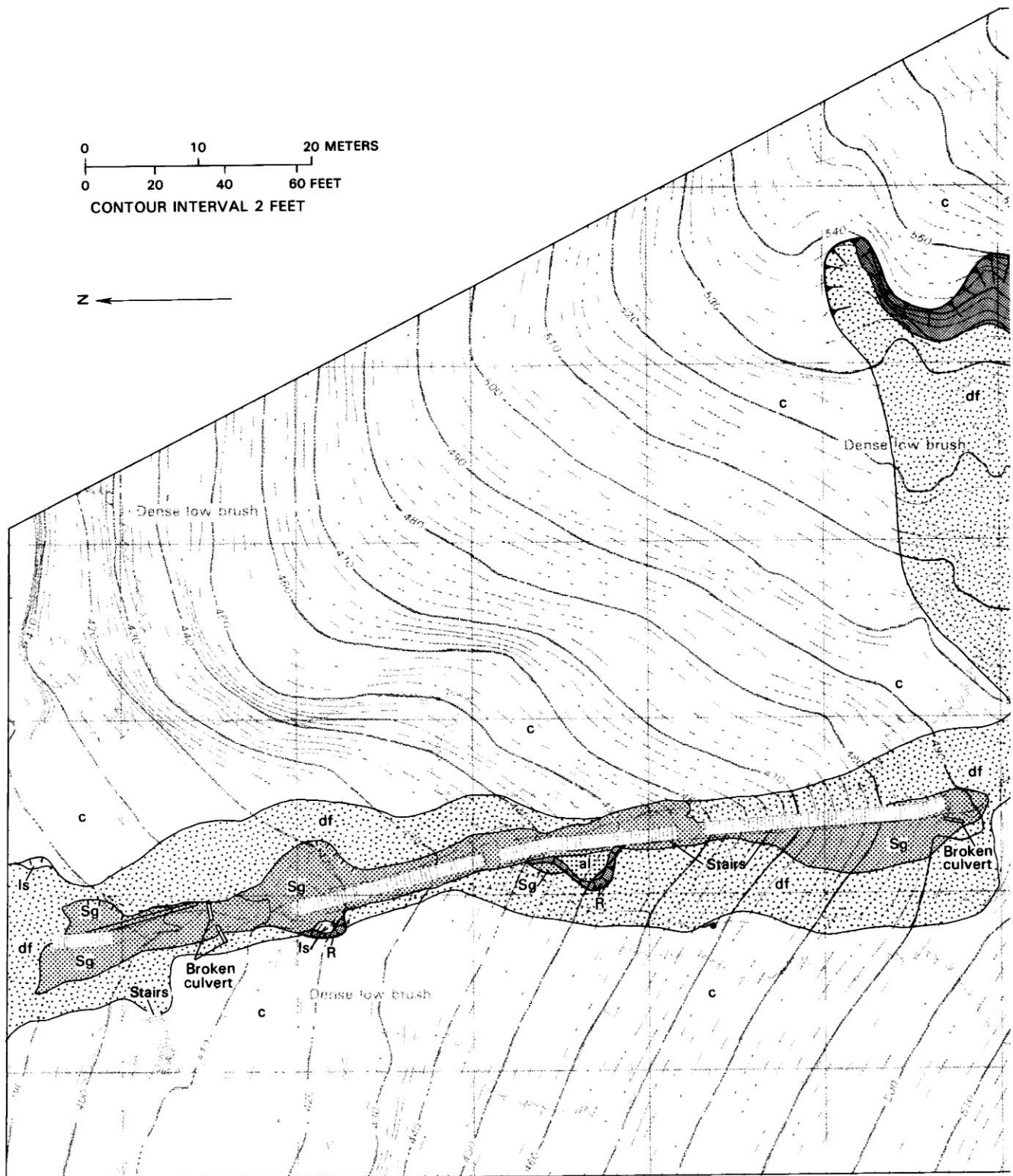


FIGURE 9.8.—Yosemite site, showing landslide on a natural north-facing hillside. See figure 9.4 for explanation of symbols. Original topographic base prepared for the city of Pacifica by Hammon-Jensen-Wallen & Associates, Oakland, Calif., 1982.

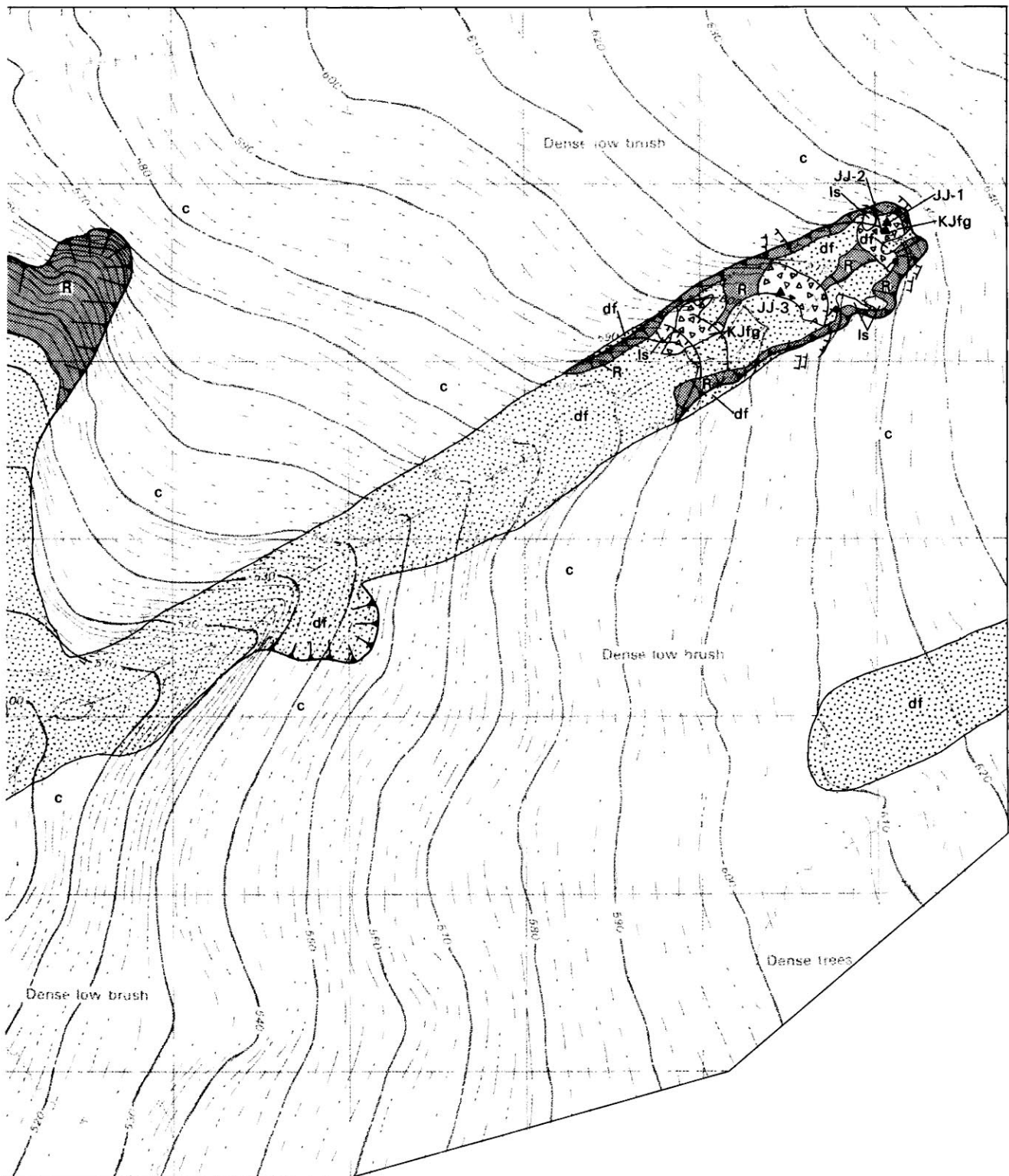


FIGURE 9.8.—Continued

## DISCUSSION

### LANDSLIDE DISTRIBUTION AND TYPE

The 475 landslides related to the January 3-5, 1982, storm were widely distributed within the city limits of Pacifica (fig. 9.3; see chaps. 8, 10). Most of these landslides occurred on hillsides near and within the Linda Mar district, namely, in the area west of Sweeney Ridge, east of California Highway 1, and south of Sharp Park (fig. 9.2). Distinguishable concentrations of landslides were mapped on a generally northwest-trending ridge that extends from northeast of the Highway 1 roadcut landslide to the Oddstad landslide (fig. 9.2). Another concentration of landslides was mapped in the southeast corner of the city in the headwaters of San Pedro Creek. North of Sharp Park, landslides were sparse. Most of the landslides occurred on natural slopes; engineered slopes performed relatively well.

Four principal types of landslides were mapped, including (1) translational slide/debris flow, (2) rotational slide/debris flow, (3) rotational slide, and (4) solifluction. Types 1 and 2, which are complex landslides (Varnes, 1978), resulted in the debris flows and debris avalanches. These complex landslides totaled 85 percent of all mapped landslides. They commonly occurred on natural slopes, although several were mapped on oversteepened cut slopes underlain by soil.

Rotational slides make up about 15 percent of the total landslide inventory. This type of landslide occurred on cut slopes and natural slopes underlain by soil or intensely weathered bedrock. They differed from the complex landslides in that flow subsequent to sliding did not occur. Rotational slides were commonly observed on hillslopes that also contained nearby debris-flow or debris-avalanche scars. Deeper rotational slides were observed locally along high, oversteepened cut slopes.

One occurrence of solifluction was mapped on a slope adjacent to Grand Teton Avenue. This type of failure resulted in a rippled ground surface without distinct boundaries; it can be considered a creep process that is capable of generating a debris flow or a rotational landslide as movement proceeds to locally oversteepen the slope.

### TOPOMORPHOLOGY

The preponderance of flows originated near the heads of first-order drainages (swales) which in some places were so subtle that they showed less than 1 m of relief in transverse profile (see chaps. 7, 10).

Original slope angle plays an important role in the distribution of failures (fig. 9.9; see chaps. 6, 7). The slope angles at the sources of the nine landslides mapped in detail all fall within the range  $26^{\circ}$ - $45^{\circ}$ . This range of slope

angle was suggested by Campbell (1975) as the most common range for soil slides that transform into flows. Although gentle slopes also generated flows in Pacifica, invariably the toe of the landslide coincided with an artificial or natural steepening of slope. Slope failure generally appeared to be independent of slope orientation.

### SOIL CHARACTERISTICS

The presence of soil, ranging in thickness from 0.45 to more than 3.7 m, was a common denominator of the source areas of the slope failures mapped in detail. Most soils examined had been transported from an upslope source (colluvial), but some had been formed in place from the underlying bedrock (residual). Debris-flow source areas generally exposed an upper dark layer, 0.6 m or less thick, of slightly expansive colluvium, underlain by a homogeneous lower layer of granular colluvium.

Engineering properties of the landslide soils were comparable (table 9.1; see table 6.1). Figure 9.10 illustrates the grain-size distribution of soils involved in the nine slope failures that we mapped in detail. Of the soils tested, 58 percent contained 40 to 60 percent sand, 20 to 40 percent silt, and 10 to 30 percent clay. In general, the representative soils involved in debris flows contained 30 to 70 percent sand, 15 to 50 percent silt, and 10 to 45 percent clay. For these ranges in gradation, the shear-strength parameters were a cohesion commonly less than 20 kPa and an angle of internal friction averaging  $35^{\circ}$ .

### LANDSLIDE GEOMETRY

Tension cracks commonly appear to have controlled the configuration of the source areas. Tension cracks were commonly observed on the flanks of the source areas, where they extended downward to become concordant with the basal rupture surface. The cracks were generally lined with fine roots and contained relatively loose soil. Projection of the tension cracks from source-area scars to the adjacent ground surface generally aligned with sub-parallel, 5- to 15-cm-high scarplets observed on the ground surface.

Most debris-flow source areas clearly exposed the geometry of the basal rupture because most of the overlying soil was removed during failure. The rupture surface occurred at or about 0.6 m above the soil-bedrock contact and was commonly subparallel to the adjacent natural ground surface. Bedrock was commonly exposed in "windows" on the floor of the source area, and springs were observed discharging from fractured rock or soil.

Rupture-surface profiles were very irregular; some profiles had a relief of as much as 0.6 m. Locally, steep reaches of the rupture surface coincided with root-lined tension cracks exposed in the adjacent flanks of the source

area. This relation may represent the headscarps of individual landslide blocks that failed retrogressively, probably nearly simultaneously.

#### SLOPE-STABILITY ANALYSES

Slope-stability analyses, using prefailure geometry, were conducted for the nine slope failures studied in detail. An infinite-slope model was used initially to represent the landslide geometries, and calculations were made using the soil unit weights and shear-strength parameters listed in table 9.1. These calculations were accomplished by using the charts from Duncan and Buchignani (1975), which assume seepage parallel to the slope. In some cases, the stability analyses showed that total saturation with seepage parallel to the slope was insufficient to cause landsliding. For these cases, it was necessary to assume

seepage out of the slope to obtain a factor of safety (FS) less than or equal to one.

However, as shown in figure 9.12A, the failure surface is finite rather than infinite. In addition, numerous tension cracks were observed during the field investigation, and we believe that these tension cracks preceded landsliding. Therefore, we reanalyzed the failures, using a method of slices that incorporates prefailure geometries with finite downslope length and total-stress conditions. Again, in some cases an FS greater than 1 was obtained. For these cases, lowering the effect of cohesion by assuming a tension crack at the headscarp, extending from the ground surface to the basal rupture surface, was sufficient to reduce the FS to within 10 percent of 1.0. We consider this FS value sufficient for failure under the given conditions and method of analysis. However, the FS can be further reduced by adding the hydrostatic force

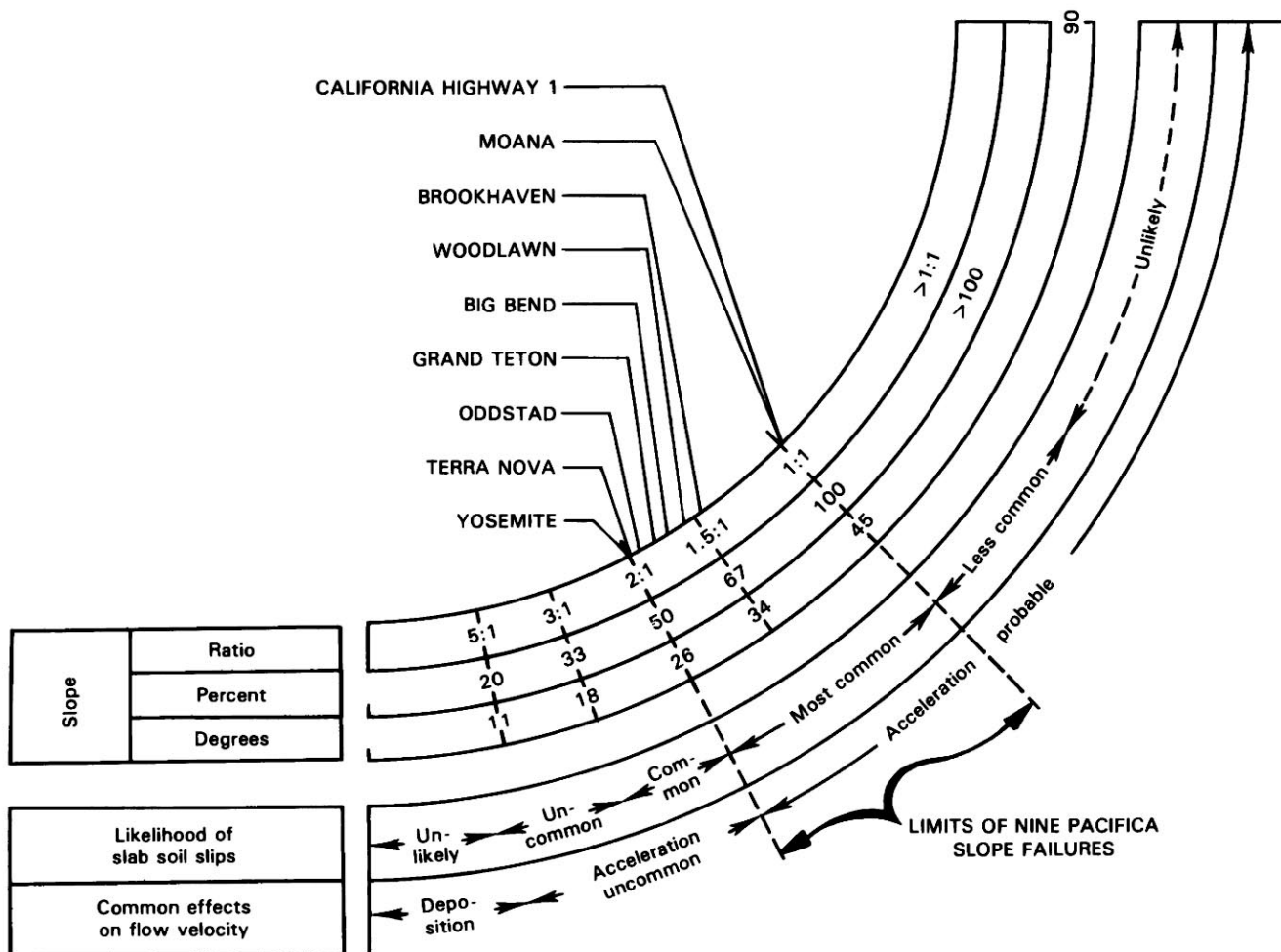


FIGURE 9.9.—Slopes at sources of nine landslides in Pacifica compared with the range of natural slopes, the likelihood of shallow slides, and the effects of slope on the velocity of debris flows (modified from Campbell, 1975, fig. 8).



TABLE 9.1—Engineering characteristics of soil samples at nine slope failures near Pacifica, Calif.

[C, cohesion; FI, silt and clay; GR, gravel; LL, liquid limit; PI, plasticity index; PL, plastic limit; SA, sand;  $\phi$ , angle of internal friction]

Sample	Depth (m)	Dry density (g/cm <sup>3</sup> )	Moisture content (percent)	Atterberg limits			Gradation (pct)			Direct shear	
				LL	PL	PI	GR	SA	FI	C (kPa)	$\phi$ (°)
Grand Teton-BB 3-----	1.89	1.52	26.2	50.3	26.8	23.5	3	27	70	7.66	25
Brookhaven-DD 1-----	1.52	1.70	19.7	---	---	---	---	---	---	11.97	40
Brookhaven-DD 3-----	.61	1.76	13.4	---	---	---	---	---	---	0	50
Brookhaven-DD 7A-----	1.98	1.70	19.8	41	23	18	4	57	39	12.93	34
Moana-HH 1-----	3.05	1.41	31.6	53	22	31	4	57	39	23.94	26
Big Bend-EE 2-----	.91	1.76	20.1	42	22	20	10	41	49	9.72	28
Woodlawn-FF 1-----	3.05	1.63	19.4	35	19	16	7	53	40	11.97	37
Terra Nova School-GG 4---	.61	1.36	24.3	40	22	18	4	46	50	0	35
Terra Nova School-GG 7---	.91	1.49	28.8	34	24	10	3	37	60	0	44
Yosemite-JJ 2-----	.91	1.54	26.9	33	19	14	1	58	41	3.35	47
Yosemite-JJ 3-----	1.52	1.94	10.0	18	15	3	2	55	43	12.45	36
Highway 1 roadcut-II 1---	1.22	1.68	20.2	37	16	21	2	34	64	4.79	25
Oddstad-AA 1-----	1.22	1.62	24.0	---	---	---	---	---	---	9.58	37
Oddstad-AA 2A-----	4.57	1.65	22.4	36	20	16	0	60	40	23.94	39
Oddstad-AA 5A-----	2.44	1.57	23.7	30	25	5	---	---	---	18.19	26
Oddstad-AA 9-----	1.22	---	---	39	19	20	0	42	58	---	---

caused by surface water filling the tension crack. This additional force is sufficient to lower the calculated FS to below 1.0.

As movement takes place, however, the tension crack widens, the height of water in the tension crack decreases, and, in turn, the driving force decreases. Several episodes of movement may be necessary to decrease the shear strength from the peak toward the residual value and thus to initiate the landslide. This sporadic type of movement could account for the addition of large volumes of water to the sliding mass.

These calculations show that both effective-stress and total-stress analyses can be used to calculate an FS that indicates failure.

#### MECHANICS AND MODE OF FAILURE

Intense rainfall during the January 3-5, 1982, storm was evidently the triggering mechanism for the landslides. Cumulative values for the storm, as well as antecedent rainfall data, are given in chapter 2; one measurement of cumulative storm rainfall near Sharp Park indicated a total of 221 mm (8.7 in.) (chap. 2). A regional estimate of rainfall by J.P. Monteverdi (written commun., 1982) shows a range of 150 to 200 mm (6-8 in.) for the city of Pacifica during the storm.

Much work has been done to relate debris-flow occurrences to rainfall (see chaps. 2-5, 8). Campbell (1975) suggested that in southern California at least 267 mm (10.5 in.) of rainfall is necessary after an average dry season to bring the soil to field capacity, the water content at which water drains from the soil at the same rate as it is added. Campbell demonstrated that a critical rain-

fall intensity of 5 to 6 mm/h (0.20-0.25 in/h) is necessary to trigger flows, once field capacity is achieved. Govi and Sorzana (1980) indicated that storm-rainfall totals sufficient to trigger debris flows increase with an increasing mean annual precipitation (see chaps. 2-4, 8). They also showed that critical storm rainfall is lower for wet antecedent than for dry antecedent conditions.

The role of intense rainfall in triggering debris flows is illustrated in figure 9.11. Kesseli (1943) postulated that slope failure occurs during rainfall sufficiently intense that

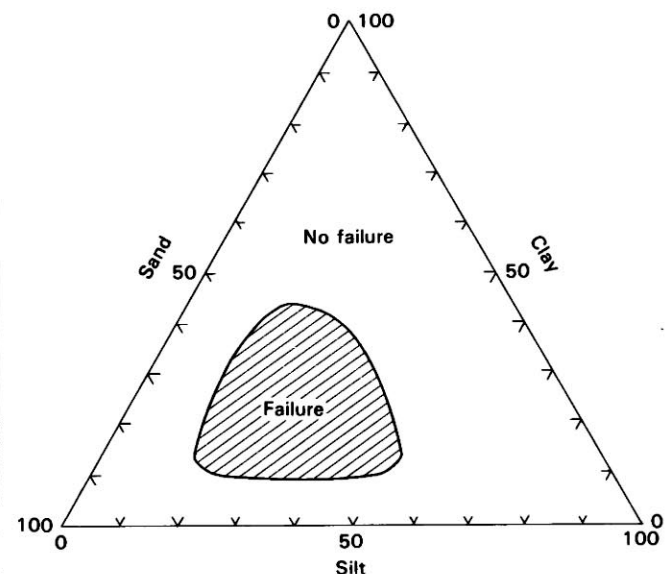


FIGURE 9.10.—Grain-size distribution for unstable soils at nine sites studied in detail. All values in weight percent.

water percolates into overburden soils at a rate greater than into bedrock. This condition develops a temporary perched water table in the soil. The height of this water table increases with continued intense rainfall, and a downslope seepage force develops in the soil mass. As saturation occurs, excess rainfall is distributed as surface runoff. In response to the pore pressures that develop, the soil becomes buoyant, and the resisting forces decrease.

The model of Kesseli, applied to debris flows in southern California by Campbell (1975), assumes that debris flows are initiated by sliding. Johnson and Rahn (1970) and Govi and Sorzana (1980) reported similar failure modes for other areas. Their model seems reasonable to apply to the flows in Pacifica, on the basis of rupture-surface geometry, the presence of remnant slide blocks exposed in the source areas of many slope failures, and the results of our stability analyses.

Once a saturated, noncohesive or slightly cohesive, granular soil mass fails by sliding, it commonly disaggregates into a debris flow (see chap. 6). Transformation of

an initially rigid slide block into a flow is shown diagrammatically in figure 9.12. The first stage (fig. 9.12A) occurs when the slide mass begins gliding along or just above the soil-bedrock contact. At this stage, high pore-water pressure, caused by the permeability differences between soil and bedrock, and tension cracks are the primary controls. As the slide mass moves, plastic deformation (fig. 9.12B) occurs in the formerly rigid mass as internal shearing causes a reduction in strength (Johnson and Rahn, 1970; Campbell, 1975). Water filling tension cracks as the mass dilates could aid in mobilization of a debris flow from the slide. Further disaggregation reduces the strength of the slide mass and initiates flowage over the original ground surface (fig. 9.12C). As the flow moves farther downslope, it may accelerate to debris-avalanche speed, and it may incorporate vegetation and soil (fig. 9.12D). If the slide occurs as separate blocks, one surge may overtake another during descent of the slope, or separate surges may occur. Decrease in slope gradient at the base of the hill initiates deposition of the debris (fig. 9.12E).

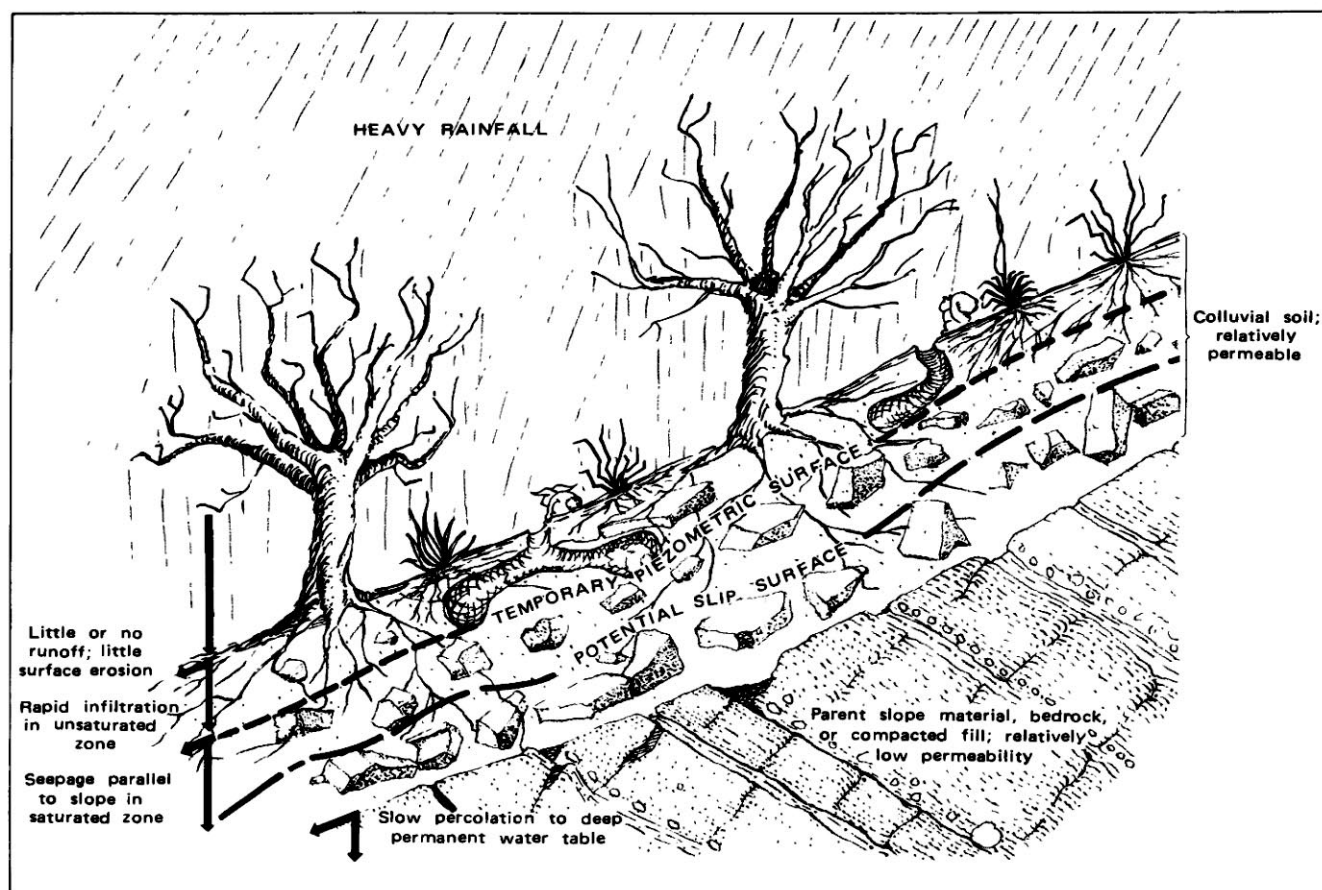


FIGURE 9.11.—Buildup of a perched water table in soil cover during heavy rainfall (from Campbell, 1975, fig. 16).

## CONCLUSIONS

1. Complex landslides involving both sliding and flow totaled 85 percent of the mapped landslides.
2. Most of these complex landslides originated near the heads of first-order drainages on slopes between  $26^{\circ}$  and  $45^{\circ}$ , independently of slope orientation.
3. Engineering properties of the landslide soils were comparable.
4. Tension cracks were common to all the landslides and probably could serve as precursors.
5. Rupture surfaces at the sources of flows occurred in soil at or slightly above the soil-bedrock contact.
6. A tension crack and (or) water filling the tension crack was necessary in some cases for failure to occur.

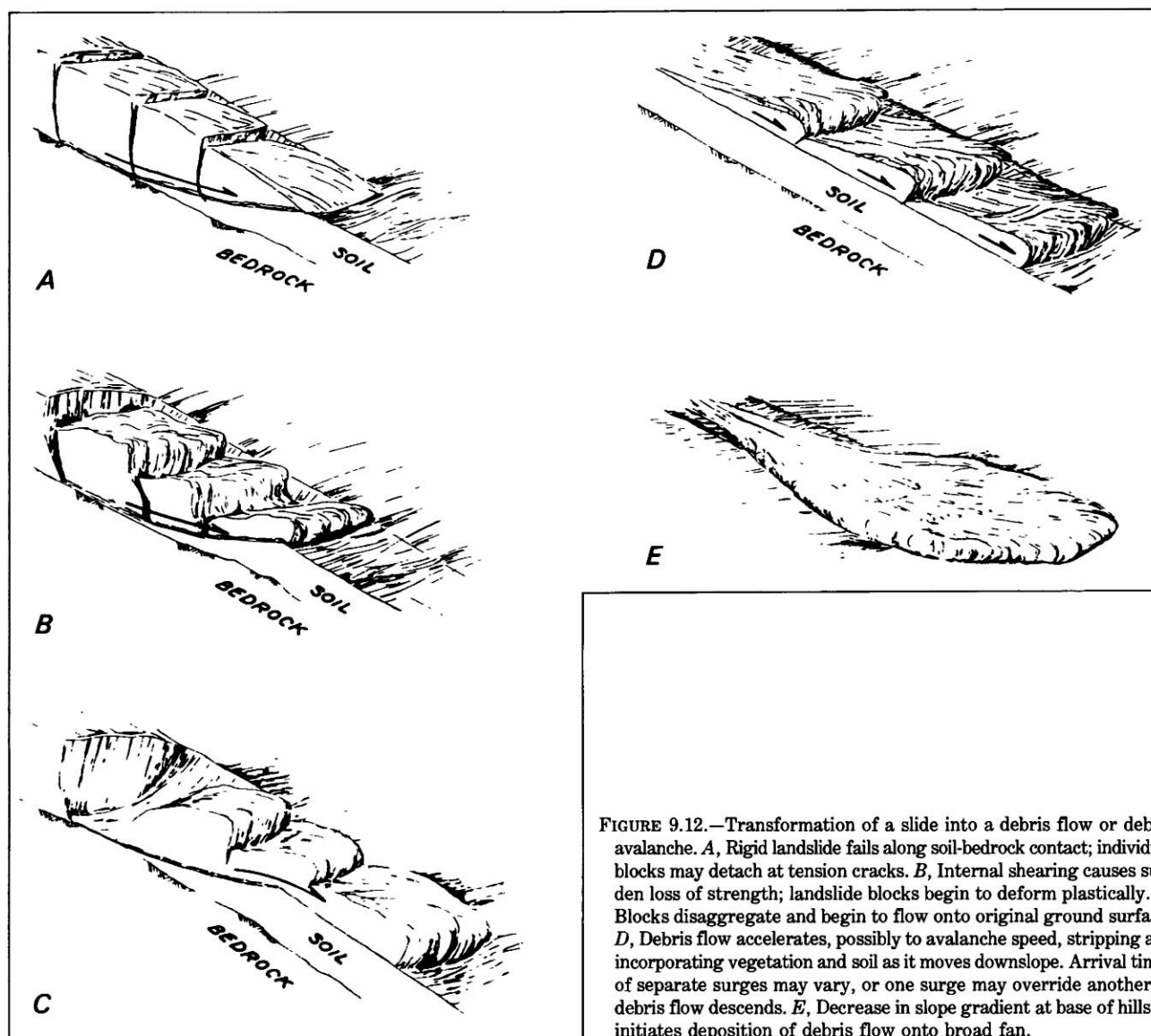


FIGURE 9.12.—Transformation of a slide into a debris flow or debris avalanche. *A*, Rigid landslide fails along soil-bedrock contact; individual blocks may detach at tension cracks. *B*, Internal shearing causes sudden loss of strength; landslide blocks begin to deform plastically. *C*, Blocks disaggregate and begin to flow onto original ground surface. *D*, Debris flow accelerates, possibly to avalanche speed, stripping and incorporating vegetation and soil as it moves downslope. Arrival times of separate surges may vary, or one surge may override another as debris flow descends. *E*, Decrease in slope gradient at base of hillside initiates deposition of debris flow onto broad fan.

## REFERENCES CITED

- Bonilla, M.G., 1960, Landslides in the San Francisco South quadrangle, California: U.S. Geological Survey open-file report, 44 p.
- Brabb, E.E., and Pampeyan, E.H., compilers, 1972, Preliminary geologic map of San Mateo County: U.S. Geological Survey Miscellaneous Field Studies Map MF-328, 10 p., scale 1:62,500.
- Campbell, R.H., 1975, Soil slips, debris flows, and rainstorms in the Santa Monica Mountains and vicinity, southern California: U.S. Geological Survey Professional Paper 851, 51 p.
- Darrow, R.L., 1951, The geology of the northwest part of Montara Mountain quadrangle: California Division of Mines and Geology Special Report 78, 23 p.
- Duncan, J.M., and Buchignani, A.L., 1975, An engineering manual for slope stability studies: Berkeley, University of California, Department of Civil Engineering, 83 p.
- Fowler, W.L., 1984, Potential debris flow hazards of the Big Bend Drive drainage basin, Pacifica, California: Stanford, Calif., Stanford University, M.S. thesis, 101 p.
- Govi, Mario, and Sorzana, M.G., 1980, Landslide susceptibility as a function of critical rainfall amount in Piedmont basins (North-Western Italy): *Studia Geomorphologica Carpatho-Balcanica*, v. 14, p. 43-61.
- Johnson, A.M., and Rahn, P.H., 1970, Mobilization of debris flows, *in* Macar, Paul, ed., New contributions to slope evolution: *Zeitschrift für Geomorphologie*, supp. v. 9, p. 168-186.
- Kesseli, J.E., 1943, Disintegrating soil slips of the Coast Ranges of Central California: *Journal of Geology*, v. 51, no. 5, p. 342-352.
- Lawson, A.C., 1914, San Francisco [district], Tamalpais, San Francisco, Concord, San Mateo, and Haywards quadrangles, folio 193 of Geologic atlas of the United States: Washington, U.S. Geological Survey, 24 p., scale 1:62,500.
- Pampeyan, E.H., 1981, Geologic map of the Montara Mountain quadrangle, San Mateo County, California: U.S. Geological Survey Open-File Report 81-451, 15 p., scale 1:12,000.
- Shlemon, R.J., Wright, R.H., and Montgomery, D.R., 1987, Anatomy of a debris flow, Pacifica, California, *in* Costa, J.E., and Wieczorek, G.F., eds., Debris flows/avalanches: Process, recognition, and mitigation: Geological Society of America Reviews in Engineering Geology, v. 7, p. 181-199.
- Varnes, D.J., 1978, Slope movement types and processes, chap. 2. *of* Schuster, R.L., and Krizek, R.J., eds., Landslides: Analysis and control: U.S. National Academy of Sciences, National Research Council, Transportation Research Board Special Report 176, p. 11-33.
- Wagner, R.J., and Nelson, R.E., 1961, Soil survey of the San Mateo area, California: U.S. Department of Agriculture, Soil Conservation Service ser. 1954, no. 13, 111 p.





# 10. A METHOD FOR MAPPING RELATIVE SUSCEPTIBILITY TO DEBRIS FLOWS, WITH AN EXAMPLE FROM SAN MATEO COUNTY

By THEODORE C. SMITH,  
CALIFORNIA DIVISION OF MINES AND GEOLOGY

## CONTENTS

	Page
Abstract - - - - -	185
Introduction - - - - -	185
Previous work in the San Francisco Bay region - - - - -	186
Factors that influence the locations of debris flows - - - - -	186
Topographic form - - - - -	186
Slope inclination - - - - -	188
Vegetation - - - - -	188
Bedrock materials - - - - -	189
The method - - - - -	190
Test of the method - - - - -	192
Summary - - - - -	192
References cited - - - - -	193

## ABSTRACT

The method described herein principally consists of the preparation of a geomorphic map by a geologist, once it has been established that the regolith and bedrock materials in a given area may be susceptible to debris flows that develop from shallow slides. Areas that appear most prone to debris-flow failure are hollows and concave areas on slopes steeper than about 20°. Debris flows also commonly originate on side-slopes steeper than about 20°, although they may also occur on slopes that are less steep. Convex surfaces, such as ridge spurs, are least likely to generate debris flows. In addition to the delineation of areas with the above-mentioned characteristics, drainages downstream from potential source areas are identified as prone to inundation by debris flows or debris floods.

Using elements of this method, I prepared a debris-flow-susceptibility map for part of San Mateo County, Calif. (Smith, 1977), 5 years before the January 3-5, 1982, storm hit the San Francisco Bay region. During and immediately after this storm, about 85 debris flows occurred in the area of my pilot study. Almost all (98 percent) of these flows originated in areas designated on the map as most susceptible to debris-flow formation. On the basis of this experience, debris-flow-susceptibility maps sufficiently detailed for land-use planning at the local level apparently can be prepared for at least some areas.

## INTRODUCTION

The purpose of this chapter is to report on one method that appears to be useful for delineating areas susceptible to rapid flows that develop from shallow slides, which are here called simply debris flows (see "Introduction" to this volume for landslide terminology). Because debris flows and related phenomena differ significantly from the more commonly recognized rotational and translational

slides, the hazards posed by debris flows differ substantially from those posed by slides, especially in a spatial context. Therefore, slope-stability maps that incorporate or present data solely on rotational or translational slides do not normally depict the potential hazards from debris flows, debris floods, and mud floods.

A typical debris flow begins as a slide that leaves a distinct, commonly spoon-shaped scar at its source (fig. 10.1). The slide material may immediately mobilize as a slurry or be quickly transformed from a relatively coherent slide mass into a slurry. Once mobilized, the soil material flows rapidly downslope, commonly gathering speed and, possibly, more soil material. This soil material eventually is deposited as the debris flow slows, commonly when gentler slopes are reached. These areas of deposition are sometimes far from the point of origin.

During the early part of this study, I reviewed the literature to determine whether a consensus exists regarding the factors controlling formation of debris flows. On the basis of this initial review and independent field observations, it became apparent that several factors control the formation of debris flows and that some of these factors can be mapped. I selected an area in northern San Mateo County and prepared a sample debris-flow-susceptibility map (Smith, 1977). I compared this initial map (hereafter referred to as the 1977 version) with older aerial photographs on which scars and tracks from earlier debris flows are apparent. In early 1982, after the January 3-5 storm, I checked this map again, using infrared aerial photographs and limited field reconnaissance. On the basis of

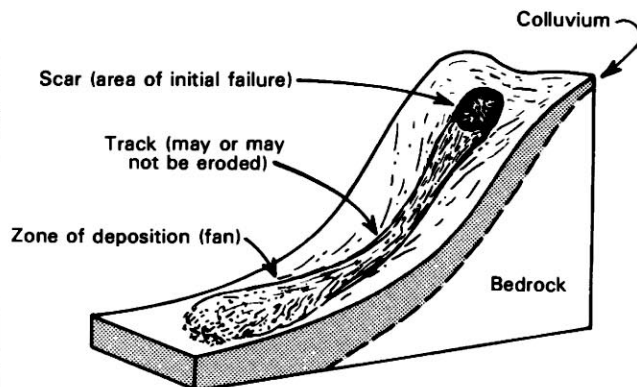


FIGURE 10.1.—Principal features of a debris flow.

these additional data, I have refined the 1977 version slightly to better portray the relative hazards from debris flows.

### PREVIOUS WORK IN THE SAN FRANCISCO BAY REGION

January 1982 was not the first time that debris flows occurred in the San Francisco Bay region. Lawson (1908), in his report on the effects of the great 1906 San Francisco earthquake, referred to several "earth-flows" that occurred near Half Moon Bay. It is apparent from the photographs included in his report that these "earth-flows" would here be called debris flows.<sup>1</sup> Rice and others (1976) indicated that debris flows constitute a major hazard in much of Marin County, but they were unable to adequately reflect this hazard on the slope-stability maps they prepared. Thomas (1939), Bonilla (1960), Radbruch and Weiler (1963), Stromberg (1967), and Smith (1977) all briefly addressed debris-flow phenomena in the bay region. Rodine (1975) and Johnson and Hampton (1969) discussed, in considerable detail, selected debris flows that have occurred in parts of the region. Before the January 3-5, 1982, storm, however, none of these reports, except that by Lawson (1908), had been widely distributed or received much attention either by the public or by the geologists and engineers who work in the bay region.

To date, most of the landslide-hazard-mapping effort in the San Francisco Bay region has been directed toward delineating large landslides that leave fairly well-defined deposits which, for the most part, remain virtually where they originated—at or near the landslide source. In contrast, debris flows generally are not very large and do not leave well-defined deposits, particularly near the points of origin. For these reasons, and because the source scars commonly are quickly revegetated (within a few months or years), much of the evidence of past debris flows has been overlooked, and the potential hazard has gone unrecognized or unreported.

Furthermore, the effects of debris flows differ significantly from those of the more commonly recognized larger landslides. Because many debris flows occur with relatively little or no warning and commonly attain velocities of 10 m/s or more, they pose a substantial threat to life and property—a threat that can only be minimized if it is recognized before the landslide occurs. In contrast, most of the more commonly recognized landslides, though larger, move more slowly and thus allow persons and, in some places, structures to be removed from the hazardous area after landslide movement begins.

The combined result of all these factors was that virtually no one in the bay region was prepared for the types of landslides that occurred during and immediately after the January 3-5, 1982, storm. In view of the serious hazard of debris flows and their widespread occurrence in populated areas, the identification of areas susceptible to debris flows is an important step in the effort to protect the public from these destructive landslides.

*Acknowledgments.*—I thank Earl W. Hart and Salem J. Rice (retired) of the California Division of Mines and Geology, and Joel W. Baldwin of Baldwin Consultants, Pacifica, Calif., for discussions on this topic.

### FACTORS THAT INFLUENCE THE LOCATIONS OF DEBRIS FLOWS

A wealth of literature exists describing debris flows. However, any review of this literature is hindered by the fact that more than 40 names have been used by experts in various disciplines (including geology, hydrology, engineering, and forestry, to name only a few), working in different parts of the world, to refer to debris flows and similar phenomena. Also, many investigators do not fully describe debris-flow events, although photographs accompanying their reports sometimes permit inferences to be made.

On the basis of the literature available, several factors appear to control the origin of the debris flows discussed here, which originate from shallow slides. Basically, debris flows are triggered by high pore-water pressure. Thus, the characteristics of the materials at the point of origin and the volume of water available at the site are of primary importance (see chaps. 5, 6, 7). In turn, the characteristics of the materials and the volume of water at the site of origin are controlled to varying degrees by other factors, including topographic form, slope inclination, vegetation, and bedrock materials and structure. There appears to be a consensus on the importance of some, but not all, of these factors.

### TOPOGRAPHIC FORM

Many authors (Holmes, 1917; Hack and Goodlett, 1960; Swanston, 1969; Pain, 1972; Swanston and Swanson, 1976; Bogucki, 1977; Eyles and others, 1978; Rapp and Stromquist, 1979; Govi and Sorzana, 1980; McConchie, 1980; Hollingsworth and Kovacs, 1981; Zeimer, 1981) have reported that most debris flows originate in hollows,<sup>2</sup>

<sup>1</sup>Some of these phenomena might also be classified as debris slides according to Varnes (1978).

<sup>2</sup>A hollow is defined as the central part of a valley that contains the head of a stream. On a topographic map, any area in which the contours are concave outward (away from the hillside) constitutes a hollow (fig. 10.2). Commonly, more hollows are apparent on high-resolution aerial photographs than on topographic maps. Noses appear as areas where the contours are convex outward. Areas where the contours are essentially straight constitute the sideslopes.

at the heads of first-order drainages, or in incipient hollows on sideslopes (fig. 10.2). Almost all these authors concluded that such sites are particularly susceptible because water concentrates in these areas. In the study area of this report, 60 percent of the debris flows triggered by the January 3–5, 1982, storm occurred adjacent to first-order drainages, and 9 percent along drainages of higher order. Similar conclusions are reported in chapters 7 and 9.

Hack and Goodlett (1960) suggested two major reasons why hollows appear to be the areas most susceptible to debris-flow failure. First, they theorized that during and immediately after rainstorms, hollows should be the wettest areas of a hillslope because the slopes above converge toward the hollow. They likewise envisioned that the ridge nose or spur should be drier than either the hollow or the sideslope areas. These hypotheses were largely verified in the field by Dunne and Black (1970) and Pierson (1980).

Second, hollows theoretically are also the areas on hillslopes where the regolith is thickest because material moved from the surrounding slopes by water or soil creep tends to converge there. Hack and Goodlett (1960) found that the regolith in hollows in some mountainous areas is generally coarser and better sorted than that on sideslopes and noses, although they cautioned that studies of valleys in lowland areas have revealed that such generalizations do not everywhere apply.

In considering the effects of water on debris-flow failures, most workers have considered only the contributions of surface runoff and water flow through near-surface soils (throughflow). Some geologists (E.W. Hart and S.J. Rice, oral commun., 1982) believe that deeper, subsurface flow along joints or beds is more important than shallower flow in triggering debris flows. Such appears to be the case at least locally (see chaps. 6, 7; Bogucki, 1977; Bevin and others, 1978). In places where deep flow through bedrock has caused debris flows, telltale depressions (scars) remain after the event. Over time, either these scars gradually fill with colluvium, or a first-order drainage develops downslope. If a drainage develops, it may be inferred from the existence of the hollow at the head of the drainage that another debris flow may occur in the future. If the scars fill with colluvium, similar peak subsurface flows might be anticipated in the future—flows that would be capable of triggering another debris flow once sufficient colluvium has accumulated. In either case, a similar failure appears likely at some future time in the same place.

Regardless of the means of water concentration, the time required for a debris flow to recur at a given site depends on local topography, the size of the “initial” failure, and the local soil-forming or colluvial processes. For example, in January 1982, during cleanup of a small debris flow in western Marin County, a wooden flume was

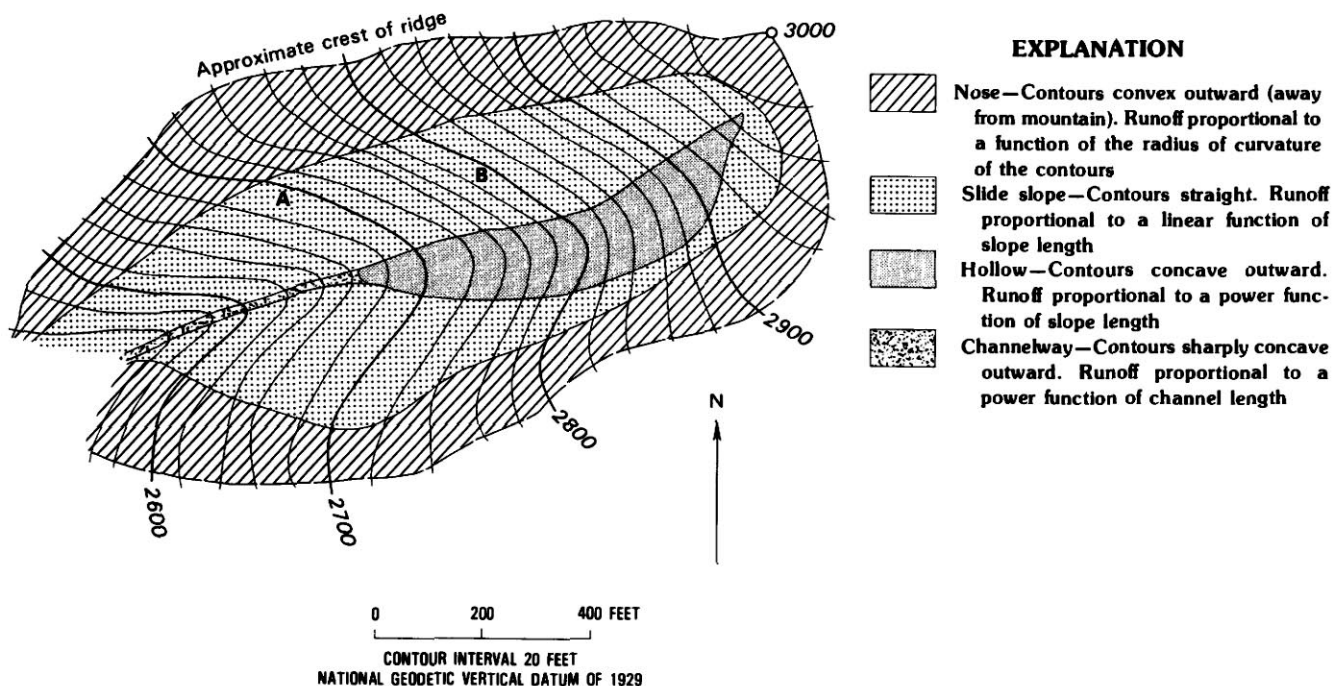


FIGURE 10.2.—Classification of various parts of a drainage. Slight inflections in contours at sites A and B in this planimetric map (modified from Hack and Goodlett, 1960, fig. 2) indicate locations of incipient hollows.



uncovered below the scar. Discussions with the property owner revealed that this flume had been constructed in January 1956 after a similar debris flow had occurred. Examination of the site, the relation of the flume to the scar, and recollections of the previous owner of the property strongly suggest that the scar had filled during the intervening 26 years and had failed again. High-resolution aerial photographs of the site taken in 1978 show no evidence of the 1956 scar, although some larger scars nearby had not filled in during that same period. Examination of other debris-flow scars created in 1982 revealed soil features that appear to be remnants of debris-flow scars which developed decades or centuries earlier (J.E. Baldwin, oral commun., 1982; see section entitled "Scars and Individual Habitats of Previous Soil Slips," chap. 7).

Until now, most of this discussion has dealt with debris flows triggered by "small" catastrophic storms or, in other words, the areas most likely to fail first. A slightly different approach can also be taken, namely, determining which areas are most likely to fail "last" or not at all, even given the most extreme weather conditions. Photographs similar to those presented by Jones (1973) lend themselves to such an analysis (figs. 10.3, 10.4). As might be anticipated from the preceding sections, ridgetops remain intact most of the time, although ridgetop areas may be extremely narrow and occasionally fail (fig. 10.4). Ridge spurs or noses appear to fail less frequently than hollows or sideslopes; noses generally fail only near the base of the slope or at other significant breaks in slope (see section entitled "Concentration of Water," chap. 6).

#### SLOPE INCLINATION

Most workers documenting debris-flow failures provide data on the inclination of the hillslope(s) that failed. Most reported failures occurred on slopes of 20° to 45°. Except for unusual conditions (discussed below), the lowest reported slope angle of failure was 26 percent (14.56°) (Schneider, 1973; see "Grant Road," chap. 8). The upper inclination limit of susceptible slopes appears to be controlled largely by the tendency of regolith to slip off steep slopes. Thus, we may conclude that if regolith exists on a steep slope, a debris flow may occur. Although such observations suggest that debris-flow-susceptibility maps may be prepared by simply using slope maps, Bailey and Rice (1969) cautioned that slope maps depict only the average slope rather than the local maximum slope, which is a more important factor (see chap. 7).

#### VEGETATION

The relation between type of vegetation and the occurrence of debris flows is not entirely clear. Some workers (Bailey and Rice, 1969; Clark, 1973) claimed a clear rela-

tion, whereas others (Holmes, 1917; Bogucki, 1970) reported no relation. This disagreement suggests that vegetation may locally reflect subsurface conditions (such as soil type and permeability) and that we may be able to determine which slopes are more susceptible to debris-flow failure in some places by mapping vegetation types.

Gray and Leiser (1982) reported that the binding power of roots affects the stability of slopes underlain by cohesionless regolith (see chap. 5). Indeed, Gray and Megahan (1980) concluded that root reinforcement is an important, if not the most important, source of cohesion for regolith on steep slopes in granitic terrane. Scott (1975) observed that the rooting depths of different plants partly control how thick a regolith can develop on steep slopes before failure occurs. If these observations and hypotheses are correct, then the susceptibility of a given slope to debris-flow failure could be significantly altered by altering the type of vegetation covering the slope. Such an occurrence has been documented in southern California, where conversion of slope cover from brush to grass was accompanied by an increase in the number of debris flows triggered during a single storm (Corbett and Rice, 1966).

Intuitively, we might expect a slope covered with cohesionless regolith and lacking vegetation to erode grain by grain, rather than fail catastrophically, unless some cohesive layer, such as a compacted soil horizon, covers the surface. Pain (1971) documented the occurrence of debris-flow phenomena in an overgrazed area in New Zealand and postulated that compaction of the soil by cattle was an important factor in the formation of these failures at the site he studied. A dense root mat of grass or similar vegetation might also act as a confining upper horizon to inhibit the flow of water from regolith to the surface. Observations by Cumberland (1944) and Stewart (1952, p. 75-78) support this hypothesis. Such a mat might also delay failure and thus allow additional water to enter the slide mass, either (1) allowing more material to liquefy (causing a larger failure) or (2) making the slurry more fluid (see section entitled "Mobilization," chap. 6). A slight change in water content can strongly affect the properties of slurries formed from cohesionless regolith (Johnson and Hampton, 1969).

Thus, vegetation appears to be a significant factor, at least locally. However, vegetation mapping does not consistently provide additional information valuable for preparing debris-flow-susceptibility maps, except, possibly, in areas which have been converted from one type of vegetative cover to another.<sup>3</sup>

<sup>3</sup>Vegetation can be useful in documenting past events. For example, after the January 3-5, 1982, storm, investigations in Mount Tamalpais State Park revealed several debris-flow deposits (presumed to be the products of 1956 or earlier events) at the mouths of several low-order drainages. In each place, these deposits were covered with Russian thistle (*Salsola kali* var. *tenuifolia*), which is easily detected on the California Department of Parks and Recreation's color aerial photographs taken in 1978.

#### BEDROCK MATERIALS

Debris flows have commonly been reported in areas underlain by granitic rocks and various types of sandstone. Although some workers (for example, Bogucki, 1977; Crozier and others, 1980; Govi and Sorzana, 1980) concluded that bedrock type is not a significant factor controlling the location of debris flows, I disagree.

Regolith is derived from bedrock, and bedrock characteristics are major factors contributing to the properties of the regolith. However, because cohesionless regolith develops over or downslope from many kinds of bedrock (for example, sandstone, granite, and chert), debris flows can occur over many types of rock. In areas where most of the bedrock yields cohesionless regolith, such as the hillside areas selected for my pilot mapping

project, debris flows may appear to occur independently of bedrock type. A more regional analysis, however, indicates that some types of bedrock, such as the smectite-rich melange matrix of the Franciscan assemblage, yield regolith that typically fails as slower moving translational or rotational slides. Debris flows rarely originate in such terrane, except where isolated blocks of sandstone, greenstone, or other types of bedrock that commonly yield cohesionless regolith exist (Rice and others, 1976; Ellen and others, 1982; see chap. 7).

In unusual cases, the regolith may have characteristics that particularly favor the formation of debris flows. For example, Bucher (1980) identified a pumice gravel that appeared to be particularly susceptible to debris-flow failure because the density of the pumice was so low that



FIGURE 10.3.—Landslides in area of upper part of old road across the Serra das Araras escarpment, Brazil (from Jones, 1973, fig. 20). Analysis of such photographs of areas affected by larger, catastrophic storms suggests that ridgetops and spurs are less susceptible to debris-flow failure than are swales and sideslopes.

it floated in water. He found that most slope failures that did not involve pumice occurred only where an impervious layer permitted the piezometric head to rise above ground level. In contrast, where sufficient pumice was present, debris flows occurred on slopes as gentle as  $7^\circ$  at times when the piezometric head was well below the ground level.

#### THE METHOD

This method of delineating areas susceptible to debris flows consists of two separate but related parts. First, the predictive factors that are relevant and mappable for a given study area must be determined. Second, these factors must be mapped.



FIGURE 10.4.—Debris flow in Fazenda Creek valley, Brazil (from Jones, 1973, fig. 23). Although ridgetops remain intact most of the time, these “stable” areas may be extremely narrow and occasionally fail.

To illustrate the process of creating a debris-flow-susceptibility map, I made such an analysis in 1976–77 for a 9.8-km<sup>2</sup> area near Pacifica, Calif. (pl. 13A; Smith, 1977). This area was selected because several generations of aerial photographs were available covering the area and debris-flow scars were clearly discernible on these photographs. The boundary of the study area was drawn so that a legible 35-mm Kodachrome slide (for a 1977 lecture) could be obtained.

As summarized above, several factors may influence or control the origin of debris flows. Rather than mapping all the factors that might influence the origin of such failures—a rather time-consuming task—a brief review of the project area should first be made. Ideally, this review should use aerial photographs of varying ages, field reconnaissance, and, where appropriate, sample collection and testing. During this initial review, the locations of debris-flow scars and tracks should be noted, along with information concerning bedrock type and (or) soil type, vegetation, and slope inclination.

Review of the aerial photographs suggests that debris flows have originated over almost all the various bedrock units in my study area (principally granodiorite and Franciscan sandstone, shale, and greenstone). Soil maps of the study area, however, were unavailable. In areas where only some of the regolith or geologic units are subject to debris-flow formation, the susceptibility maps have to reflect such a condition (for an example, see Smith, 1985). Vegetation maps were also unavailable, although no relations between vegetation and debris-flow sites were readily apparent (furthermore, the services of a botanist were not readily available). Thus, the study area selected here appears to represent a relatively simple case in which, given the propensity for debris flows to occur in hollows and along first-order drainages and not to involve ridgetops, areas susceptible to debris-flow failure may be delineated by using morphologic factors alone. Although morphologic maps can be quite complex (for example, Klimaszewski, 1963; Starkel, 1965), matters can be simplified by limiting the effort to identifying only those morphologic features significant to the formation of debris flows. This simplified morphologic analysis can be accomplished with varying levels of accuracy by using topographic maps and stereoscopically paired aerial photographs.

Plate 13A presents the 1977 version, with a minor correction along one margin. The units delineated are: (1) ridgetops, ridge noses, and lowland areas with slopes of less than about 20°, the areas least susceptible to debris-flow formation; (2) ridgetops and ridge noses steeper than approximately 20°; and (3) sideslopes and hollows, the areas hypothesized at that time as most susceptible to debris-flow formation. The slope classifications (nose, hollow, and sideslope) are defined in figure 10.2.

The method used to prepare the 1977 version addressed only the sites of origin of future debris flows. However, the major hazard posed by debris flows is from impact and inundation. Detailed maps showing inundation areas have to date been based only on eyewitness accounts or written records of past events (for example, Mears, 1977) and cannot yet be reliably developed by other means. However, just as water flows downhill, debris flows also flow downhill and commonly down drainages. As illustrated in figure 10.5, the probability that a given site will be overrun by a debris flow can generally be deduced from its spatial relation to potential source areas. Such a deduction may not be valid everywhere because the distance a debris flow travels depends on the velocity and volume it attains (Johnson and Hampton, 1969; Smith and Hart, 1982).

In spite of our inability to predict the precise areas that will be inundated by debris flows, the areas of greatest hazard can be delineated in a general way simply by delineating drainage channels. If this method were to be

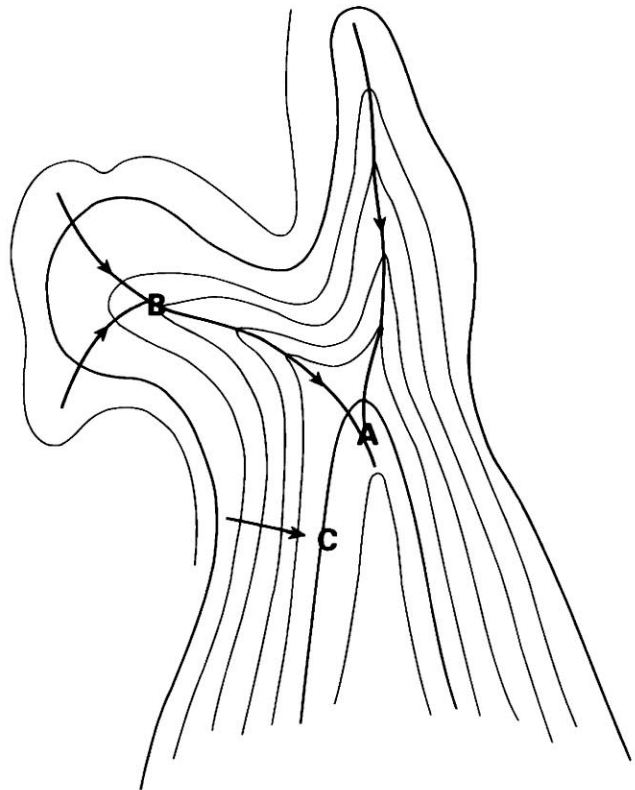


FIGURE 10.5.—Schematic map showing hypothetical routes of debris flows originating from various parts of a hillslope. A structure located at point A could be affected by more debris flows than one at point B; a structure located at point B could, in turn, be overrun by more debris flows than one at point C. Arrows show hypothetical debris-flow tracks; lines are contours.



used for preparation of the hazard maps required by the National Flood Insurance Program, streams that are susceptible to inundation by debris flows in their upper reaches would probably be declared susceptible to debris flooding in their lower reaches. Arguments about whether a given site may be inundated by a debris flow or by debris flooding may be moot in many areas; the site is likely to be inundated by some form of flowing-debris phenomenon. In any case, it is prudent to assume that at some future time, a debris flow may inundate any and all areas inundated by debris flows in the past.

By delineating drainage channels, the hollows, which are expected to be the sources of about 60 percent of debris flows, are indirectly identified at the upper ends of the drainage channels. Most of the remaining 40 percent of debris flows will originate on the sideslopes and quickly flow into and down the drainages.

### TEST OF THE METHOD

As part of my earlier study, I compiled the locations of debris-flow scars and tracks from aerial photographs taken in 1941, 1969, and 1970. Plate 13B shows the relations between the locations of pre-1970 scars and the morphologic zones delineated on the 1977 version. Note the large number of scars on sideslopes and swales (slope category 3) and along the boundary between slope category 3 and the adjacent slope categories.

The January 3-5, 1982, storm provided a further check on this method (pls. 13C, 13D; table 10.1). Note that: (1) none of the 1982 debris flows initiated at the scars previously identified (see section entitled "Scars and Individual Habitats of Previous Soil Slips," chap. 7), (2) not all the drainages affected by earlier storms produced debris flows in January 1982, and (3) about two-thirds of the debris flows originated in hollows or along other parts of the drainages (see section entitled "Local Topographic Setting," chap. 7). The fact that, in graded areas, a greater proportion of debris flows appeared to originate on or near former drainages (subsequently obliterated by human activity) suggests that grading had not significantly reduced the debris-flow susceptibility of these sites. This observation probably reflects the fact that the regolith was thicker on the finished slope in areas beneath former drainages or that more water flowed through the regolith in such areas, or both.

To determine whether the susceptibility zones delineated on the original predictive map are significant, I counted the number of pre-1982 and 1982 events originating in each zone. I estimated the areal extent of each zone by placing a 10-to-the-inch grid over the susceptibility map and counting the number of cells in which the

TABLE 10.1.—Summary of the number of 1982 debris flows in relation to the 1977 debris-flow-susceptibility map

[Number in parentheses indicates percentage of total number of events. Slope categories: 1, area of low susceptibility to debris-flow failure; morphology does not favor the formation of debris flows, and slope is normally insufficient for debris flows to occur; 2, area of intermediate susceptibility to debris-flow failure; morphology favors the formation of debris flows, or slopes are sufficiently steep (more than approx 20°) for debris flows to originate; 3, area of high susceptibility to debris-flow failure; both the morphology and the inclination of a slope favor the formation of debris flows; 1-2, 1-3, and 2-3, areas of intervening slope category. Note that about two-thirds of all debris flows originated on drainage channels (including hollows as parts of drainage channels)]

Slope category	1	1-2	2	1-3	2-3	3	All
<b>Slopes</b>							
<b>Graded:</b>							
On drainage	0(0)	0(0)	0(0)	1(1)	0(0)	3(4)	4(5)
Off drainage	0(0)	0(0)	0(0)	0(0)	0(0)	2(2)	2(2)
<b>Natural:</b>							
On drainage	0(0)	0(0)	0(0)	5(6)	9(11)	42(49)	56(66)
Off drainage	1(1)	0(0)	1(1)	1(1)	12(14)	8(9)	23(27)
<b>All:</b>							
On drainage	0(0)	0(0)	0(0)	6(7)	9(11)	45(53)	60(71)
Off drainage	0(0)	0(0)	1(1)	1(1)	12(14)	10(12)	25(29)
<b>Total</b>	<b>1(1)</b>	<b>0(0)</b>	<b>1(1)</b>	<b>7(8)</b>	<b>21(25)</b>	<b>55(65)</b>	<b>85(100)</b>

various zones dominated. Zone 1 includes two geomorphically distinct settings—wide valley bottoms and broad ridgetops. Because the valley bottoms could not conceivably produce debris flows, it appears appropriate to eliminate the 1,781 cells in valley bottoms from the analysis. Furthermore, because the boundaries of the zones may be thought of as delimiting the edge of the less stable categories, I included events plotting on the zone boundaries as originating within the less stable (more susceptible) zones. The resulting data are listed in table 10.2. These data reveal that about 97 percent of the events originated within zone 3, which constitutes about 70 percent of the upland slopes—a relation suggesting that the method is reasonably valid.

### SUMMARY

Although it appears to be beyond our current abilities to pinpoint precisely which sites are likely to fail next as debris flows, maps showing general areas susceptible to debris-flow failure can rather quickly and easily be developed for at least some areas. The method summarized herein is one way by which potential source areas and areas that may potentially be inundated by debris flows might be delineated. As noted above, this method should, ideally, be tailored to suit the areas studied by initially identifying those factors that significantly affect the formation of debris flows in any given area. Once identified, these factors can then be considered in preparing debris-flow-susceptibility maps.

TABLE 10.2.—*Comparison of the areal extent of susceptibility zones within the hillside area with the number of events originating within each zone*

[The 1,781 cells within valley bottoms are omitted from comparison. Events that originated on zone boundaries are included in the totals for less stable (more susceptible) zones. Numbers in parentheses are percentages of totals]

Zone-----	1	2	3	Total
Number of cells-----	1,131(13.76)	1,425(17.34)	5,663(68.90)	8,219(100.00)
Number of 1982 events---	1(1.18)	1(1.18)	83(97.65)	85(100.00)
Number of pre-1982 events.	2(0.63)	8(2.50)	310(96.88)	320(100.01)
Total number of events.	3(0.74)	9(2.22)	393(97.04)	405(100.00)

It appears that the volume of future debris flows depends considerably on site-specific factors which may defy analysis, at least given our present understanding. I have not incorporated size factors into the method outlined here, and so the maps (pl. 13) may not accurately portray the total runoff of future debris-flow phenomena. Such estimates may be desirable for site-specific design and hazard assessments.

I have not attempted to indicate when in the future such events will occur. Also, on the basis of the aerial photographs analyzed during the course of this study and other information summarized herein, I believe that the site-specific recurrence interval may be shorter for smaller than for larger debris flows, although further work is necessary to confirm this hypothesis.

## REFERENCES CITED

- Bailey, R.G., and Rice, R.M., 1969, Soil slippage: An indicator of slope instability on chaparral watersheds of southern California: *Professional Geographer*, v. 21, no. 3, p. 173-177.
- Bevin, Keith, Lawson, Andrew, and McDonald, Adrian, 1978, A landslide/debris flow in Bilsdale, North York Moors, September 1976: *Earth Surface Processes*, v. 3, no. 3, p. 407-419.
- Bogucki, D.J., 1970, Debris slides and related flood damage associated with the September 1, 1951, cloudburst in the Mt. LeConte-Sugarland Mountain area, Great Smokey Mountains National Park: Knoxville, University of Tennessee, Ph.D. thesis, 165 p.
- , 1977, Debris slide hazards in the Adirondack province of New York State: *Environmental Geology*, v. 1, no. 6, p. 317-328.
- Bonilla, M.G., 1960, Landslides in the San Francisco South quadrangle, California: U.S. Geological Survey open-file report, 44 p.
- Bucher, F., 1980, Landslides caused by liquefaction of pumice gravel in Tukuyu District, Tanzania: Soil Mechanics and Foundation Engineering Regional Conference for Africa, 7th, Accra, Ghana, 1980, Proceedings, p. 441-448.
- Clark, G.M., 1973, Appalachian debris slide-debris flow characteristics and distribution south of the glacial border: Actualization of knowledge in mapping high risk sites [abs.]: Geological Society of America Abstracts with Programs, v. 5, no. 5, p. 386-387.
- Corbett, E.S., and Rice, R.M., 1966, Soil slippage increased by brush conversion: U.S. Department of Agriculture, Forest Service, Pacific Southwest Forest and Range Experiment Station Note PSW-128, 8 p.
- Crozier, M.J., Eyles, R.J., Marx, S.L., McConchie, J.A., and Owen, R.C., 1980, Distribution of landslips in the Wairarapa hill country: New Zealand Journal of Geology and Geophysics, v. 23, no. 5-6, p. 575-586.
- Cumberland, K.B., 1944, Contrasting regional morphology of soil erosion in New Zealand: *Geographical Review*, v. 34, p. 77-95.
- Dunne, Thomas, and Black, R.D., 1970, Partial area contributions to storm runoff in a small New England watershed: *Water Resources Research*, v. 6, no. 5, p. 1269-1311.
- Ellen, S.D., Peterson, D.M., and Reid, G.O., 1982, Map showing areas susceptible to different hazards from shallow landsliding, Marin County and adjacent parts of Sonoma County, California: U.S. Geological Survey Miscellaneous Field Studies Map MF-1406, 8 p., scale 1:62,500.
- Eyles, R.J., Crozier, M.J., and Wheeler, R.H., 1978, Landslips in Wellington City: *New Zealand Geographer*, v. 34, no. 2, p. 58-74.
- Govi, Mario, and Sorzana, P.F., 1980, Landslide susceptibility as a function of critical rainfall in Piedmont basins (North-Western Italy): *Studia Geomorphologica Carpatho-Balcanica*, v. 14, p. 43-61.
- Gray, D.H., and Leiser, A.T., 1982, Biotechnical slope protection and erosion control: New York, Van Nostrand-Reinhold, 271 p.
- Gray, D.H., and Megahan, W.F., 1980, Forest vegetation removal and slope stability in the Idaho Batholith: U.S. Department of Agriculture, Forest Service, Intermountain Forest and Range Experiment Station Research Paper INT-271, 23 p.
- Hack, J.T., and Goodlett, J.C., 1960, Geomorphology and forest ecology of a mountain region in the central Appalachians: U.S. Geological Survey Professional Paper 347, 66 p.
- Hollingsworth, Robert, and Kovacs, G.S., 1981, Soil slumps and debris flows: Prediction and protection: *Association of Engineering Geologists Bulletin*, v. 18, no. 1, p. 17-28.
- Holmes, J.S., 1917, Some notes on the occurrence of landslides: *Elisha Mitchell Science Society Journal*, v. 33, no. 3, p. 100-105.
- Johnson, A.M., and Hampton, M.A., 1969, Subaerial and subaqueous flow of slurries, with shorter contributions by Fred Molz, T.A. Ogawa, and Richard Weiss: Stanford, Calif., Stanford University, School of Earth Science, 137 p.
- Jones, F.O., 1973, Landslides of Rio de Janeiro and the Serra das Araras escarpment, Brazil: U.S. Geological Survey Professional Paper 697, 42 p.

- Klimaszewski, Mieczysław, 1963, Landform list and signs used in the detailed geomorphological map, annex to Problems of geomorphological mapping: Polska Akademia Nauk, Prace Geograficzne (Polish Academy of Sciences, Institute of Geography Geographical Studies), no. 46, p. 139-179.
- Lawson, A.C., chairman, 1908, The California earthquake of April 18, 1906, Report of the State Earthquake Investigation Commission: Carnegie Institution of Washington Publication 87, 2 v.
- McConchie, J.A., 1980, Implication of landslide activity for urban drainage: Journal of Hydrology (New Zealand), v. 19, no. 1, p. 27-34.
- Mears, A.I., 1977, Debris-flows hazard analysis and mitigation, an example from Glenwood Springs, Colorado: Colorado Geological Survey Information Series 8, 45 p.
- Pain, C.F., 1971, Rapid mass movement under forest and grass in the Honua Ranges, New Zealand: Australian Geographical Studies, v. 9, no. 1, p. 77-84.
- , 1972, Characteristics and geomorphic effects of earthquake-initiated landslides in the Adelbert Range, Papua, New Guinea: Engineering Geology, v. 6, no. 4, p. 261-274.
- Pierson, T.C., 1980, Piezometric response to rainstorms in forested hillslope drainage depressions: Journal of Hydrology (New Zealand), v. 19, no. 1, p. 1-10.
- Radbruch, D.H., and Weiler, L.M., 1963, Preliminary report on landslides in a part of the Orinda Formation, Contra Costa County, California: U.S. Geological Survey open-file report, 49 p.
- Rapp, Anders, and Stromquist, Lennart, 1979, Field experiments on mass movements in the Scandinavian Mountains with special reference to Karkebagge, Swedish Lapland: Studia Geomorphologica Carpatho-Balcanica, v. 13, p. 23-38.
- Rice, S.J., Smith, T.C., and Strand, R.G., 1976, Geology for planning, central and southeastern Marin County, California: California Division of Mines and Geology Open-File Report 76-2SF, 103 p.
- Rodine, J.D., 1975, Analysis of the mobilization of debris flows: Stanford, Calif., Stanford University, Ph.D. thesis, 226 p.
- Schneider, R.H., 1973, Debris slides and related flood damage resulting from hurricane Camille, 19-20 August, and subsequent storm, 5-6 September, 1969, in the Spring Creek drainage basin, Greenbrier County, West Virginia: Knoxville, University of Tennessee, Ph.D. thesis, 131 p.
- Scott, G.A.J., 1975, Relationships between vegetation cover and soil avalanching in Hawaii: Association of American Geographers Proceedings, v. 7, p. 208-212.
- Smith, T.C., 1977, The debris avalanche: A commonly overlooked geologic hazard: Geological Society of America Abstracts with Programs, v. 9, no. 4, p. 502.
- Smith, T.C., 1985, Landslide hazards in the southeastern part of the Petaluma Dairy Belt, Sonoma County, California: California Division of Mines and Geology Open-File Report 86-5SF, scale 1:24,000, 4 sheets.
- Smith, T.C., and Hart, E.W., 1982, Landslides and related storm damage, January 1982, San Francisco Bay region, *with a contribution by J.E. Baldwin and R.J. Rodrigues*: California Geology, v. 35, no. 7, p. 139-152.
- Starkel, Leszek, 1965, [Geomorphological development of the Polish Eastern Carpathians (upon the example of the upper San Basin)] [in Polish]: Polska Akademia Nauk, Prace Geograficzne (Polish Academy of Sciences, Institute of Geography Geographical Studies), no. 50, 160 p.
- Stewart, J.E., 1952, Descriptive details of the storm and floods, in Eisenlohr, W.S., Jr., Floods of July 18, 1942, in north-central Pennsylvania: U.S. Geological Survey Water-Supply Paper 1134-B, p. 66-78.
- Stromberg, P.A., 1967, Landslide problems related to housing development in central California: San Francisco, Calif., San Francisco State University, M.A. thesis, 137 p.
- Swanston, D.N., 1969, Mass wasting in coastal Alaska: U.S. Department of Agriculture, Forest Service, Pacific Northwest Forest and Range Experiment Station Research Paper PNW-83, 15 p.
- Swanston, D.N., and Swanson, F.J., 1976, Timber harvesting, mass erosion and steepland forest geomorphology in the Pacific Northwest, in Coates, D.R., ed., Geomorphology and engineering: Stroudsburg, Pa., Dowden, Hutchinson & Ross, p. 199-221.
- Thomas, E.S., 1939, Landslide forms and their origin in the middle Coast Ranges: Berkeley, University of California, M.A. thesis, 65 p.
- Varnes, D.J., 1978, Slope movement types and processes, chap. 2 of Schuster, R.L., and Krizek, R.J., eds., Landslides: Analysis and control: U.S. National Academy of Sciences, National Research Council, Transportation Research Board Special Report 176, p. 11-33.
- Ziemer, R.R., 1981, Management of steeppland erosion: An overview: Journal of Hydrology (New Zealand), v. 20, no. 1, p. 8-16.

## 11. LANDSLIDE DAMAGE: A COSTLY OUTCOME OF THE STORM

By CAROL LAVOPA CREASEY,<sup>1</sup>  
U.S. GEOLOGICAL SURVEY

### CONTENTS

	Page
Abstract - - - - -	195
Introduction - - - - -	195
Procedure - - - - -	195
Acknowledgments - - - - -	196
Categories of damage costs - - - - -	197
Damage costs by county - - - - -	197
Alameda County - - - - -	197
Contra Costa County - - - - -	199
Marin County - - - - -	199
San Francisco County and city - - - - -	200
San Mateo County - - - - -	200
Santa Clara County - - - - -	200
Santa Cruz County - - - - -	201
Solano County - - - - -	201
Sonoma County - - - - -	201
Limitations - - - - -	202
Financial assistance - - - - -	202
Conclusion - - - - -	202
References cited - - - - -	203

### ABSTRACT

The January 3-5, 1982, storm triggered landslides that caused extensive damage in the San Francisco Bay region of California. Total direct costs of landslide damage from the storm in the counties of Alameda, Contra Costa, Marin, San Francisco, San Mateo, Santa Clara, Santa Cruz, Solano, and Sonoma exceeded \$66 million. Santa Cruz County suffered the most damage—40 percent of the total for the bay region. The economic losses resulting from landsliding are tabulated here according to damage to transportation, utilities, parks and open spaces, private property and other businesses, and miscellaneous. The category of private property and other businesses accounted for 56 percent of the total landslide-damage costs. Landslide damage was concentrated along roads and in the developed parts of hilly and mountainous areas of the San Francisco Bay region.

### INTRODUCTION

Extensive damage in the San Francisco Bay region occurred during the January 3-5, 1982, storm. Shortly after this storm, the Federal Emergency Management Agency (FEMA) estimated the total damage at \$300 million (U.S. Federal Emergency Management Agency, 1982). Although most of this damage was caused by

flooding, considerable damage also resulted from landslides. This study quantifies the damage caused by landslides during the storm and identifies the distribution of landslide damage throughout the San Francisco Bay region.

### PROCEDURE

In the winter and spring immediately following the January 3-5, 1982, storm, I compiled damage costs for the San Francisco Bay region counties of Alameda, Contra Costa, Marin, San Francisco, San Mateo, Santa Clara, Santa Cruz, Solano, and Sonoma. Unlike two previous U.S. Geological Survey landslide-cost studies (Taylor and Brabb, 1972; Taylor and others, 1975), Napa County was excluded and Santa Cruz County was included. Napa County was excluded because it had sustained relatively few landslides and because of time constraints; Santa Cruz County was included because of the extensive landslide damage that had occurred there.

Three basic criteria were used to qualify landslide damage for inclusion in this study. First, the damage had to have occurred during the January 3-5, 1982, storm; damage before or after this period was not considered.

Second, the damage had to have resulted from a landslide, defined by Varnes (1958, p. 20) as the " \* \* \* downward and outward movement of slope-forming materials composed of natural rock, soils, artificial fills, or combinations of these materials. The moving mass may proceed by any one of three principal types of movement: falling, sliding, or flowing, or by their combinations." The landslides that caused damage during the storm were mostly debris flows (see "Introduction" to this volume for landslide terminology) but included rock slides, slumps, and other landslide types. Damage from slipouts was considered as landslide damage (many agencies use the word "slipout" to denote a minor landslide or the downward movement of material below a roadway). Damage from washouts, creek and river erosion, sloughing, subsidence, and creep was not considered because the mechanism of damage is not a landslide as defined.

Third, economic loss was defined as the direct cost attributed to landsliding. The category of direct cost includes temporary and permanent repairs, replacement costs, and debris removal. Stabilization of landslides was counted as a direct cost if the stabilization was complete or underway at the time of this study.

<sup>1</sup>Current affiliation: Dames & Moore, San Francisco, CA 94105.



As a result of the widespread flooding and landsliding during the period December 19, 1981-January 8, 1982, President Reagan designated nine of the San Francisco Bay region counties as a declared major disaster area eligible for Federal assistance. Thus, disaster-assistance records were available from FEMA, the Small Business Administration (SBA), the Individual and Family Grant Program, and the Federal Highway Administration (FHA). These records provided most of the information for this study.

Other agencies believed to have sustained landslide damage or to have knowledge of landslide damage were also contacted. Such State agencies as the California Department of Transportation (Caltrans) and the California Department of Forestry, as well as county and municipal departments of public works, building inspection, planning, community development, parks and open spaces, and emergency services, in addition to various city offices, helped identify areas of landslide damage and the costs of such damage. Utilities, railroads, and communication agencies provided additional landslide-damage information.

An accurate assessment of private-property damage—that is, losses to private businesses or individuals—was difficult to obtain. Such information was commonly inaccessible because much of the damage was unreported; even when such damage was reported, the direct cost was in many cases unobtainable owing to the Privacy Act of 1974. The estimates of private-property damage made in this study were computed by adding the total landslide-damage costs reported by the Individual and Family Grant Program to a statistically estimated total of the damage reported in the SBA applications for each county. Care was taken to avoid any duplication of damage costs.

I have assumed the information on the costs and locations of landslide damage supplied by public and private agencies and individuals to be correct. Field checks to verify damage reports were not feasible in most cases because of time restrictions and the extent of area to be covered. Wherever possible, estimates were verified by secondary sources and reviewed for consistency with reports from the media, public agencies, or assistance organizations.

### ACKNOWLEDGMENTS

This investigation would not have been possible without the cooperation of the public and private agencies and individuals contacted. The following list acknowledges those who contributed; their help is greatly appreciated.

#### *Multicounty Sources:*

Federal Emergency Management Agency; U.S. Small

Business Administration; Individual and Family Grant Program; Pacific Gas and Electric Co.; Pacific Telephone; Atchison, Topeka & Santa Fe Railroad Co.; Southern Pacific Transportation Co.; Association of Engineering Geologists, Landslide Committee; U.S. Department of Agriculture, Soil Conservation Service; California Department of Forestry; California Department of Transportation; San Francisco Water Department; Citizens Utility Co. of California; California Water Service Co.; California Public Utilities Commission; U.S. Department of the Interior, National Park Service; Federal Highway Administration; California Division of Mines and Geology; Golden Gate National Recreation Area; California Parks and Recreation Department; U.S. Department of Agriculture, Stabilization and Conservation Service; U.S. Bureau of the Census; East Bay Regional Park District; East Bay Municipal Utility District.

#### *Alameda County:*

County Public Works Agency, County Flood Control & Water Conservation District, County Parks and Recreation, County Office of Emergency Services, County Engineering Geologist, County Resource Conservation District, Albany Public Works, Berkeley Public Works, Oakland Park System, Oakland Office of Public Works Agency, Piedmont Public Works, San Leandro Building Department.

#### *Contra Costa County:*

County Public Works, County Building Inspection Department, County Office of Emergency Services, Clayton Public Works, Concord Public Works Administration, El Cerrito Community Development Department, Hercules City Engineer, Martinez Public Works Department, Moraga City Engineer, Pinole Public Services, Pittsburg Public Services and Maintenance, Pleasant Hill City Engineer, San Pablo Public Works, Walnut Creek Community Development.

#### *Marin County:*

County Public Works, County Building Inspection Department, County Parks and Recreation Department, County Open Space District, County Office of Emergency Services, County Administration, Belvedere City Manager, Corte Madera Engineering and Public Works, Larkspur Public Works Department, Mill Valley Public Works Department, Novato Public Works, Ross Public Works, San Rafael Public Works, Sausalito Public Works, Tiburon Public Works, Point Reyes National Seashore.

#### *San Francisco County and City:*

Department of Public Works, Building Inspection Department, Recreation and Park Department, Assessor's Office.

*San Mateo County:*

County Public Works Department; County Building Inspection Department; County Civil Defense Operational Office; County Geologist; Atherton City Manager; Belmont Public Services Department; Brisbane Public Works; Burlingame Public Works Office; Colma Public Works; City Attorney of Daly City; Hillsborough City Manager; Menlo Park City Manager; Millbrae Public Works; Pacifica Department of Community Development and Services; San Bruno Public Works; San Carlos City Engineer; San Mateo Parks and Recreation Department; San Mateo Public Works Department; South San Francisco Department of Public Services; Woodside Town Manager; University of California, Berkeley, Cooperative Extension Program, Elkus 4-H Ranch.

*Santa Clara County:*

County Environmental Management & General Services Agency, County Building Department, County Parks and Recreation, County Office of Emergency Services, County Transportation Agency, County Geologist, Monte Sereno City Offices.

*Santa Cruz County:*

Much of the data for Santa Cruz County was collected by Mark Foxx (written commun., 1982); this information was supplemented by other multicounty sources.

*Solano County:*

County Public Works Department, County Planning Department, County Operations Manager, County Parks, County Office of Emergency Services, Benicia Public Works, Vallejo Public Works.

*Sonoma County:*

County Department of Public Works, County Community & Environmental Services, County Parks-Regional, County Office of Emergency Services-Civil Defense, Cloverdale Public Works, Healdsburg Public Works.

I also thank the many people at the U.S. Geological Survey who compiled an initial damage map after the storm. I especially thank Earl Brabb, Stephen Ellen, Catherine McMasters, Robert Mark, and Evelyn Newman for their contributions.

### CATEGORIES OF DAMAGE COSTS

I have quantified the landslide-damage costs according to land use or ownership. Costs were categorized as damage to either transportation, utilities, parks, private property and other businesses, or miscellaneous. "Transportation" includes railroads and State, county, and municipal roads. (Roads considered as Federal are actually

Federally funded State or local highways.) "Utilities" includes both private and public: private utilities are those that are investor owned, for example, the Pacific Gas and Electric Co. and Pacific Telephone; public utilities include water, power, sewage, and drainage services publicly owned and maintained by governmental agencies, such as the East Bay Municipal Utility District and the Central Contra Costa County Sanitary District. "Parks" includes damage to Federal, State, county, and municipal parks and open spaces. "Private property and other businesses" consists mostly of personal residences but includes private access roads, private businesses other than railroads and utilities, and other private real estate and personal property.

### DAMAGE COSTS BY COUNTY

Damage costs are listed by county in the following sections. All costs have been rounded to the nearest thousand dollars. Plate 14 and figure 11.1 show the distribution of landslide damage and landslide-damage costs, respectively, in the San Francisco bay region; and table 11.1 summarizes the costs for each county.

#### ALAMEDA COUNTY

Category	Cost
Transportation	
State roads - - - - -	\$ 90,000
County roads - - - - -	340,000
City roads - - - - -	688,000
Railroads - - - - -	20,000
Total - - - - -	\$1,138,000
Percent - - - - -	32.0
Utilities	
Private - - - - -	\$ 299,000
Public - - - - -	70,000
Total - - - - -	\$ 369,000
Percent - - - - -	10.4
Parks	
Regional - - - - -	\$ 67,000
City - - - - -	73,000
Total - - - - -	\$ 140,000
Percent - - - - -	3.9
Private property - - - - -	\$1,880,000
Percent - - - - -	52.8
Miscellaneous	
Other city damage - - - - -	\$ 33,000
Percent - - - - -	0.9
County total - - - - -	\$3,560,000

Damage in Alameda County was concentrated in Oakland, Piedmont, and Berkeley.

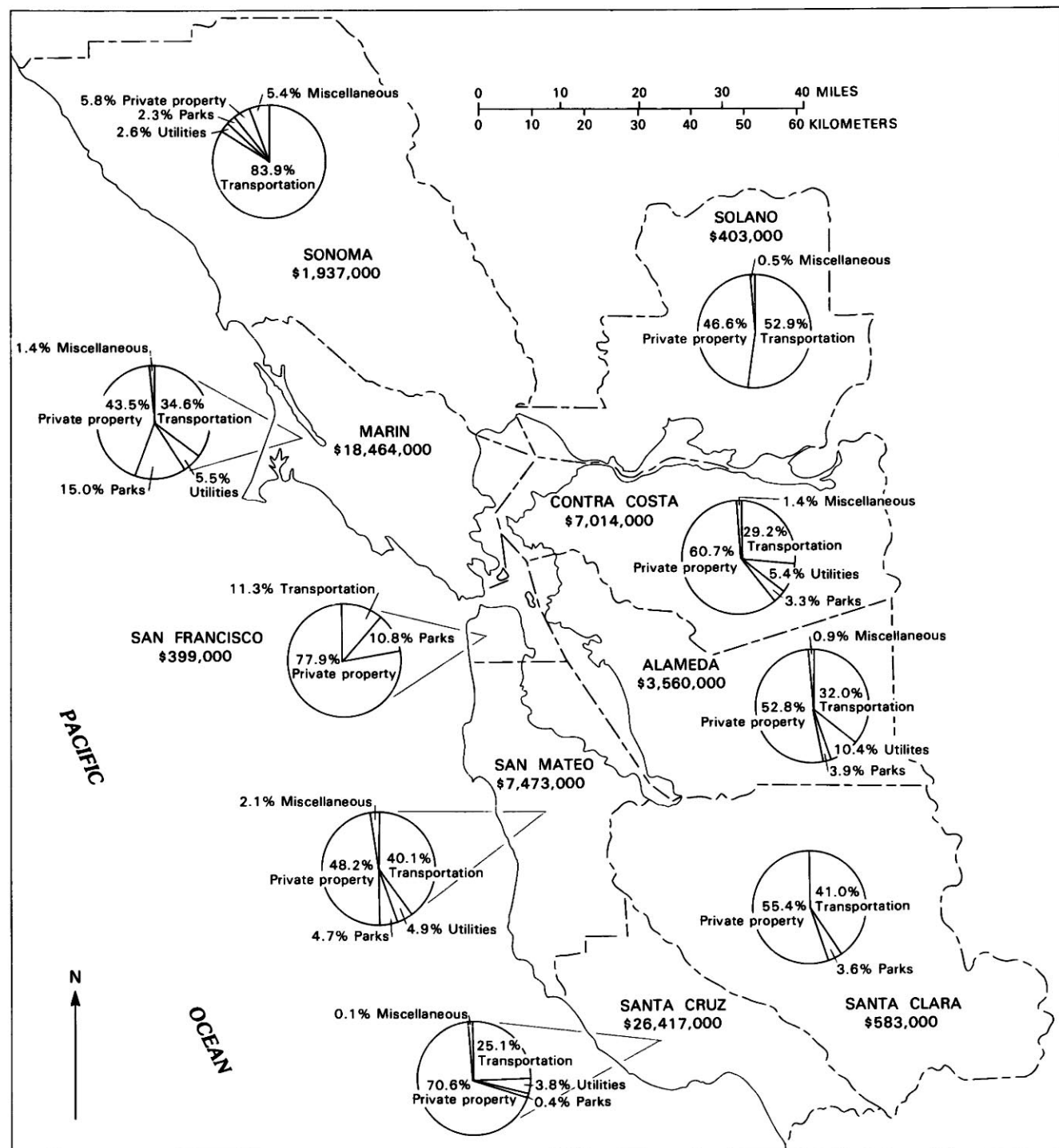


FIGURE 11.1.—San Francisco Bay region, showing landslide-damage costs from the January 3-5, 1982, storm for each county. Pie charts illustrate proportions of total costs for each category.

TABLE 11.1.—Summary of landslide-damage costs in the San Francisco Bay region from the January 3-5, 1982, storm, by county

[Population figures from U.S. Bureau of the Census, 1980]

County	Trans- portation	Utilities	Parks	Private property and other businesses	Miscellaneous	Total	Population	Per capita	Land area (km <sup>2</sup> )	Land area (mi <sup>2</sup> )	Per square kilometer	(Per square mile)
Alameda	\$ 1,138,000	\$ 369,000	\$ 140,000	\$ 1,880,000	\$ 33,000	\$ 3,560,000	1,105,379	\$ 3.22	1,898	(733)	\$1,875.66	(\$4,856.75)
Contra Costa	2,044,000	381,000	234,000	4,256,000	199,000	7,014,000	656,380	10.69	1,901	(734)	3,689.64	(9,555.86)
Marin	6,384,000	1,021,000	2,778,000	8,030,000	1,251,000	18,464,000	222,568	82.96	1,347	(520)	13,707.50	(35,507.69)
San Francisco	45,000	0	43,000	311,000	0	399,000	678,974	.59	126	(49)	3,166.67	(8,142.86)
San Mateo	2,999,000	364,000	355,000	3,600,000	2,344,000	7,473,000	587,329	12.72	1,176	(454)	6,354.59	(16,460.35)
Santa Clara	239,000	0	21,000	323,000	0	583,000	1,295,071	.45	3,372	(1,302)	172.89	(447.77)
Santa Cruz	6,636,000	1,016,000	98,000	18,652,000	215,000	26,417,000	188,141	140.41	1,137	(439)	23,233.95	(60,175.40)
Solano	213,000	0	0	188,000	42,000	403,000	235,203	1.71	2,142	(827)	188.14	(487.30)
Sonoma	1,624,000	51,000	45,000	112,000	2105,000	1,937,000	299,681	6.46	4,090	(1,579)	473.59	(1,226.73)
Total	\$21,322,000	\$3,202,000	\$3,714,000	\$37,352,000	\$ 660,000	\$66,250,000	5,268,726	\$ 12.57				

1 Fire Protection District.

2 California Department of Forestry.

3 University of California, Berkeley, Cooperative Extension Program.

4 Miscellaneous county and city expenses.

## CONTRA COSTA COUNTY

Category	Cost
Transportation	
State roads	\$ 127,000
County roads	678,000
City roads	303,000
Railroads	936,000
Total	\$2,044,000
Percent	29.2
Utilities	
Private	\$ 355,000
Public	26,000
Total	\$ 381,000
Percent	5.4
Parks	
State	\$ 54,000
Regional	132,000
City open space	48,000
Total	\$ 234,000
Percent	3.3
Private property	\$4,256,000
Percent	60.7
Miscellaneous	
Other city damage	\$ 85,000
Fire-protection district	14,000
Total	\$ 99,000
Percent	1.4
County total	\$7,014,000

Damage in Contra Costa County was concentrated in the areas of Richmond, El Sobrante, El Cerrito, Martinez, Orinda, Walnut Creek, and Lafayette. This county sustained the most railroad damage of all the counties studied; 13 percent of the total county damage occurred to two railroads. Total damage in Contra Costa County was almost as great as in San Mateo County. Surprisingly, during and after the storm, media coverage of the storm events in Contra Costa County was rather limited.

## MARIN COUNTY

Category	Cost
Transportation	
State roads	\$ 4,095,000
County roads	1,400,000
City roads	889,000
Total	\$ 6,384,000
Percent	34.6
Utilities	
Private	\$ 370,000
Public	651,000
Total	\$ 1,021,000
Percent	5.5
Parks	
Federal	\$ 2,635,000
State	49,000
County	90,000



City -----	4,000
Total -----	\$ 2,778,000
Percent -----	15.0
Private property -----	\$ 8,030,000
Percent -----	43.5
Miscellaneous -----	
Other county damage -----	\$ 199,000
Other city damage -----	50,000
Fire-protection district -----	2,000
Total -----	\$ 251,000
Percent -----	1.4
County total -----	\$18,464,000

Damage in Marin County (see section entitled "Case Studies," chap. 6) was concentrated in the southeastern part of the county between Sausalito and Fairfax. Other areas with high concentrations of damage were near Inverness, Novato, and Lagunitas. A total of 15 percent of the damage in the county occurred in parks and open spaces; 91 percent of the park damage occurred in Point Reyes National Seashore, where landslide damage to roads and trails was the major problem.

Although costs from unconducted business, unearned wages, and general inconvenience were not included in this study, Marin County experienced such losses to a greater degree than the other counties. For example, U.S. Highway 101, the major route connecting Marin County to San Francisco, was closed for 24 hours as a result of a landslide on the Waldo Grade. This closure isolated Marin County from the San Francisco peninsula and stranded thousands of Marin County residents in San Francisco.

#### SAN FRANCISCO COUNTY AND CITY

Category	Cost
Transportation	
County roads-----	\$ 45,000
Percent -----	11.3
Utilities -----	\$ 0
Percent -----	0
Parks	
Federal-----	\$ 24,000
County -----	19,000
Total -----	\$ 43,000
Percent -----	10.8
Private property -----	\$311,000
Percent -----	77.9
County total -----	\$399,000

Most landslides in San Francisco County were located in the center of the city in the Twin Peaks, Mount Davidson, and Glen Canyon Park areas. Most of the damage was to private dwellings.

#### SAN MATEO COUNTY

Category	Cost
Transportation	
State roads-----	\$1,278,000
County roads-----	890,000
City roads -----	831,000
Total -----	\$2,999,000
Percent-----	40.1
Utilities	
Private-----	\$ 64,000
Public -----	300,000
Total -----	\$ 364,000
Percent-----	4.9
Parks	
State -----	\$ 324,000
County -----	28,000
City -----	3,000
Total -----	\$ 355,000
Percent-----	4.7
Private property -----	\$3,600,000
Percent-----	48.2
Miscellaneous	
California Department of Forestry -----	\$ 51,000
University of California, Berkeley -----	35,000
Other city damage -----	69,000
Total -----	\$ 155,000
Percent-----	2.1
County total -----	\$7,473,000

The most extensive damage in San Mateo County occurred in Pacifica (see chap. 9), South San Francisco, Brisbane, Daly City, and west of Woodside. A total of 40 percent of the county's damage was to roads; the private sector sustained an estimated 48 percent of the total damage. In the area around Pescadero, many farms had landslide damage that remained unreported, and so it is omitted from the totals listed above. Damage to property of the University of California, Berkeley, occurred at the Elkus 4-H Ranch (see chap. 8).

#### SANTA CLARA COUNTY

Category	Cost
Transportation	
State roads-----	\$ 81,000
County roads-----	152,000
City roads -----	6,000
Total -----	\$239,000
Percent -----	41.0
Utilities -----	\$ 0
Percent -----	0
Parks	
County -----	\$ 21,000
Percent -----	3.6
Private property -----	\$323,000
Percent -----	55.4

County total ----- \$583,000

Damage in Santa Clara County was more scattered than in the other counties. Pockets of damage occurred near Morgan Hill, in Saratoga and Gilroy, and near the Anderson and Lexington Reservoirs.

#### SANTA CRUZ COUNTY

Category	Cost
Transportation	
State roads -----	\$ 865,000
County roads -----	5,709,000
City roads -----	17,000
Railroads -----	45,000
Total -----	\$ 6,636,000
Percent -----	25.1
Utilities	
Private -----	\$ 816,000
Public -----	200,000
Total -----	\$ 1,016,000
Percent -----	3.8
Parks	
State -----	\$ 98,000
Percent -----	0.4
Private property -----	\$18,652,000
Percent -----	70.6
Miscellaneous	
California Department of Forestry -----	\$ 15,000
Percent -----	0.1
County total -----	\$26,417,000

Damage in Santa Cruz County (see chap. 8) was more widely dispersed. Areas greatly damaged by landslides were Boulder Creek, Felton, Ben Lomond, Scotts Valley, Soquel, and Aptos. A total of 69 percent of the damage was to dwellings and private roads.

As previously mentioned, most of the damage costs for Santa Cruz County were compiled by Mark Foxx (written commun., 1982). I have modified his data to conform with the format of this chapter and combined them here with additional information that I collected. Foxx cited additional, unspecified private damage approximating \$7 million, a figure based on his estimate of the probable unreported private damage; this figure is omitted from this study because it could not be verified.

#### SOLANO COUNTY

Category	Cost
Transportation	
State roads -----	\$179,000
County roads -----	15,000
City roads -----	19,000
Total -----	\$213,000
Percent -----	52.9

Utilities -----	\$ 0
Percent -----	0
Parks -----	\$ 0
Percent -----	0
Private property -----	\$188,000
Percent -----	46.6
Miscellaneous	
Other city and county damage -----	\$ 2,000
Percent -----	0.5
County total -----	\$403,000

Damage in Solano County was reported near Vallejo and Vacaville.

#### SONOMA COUNTY

Category	Cost
Transportation	
State roads -----	\$ 941,000
County roads -----	531,000
City roads -----	2,000
Railroads -----	150,000
Total -----	\$1,624,000
Percent -----	83.9
Utilities	
Private -----	\$ 13,000
Public -----	38,000
Total -----	\$ 51,000
Percent -----	2.6
Parks	
State -----	\$ 45,000
Percent -----	2.3
Private property -----	\$ 112,000
Percent -----	5.8
Miscellaneous	
California Department of Forestry -----	\$ 105,000
Percent -----	5.4
County total -----	\$1,937,000

Landslide damage in Sonoma County was concentrated in the areas of Bodega, Bodega Bay, Salmon Creek, Occidental, and along the Russian River. Unlike the other counties in this study, private-property damage in Sonoma County accounted for only a small proportion of the total. Although significant damage to private farm and pasture land was reported, this information was not communicated to public agencies, and so it was omitted from this study.

Two previous studies of landslide damage in the San Francisco Bay area (Taylor and Brabb, 1972; Taylor and others, 1975) classified damage costs as public or private. For comparison with these earlier studies, the damage estimates in this study were also divided by county into public and private costs, as listed in table 11.2. Public-damage costs are defined as costs to Government agencies; conversely, private-damage costs are losses to the

non-Government sector, such as private property and private businesses. In table 11.2, public costs are divided into costs to Federal, State, county, and city governments and to municipal utilities. Damage to the Federal Government occurred in Federal parks. "Miscellaneous" includes damage to Government agencies, such as the special districts of regional parks and fire-protection districts. The reader should note that the present study is based on a different criterion from that used in these other two studies, and so adjustments must be made for any direct comparisons.

### LIMITATIONS

The estimated total economic loss of \$66 million from the January 3-5, 1982, storm in the San Francisco Bay region is a conservative figure. Agencies commonly combined flooding, erosion, wind, landslide, and other storm-related damage into one budgetary category. Unless the landslide damage could be separated from other damage or estimated accurately, its cost was omitted from this study.

Some landslide-damage information was unobtainable. Damage that was not reported until months after the storm could have been missed by this study. Some damage was not reported at all, especially if the damage was small or occurred on farm or pasture land.

Because this information was undertaken in the winter and spring following the storm, final costs for repair were not everywhere available. Estimates were obtained whenever possible, but the actual cost of the damage may vary from these estimates.

The costs of labor by public servants, such as policemen, firemen, the California Conservation Corps, and the National Guard, were omitted from this study. Records are rarely kept that distinguish the time spent directly for landslides. Nonprofit organizations, such as the American Red Cross and the Mennonites, contributed labor and supplies to landslide victims; their costs also were omitted.

Although landslides caused a loss of revenue to many businesses, these costs were omitted here. For example, a section of the Southern Pacific Railroad's main line between Point Costa and Martinez in Contra Costa County was closed. The Golden Gate Bridge Authority lost revenue owing to the closing of U.S. Highway 101 as a result of the Waldo Grade slide.

Other costs omitted here are the inconvenience of closed roads and the loss of production as workers took leave from work to rectify landslide damage. Depreciation of property and litigation costs also were excluded because they were indeterminate at the time of this study. This

study does not estimate the losses related to death or personal injury of landslide victims.

### FINANCIAL ASSISTANCE

Because the January 3-5, 1982, storm was declared a national disaster, the costs of landslide damage were not borne totally by the State, counties, municipalities, and local residents. Federal disaster assistance compensated part of the economic losses due to landslides. The counties of Alameda, Contra Costa, Marin, San Mateo, Santa Cruz, Solano, and Sonoma were declared eligible for Individual and Public Assistance; Santa Clara County was designated for Public Assistance; and San Francisco County was eligible for the SBA loan program. For landslide damage that qualified according to FEMA guidelines, public agencies received 75-percent funding. The FHA declared Alameda, Contra Costa, Marin, San Mateo, Santa Cruz, and Sonoma Counties available for Federal Emergency Relief funding; this declaration allowed certain roads to be repaired entirely with Federal funds.

Landslide damage to public agencies other than Federal agencies in Alameda, Contra Costa, Marin, San Mateo, Santa Clara, Solano, and Sonoma Counties has been estimated at \$16,197,000. Federal Government agencies, such as FEMA and FHA, funded an estimated \$13,043,000, or 81 percent, of that total.

Eligibility for Individual Assistance allowed private individuals and businesses to participate in 8- and 16-percent SBA loans and in Individual and Family Grants. These SBA loans enable individuals to finance repair and reconstruction at rates below the current bank lending rates.

Additional factors reduced the local economic impact of the storm. Losses to private utilities and railroads were borne by investors or transferred to consumers system-wide. Help to individuals was granted by the American Red Cross, the Mennonites, the Buck Foundation of Marin, and other nonprofit organizations. The National Guard and the California Conservation Corps also helped during and after the storm.

### CONCLUSION

On the basis of the data collected, landslide damage in the San Francisco Bay region from the January 3-5, 1982, storm is estimated to be at least \$66 million. The various counties suffered damage, in decreasing order, as follows: Santa Cruz, Marin, San Mateo, Contra Costa, Alameda, Sonoma, Santa Clara, Solano, and San Francisco. Santa Cruz County reported the greatest damage per capita and

TABLE 11.2.—Public and private landslide-damage costs in the San Francisco Bay region from the January 3–5, 1982, storm, by county

[Per capita costs calculated from U.S. Bureau of the Census population figures, 1980]

County	Public						Private	Total	Per capita
	Federal	State	County	City	Municipal utility	Miscellaneous			
Alameda-----	\$ 0	\$ 90,000	\$ 340,000	\$ 1,835,000	\$ 29,000	\$ 67,000	\$ 2,199,000	\$ 3,560,000	\$ 3.22
Contra Costa-----	0	181,000	678,000	1,243,000	25,000	146,000	5,547,000	7,014,000	10.69
Marin-----	2,635,000	4,144,000	1,689,000	2,953,000	641,000	2,000	8,400,000	18,464,000	82.96
San Francisco-----	24,000	0	64,000	0	0	0	311,000	399,000	.59
San Mateo-----	0	1,391,000	1,216,000	943,000	259,000	0	3,664,000	7,473,000	12.72
Santa Clara-----	0	81,000	173,000	6,000	0	0	323,000	583,000	.45
Santa Cruz-----	0	978,000	5,709,000	17,000	200,000	0	19,513,000	26,417,000	140.41
Solano-----	0	179,000	16,000	20,000	0	0	188,000	403,000	1.71
Sonoma-----	0	1,091,000	531,000	5,000	38,000	0	272,000	1,937,000	6.46
Total-----	\$2,659,000	\$8,135,000	\$10,416,000	\$3,216,000	\$1,192,000	\$215,000	\$40,417,000	\$66,250,000	\$ 12.57

<sup>1</sup>Regional parks.<sup>2</sup>Fire-protection districts.

per unit area of the nine counties studied. Contra Costa County sustained more landslide damage than has been popularly perceived.

Most of the reported landslide damage corresponds to the concentration of development and roads in hilly and mountainous areas of the nine counties (pl. 14). Although many landslides occurred in undeveloped areas, these landslides caused relatively minor economic loss and thus were not so critical to this study.

The greatest amount of landslide damage was to private residences. Damage to private property and other businesses accounted for 56 percent of the total landslide damage. Few businesses were directly affected by landslides, probably because businesses are generally located in flat areas. Those businesses that did sustain landslide damage were railroads, utilities, and farms located on steeper slopes.

## REFERENCES CITED

- Taylor, F.A., and Brabb, E.E., 1972, Map showing distribution and cost by counties of structurally damaging landslides in the San Francisco Bay region, California, winter of 1968–69: U.S. Geological Survey Miscellaneous Field Studies Map MF-327, scales 1:500,000, 1:1,000,000.
- Taylor, F.A., Nilsen, T.H., and Dean, R.M., 1975, Distribution and cost of landslides that have damaged manmade structures during the rainy season of 1972–1973 in the San Francisco Bay region, California: U.S. Geological Survey Miscellaneous Field Studies Map MF-679, scales 1:500,000, 1:1,000,000.
- U.S. Federal Emergency Management Agency, 1982, Interagency flood hazard mitigation report in response to the January 7, 1982, disaster declaration: Report FEMA-651-DR-CA, 43 p.
- Varnes, D.J., 1958, Landslide types and processes, chap. 3 of Eckel, E.B., ed., Landslides and engineering practice: Washington, U.S. National Research Council, Highway Research Board Special Report 29, p. 20–47.





## 12. IMPACT OF THE JANUARY 1982 FLOOD IN SANTA CRUZ COUNTY

By GARY B. GRIGGS,  
UNIVERSITY OF CALIFORNIA, SANTA CRUZ

### CONTENTS

	Page
Abstract - - - - -	205
Introduction - - - - -	205
Flooding in the Santa Cruz Mountains - - - - -	205
Flooding and flood damage on the San Lorenzo River - - -	207
Basin description and potential for flooding - - - - -	207
Magnitude of the 1982 flood - - - - -	207
Inundation and damage - - - - -	208
City of Santa Cruz - - - - -	208
Felton and vicinity - - - - -	210
Lockhart Gulch - - - - -	212
Flooding and flood damage on Soquel Creek - - - - -	212
Basin description - - - - -	212
Magnitude of the 1982 flood - - - - -	213
Inundation and damage - - - - -	214
Flooding and flood damage on Aptos Creek - - - - -	217
Basin description - - - - -	217
Magnitude of the 1982 flood - - - - -	218
Inundation and damage - - - - -	219
Lessons learned - - - - -	222
Utility of flood-plain maps - - - - -	222
Reliability of flood-plain maps - - - - -	223
Conclusions - - - - -	223
References cited - - - - -	223

### ABSTRACT

Santa Cruz County, along with most of the San Francisco Bay region, experienced prolonged and intense precipitation during January 3-5, 1982, and this precipitation resulted in heavy flood damage. The storm followed 2 months of abnormally high rainfall and produced 24-hour rainfall totals in excess of the 100-year event at many stations in the county. Flood levels along the upper San Lorenzo River, Soquel Creek, and Aptos Creek approached the largest flood on record. Log and debris jams at numerous bridge constrictions and culverts contributed significantly to flooding and flood damage in the heavily wooded basins. Development on flood plains and streambanks sustained heavy damage as floodwaters undercut their banks and inundated their flood plains. Continuing construction on flood plains necessitates accurate flood-plain mapping, especially for events with recurrence intervals of less than 100 years. Mapping of the areas flooded in 1982 can be used to revise and update existing flood-hazard maps, so that flood-prone areas can be more accurately delineated.

### INTRODUCTION

The central coast of California, particularly in Santa Cruz County, received prolonged and intense precipitation during January 3-5, 1982. Heavy rainfall lasted about 28 hours over most of the Santa Cruz Mountains; some localities received 25 mm/h (1 in/h) for more than 8 hours.

High-intensity precipitation was not confined to steep mountainous areas; at sea level, the city of Santa Cruz received 209 mm (8.23 in.) of rain in the 24 hours ending 7 p.m. P.s.t. January 4 (Santa Cruz *Sentinel*, Jan. 10, 1982). This total exceeded any other 24-hour measurement since record keeping began in 1891, and it also exceeded the 100-year 24-hour event (Rantz, 1971). Rainfall stations at higher elevations in the Santa Cruz Mountains received considerably more precipitation; most values exceeded that for the projected 100-year 24-hour storm (table 12.1). Storm rainfall, therefore, was extreme throughout the area (see chap. 2).

Antecedent rainfall had been high as well (see chap. 2). Some communities in the San Lorenzo River valley, such as Lompico, Ben Lomond, and Boulder Creek, had received 840 to more than 990 mm (33-39 in.) of rain during November and December (table 12.1). This 2-month rainfall has an average return period of 5 to 15 years (Rantz, 1971). Such high antecedent rainfall created conditions favorable for rapid runoff at the time the January 3-5, 1982, storm hit these steep basins.

### FLOODING IN THE SANTA CRUZ MOUNTAINS

Flood season in the Santa Cruz Mountains extends from November through April, although most historical flooding has taken place in either December or January. At least 11 major historical floods have been recorded in this area during the past 120 years. These floods have generally been of short duration, largely because of the steepness and small size of the drainage basins. Damaging flood stages generally last less than 18 to 36 hours; in contrast, during the 1973 floods on the lower Mississippi River, flood stages persisted for a record 77 days. Those same basins that generate short-duration floods also cause very rapid rises in river stage, and little warning is possible before overbank flooding.

Flood plains have been utilized and populated on a worldwide basis for centuries, and Santa Cruz County is no exception. Flat land, fertile soil, and the availability of water have all contributed to intense use of these areas. Downtown Santa Cruz and Soquel, and sections of Felton, Ben Lomond, Boulder Creek, Aptos, and Capitola, all lie on flood plains (fig. 12.1). Although generalized flood-plain maps exist for urbanized parts of the San Lorenzo River, Soquel Creek, and Aptos Creek (U.S. Army Corps of Engineers, 1973a, b, c), construction in these areas has

TABLE 12.1.—Rainfall data for the January 3-5, 1982, storm in the San Lorenzo Valley, Santa Cruz County, Calif.

[Storm rainfall is for 24-hour period ending 8 a.m. P.s.t. January 5 (Santa Cruz, Calif., *Sentinel*, Jan. 10, 1982). Recurrence intervals from Rantz (1971)]

Station	Mean annual precipitation (mm)	Nov.-Dec. 1980-81 rainfall (mm)	1981-82 prestorm period		January 1982 storm (24 hours)	
			Rainfall (mm)	Recurrence interval (years)	Rainfall (mm)	Recurrence interval (years)
Ben Lomond-----	1,168	179	847	6-7	292	>100
Boulder Creek----	1,473	207	1,009	5	324	>100
Lompico-----	1,118	221	968	15-20	394	>100

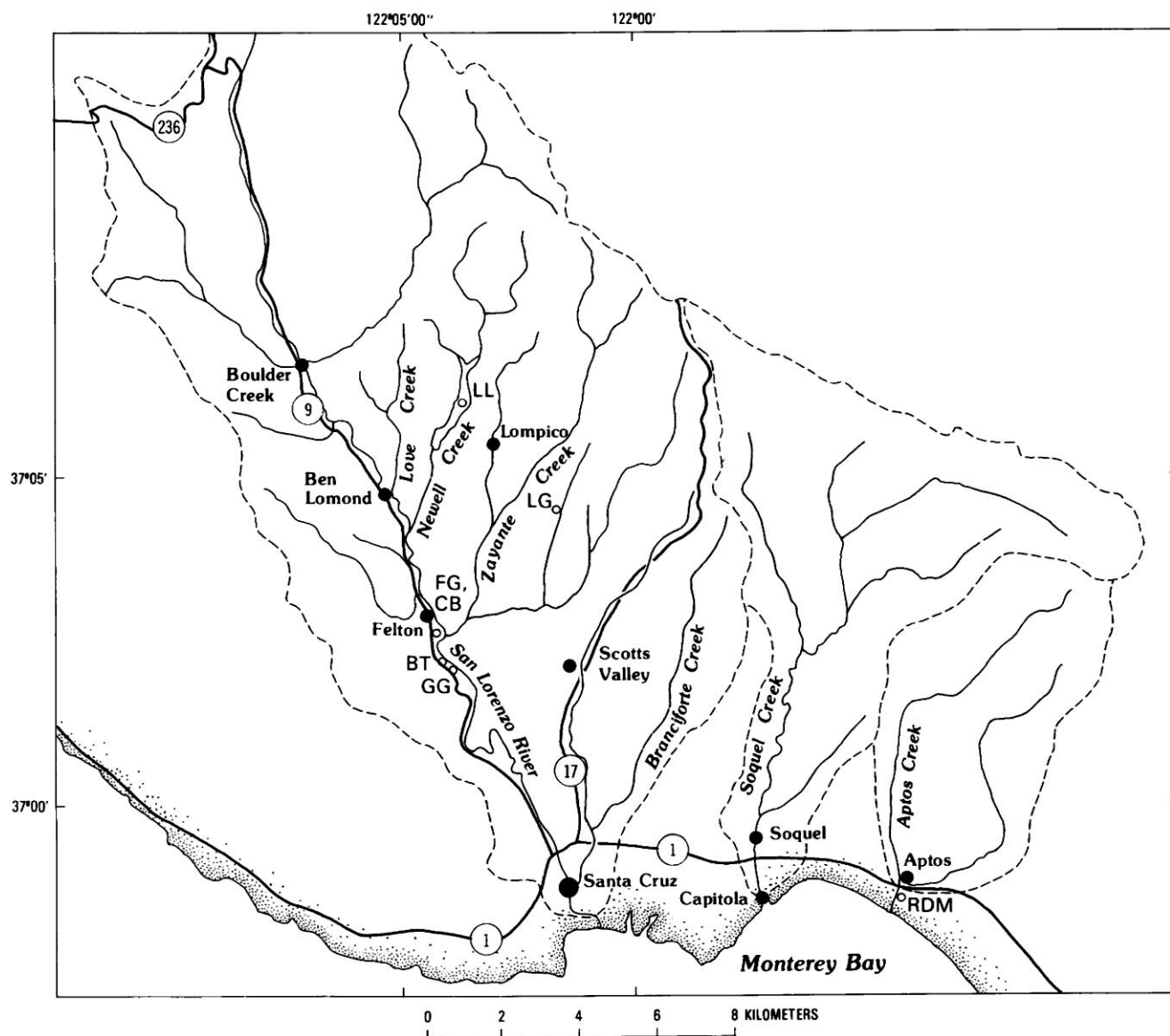


FIGURE 12.1.—Santa Cruz County, showing major areas affected by the January 1982 flood. BT, Big Trees gaging station; CB, Covered Bridge; FG, Felton Grove; GG, Gold Gulch; LG, Lockhart Gulch; LL, Loch Lomond; RDM, Rio Del Mar Flats. Dashed lines, watershed boundaries.

not been deterred. The last major flood to affect the area occurred in December 1955, when the San Lorenzo River topped its banks and inundated the downtown area of the city of Santa Cruz; 7 lives were lost, 2,830 persons were displaced from their homes, and damage amounted to \$8.7 million.

## FLOODING AND FLOOD DAMAGE ON THE SAN LORENZO RIVER

### BASIN DESCRIPTION AND POTENTIAL FOR FLOODING

The San Lorenzo River drains 357 km<sup>2</sup> of the central California Coast Ranges (fig. 12.1). Its steep, redwood-forested basin extends about 33 km in a northwesterly direction from the river mouth; the lower 5 km flows across a flood plain occupied by the city of Santa Cruz. Elevations range from sea level to 1,000 m, and annual precipitation in the basin averages 1,200 mm (47 in.). Stream gradients range from 0.0008 near the river mouth to 0.06 in the upper watershed.

The watershed, excluding the city of Santa Cruz, is home to 33,000 people. Owing to the prevalence of extremely steep hillsides, most of this population is concentrated near the river and its tributaries, where flooding has been common. Steep slopes, landsliding, and unstable soils, in combination with high-intensity precipitation, have led to severe erosion in parts of the basin. Logging, quarrying, and the removal of vegetation, grading, and impermeable surfaces that accompany development have increased both runoff and sediment production (Brown, 1973; Santa Cruz County Office of Watershed Management, 1976).

Logging and land clearing can contribute directly to flood problems in the basin. Organic-debris jams, formed where logs and other debris pile up at bridge constrictions, commonly result in stream impoundment and overbank flooding. Debris may also collect against culverts, which are designed to carry only water and are normally undersized for major floods.<sup>1</sup> Where a culvert is plugged, upstream or roadway flooding occurs, commonly followed by erosion and failure of fill or roadbeds. Flooding caused by obstruction of culverts and bridges by organic debris was a major factor in the damage from both the 1955 flood (U.S. Army Corps of Engineers, 1973b) and the 1982 flood. Logs and trees as much as 20 m long, carried down the San Lorenzo River during the January 1982 flood, lodged against the five major bridges that span the river within the city of Santa Cruz. Two cranes worked throughout the flood peak removing logs and thus prevented logjams downstream (fig. 12.2).

### MAGNITUDE OF THE 1982 FLOOD

The magnitude of the January 1982 flood was close to that of the last preceding disastrous flood, which occurred in December 1955 (see chap. 13). U.S. Geological Survey slope-area calculations near the Big Trees gaging station at Felton indicated a peak flow of 841 m<sup>3</sup>/s on January 4; the calculated 1955 peak flow was 861 m<sup>3</sup>/s (table 12.2).

Floodwater elevations at specific points can also be used for comparison. The San Lorenzo River above Felton is crossed by several bridges, which provide permanent datums (fig. 12.3). Flood levels from 1955 and the projected 100-year flood (also referred to as intermediate regional flood) were determined at each location by the U.S. Army Corps of Engineers (1973a, b, c). The maximum 1982 levels measured at many of these bridges are listed in table 12.3. Proceeding down the San Lorenzo River from Ben Lomond to Felton, a reversal occurs in the relation between 1982 and 1955 flood levels. Between Ben Lomond and Brackney south (a 4.5-km reach), 1955 flood peaks were 120 to 150 cm above 1982 levels. However, beginning at the San Lorenzo Way Bridge (0.7 km upstream from Felton) and proceeding through Felton to the Big Trees gaging station and bridge, 1982 levels were about 30 to 40 cm above 1955 levels. This downstream increase in the 1982 flood peak relative to the 1955 flood peak appears to result from more intense rainfall along the east flank of the middle reaches of the watershed in 1982, in contrast to the longer duration rainfall throughout the basin in 1955. The cumulative contribution of high discharges from east-side drainages, principally Love, Newell, and Zayante Creeks, during 1982 led to the higher downstream stages. At the Big Trees gaging-station bridge just south of Felton (figs. 12.1, 12.3), the 1982 event was actually 43 cm higher than the 1955 peak; 1,000 m upstream at the historic Covered Bridge (East San Lorenzo Way), the 1982 peak was 30 cm above the 1955 peak. Although no major organic-debris jams are known to have occurred at any of these upstream bridges during the 1982 flood, this may not have been the case in 1955 (U.S. Army Corps of Engineers, 1973b); river impoundment at these bridge constrictions in 1955 may have created anomalous elevations. The foundation for an inflatable diversion dam, constructed in 1976 just upstream from the gaging-station bridge, may have affected 1982 flood stages in the Felton area. No major logjams or backwater occurred in the Felton reach of the watershed in 1982. It is reasonable to conclude, therefore, that the 1982 peak discharge was slightly higher than the 1955 peak in this area, despite the differences in discharge calculations at the Big Trees gage (table 12.2).

According to WRC Log Pearson type III flood-frequency analyses performed by the U.S. Geological Survey (see chap. 13), the 1982 and 1955 flood peaks at

<sup>1</sup>Most culverts, if engineered at all, are sized only to carry runoff from 5- to 10-year events.



Big Trees in Felton represent approximately 33- and 36-year events, respectively (table 12.2). These discharges are 3.6 to 3.7 times the mean annual flood.

#### INUNDATION AND DAMAGE

##### CITY OF SANTA CRUZ

On January 4, 1982, overbank flooding occurred along much of the San Lorenzo River and its tributaries. Because of a major flood-control project within the city of Santa Cruz, that city was spared the heavy damage inflicted on the county's other riverside communities. The river rose to within about 1 m of the top of the levees in Santa Cruz (fig. 12.4), and it actually flowed onto parklands and a roadway at one point. Surface velocities, determined from the transit times of floating objects between bridges, reached as much as 4.2 m/s in the downtown reach and caused considerable scouring in the silted channel.

The flood-control channel along the lower San Lorenzo River in the city of Santa Cruz was constructed by the

U.S. Army Corps of Engineers in 1958 after the flood of 1955 (fig. 12.5). Levees were constructed for 4 km upstream from the mouth, and about 590,000 m<sup>3</sup> of sediment was excavated from the existing channel to increase the slope and capacity of the new channelled reach. The design channel bottom was lowered by as much as 2.1 m from the natural or original river bottom. The city agreed to maintain the channel to design specifications and was provided with a maintenance plan; annual maintenance costs, including sediment removal, were estimated at \$25,000. However, the sediment yield from the steep slopes of the watershed had not been considered in the channel design for below-bed flood containment, and the city did not initiate a sediment-removal program. During subsequent years, about 370,000 m<sup>3</sup> of sediment was deposited in the lower 5 km of the river channel, and this sediment significantly reduced the flood-control capacity (Griggs and Paris, 1982).

The high flows of January 3-4, 1982, scoured about 143,000 m<sup>3</sup> of sediment from the channel. The depth and volume of scour reached maximums in the last kilometer



FIGURE 12.2.—Crane working on the Riverside Avenue Bridge on the afternoon of January 4, 1982, removing logs and other debris from the San Lorenzo River in the city of Santa Cruz to prevent logjams from forming. See figure 12.5 for location. Photograph by Pete Amos and Bill Lovejoy, Santa Cruz, Calif., *Sentinel*.

TABLE 12.2.—Flood statistics for gaged streams in northern Santa Cruz County, Calif.

[Ratios are of peak flow to mean annual flood. Most discharges and recurrence intervals from table 13.3; other flood data from U.S. Geological Survey, Water Resources Division (Ken Lee and Bud Hoffard, written commun., 1982). Recurrence intervals were determined using WRC log Pearson type III flood-frequency analysis]

Stream and gaging station	Years of record (period)	Mean annual flood ( $m^3/s$ )	1955 flood peak			1982 flood peak		
			Discharge ( $m^3/s$ )	Recurrence interval (years)	Ratio	Discharge ( $m^3/s$ )	Recurrence interval (years)	Ratio
Zayante Creek at Zayante.	23 (1958-80)	41.71	( <sup>1</sup> )	( <sup>1</sup> )	( <sup>1</sup> )	104	7	2.5
San Lorenzo River at Big Trees.	46 (1937-82)	232.5	861	36	3.7	841	33	3.6
Branciforte Creek at Market Street.	19 (1941-43, 1953-68)	59.15	229	77	3.9	188	29	3.2
Soquel Creek at Bridge Street.	27 (1937, 1952-80)	89.74	447	62	5.0	275	14	3.1
Aptos Creek at Aptos.	22 (1959-80)	16.48	99	35	6.0	113	40	6.9

<sup>1</sup>No gaging station.

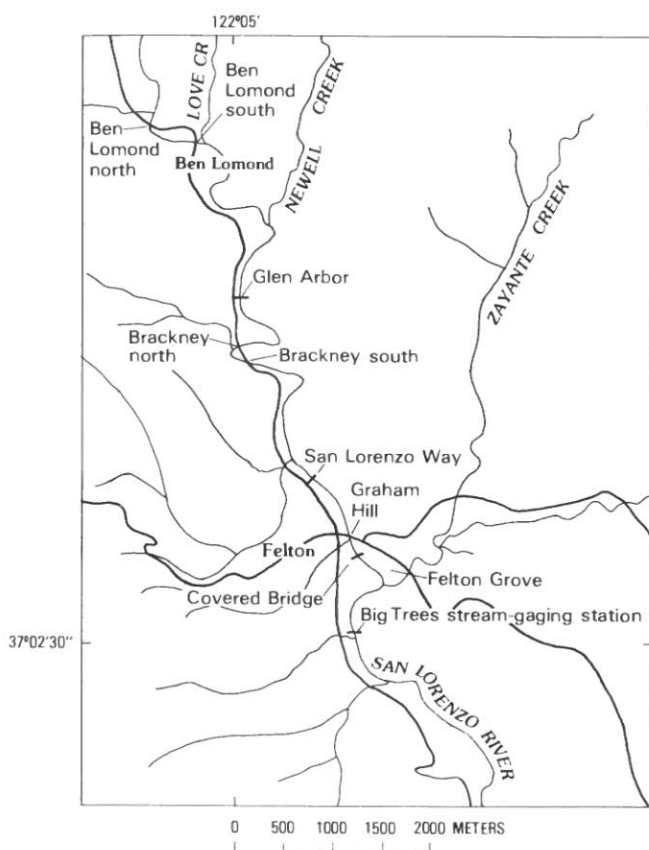


FIGURE 12.3.—San Lorenzo River area, showing locations of bridges where comparative levels for 1955 and 1982 floods have been measured. See table 12.3 for elevations.

TABLE 12.3.—Comparative floodwater elevations along the San Lorenzo River

[All elevations relative to mean sea level. 1955 and intermediate regional or 100-year flood levels from U.S. Army Corps of Engineers (1973b)]

Bridge location	1982 flood level (m)	1955 flood level (m)	Intermediate regional or 100-year-flood level (m)
Ben Lomond North (BR 36-49).	98.47	99.69	100.30
Ben Lomond South (BR 36-48).	95.41	96.94	98.47
Glen Arbor Bridge-----	88.99	<sup>1</sup> 92.05	91.42
Brackney North (BR 36-47).	87.46	<sup>1</sup> 91.74	89.76
San Lorenzo Way-----	84.40	83.49	84.71
Graham Hill Road-----	80.73	80.43	80.73
Felton Covered Bridge-----	80.12	79.82	80.43
Henry Cowell State Park (Big Trees gage).	78.10	77.68	79.20

<sup>1</sup>Error in U.S. Army Corps of Engineers data or elevated water level due to logjam.

of channel and decreased gradually upstream. Part of the Riverside Avenue Bridge (0.8 km from the mouth) was damaged by scour. This old bridge also forms the greatest constriction to floodwaters, owing to its low arches; the peak flow of January 4 was barely contained at this point (fig. 12.2).

Branciforte Creek enters the San Lorenzo River 1.8 km upstream from its mouth, at the point where the Soquel

Avenue Bridge crosses the river. The rectangular, concrete flood-control channel designed to convey Branciforte Creek through Santa Cruz to its confluence with the San Lorenzo River was filled to capacity by the storm (fig. 12.6).<sup>2</sup> The combined discharge from the San Lorenzo River and Branciforte Creek caused severe scouring that undermined an older pier of the Soquel Avenue Bridge. One span of the bridge collapsed (fig. 12.7), taking with it half of Santa Cruz' telephone circuits.

#### FELTON AND VICINITY

*Upstream from the city of Santa Cruz, no flood protection exists, and inundation of homes along the banks and flood plain of the river and its tributaries was widespread.*

<sup>2</sup>Although the Branciforte Creek flood-control channel was designed to carry 238 m<sup>3</sup>/s, its maximum capacity was reduced to about 200 m<sup>3</sup>/s owing to backwater effects of the San Lorenzo River. Thus, the Branciforte channel can contain only the 30-year flood, rather than the 100-year flood, during high water on the San Lorenzo River (K.W. Lee, written commun., 1982).

Between the city of Santa Cruz and Felton, individual developments adjacent to the river, including Paradise Park, Gold Gulch, and Felton Grove, were especially severely damaged.

Felton Grove provides an example of flood-plain development in the study area (figs. 12.3, 12.8). The group of more than 50 cabins and homes adjacent to the historic Covered Bridge is only 4 to 5 m vertically above the river bottom at this point, and most homes have been there for at least 25 years. The houses closest to the river have been inundated four times in the past 12 years (1969, 1973, 1978, 1982). Discharge data for the Big Trees station indicate that flows large enough to inundate part of Felton Grove have occurred 14 times in the past 46 years; this calculation is based on major flooding in 1978, during a peak discharge of 320 m<sup>3</sup>/s, and 14 annual floods in excess of this volume since 1937. During the 1955 floods, "Felton Grove, near Felton Road, was nearly wiped out. Five cabins were carried away, some 20 were destroyed,



FIGURE 12.4.—San Lorenzo River from the Water Street Bridge in the city of Santa Cruz at 1:00 p.m. P.s.t. January 4, 1982. River came within about 1.7 m of topping the levees here.

crushed by the rushing current" (Santa Cruz, Calif., *Sentinel*, December 25, 1955, p. 1).

Virtually all the houses in Felton Grove were inundated by the high water on January 4; this was the first area along the San Lorenzo River to be flooded and evacuated in the January 1982 storm. Water levels quickly reached 1 to 2 m in many homes (fig. 12.9), and a meter or more of sand was left behind. Most damage was due to the deposition of sediment in homes and automobiles. Residents who were evacuated have since dug out the mud, sand, and debris and reoccupied their homes. No major structural damage was received, and so no permits or permission was required to again take up residency in this flood-prone area.

In Gold Gulch, 1.8 km south of Felton, a group of about 25 homes was inundated and damaged along the southwest bank of the river. In 1955, 30 homes in Gold Gulch

were reported pushed off their foundations, and 3 were reported carried down the river (Santa Cruz, Calif., *Sentinel*, December 25, 1955, p. 1).

In the town of Felton itself, water entered some businesses and reached a depth of 0.3 m in the firehouse. This flooding resulted from overflow of a small tributary stream, Bull Creek, rather than the San Lorenzo River.

Between Felton and Ben Lomond, 60 to 70 homes and other structures built along the San Lorenzo River were flooded. One downtown business section of Ben Lomond (Mill Street) was inundated by 30 cm of water.

The effects of flooding in the San Lorenzo Valley were felt by the entire population of the city of Santa Cruz because overflow from the Loch Lomond Reservoir on Newell Creek broke the principal waterline to the city. A total of 70,000 users were ordered to ration water for about a week until repairs could be made.



FIGURE 12.5.—San Lorenzo River in the city of Santa Cruz, showing flood-control channel and bridge crossings. RA, Riverside Avenue Bridge; SA, Soquel Avenue Bridge; WS, Water Street Bridge.



## LOCKHART GULCH

A graphic example of flooding due to undersized culverts can be documented along Lockhart Gulch, a small watershed that parallels Zayante Creek northwest of the city of Scotts Valley. Many cabins and small homes have been built over the years along the narrow flood plain of this creek. In some places, the streamcourse has been severely confined between concrete retaining walls and capped with concrete driveways. This part of the San Lorenzo watershed received some of the heaviest rainfall in the January 1982 storm, and the flow of water and debris down Lockhart Gulch exceeded the capacities of the culverts and channel constrictions. Thus, the creek overtopped a culvert and flowed down Lockhart Gulch Road, across driveways, and through houses and garages. At least 20 homes in this area were reported destroyed or heavily damaged by flooding and mud.

Two homes had been built directly at the confluence of Lockhart Gulch with a small intermittent tributary that drains about 1 km<sup>2</sup>. This tributary had been placed underground in this area within a 1-m-square box culvert.

Flood flows on January 4 reached depths of over 2 m at this site and spanned the entire 15 m of the stream bottom (fig. 12.10). The culvert was simply bypassed as flow from the small tributary swept through one home and filled it with debris.

**FLOODING AND FLOOD DAMAGE  
ON SOQUEL CREEK****BASIN DESCRIPTION**

Soquel Creek drains a triangular basin, 18 km long and about 104 km<sup>2</sup> in area (fig. 12.1). Maximum elevations in this basin are more than 900 m. The upper reaches of the basin are steep and heavily forested, and the stream channel occupies a deep narrow canyon that can contain all expectable flood flows. The lower 8 km of the basin opens up into a broad valley, much of which is used for agriculture. Two towns, Soquel and Capitola, with populations totaling about 15,000 people, lie on the lower 3 km of the flood plain. Channel gradient ranges from about 0.004 in the lower reaches to 0.038 in the upper reaches, and some



FIGURE 12.6.—Branciforte Creek flood-control channel at peak capacity on the afternoon of January 4, 1982. Photograph by Pete Amos and Bill Lovejoy, Santa Cruz, Calif., *Sentinel*.

of the tributaries have gradients of at least 0.15. Mean annual precipitation over the entire basin is 1,020 mm (40 in.) (U.S. Army Corps of Engineers, 1973c). Although the wet season normally extends from October to May, most flooding has occurred in the months of December through February. Streamflows can rise to flood peaks within a few hours, and so the effectiveness of flood warnings is limited.

Soquel Creek is spanned four times by bridges in its lower reaches; two of these bridges, in the town of Soquel, have restricted clearances and thus form obstructions to floodflow and associated debris. Streambank vegetation in the basin, particularly large trees, in addition to logs and other organic debris, has the potential to form debris jams that can cause overbank flow in unpredictable places.

#### MAGNITUDE OF THE 1982 FLOOD

Peak discharge of Soquel Creek, calculated 3 km upstream from the gaging station located in the town of

Soquel, was  $275 \text{ m}^3/\text{s}$  on January 4, 1982, corresponding to a stage of 6.66 m. The peak discharge of the 1955 flood has been calculated at  $447 \text{ m}^3/\text{s}$  at only a slightly higher stage of 6.81 m (table 12.2). The significantly lower discharge in 1982 at nearly the same stage as in 1955 is ascribed to backwater effects of a massive logjam at the Soquel Avenue Bridge in downtown Soquel on January 4, 1982; the gaging station is only 275 m upstream from this bridge. Nonetheless, a major debris jam in 1955 had similar effects. The 1955 discharge value was obtained at a location only 150 to 250 m upstream from the gaging station by using the slope-area method and is probably too high.

Downstream evidence gives a clearer picture of the relative flood peaks and discharge volumes. At the California Highway 1 Bridge (0.9 km downstream from the Soquel Avenue Bridge), surveys indicate that the 1982 peak was only 28 cm below the 1955 peak. Because the channel is confined at this point by the freeway-bridge



FIGURE 12.7.—Soquel Avenue Bridge in the city of Santa Cruz, showing collapsed span. Scour at confluence of the San Lorenzo River and Branciforte Creek led to subsidence of an older bridge pier. Arrow denotes high-water line.

constriction, the 28 cm greater stage at this point in 1955 could not have caused the additional  $172 \text{ m}^3/\text{s}$  that official discharge figures indicate. Thus, peak discharge for the 1955 event probably was only slightly greater than for the 1982 event.

The calculated January 1982 peak flow has a recurrence interval of about 15 years (table 12.2) and is 3 times the mean annual flood.

#### INUNDATION AND DAMAGE

The areas inundated along Soquel Creek in January 1982 were nearly identical to those inundated in 1955. Creek levels rose so quickly on January 4, 1982, that some residents of the two mobile-home parks adjacent to the stream in downtown Soquel had to wade out through knee-deep water. At about noon on that day, Soquel

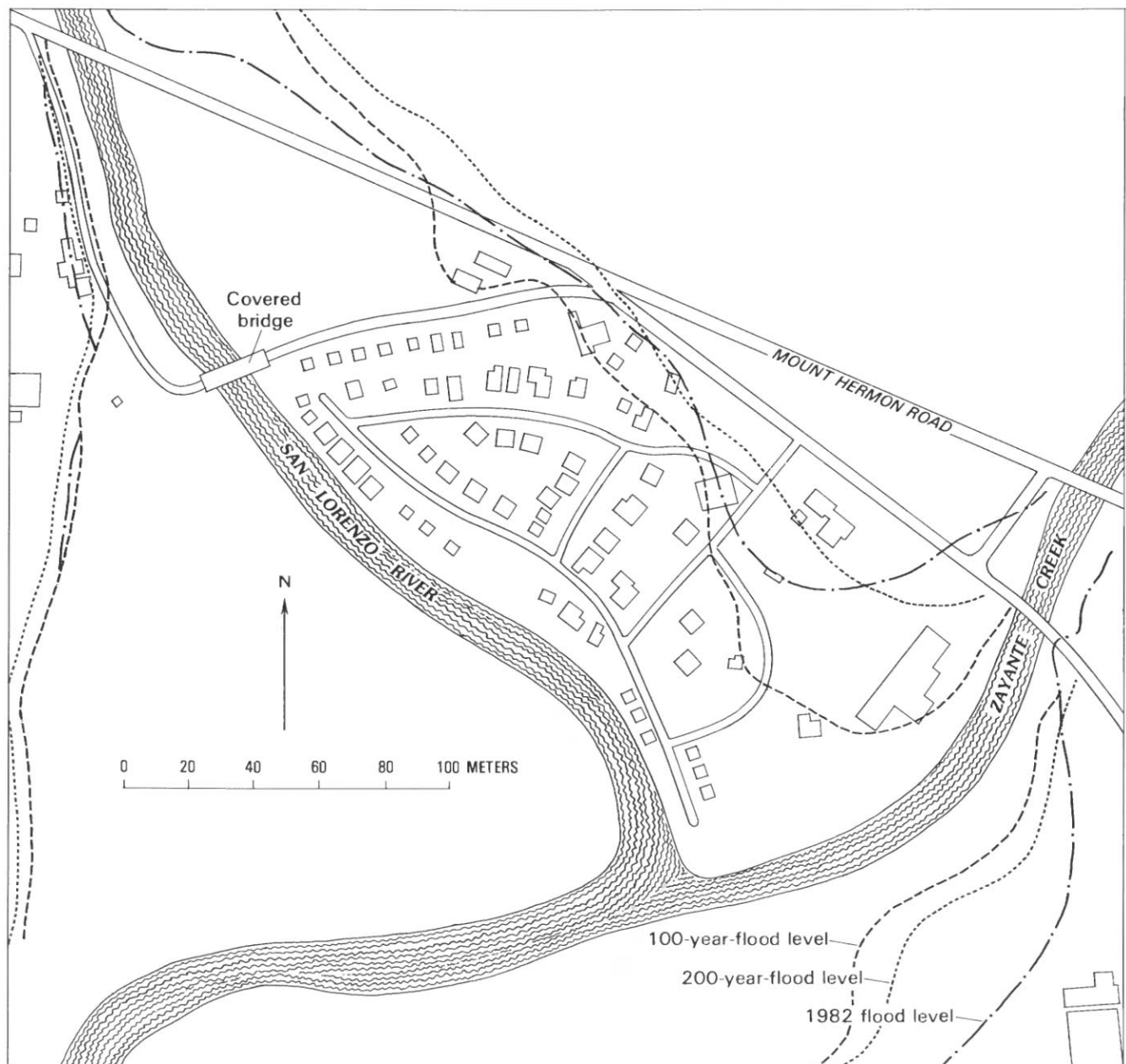


FIGURE 12.8.—Felton Grove, showing projected 100- and 200-year-flood levels and high water of January 4, 1982.

Creek, flowing at  $114 \text{ m}^3/\text{s}$ , entered the Heart of Soquel trailer park. One resident was not aware of a flood problem until water began to flow under the door of his mobile home. By 2:30 p.m. P.s.t., water began to enter the downtown business district. About 3 hours later, the logs and trees being carried downstream began to get caught at a constricted downtown bridge (maximum horizontal span, 18 m) spanning the creek at Soquel Drive (see fig. 12.15). A repeat of the 1955 flood occurred at this point. In that earlier flood, at an older bridge on the

same site, a tremendous logjam, which included a four-room house and five auto-court apartments, diverted the muddy floodwaters into downtown Soquel.

By 10:00 p.m. P.s.t. January 4, 1982, the logjam extended the entire width of the creek and about 120 m upstream (fig. 12.11). County fire officials considered using plastic explosives to break up the logjam but, instead, called for a crane from the county. The crane broke down on route and never arrived. Much of the approximately  $275 \text{ m}^3/\text{s}$  of discharge of Soquel Creek was



FIGURE 12.9.—Flood level and sand deposits along the San Lorenzo River in Felton Grove. High-water mark (arrow) is about 1 m above sediment fill. This particular area was flooded four times during the period 1970–82.



diverted through the Old Mill Trailer Park and then through the town's main street (figs. 12.11, 12.12). Floodwaters reached depths as great as 1.5 m and left as much as 1.2 m of sand and mud behind. Two mobile-home parks adjacent to the creek received major damage. Trailers were swept off their piers and broken up by logs and other debris (fig. 12.13); only 17 out of the 39 mobile homes damaged were determined to be salvageable. In addition, 58 businesses, 21 homes, the firehouse, post office, library, and Grange Hall were damaged by floodwaters and the debris they left behind (fig. 12.14). The bridge at Soquel Drive sustained an estimated \$270,000 in damage, due principally to scour and roadway collapse at the abutments, but the low structure remained standing and was soon back in use.

The size of the flood and the presence of the debris jam were almost identical to conditions in 1955. A resident who had also experienced the 1955 flood stated that the 1982 flood, though slightly lower in elevation, was much worse because "it hit harder and quicker" and because so much growth had occurred in the business district since the 1955 event.

Although logjams here and elsewhere in Santa Cruz County contributed to and exacerbated flooding, overbank flow along Soquel Creek occurred both before the logjam and at sites unaffected by that obstruction. The chronology of events of January 4 indicates that overbank flow had inundated the two trailer parks and the downtown business district by late afternoon on that day; by that time, the entire downtown area had been evacuated. At



FIGURE 12.10.—Culvert overflow in Lockhart Gulch. This box culvert was totally inadequate to handle the runoff from this small ephemeral stream. At peak discharge, flow was approximately 15 m wide and more than 2 m deep. Arrow denotes high-water mark.

about 5:15 p.m., water in the creek had risen high enough that logs and other organic debris were beginning to jam against the underside of the Soquel Drive Bridge, and not until 10:00 p.m. did this logjam divert much of the creek through the downtown area (fig. 12.12).

Flooding unrelated to the logjam also occurred 350 m downstream. Homes built within the past 5 years on a flood terrace along Soquel Wharf Road (fig. 12.15), downstream from the Porter Street Bridge, were inundated by more than a meter of water and mud as the creek topped its banks (fig. 12.16). This area had been recognized as flood prone, and specially designed elevated structures had been permitted in recent years. The second-story living structures were not inundated, but the first-floor carports, many of which had been remodeled as solid garages, were damaged by water and mud, as were automobiles.

After the flood, local residents and business owners washed out their residences and businesses, trucked away the sand and mud, and made the necessary repairs. The two mobile-home parks have again been filled with

coaches. Most of the residents of downtown Soquel apparently do not realize that they live on a flood plain. The historical record indicates that Soquel has been flooded at least eight times since 1890 (Singer and Swanson, 1983); severe damage was incurred during the floods of 1931, 1937, 1940, and 1955. Flood-frequency data indicate that the 1982 flood was not an extreme event; similar floods can be expected every 15 years on an average. Overbank flooding would still have occurred without a constricted bridge opening. Most of the community occupies the flood plain, and flooding will continue to occur in the same areas (fig. 12.15).

### FLOODING AND FLOOD DAMAGE ON APTOS CREEK

#### BASIN DESCRIPTION

Aptos Creek drains a basin of about 63 km<sup>2</sup> of south-central Santa Cruz County (fig. 12.1). The drainage extends inland 11 km from the coast to a maximum elevation of 765 m. Channel gradients range from 0.0015 near



FIGURE 12.11.—Logjam on Soquel Creek and path of diverted floodwaters through the Old Mill Trailer Park (arrows). Photograph by Pete Amos and Bill Lovejoy, Santa Cruz, Calif., *Sentinel*.

the creek mouth to as high as 0.284 in some of the steeper canyons of the upper watershed. Near the coast, Aptos Creek and its tributaries are flanked by a marine terrace and low hills, which are occupied by the communities of Aptos and Rio Del Mar. Only in the lowermost reaches of the creek, between California Highway 1 and the ocean, has construction occurred on the flood plain.

Upstream from California Highway 1, Aptos Creek enters the steep, heavily forested mountains of the central Coast Ranges. Approximately 1.5 km above its mouth, the creek enters the Forest of Nisene Marks, an undeveloped State park that has been virtually untouched by human activity for nearly 50 years. This park constitutes most of the Aptos Creek watershed upstream from this point. The condition of this watershed stands in marked contrast to that of the San Lorenzo River basin, which has been heavily altered by quarrying, logging, and the land clearing and grading that accompany development. Although the Aptos Creek drainage was logged 50 to 100 years ago, it appears to have regenerated to a natural, relatively undisturbed secondary-growth-redwood-covered basin. The runoff from this basin provides a useful datum for comparison with the heavily altered drainages in the area.

#### MAGNITUDE OF THE 1982 FLOOD

The U.S. Geological Survey has maintained a stream gage on Aptos Creek, about 1 km upstream from the mouth, since 1959. In 1971, this gage was moved farther upstream. Owing to the steep slopes and short length of the basin, creek levels can rise to flood stage within a few hours. For these same reasons and because peak precipitation intensities do not persist for long periods, floodwaters generally do not persist for more than 6 to 12 hours.

The last major flood to affect the drainage was during December 1955, when estimated peak discharge was  $99 \text{ m}^3/\text{s}$ . The 1982 flood peaked on January 4 at  $113 \text{ m}^3/\text{s}$ , according to U.S. Geological Survey slope-area calculations. At the California Highway 1 Bridge, the flood level from the 1982 flood was about 15 cm above the 1955 peak.

The 1982 flood has a recurrence interval of about 40 years and a peak discharge 6.9 times the mean annual flood (table 12.2). The 1955 flood, by comparison, ranked as approximately the 35-year event, with a discharge 6.0 times the mean annual event. The 1982 flood peak on Aptos Creek had the largest return period for any major gaged stream in Santa Cruz County (table 12.2).



FIGURE 12.12.—Downtown Soquel being inundated by waters of Soquel Creek on the evening of January 4, 1982. Floodwaters rose another meter after this photograph was taken. Photograph by Pete Amos and Bill Lovejoy, Santa Cruz, Calif., *Sentinel*.



## INUNDATION AND DAMAGE

During the December 1955 flood, major damage to the houses along Aptos Creek was apparently limited to four homes that were flooded along Moosehead Drive. The Southern Pacific Railroad bridge sustained damage due to roadbed undermining, and underground telephone lines in the flood plain were also damaged. Damage in 1955 totaled about \$62,000.

Small organic-debris jams formed throughout the park portion of the basin in 1982, and a massive debris jam formed nearly at the park entrance. This mass consisted both of cut logs and of trees with their roots intact; it measured 180 m long, 60 m wide, and 6 to 9 m high. In contrast to the overbank flood damage that resulted from the debris jam in Soquel Creek, however, Aptos Creek flowed around the debris jam across an undeveloped part of the flood plain.

Downstream from the California Highway 1 Bridge (fig. 12.17), the 1982 flood inflicted much damage to older homes that had been rebuilt after the 1955 flood and to newer homes that had been built on streamside fill brought in after the 1955 flood. Aerial photographs flown directly after the 1955 flooding show that at that time Aptos Creek meandered in its course between the California Highway 1 Bridge and the Spreckels Drive Bridge, and that two cutbank areas were clear. After those floods, the creek channel was constricted and straightened by fill in these areas, and additional houses were constructed. In January 1982, the two former meanders were again sites of bank cutting. Water levels rose throughout January 4 and began undermining the foundations of the homes along Moosehead and Spreckels Drive at these two sites (figs. 12.17, 12.18). At 7:00 p.m. that evening, foundations started to fail because these houses were built on



FIGURE 12.13.—Row of damaged mobile homes along Soquel Creek in the Heart of Soquel Trailer Park. Arrow denotes high-water mark.



perimeter foundations, which collapsed as the loose fill and unconsolidated flood-plain sediment were eroded, rather than on caissons or piers. At least seven homes sustained major damage. One heavily damaged home had been rebuilt after the 1955 floods. Two other homes broke in half owing to undermining (fig. 12.19); the detached part of one ended up in the creek, and the other floated downstream. A third home on the north bank totally collapsed into the creek at 8:00 p.m.; part of the house ended up on a nearby bridge (fig. 12.20), and the rest floated downstream to the ocean.

Further downstream, major sections of the two streets paralleling Aptos Creek, along with their associated utilities, collapsed into the floodwaters owing to stream-bank erosion, as did the entire lower floor of a creekside home.

All these heavily damaged areas are delineated on the existing flood-plain map (U.S. Army Corps of Engineers, 1973a). In contrast to construction on the flood plains of the San Lorenzo River and Soquel Creek, houses along Aptos Creek were built on the streambanks, directly in the floodway; and some were built partly on artificial fill placed in the stream channel. Structural damage and passive inundation occurred as a result.

Where less than 50 percent of a structure has been damaged or destroyed, local government cannot require relocation, floodproofing, or elevation of a damaged home. Thus, before winter was over, residents applied for emergency permits, dumped fill into the stream channel, poured new foundations, and rebuilt homes (fig. 12.21). Some riprap was brought in to protect the new fill and rebuilt homes, but rocks of the same size had been swept

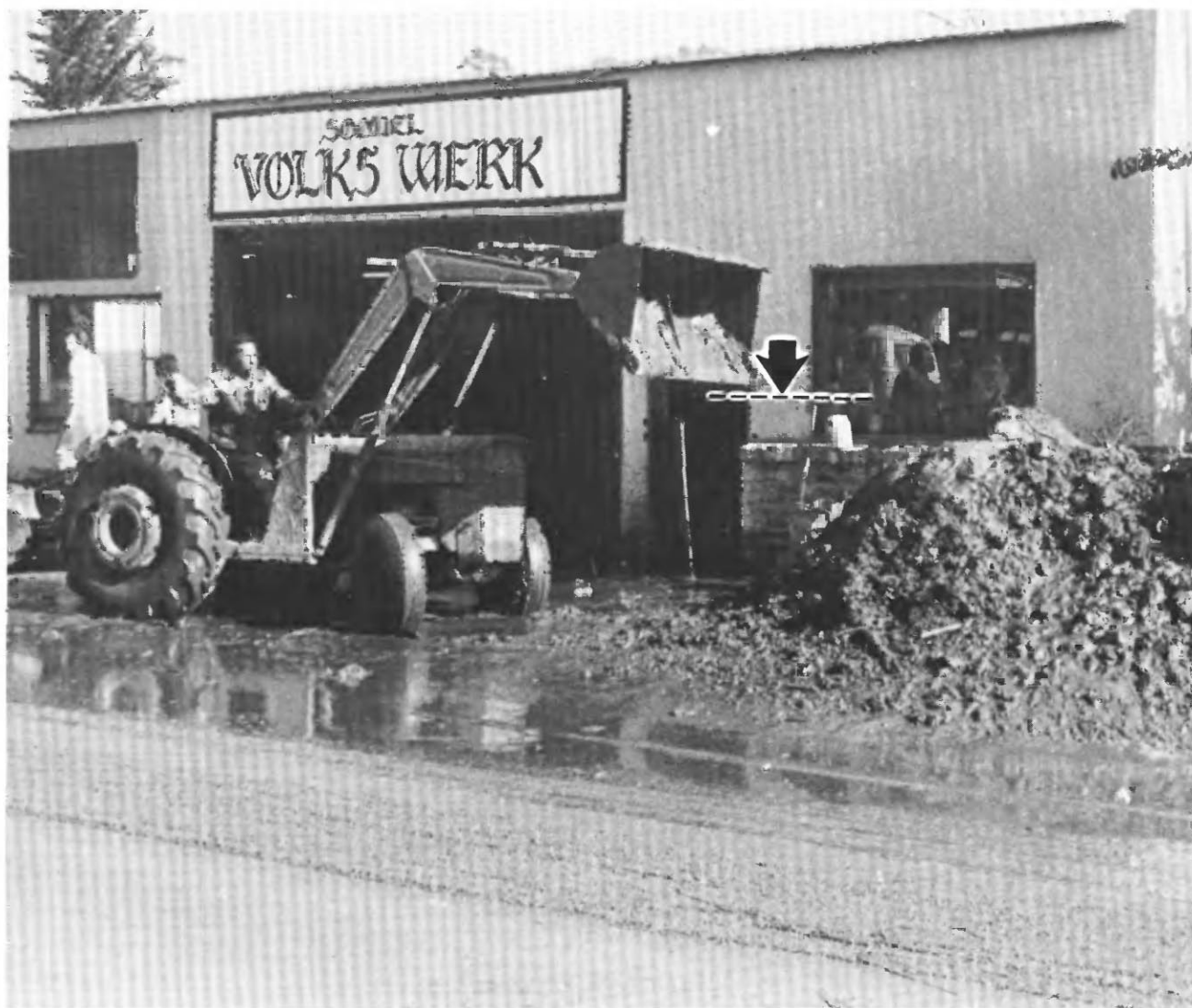


FIGURE 12.14.—Mud being removed from automotive garage in downtown Soquel. High water (arrow) here reached a depth of 1.43 m.

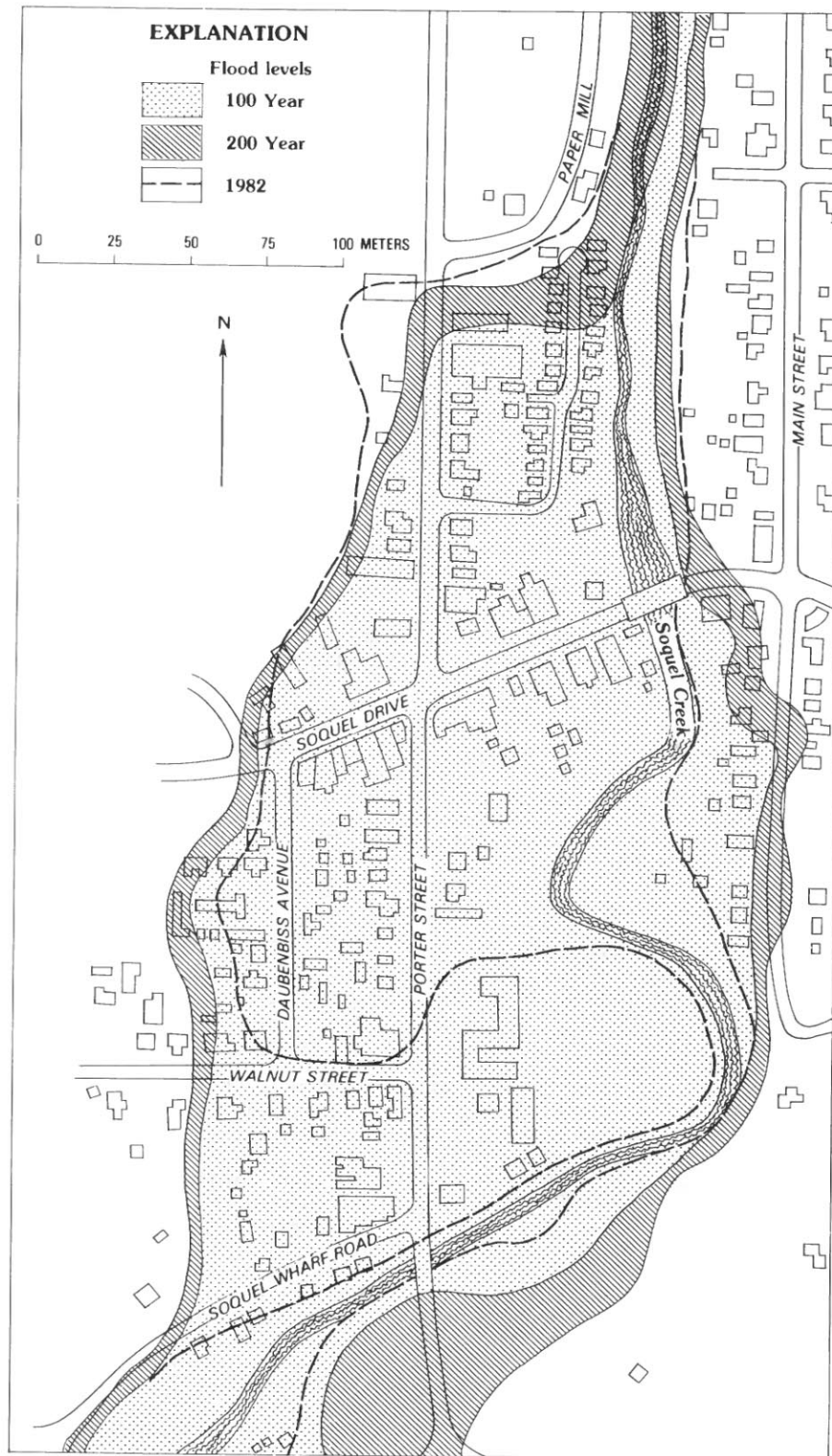


FIGURE 12.15.—Downtown Soquel, showing projected 100- and 200-year-flood levels and January 4, 1982, high water. California Highway 1 is located along south edge of map.

away by the January floodwaters. The course of Aptos Creek has again been straightened, and rebuilding has been done in the same flood-prone locations.

### LESSONS LEARNED

Although some of the flood damage in 1982 was to structures built long before flood-plain maps were published by the U.S. Army Corps of Engineers (1973a), many of the damaged structures had been built or rebuilt in areas inundated by the 1955 flood. The availability of accurate and useful flood-plain maps, combined with building restrictions in these areas, would certainly have reduced this winter's damage.

### UTILITY OF FLOOD-PLAIN MAPS

One shortcoming in flood-plain mapping for planning purposes is the preoccupation with a single event, the 100-year (or intermediate regional) flood. U.S. Army Corps of Engineers maps also project the limits of a

standard-project flood, approximately a 200-year event. For land-use and risk-assessment purposes, designation of those areas inundated more frequently than the 100-year event—for example, the 10- or 25-year flood levels—would be of equal or greater significance. In the mind of the public, the 100-year flood plain is an area that will be flooded each 100 years or so. A wide range of hazard exists, however, across the 100-year flood plain. At Felton Grove, for example, homes adjacent to the river have been flooded four times since 1969, and they received more than 2 m of water and a meter of sand in 1982. Structures on the very periphery of the designated flood plain, however, may receive only several centimeters of water every 100 years on the average; yet both areas have the same flood-plain designation. Nothing on existing maps or in existing policies or restrictions draws distinctions between areas of vastly different flood frequency within the designated 100-year flood plain. Such distinctions would allow for considerable improvement and resolution in planning efforts for flood-prone areas and might present a clearer picture of risk to the general public.



FIGURE 12.16.—Flooding and mud deposition along Soquel Wharf Road. Construction was approved on Soquel Creek flood plain at this site because structures were to be elevated. Arrow denotes high-water mark.

## RELIABILITY OF FLOOD-PLAIN MAPS

Areas outside 100-year-flood-plain boundaries on existing maps were also inundated during the 1982 flood. Along the San Lorenzo River, major discrepancies exist along the urbanized 1.6 km of river from Felton to the gaging station at Big Trees. Along the northeast side of the river from Mount Hermon Road to the confluence with Zayante Creek, 1982 levels were generally well above the 100-year floodline (fig. 12.8). At the confluence itself, flood levels extended as much as 35 m laterally beyond the projected 200-year event. Downchannel at the Big Trees gaging station and Gold Gulch, levels for 1982 remained at the 200-year line. On the southwest side of the river, flood levels followed the 100-year line to the gaging station and then reached the projected 200-year level from there to Gold Gulch. Local discrepancies also exist upstream at Glen Arbor and at the Newell Creek confluence. In all these places, 1982 flood levels, which represent approximately a 33-year event, were well above the levels that existing maps would have projected. Clearly, either the data available on flood-recurrence intervals or the methods used in constructing the maps (or both) were limited.

In Soquel, a similar discrepancy exists between flood-map boundaries and the areas inundated in 1982 (fig. 12.15). The downtown area occupies the broad flood plain west of the creek. North of Soquel Drive, 1982 levels exceeded projected 200-year levels (fig. 12.15). Midway through town at Soquel Drive, water reached the 100-year level; but at the California Highway 1 Bridge, high water was somewhat below this level. Because the 1982 peak represents approximately a 15-year event, the existing maps appear to have significantly underestimated the 100-year-flood levels in much of downtown Soquel. Certainly the debris jam at the Soquel Drive played a role here, as it has in at least four earlier floods (Singer and Swanson, 1983).

Along Aptos Creek, 1982 high-water levels in the principal areas of flooding (between California Highway 1 and Spreckles Drive) were above the projected 100-year level and close to the 200-year mark (fig. 12.17). Although the peak on Aptos Creek had a higher return period (approx 40 years) than on other county streams, the existing maps again are inadequate in accurately assessing inundation frequency or flood hazard.

The reliability of existing maps can now be assessed because most major areas of 1982 flooding along the San Lorenzo River, Soquel Creek, and Aptos Creek have been mapped by the Earth Sciences Department of the University of California, Santa Cruz, as well as by the U.S. Geological Survey. With a well-documented 30- or 40-year-flood level, we now can develop a more accurate 100-year inundation line.

## CONCLUSIONS

The extensive flooding and flood damage in Santa Cruz County from the January 3-5, 1982, storm in the San Francisco Bay region demonstrate that existing flood-hazard maps are inaccurate in many critical areas and furthermore, delineate only 100-year-flood levels. A definite need exists both (1) to accurately map inundation levels of more frequent floods, such as 10- or 25-year floods, and (2) to continually update the 100-year hazard zone in the light of data gathered during smaller, more frequent events. Flood-inundation mapping is relatively quick and inexpensive immediately after a flood. Such information can be used to update and revise existing flood-hazard maps, so that flood-prone areas can be more accurately delineated.

## REFERENCES CITED

- Brown, W.M., III, 1973, Erosion processes, fluvial sediment transport, and reservoir sedimentation in a part of the Newell and Zayante Creek basins, Santa Cruz County, California: U.S. Geological Survey, Water Resources Division open-file report, 31 p.

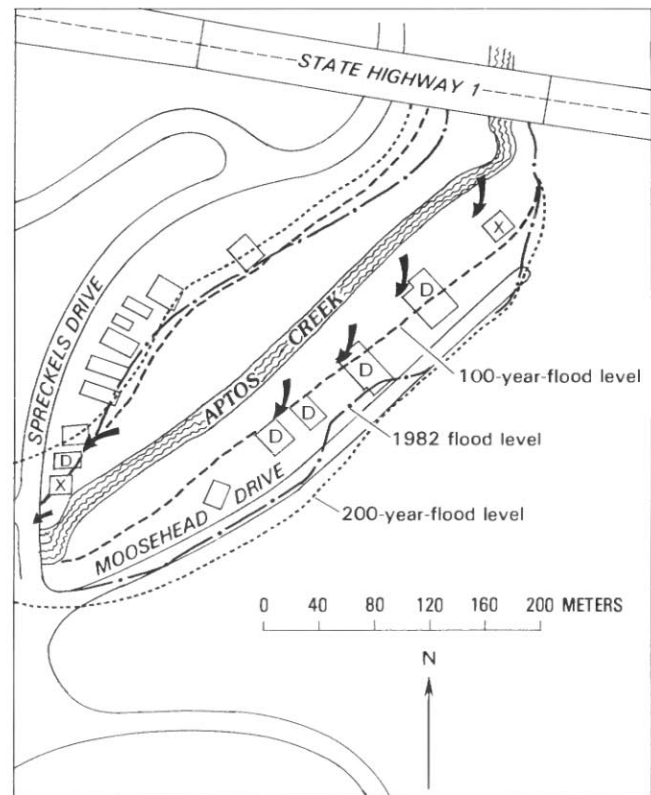


FIGURE 12.17.—Aptos Creek flood plain, showing area inundated by the January 1982 flood and projected inundation areas of 100- and 200-year floods. D, damaged structures; X, destroyed structure. Arrows denote sites of bank erosion.



- Griggs, G.B., and Paris, L., 1982, The failure of flood control along the San Lorenzo River, Santa Cruz County, California: *Environmental Management*, v. 6, no. 4, p. 407-419.
- Rantz, S.E., 1971, Mean annual precipitation and precipitation depth-duration-frequency data for the San Francisco Bay region, California: U.S. Geological Survey, San Francisco Bay Region Environment and Resources Planning Study Basic Data Contribution 32, 23 p.
- Santa Cruz County Office of Watershed Management, 1976, Preliminary report on the San Lorenzo River watershed planning process: Santa Cruz, Calif., 115 p.
- Singer, S., and Swanson, M.L., 1983, Soquel Creek storm damage recovery plan: Aptos, Calif., U.S. Department of Agriculture, Soil Conservation Service, 71 p.
- U.S. Army Corps of Engineers, 1973a, Flood plain information, Aptos, Trout and Valencia Creeks, city of Aptos, California, Santa Cruz County, California: San Francisco, 17 p.
- 1973b, Flood plain information, San Lorenzo River, Boulder Creek-Felton, Santa Cruz County, California: San Francisco, 23 p.
- 1973c, Flood plain information, Soquel Creek, Santa Cruz County, California: San Francisco, 20 p.



FIGURE 12.18.—View upstream along Aptos Creek from the Spreckels Drive Bridge, showing bank erosion, foundation failure, and house collapse.



FIGURE 12.19.—Bank erosion from lateral cutting during the January 1982 flood on Aptos Creek. Much of this house fell into the creek and was carried downstream. Bank erosion occurred at this same site during the 1955 flood, and fill was subsequently brought in.



FIGURE 12.20.—Wreckage of a house sits atop the Spreckles Drive Bridge across Aptos Creek. Timber in foreground was part of foundation for another house that was totally destroyed. House was built after 1955 flood in an area where bank erosion had previously occurred.



FIGURE 12.21.—View upstream along Aptos Creek from the Spreckles Drive Bridge in August 1982, showing filling and reconstruction that have taken place since the January 1982 flood. Compare with figure 12.18.





# 13. PEAK DISCHARGE, VOLUME, AND FREQUENCY OF THE JANUARY 1982 FLOOD IN THE SANTA CRUZ MOUNTAINS AND VICINITY

By JAMES C. BLODGETT and KAREN R. POESCHEL,  
U.S. GEOLOGICAL SURVEY

## CONTENTS

	Page
Abstract - - - - -	229
Introduction - - - - -	229
Sources of data - - - - -	230
Antecedent conditions - - - - -	230
Description of the storm - - - - -	232
Regional characteristics of precipitation - - - - -	232
Precipitation depth-duration-frequency - - - - -	234
Analysis of flow frequency - - - - -	234
Regional characteristics of flooding - - - - -	234
Frequency of the flood - - - - -	235
Effect of antecedent precipitation on flooding of the San Lorenzo River at Big Trees - - - - -	238
Summary - - - - -	243
References cited - - - - -	243

## ABSTRACT

In many parts of the Santa Cruz Mountains, the flooding and landslides caused by the January 3-5, 1982, storm were the most severe since December 1955. To assess the severity of the January 1982 flood, this chapter compares this flood with other historical floods, including that of December 1955.

The areal distribution of precipitation during the January 1982 storm in the Santa Cruz Mountains and vicinity was chiefly influenced by the topography. On the west side near Boulder Creek, the 1-day precipitation depth reached 310 mm (12.2 in.), with a recurrence interval of 67 years. In the rain shadow of the mountains, by contrast, the 1-day precipitation depth at San Jose was 34 mm (1.33 in.), with a recurrence interval of less than 2 years.

The rain shadow of the Santa Cruz Mountains also influenced flooding during the storm. For example, the flow, calculated as unit peak discharge, ranged from 0.91 (m<sup>3</sup>/s)/km<sup>2</sup> for Pescadero Creek near Chittenden on the east side of the mountains to 6.84 (m<sup>3</sup>/s)/km<sup>2</sup> for a tributary to the San Lorenzo River near Boulder Creek on the west side. The median recurrence interval for the peak discharge on the west side of the mountains is 21 years, whereas on the east side it is only 6 years.

During the January 1982 flood, peak discharges of many streams were similar to those observed during the December 1955 flood. Although precipitation and flood magnitude for both the December 1955 and January 1982 floods are similar, the damages caused by landslides, inundation, and channel changes during the 1982 storm and flood are considered more severe.

A study of historical floods and precipitation characteristics in the San Lorenzo River basin suggests that major floods in the area are the product of (1) greater than normal antecedent precipitation for as many as 60 days before the flood and (2) subsequent intense frontal-type storms immediately preceding the peak.

## INTRODUCTION

During January 3-5, 1982, an intense storm system passed through the coastal area of central California and caused record amounts of precipitation, which resulted in flooding in the Santa Cruz Mountains and vicinity. This storm originated from the merger of a cold front from Alaska with another storm originating in the warmer midlatitudes. Rainfall rates of more than 25 mm/h (1 in/h) for more than 8 hours were recorded in the Santa Cruz Mountains south of San Francisco. The 1-day rainfall of 291 mm (11.47 in.) at the Ben Lomond precipitation station on January 4, 1982, was the highest daily rainfall total since the beginning of record in 1938.

The introduction of large amounts of sediment and debris into the waterways by heavy runoff, together with debris flows and other landslides in steep terrain, resulted in reduction in channel capacity, logjams, blockage of bridges, channel scouring and filling, changes in channel alignment, and overflow of the banks. High-water levels caused inundation of the flood plain and damaged residences, commercial establishments, roadways, and bridges (see chap. 12).

On the west side of the Santa Cruz Mountains, only the peak discharges from the December 19-26, 1955, storm exceeded those of January 1982. Flooding on the east side of the mountains during January 1982 was less severe; peak discharges there were comparable to those in the floods of January 1952 and April 1958.

Normally, a frequency analysis of historical peak discharges of streams in the flood area provides a good indication of the severity of a given event. During the January 1982 flood, however, peak discharges of many streams were similar to those observed during the December 1955 flood, whereas damage resulting from landslides and channel changes was considered much more severe. The greater severity of damage from the 1982 storm relative to that of previous events may have been due to antecedent (prestorm) conditions and to the storm duration and intensity. In addition, increased cultural development in the study area, including construction of buildings, roads, fills, and benching in hillside areas, may have contributed to damages from the 1982 storm.

In this chapter, we use data from 5 precipitation stations and 37 streamflow sites located in the Santa Cruz

Mountains, along the coast northward to San Francisco and inland eastward to the San Francisco Bay and the Santa Clara Valley (fig. 13.1), to compare the January 1982 and December 1955 floods. The study area includes basins that underwent major flooding, as well as adjacent basins both east and west of the Santa Cruz Mountains divide and south of the major areas of flooding. Areas north and east of the San Francisco Bay were also subject to extensive flooding by the storm, but flooding in those areas is not discussed in this volume. Gaging stations are located in mountainous terrain, except those on terraces directly adjacent to the coast. Most stations east of the divide are located near the base of the Santa Cruz Mountains and in the Santa Clara Valley.

We compared data for the January 1982 flood with historical precipitation and streamflow records to assess the magnitude of the storm. Our specific objectives were (1) to evaluate the effects of prestorm conditions, such as antecedent precipitation, on runoff; (2) to document peak discharge and runoff for selected durations; (3) to estimate the frequency of occurrence of peak discharges and runoffs; (4) to indicate the areal variation of flooding; and (5) to compare the magnitudes of the January 1982 and December 1955 floods.

#### SOURCES OF DATA

We used daily precipitation data (U.S. National Oceanic and Atmospheric Administration, 1938-82) for stations in San Francisco, San Jose, Santa Cruz, Ben Lomond, and Boulder Creek (Locatelli Ranch) to compare the 1982 storm with other historical storms (fig. 13.1). To supplement the streamflow-data base, as well as for purposes of comparison, precipitation data from these stations were analyzed for frequency of occurrence.

Streamflow data were obtained at 33 continuously recording gaging stations, 3 discontinued crest-stage gages, and 1 miscellaneous site near a former crest-stage gage (U.S. Geological Survey, 1937-70, 1971-74, 1975-80). The lengths of record, basin sizes, and comparative flood data for these stations are listed in table 13.1. Only six stations in the vicinity of the Santa Cruz Mountains have streamflow records of 25 years or longer. We consider the selected gaged streams throughout the Santa Cruz Mountains and vicinity to provide a reasonable sample of the various hydrologic conditions in the study area. The largest flow recorded during the flood was 841.1 m<sup>3</sup>/s on the San Lorenzo River at Big Trees, and the smallest was 1.2 m<sup>3</sup>/s on a Pescadero Creek tributary near La Honda. All the gaging stations listed in table 13.1 are

located on streams that are generally unaffected by regulation and diversion upstream from the gage.

The crest-stage gages (stas. 11153800, 11159770, 11162470) are devices that record the peak stage, which can then be converted to a peak discharge. These gages were operated on a systematic basis between 1958 and 1972. Peak discharge data obtained at crest-stage gages located throughout California were summarized by Waananen (1973).

The January 1982 peak discharge was determined by indirect measurements at the crest-stage-gage sites and several inactive gaging stations. These measurements of peak discharge were used to extend the period of historical record at these sites from the date of discontinuance to January 1982.

#### ANTECEDENT CONDITIONS

Flooding in the coastal areas of central California during early January 1982 was preceded by a series of storms that moved eastward from the Pacific Ocean during October through December 1981. The rainfall resulting from these storms is shown in plate 1. These storms provided greater than normal amounts of cumulative precipitation to the region. The accumulated precipitation from October 1, 1981, to January 31, 1982, is shown in intervals of 5 days in figure 13.2 as a percentage of the norm for each month at three precipitation stations in the Santa Cruz Mountains and vicinity. Norms for each month were obtained from data published by the U.S. National Oceanic and Atmospheric Administration (1938-82). By November 12, 1981, the accumulated precipitation at all stations was near or above 100 percent of normal for November. Precipitation later in November and December continued at a greater than normal rate, and by the end of December, soils were generally saturated. The Santa Cruz precipitation station recorded 111 mm (4.36 in.) for December 1981, of which 58 mm (2.29 in.) fell on December 30. This greater than normal precipitation in November and December significantly increased the potential for flooding during the subsequent winter months.

Streamflow in the study area responded to the greater than normal rainfall during the 3 months preceding the January 1982 storm with a rapid increase in accumulated flow (fig. 13.2) after the storms of October 25 to November 12. Runoff was near or above normal for the three stations shown in figure 13.2 during part of November and all of December. During the first 4 days of January, runoff increased rapidly to peak discharges, from about 120 to 400 percent of normal for January.

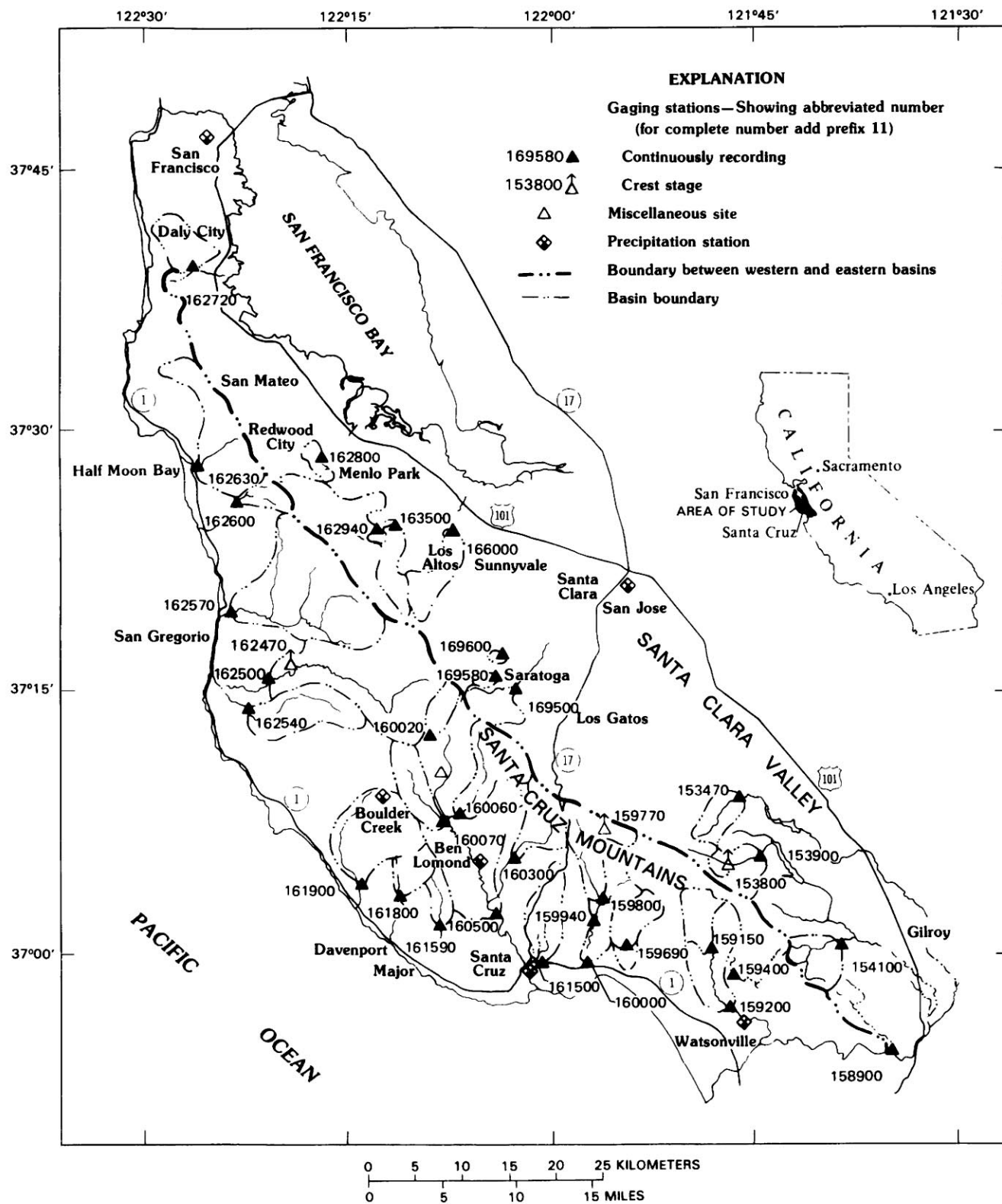


FIGURE 13.1.—Southern San Francisco Bay region, showing locations of data-collection sites in the study area in the Santa Cruz Mountains.



TABLE 13.1.—Summary of flood stages and discharges

Station	Stream	Drainage area (km <sup>2</sup> )	Maximum previously known				Maximum, January 1982			
			Period	Year	Gage height (m)	Discharge (m <sup>3</sup> /s)	Date	Gage height (m)	Discharge	
									(m <sup>3</sup> /s)	(m <sup>3</sup> /s)/km <sup>2</sup>
11153470	Llagas Creek above the Chesbro Reservoir, near Morgan Hill.	24.94	1971-81	1978	2.29	27.44	4	2.09	27.75	1.12
<sup>1</sup> 11153800	Alec Canyon near Morgan Hill-----	2.36	1961-73	1963	---	10.39	4	17.97	4.48	1.90
11153900	Uvas Creek above the Uvas Reservoir, near Morgan Hill.	54.39	1961-81	1962	4.02	186.35	4	3.65	147.26	2.71
11154100	Bodfish Creek near Gilroy-----	19.17	1959-81	1963	2.52	35.12	4	2.70	33.42	1.74
11158900	Pescadero Creek near Chittenden---	26.42	1970-81	1981	1.85	12.04	4	2.48	23.96	.91
11159150	Corralitos Creek near Corralitos.	27.45	1957-72	1958	2.30	55.79	4	3.16	60.04	2.19
11159200	Corralitos Creek at Freedom-----	72.00	1955-81	1955	4.76	102.52	4	5.08	158.88	2.21
11159400	Green Valley Creek near Corralitos.	18.26	1961-73	1963	17.26	26.20	4	17.57	33.98	1.86
11159690	Aptos Creek near Aptos-----	26.42	1959-81	1963	---	54.37	4	3.69	112.71	4.26
<sup>1</sup> 11159770	Laurel Creek near Laurel-----	2.41	1961-73	1963	9.85	8.21	4	9.73	7.65	3.17
11159800	West Branch Soquel Creek near Soquel.	31.60	1959-72	1967	3.50	128.29	4	3.81	106.2	3.36
11159940	Soquel Creek near Soquel-----	82.88	1968-72	1969	2.75	76.46	4	4.99	169.92	2.06
11160000	Soquel Creek at Soquel-----	104.12	1937, 1951-81	1955	6.81	447.46	4	6.66	274.70	2.64
11160020	San Lorenzo River near Boulder Creek.	15.98	1968-81	1973	2.77	19.03	4	3.50	29.74	1.86
( <sup>2</sup> )	San Lorenzo River tributary near Boulder Creek.	.30	---	---	---	---	4	---	2.04	6.84
11160060	Bear Creek at Boulder Creek-----	41.44	1977-81	1980	3.16	58.91	4	4.05	126.87	3.06
11160070	Boulder Creek at Boulder Creek----	29.27	1976-81	1978	2.45	46.16	4	2.90	99.12	3.39
11160300	Zayante Creek at Zayante-----	28.75	1957-81	1978	2.60	130.84	4	2.70	103.93	3.62
11160500	San Lorenzo River at Big Trees-----	274.54	1936-81	1955	6.87	860.93	5	8.79	841.10	3.06
11161500	Branciforte Creek at Santa Cruz---	44.81	1940-43, 1952-68	1955	6.72	229.39	4	6.39	188.33	4.20
11161590	Laguna Creek near Davenport-----	7.95	1969-76	1974	1.12	8.01	4	1.54	18.41	2.32
11161800	San Vicente Creek near Davenport.	15.72	1969-81	1974	1.78	26.54	4	2.71	64.57	4.11
11161900	Scott Creek above Little Creek, near Davenport.	65.01	1937-41, 1958-73	1940	---	205.04	4	3.07	119.51	1.84
<sup>1</sup> 11162470	Pescadero Creek tributary near La Honda.	.57	1961-73	1973	15.77	1.44	4	15.61	1.19	2.09
11162500	Pescadero Creek near Pescadero----	118.88	1951-82	1955	6.48	266.77	4	6.38	266.21	2.24
11162540	Butano Creek near Pescadero-----	47.40	1961-74	1962	3.06	45.31	4	6.85	59.47	1.26
11162570	San Gregorio Creek at San Gregorio.	131.83	1969-81	1973	5.33	105.63	4	6.49	224.01	1.69
11162600	Purisima Creek near Half Moon Bay.	12.51	1958-69	1967	1.65	9.71	4	2.07	31.15	3.15
11162630	Pilarcitos Creek at Half Moon Bay.	70.45	1966-81	1968	3.41	36.53	4	3.99	134.52	1.91
11162720	Colma Creek at South San Francisco.	27.97	1963-81	1973	3.60	81.56	4	3.54	72.22	2.58
11162800	Redwood Creek at Redwood City-----	4.71	1959-81	1963	2.85	18.24	4	2.12	10.73	2.27
11162940	San Francisquito Creek below the Ladera damsite, near Stanford University.	73.82	1961-70	1967	4.51	81.84	4	3.79	147.83	2.00
11163500	Los Trancos Creek at Stanford University	19.32	1931-41	1940	1.24	18.32	4	1.31	26.34	1.37
<sup>3</sup> 11166000	Matadero Creek at Palo Alto-----	18.80	1952-81	1973	1.70	39.08	4	1.12	17.78	.95
11169500	Saratoga Creek at Saratoga-----	23.88	1933-81	1955	1.95	77.31	4	2.15	48.71	2.04
11169580	Calabazos Creek tributary at Mount Eden Road, near Saratoga.	.96	1972-78	1978	1.68	3.40	4	1.49	3.12	3.25
11169600	Prospect Creek at the Saratoga Golf Course, near Saratoga.	.70	1972-78	1978	1.56	1.78	4	1.52	1.56	2.23

<sup>1</sup>Crest-stage gage.<sup>2</sup>Miscellaneous site.<sup>3</sup>January 4, 1982, flood not maximum for water year.

## DESCRIPTION OF THE STORM

## REGIONAL CHARACTERISTICS OF PRECIPITATION

About 85 percent of the annual precipitation in the Santa Cruz Mountains and vicinity occurs from November through March (Rantz, 1971). Mean annual precipitation

in the area ranges from about 356 mm (14 in.) at San Jose to more than 1,321 mm (52 in.) at the towns of Boulder Creek and Ben Lomond. This range from east to west results from the orographic influence of the Santa Cruz Mountains, which rise abruptly from the coastline to more than 1,200 m, causing high annual depths of precipitation

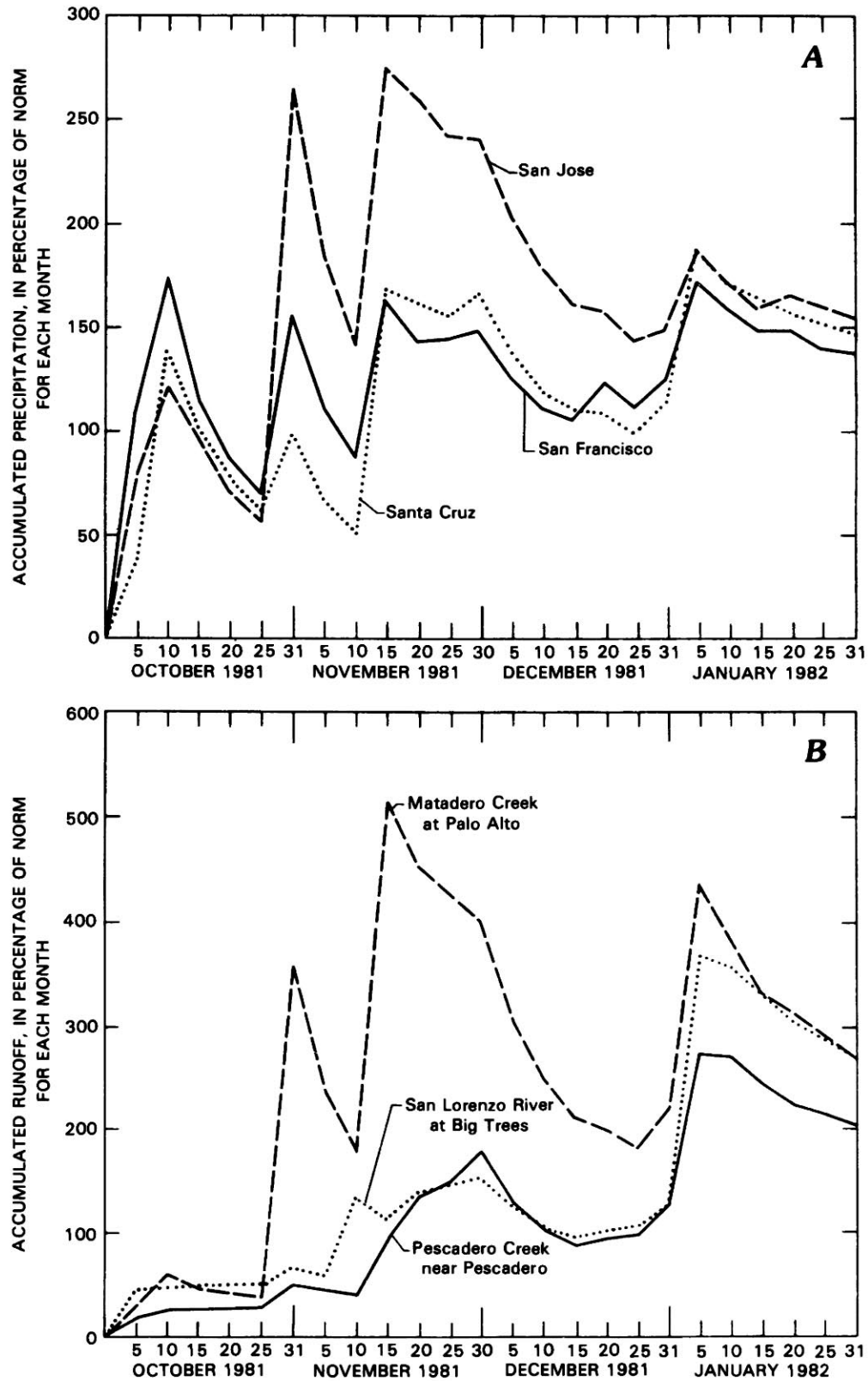


FIGURE 13.2.—Accumulated precipitation and runoff from October 1, 1981, to January 31, 1982, for precipitation stations (A) and stream-gaging stations (B) in the Santa Cruz Mountains and vicinity.

in some areas of the mountains and creating a rain shadow on the leeward side. The location of the divide between the west and east sides of the Santa Cruz Mountains is shown in figure 13.1. The orographic effect of the Santa Cruz Mountains is reflected in the areal variation in precipitation during the 1955 and 1982 storms. The 1-day precipitation at Boulder Creek during the 1955 and 1982 storms was more than 6 times that recorded in the valley at San Jose (table 13.2). The 1982 storm-rainfall isohyetal map shows this same effect (pl. 2).

#### PRECIPITATION DEPTH-DURATION-FREQUENCY

To compare the intensity, duration, and frequency of the storms of December 1955 and January 1982, we assembled precipitation-depth data from the five stations listed in table 13.2 for 1-, 3-, and 8-day intervals. The 1-day depth was selected as an indicator of maximum rainfall associated with peak discharge. The 3- and 8-day precipitation depths were selected to identify the largest segment of precipitation during a storm that can be related to runoff for a typical flood. Many major storms in the vicinity of the Santa Cruz Mountains last for 8 or 9 days, as did the December 1955 and January 1982 storms (fig. 13.3).

The data listed in table 13.2 suggest that the maximum 1-day precipitation of the December 1955 storm averaged 26 mm (1 in.) less than that of the January 1982 storm, although the average precipitation measured in 3- and 8-day periods was about 38 mm (1.5 in.) greater for the December 1955 than for the January 1982 storm.

The areal variation of precipitation for a given storm can be described by the standard deviation of observed precipitation at various locations. For example, the standard deviations of 1-day rainfall for the December 1955 and January 1982 storms at selected stations in the study area (table 13.2) differed by about 2 percent. This small difference indicates that both storms had a similar areal variation in precipitation. The standard deviations of the ratios of 3- and 8-day rainfall to 1-day rainfall of the two storms differed by 6 and 12 percent, respectively, a difference indicating that both storms also had a similar areal variation of precipitation over the longer period. The similarity of precipitation intensity and duration for the December 1955 and January 1982 storms suggests that areal-streamflow patterns of the two floods should have comparable characteristics, provided that antecedent conditions and hydrologic features are similar.

We used a frequency analysis of the precipitation totals at 1, 3, and 8 days for each precipitation station in the study area to estimate the average recurrence interval of the December 1955 and January 1982 storms. General precipitation depth-duration-frequency relations developed by Rantz (1971) for the San Francisco Bay region

were applied to these five stations to obtain the recurrence intervals listed in table 13.2. During the January 1982 storm, the 1-day rainfall depth at the Ben Lomond station was 291 mm (11.5 in.), with a recurrence interval of 95 years. The 1-day precipitation depth for a 100-year recurrence interval is about 293 mm (11.5 in.). By comparison, on the basis of an interpretation of precipitation maps by the U.S. National Oceanic and Atmospheric Administration (1973), the 100-year precipitation depth for this location is about 356 mm (14 in.).

The recurrence intervals of the 3- and 8-day precipitation depths for the December 1955 storm were longer than those for the January 1982 storm (table 13.2) at three of the five stations. Stations at which precipitation in 1955 was less than in 1982 are located on the perimeter of the study area.

#### ANALYSIS OF FLOW FREQUENCY

##### REGIONAL CHARACTERISTICS OF FLOODING

Floods in the Santa Cruz Mountains result from precipitation during winter-frontal storms, which are greatly influenced by orographic uplift. Floods in basins in the eastern part of the study area, however, reflect the rain shadow of the mountains. During years in which winter-frontal storms are less intense, as in 1977 and 1981, floods in basins along the eastern part of the study area may result from isolated storm systems occurring at different times from those centered along the west side of the mountains.

This rain-shadow effect is demonstrated by the variation in unit peak discharge<sup>1</sup> observed at the gaging stations during the January 1982 flood (fig. 13.4). For example, the unit peak discharge was 4.11 (m<sup>3</sup>/s)/km<sup>2</sup> for San Vicente Creek near Davenport (sta. 11161800), but on the east side of the mountains it was only 1.12 (m<sup>3</sup>/s)/km<sup>2</sup> for Llagas Creek above the Chesbro Reservoir near Morgan Hill (sta. 11153470; fig. 13.4). The January 1982 flood also suggests a north-southward trend in the magnitude of unit peak discharge. Unit peak discharge from streams near the northern part of the study area was about 2.2 (m<sup>3</sup>/s)/km<sup>2</sup>, in comparison with about 3.3 (m<sup>3</sup>/s)/km<sup>2</sup> near the southwestern part of the study area. The highest unit peak discharge measured was 6.84 (m<sup>3</sup>/s)/km<sup>2</sup> at the miscellaneous site on the San Lorenzo River tributary near Boulder Creek; this site was selected to indicate the peak discharge from a very small basin near a former crest-stage gage.

Although some snow falls during the winter in the study area at altitudes above about 610 m, it generally does not

<sup>1</sup>Because discharge varies with basin size, flow is expressed here in terms of unit peak discharge to discount this effect.

TABLE 13.2.—*Precipitation depth, duration, and frequency for selected precipitation stations, December 19–26, 1955, and December 29, 1981–January 5, 1982*

Station	Length of record (yr)	Mean annual precipitation (mm)	Year	1-day precipitation		3-day precipitation			8-day precipitation		
				(mm)	Recurrence interval (yr)	(mm)	Recurrence interval (yr)	Ratio to 1-day	(mm)	Recurrence interval (yr)	Ratio to 1-day
Boulder Creek at the Locatelli Ranch, near Boulder Creek.	36 ---	1,480 ---	1955 1982	308 310	63 67	496 333	46 5.3	1.61 1.07	676 531	53 11	2.19 1.71
Bon Lomond-----	43 ---	<sup>1</sup> 1,328 ---	1955 1982	265 291	43 95	431 409	35 25	1.63 1.41	605 564	55 32	2.29 1.94
Santa Cruz-----	105 ---	797 ---	1955 1982	112 176	5 70	226 240	16 23	2.03 1.37	281 330	10 26	2.52 1.88
San Francisco-----	133 ---	525 ---	1955 1982	57 107	2 27	107 120	3.7 5.5	1.86 1.12	148 170	3.9 6.7	2.58 1.58
San Jose-----	109 ---	347 ---	1955 1982	48 34	3.3 <2	85 50	7.8 <2	1.76 1.48	147 86	32 2.5	3.05 2.54
Average-----			1955 1982	158 184	--- ---	269 230	--- ---	1.78 1.29	371 336	--- ---	2.53 1.93
Standard deviation-----			1955 1982	121 118	--- ---	187 148	--- ---	.17 .18	253 212	--- ---	.33 .37

<sup>1</sup>Average of data collected at four sites in the vicinity of Ben Lomond during the period 1937–82.

remain on the ground for more than a few days. Snowmelt was not a significant factor during the January 1982 flood.

We used the flows for durations of 1, 3, and 8 days and the peak discharges to define the magnitude of the flood and to compare the precipitation and streamflow data. Most of the storm runoff occurs within an 8-day period for streams in the study area. To analyze a complete storm system, therefore, streamflow data were developed for periods as long as 8 days.

Some maximum 1-day flows for the year do not coincide with the periods of maximum 3- and 8-day flows. For determining frequency relations, runoff was defined by selecting consecutive daily flows that gave the greatest flow for periods of 1, 3, and 8 days, whether or not the maximum 1-day flows coincided with the maximum 3- and 8-day flows.

We compared runoff and precipitation by using flows and precipitation for durations of 1, 3, and 8 days as well. To relate a particular flood to the precipitation that caused it, however, the maximum 1-day flow was made to coincide with the 3- and 8-day flows.

#### FREQUENCY OF THE FLOOD

For many streams in the Santa Cruz Mountains and vicinity, peak discharges during the January 1982 flood were among the largest since the December 1955 flood. To determine the magnitude of the January 1982 flood, data for 37 streamflow sites in the study area (fig. 13.1) were analyzed. Flood-frequency relations were developed for stations that have systematic records of at least 10

years' duration. The annual flow and flood volumes for selected periods were analyzed for frequency of occurrence. The recurrence interval is defined as the average number of years between exceedences of a flood of a given magnitude; it is also the reciprocal of the probability of exceedence. A log-Pearson type III distribution of annual floods was used to define the frequency curves from which recurrence intervals for peak discharges and 1-, 3- and 8-day flow volumes were determined.

In determining the recurrence intervals of floods from the frequency relations, historical data were used to lengthen the period of record and to improve the reliability of estimates of flow frequency. For sites with historical data, the period of record used in the flood-frequency analysis was expanded to include historical periods that preceded or followed the period of systematic record. To determine the number of years of historical record that could be included as unrecorded peaks smaller than the flood magnitude of interest—in this case, the January 1982 floodflow—it was necessary to estimate by regression analysis the historical period of record. Annual peak discharges for stations with gaps in the record (dependent stations) were estimated from data from stations with more complete records (independent stations). Independent stations were selected that yielded the highest correlation coefficient when correlations with several stations were attempted.

Estimated annual peak discharges were not incorporated into the flow record but were used solely as an indication of the historical period during which peaks were less than the January 1982 floodflow. The systematic data



base was extended as much as 8 years for 14 stations, on the basis of estimated historical information.

To estimate the frequency relations of peak discharges, a generalized skew coefficient of  $-0.78$  was calculated by the procedures of the U.S. Water Resources Council (1981). To estimate the frequency of flow volumes for the selected durations, using comparable procedures, it was necessary to determine the generalized skew coefficients applicable for flow volumes as well as flood peaks.

However, the U.S. Water Resources Council (1981) did not present methods for estimating the generalized skew coefficient of flow volumes. For the present report, we assumed that the appropriate generalized skew coefficients are  $-0.73$ ,  $-0.80$ , and  $-0.84$ , which were derived from 1-, 3-, and 8-day flow volumes in the same manner as for peak discharges.

The peak discharge and 1-, 3-, and 8-day flow volumes of the January 1982 flood and their associated recurrence

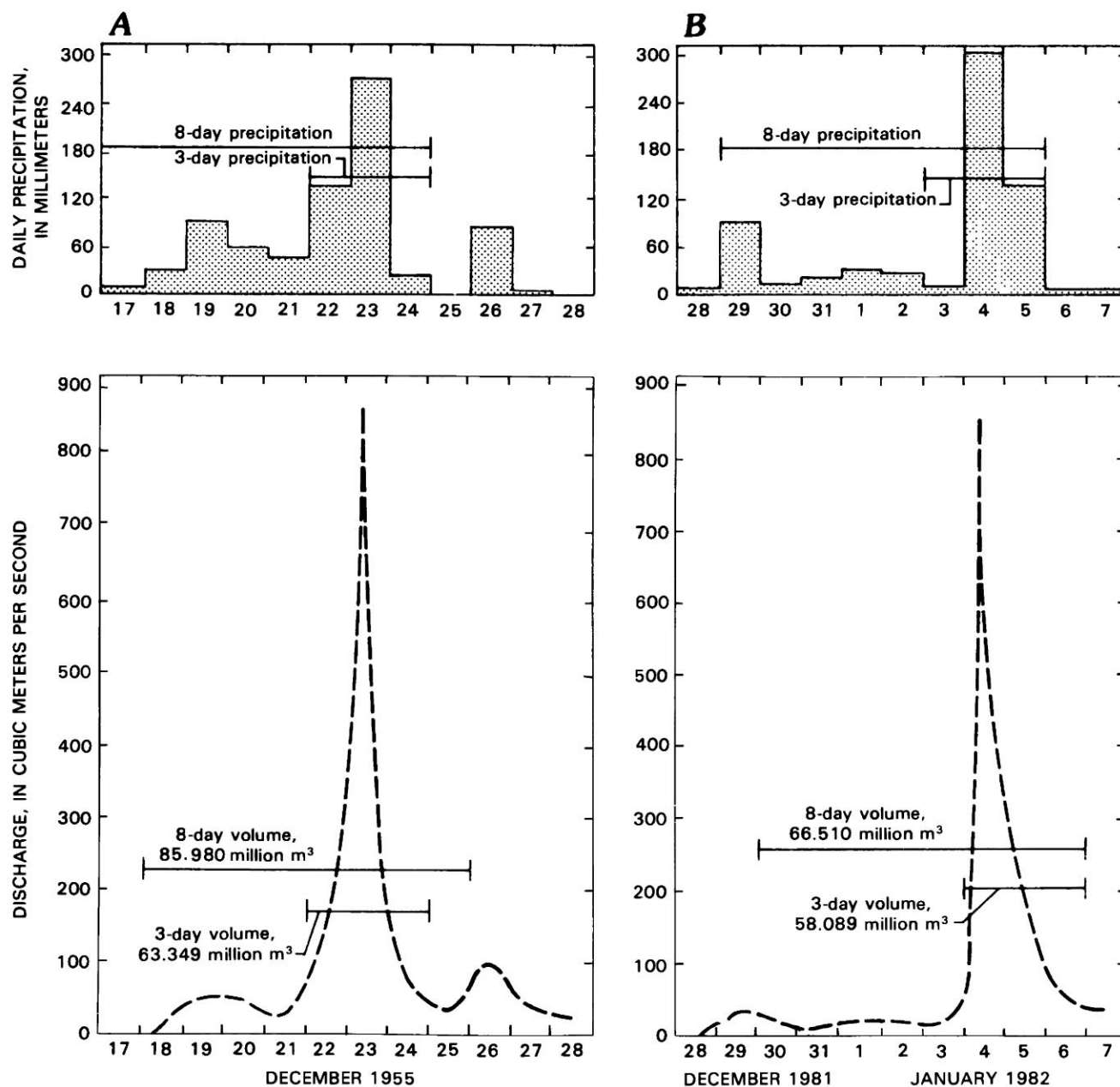


FIGURE 13.3.—Daily precipitation at Ben Lomond and discharge of the San Lorenzo River at Big Trees for the storms of December 1955 (A) and January 1982 (B).

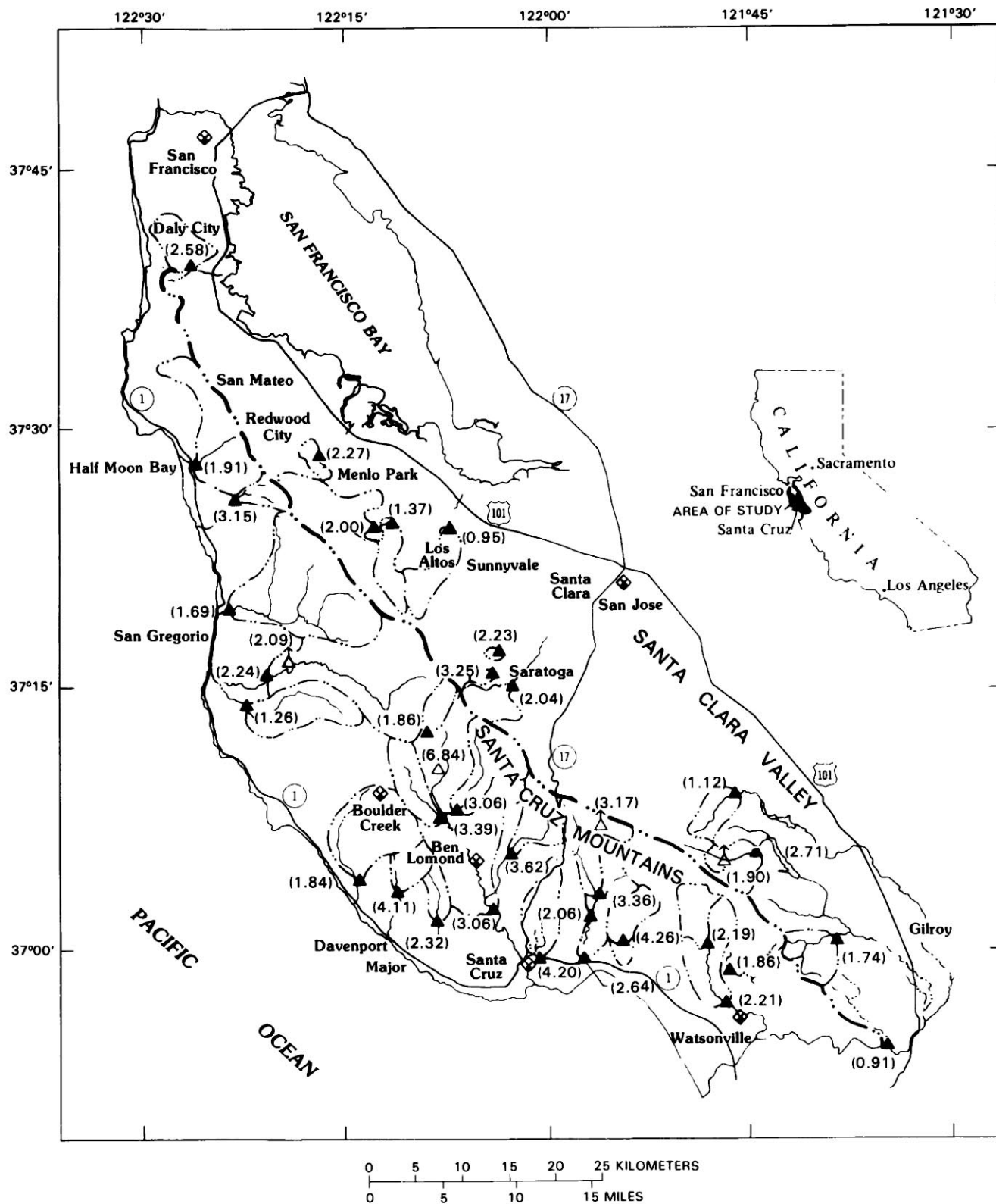


FIGURE 13.4.—Southern San Francisco Bay region, showing areal distribution of unit peak discharge (in cubic meters per second per square kilometer) during the January 1982 flood. See figure 13.1 for explanation.

intervals for selected gaging stations in the Santa Cruz Mountains and vicinity are listed in table 13.3. Where available, the recurrence intervals of peak discharge and flood volume for the December 1955 flood are listed for comparison. The median recurrence interval of the January 1982 peak discharge for 33 stations in the study area is 14 years. On the basis of data from six stations, the median recurrence for the December 1955 flood is 36 years. Only one of the seven sites with comparable data—Corralitos Creek at Freedom (sta. 11159200)—had a higher peak discharge in January 1982 than in December 1955.

The peak discharges of the January 1982 flood for San Vicente Creek near Davenport (sta. 11161800, table 13.3) and Purisima Creek near Half Moon Bay (sta. 11162600) indicate recurrence intervals longer than 100 years, but flows expressed as unit runoff are comparable to flows for nearby basins. Most of the other basins in areas of high flow had peak discharges with recurrence intervals of about 40 to 50 years.

Flood volumes during January 1982 for a 1-day period had a longer recurrence interval than peak discharges at 10 of the 15 stations. Recurrence intervals of flows for a 3-day period, however, were longer than those for the peak discharge at only 5 of these 15 stations. In terms of flow volumes (table 13.3), the median recurrence intervals of the January 1982 flood for 1-, 3-, and 8-day periods are 22, 18, and 10 years, respectively. Corresponding recurrence intervals of the December 1955 flood are 62, 22, and 30 years. In comparison, the recurrence intervals of runoffs of 3- and 8-day periods on the west side of the Santa Cruz Mountains were similar to or shorter than those of peak discharges, as indicated in table 13.3, whereas on the east side they were longer.

The median recurrence intervals of peak discharges at selected stations listed in table 13.3 indicate that the December 1955 flood was much larger and longer in duration than the January 1982 flood. Although precipitation records (table 13.2) indicate that 1-day precipitation during the January 1982 storm generally was greater than that recorded during the December 1955 storm, the peak discharge and runoff of the January 1982 flood for 1-, 3-, and 8-day periods were less than those of the December 1955 flood. This difference in the flow characteristics of the two floods may be attributable to differences in total precipitation.

#### EFFECT OF ANTECEDENT PRECIPITATION ON FLOODING OF THE SAN LORENZO RIVER AT BIG TREES

Streamflow-related damages in the Santa Cruz Mountains and vicinity caused by the January 1982 storm were the greatest since the December 1955 flood. Precipitation

data at Ben Lomond and flood data for the San Lorenzo River at Big Trees indicate that the amount of precipitation and corresponding runoff for these two floods are similar (table 13.4). For comparison, we note that both the January 1963 and February 1945 floods, which had similar amounts of precipitation, also had similar-size peak discharges and runoffs (table 13.4). These comparisons suggest that for certain precipitation patterns, the resulting floods may be of similar magnitude and volume. Although the storm in January 1963 was more severe (in terms of 3-day duration) than either the 1955 or 1982 storm (table 13.4), the resulting runoff was about half that recorded during the 1955 and 1982 floods. Because it has been established that locally intense convective-type storms and snowmelt are not factors in causing floods in the Santa Cruz Mountains (Rantz, 1971), the variation in runoff of a flood for a given amount of storm precipitation is attributable to antecedent precipitation.

A review of the dates of annual peak discharges of the San Lorenzo River at Big Trees (table 13.4) indicates that all the floods occurred during the winter months November through March, except for two floods that occurred in April, the largest of which was very early in the month. October and November are the only two months with storm activity that precede the period of major precipitation and flooding, December through March (fig. 13.5); September is omitted from the analysis of antecedent precipitation because it is a low-precipitation month (fig. 13.5).

The data in figure 13.3 indicate that most of the runoff for two major floods on the San Lorenzo River at Big Trees occurred during a 3-day period. To compare the precipitation at Ben Lomond and the corresponding runoff of the San Lorenzo River for different floods, the 3-day period that includes the annual peak discharge was selected. Using the precipitation and runoff data in table 13.4 for this 3-day period, the variation in runoff of the San Lorenzo River versus the precipitation at Ben Lomond is plotted in figure 13.6.

The enveloping lines for minimum and maximum 3-day runoff on figure 13.6 indicate that the runoff for a given amount of precipitation may vary by a factor of as much as 18, depending on antecedent conditions. For example, with a 3-day precipitation of 114 mm (4.5 in.), the flow of the San Lorenzo River may range from 0.9 million to 16 million m<sup>3</sup>. The water years<sup>2</sup> in which the runoff was minimal for a given amount of precipitation, 1963 and 1976 (fig. 13.6), had antecedent precipitations for the 15 days preceding the flood that were the lowest on record (table 13.4). Water years with maximum runoff, 1965,

<sup>2</sup>A water year is the 12-month period from October 1 to September 30, designated by the calendar year in which it ends. All references to years in this chapter are to water year unless otherwise noted.

TABLE 13.3.—Peak discharges, volumes, and recurrence intervals during various durations of flow at selected stream-gaging stations, December 19–26, 1955, and December 30, 1981–January 6, 1982

["Side" refers to side of the Santa Cruz Mountains drained by the stream]

Station		Side	Peak discharge			1-day volume		3-day volume		8-day volume	
No.	Name		Date	(m <sup>3</sup> /s)	Recur- rence interval (yr)	(10 <sup>3</sup> m <sup>3</sup> )	Recur- rence interval (yr)	(10 <sup>3</sup> m <sup>3</sup> )	Recur- rence interval (yr)	(10 <sup>3</sup> m <sup>3</sup> )	Recur- rence interval (yr)
11153470	Llagas Creek above Chesbro Reservoir, near Morgan Hill.	East---	1- 4-82	27.75	4	---	---	---	---	---	---
<sup>1</sup> 11153800	Alec Canyon near Morgan Hill.	do---	1- 4-82	4.47	4	---	---	---	---	---	---
11153900	Uvas Creek above Uvas Reservoir.	do---	1- 4-82	147.26	5	6,699	15	12,324	22	14,310	9
11154100	Bodfish Creek near Gilroy.	do---	1- 4-82	33.42	10	1,130	12	1,678	9	2,110	7
11158900	Pescadero Creek near Chittenden.	do---	1- 4-82	23.96	6	---	---	---	---	---	---
11159150	Corralitos Creek near Corralitos.	West---	1- 4-82	60.04	9	---	---	---	---	---	---
11159200	Corralitos Creek at Freedom.	do---	12-22-55	102.52	12	---	---	---	---	---	---
			1- 4-82	158.88	40	5,603	30	9,822	19	10,887	10
11159400	Green Valley Creek near Corralitos.	do---	1- 4-82	33.98	15	---	---	---	---	---	---
11159690	Aptos Creek near Aptos.	do---	1- 4-82	112.71	40	4,083	37	5,095	21	5,971	14
<sup>1</sup> 11159770	Laurel Creek near Laurel.	do---	1- 4-82	7.65	6	---	---	---	---	---	---
11159800	West Branch Soquel Creek near Soquel.	do---	1- 4-82	106.20	9	---	---	---	---	---	---
11159940	Soquel Creek near Soquel.	do---	1- 4-82	169.92	9	---	---	---	---	---	---
11160000	Soquel Creek at Soquel.	do---	12-23-55	447.46	62	21,588	>100	34,911	>100	43,423	>100
			1- 4-82	274.70	14	10,523	18	14,927	11	17,517	6
11160020	San Lorenzo River near Boulder Creek.	do---	1- 4-82	29.74	11	1,234	8	2,085	7	2,295	5
11160060	Bear Creek at Boulder Creek.	do---	1- 4-82	126.87	7	4,478	---	6,538	---	7,648	---
11160070	Boulder Creek at Boulder Creek.	do---	1- 4-82	99.12	14	2,233	6	4,404	6	5,502	4
11160300	Zayante Creek at Zayante.	do---	1- 4-82	103.93	7	4,182	16	5,428	10	5,909	6
11160500	San Lorenzo River at Big Trees.	do---	12-23-55	860.93	36	41,573	62	63,408	30	85,983	30
			1- 5-82	841.10	33	36,022	36	58,103	24	66,492	11
11161500	Branciforte Creek at Santa Cruz.	do---	12-22-55	229.39	77	---	---	---	---	---	---
			1- 4-82	188.33	29	---	---	---	---	---	---
11161800	San Vicente Creek near Davenport.	do---	1- 4-82	64.57	>100	2,085	38	2,813	27	3,158	10
11161900	Scott Creek above Little Creek, near Davenport.	do---	1- 4-82	119.51	20	---	---	---	---	---	---
<sup>1</sup> 11162470	Pescadero Creek tributary near La Honda.	do---	1- 4-82	1.19	23	---	---	---	---	---	---
11162500	Pescadero Creek near Pescadero.	do---	12-23-55	266.77	21	13,570	41	21,342	31	31,334	25
			1- 4-82	266.21	21	8,561	14	12,336	7	14,927	6
11162540	Butano Creek near Pescadero.	do---	1- 4-82	59.47	11	---	---	---	---	---	---
11162570	San Gregorio Creek at San Gregorio.	do---	1- 4-82	224.01	43	---	---	---	---	---	---
11162600	Purisima Creek near Half Moon Bay.	do---	1- 4-82	31.15	>100	---	---	---	---	---	---
11162720	Colma Creek at South San Francisco.	East---	1- 4-82	72.22	40	2,011	>100	2,677	>100	3,417	>100
11162800	Redwood Creek at Redwood City.	do---	1- 4-82	10.73	5	421	29	528	9.2	738	9.1
11163500	Los Trancos Creek at Stanford University.	do---	1- 4-82	26.34	21	---	---	---	---	---	---
11166000	Matadero Creek at Palo Alto.	do---	12-22-55	24.19	7	819	15	1,332	16	1,776	11
			1- 4-82	17.78	4	801	13	1,021	8	1,283	8
11169500	Saratoga Creek at Saratoga.	do---	12-22-55	77.31	46	1,468	14	3,306	22	5,662	20
			1- 4-82	48.71	13	1,194	25	2,788	11	4,108	9
11169580	Calabazas Creek tributary at Mount Eden Road, near Saratoga.	do---	1- 4-82	3.12	4	---	---	---	---	---	---
11169600	Prospect Creek at the Saratoga Golf Course, near Saratoga.	do---	1- 4-82	1.56	5	---	---	---	---	---	---
Median values, 1982											
Study area-----					13.5	---	21.5	---	17.5	---	9.6
West side-----					20.5	---	33.0	---	20.0	---	10.0
East side-----					5.5	---	15.0	---	13.5	---	9.0
Median, 1955-----					36	---	62	---	22	---	30

<sup>1</sup>Crest-stage gage.



TABLE 13.4.—Precipitation at Ben Lomond and annual flood discharge of the San Lorenzo River at Big Trees, Calif. for the years 1938-82

Water year	Date of flood	Precipitation (mm)			Antecedent precipitation (mm)			Discharge (m <sup>3</sup> /s)	Volume (10 <sup>3</sup> m <sup>3</sup> )		
		1-day	3-day	8-day	15-day	45-day	60-day		1-day	3-day	8-day
38	1-31-38	138	190	303	122	---	---	390.8	11,867	21,924	40,025
39	3-09-39	80	118	123	36	252	252	19.2	1,301	2,476	3,624
40	2-27-40	159	300	367	358	533	1,330	679.7	33,522	53,781	68,568
41	2-09-41	99	208	355	144	425	805	439.0	18,057	37,657	54,328
42	1-24-42	182	279	373	44	558	628	379.5	18,278	27,869	42,362
43	1-21-43	171	300	402	112	276	443	393.6	18,180	28,750	35,670
44	3-04-44	63	99	170	195	498	521	53.5	3,817	6,631	11,880
45	2-02-45	261	420	496	77	189	190	373.8	17,739	32,397	40,050
46	12-27-45	76	124	308	185	447	577	79.6	3,769	8,337	15,654
47	11-22-46	162	129	302	91	94	117	41.1	1,292	2,219	3,707
48	4-29-48	65	113	114	62	320	371	39.4	1,343	3,306	5,016
49	3-10-49	95	180	210	173	356	447	109.9	5,750	15,024	20,955
50	2-06-50	135	239	254	80	393	547	175.3	6,289	16,097	21,716
51	11-18-50	180	368	551	177	318	319	300.2	10,693	23,612	30,459
52	1-12-52	160	225	369	339	800	910	422.0	15,659	29,827	48,986
53	12-07-52	197	240	256	171	569	701	262.0	8,075	9,753	11,527
54	1-17-54	124	144	145	120	393	393	76.7	22,594	3,193	3,836
55	12-02-54	133	200	265	58	280	283	93.5	2,447	5,848	8,877
56	12-23-55	265	431	670	236	488	488	860.9	41,596	63,349	82,327
57	2-24-57	76	161	222	66	285	365	72.5	3,132	6,956	8,867
58	4-02-58	124	210	296	263	656	1,016	487.1	15,366	32,250	51,109
59	2-16-59	76	123	197	208	421	528	189.5	6,558	10,910	17,502
60	2-01-60	117	138	183	253	482	566	84.7	2,570	4,078	6,599
61	11-26-60	89	106	106	36	141	220	18.1	661	893	1,192
62	2-14-62	130	224	319	288	416	416	172.5	5,799	15,121	23,764
63	1-31-63	247	487	496	9	59	148	368.2	18,107	36,458	43,093
64	1-21-64	63	146	215	19	329	329	75.3	2,814	5,583	7,456
65	1-05-65	69	115	210	147	330	482	239.3	7,365	16,027	28,782
66	12-29-65	---	---	---	105	157	158	30.6	1,403	3,262	5,217
67	1-21-67	275	320	407	22	29	351	294.5	15,537	23,475	35,087
68	1-30-68	125	195	203	96	185	285	247.0	8,833	11,738	13,815
69	2-15-69	120	128	161	185	441	452	325.7	13,653	20,236	30,813
70	1-16-70	102	200	249	105	331	331	231.9	9,151	18,033	26,205
71	11-29-70	70	136	257	188	340	340	71.6	3,352	6,680	13,566
72	12-27-71	56	88	184	138	293	293	30.0	1,565	3,262	5,427
73	1-16-73	89	137	150	171	261	265	334.2	11,231	22,732	30,268
74	3-28-74	84	144	256	42	81	202	119.5	5,138	12,007	14,131
75	3-21-75	58	94	126	32	329	355	142.7	3,645	7,653	13,509
76	2-29-76	76	117	122	0	100	124	13.0	396	903	1,301
77	3-15-77	34	67	72	9	60	60	7.4	313	540	796
78	1-14-78	139	287	399	272	539	661	320.0	14,656	32,861	46,177
79	2-13-79	116	147	208	27	333	374	143.9	4,062	7,986	11,312
80	2-19-80	137	241	483	424	767	1,024	297.4	15,636	28,848	51,516
81	3-21-81	82	128	144	126	138	289	68.3	3,645	5,762	8,523
82	1-05-82	291	427	582	253	396	645	841.1	35,968	58,088	66,510
Mean-----		127	202	279	139	343	446	231.5	9,618	17,431	24,713

1969, 1973, and 1975, had average antecedent precipitation for a 15-day period, but the 60-day antecedent precipitations were above average (table 13.4).

We note that major floods during the years 1940, 1955, and 1982 fall midway between the enveloping curves in figure 13.6. Although these floods were larger than average, an even greater flood might occur in the future, given the right combination and storm intensity. For example, under antecedent conditions observed before the 1940 flood and with a 3-day precipitation similar to that of the 1982 storm (table 13.4), a flood greater than any other observed to date would be likely.

To determine which periods of antecedent precipitation were most influential on subsequent runoff under different storm conditions, we developed a rainfall-runoff model based on precipitation data from the Ben Lomond station and flow data from the stream-gaging station (11160500) on the San Lorenzo River at Big Trees. An equation relating flood magnitude to various periods of antecedent precipitation was developed from a linear multiple regression:

$$Q = a + bP_n + cAP_n,$$

where  $Q$  is the peak discharge (in cubic meters per second) or runoff (in cubic meters) for a selected duration for the stream-gaging station on the San Lorenzo River at Big Trees,  $P_n$  is the precipitation depth (in millimeters) for the selected period, concurrent with the annual maximum flow of a similar period,  $AP_n$  is the antecedent precipitation (in millimeters) preceding the beginning of the selected flood period (generally, the beginning day of a 60-day period is 62 to 64 days before the date of the peak discharge),  $n$  is the number of days in a period, and  $a$ ,  $b$ , and  $c$  are constants. Various transformations, such as logarithms or use of a polynomial expansion in the regression analysis, did not improve the accuracy of this regression. Inclusion of other hydrologic variables, such as those that tend to define the shape of the precipitation hydrograph, also did not improve the regression.

Precipitation data from the Ben Lomond station were used to regress with streamflow data from the stream-gaging station on the San Lorenzo River at Big Trees because the Ben Lomond station is located near the center of the basin. We found that antecedent precipitation for 15- and 30-day periods was statistically insignificant. Because the largest floods on record occurred either in late December or in January and February (table 13.4), a period of antecedent precipitation longer than 45 days was considered a possible influence on the flood magnitude.

The data in table 13.5 are based on antecedent precipitation for a 60-day period. The highest correlation coefficient of the various regressions was 80 percent. On the basis of the standard estimation error, use of a 60-day period instead of a 15- or 45-day period improved all the regressions by an average of 10 percent. We note that the 60-day period of antecedent precipitation was significant for all the durations of floods listed in table 13.5, including the annual peak discharge.

The regression analysis and a comparison of the precipitation and flood data listed in table 13.4 indicate that major floods (those with a 3-day flood volume greater than 50 million  $m^3$  or with an annual peak discharge exceeding 566  $m^3/s$ ) on the San Lorenzo River reflect a combination of two climatic conditions, in the following sequence: (1) a prolonged period of continual greater than normal storm activity, as occurred during winter 1981–82; this precipitation saturated the ground and reduced the infiltration capacity of the soil; and (2) a period of intense storm activity near the end of this prolonged period of precipitation, in which large amounts of precipitation fall within a short period (generally more than 254 mm [10 in.] within 3 days).

For example, the February 1980 flood season had a high 60-day antecedent precipitation of 1,024 mm (40.3 in.) but a low 3-day storm intensity of 241 mm (9.5 in.), and the recurrence interval of the resulting 3-day flood volume

is 5 years (fig. 13.7). By comparison, the flood season before February 1945, which had a low 60-day antecedent precipitation of 190 mm (7.48 in.), had a strong 3-day storm that produced 420 mm (16.54 in.) of rainfall, and the recurrence interval of this flood is 7 years. This analysis suggests that major floods on the San Lorenzo River are not the result of isolated severe storm events during winter months but are the combined effect of greater than normal antecedent precipitation and subsequent intense frontal-type storms.

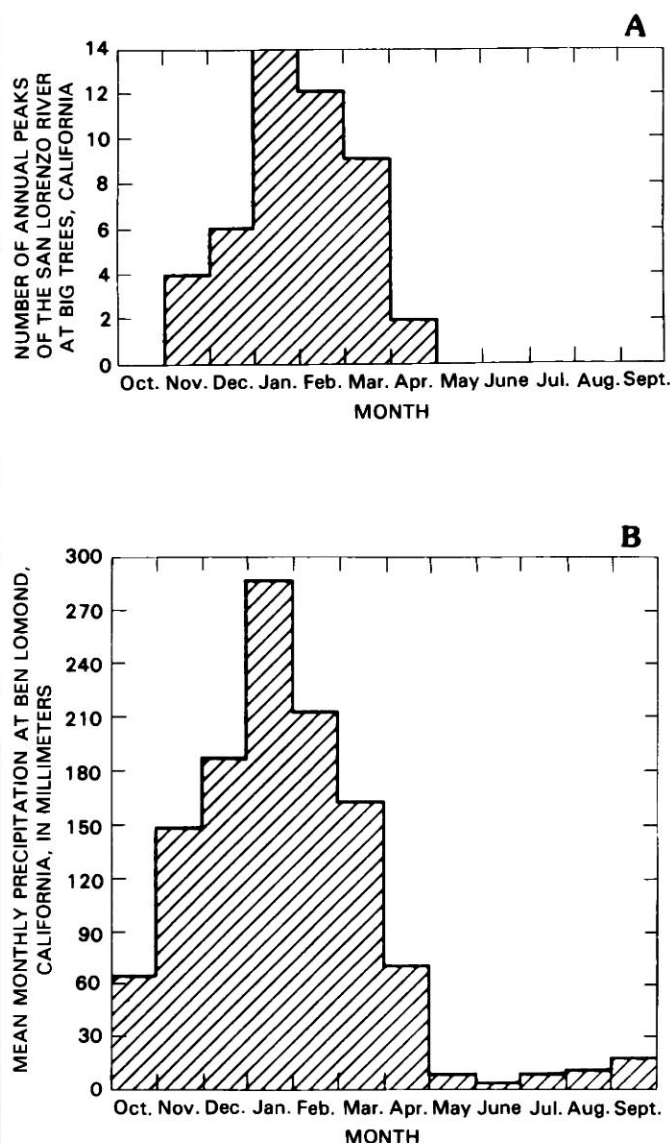


FIGURE 13.5.—Patterns of streamflow and annual rainfall in the study area. A, Monthly distribution of annual peak discharge of the San Lorenzo River at Big Trees for the period 1938–82. B, Mean monthly precipitation at Ben Lomond for the period 1968–82.

TABLE 13.5.—Regression of discharge of the San Lorenzo River at Big Trees and precipitation at Ben Lomond, Calif., to determine the effect of antecedent precipitation on streamflow

[Form of equation:  $Q = a + bP_n + cAP_n$ , where  $P$  is the precipitation depth (in millimeters) for the selected period,  $AP$  is the antecedent precipitation (in millimeters) preceding the day of peak discharge or the beginning of the flood period,  $n$  is the number of days, and  $Q$ ,  $a$ ,  $b$ , and  $c$  are defined below]

Peak discharge or runoff	Mean flow for period 1938-82	Intercept $a$	Coefficient $b$ for duration of flood	Coefficient $c$ for antecedent period of 60 days	Statistical measure of regressions	
					Correlation coefficient ( $r^2$ )	Standard error of estimate ( $S_e$ )
Peak discharge ( $m^3/s$ )---	$0.232 \times 10^3$	$-0.188 \times 10^3$	$2.72 \times 10^3$	56.0	.71	$0.125 \times 10^3$
1-day runoff ( $m^3$ )-----	$9.62 \times 10^6$	$-9.61 \times 10^6$	$127 \times 10^6$	$2.40 \times 10^6$	.71	$5.10 \times 10^6$
3-day runoff ( $m^3$ )-----	$17.4 \times 10^6$	$-14.9 \times 10^6$	$119 \times 10^6$	$16.7 \times 10^6$	.80	$6.96 \times 10^6$
8-day runoff ( $m^3$ )-----	$24.7 \times 10^6$	$-17.0 \times 10^6$	$122 \times 10^6$	$10.4 \times 10^6$	.80	$9.17 \times 10^6$

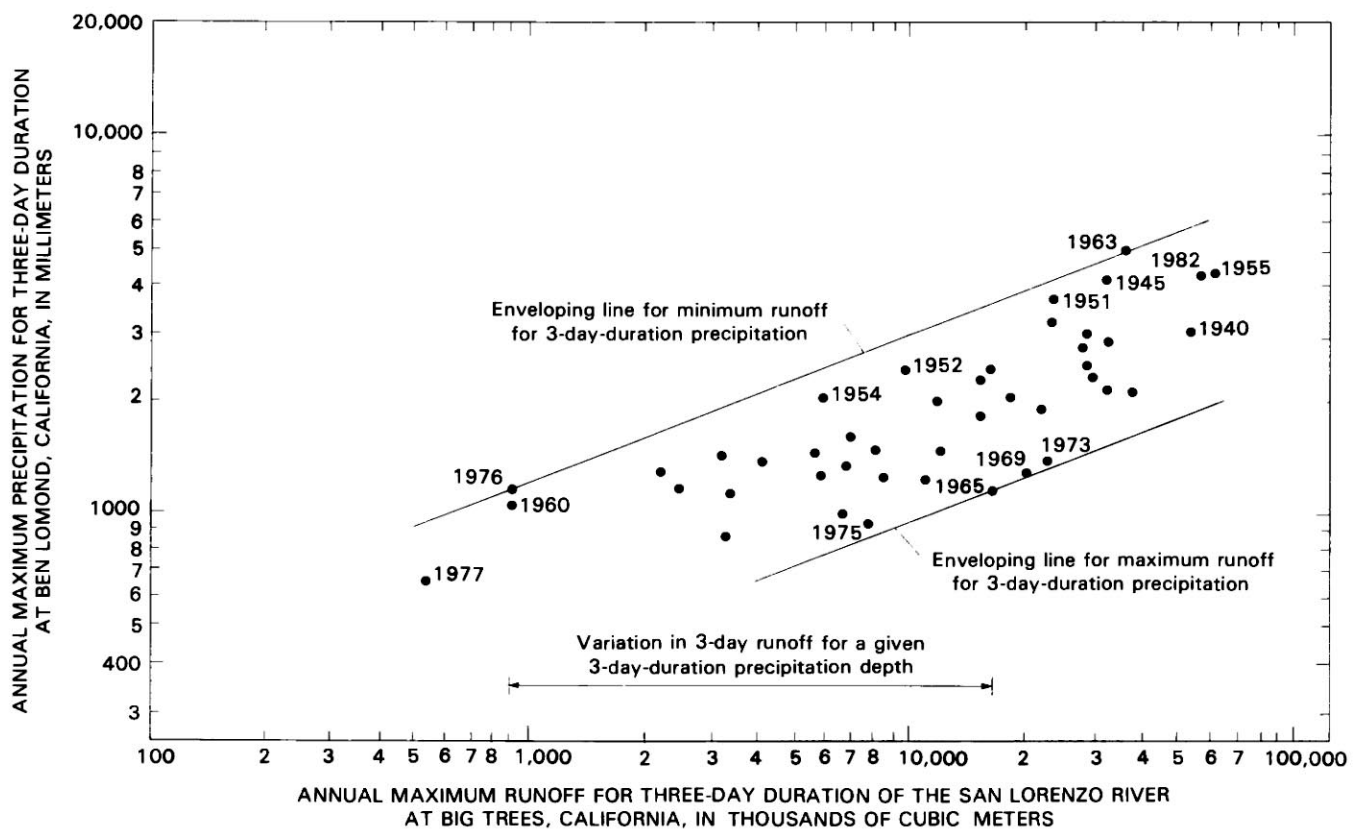


FIGURE 13.6.—Runoff of the San Lorenzo River at Big Trees for a 3-day period, versus precipitation at Ben Lomond. Dates indicate year of flood.

## SUMMARY

1. Antecedent precipitation for 2 months before the January 3-5, 1982, storm was more than 100 percent of normal.
2. The maximum 1-day precipitation of the December 1955 storm averaged 26 mm (1 in.) less than that of the January 1982 storm.
3. For 3- and 8-day periods, precipitation during the December 1955 storm was about 38 mm (1.5 in.) greater than during the January 1982 storm.
4. Unit peak discharge of the January 1982 flood for the study area ranged from 0.91 to 6.84 ( $\text{m}^3/\text{s}/\text{km}^2$ ); the smaller amounts were on the east side of the Santa Cruz Mountains.
5. The median recurrence interval of the January 1982 peak discharge for 33 stations in the study area is 14 years. On the basis of data from six stations, the median recurrence interval for the December 1955 flood is 36 years.
6. In terms of flow volumes, the median recurrence intervals of the January 1982 flood for 1-, 3-, and 8-day periods are 22, 18, and 10 years, respectively. Corresponding recurrence intervals for the December 1955 flood are 62, 22, and 30 years.
7. Major floods on the San Lorenzo River are the result of greater than normal antecedent precipitation for a period as long as 60 days, combined with subsequent intense frontal-type storms.

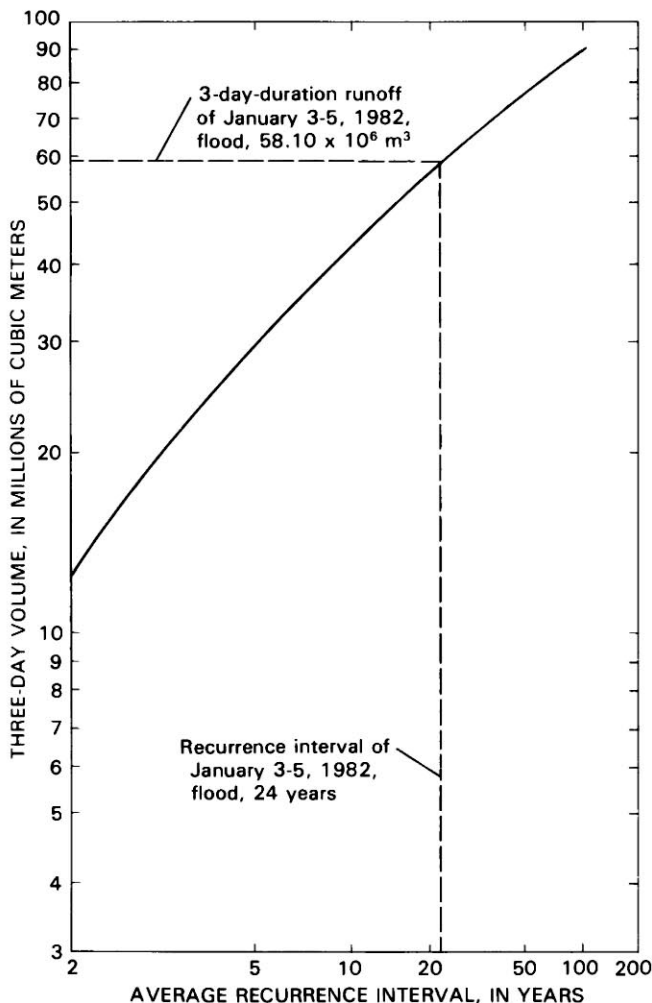


FIGURE 13.7.—Runoff for 3-day duration versus average recurrence interval for the San Lorenzo River at Big Trees. Curved line represents flood-frequency relation for 3-day flood volume based on 44 years of record.

## REFERENCES CITED

- Rantz, S.E., 1971, Precipitation depth-duration-frequency relations for the San Francisco Bay region, California: U.S. Geological Survey Professional Paper 750-C, p. C237-C241.
- U.S. Geological Survey, 1937-70, Surface-water supply of the United States: Water-Supply Papers 831, 861, 881, 901, 931, 961, 981, 1011, 1041, 1061, 1091, 1121, 1151, 1181, 1215, 1245, 1285, 1345, 1395, 1445, 1515, 1565, 1635, 1715, 1928, 1929, 1930, 1931, 2128, 2129, 2130, 2131.
- 1971-74, Water resources data for California, water years 1971-74, Part 1, volume 1, Colorado River basin, southern Great Basin, and Pacific slope basin, excluding Central Valley: Water-Data Reports CA 71-1 through CA 74-1.
- 1975-80, Water resources data for California, water years 1975-80, volume 2, Pacific slope basins from Arroyo Grande to Oregon State line except Central Valley: Water-Data Reports CA 75-2 through CA 80-2.
- U.S. National Oceanic and Atmospheric Administration, 1938-82, Climatological data, California: Asheville, N.C., v. 42-86.
- U.S. Water Resources Council, 1981, Guidelines for determining flood flow frequency: Hydrology Committee Bulletin 17B.
- Waananen, A.O., 1973, Floods from small drainage areas in California: A compilation of peak data, October 1958 to September 1973: Geological Survey open-file report, 261 p.





# 14. STREAM-CHANNEL RESPONSE TO THE STORM IN THE SANTA CRUZ MOUNTAINS

By K. MICHAEL NOLAN and DONNA C. MARRON,  
U.S. GEOLOGICAL SURVEY

## CONTENTS

Abstract	245
Introduction	245
Description of the study area	245
Location and physical characteristics	245
Climate, vegetation, and land use	246
Geology	247
Landslides	247
Storm effects on stream-channel morphology	247
Methods used to assess channel changes	248
Poststorm field observations	250
Low-order channels	250
Intermediate-order channels	251
High-order channels	254
Channel-geometry changes at gaging stations	254
Variations in channel response to previous storms	255
Sediment transport	257
Storm sediment transport	257
San Lorenzo River	257
Sediment transport at ungaged sites	258
Regional comparison of sediment transport	259
Interactions of processes within watersheds	260
Relations between sediment transport and channel changes	260
Interaction of hillslope and stream-channel processes	260
Contrast with hillslope and stream-channel interaction in other steep terrains	261
Geomorphic effectiveness of the storm	261
Summary	263
References cited	263

## ABSTRACT

Intense rainfall on January 3-5, 1982, in the Santa Cruz Mountains caused high streamflow and widespread landsliding. In the watersheds studied, recurrence intervals for peak streamflows were as much as 33 years, and recurrence intervals for maximum rainfall intensities were more than 100 years. Generalized channel response in these basins included scour in steep low-order channels and moderate filling in higher order channels. Large volumes of channel fill were noted along some channels, but this observation was limited to reaches that received large amounts of colluvium from debris flows and streamside debris slides. Such major effects were generally local and did not extend great distances upstream or downstream. The localization of these effects on channel geometry contrasts with the widespread depositional effects observed after major storms in steep terrain in other parts of California. This contrast may be related to the manner in which channel and hillslope processes interact.

Storm-related changes in channel morphology, coupled with frequency analysis of sediment transport, indicate that the morphology of most intermediate- and high-order channels is formed at least as much by events with moderate recurrence intervals as by extreme events. Along

low-order channels that were scoured during the storm and along isolated reaches of some intermediate- and high-order channels where filling was severe, however, storm effects will probably persist for long periods. Individual high-magnitude storms are therefore effective in modifying channel geometry, but only in some places. Because the localized effects of high-magnitude storms can persist longer than the recurrence interval of the storms themselves, channel morphology throughout the area probably reflects the effects of several storms.

## INTRODUCTION

The January 3-5, 1982, storm brought as much as about 600 mm (23.6 in.) of rain within a 36-hour period in the steep drainage basins of the Santa Cruz Mountains. This intense rainfall generated record or near-record flood peaks throughout the area and caused widespread shallow landsliding. This chapter assesses the effects of high streamflow on stream-channel geometry and sediment transport in three drainage basins within this steep terrain, and relates these effects to hillslope processes operating during the storm. The data presented have been collected from sites of previously established stream-gaging stations, as well as from postflood field investigations. Land use does not appear to have altered the natural response of stream channels to the storm, and so storm effects on manmade structures, though locally extensive, are described here only briefly (see chap. 12).

## DESCRIPTION OF THE STUDY AREA

### LOCATION AND PHYSICAL CHARACTERISTICS

Effects of the January 1982 storm were studied in the drainage basins of Soquel Creek, San Lorenzo River, and Pescadero Creek. These streams drain 300 km<sup>2</sup> in the Santa Cruz Mountains and are situated approximately 50 km southeast of San Francisco and 25 km west of San Jose (fig. 14.1). Elevations in the study basins range from sea level to more than 800 m along the crest of Ben Lomond Mountain. The San Lorenzo River watershed, which encompasses much of the study area, is highly asymmetric; short steep tributaries feed the main channel from the west, and longer, more gently sloping tributaries feed the main channel from the northeast. Several levels of marine terraces extend along some coastal sections of the study area.

Hillslopes within the study basins are relatively steep; average gradients range from 30 to more than 50 per cent, and stream gradients from 3 to 200 m/km. The steepest gradients occur along small low-order tributaries in the extreme upper parts of drainage basins. These small channels are only slightly incised into surrounding hillslopes, and bedrock is common along such channels. Low-order channels generally contain a relatively thin deposit of alluvium over the underlying bedrock. Larger, intermediate-order channels in the middle of the watersheds are typically V shaped and narrow, and are incised into the surrounding landscape more than the lower order channels. Because of this incision, steep hillslopes are common adjacent to these intermediate-order channels. Varying amounts of bedrock are exposed in the channel. Alluvium is commonly composed of sand or boulders surrounded by sand. The bedrock along intermediate-order channels is effective in reducing the rate of bank erosion in many localities. High-order channels in the downstream

parts of the study basins flow through alluviated valleys and show well-defined meander and point-bar morphology. The lowest stream gradients within the study basins are found along these channels. Flood plains developed adjacent to high-order channels generally buffer them from the direct input of colluvium from landslides.

#### CLIMATE, VEGETATION, AND LAND USE

The Santa Cruz Mountains have a Mediterranean climate, with moist cool winters and warm dry summers. Mean annual precipitation ranges from about 500 mm (19.7 in.) near the coast to about 1,500 mm (59.0 in.) on top of Ben Lomond Mountain. Rainfall occurs almost exclusively from November to March. The area frequently has coastal fog during the summer months.

Most ridgetops and hillslopes are densely vegetated by second-growth coastal redwood and associated Douglas-fir, oak, and madrone. Riparian vegetation is dominated

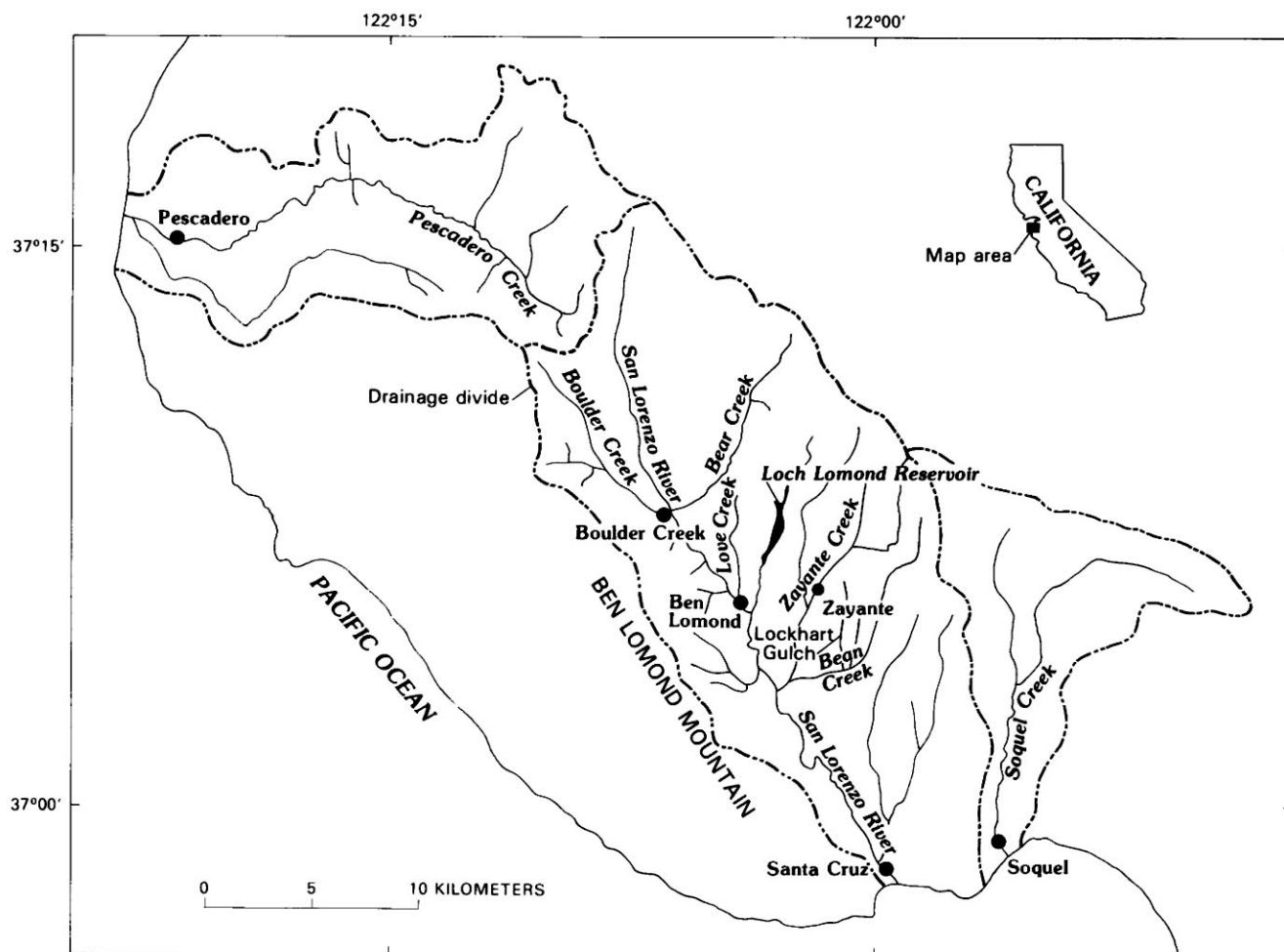


FIGURE 14.1.—Sketch map of study area in the Santa Cruz Mountains, west-central California.

by alder, willow, and cottonwood. Open prairies occur on some ridgetops and marine terraces.

Timber was harvested from most slopes in the study area during the early and middle 1900's. At present, low-density suburban development is the major land use. Artificial flow constrictions in stream channels and structures on low flood plains are common. The Santa Margarita Sandstone is quarried in parts of the Zayante Creek watershed.

#### GEOLOGY

Bedrock in the study area is dominated by a thick sequence of Tertiary units consisting of marine arkosic sandstone, mudstone, and interbedded volcanic rocks (Clark, 1981). Weathered materials from most units are predominately sand to gravel size and are readily transported by streams. The most common rock types are bedded mudstone, and sandstone with abundant mudstone interbeds. These stratigraphic units, which include the Santa Cruz Mudstone of late Miocene age and the Monterey Formation of middle Miocene age, are highly susceptible to landsliding and typically shed colluvium and alluvium that consist mostly of sand, gravel, and some boulders. Massive sandstone units, such as the Santa Margarita Sandstone of late Miocene age and the Lompico Sandstone of middle Miocene age, contribute predominately sand-size material to streams. These units are highly susceptible to dry raveling, sheetwash, and gullying, particularly where disturbed by quarrying and roadbuilding (Brown, 1973). Several Tertiary marine units crop out in most tributary drainages.

Stratigraphically beneath the Tertiary marine section are Cretaceous granitic and metasedimentary rocks, which crop out along the summit and on the flanks of Ben Lomond Mountain. Alluvium in creeks draining these rocks is rich in sand-size particles but contains more cobbles and boulders than does alluvium derived from the overlying Tertiary sedimentary rocks.

According to Clark (1981), major active faults in the Santa Cruz Mountains include the San Andreas fault, which lies inland of the study area, and the San Gregorio fault, which crosses Pescadero Creek approximately 5 km upstream from its mouth. Most folds and faults in the study area trend northwest. Some ridgetops and stream channels, particularly Ben Lomond Mountain, the San Lorenzo River downstream from Boulder Creek, and a tributary of Zayante Creek called Mountain Charlie Gulch, follow bedrock structures so aligned.

#### LANDSLIDES

Landslides are numerous throughout the study area (see "Introduction" to volume for landslide terminology).

Steep hillslopes combine with friable regolith in many places to give a high susceptibility to debris flows. Where the dip surfaces of bedding planes parallel hillslopes, the susceptibility to block slides is great. Debris slides are also common. Debris flows, block slides, and debris slides are triggered both by high pore-water pressures induced by intense rainfall and by undercutting due to streambank erosion. The role of streambank erosion, however, is somewhat limited because bedrock along many stream channels limits bank erosion. Such persistently active landslides as earth flows are sparse.

#### STORM EFFECTS ON STREAM-CHANNEL MORPHOLOGY

The January 1982 storm generated short-lived flood peaks on the study streams. Recurrence intervals of peak discharges in the Santa Cruz Mountains ranged from 4 to greater than 100 years (see chap. 13). The recurrence intervals of flood peaks varied as a result of the distribution of rainfall. Reported storm-rainfall totals ranged from 135 mm (5.3 in.) to 616 mm (24.3 in.) (Mark and others, 1983; see chap. 2). Maximum 24-hour precipitation intensities recorded during the storm were associated with recurrence intervals of greater than 100 years (J.P. Monteverdi, written commun., 1982). Maximum precipitation values were recorded along a northwest-southeast line running through the lower two-thirds of basins draining into the San Lorenzo River from the northeast.

The storm triggered numerous landslides throughout the study area. The most common features were debris flows and debris slides that were caused by high pore-water pressures induced in soils during the storm. Variations in precipitation intensity resulted in considerable variation in the spatial distribution of landslides and thus in the amount of colluvium introduced to different stream systems. The distribution of storm-related landslides is shown on plates 8 and 9 and discussed in chapter 8.

General effects of the storm on channel morphology included scour in small first- and second-order channels and filling in larger, higher order channels. In most places, effects from channel filling were either not particularly severe or are not likely to persist for a long period. In localized reaches, however, deposition caused severe decreases in stream cross-sectional area that may persist for long periods. This deposition occurred adjacent to large individual streamside debris slides and where small-scale landsliding was particularly abundant. Landsliding was most abundant in the basins that drain into the San Lorenzo River from the east and in the Soquel Creek basin (see chap. 8).



## METHODS USED TO ASSESS CHANNEL CHANGES

We assessed the effects of the January 1982 storm on stream channels in the San Lorenzo River, Soquel Creek, and Pescadero Creek watersheds, using field and airphoto observations and measurements, in addition to information from U.S. Geological Survey stream-gaging stations. To assess basinwide effects of the storm, stream reaches were described at study sites chosen to represent a range in stream size, bedrock type, and impact severity (fig. 14.2). The length of channel investigated at each study site equaled approximately five channel widths. We estimated sediment accumulation and scour in each reach, using botanical and physical evidence. Botanical evidence included burial of vegetation and exposure of roots in streambanks; physical evidence included burial of pre-flood surfaces by alluvium, burial of culverts and bridge aprons, and exposure of fresh bedrock, waterpipes, drains, and drainlines.

Table 14.1 lists the measured channel changes and basic physiographic parameters of the study sites. The measures of channel change listed in table 14.1 include average filling within the active channel, average decrease in cross-sectional area, and weighted sediment accumulation. The average decrease in channel cross-sectional area was calculated by dividing the total volume of flood deposits in each reach by the reach length; this area change includes both inchannel and overbank deposition. Because location of pre-flood channel levels along reaches characterized by scour proved to be difficult, no estimates of the volume of material removed by scour were made. Thus, table 14.1 contains only the word "scour" for those sites where evidence of pervasive channel scour was found. The weighted decrease in cross-sectional area represents the average decrease in cross-sectional area divided by the drainage area; this value was calculated to provide perspective on the amount of cross-sectional change relative to channel size. Gradients of stream

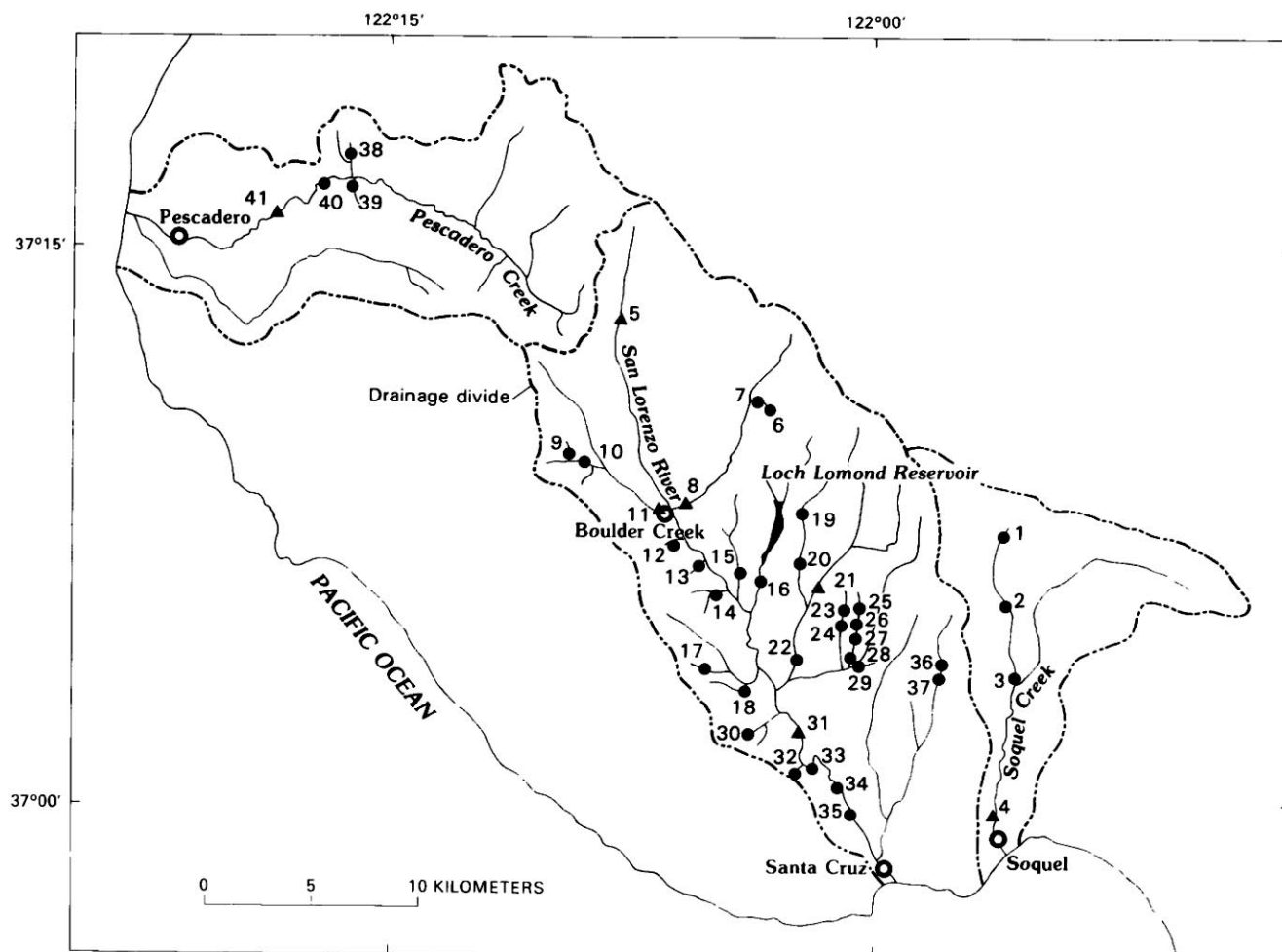


FIGURE 14.2.—Sketch map of study area, showing locations of study sites (dots) and U.S. Geological Survey stream-gaging stations (triangles). Numbers refer to tables 14.1 and 14.2.

TABLE 14.1.—Summary of physiographic parameters and channel scour or filling due to the January 3–5, 1982, storm at study sites in the Santa Cruz Mountains

Study site (see fig. 14.2)	Drainage basin	Drainage area (km <sup>2</sup> )	Average bankfull width (m)	Channel gradient (m/m)	Average depth of channel fill (m)	Average decrease in cross-sectional area (m <sup>2</sup> )	Weighted decrease in cross-sectional area (m <sup>2</sup> /km <sup>2</sup> )
1	Hester Creek-----	0.3	1.3	0.15	0.06	0.09	0.30
2	do-----	2.8	5.5	.023	.23	3.19	1.14
3	do-----	5.3	4.1	.0033	.08	.33	.06
14	Soquel Creek-----	104.1	---	.0050	.39	---	---
15	San Lorenzo River---	16.0	---	.021	.41	---	---
6	Unnamed tributary---	.3	1.2	.20	.08	.38	1.27
7	do-----	.4	.9	.11	0	-----Scour-----	---
18	Bear Creek-----	38.5	8.4	.0070	.31	.26	.01
9	Unnamed tributary---	.2	---	.20	0	-----Scour-----	---
10	Jamison Creek-----	3.4	4.2	.050	.16	.73	.21
111	Boulder Creek-----	29.3	8.4	.16	.03	.55	.02
12	Unnamed tributary---	.1	---	.36	0	-----Scour-----	---
13	do-----	.1	---	.20	---	---	---
14	Marshall Gulch-----	2.8	3.5	.011	.07	.99	.35
15	Love Creek-----	7.3	4.0	.025	.15	.92	.13
16	Newell Creek-----	23.2	7.6	.015	0	.30	.01
17	South Fall Creek----	1.1	1.1	.73	0	-----Scour-----	---
18	Bennett Creek-----	1.0	1.2	.011	.04	.06	.06
19	Lompico Creek-----	2.8	2.9	.033	.22	2.33	.83
20	do-----	5.5	2.2	.029	.42	2.82	.51
21	Zayante Creek-----	28.7	7.9	.017	.05	.78	.03
22	do-----	32.9	6.9	.010	.31	3.27	.10
23	Lockhart Gulch-----	1.7	2.8	.040	.49	1.53	.90
24	do-----	2.0	2.0	.022	.84	11.97	5.99
25	Ruins Creek-----	.8	1.5	.030	.51	4.19	5.24
26	do-----	1.0	1.7	.039	.08	.92	.92
27	do-----	1.9	2.5	.029	.72	3.09	1.63
28	do-----	2.0	2.4	.023	.17	.65	.33
29	Bean Creek-----	13.7	4.6	.010	.30	5.34	.39
30	Gold Gulch-----	2.2	2.1	.043	.09	.90	.41
131	San Lorenzo River---	288.8	19.0	.017	.47	8.67	.03
32	Unnamed tributary---	.1	---	.82	0	-----Scour-----	---
33	San Lorenzo River---	291.8	15.2	.0050	.46	40.02	.14
34	do-----	297.4	25.9	.0030	.46	23.04	.08
35	do-----	300.8	18.6	.0020	.46	21.88	.07
36	Branciforte Creek---	5.8	5.2	.013	.20	2.32	.40
37	do-----	7.3	5.4	.0090	.11	.68	.09
38	McCormick Creek----	2.9	3.8	.034	.13	.59	.20
39	Hoffman Creek-----	.8	1.2	.10	0	-----Scour-----	---
40	Pescadero Creek-----	107.8	12.6	.0030	.07	2.81	.03
141	do-----	118.9	13.9	.0040	.22	8.6	.07

<sup>1</sup>U.S. Geological Survey stream-gaging station.

reaches were measured on 1:24,000-scale topographic maps and thus represent average gradients above reaches. Local irregularities in gradient are not represented in these data.

Channel conditions portrayed on vertical aerial photographs taken on February 15, 1982, at a scale of 1:8,000 were compared with conditions depicted on preflood photographs. The steep, redwood-dominated hillslopes in the study area, coupled with low midwinter sun angles, made airphoto identification of flood effects possible only at the wider reaches of high-order channels.

Changes in channel geometry were more rigorously quantified at U.S. Geological Survey stream-gaging stations (fig. 14.2) by comparing changes in channel profiles drawn normal to the direction of streamflow (crossprofile). We compared preflood channel crossprofiles at these sites with postflood crossprofiles measured at similar discharges and at similar times of the year at the same locations. Crossprofile information was also used to gain a historical perspective on the channel changes caused by floodflows during the previous 42 years.

## POSTSTORM FIELD OBSERVATIONS

## LOW-ORDER CHANNELS

Most small stream channels observed after the storm showed evidence of recent scour (table 14.1). These first- and second-order channels (Strahler, 1954) have drainage areas of less than 0.10 km<sup>2</sup> and local gradients of more than 100 m/km. Many of these channels were scoured through older alluvium, so that underlying bedrock is now exposed (fig. 14.3). Channel fill was prevalent only above artificial constrictions, such as culverts blocked by sediment and by such organic debris as trees and bushes. Most accumulations of organic debris in unconstricted channel reaches formed open frameworks that were ineffective in trapping sediment (fig. 14.4).

Sediment was removed and transported through these steep channels by both high streamflow and debris flows. The effects of debris flows on channel morphology resembled those described by Campbell (1975) and Swanston

and Swanson (1976). Some debris flows apparently were highly fluid, and although they transported large volumes of sediment through steep reaches, they caused only minimal channel scour (fig. 14.5). In contrast, other in-channel debris flows stripped large amounts of alluvium and colluvium from steep reaches, commonly exposing bedrock and leaving much more obvious scars on the landscape (fig. 14.6). These effects closely resemble the scouring debris flows described by Campbell (1975), as well as the debris torrents described by Swanston and Swanson (1976). Campbell (1975) attributed variations in the erosive potential of debris flows to gradient steepness and, therefore, flow velocity, and to the moisture content of the moving material. Along low-gradient reaches at the mouths of some channels that received debris flows, large volumes of channel fill were spread over wide areas (fig. 14.7).



FIGURE 14.3.—Scour in second-order channel near Ben Lomond.



FIGURE 14.4.—Open framework of debris jam near Ben Lomond. Note nondeposition behind debris.



FIGURE 14.5.—Minor channel changes resulting from debris flow near the town of Boulder Creek. Note that most soil and vegetation remains in place upstream of house on left. Downstream deposition resulting from this activity is visible in figure 14.7.



FIGURE 14.6.—Scoured trail of debris flow in San Lorenzo River basin near Ben Lomond. Note removal of large amounts of vegetation and colluvium.



FIGURE 14.7.—Deposition and damage on low-gradient slopes below channel shown in figure 14.5. Despite absence of major channel changes upstream, large amounts of debris were transported through the channel and deposited on the low-gradient slopes shown here.

#### INTERMEDIATE-ORDER CHANNELS

Flood effects in intermediate-order channels varied considerably. Such observations were made primarily along third- and fourth-order channels with drainage areas of 1 to 50 km<sup>2</sup>. Although many reaches along these streams showed little or no effects from the storm, significant channel modification was observed along some reaches (table 14.1). Most of these channel modifications occurred where input of colluvium from large streamside debris slides or large debris flows overwhelmed the sediment-transport capacity of the affected channel (fig. 14.8). These effects were generally confined to the immediate area of colluvial input. In such places, large volumes of introduced colluvium were removed by streamflow with little or no effect on downstream reaches (fig. 14.9).



FIGURE 14.8.—Streamside debris slide in Soquel Creek. This slide, which entered the creek from the left side of the photograph, caused locally severe channel changes typical of those observed in many places that received exceptionally intense rainfall.



FIGURE 14.9.—Channel of Soquel Creek, 1.4 km downstream of severe channel changes shown in figure 14.8, showing absence of channel effects downstream of streamside landslide. Nonburial of pre-flood bouldery alluvium and minimal effects on riparian vegetation indicate a general absence of channel changes in this reach.



The most numerous and severe channel modifications were observed along the midbasins of Zayante and Bean Creeks. Figure 14.10 maps the distribution of weighted changes in cross-sectional area at all the study sites. Comparison of figure 14.10 with plate 2, which shows storm-rainfall totals, and with plates 8 and 9, which show the locations of storm-related landslides, indicates that the most numerous and severe channel modifications occurred in areas that were also characterized by the most landslides and the most storm rainfall. The relation between landslides and rainfall becomes particularly significant when normalized storm rainfall is considered (see chap. 8; table 8.3).

In a few areas, such as at study sites 19, 23, and 24, major channel modifications extended beyond the areas immediately adjacent to individual landslides. The deposits in these areas, which were characterized by poorly sorted, angular to subangular cobbles and gravel, suggested inchannel debris-flow activity (figs. 14.11, 14.12).

These deposits were commonly found overlying well-sorted sandy deposits, interpreted to be water-worked alluvium that was deposited before the debris flows. Debris-flow deposits were found only in the higher areas bordering stream channels, such as in overbank areas or on the tops of point bars. Post-debris-flow streamflow probably obscured evidence of debris-flow deposits in lower stream-channel positions.

Debris-flow deposits were found only along reaches adjacent to the most abundant landsliding. The mechanisms for formation of these inchannel debris flows are unclear. The debris flows may have been downchannel continuations of flows that started high in steep tributaries (Takahashi, 1980), or they may have been formed within intermediate-order channels, owing to sudden large increases in sediment load from abundant streamside debris slides and debris flows (Ashida and others, 1981). Some lithologic control was apparent on the occurrence of in-channel debris flows. Debris-flow deposits were found only

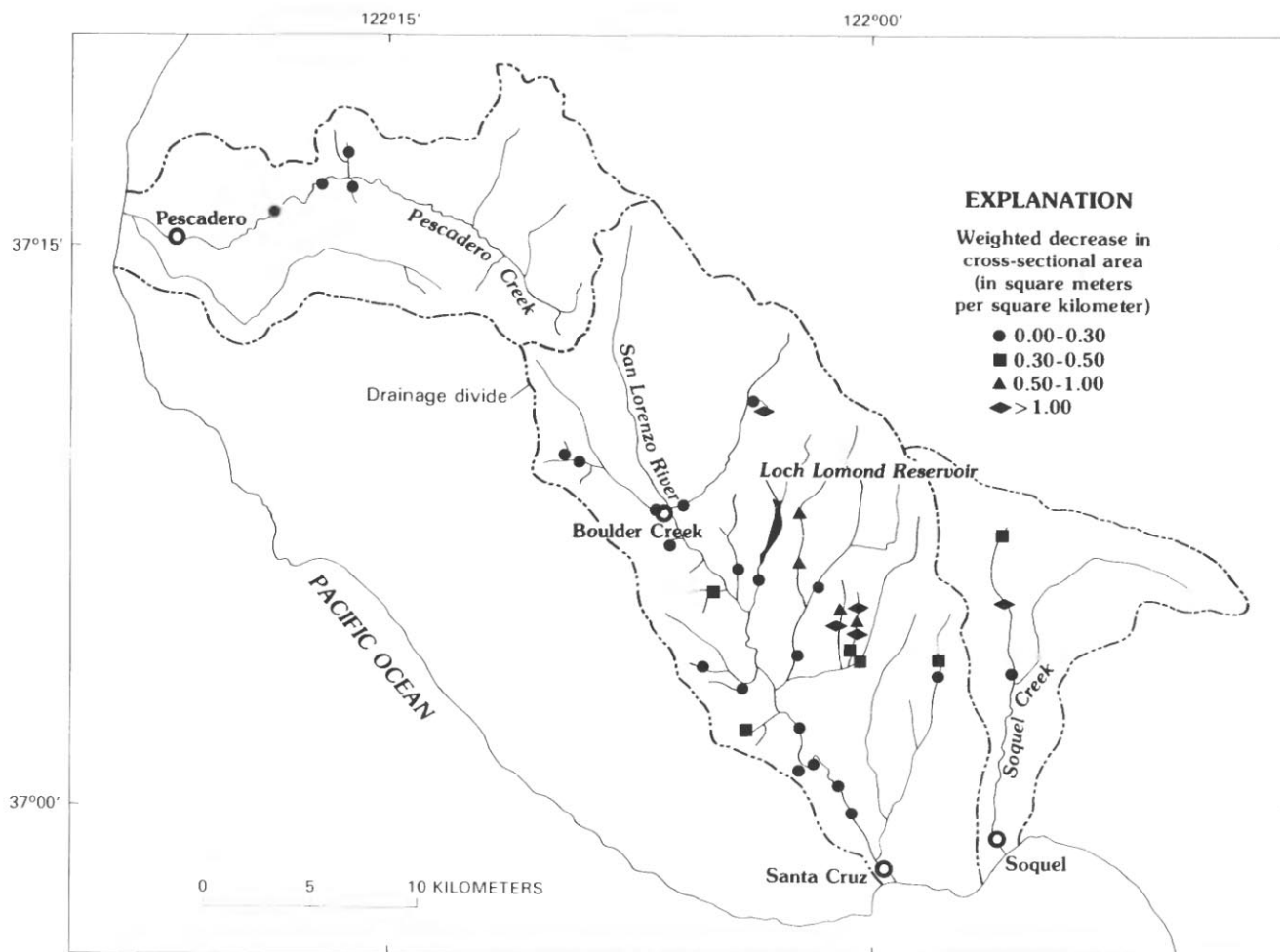


FIGURE 14.10.—Sketch map of study area, showing distribution of measured sediment accumulation. Weighted decrease in cross-sectional area at each site was calculated by dividing the volume of flood deposits by the product of the reach length times the drainage area.

in reaches receiving colluvium derived predominately from well-consolidated mudstone, siltstone, and sandstone. Well-sorted, noncohesive sandy colluvium introduced from the Santa Margarita Formation, though exceptionally voluminous in some places, either was not conducive to debris-flow initiation or did not generate deposits that were easily recognizable as resulting from debris flows. As much as 0.84 m of average channel fill was observed in reaches subjected to debris flows.

Where landslides were numerous but evidence of inchannel debris flows was absent, the transport of colluvium and alluvium by floodwaters generated as much as 0.72 m of average channel fill. The most extensive and voluminous channel fill and overbank-flood deposits in

these areas were observed at or near study sites 20, 25, 27, and 29 (figs. 14.13, 14.14). Fluvially reworked deposits consisted predominantly of well-sorted sand and gravel. Naturally extensive deposition appeared to have been augmented by the blocking or overloading of artificial flow constrictions (bridges and culverts) by organic and inorganic debris (fig. 14.15). Some local bank erosion occurred where channel filling was great because stream-flow was affected by landslides and (or) organic debris (fig. 14.16).

Changes in intermediate-order channels throughout the rest of the study area were due predominantly to deposition of moderate amounts of well-sorted alluvium. Average channel fill ranged from 0 to 0.30 m in thickness.

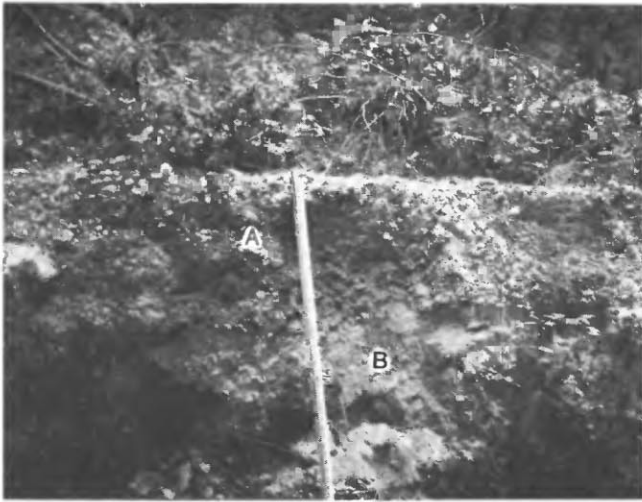


FIGURE 14.11.—Debris-flow deposit in Lockhart Gulch at study site 23. Deposit consists of approximately 0.50 m of poorly sorted material composed predominantly of sand and gravel (A) over approximately 0.25 m of well-sorted sand (B).



FIGURE 14.12.—Massive flood berms in Lockhart Gulch at study site 24. The sedimentology of the deposits at this site and immediately upstream (fig. 14.11) suggests that the massive deposits along this reach resulted from inchannel debris-flow activity.



FIGURE 14.13.—Channel fill in Bean Creek at study site 29. Note absence of streambanks and burial of riparian vegetation.



FIGURE 14.14.—Overbank deposits in Bean Creek near study site 29. This area contained some of the thickest overbank deposits observed in the study area.

Hydrologists who have a long-term familiarity with the stream-gaging sites in the area noticed a postflood increase in the amount of sandy alluvium filling interstices between cobbles and boulders in many channels (S.H. Holford, oral commun., 1982). Although such changes may be pervasive throughout the study area, they generally are too subtle to be documented by the available data. Streambank scour was evident in both highly and moderately affected reaches, but major changes in bank-to-bank channel width were uncommon. Streambanks in the study area are typically quite stable, owing to bedrock control and buttressing by riparian vegetation (fig. 14.17).

#### HIGH-ORDER CHANNELS

Moderate channel filling was common in larger high-order channels as a result of the storm. Observations were

made along channels with drainage areas of 100 to 300 km<sup>2</sup>. Average channel fill recorded in these places ranged from 0.07 to 0.47 m; much of this sediment was transported from upstream reaches and deposited in wide, low-gradient reaches characteristic of the high-order channels. Point-bar and overbank deposits of well-sorted sand, though not everywhere particularly thick, were extensive (figs. 14.18, 14.19). Direct colluvial input to the reaches was minimal because flood plains were wider than those of smaller streams and prevented most landslide material from directly entering stream channels. Large amounts of organic debris were removed from and redeposited along many infrequently occupied portions of floodways (fig. 14.20). Because the last major flood to occupy many floodway areas occurred in 1955, vegetation had 27 years to become established in such areas.

#### CHANNEL-GEOMETRY CHANGES AT GAGING STATIONS

We also assessed storm-related changes in the geometry of intermediate- and high-order channels at seven stream-gaging stations operated by the U.S. Geological Survey (see fig. 14.2), using techniques similar to those of Hickey (1969) and Lisle (1981). We assessed changes in channel crossprofiles and median streambed elevations at five of these stations, using data collected during water-discharge measurements at fixed locations, such as bridges and cableways, and during leveling surveys conducted during indirect measurements of water discharge. When data collected during water-discharge measurements at fixed locations were used, preflood data were selected to conform as closely as possible to the time of year and to the rate of water discharge associated with the available postflood data. This selection limited any



FIGURE 14.15.—Damage to manmade structures along tributary to Lockhart Gulch. The volume of water and debris transported during the storm totally overwhelmed the small box culvert (arrow) and destroyed some streamside structures.



FIGURE 14.16.—Streambank erosion caused by deflection of streamflow by organic debris in Love Creek.



FIGURE 14.17.—Channel widening limited by bedrock along streambanks in Zayante Creek. Although high water along this and many other reaches extended from bank to bank and removed riparian vegetation, it did not cause streamside instability.

ambiguity that might be caused by scour and fill associated with variations in the rate of water discharge or seasonal variations in bed elevations. Median streambed elevations were used rather than mean elevations, to deemphasize the effects of extreme elevations associated with streambanks. Lisle (1981) discussed more completely the ambiguities caused by scour and fill and the use of median streambed elevations.

At two gaging stations, the fixed location for highwater measurements was inappropriate for assessing changes in channel geometry. Discharge measurements on the San Lorenzo River near Boulder Creek were made at a culvert, and those at Zayante Creek at a bridge that severely constricted the channel. At these two locations, changes in channel geometry were assessed by using

mean streambed elevations, which were determined during low-flow measurements by wading. This technique introduces additional error because the locations of wading measurements are not precisely fixed in space; Hickey (1969) suggested that an error of  $\pm 0.15$  m is associated with such comparisons. Thus, we used mean streambed elevations, rather than median elevations, for these comparisons because of the limited streambank heights associated with these low-flow wading measurements. These elevations were calculated by subtracting the mean depth during the discharge measurement from the gage height associated with the measurement. Elevations of the thalweg (the deepest part of the channel) were also calculated for all study sites by subtracting the greatest depth during a given discharge measurement from the gage height associated with that measurement. The data on channel geometry at the stream-gaging stations are summarized in table 14.2. Preflood and postflood cross-profiles of Boulder Creek and the San Lorenzo River are shown in figures 14.21 and 14.22.

Five of the seven stream-gaging stations showed some degree of poststorm channel filling. The greatest measured changes were on the San Lorenzo River at Big Trees, on Pescadero Creek, and on Soquel Creek. The median streambed elevation of the San Lorenzo River rose 0.85 m, the bed of Pescadero Creek rose 0.56 m, and the bed of Soquel Creek rose 0.39 m. Changes in streambed elevations at the other stations ranged from 0.46 m of scour on Bear Creek to 0.06 m of fill on the San Lorenzo River near Boulder Creek.

#### VARIATIONS IN CHANNEL RESPONSE TO PREVIOUS STORMS

Available data from 1936 to 1982 for the stream-gaging station on the San Lorenzo River at Big Trees indicate that the January 1982 storm affected that channel at least



FIGURE 14.18.—Flood berm in downstream reach of Pescadero Creek near study site 40. This berm was typical of many observed along downstream reaches of high-order channels in the study area.



FIGURE 14.19.—Detail of flood berm shown in figure 14.18. This and most other such deposits observed along high-order channels in the study area consisted of well-sorted crossbedded sand. Lens cap for scale.



FIGURE 14.20.—Organic debris deposited along downstream reach of Soquel Creek.



TABLE 14.2.—*Prestorm and poststorm stream-bed elevations at U.S. Geological Survey stream-gaging stations*

[Median and mean bed elevations are heights above gage datum. Do., ditto; n.a., not available]

Stream-gaging station	Location	Study site (fig. 14.2)	Date	Median bed elevation (m)	Mean bed elevation (m)	Thalweg elevation (m)	Water discharge (m <sup>3</sup> /s)	Type of measurement	Location
11160000	Soquel Creek at Soquel.	4	1/15/80 2/17/82	0.52 .91	--- ---	0.32 .84	10.5 10.2	Cable-----	Cable.
11160020	San Lorenzo River near Boulder Creek.	5	12/16/81 1/07/82	--- ---	.50 .56	.41 .35	.04 1.09	Wading-----	15 m above gage.
11160060	Bear Creek near town of Boulder Creek.	8	3/21/78 1/15/82	1.18 .72	--- ---	-.15 -.21	n.a. n.a.	Survey-----	60 m above gage.
11160070	Boulder Creek near town of Boulder Creek.	11	3/24/78 3/10/82	1.49 1.34	--- ---	.94 .92	n.a. n.a.	do-----	8 m above gage.
11160300	Zayante Creek at Zayante. <sup>1</sup>	21	11/25/81 1/19/82	--- ---	.31 .31	.21 .24	.15 .30	Wading-----	55 m above gage.
11160500	San Lorenzo River at Big Trees.	31	1/11/80 1/06/82 3/16/82	.45 1.30 .98	--- --- ---	.33 .90 .68	29.2 40.8 15.0	Bridge-----	At bridge.
11162500	Pescadero Creek near Pescadero.	41	2/21/80 1/06/82	-.27 .29	--- ---	-.40 -.14	30.6 15.6	do-----	Do.

<sup>1</sup>Bed elevation controlled by concrete weir with dropoff on downstream side.

as much as any other storm did during the period of record. Effects of previous floods in February 1940 and December 1955 are evident in the variation of mean low-flow streambed elevations (fig. 14.23) and by comparison of channel crossprofiles before and after those floods (figs. 14.24, 14.25). The data plotted in figure 14.23 indicate that the effects of these earlier storms were no greater than those associated with moderate flows during the rest of the record. Figures 14.23 and 14.24 show

that the 1940 storm caused slight channel filling, which persisted to some degree until 1943. Figure 14.25 shows that the 1955 storm, unlike the 1940 and 1982 storms, caused moderate channel scour.

Differences in storm characteristics may have caused the observed contrast in channel response. The 1940 storm was a short, discrete event that occurred late in the rainy season. In contrast, the 1955 storm was a longer event that occurred early in the rainy season. The greater

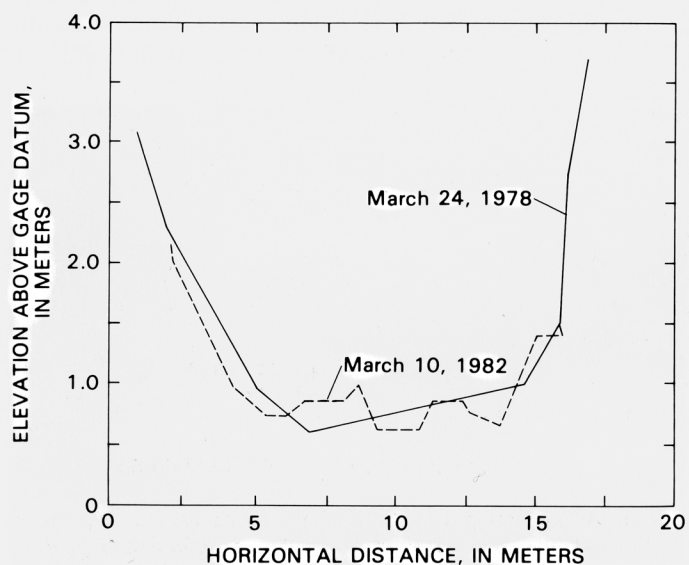


FIGURE 14.21.—Crossprofiles of Boulder Creek before and after the storm, showing dates of survey.

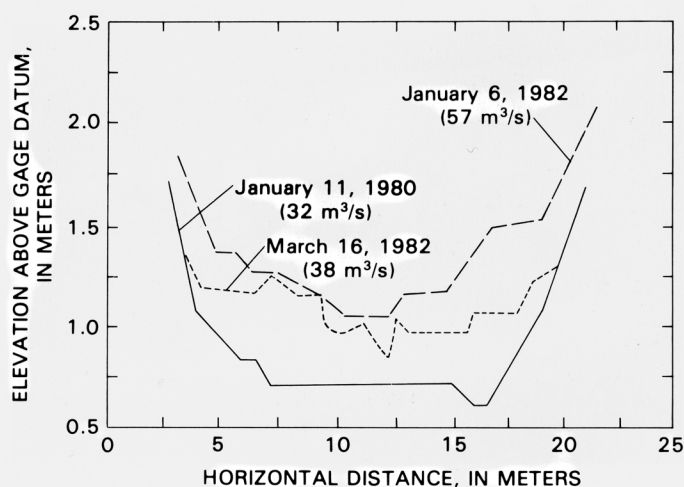


FIGURE 14.22.—Crossprofiles of the San Lorenzo River at Big Trees before and after the storm, showing dates of survey and discharges.

volume of streamflow associated with the 1955 storm may have been sufficient to transport all the available sediment and thus cause net channel scour at the stream-gaging station on the San Lorenzo River. Total 7-day streamflow during the 1955 storm was 81.4 million  $\text{m}^3$ , whereas that during the 1940 storm was only 65.3 million  $\text{m}^3$ .

Streams may also have carried additional sediment supplied by landslides during the 1940 storm. Because that storm occurred later in the rainy season, soil moisture may have been higher, and hillslopes more prone to landsliding. No definitive means exist, however, for assessing the relative amount of landsliding associated with these two storms. Examination of available preflood and postflood aerial photographs was inconclusive, owing to the small scale of the photographs, dense vegetal cover, and the small size of most landslide features.

## SEDIMENT TRANSPORT

### STORM SEDIMENT TRANSPORT

#### SAN LORENZO RIVER

Despite the short duration of the January 1982 storm, large amounts of sediment were transported by all stream systems throughout the study area. The total suspended-sediment transport of the San Lorenzo River at the Big Trees stream-gaging station from January 4 to 6 was 940,700 Mg, or 3,420  $\text{Mg}/\text{km}^2$ . Bedload discharge for these three days has been estimated at 3,320 Mg, or 12.1  $\text{Mg}/\text{km}^2$  (L.F. Trujillo, written commun., 1982). The water and sediment discharges for this event are plotted in figure 14.26. The importance of these data may best be viewed from the perspective of the sediment record at this station. The 3-day total of 944,000 Mg is 5.8 times

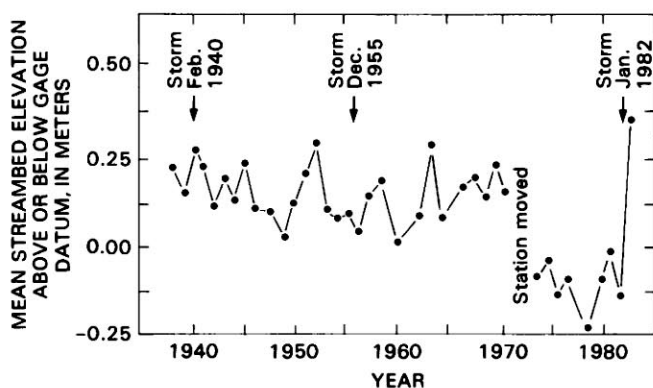


FIGURE 14.23.—Variations in mean streambed elevation of the San Lorenzo River at Big Trees, determined from low-flow water-discharge measurements between April and October at sites from 30 to 60 m upstream from the gage (pre-1973) and from 0 to 10 m downstream from the gage (post-1973).

the average annual total-sediment load at this station for the period 1973–80 (table 14.3) and represents 42 percent of all the sediment transported between 1973 and 1980 plus the 3 days of January 4–6, 1982.

The role of extreme events in transporting sediment in the San Lorenzo River resembles that in other mountainous areas of California. Hawkins (1982) assessed the magnitude and frequency of suspended-sediment transport at five stream-gaging stations in northwestern California. His data indicate that 50 percent of the sediment transported by northern California streams is carried by daily discharges that occur on the average of at least 1.9 days per year and that 90 percent is carried

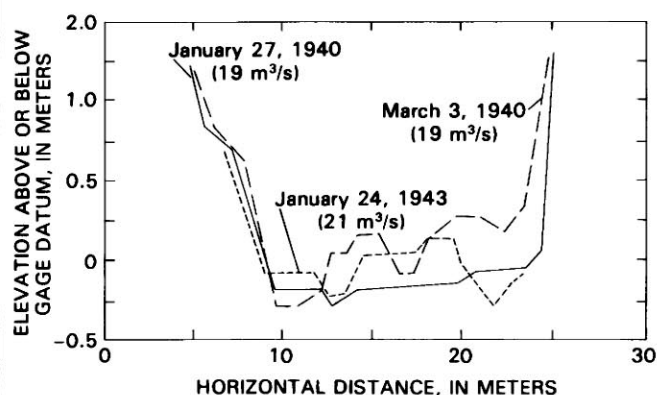


FIGURE 14.24.—Crossprofiles of the San Lorenzo River at Big Trees before and after flood of February 27, 1940, determined during discharge measurements at stream-gaging station. Dates of survey and discharges are given. Note tendency toward channel filling as a result of the flood.

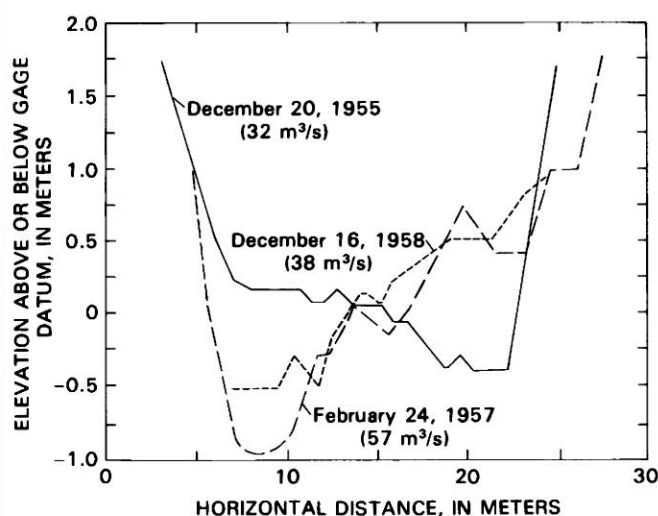


FIGURE 14.25.—Crossprofiles of the San Lorenzo River at Big Trees before and after flood of December 23, 1955, determined during water-discharge measurements at stream-gaging station. Dates of survey and discharges are given. Note tendency toward channel scouring as a result of the flood.

by flows that occur on the average at least once every 12.5 years or 0.08 days per year. Similar analysis of suspended-sediment data collected between water years 1973 and 1980 and January 4-6, 1982, on the San Lorenzo River indicate that 50 percent of the suspended sediment is transported by daily discharges that occur on the average of 2.0 days per year and that 90 percent is carried by flows that occur on the average of once every 15 years or 0.07 days per year. Infrequent flows appear to be more important in determining the magnitude and frequency of sediment transport in both these areas than in many other areas for which data are available (Wolman and Miller, 1960; Webb and Walling, 1982). The effectiveness of infrequent flows probably results from the large amounts of sediment delivered to channels by hillslope processes operating during high-flow periods, the steepness of stream channels in these mountainous areas, and the effects of highly varying flow, as described by Baker (1977).

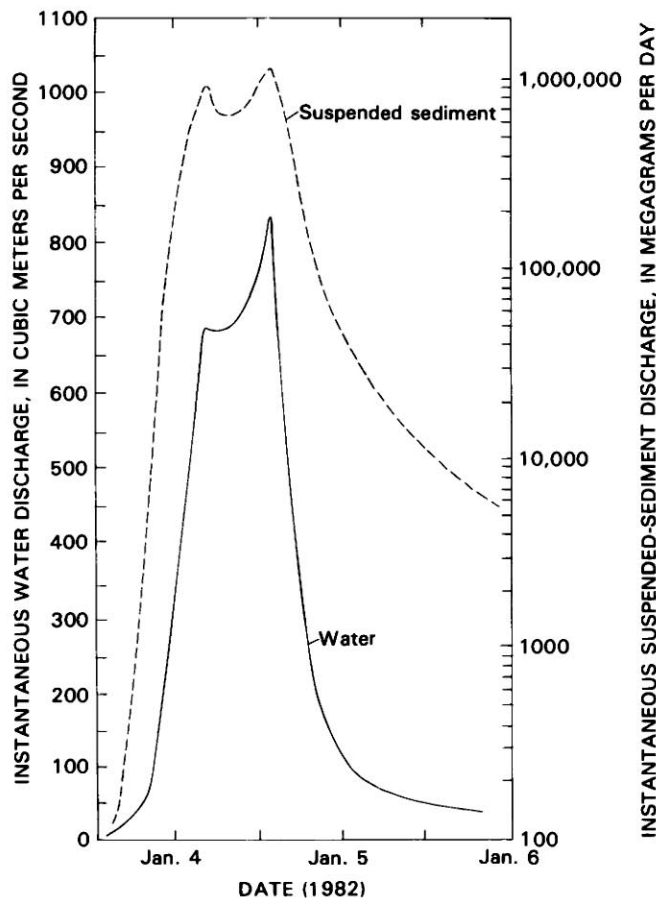


FIGURE 14.26.—Water and sediment discharge from the San Lorenzo River at Big Trees during period of the January 1982 storm.

TABLE 14.3.—Sediment discharge of the San Lorenzo River at Big Trees (sta. 11160500)

[Time interval is water year unless otherwise noted.  
All values in megagrams; n.a., not available]

Time interval	Suspended-sediment discharge	Bedload discharge	Total sediment discharge
1973	397,500	13,450	411,000
1974	84,700	10,600	95,300
1975	58,200	5,540	63,740
1976	481	94	575
1977	510	7	517
1978	304,400	12,400	316,800
1979	26,200	655	26,850
1980	383,500	3,740	387,300
1981	16,900	n.a.	---
Jan. 4-6, 1982	940,700	3,320	944,000

#### SEDIMENT TRANSPORT AT UNGAGED SITES

Although the most easily quantifiable information on sediment transport is from the San Lorenzo River, post-flood field observations indicate that sediment transport throughout the entire study area was high. Scour in lower order channels, deposition of midchannel and overbank alluvium and debris-flow deposits, and accumulation of large volumes of alluvium behind such flow constrictions as culverts and bridges all indicate that large amounts of sediment were transported by nearly all the stream systems.

The massive accumulations of sediment behind such flow constrictions as culverts and debris jams indicate that large amounts of sediment were transported through reaches where the flood caused minimal effects on channel geometry or riparian conditions. The amount of sediment transported by one small steep tributary (study site 13, fig. 14.2) was estimated by measuring the amount of sediment deposited behind a small-diameter (1 m) culvert that plugged during the storm (fig. 14.27). High-water marks indicate that the wingwall surrounding this culvert was overtopped by flow and that water was ponded 40 m upstream from the culvert. The flat tops of the backwater deposits, their concordant tops, and the sediment adhering to a tree in the center of the deposit (fig. 14.27) suggest that backwater deposits filled the entire area and that the void now present in the middle represents scour by flow after unplugging of the culvert. Field measurements indicate that approximately 145 m<sup>3</sup> of sediment remained behind the culvert and that, assuming that sediment once filled the void between the flat-topped lateral berms, scour has removed approximately

575 m<sup>3</sup> of sediment. Using a specific weight<sup>1</sup> of sediment of 1.3 g/cm<sup>3</sup>, these data indicate a possible 3-day unit-sediment yield of 9,400 Mg/km<sup>2</sup>, approximately 2.7 times the 3-day unit-sediment yield of the San Lorenzo River at Big Trees. Unit-sediment yields, which are calculated by dividing sediment yields by the drainage area, are used in drainage-basin comparisons. The estimated 3-day unit-sediment yield for this small tributary seems high but is not unreasonable in comparison with the suspended-sediment data collected on Zayante and Newell Creeks between water years 1970 and 1973 (Brown, 1973; U.S. Geological Survey, 1973). The maximum annual yield reported for these two study sites was 2,760 Mg/km<sup>2</sup> for Zayante Creek during the moderate-flow year 1973. The episodicity of sediment transport in this terrain and the somewhat lower gradient of Zayante Creek (table 14.1) indicate that yields of far more than 2,760 Mg/km<sup>2</sup> can be expected from the tributary at study site 13. Sediment yields from tributaries in which storm effects were particularly severe may have been significantly higher than that estimated at study site 13, particularly in stream reaches subjected to debris flows.

#### REGIONAL COMPARISON OF SEDIMENT TRANSPORT

Despite apparently high sediment yields during storms in the Santa Cruz Mountains, from a regional perspective, annual unit-sediment yields of the San Lorenzo River are not exceptionally high. Low average annual runoff, rather than sediment-transport capacity, accounts for this discrepancy. In comparison, the 720-km<sup>2</sup>-area Redwood Creek watershed in northwestern California has one of the highest annual unit-sediment yields in the conterminous United States (Janda and Nolan, 1979b). The San Lorenzo River's suspended-sediment-transport curve, which relates volume of water to suspended-sediment discharge, resembles that of Redwood Creek (fig. 14.28). Although the San Lorenzo River has a potential for high annual sediment transport, annual unit-sediment yields are limited by the amount of annual runoff. For example, the average annual runoff for Redwood Creek between water years 1973 and 1980 was 1,200 mm, whereas the average annual runoff from the San Lorenzo River during the same period averaged 420 mm. Average annual unit-sediment yields of the San Lorenzo River and Redwood Creek reflect their difference in average annual runoff. The average annual unit-sediment yield between 1973 and 1980 for Redwood Creek was 1,333 Mg/km<sup>2</sup>, whereas that for the San Lorenzo River was only 590 Mg/km<sup>2</sup>.

<sup>1</sup>Specific weight is from data presented by Brown (1973, fig. 1); 1.3 g/cm<sup>3</sup> is the density of the most sand rich deposit collected by Brown in the Loch Lomond Reservoir. This density was used because its grain-size distribution most nearly resembles that of sediment transported by the tributary studied.

The suspended-sediment discharge associated with a given water discharge on the San Lorenzo River increased after the January 1982 storm (fig. 14.29). Other investigators have noticed similar effects of storms on suspended-sediment-transport curves elsewhere (Anderson, 1968; Brown and Ritter, 1971; Knott, 1971). Janda and Nolan (1979a) suggested that the sediment discharge associated with a given water discharge directly depends on the amount of sediment readily available for transport. This observation is consistent with the poststorm situation in the San Lorenzo River because much of the sediment responsible for poststorm channel fill is in mid-channel areas and thus is available for transport during a wide range of flow conditions.

The suspended-sediment-transport curve of the San Lorenzo River did not shift upward until after the storm, as confirmed by the fact that a sample taken on January 6 falls within the prestorm relation. Because no suspended-sediment samples were taken during the slow recession in streamflow that occurred from January 6 to 20, it is not known exactly when the shift in the suspended-sediment-transport curve occurred. It seems reasonable, however, to assume that this shift occurred in response to a rise in streamflow on January 19–20. This shift may have been caused by downstream migration of sediment from upstream areas during the January 19–20 event. The higher position of the suspended-sediment-transport curve of the San Lorenzo River in figure 14.29 is probably temporary, as was the case elsewhere. The shift will last only as long as excessive sediment deposited during the storm remains in the channel.



FIGURE 14.27.—Backwater deposits resulting from plugging of culvert at study site 13.



## INTERACTIONS OF PROCESSES WITHIN WATERSHEDS

### RELATIONS BETWEEN SEDIMENT TRANSPORT AND CHANNEL CHANGES

The relation between sediment transport in tributary and mainstem channels displayed during the January 1982 storm seems to be consistent with that observed in other steep-land watersheds (Kelsey, 1977; Nolan and Janda, 1981). Steep stream gradients and relatively high water discharge per unit area from smaller areas generally caused the sediment-transport capacity of small streams to be exceptionally high during the storm and resulted

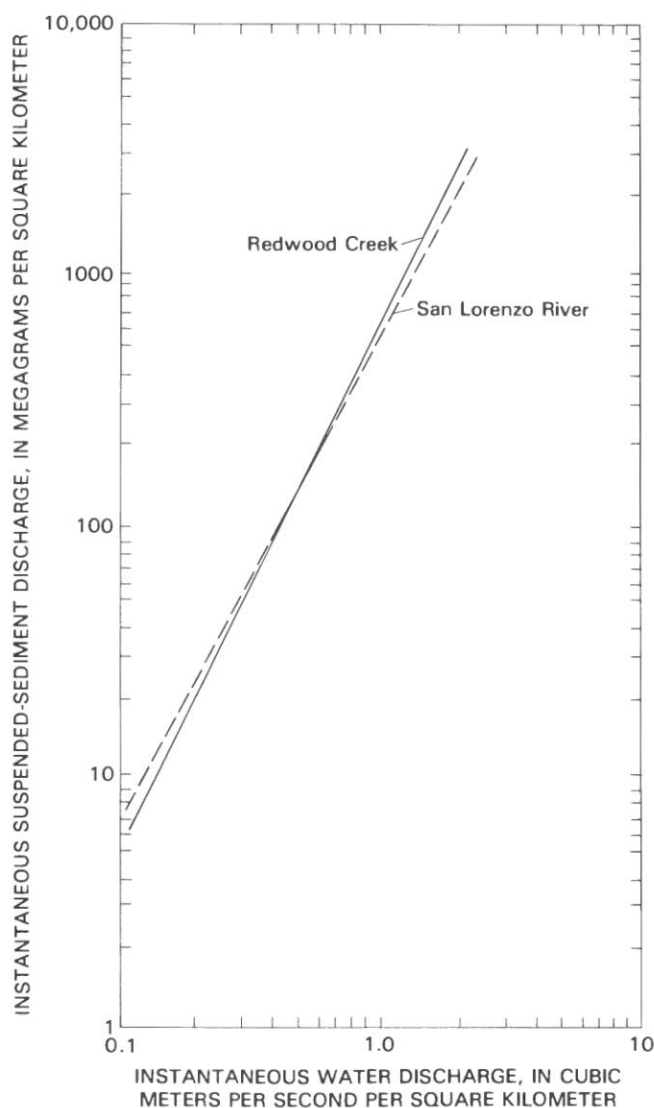


FIGURE 14.28.—Suspended-sediment transport during 1973-80 for the San Lorenzo River at Big Trees and for Redwood Creek at Orick. Curves were fitted to data by regression analysis; coefficients of determination: San Lorenzo River, 0.94; Redwood Creek, 0.95.

in channel scour. The propensity for scour in these steep first-order channels was aided by minimal colluvial input. These streams are only slightly incised into the surrounding hillslopes, hillslope segments adjacent to them are not particularly expansive or steep, and streamside landslides are relatively scarce. The sediment removed from these steep streams was transported to higher order channels, which generally have gentler gradients and lower unit runoff. Where sediment delivery from tributaries exceeded the transport capacity of higher order channels, filling resulted.

### INTERACTION OF HILLSLOPE AND STREAM-CHANNEL PROCESSES

Although the link between channel processes in the Santa Cruz Mountains appears to resemble that in steep terrain elsewhere, the interactions of physical processes in stream channels and on hillslopes contrast with such interactions in other areas. In the Santa Cruz Mountains, local geology and the distribution of rainfall intensity apparently control the extent of changes in channel geometry during major events. During the January 1982 storm, major depositional effects on stream channels were limited to reaches that received massive amounts of colluvium from landslides. Areas of most abundant sliding were, in turn, limited to areas of maximum precipitation intensity.

Although large volumes of sediment were transported out of highly affected channel reaches, this sediment did

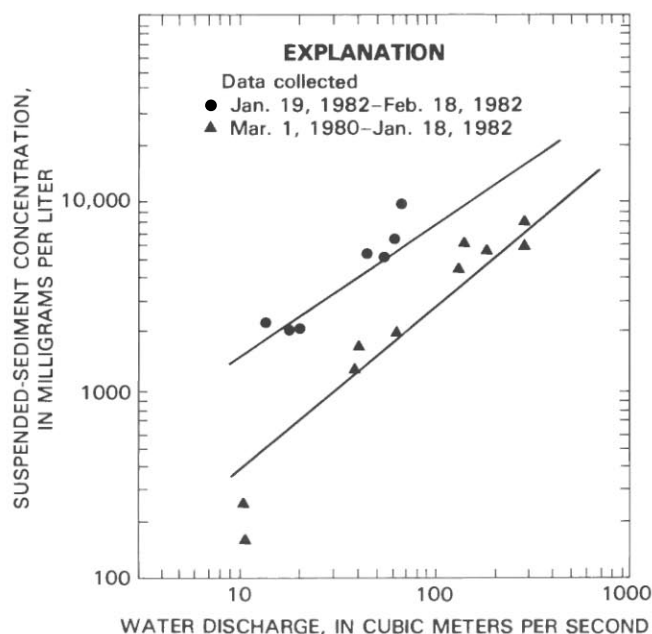


FIGURE 14.29.—Suspended-sediment transport of the San Lorenzo River at Big Trees. Curves were fitted by eye.

not cause widespread downstream channel modification. The high sediment-transport capacity of streams, due at least in part to steep gradients and the sandiness of the sediment load, limited downstream effects. Bedrock banks or dense and well-rooted riparian vegetation limited channel widening in most reaches. The absence of major increases in channel width, coupled with the relative stability of the lower parts of many streamside hillslopes, limited the amount of streamside landsliding. Much of the landsliding related to the storm apparently resulted from failures initiated in the upper parts of hillslopes in response to high-soil-moisture conditions (see chap. 5) and not from undercutting associated with channel widening.

#### CONTRAST WITH HILLSLOPE AND STREAM-CHANNEL INTERACTION IN OTHER STEEP TERRAINS

The interactions between hillslope and stream-channel processes in the Santa Cruz Mountains contrast with the interactions of these physical processes in steep terrains elsewhere in California. Studies by Stewart and LaMarche (1967), Janda and others (1975), Kelsey (1977), Harden and others (1978), and Lisle (1981) have illustrated that storms in northwestern California have had catastrophic effects on channel morphology throughout large drainage basins. High streamflow during these storms initiated numerous streamside debris slides by undercutting the toes of the inherently unstable hillslopes that occur throughout the area (Harden and others, 1978). The large volumes of colluvium from these debris slides overloaded the transport capacity of most channels and resulted in massive channel filling. Evidence has been reported for as much as 4 m of fill and channel widening by more than 100 percent in the Redwood Creek drainage basin as the results of a major storm in 1964 (Harden and others, 1978).

Stream channels in the rapidly eroding terrain common in northwestern California are particularly prone to aggradation because they commonly contain large amounts of sediment even without the effects of storms. This sediment includes deposits from previous storms (Janda and others, 1975), in addition to yearly input from persistently active mass movement (Harden and others, 1978; Janda and Nolan, 1979b). When this terrain is subjected to a major storm, stream channels already contain large amounts of readily transportable alluvium, and unstable streamside hillslopes found throughout the area fail easily when undercut by streamflow. This set of conditions appears to be responsible for initiating a series of positive-feedback loops during which colluvium from landslides causes channel aggradation and widening, which initiates further bank undercutting and streamside landsliding (Colman, 1973). This loop can result in widespread channel aggradation and hillslope failures even away from the locus of initial failure and channel fill.

Unlike stream channels in northwestern California, intermediate- and high-order streams in the Santa Cruz Mountains can transport a high percentage of the sediment supplied to them during storms because of their high transport capacity, because the sediment is commonly sand size, and because, before a major storm, channels do not contain exceptional amounts of sediment. Large volumes of storm-related sediment can be introduced into a channel before its transport capacity is reached. When channel modification does occur in the Santa Cruz Mountains, it does not propagate downstream. Limitation of bank undercutting by the bedrock along streambanks effectively prevents the positive-feedback effects seen in northwestern California.

#### GEOMORPHIC EFFECTIVENESS OF THE STORM

As discussed in the preceding sections, the effects of the January 1982 storm on channel geometry in the studied basins varied considerably. Scour was pervasive in lower order channels. In most of the study area, however, the effects of this storm on intermediate and high-order channels were minimal and generally no more severe than those of more frequently occurring events. In some localities, the storm caused severe channel modification that can be expected to last for a long time. Because of these varying effects, both the concept of geomorphic work suggested by Wolman and Miller (1960) and that of geomorphic effectiveness suggested by Wolman and Gerson (1978) seem to be relevant in assessing the role of the storm in shaping channel morphology throughout the study area.

Wolman and Miller (1960) suggested that the amount of geomorphic work done during individual events is measurable, at least in part, by the amount of sediment transported in such events. Their data indicate that for such streams as the Rio Puerco in New Mexico and Brandywine Creek in Delaware, daily discharges which recur more frequently than 6 and 11 times per year, respectively, transport 50 percent of the sediment and that these moderate flows control the shape of some fluvial landforms. Although the flows that transport 50 percent of the sediment in the Santa Cruz Mountains recur only 2 days per year and are therefore less frequent than in the study areas cited by Wolman and Miller, flows with such moderate recurrence intervals appear to have the potential to influence the morphology of channels in the Santa Cruz Mountains. The data presented here indicate that channel morphology along most intermediate- and high-order reaches is probably shaped at least as much by frequently occurring flow events as by catastrophic events. The morphology of such reaches either was not

modified significantly by the flood or is expected to return quickly to the preflood configuration. In such reaches, the concepts of Wolman and Miller (1960) probably apply.

In other reaches, however, channel geometry was severely modified by the flood of January 1982. These were the reaches scoured to bedrock by exceptionally high runoff or subjected to severe deposition related to the influx of overwhelming volumes of colluvium. Although most of these severe changes will subsequently be modified during more moderate events, the imprint of the storm will remain for a long time. In these areas, the concept of impact persistence proposed by Wolman and Gerson (1978) seems to apply. This concept suggests that if effects produced by a high-magnitude storm persist longer than the recurrence interval of the storm itself, the storm has long-term geomorphic significance. In such cases, the landscape always reflects the effects of high-magnitude storms. Channel geometry in these areas cannot be totally attributed to effects of more moderate events.

Storm-related changes in highly affected reaches persist because the forces tending to restore channel geometry to prestorm conditions either are not totally able to remove storm-related effects, act very slowly, or act only intermittently. The massive amounts of colluvium supplied to highly affected intermediate-order reaches by debris flows and debris slides totally rearrange channel morphology. The effects of this large volume of material are probably visible in the crossprofiles and longitudinal profiles of these channels for long periods. Channels incise through this debris and leave colluvial remnants along channel margins. Filling of voids left by scouring debris torrents or by simple scour in some first-order channels depends on slowly operating processes, such as soil creep. Although most overbank deposits in the study area are not particularly massive, some of the more massive of these deposits may persist for a long time. The degree to which the less massive overbank deposits can resist weathering and subsequent overbank flooding is uncertain.

The long-term persistence of effects of previous storms was evident in the landscape before the January storm. Field observations revealed multiple sites along intermediate-order streams where channels are exceptionally wide and gently sloped and where colluvium mantles adjacent hillslopes. Channels in these reaches are lined with well-established vegetation. These observations indicate that such reaches were probably the depositional sites of ancient landslides. Channels upstream and downstream of these sites are typically much steeper and narrower, and abut directly against steep hillslopes.

The persistence of storm-related effects also depends on the sequence of future events (Bevin, 1981). If the 1982 storm is followed by an exceptionally long storm-free

period, the effects of moderate events will become more obvious within the studied watersheds than will the effects of extreme events. The effects associated with future storms will also depend somewhat on the sequencing of those storms. For example, effects of another storm that might follow the one of January 1982 closely in time with maximum precipitation intensities in similar locations may cause substantially less impact than one with maximum precipitation intensities located elsewhere, or one that occurs hundreds or even thousands of years in the future.

In such areas as the Santa Cruz Mountains where debris slides and debris flows can contribute volumes of colluvium sufficient to modify channel geometries, it may be more appropriate to measure the persistence of impacts against the recurrence intervals associated with precipitation intensity than those associated with streamflow. The occurrence of debris slides and debris flows similar to those observed in the studied watersheds depends more on short-duration precipitation intensity (Campbell, 1975) than on the volume of water necessary to produce exceptionally high streamflow. Recurrence intervals associated with peak rainfall intensity for the January storm were considerably higher than those associated with peak streamflow. Although 24-hour precipitation recorded during the storm had estimated recurrence intervals of more than 100 years (J.P. Monteverdi, written commun., 1982), peak streamflows in the study area had estimated recurrence intervals between 7 and 33 years (see chap. 13).

Because of the high precipitation intensity associated with the January 1982 storm, postflood observations of channel behavior probably permitted assessment of the effects of a particularly effective geomorphic event with a relatively rare frequency of occurrence. Observations of the response of stream channels to this event and of gross preflood channel morphology indicate that the morphology of stream channels in the Santa Cruz Mountains reflects the effects of both moderate and catastrophic events. The morphology of most intermediate- and high-order channels appears to reflect the effects of moderate, at least as much as of catastrophic, events. However, the morphology of most steep low-order channels and of localized reaches along higher order channels strongly reflects the effects of extreme events because the scour along these low-order channels and the fill along these isolated reaches of larger channels can persist as long as or longer than the recurrence interval of the storm itself. If such storm-related effects persist for periods exceeding the recurrence interval of the storm, there is a reasonable probability that the effects of multiple storms could be found throughout the studied watersheds. This appears to be the case because the morphology of some reaches shows the influence of deposition of colluvium during previous storms.



## SUMMARY

In most of the channels studied, channel changes resulting from the January 3–5, 1982, storm in the Santa Cruz Mountains were not particularly severe and are not expected to persist for a long time. This absence of channel response occurred despite streamflow recurrence intervals of as much as 33 years and the large volumes of sediment that were transported through most stream systems in the study area. Significant channel changes did occur where low-order channels were scoured to bedrock and where colluvial input from debris slides and (or) debris flows was exceptionally voluminous. Depositional changes were mostly observed in areas characterized by maximum precipitation intensities because high pore-water pressures induced by this intense precipitation were a dominant triggering mechanism of landsliding. These major channel changes were commonly local because the positive-feedback loop between hillslope and stream-channel processes that is responsible for downstream propagation of storm-related channel changes elsewhere in California was not found to be effective in the Santa Cruz Mountains. In the Santa Cruz Mountains, bedrock along many stream channels limits the importance of channel widening as a mechanism for triggering stream-side debris sliding; stream-transport capacities are high, owing to steep gradients and sand-size alluvium and colluvium; and channels are relatively clear of sediment before major storms, owing at least in part to the absence of persistently active landslides.

Consideration of channel response to this and previous major storms suggests that channel morphology in the Santa Cruz Mountains is formed by both moderate and extreme events. For example, steep low-order channels generally contain only small amounts of alluvium because alluvium is periodically flushed from them during major storms. Some intermediate-order streams flow through alluvial channels that are relatively wide and flat, owing to deposition related to the influx of overwhelming volumes of colluvium. Elsewhere, channels of this size generally are V shaped and relatively steep, and appear to reflect the effects of moderate, at least as much as of extreme, events. Because the localized effect of a high-magnitude storm can persist longer than the recurrence interval of the storm itself, channel morphology throughout the study area probably reflects the effects of many storms. These effects are apparently scattered throughout the study area, owing to variation in the spatial distribution of maximum precipitation intensity.

## REFERENCES CITED

- Anderson, H.W., 1968, Major flood effect on subsequent suspended sediment discharge [abs.]: *American Geophysical Union Transactions*, v. 49, no. 1, p. 175.
- Ashida, Kazuo, Takahashi, Tamotsu, and Sawada, Toyooki, 1981, Processes of sediment transport in mountain stream channels, in Davies, T.R.H., and Pearce, A.J., eds., *Erosion and sediment transport in Pacific rim steeplands*: International Association of Hydrological Sciences Publication 132, p. 166–178.
- Baker, V.R., 1977, Stream-channel response to floods, with examples from central Texas: *Geological Society of America Bulletin*, v. 88, no. 8, p. 1057–1071.
- Bevin, Keith, 1981, The effects of ordering on the geomorphic effectiveness of hydrologic events, in Davies, T.R.H., and Pearce, A.J., eds., *Erosion and sediment transport in Pacific rim steeplands*: International Association of Hydrological Sciences Publication 132, p. 510–526.
- Brown, W.M., III, 1973, Erosion processes, fluvial sediment transport, and reservoir sedimentation in a part of the Newell and Zayante Creek basins, Santa Cruz County, California: U.S. Geological Survey open-file report, 31 p.
- Brown, W.M., III, and Ritter, J.R., 1971, Sediment transport and turbidity in the Eel River basin, California: U.S. Geological Survey Water-Supply Paper 1986, 70 p.
- Campbell, R.H., 1975, Soil slips, debris flows, and rainstorms in the Santa Monica Mountains and vicinity, southern California: U.S. Geological Survey Professional Paper 851, 51 p.
- Clark, J.C., 1981, Stratigraphy, paleontology, and geology of the central Santa Cruz Mountains, California Coast Ranges: U.S. Geological Survey Professional Paper 1168, 51 p.
- Colman, S.M., 1973, The history of mass movement processes in the Redwood Creek basin, Humboldt County, California: University Park, Pennsylvania State University, M.S. thesis, 180 p.
- Harden, D.R., Janda, R.J., and Nolan, K.M., 1978, Mass movement and storms in the drainage basin of Redwood Creek, Humboldt County, California—a progress report: U.S. Geological Survey Open-File Report 78–486, 161 p.
- Hawkins, R.H., 1982, Magnitude and frequency of sediment transport in three northern California coastal streams: Arcata, Calif., Humboldt State University, M.S. thesis, 68 p.
- Hickey, J.J., 1969, Variations in low-water streambed elevations at selected stream-gaging stations in northwestern California: U.S. Geological Survey Water-Supply Paper 1879-E, p. E1–E33.
- Janda, R.J., and Nolan, K.M., 1979a, Geomorphic controls on the form of suspended-sediment transport curves [abs.]: *Geological Society of America Abstracts with Programs*, v. 11, no. 6, p. 113.
- , 1979b, Stream sediment discharge in northwestern California, in *Natural and management-related erosion in Franciscan terrane of northern California*: Geological Society of America, Cordilleran Section Guidebook, Field Trip 12, p. 4–1 to 4–27.
- Janda, R.J., Nolan, K.M., Harden, D.R., and Colman, S.M., 1975, Watershed conditions in the drainage basin of Redwood Creek, Humboldt County, California, as of 1973: U.S. Geological Survey Open-File Report 75–568, 266 p.
- Kelsey, H.M., 1977, Landsliding, channel changes, sediment yield and land use in the Van Duzen River basin, north coastal California, 1941–1975: Santa Cruz, University of California, Ph.D. thesis, 370 p.
- Knott, J.M., 1971, Sedimentation in the Middle Fork Eel River basin, California: U.S. Geological Survey open-file report, 60 p.
- Lisle, T.E., 1981, Recovery of aggraded stream channels at gauging stations in northern California and southern Oregon, in Davies, T.R.H., and Pearce, A.J., eds., *Erosion and sediment transport in Pacific rim steeplands*: International Association of Hydrological Sciences Publication 132, p. 189–211.
- Mark, R.K., Newman, E.B., Northcut, C.R., and Hamachi, B.R., 1983, Rainfall associated with the January 1982 rainstorm in the San Francisco Bay region, California: U.S. Geological Survey Open-File Report 83–16, scale 1:250,000, 2 sheets.
- Nolan, K.M., and Janda, R.J., 1981, Use of short-term water and



- suspended-sediment discharge observations to assess impacts of logging on stream-sediment discharge in the Redwood Creek basin, northwestern California, U.S.A., in Davies, T.R.H., and Pearce, A.J., eds., *Erosion and sediment transport in Pacific rim steepplands*: International Association of Hydrological Sciences Publication 132, p. 415-437.
- Stewart, J.H., and LaMarche, V.C., Jr., 1967, Erosion and deposition produced by the flood of December, 1964, on Coffee Creek, Trinity County, California: U.S. Geological Survey Professional Paper 422-K, p. K1-K22.
- Swanston, D.N., and Swanson, F.J., 1976, Timber harvesting, mass erosion, and steeppland forest geomorphology in the Pacific Northwest, in Coats, D.R., ed., *Geomorphology and engineering*: Stroudsburg, Pa., Dowden, Hutchinson & Ross, p. 199-221.
- Strahler, A.N., 1954, Quantitative geomorphology of erosional landscapes: International Geological Congress, 19th, Algiers, 1952, Proceedings, sec. 13, pt. 3, p. 341-354.
- Takahashi, Tamotsu, 1980, Debris flow on prismatic open channel: American Society of Civil Engineers Proceedings, Hydraulics Division Journal, v. 106, no. HY3, p. 381-396.
- U.S. Geological Survey, 1973, Water resources data for California, water year 1973—part 2. Water quality records: Menlo Park, Calif., Water-Data Report CA-73-3, 654 p.
- Webb, B.W., and Walling, D.E., 1982, The magnitude and frequency characteristics of fluvial transport in a Devon drainage basin and some geomorphic implications: *Catena*, v. 9, no. 1, p. 9-23.
- Wolman, M.G., and Gerson, R., 1978, Relative scales of time and effectiveness of climate in watershed geomorphology: *Earth Surface Processes*, v. 3, no. 2, p. 189-208.
- Wolman, M.G., and Miller, J.C., 1960, Magnitude and frequency of forces in geomorphic processes: *Journal of Geology*, v. 68, no. 1, p. 54-74.

# 15. EPHEMERAL DELTA DEVELOPMENT AT THE MOUTH OF APTOS CREEK, NORTHERN MONTEREY BAY

By BRUCE M. RICHMOND,  
U.S. GEOLOGICAL SURVEY

## CONTENTS

	Page
Abstract - - - - -	265
Introduction - - - - -	265
Physical setting - - - - -	265
Location - - - - -	265
Climate - - - - -	266
Drainage-basin characteristics - - - - -	266
Waves and tides - - - - -	267
Geology - - - - -	268
The January 3-5, 1982, storm - - - - -	268
The flood delta - - - - -	268
Analysis of storm deposits - - - - -	269
Surface features - - - - -	269
Vertical distribution of sedimentary features - - - - -	271
Sediment composition - - - - -	275
Discussion - - - - -	275
Flood-delta morphology - - - - -	276
Current velocities - - - - -	277
Interpretation of sedimentary structures - - - - -	277
Vertical sequence - - - - -	278
Summary and conclusions - - - - -	279
References cited - - - - -	279

## ABSTRACT

The high-intensity rainfall and runoff associated with the January 3-5, 1982, storm led to substantial deposition of sediment at river mouths along the central California coast. This chapter examines the deposition induced by the storm at the mouth of Aptos Creek in northern Monterey Bay.

During and immediately after the peak-rainfall period, a delta formed on the previously straight beach. This delta, which prograded as much as 90 m, deposited an intertidal volume of material of about 23,000 m<sup>3</sup>. The clasts deposited from this flood ranged in size from clay to boulders more than 50 cm in median dimension. The flood deposits formed a fining-upward sequence composed of basal flood gravel in a poorly sorted muddy-sand matrix, overlain by horizontally laminated and nonlaminated beds of slightly muddy sand. Immediate reworking of the flood-delta deposits by waves contributed to coarsening of the delta surface.

## INTRODUCTION

The January 3-5, 1982, storm, which caused severe landsliding and erosion in onland parts of the northern Monterey Bay area, was responsible for the deposition of large amounts of sediment at nearby river mouths. The purpose of this study was to examine some of the effects on coastal sedimentation at the mouth of one small stream in this area, Aptos Creek (fig. 15.1), including sedimen-

tary structures, grain-size variations, and morphology of the flood deposits.

Larger rivers, such as the San Lorenzo, commonly develop river-mouth bars or deltas annually in response to seasonal winter rains. The high sediment discharge (average sediment load for the San Lorenzo River is 140,000 Mg/yr; Janda and Nolan, 1979) forms seasonal delta deposits that generally are beyond the capacity of the waves to redistribute rapidly. Aptos Creek, however, rarely has any significant deltaic buildup because of its open exposure to waves and its small sediment discharge; thus, this setting is advantageous for determining the effects of a single event (or a closely timed series of events). Other advantages to choosing the Aptos Creek mouth as a study site include: (1) its position on an otherwise relatively straight, unbroken stretch of sandy beach; (2) extensive subaerial exposure of the delta surface at spring low tides; (3) a wide variation in particle size in the flood sediment (from mud through boulder-size clasts); and (4) easy and safe access.

Although numerous investigations have been directed toward sediment source and distribution within Monterey Bay (for example, Arnal and others, 1973), most have focused either on southern Monterey Bay (for example, Dorman, 1968; Combellick and Osborne, 1977; Porter and others, 1979; Clark and Osborne, 1981), an area of extensive sand-mining operations, or on the coastline near the Santa Cruz Yacht Harbor (Griggs and Johnson, 1976, 1979). None of these studies has dealt with the sediment derived from a single storm.

*Acknowledgments.*—For their assistance in the fieldwork, I thank Beth Laband, Jeff List, Tom Reiss, Don Hirschaut, Bob Mallonee, Roberto Anima, and Ed Kempema. Zenon Valin, Jr., performed the grain-size analyses and sand-grain point counts.

## PHYSICAL SETTING

### LOCATION

Aptos Creek debouches into northern Monterey Bay at Seacliff State Beach, approximately 10 km east of Santa Cruz (fig. 15.1). Seacliff State Beach is part of a continuous stretch of sandy coastline that extends from New Brighton State Beach, 3.2 km to the northwest, to Del Mar Beach near Monterey, 47 km to the south. This concave-seaward coastline is broken only by the mouths

of the Pajaro and Salinas Rivers and by the inlet to Elkhorn Slough at Moss Landing. At the mouth of Aptos Creek, the beaches are backed by 30-m-high cliffs composed of semiconsolidated Pleistocene Aromas Sand (Dupre, 1975).

#### CLIMATE

The Mediterranean climate of the Monterey Bay area is characterized by dry summers, precipitation that exceeds potential evaporation, and more than 30 days of fog per year (Donley and others, 1979). The annual range of mean temperature is less than 9 °C, and the average temperature of the coldest month is above 12 °C. Mean annual precipitation near the coast is 660 mm (26 in.), and about 1,000 mm (40 in.) in the upper watershed (Rantz, 1971).

#### DRAINAGE-BASIN CHARACTERISTICS

The following pertinent hydrologic information is summarized from the U.S. Army Corps of Engineers (1973). The Aptos Creek drainage basin (including Valencia Creek, Trout Creek, Bridge Creek, and Mangles Gulch) is typical of the small coastal basins of central California in its limited areal extent (63 km<sup>2</sup>) but high relief (762 m). Streambed slopes are 1.5 m/km in the lower reaches, 57 m/km in the middle reaches, and 286 m/km in the upper canyons. The lower part of the basin is an area of low-density residential development, whereas the upper part of the basin, which extends 11 km inland, includes parts of Nisene Marks State Park, where development is very sparse.

Flow within the Aptos Creek system varies seasonally. The bulk of precipitation is between October and May,

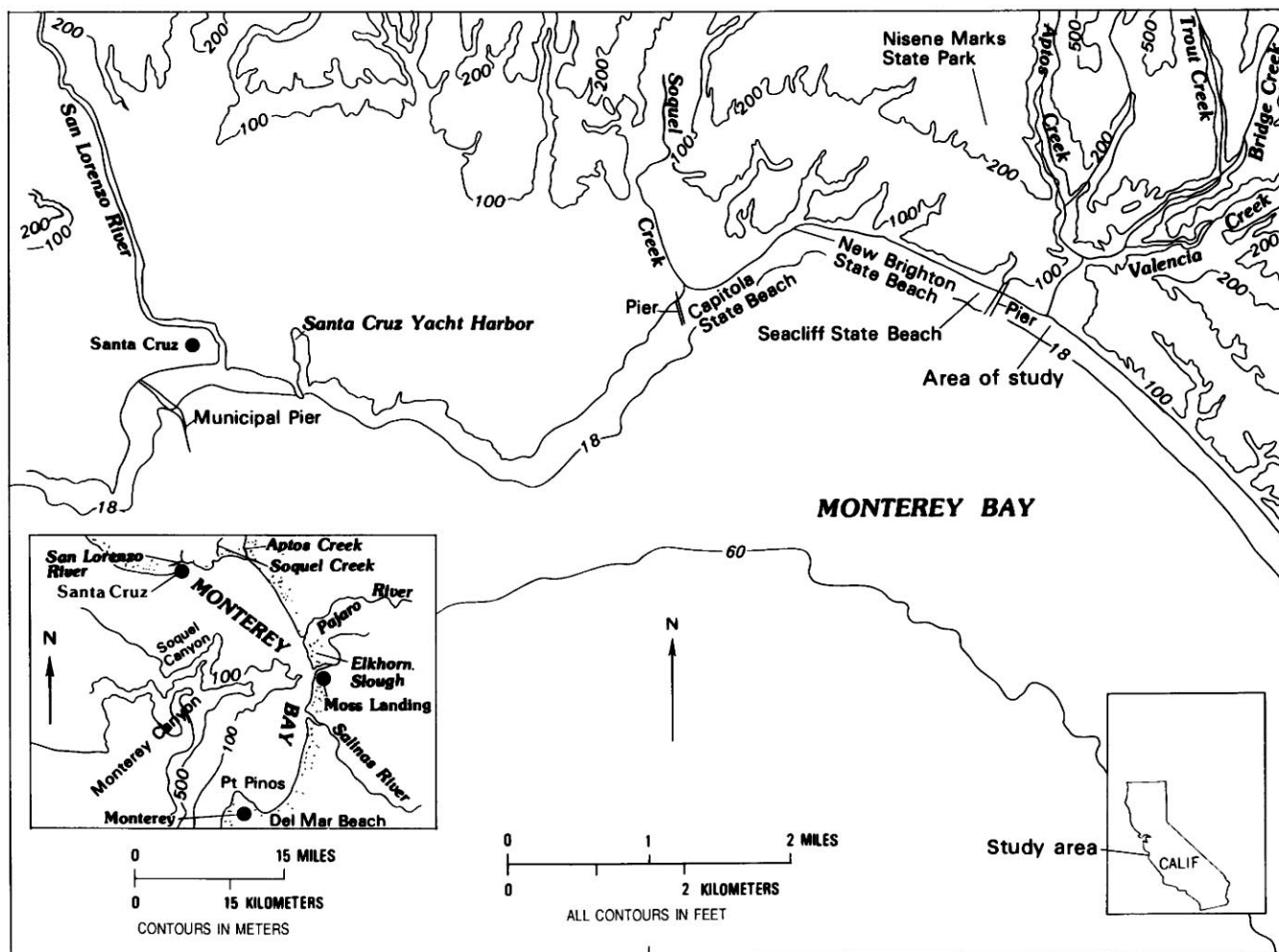


FIGURE 15.1.—Index map of Monterey Bay, Calif., showing location of study area.

and the heaviest rains generally fall between December and March. The drainage system responds rapidly to storms; the water level can rise to flood stage within hours (fig. 15.2). The estimated peak discharge from the creek in previous storms is as follows:

Date	Estimated peak discharge ( $\text{m}^3/\text{s}$ )
Jan. 31, 1963	60
Dec. 22, 1964	27
Mar. 16, 1967	37
Jan. 16, 1970	32

During the dry summer season, buildup of the beach berm commonly blocks the river mouth and creates a shallow pond behind the beach. Freshwater discharged into the pond during such blocked conditions presumably percolates through the beach into the sea.

#### WAVES AND TIDES

The central California coast receives high-energy swell from the North Pacific throughout much of the year. Half of all waves (both sea and swell) that are greater than 1 m in amplitude arrive from azimuths between  $300^\circ$  and  $340^\circ$  (Meteorology International Inc., 1977a, b). The California Coastal Data Collection Program operated a wave-gaging station near the Seacliff Beach Pier sporadically from August 1978 to May 1980. Figure 15.3, a composite of several years' data, illustrates the seasonal probability of exceeding various significant wave heights. Wave heights between January and March typically exceed 1 m 25 percent of the time, and 1.5 m slightly less than 5 percent of the time. The wave direction is predominantly from the northwest at peak periods of 13 to 17 s for swell

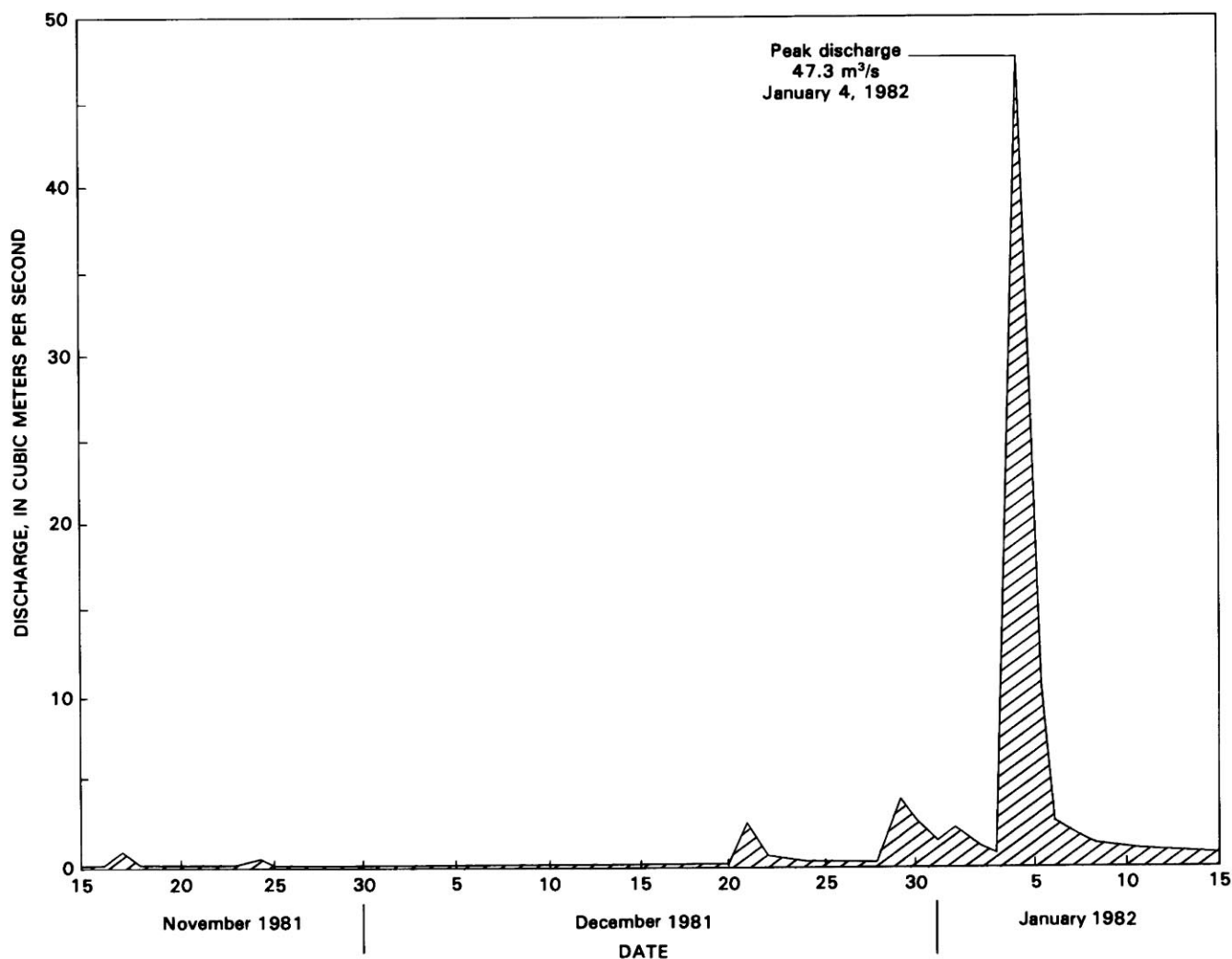


FIGURE 15.2.—Stream discharge from Aptos Creek from November 1981 to January 1982 (Ken Lee, written commun., 1982). U.S. Geological Survey stream-gaging station is just above the Aptos Creek/Valencia Creek junction; the discharge from the entire drainage is about 2.3 times that shown.



and of 5 to 7 s for seawaves. Net longshore drift near the study area is generally regarded as from north to south (Arnal and others, 1973).

The tides in Monterey Bay are semidiurnal and have maximums of 2.6 m during spring tides and of about 0.5 m during neap tides (U.S. National Ocean Survey [NOS] tide tables).

### GEOLOGY

Tertiary and Quaternary marine and nonmarine rocks overlie a Mesozoic basement complex composed chiefly of granodiorite. The outcrop area of granodiorite within the drainage basin is small. Of largest areal extent within the basin is the upper Miocene and Pliocene Purisima Formation (Greene and Clark, 1979), composed of semiconsolidated to consolidated, locally fossiliferous marine mudstone, siltstone, and sandstone. The semiconsolidated Pleistocene Aromas Sand, a unit of fluvial, eolian, and shallow-marine depositional environments (Dupre, 1975), composes most of the sequence that is late Pliocene and younger in age. Other Quaternary deposits consist of undifferentiated alluvium and terrace deposits.

### THE JANUARY 3-5, 1982, STORM

The Aptos Creek drainage basin was near the center of maximum rainfall from the January 1982 storm. As much as 300 mm (11.8 in.) of rain fell in the lower reaches of the drainage basin (see chap. 2); this amount was probably exceeded in the higher elevations of the basin, inasmuch as the upper parts of nearby basins received more rainfall than did their lower parts.

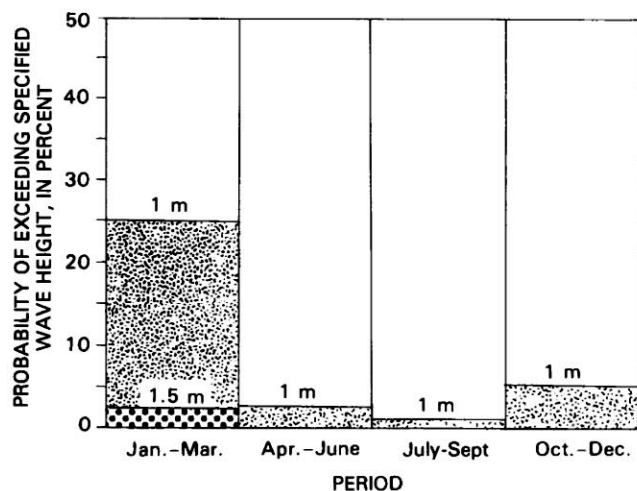


FIGURE 15.3.—Seasonal probability of exceeding wave heights of 1 and 1.5 m at Seacliff Beach. Composite diagram modified from Seymour and others (1979, fig. 21; 1980, fig. 26).

Peak flow for Aptos Creek during the storm was measured at about 110 m<sup>3</sup>/s (Ken Lee, written commun., 1982), using slope-area calculations. As shown in figure 15.2, the January 1982 storm far exceeded any previous discharges for the 1981-82 rainy season. The previous high flow at the U.S. Geological Survey stream-gaging station (located 1 km upstream from the creek mouth) was 54 m<sup>3</sup>/s in 1963; however, the 1955 floodflow was estimated at 99 m<sup>3</sup>/s. The 1982 floodflow had a recurrence interval of 40 years for Aptos Creek, as determined using WRC Log Pearson type III flood-frequency analysis (see chap. 12), and the peak discharge was 6.8 times larger than the mean annual flood.

The principal morphologic effect of the storm in the lower reaches of the creek was a widening of the channel. Bank erosion in some areas exceeded 5 m. Because of the numerous artificial channel-stabilization structures (concrete walls, riprap, and so on), it is difficult to identify how much bank erosion would have occurred in the natural state.

The Santa Cruz Harbor array (which provides wave height, period, and direction information) recorded a sizable increase in wave height during passage of the storm front. On January 3, the maximum daily significant wave height was 0.9 m, whereas on January 4 it had increased to 3.2 m (Coastal Data Information Program, 1982). Wave data after January 4 were not transmitted because telephone lines were damaged by the storm. Dominant wave periods during the storm, ranging from 4 to 10 s, indicate seawaves generated from the storm rather than long-distance swell waves. By January 7, the wave height (visual observations) at the mouth of Aptos Creek was approximately 0.5 m. My own observations indicated a rapid decrease in wave size on January 5 and 6. The maximum tidal range during this period (as determined from NOS tide tables, uncorrected for any storm surge that may have occurred during the storm) was 1.75 m. Spring tides occurred on January 7 with a range of 2.6 m.

### THE FLOOD DELTA

Flooding on January 4, 1982, generated a deltaic deposit (fig. 15.4) at the mouth of Aptos Creek, where before the storm the beach was essentially linear. The initial cusped delta was centrally bisected by a slightly sinuous channel bounded by natural levees that were submerged at higher tides. On January 7, the vertical distance between the channel bottom and these levees was less than half a meter. The vertical relief of the channel during peak streamflow is not known. Initial progradation of the subaerially exposed shoreline was approximately 90 m at its maximum point. Pronounced wave refraction seaward

of the delta (delta front and prodelta) indicates that significant amounts of deposition occurred in this area as a result of the flood. Wave refraction and shoaling continued on the delta front for another 4 to 6 weeks after the storm.

Initial northward displacement of the deltaic buildup (fig. 15.5) is consistent with waves traveling from the south-southwest, the direction reported by the Santa Cruz Harbor array. Aerial photographs taken on January 7, 1982 (fig. 15.5), show suspended-sediment plumes deflected to the north at the mouth of Aptos Creek.

On the delta flanks at midbeach level, ridge-and-runnel-type swash bars developed, similar to those described by Wright (1977) and Wright and others (1980). These swash bars, which probably developed within one or two tidal cycles of the initial delta progradation, most likely represent the first pulse of landward and longshore wave-transported sediment.

The volume of deltaic intertidal sediment deposited from this single storm is estimated at about 23,000 m<sup>3</sup>. This volume is based on ground measurements using a hand-held Abney level in a pace-and-compass survey, and on areal boundaries determined from aerial photographs, assuming that, before the flood, the intertidal beach configuration at the creek mouth was nearly linear, without large three-dimensional topographic perturbations (U.S. National Aeronautics and Space Administration aerial photographs taken on December 11, 1981, about 3 weeks before the storm, depict a nearly linear beach). The

estimate of 23,000 m<sup>3</sup> is probably conservative because the aerial photographs and pace-and-compass survey were not done until 3 days after the storm, when some material had probably been removed by waves. The amount of material transported through the creek mouth was certainly greater than the amount deposited intertidally on the delta. The subtidal part of the delta (the delta front and prodelta) equaled, or possibly exceeded, that of the intertidal delta. Drake and others (1972), in their study of flood-derived shelf sediment from the Santa Clara River, estimated that about twice as much detritus was deposited in offshore areas as retained in the river-mouth delta.

#### ANALYSIS OF STORM DEPOSITS

Surficial (upper 2 cm) sediment samples were collected from deltaic, fluvial, beach (primarily the active swash zone), and prestorm (dry backbeach) environments (fig. 15.4). Oriented and undisturbed pipe cores (90 mm diam), with an average length of 0.7 m, were also taken from the sediment deposited in each of these environments. Percentages of gravel, sand, and mud were determined for each surface sample and core subsample. Selection of subsamples from each core was based on stratigraphic intervals of relatively uniform texture and sedimentary-structure characteristics. Sand-textural parameters were determined using standard Rapid Sediment Analyzer (RSA) techniques, and the percentages of mud and of silt and clay were determined using pipette analysis. Textural terms follow the usage of Folk (1980). Epoxy-resin peels of all the pipe cores were made, and selected peels underwent X-ray radiography for analysis of sedimentary structures.

#### SURFACE FEATURES

Most surficial deposits in the subaerial delta consisted of medium sand, but large areas of this sand were overlain by a deposit, as much as about 30 cm thick, composed primarily of a coarse-textured woodpulp. This woodpulp probably represents the remnants of vegetative debris that was fragmented during its short but active fluvial journey. In addition to the woodpulp, many sticks and logs collected on the beaches and within the sediment adjacent to the creek mouth (fig. 15.6). Scattered pebbles and cobbles were also present on the delta surface.

Bedforms observed on the exposed delta surface after the initial (storm) phase of deposition (Jan. 7, 1982) included those formed both by swash-zone and by fluvial processes. Swash-zone bedforms, such as rhomboid ripple marks, swash marks (Sallenger, 1981), and V-swash marks (Komar, 1976), were widespread on the delta surface except within the active fluvial channels. The swash

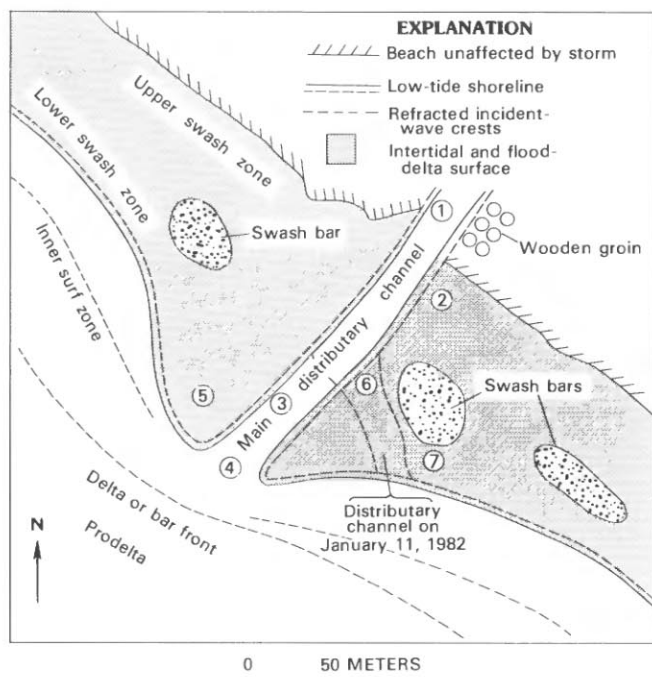


FIGURE 15.4.—Sketch map of mouth of Aptos Creek, showing relative positions of various geomorphic features of the flood delta. Numbers denote locations of cores in figure 15.8.



FIGURE 15.5.—Mouth of Aptos Creek on January 7, 1982. Wave height is approximately 0.5 m. U.S. Geological Survey aerial photograph.

marks were composed of coarser sand grains, shell fragments, and such low-density material as woody debris. By 3 days after the peak flow, the main channel had started to meander and branch into several smaller distributary channels. Within each of these smaller channels, various ripple types were observed, including straight to sinuous long-crested ripples, three-dimensional ripples, and, where wave influences were strong, near-symmetrical and flat-topped ripples. In shallow swift flows, standing waves and antidunes were present. A small abandoned channel on the delta flank contained two intersecting ripple sets draped by a thin mud layer. The same channel at the level of the low-tide swash zone also contained large (approx 1.2 m diam and 15 cm deep) lunate megaripples, commonly covered with a thin mud layer (fig. 15.7). These megaripples faced in a southerly (east-southeastward to southwestward) direction indicating oblique onshore, shore-parallel, and oblique offshore bedform migration. The bedforms occurred as

isolated features, commonly with several meters' spacing between individuals and different facing directions amongst neighbors. Formed during higher tides, they occurred in an area influenced by waves and streamflow.

I examined the sea floor below the surf zone by wading at low tide where a coarse-gravel pavement covered the floor opposite the main stream channel. Any overlying sand was presumably winnowed away by waves.

#### VERTICAL DISTRIBUTION OF SEDIMENTARY FEATURES

The initial coring (Jan. 11, 1982) established that much of the delta deposit consisted of a sand body (max 80 cm thick, fig. 15.8) containing scattered pebbles, overlying a much coarser gravel deposit. The cores were unable to penetrate this gravel, and probing indicated that it was widespread within the delta. Subsequent erosion of the sand veneer confirmed that gravel underlay most of the delta. Thus, all the cores from the initial coring program,



FIGURE 15.6.—Vegetative debris (mainly twigs and branches) deposited on beach face near mouth of Aptos Creek after a winter flood.



with the possible exception of the one from the upper stream channel (core 1, fig. 15.8), record only the waning phases of flood deposition, that is, postgravel deposition. The relative positions of the sand and gravel and approximate core locations are schematically illustrated in figure 15.9. The length of each core (except the one from the upper stream channel) approximates the thickness of sand overlying the gravel.

The core subsample intervals used for textural analysis are shown in figure 15.8, and the results of the statistical analysis are listed in table 15.1. Composed primarily of sand, the samples also contained as much as 6 weight percent of gravel (mainly granules) and as much as 3.5 weight percent of mud (mostly silt). The mean grain size of the sand fraction for 22 samples ranged from 1.48 to 2.02 $\phi$  (fine to medium sand). Measures of sorting (standard deviation) indicated that the sand analyzed was, at worst,

moderately well sorted and that most was well or very well sorted (0.29–0.61 $\phi$ ). Skewness values ranged from strongly coarse skewed through fine skewed. About half the samples exhibited near-symmetry in their skewness values.

Sedimentary structures recognized in the Epoxy peels include (fig. 15.8) (near) horizontal planar stratification, low-angle (less than 15°) and high-angle (more than 20°) cross-stratification, and nonlaminated beds that appear somewhat massive.

The horizontal planar stratification comprised distinct laminae ranging from a few millimeters to more than 20 mm in thickness (for example, intervals 1c, 2c, 3c, fig. 15.8). Some of the near-horizontal laminae exhibit subtle truncations and are probably analogous to the horizontal discontinuous stratification of Picard and High (1973). The sediment is composed of well-sorted medium

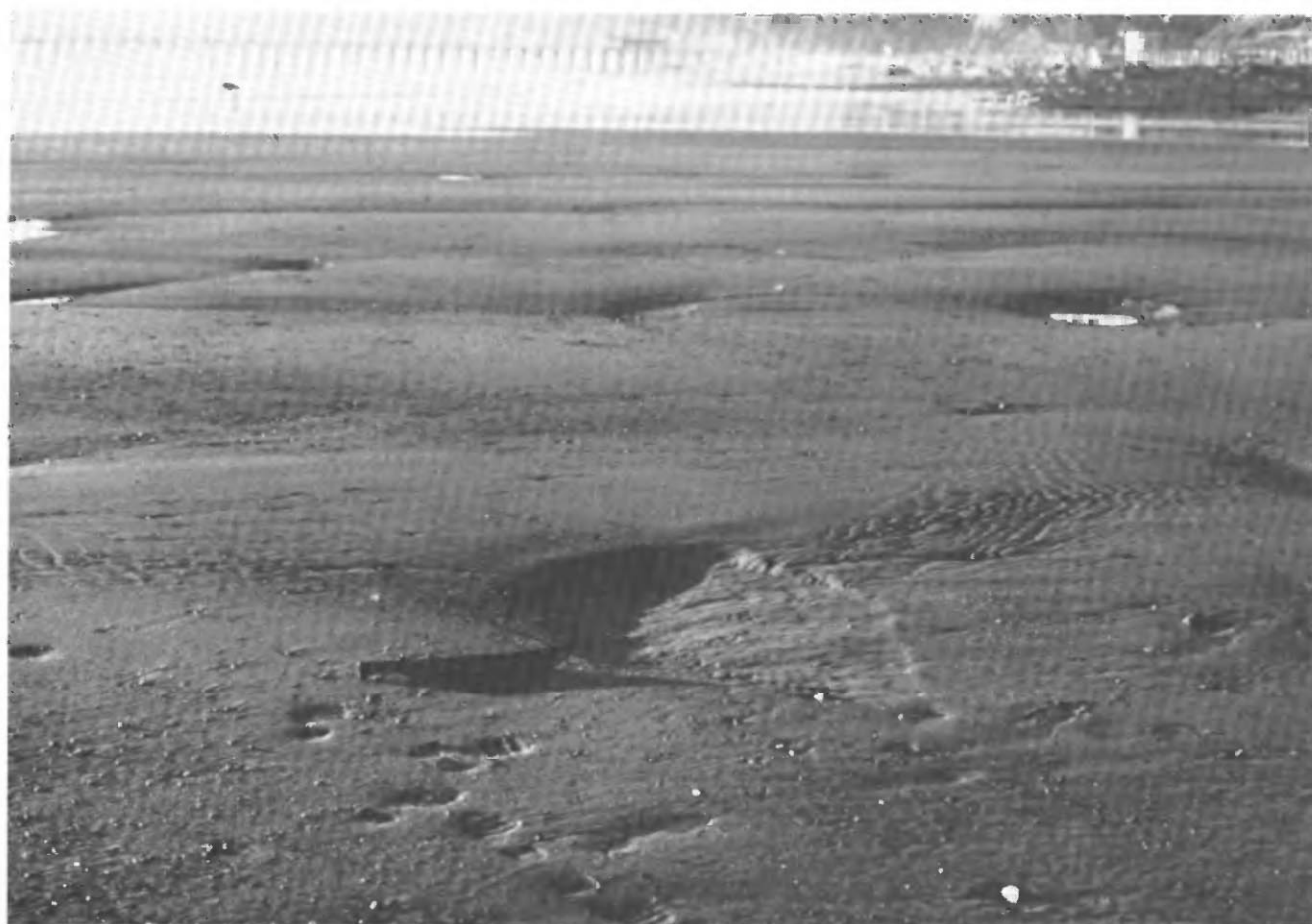


FIGURE 15.7.—Lunate megaripples near a meandering distributary channel at mouth of Aptos Creek. View westward toward ocean. Photograph by H.E. Clifton, taken January 9, 1982.

sand (table 15.1) containing a small percentage of mud that increases downcore. Grading within the laminations commonly is poorly developed, but where the laminations are present, both normal and inverse grading occurs. Contacts between laminae are generally sharp.

Interbedded with the planar-laminated sediment are beds, as much as 10 cm thick, similar in texture to the planar beds but containing no obvious sedimentary structures and appearing somewhat massive (for example, within interval 2c, fig. 15.8). Crude layering, where

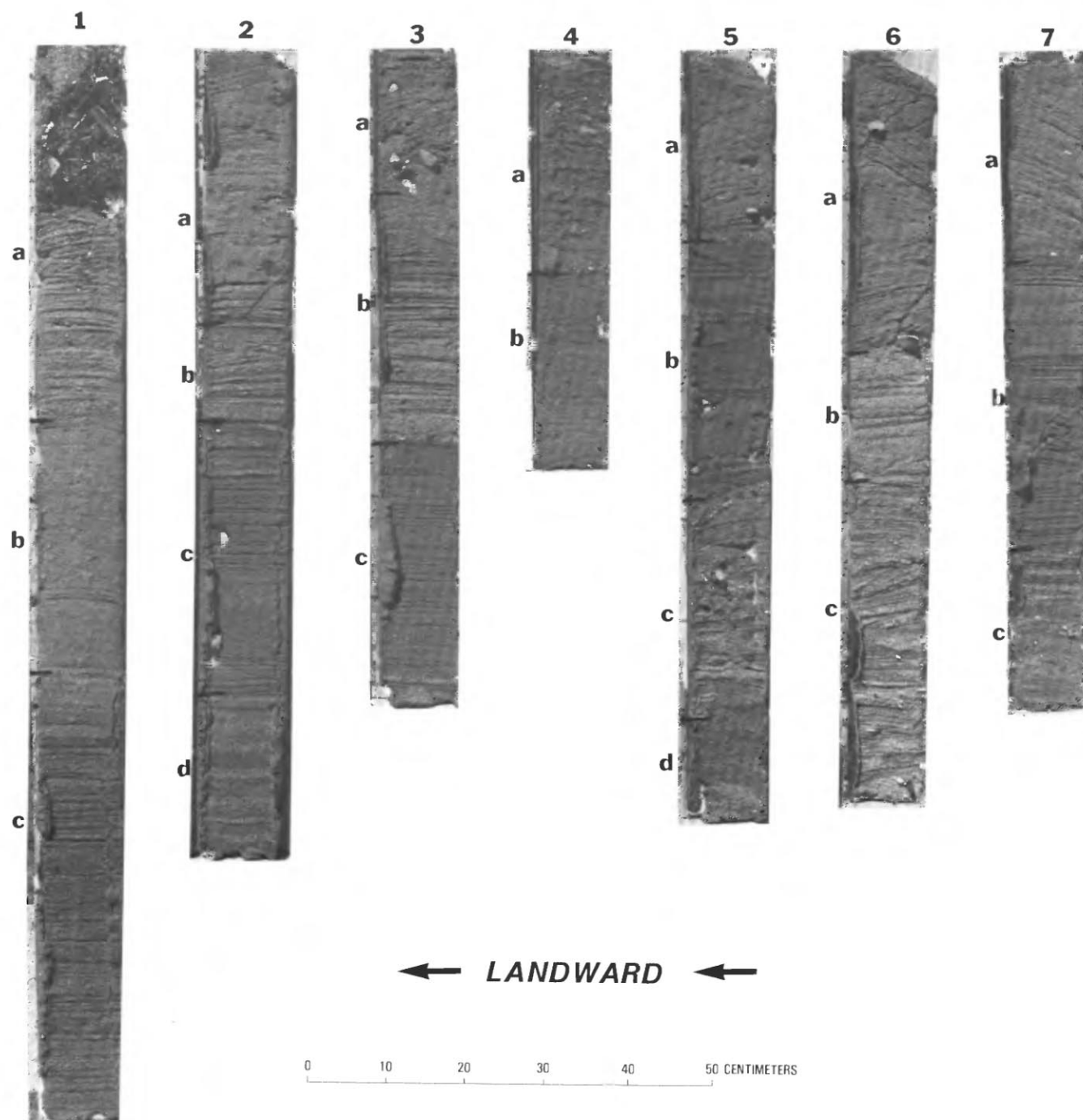


FIGURE 15.8.—Epoxy-resin peels of initial (Jan. 11, 1982) set of oriented pipe cores; landward direction is to left in all cores (see fig. 15.4 for locations). Core numbers and lettered subsample intervals same as for samples in table 15.1.

TABLE 15.1.—*Surficial and downcore sediment-texture parameters*

[All sedimentary-component values in weight percent; statistical parameters for sand fraction only]

Sample	Mean size ( $\phi$ )	Skewness	Standard deviation	Gravel	Sand	Silt	Clay
1a	1.52	-0.06	0.50	1.75	96.96	0.82	0.47
1b	1.85	.04	.44	---	96.97	2.38	.66
1c	1.75	.19	.55	---	96.86	2.90	.24
2a	1.72	-.35	.52	5.52	94.31	.17	---
2b	1.76	-.34	.61	1.66	97.43	.90	---
2c	1.80	-.04	.54	1.54	95.52	1.93	1.01
2d	1.79	.10	.50	---	96.65	2.06	1.29
3a	1.48	-.36	.57	6.00	93.75	.25	---
3b	1.83	-.11	.40	---	99.61	.39	---
3c	1.75	.09	.42	---	97.14	1.89	.67
4a	1.77	-.16	.44	1.40	98.60	---	---
4b	1.86	-.01	.61	1.64	95.50	2.07	0.79
5a	1.79	-.15	.40	2.33	96.83	.30	.54
5b	2.02	.09	.44	---	96.46	2.53	1.02
5c	1.48	-.23	.53	5.41	94.21	.21	.17
5d	1.71	-.08	.38	---	99.18	.48	.34
6a	1.80	-.30	.51	2.54	96.46	.49	.50
6b	1.51	-.01	.50	1.35	98.54	.11	---
6c	1.57	-.08	.49	1.07	98.82	.11	---
7a	1.65	-.21	.41	---	99.43	.15	.42
7b	1.78	-.11	.52	---	97.96	1.18	.86
7c	1.64	-.29	.61	2.80	95.83	.47	.90
North beach.	1.81	-.12	.29	---	100	---	---
South beach.	1.60	-.12	.31	---	100	---	---

developed, does not have the same degree of grain segregation as within the planar-laminated sediment. Normal grading is present within some beds. Contacts with adjacent beds are both sharp and gradational.

Cross-stratification within the cores occurs as: (1) low-angle (less than 15°) sets, generally less than 10 cm thick, commonly associated with horizontal planar-laminated

beds (interval 2b, fig. 15.8); and (2) high-angle (more than 20°) sets, possibly as much as 20 cm thick (interval 7a). Texturally coarser than the planar-laminated and nonlaminated beds, the crossbedded sediment commonly contains small amounts of gravel (mostly granules or a few pebble clasts) and only very small amounts of mud. Most of the low-angle crossbeds have a landward component of dip,

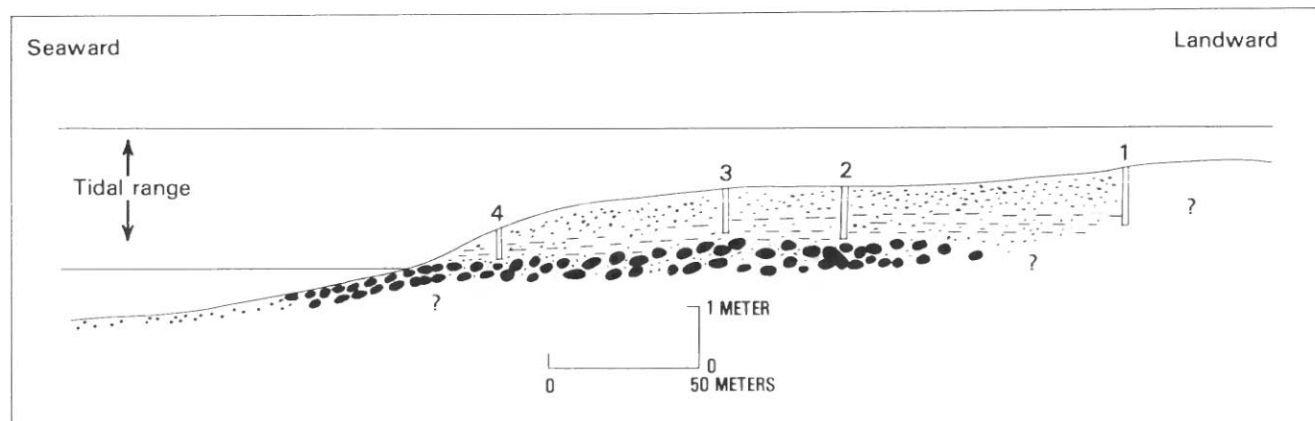


FIGURE 15.9.—Schematic cross section of flood delta, showing relative locations of cores and approximate thicknesses of deposited sand (dots), gravel (ovals), and mud (dashes).

whereas the high-angle crossbeds show both landward (upstream; interval 5a) and seaward (downstream; intervals 6a, 7a) dip directions.

The beach sand sampled (from a section of dry, pre-storm backbeach) contained no mud or gravel, was very well sorted, and was negatively skewed (table 15.1). Planar laminations, some of which are inversely graded, are the dominant sedimentary structure.

The above sedimentary structures typically occur in assemblages commonly arranged in a vertical succession. Slightly muddy sand, containing horizontal planar laminations intermixed with nonlaminated beds (lowermost units of cores 1-4), directly overlies the gravel. These muddy-sand beds, which probably consist of distributary-channel fill and subaqueous-levee sand deposited during the waning stages of the flood (see section below entitled "Discussion"), are here referred to as the "flood sand."

Low-angle cross-stratified, horizontal planar-laminated, and nonlaminated, slightly gravelly sand that overlies the flood sand probably represents flood-derived fluvial sediment mixed with marine sediment. Some units are more marinelike, such as core interval 6c (fig. 15.8), which contains shell fragments and onshore- and offshore-dipping low-angle crossbeds.

The upper units of most cores contain medium-scale crossbedding, formed by migration and deposition of lower-flow-regime bedforms (see section below entitled "Discussion"). Both seaward- and landward-dipping cross-strata are present. Although more gravel and less mud distinguishes this sediment from the underlying material, the sediment can still be regarded as deposits of delta reworking.

Fabric, stratification, and grading within the gravel deposits could not be determined quantitatively because the flood gravel occurred below the water table, where trench faces could not be maintained. Although shallow trenching was inadequate for observing sedimentary structures, it did indicate at least two types of gravel-rich deposits. The flood gravel of the intertidal delta (the first type) contained a wide variety of clast sizes and an abundant muddy-sand matrix. As best as could be determined by trenching, most of these gravel beds were not clast supported but, instead, were matrix supported or, at least, lacked a tight gravel framework. In contrast, the gravel beds in the subtidal part of the inner surf zone (the second type) formed a tightly packed network or pavement at least two layers thick. Mud was absent, and sand (much of it coarse) formed a matrix between the clasts. Though probably originally deposited as flood gravel, these beds were quickly reworked and redistributed within the surf zone. Pebble segregation and bed lenticularity, used by Clifton (1973) to differentiate wave-worked from fluvial gravel, could not be properly assessed in the present deposits because of inadequate exposure.

Maximum clast size was greater than 50 cm (median dimension). The average size of the larger clasts was approximately 18 cm (average median dimension of 100 measured clasts in the reworked gravel).

#### SEDIMENT COMPOSITION

Examination of the core subsamples under a binocular microscope revealed some differences in characteristics between the sand layers. Point-count histograms for the flood, prestorm beach, and deltaic (mixed marine-fluvial) sediment are shown in figure 15.10. The flood sand is characterized by abundant light minerals and lithic fragments (predominantly siltstone and sandstone), and moderate amounts of dark minerals. The beach sand (taken from a non-storm-affected section of backbeach) contains abundant dark minerals and very few lithic fragments. Most of the samples examined contained a mixture of the flood-type (fluvial) and beach-type sand-grain compositions and morphologies (fig. 15.10). This mixture is expectable because the riverborne sediment is rapidly reworked by wave and tidal processes; as the material is deposited at the creek mouth, it immediately undergoes wave reworking. Grain angularity proved to be of little value in distinguishing between sand types; most of the grains examined were either angular, subangular, or subrounded (fig. 15.10). The relatively high percentages of angular grains suggest little abrasion and, therefore, recent introduction to the high-energy coastal environments where the samples were gathered.

The cobble and gravel clasts consisted predominantly of well-indurated fine-grained sandstone and mudstone, in some samples highly fossiliferous, most likely from the Purisima Formation, which forms extensive outcrops within the drainage basin. Other clasts consisted of such manmade materials as concrete and asphalt, and several types of crystalline rock (marble and (or) granite) that could have come either from the riprap used in artificial-stabilization measures along the channel (marble) or from the Mesozoic basement outcrops (granite) within the drainage basin. Because both angular (riprap?) and well-rounded (stream gravel?) crystalline clasts were observed, both of these sources are probable. Additional evidence for recent deposition included angular concrete clasts with painted surfaces and angular blocks of asphalt roadway. It is highly unlikely that painted surfaces and angular corners on soft asphalt would last long under the rigorous conditions in the surf zone. Observations over a 4-month period indicated a deterioration of these features.

#### DISCUSSION

Although neither accurate measurements nor sediment samples were taken from the delta until 4 days after the



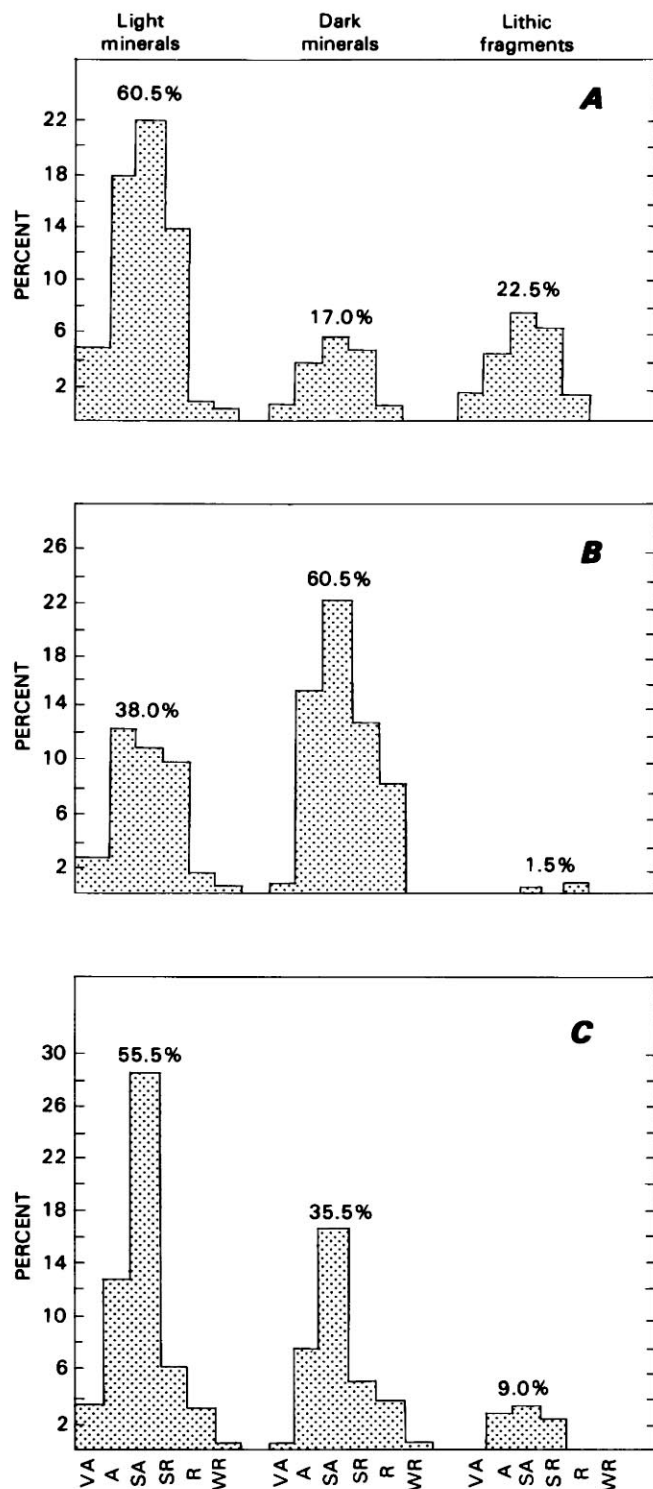


FIGURE 15.10.—Point-count histograms of light (predominantly quartz and feldspars) and dark (opaque and nonopaque) minerals and lithic fragments from three samples (500 grains per sample). A, Flood sand. B, Prestorm beach sand. C, Mixed deposits. A, angular; R, rounded; SA, subangular; SR, subrounded; VA, very angular; WR, well rounded.

storm, some of the processes that occurred during the flood can be deduced from the delta morphology, sedimentary structures, and particle characteristics.

#### FLOOD-DELTA MORPHOLOGY

Most of the flood delta was built within less than 24 hours. The resulting morphology was a product of the interaction between stream discharge, incident-wave characteristics, and tidal stage (Mikhailov, 1966; Clifton and others, 1973). Because these parameters changed continually during passage of the storm front, delta morphology evolved rapidly. Any discussions of delta form, therefore, must include generalizations based on observations taken at different stages of delta development.

Channel-stabilization measures in the lower half-kilometer of the stream prevent channel meandering and constrain the creek mouth to a fixed position. As the stream channel enters the shoreface, the channel is no longer bounded by rigid artificial levees, and so the streamflow can expand, and its competence to transport sediment is reduced (Harms and others, 1982). In addition, the collision between the outgoing discharge and incoming waves promotes mixing and rapid deceleration of the sediment load (Wright, 1977). The resulting flood deposition proceeded by vertical accretion within the channel and lateral progradation on an essentially undisturbed shoreface. Wave refraction around the prodelta and delta front acted to confine the deposits because of lateral convergence of the breaking waves (fig. 15.5; see Wright, 1977). Observations 2 days after the storm (at low tide) suggest that as the stream channel crossed the beach, it scoured to a depth approximating the low-tide level. As streamflow decreased, the bed aggraded vertically. The actual locus of deposition probably varied longitudinally, depending on the tidal stage. During the storm, the tidal range of 1.75 m could have been responsible for as much as 175 m of difference in mean shoreline position at the creek mouth and have resulted in elongation of the delta. Elongation of the flood-delta perpendicular to the shoreline trend was thus enhanced by (1) unusually high sediment discharge at the creek mouth, (2) a 1.7-m tidal range during the storm, and (3) relatively low wave heights combined with wave refraction and convergence of transport around the delta front.

Between January 5 and 9, the low-tide position of the mouth of Aptos Creek migrated approximately 60 m to the south. In addition, the main distributary channel changed from nearly linear to more sinuous as stream discharge declined. Division of the channel into several branches accompanied this increase in sinuosity. The sequence of channel straightening during peak flows followed by increased meandering as discharge declined

was also observed during storms in February and April 1982. One effect of the change in creek-mouth position will be to deposit sediment laterally along the shoreline.

#### CURRENT VELOCITIES

Mean flow velocity for the January 1982 flood 0.29 km upstream from the mouth of Aptos Creek can be estimated from discharge data, high-water marks (Ken Lee, written commun., 1982), and published stream cross sections (U.S. Army Corps of Engineers, 1973). The resulting mean flow velocity was about 1.70 m/s. Maximum flow velocities can be estimated by calculating the current needed to transport large clasts at the creek mouth. Calculation of  $U_{100}$ , the threshold flow velocity 100 cm above the bed, using the empirical relation  $U_{100} = 160 D^{0.45}$  (Miller and others, 1977), where  $D$  is the grain diameter (in centimeters), yields a value of  $U_{100} = 9.30$  m/s, or 5.4 times the mean flow velocity. Here, 50 cm was used as the median diameter of the largest clasts transported. This modified Sundborg equation assumes, among other things, material of quartz density, a water temperature of 20 °C, and a kinematic viscosity of 0.01 cm<sup>2</sup>/s (Miller and others, 1977). Although most of the clasts are probably close to quartz density, the water temperature and viscosity of Aptos Creek during the storm were very unlikely to be at these typical values. A change in the temperature from 21 to 10 °C (a more probable temperature for Aptos Creek) can affect the discharge of sand by as much as 20 percent (Colby, 1964). Very high suspended-sediment concentrations will also increase the fluid viscosity and thus reduce the threshold velocity (Colby, 1964). Another complicating factor is the composition of the bed during high-flow conditions; did it consist of a gravel pavement, or was it essentially a sandy bottom with gravel material sporadically dispersed? Poststorm observations of the channel bottom in the lower reaches of the stream revealed a primarily sandy bottom with a few gravel clasts. The current needed to transport gravel on a sandy bed is less than that needed to transport it on a gravelly bed (Harms and others, 1982). The calculated maximum flow velocity of 9.30 m/s would most likely represent an upper limit, and on the basis of the above considerations, the maximum current velocity was most likely below that limit.

The calculated  $U_{100}$  value for gravel clasts 18 cm in diameter (mean of 100 larger clasts exposed as a post-storm lag) is about 5.90 m/s, or 3.4 times the mean flow velocity. Even though many of the assumptions used to calculate current velocities from clast size may overestimate the streamflow associated with the January 1982 storm, it appears that current velocities significantly greater than the mean flow velocity did occur.

#### INTERPRETATION OF SEDIMENTARY STRUCTURES

The analysis of sedimentary structures can be an important interpretative tool in reconstructing processes operating at the time of sediment deposition (Harms and others, 1982). However, because the cores taken represent such a limited area of the overall feature, some caution must be exercised in such interpretations. For example, low-angle cross-stratification in the cores may be real (that is, deposition on a gently inclined surface), or it could be high-angle cross-stratification observed in a plane other than the one perpendicular to the direction of bedform migration. Care was taken during the coring operation to note surface bedform type and orientation at each core location, so that any structures preserved in the core tops could be related to known bedforms. Most of the peels are sufficiently thick (1+ cm) that any large component of inclination perpendicular to a major peel face (that is, the photographed surface) is recognizable.

Horizontal planar stratification developed in medium sand can form under various flow conditions and in various environments (for example, Harms and others, 1982), and so its interpretation can be difficult. The planar laminations in core intervals 1c, 2c, 2d, and 3c (fig. 15.8) (the flood sand) probably result from bed aggradation under upper-flow-regime plane-bed transport. The mean grain size (medium sand), water depth (max 2.5 m), and mean flow velocity (1.7 m/s) fall well within the range predicted for upper flat beds (Rubin and McCulloch, 1980). Horizontally laminated sand is a common feature of sandy streamflood deposits (McKee and others, 1967; Williams, 1971; Picard and High, 1973). Although swash lamination formed on beaches is similar in appearance (for example, Clifton, 1969; Sallenger, 1981), the plane beds observed in the lower core segments most likely represent deposition from unidirectional fluvial currents. The location of core 1 in a fluvial channel and the presence of mud in the samples, which is very uncommon in swash-zone deposits, suggest a fluvial setting. The continuation of horizontal planar laminations seaward (cores 2–4, fig. 15.8) along the trace of the main channel indicates that flood-controlled deposition extended at least 75 m from the mean shoreline position. During unidirectional upper-regime flow conditions, the bed is presumed to be planar and near-horizontal. Bedload and suspended-sediment transport is appreciable and nearly continuous (Colby, 1964). The mechanics whereby plane beds are formed under (quasi?) steady-state unidirectional flows are not fully understood but are thought to be related either to turbulent variations within boundary layers (that is, bursting cycle; Bridge, 1978) or to areal variations in sorting or packing (Moss-Kuenen hypothesis, in Harms and others, 1982).

The flood sand also contains the greatest proportion of mud (3.5 weight percent), which apparently was deposited with the sand during upper-flat-bed conditions. Many of the horizontal laminations examined in flood deposits by McKee and others (1967) likewise contain small amounts of silt and clay. Although the mechanism(s) responsible for the (near?) simultaneous deposition of sand, silt, and clay at high flow velocities are poorly understood, one possibility is that the viscous sublayer of the turbulent boundary layer accepts sediment by settling but does not eject it back into the main flow (McCave, 1970).

The nonlaminated beds present another problem in interpretation. Blatt and others (1980, p. 136) attributed the absence of lamination in sand either to very rapid deposition from suspension, to deposition from very highly concentrated sediment dispersions, or to destruction of original lamination by liquefaction soon after deposition. Complete bioturbation, though unlikely here (considering the evidently rapid rate of deposition), may also create homogenous beds (Reineck and Singh, 1980). McKee and others (1967, p. 849) observed " \* \* \* units of virtually structureless sand that contains thick laminae locally" from flood deposits, but they were unable to document the origin of this sand. The intercalation of nonlaminated beds with upper flat beds indicates variations in sediment transport and depositional rates at relatively high flow velocities. At higher tides, incoming waves could interact with stream outflow such that periodic current decelerations (Wright, 1977) could lead to rapid deposition of suspended sediment and bedload. Wave-induced setup, due to surf beat, could last for minutes (Komar, 1976). During this time, greater sediment transport to than from the creek mouth could result in a brief period of increased deposition, primarily from suspension producing non-laminated or poorly laminated deposits.

The horizontal laminations in the mixed flood and marine sediment could be formed from unidirectional flow under shallow-water upper-flat-bed conditions (Bridge, 1978), in wave-swash processes on the delta (Clifton, 1969), or by migration of low-relief bedforms (McBride and others, 1975). The spatial and temporal variations of these processes can occur over very short distances (meters) and timeframes (minutes). For example, at a low incoming tide, a small distributary channel with shallow (less than 10 cm) flow can form upper flat beds. A rise in mean sea level with the rising tide could cause deceleration of the streamflow and a change to lower-flow-regime bedforms, whereas on an adjacent delta surface, wave swash could be the dominant process.

The cross-stratification within the mixed sediment was formed by various bedforms. The medium-scale landward-dipping cross-strata (intervals 3a, 5a, fig. 15.8) are the products of landward-migrating lunate megaripples similar to that shown in figure 15.7. Core 5 was taken just

seaward of one of these lunate megaripples on a smooth sandy surface (see fig. 15.4). The cross-strata in interval 5a (fig. 15.8) record landward migration by slipface avalanching. The high-angle crossbedding near the tops of cores 6 and 7 (fig. 15.8) were formed by slipface progression of straight-crested bars within the distributary channel. The upstream-inclined low-angle crossbeds in core interval 6a (fig. 15.8) were probably formed by stoss deposition on a climbing bedform. The stoss-slope deposits are overlain, first, by lower-angle, then, by higher-angle crossbeds that are oriented downstream (the very top of core 6 was distorted during coring). The laminae in interval 6a appear to be conformable with each other and thus probably represent a continuous sequence of deposition. This core was taken just upstream from the crest of a small straight-crested bar in the main distributary channel. The high-angle cross-strata were formed by sand avalanching on the bar's slipface (cross-strata in interval 7a, fig. 15.8).

Although the cross-stratification within the cores (that is, not at the top, where it can be related to known surface features) presents uncertainties in interpretation, possible mechanisms of formation for the various types of crossbedding can be briefly discussed. Picard and High (1973) attributed low-angle cross-stratification in flood deposits to deposition of point and longitudinal bars with bed inclination in a downcurrent direction. However, most of the low-angle crossbeds at Aptos Creek are inclined upstream. Antidunes were a common feature during the waning stages of the flood, and so many of these upstream-dipping beds may be the products of antidune deposition. Alternatively, landward-migrating bedforms, driven by waves, during a rising tide could form landward-dipping crossbeds (Clifton and others, 1973). The narrow core diameter (9 cm) hampers distinction of low-angle cross-stratification. A set of cross-strata formed by antidunes would be expected to be highly lenticular (Hand and others, 1969), whereas sets formed by lunate megaripples would be trough shaped (Williams, 1971) or, possibly, approaching tabular-planar (Clifton and others, 1971).

#### VERTICAL SEQUENCE

An idealized composite vertical sequence of the flood deposits and associated reworked sediment is illustrated in figure 15.11. Two types of basal gravel deposits are probable during progradation. The lowermost gravel would be of the surf-zone type, consisting of framework-supported clasts in a clean sand matrix. Segregation of the gravel into well-defined beds that are laterally regular also is likely (Clifton, 1973). Flood-deposited gravel overlies the surf-zone gravel and is characterized by more matrix and a wider range of sediment sizes, especially finer (mud). The flood gravel was deposited during the



peak of the storm runoff, when current velocities were the highest. The surf-zone gravel was initially deposited as flood gravel under highly energetic conditions. Initial deposition of the seawardmost (and thus topographically lowest) gravel occurred at the highest flow velocities and during the lowest tidal stage. Lower streamflow and (or) higher tidal stage is responsible for a landward shift in

the center of gravel deposition. During falling tide, flood gravel will be deposited atop gravel that has been reworked by waves. Surf-zone gravel may overlie flood gravel if the entire thickness of flood gravel is not reworked.

The flood sand can overlie both flood and surf-zone gravel. The flood sand is characterized by horizontally laminated and nonlaminated beds and small (less than 3.5 weight percent) amounts of mud. The flood gravel was deposited under peak storm conditions, whereas the flood sand represents deposition under upper-flow-regime conditions during the waning stages of the flood. Plane beds and, possibly, antidunes were present at that time. The flood sand grades upward into reworked sand that contains horizontal laminations, small- to medium-scale cross-stratification, and small amounts (less than 6 weight percent) of gravel. Beds rich in organic material may also be present.

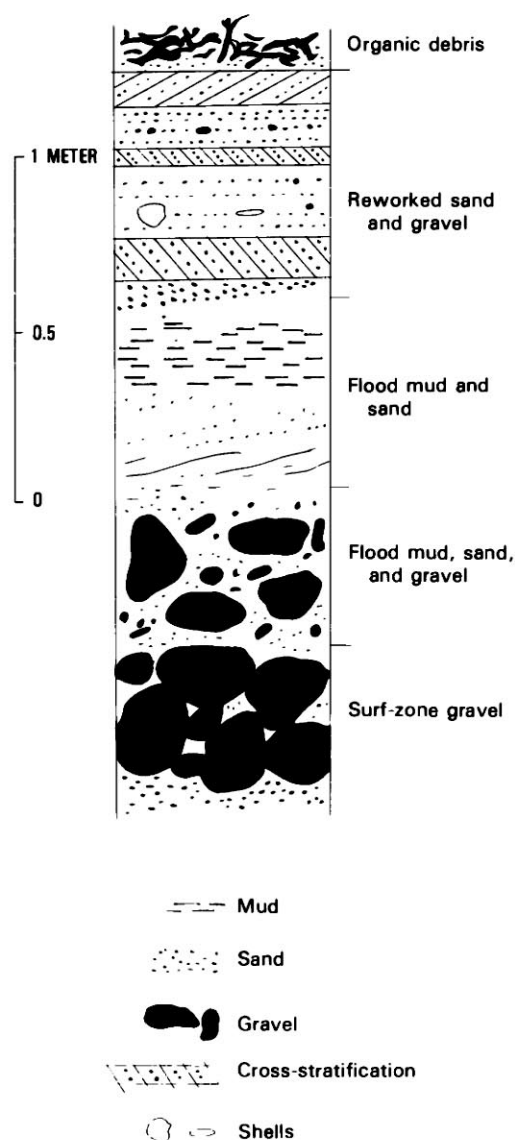


FIGURE 15.11.—Idealized vertical sequence of flood-delta deposits.

## SUMMARY AND CONCLUSIONS

An inferred sequence of events at the mouth of Aptos Creek for the January 3–5, 1982, storm, based on the data discussed in this chapter, photographs, and my own observations, is presented in table 15.2.

The following are some of the short-term consequences of a 40-year-recurrence-interval flood on sedimentation at the creek mouth. (1) A cusped delta was constructed, containing approximately 23,000 m<sup>3</sup> of intertidal sediment. (2) A wide size range of sediment was introduced, including clay and boulders. Mud was deposited on the active shoreface, and gravel was deposited as far as 250 m from the winter shoreline position; the sand fraction appeared to be enriched in lithic grains relative to the beach sand in this area. (3) The flood deposits at the creek mouth constituted a fining-upward sequence consisting of poorly sorted, matrix-supported flood gravel overlain by horizontally laminated and nonlaminated, slightly muddy sand. As flood-derived sediment was introduced to the nearshore, intense reworking by waves was common. (4) Reworked sediment was both horizontally stratified and cross-stratified, and the sand was coarser than the flood sand.

## REFERENCES CITED

- Arnal, R.E., Dittmer, E., and Shumaker, E., 1973, Sand transport studies in Monterey Bay, California: Moss Landing Marine Laboratories Technical Publication 73-5, 71 p.  
 Blatt, H., Middleton, G.V., and Murray, R.C., 1980, Origin of sedimentary rocks (2d ed.): Englewood Cliffs, N.J., Prentice-Hall, 782 p.  
 Bridge, J.S., 1978, Origin of horizontal lamination under turbulent boundary layers: *Sedimentary Geology*, v. 20, no. 1, p. 1-16.



TABLE 15.2.—*Inferred sequence of storm events at the mouth of Aptos Creek*

[River discharge is adjusted to include entire drainage basin]

Date (Jan. 1982)	Waves	River discharge (m <sup>3</sup> /s)	Sedimentation	Geomorphology
3	$H_{1/3}=0.9$ m; dominant periods, 10-16 and 4-6 s.	1.4	Very little suspended-sediment transport and even lower bed-load transport.	River mouth open through beach to sea. Beach is essentially linear.
4	$H_{1/3}=3.2$ m; dominant period, 4-10 s.	112.6	Increasing amounts of suspended sediment and traction load throughout the day, reaching extremely high amounts. Boulders with median dimensions as large as 0.5 m are transported.	Development of a well-formed cusped delta. Upstream, creek channel is undergoing significant widening.
5	$H_{1/3}=1.5$ m	<sup>1</sup> 25.1	Very high sediment discharge still occurring. All but the largest clasts are probably still being transported. Reworking of sediment at creek mouth unable to keep pace with sediment discharge.	Bank caving along stream margins still occurring (at reduced levels). Delta progradation and lateral growth occurring at reduced levels.
6	$H_{1/3}=1.0$ m	5.4	Significant amounts of suspended sediment and bedload transport of smaller sizes (probably less than boulder size).	Stream channel has been mostly stabilized. Reworking along delta surface starting to become significant.
7	$H_{1/3}=0.5$ m	3.5	Large amounts of suspended-sediment transport, as evidenced by large plumes at river mouth. Observations at beach level indicate movement of pebbles and cobbles.	Branching of distributary channels and an increase in their sinuosity. Development of swash bars on delta flanks.

<sup>1</sup>Rainfall ceased by about 11:00 a.m. P.s.t.; most discharge was from poststorm runoff.

- Clark, R.A., and Osborne, R.H., 1981, Contribution of Salinas River sand to the beaches of Monterey Bay, California, during the 1978 flood period: Fourier grain-shape analysis: *Journal of Sedimentary Petrology*, v. 52, no. 3, p. 807-822.
- Clifton, H.E., 1969, Beach lamination—nature and origin: *Marine Geology*, v. 7, no. 6, p. 553-559.
- , 1973, Pebble segregation and bed lenticularity in wave-worked versus alluvial gravel: *Sedimentology*, v. 20, no. 2, p. 173-187.
- Clifton, H.E., Hunter, R.E., and Phillips, R.L., 1971, Depositional structures and processes in the non-barred high-energy nearshore: *Journal of Sedimentary Petrology*, v. 41, no. 3, p. 651-670.
- Clifton, H.E., Phillips, R.L., and Hunter, R.E., 1973, Depositional structures and processes in the mouths of small coastal streams, southwestern Oregon, in Coates, D.R., ed., *Coastal geomorphology*: Binghamton, State University of New York, p. 115-140.
- Coastal Data Information Program, 1982, Monthly summary report no. 74, January, 1982: Sacramento, U.S. Army Corps of Engineers and California Department of Boating and Waterways, unpaginated.
- Colby, B.R., 1964, Discharge of sands and mean-velocity relationships in sand-bed streams: U.S. Geological Survey Professional Paper 462-A, p. A1-A47.
- Combellick, R.A., and Osborne, R.H., 1977, Sources and petrology of beach sand from southern Monterey Bay, California: *Journal of Sedimentary Petrology*, v. 47, no. 2, p. 891-907.
- Donley, M.W., Allen, Stuart, Caro, Patricia, and Patton, C.P., 1979, *Atlas of California*: Culver City, Calif., Pacific Book Center, 191 p.
- Dorman, C.E., 1968, The southern Monterey Bay littoral cell: A preliminary budget study: Monterey, Calif., U.S. Naval Postgraduate School, M.S. thesis, 166 p.
- Drake, D.E., Kolpack, R.L., and Fischer, P.J., 1972, Sediment transport on the Santa Barbara-Oxnard Shelf, Santa Barbara Channel, California, in Swift, D.J., Duane, D.B., and Pilkey, O.H., eds., *Shelf sediment transport: Process and pattern*: Stroudsburg, Pa., Dowden, Hutchinson & Ross, p. 307-331.
- Dupre, W.R., 1975, Quaternary history of the Watsonville lowlands, north-central Monterey Bay region, California: Stanford, Calif., Stanford University, Ph.D. thesis, 232 p.
- Folk, R.L., 1980, *Petrology of sedimentary rocks*: Austin, Tex., Hemphill, 182 p.
- Greene, H.G., and Clark, J.C., 1979, Neogene paleogeography of the Monterey Bay area, California, in Armentrout, J.M., Cole, M.R., and TerBest, Harry, eds., *Cenozoic paleogeography of the Western United States: Pacific Coast Paleogeography Symposium 3*: Los Angeles, Society of Economic Paleontologists and Mineralogists, Pacific Section, p. 277-296.
- Griggs, G.B., and Johnson, R.E., 1976, Effects of the Santa Cruz Harbor on coastal processes of northern Monterey Bay, California: *Environmental Geology*, v. 1, no. 5, p. 299-312.
- , 1979, Coastline erosion, Santa Cruz County: *California Geology*, v. 32, no. 4, p. 67-76.

- Hand, B.M., Wessel, J.M., and Hayes, M.O., 1969, Antidunes in the Mount Toby Conglomerate (Triassic), Massachusetts: *Journal of Sedimentary Petrology*, v. 39, no. 4, p. 1310-1316.
- Harms, J.C., Southard, J.B., and Walker, R.G., 1982, Structures and sequences in clastic rocks: Society of Economic Paleontologists and Mineralogists Short Course 9, 249 p.
- Janda, R.J., and Nolan, K.M., 1979, Stream sediment discharge in northwestern California, in *Field trip to observe natural and resource management-related erosion in Franciscan terrane of northwestern California*: Geological Society of America, Cordilleran Section Annual Meeting, San Jose, Calif., 1979, guidebook, p. IV-1 to IV-27.
- Komar, P.D., 1976, Beach processes and sedimentation: Englewood Cliffs, N.J., Prentice-Hall, 429 p.
- McBride, E.F., Shepherd, R.G., and Crawley, R.A., 1975, Origin of parallel, near-horizontal laminae by migration of bed forms in a small flume: *Journal of Sedimentary Petrology*, v. 45, no. 1, p. 132-139.
- McCave, I.N., 1970, Deposition of fine-grained suspended sediment from tidal currents: *Journal of Geophysical Research*, v. 75, no. 21, p. 4151-4159.
- McKee, E.D., Crosby, E.J., and Berryhill, H.L., 1967, Flood deposits, Bijou Creek, Colorado, June 1965: *Journal of Sedimentary Petrology*, v. 37, no. 3, p. 829-851.
- Meteorology International Inc., 1977a, Deep-water wave statistics for the California coast, station 3: Sacramento, California Department of Navigation and Ocean Development, 37 p.
- 1977b, Deep-water wave statistics for the California Coast, station 4: Sacramento, California Department of Navigation and Ocean Development, 37 p.
- Mikhailov, V.N., 1966, Hydrology and formation of river mouth bars, in *Scientific problems of the humid tropical zone deltas and their implications*: Proceedings of the Dacca Symposium: Paris, United Nations Educational, Scientific and Cultural Organization, p. 59-64.
- Miller, M.C., McCave, I.N., and Komar, P.D., 1977, Threshold of sediment motion under unidirectional currents: *Sedimentology*, v. 24, no. 4, p. 507-527.
- Picard, M.D., and High, L.R., 1973, *Sedimentary structures of ephemeral streams*: Amsterdam, Elsevier, 223 p.
- Porter, G.A., Ehrlich, Robert, Osborne, R.H., and Combellick, R.A., 1979, Sources and nonsources of beach sand along southern Monterey Bay, California—Fourier shape analysis: *Journal of Sedimentary Petrology*, v. 49, no. 3, p. 727-732.
- Rantz, S.E., 1971, Mean annual precipitation and precipitation depth-duration-frequency data for the San Francisco Bay Region, California: U.S. Geological Survey, San Francisco Bay Region Environment and Resources Planning Study Basic Data Contribution 32, 23 p.
- Reineck, H.E., and Singh, I.B., 1980, *Depositional sedimentary environments—with reference to terrigenous clastics* (2d ed.): Berlin, Springer-Verlag, 549 p.
- Rubin, D.M., and McCulloch, D.S., 1980, Single and superimposed bed-forms: A synthesis of San Francisco Bay and flume observations: *Sedimentary Geology*, v. 26, p. 207-231.
- Sallenger, A.H., Jr., 1981, Swash mark and grain flow: *Journal of Sedimentary Petrology*, v. 51, no. 1, p. 261-264.
- Seymour, R.J., Castel, D., Sessions, M.H., and Woods, A.E., 1979, California coastal engineering data network, third annual report, January 1978 through December 1978: Sacramento, California Department of Boating and Waterways, 105 p.
- Seymour, R.J., Thomas, J.O., Castel, D., Woods, A.E., and Sessions, M.H., 1980, California coastal data collection program, fourth annual report, January 1979 through December 1979: Sacramento, U.S. Army Corps of Engineers and California Department of Boating and Waterways Report IMR 80-4, 121 p.
- U.S. Army Corps of Engineers, 1973, Flood plain information, Aptos, Trout, and Valencia Creeks, City of Aptos, California: San Francisco, 17 p.
- Williams, G.E., 1971, Flood deposits of the sand-bed ephemeral streams of central Australia: *Sedimentology*, v. 17, no. 1, p. 1-40.
- Wright, L.D., 1977, Sediment transport and deposition at river mouths: A synthesis: *Geological Society of America Bulletin*, v. 88, no. 6, p. 857-868.
- Wright, L.D., Thom, B.G., and Higgins, R.J., 1980, Wave influences on river-mouth depositional process: Examples from Australia and Papua New Guinea: *Estuarine and Coastal Marine Science*, v. 11, no. 3, p. 263-277.



## 16. SEDIMENTOLOGIC CONSEQUENCES OF THE STORM IN TOMALES BAY

By ROBERTO J. ANIMA, JENNIFER L. BICK, and H. EDWARD CLIFTON,  
U.S. GEOLOGICAL SURVEY

### CONTENTS

	Page
Abstract - - - - -	283
Introduction - - - - -	283
Setting - - - - -	283
Location and morphology - - - - -	283
Waves and currents - - - - -	283
Streams - - - - -	286
Sediment - - - - -	286
The January 3-5, 1982, storm - - - - -	289
Rainfall - - - - -	289
Landslides - - - - -	289
Methods - - - - -	289
Flood deposits - - - - -	292
Discussion and conclusion - - - - -	297
References cited - - - - -	300

### ABSTRACT

The January 3-5, 1982, storm caused considerable damage due to increased runoff that resulted in flooding and debris flows in the Tomales Bay area. Sampling in the bay 1 month after the storm showed that flood-derived sediment was generally concentrated near the sources of sediment input (that is, stream mouths). Subsequent sampling 6 to 9 months after the storm showed that this flood layer was still discernible in some areas but totally reworked by organisms in other areas. The absence of a significant amount of sediment overlying the proposed storm layer indicates that major sedimentation in the bay occurs only during such storm events as the one of January 1982.

### INTRODUCTION

The flooding associated with the January 3-5, 1982, storm must be considered a major sedimentologic event along the central California coast. The discharge of coastal streams during and immediately after the storm increased tenfold over their normal levels (see chap. 13). This chapter examines the sedimentologic consequences of the storm to one coastal embayment in the area—Tomales Bay. Our goals were to estimate the volume of sediment introduced into the bay by the storm, to delineate the distribution of this sediment, and to assess the importance of storms in the overall pattern of sedimentation within the bay. We present data regarding the extent of physical and biologic reworking of the flood deposits during 6 months following their deposition. We also describe the impact of the storm on the shellfish industry supported by the bay.

### SETTING

#### LOCATION AND MORPHOLOGY

Tomales Bay is in Marin County, Calif., approximately 24 km south of the Russian River mouth and 64 km north of San Francisco (fig. 16.1). The entrance of the bay lies at the southeast end of Bodega Bay. Occupying the rift zone of the San Andreas fault, Tomales Bay is 20.4 km long, ranges from 650 to 2,650 m in width, and encompasses an area of approximately 28.5 km<sup>2</sup> (Daetwyler, 1965). South of Pelican Point, the bay takes the form of a broad trough that is approximately 7 m deep at mean lower low water (MLLW) and shallows to less than a meter southeast of Millerton Point. North of Pelican Point the bay consists of well-defined tidal channels, from 2 to 8 m deep, separated by intertidal or shallow subtidal banks. The depth of the bay averages 3.7 m at MLLW and reaches a maximum of 18.5 m in the main channel west of Hog Island (fig. 16.2).

Tomales Bay supports a small commercial fishing fleet stationed at Marshall and other small communities on its shores. Shellfish are produced from selected places along the east side of the bay, particularly southeast of Toms Point, on the Walker Creek delta, and north of Millerton Point (fig. 16.2).

#### WAVES AND CURRENTS

Oceanic swell is largely dissipated on the shoals at the mouth of the bay, and so the only waves to influence sediment transport within the bay are generated by local winds. The shape of the bay severely limits the wind fetch in directions other than those approximately parallel to its long axis. The largest wave likely to be generated within the bay (assuming 80-km/h winds) would have a period of about 3.1 s and a height of about 1.1 m (U.S. Army Corps of Engineers, 1973).

Mixed semidiurnal tides drive most of the water movement within Tomales Bay. The mean tidal range is about 0.85 m, and the maximum is 1.6 m (National Climatic Center, 1982, p. 172-173). Johnson and others (1961) found the tidal currents between Toms Point and Pelican Point to have a mean velocity of 37 cm/s and a maximum velocity of 67 cm/s. The tidal currents diminish sharply south of Pelican Point, where the mean velocity is 8 cm/s and the maximum velocity is 27 cm/s (Johnson and others, 1961).



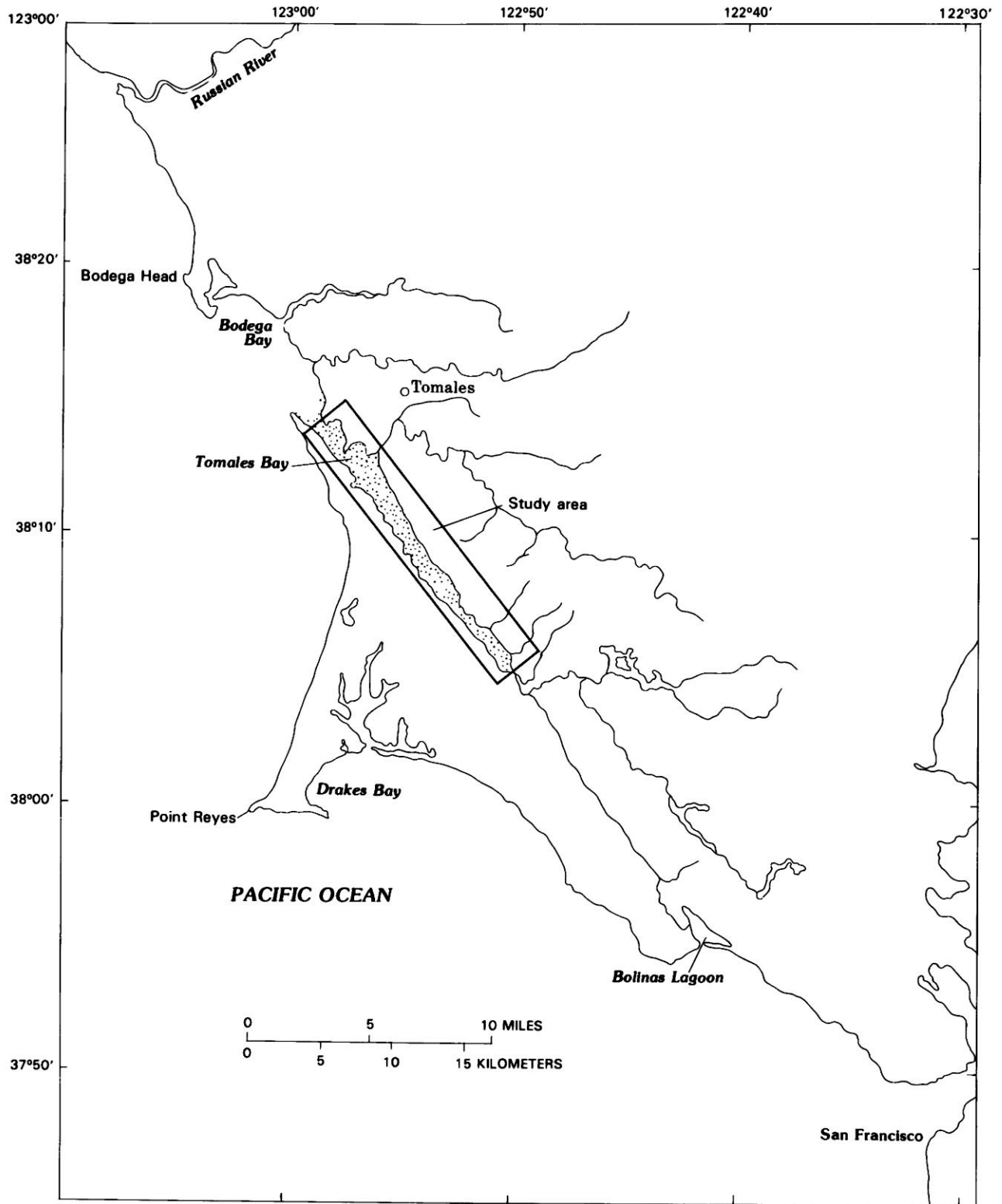


FIGURE 16.1.—Location of Tomales Bay, central California, showing major drainage systems discharging into the bay (from Daetwyler, 1966, fig. 1).

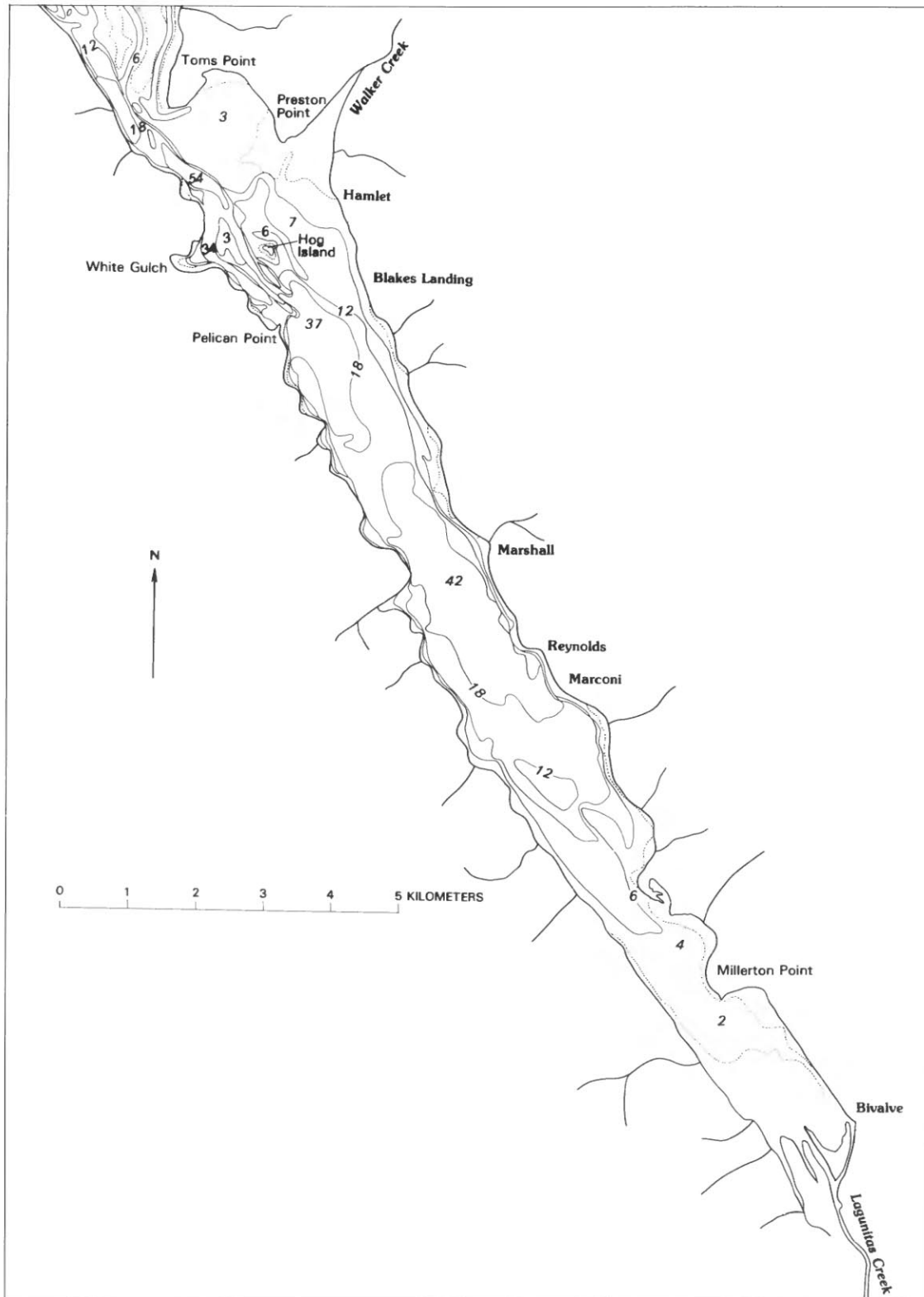


FIGURE 16.2.—Simplified bathymetric map (in feet) of Tomales Bay, showing locations of mouths of Walker and Lagunitas Creeks. Dotted lines mark edge of intertidal flats. Owing to map scale, contours are not traceable in places.

### STREAMS

Five ephemeral streams and two perennial streams drain the area surrounding Tomales Bay. The ephemeral streams are Olema, Arroyo, Nicasio, Chileno, and Salmon Creeks. These creeks deposit substantial volumes of sediment that remains near their mouths. Walker Creek, a perennial stream, enters the bay from the east approximately 4.6 km southwest of the bay mouth; it has a drainage area of 96.1 km<sup>2</sup>, and a well-defined tidal delta extends from its mouth into the bay (fig. 16.3). This creek, which has been monitored since 1965 from a stream-gaging station located 5.6 km southeast of the town of Tomales, has a mean discharge of 1.212 m<sup>3</sup>/s.

Lagunitas Creek, also a perennial stream, supplies conspicuous amounts of sediment to the bay. This stream

enters the southeast end of the bay approximately 2 km northwest of the town of Point Reyes Station (fig. 16.4). Of all the streams that enter the bay, Lagunitas Creek drains by far the largest area (211.6 km<sup>2</sup>). Flow in Lagunitas Creek is monitored at a stream-gaging station located 2.3 km northwest of Point Reyes Station; the mean discharge is 1.733 m<sup>3</sup>/s. Streamflow in the creek is regulated by several artificial lakes (Nicasio Reservoir, Kent Lake, and Alpine Lake).

### SEDIMENT

The type of sediment in Tomales Bay differs greatly, depending on its location (fig. 16.5). Daetwyler (1966) summarized the texture of the sediment on the basis of

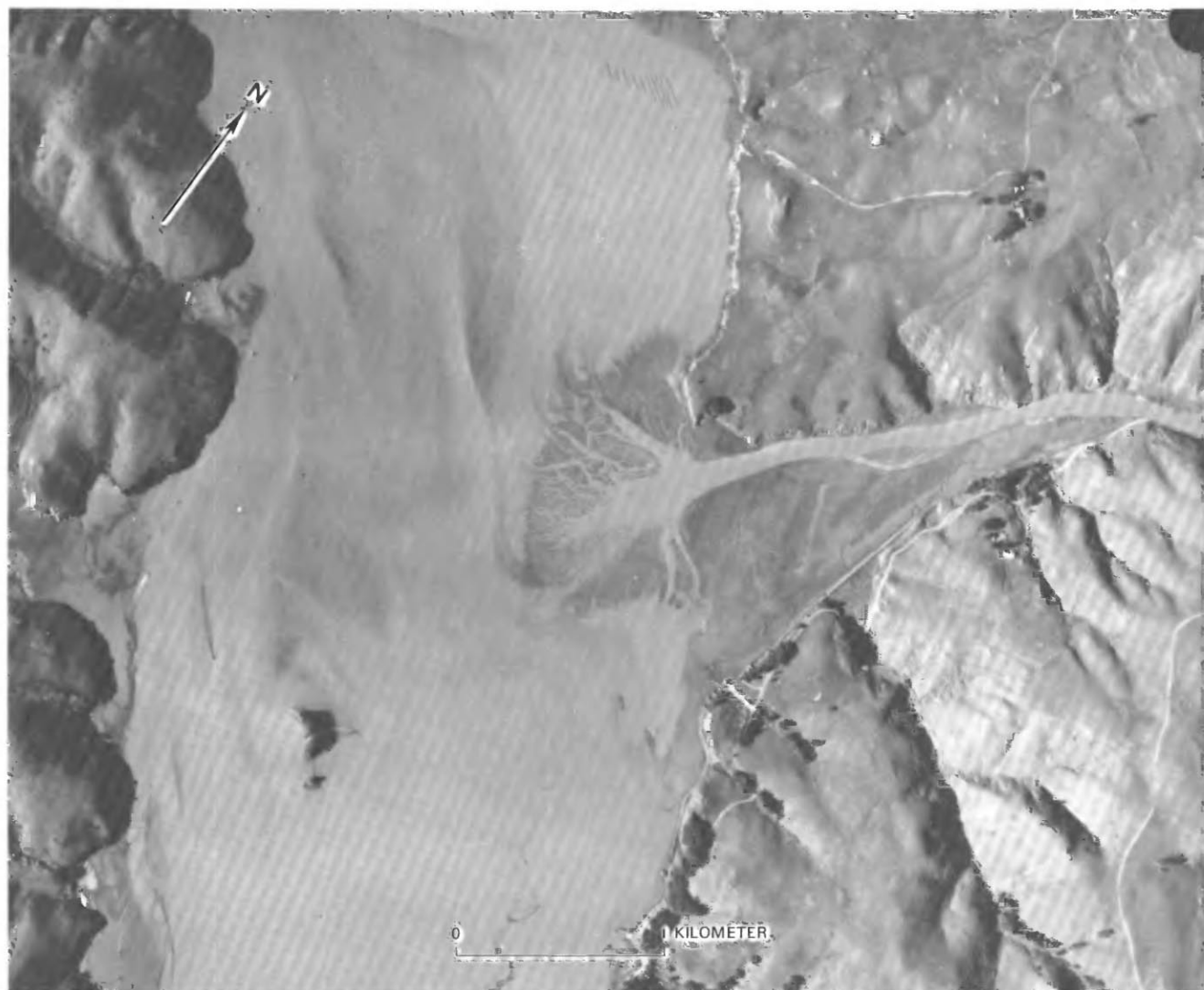


FIGURE 16.3.—Walker Creek delta. Photograph taken 2 days after the January 1982 flood.



FIGURE 16.4.—Lagunitas Creek delta.



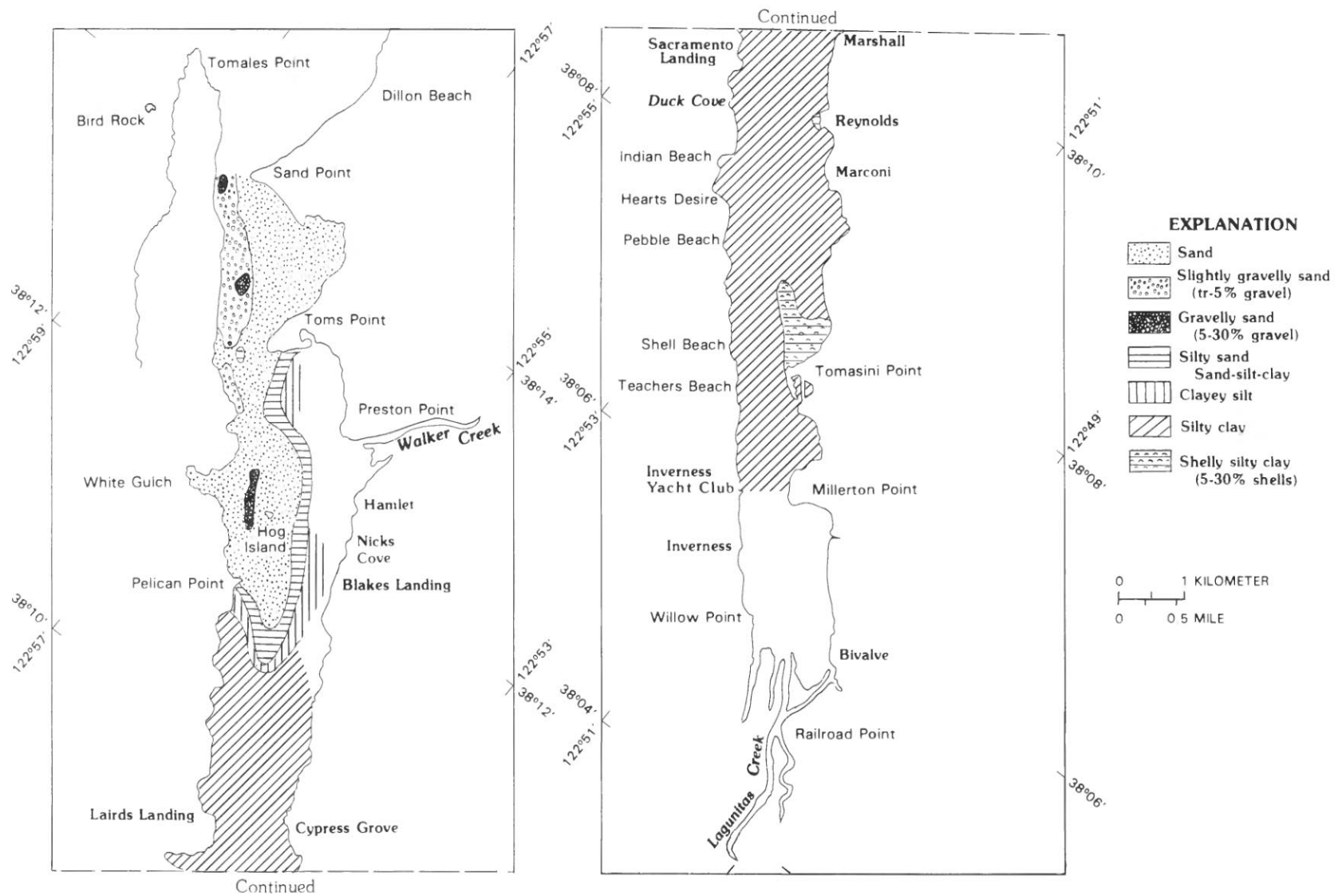


FIGURE 16.5.—Distribution of surface lithologic units in Tomales Bay (modified from Daetwyler, 1965, fig. 16).

more than 100 samples collected within the bay. Within the main body of the bay, from Millerton Point to a short distance south of Pelican Point, the sediment is silty clay and has a median grain size smaller than  $3.9\ \mu\text{m}$ . Coarser sediment is present only at the margins of the bay and tidal channels; for example, sand extends offshore for a few tens of meters from sandy beaches on the west side of the bay.

From the vicinity of Pelican Point northward to the mouth of Tomales Bay, the textural distribution is relatively complex. The tidal channels north of Pelican Point are floored by sand that grades from fine to medium and coarse near the mouth of the bay (Daetwyler, 1966, fig. 19). Sandy sediment extends into the bay from a well-defined flood-tidal delta southeast of Pelican Point. Between Toms Point and Blakes Landing, the sediment changes in a northeasterly direction from well-sorted, tidally winnowed sand to a more poorly sorted silty sand or clayey silt. South of Millerton Point, the sediment that floors the bay progressively coarsens and grades from clayey silt to sand on the intertidal part of the Lagunitas Creek delta at the southeast end of the bay.

## THE JANUARY 3-5, 1982, STORM

### RAINFALL

Rain-gage data collected January 3-5, 1982, varied between stations located inshore and those located near the open coast. Storm totals ranged from 333 mm (13.1 in.) at Point Reyes Station to 131 mm (5.2 in.) at Tomales (Edward Richmond, written commun., 1983). Other stations in the area were: Inverness, which recorded 285 mm (11.2 in.); Nicasio Reservoir, 248 mm (9.8 in.); and Bodega Bay Marine Station, 276 mm (10.9 in.). The rain-gage stations had not been established for previous years, and comparisons with other storms are not possible in terms of actual rainfall amounts; however, stream-discharge records do show relative differences between years of high discharge.

The streams that drain into Tomales Bay quickly responded to the large amounts of rainfall. Discharge in Lagunitas Creek reached  $302\ \text{m}^3/\text{s}$  on January 4, 1982, in contrast to a typical winter discharge of 0.1 to  $8.2\ \text{m}^3/\text{s}$  for the period 1972-82. Earlier records show that streamflow last approached that of the January 1982 storm in December 1955, when it reached  $255\ \text{m}^3/\text{s}$  (U.S. Geological Survey, 1954-82). Although the flood gage on Walker Creek was submerged on January 4 and the recorder fouled, an estimate of slightly more than  $230\ \text{m}^3/\text{s}$  was made by using a slope-area measurement with a normal recession to a measurement made on January 16 of  $0.78\ \text{m}^3/\text{s}$  (Kenneth Markham, written commun., 1983). Before the January 1982 flood, the only other

flood to approximate it was in January 1966, when streamflow reached a discharge rate of  $153\ \text{m}^3/\text{s}$  (U.S. Geological Survey, 1959-82). Although discharge data are unavailable for the smaller streams that empty into the bay, the presence of small, well-formed deltas immediately after the storm at the mouth of nearly every valley on the east side of the bay attests to substantial flow in even the smallest streams (fig. 16.6).

The streams generated a high level of turbidity in the bay that persisted for some time after the storm. Turbid plumes issued from the mouth of the bay as ebbs carried the suspended sediment into the ocean.

### LANDSLIDES

The effects of many debris torrents, debris flows, and other landslides were observed along the roadways and hills surrounding Tomales Bay (pl. 5). Steven L. Reneau (see Inverness area case study, chap. 6) investigated the area around Inverness, which was extensively damaged by landslides and floods. Our observations that few landslides reached the bay itself are supported by Reneau's. The only major landslide entering the bay was a log surge at Redwood Avenue (see figs. 6.7, 6.8). One landslide along the canyon onshore of Shell Beach (fig. 16.6), which Reneau did not investigate, moved debris approximately 500 m toward the bay but stopped 10 m short of the bay where the canyon widens. Reneau observed such features as erosion of soil and vegetation from a 15- to 20-m-wide swath, pileup of 1 to 2 m of mud and woody debris on the upstream side of trees within this swath, pressing down of vegetation and orientation of stems downcanyon, and banking of piles of woody debris around bends in the channel, higher on one side of the drainage axis than on the other. Many of these same features also were noted along the Shell Beach landslide. The sediment that did enter the bay accumulated in small deltas formed partly by runoff from these landslides.

### METHODS

To identify the depositional effects of the January 1982 storm, we sampled surficial sediment in the northern and central parts of Tomales Bay about a month after the storm and in the southernmost part of the bay 3 weeks later (fig. 16.7). Several types of cores were taken. A total of 31 gravity cores, 8 cm in diameter and as much as 123 cm long, were taken in the muddier sediment; by using a tensiometer, we ensured that the core barrel only partly penetrated the sediment, so that its uppermost layers were preserved. Where the sediment was sandier, a Smith-McIntire sampler, capable of engulfing and removing 9 L of sediment, was employed. Hinged flaps

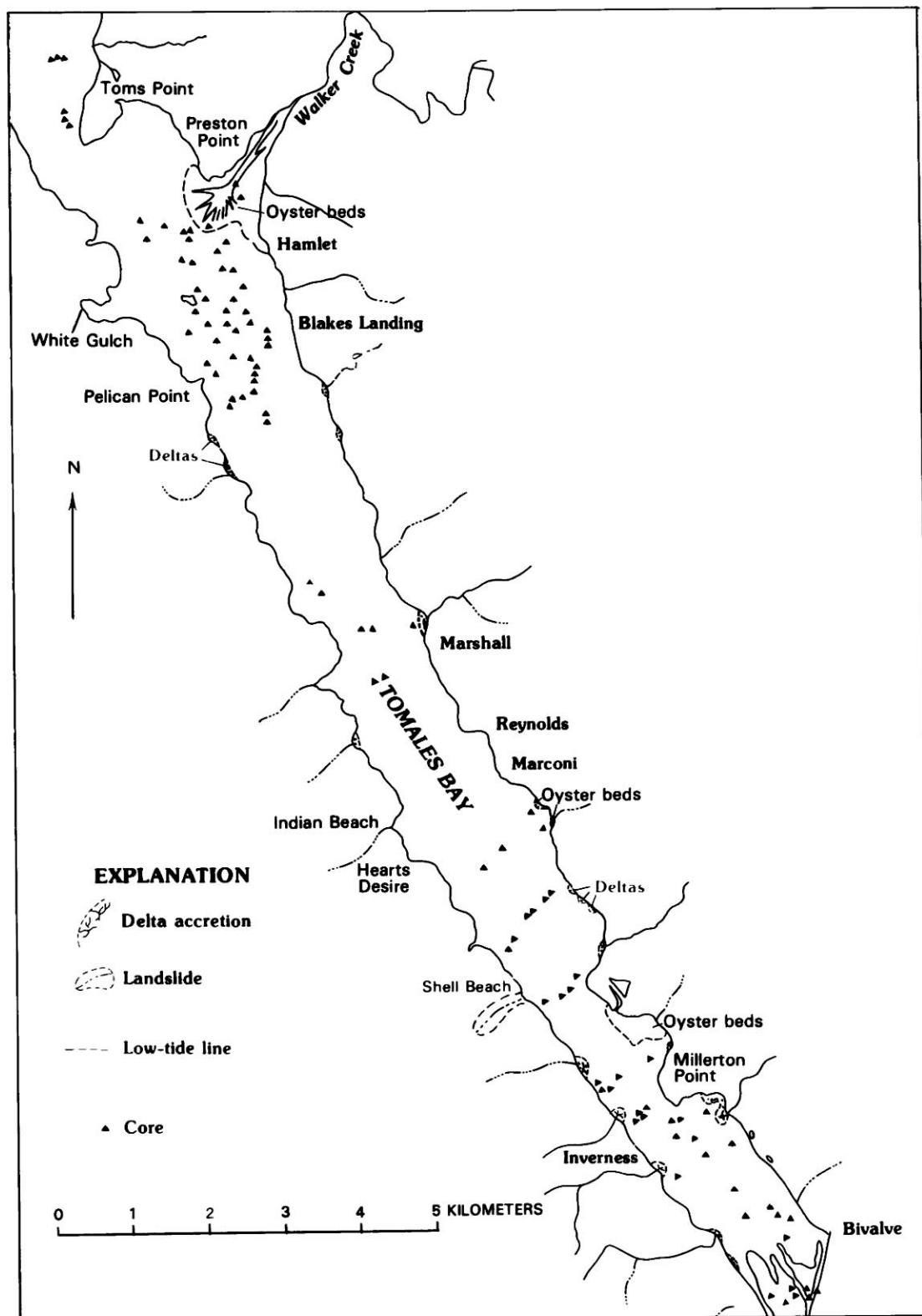


FIGURE 16.6.—Tomales Bay, showing locations of cores, shellfishing grounds, and areas of major and minor delta accretion due to the January 1982 storm.

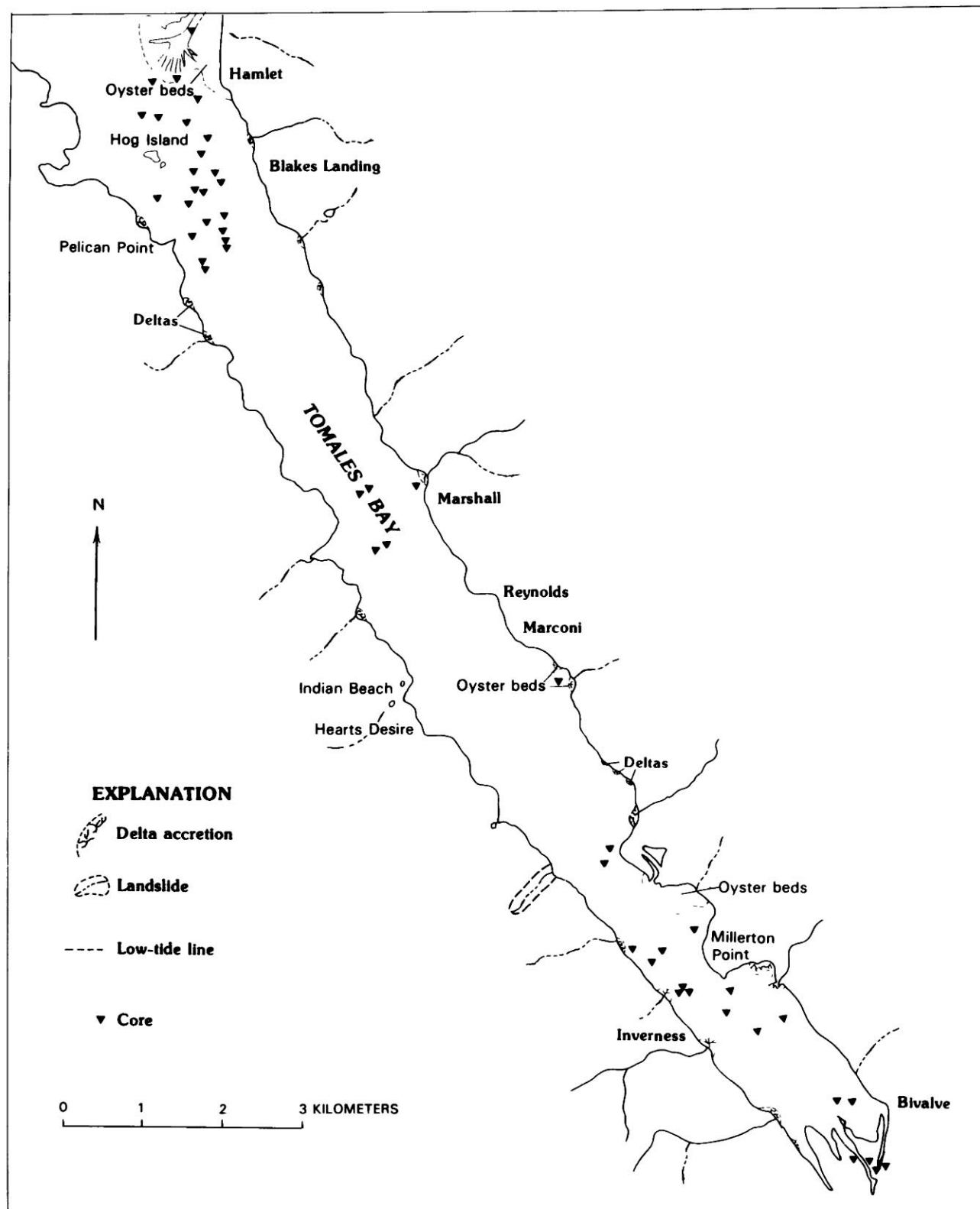


FIGURE 16.7.—Tomales Bay, showing locations of cores taken in February and March 1982.



on the top of the sampler provided access for examining the sediment surface (which typically was undisturbed) and for taking small box cores (surface area, 40 cm<sup>2</sup>) and pipe cores (2.5 cm diam) to a depth of 10 to 15 cm from the sediment enclosed in the sampler. The resulting cores were split in the laboratory, where photographs and X-ray radiographs were taken. Samples were extracted from the cores for textural and mineralogic analysis.

Samples were wet-sieved and prepared for grain-size analysis, according to the method of Thiede and others (1976). Sediment between 200 and 63  $\mu$ m in size was analyzed by a rapid sediment analyzer (RSA; Thiede and others, 1976, p. 45). The remaining sediment of less than 63  $\mu$ m size was analyzed with a hydrophotometer (Jordan and others, 1971).

The standard X-ray-diffraction method (Hein and others, 1975) was used for clay mineralogic analysis. Preparation of the sample was similar to the method used for grain size, and only the clay-size material was used. However, variations in clay mineralogy between the storm and nonstorm layers were not found.

A second round of sampling in June, July, and September 1982 provided a basis for examining the degree of reworking of probable storm deposits by physical and biologic processes (fig. 16.8). Cores collected during this sampling were processed similarly to those in the first set.

### FLOOD DEPOSITS

Many of the cores taken in Tomales Bay after the January 1982 storm contain a layer of sediment possibly attributable to the storm. In the absence of this layer (or beneath it) the sediment appeared in the X-ray radiographs to be thoroughly bioturbated. Mollusk shells or shell fragments are common in this bioturbated material.

Three lines of evidence support the inference that the surface layer resulted from the storm. First, on the Walker Creek delta front, blanketing of a surface marked by a concentration of still-green blades of the seagrass *Zostera* by such a layer indicated recent rapid sedimentation. A similar smothering of living saltgrass *Salicornia* was observed on the Lagunitas Creek delta (fig. 16.9). Second, this layer everywhere lacked mollusk shells or shell fragments (except for a few obviously active gastropods at the surface of one core). This general absence of shells suggests rapid deposition of terrigenous detritus derived from a source outside the bay. Third, of the 31 cores taken shortly after the storm, 14 contain a well-defined surficial layer, and 6 others a questionable layer. The appearance of this layer varied. Commonly, it seemed

to be texturally graded (fig. 16.10), and in many places it was internally laminated (fig. 16.11). A few burrows are visible within the layer in some X-ray radiographs, but in comparison with the underlying sediment the layer is relatively undisturbed by faunal activity. The base of the layer commonly was sharply defined, and in some cores, burrows in the underlying sediment were truncated by the contact (fig. 16.12).

A few of the cores on the Walker Creek delta contain two layers that may have formed as a result of discharge from the creek. This double layer is best defined in a core taken a short distance off the delta (fig. 16.13). The lower layer, 1.2 cm thick, shows more burrows than does the upper layer, which consists of about 1.5 cm of homogeneous fine mud. The upper surface of the lower layer is marked by a slight concentration of fine sand. The other core containing a probable double layer (fig. 16.14) was taken from the edge of the delta (fig. 16.15). The lower layer in this core consists of crosslaminated sand, is sharply overlain by 4 to 5 cm of graded laminated mud, and contains an articulated open clamshell that may have been redeposited from the top of the delta. Cores taken from the central part of the bay typically contain no surficial layer. Some of these cores show small articulated clamshells within a few millimeters of the sediment-water interface. The presence of these clamshells implies that any storm deposit here was less than a millimeter or so thick and thus too thin to be discernible in the X-ray radiographs.

The composition of the flood deposit varied with location. On the deltas of Walker and Lagunitas Creeks, deposition from bedload predominated. Lagunitas Creek, where it enters the delta, was floored with loosely packed gravel that yielded underfoot when we waded up the stream in March. Figure 16.16 shows a core taken through gravel exposed at the point where the stream bifurcates (fig. 16.17); the absence of bioturbation of this material suggests that it was recently deposited. Thin discontinuous patches of recently deposited sand atop the adjacent salt-marsh surface documents topographically higher deposition of finer material.

Sediment in the bed of Lagunitas Creek fines toward the front of the delta (fig. 16.18). West of the Bivalve area (fig. 16.17), the channel floor consists of coarse sand, and the intertidal sandflats showed evidence of recently deposited sand (fig. 16.19). On the submerged front of the delta, east of Inverness, the bay occupies a flat trough less than a meter deep at low tide. Cores taken here contain a faintly stratified surficial mud layer, 2 to 3 cm thick.

A similar pattern prevails on the Walker Creek delta. On the intertidal surface of the delta, 6 to 7 cm of faintly

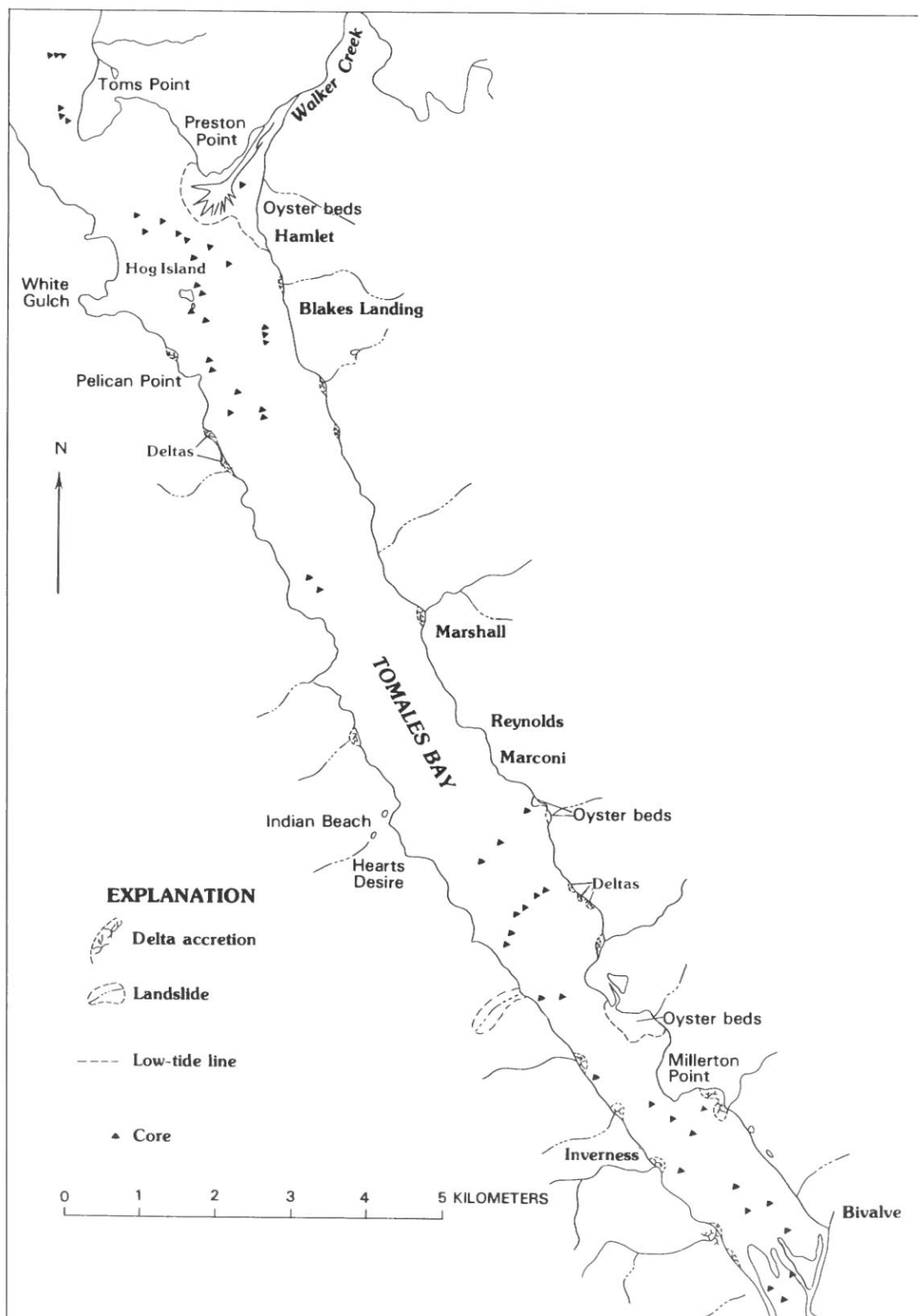


FIGURE 16.8.—Tomales Bay, showing locations of cores taken in June, July, and September 1982.

stratified sandy sediment was deposited atop bioturbated muddy sand containing abundant mollusks. On the subtidal prodelta, cores contained 3 to 12 cm of fine sand, silt, and clay attributable to flood deposition.

The flood deposits remained discernible in cores taken 6 to 9 months after the storm. Most cores showed evidence of biologic reworking, although the degree of bioturbation differed substantially among the various cores. Some cores reflected rapid and intensive colonization by an organism that constructs a U-shaped burrow (fig. 16.20), whereas others showed remarkably little bioturbation (fig. 16.21). The presence of a thin, somewhat mixed sandy layer atop a well-defined layer of clay within a few cores taken in June 1982 off the front of the Walker Creek delta implies introduction of sand by ordinary processes during the 6 months after the storm.

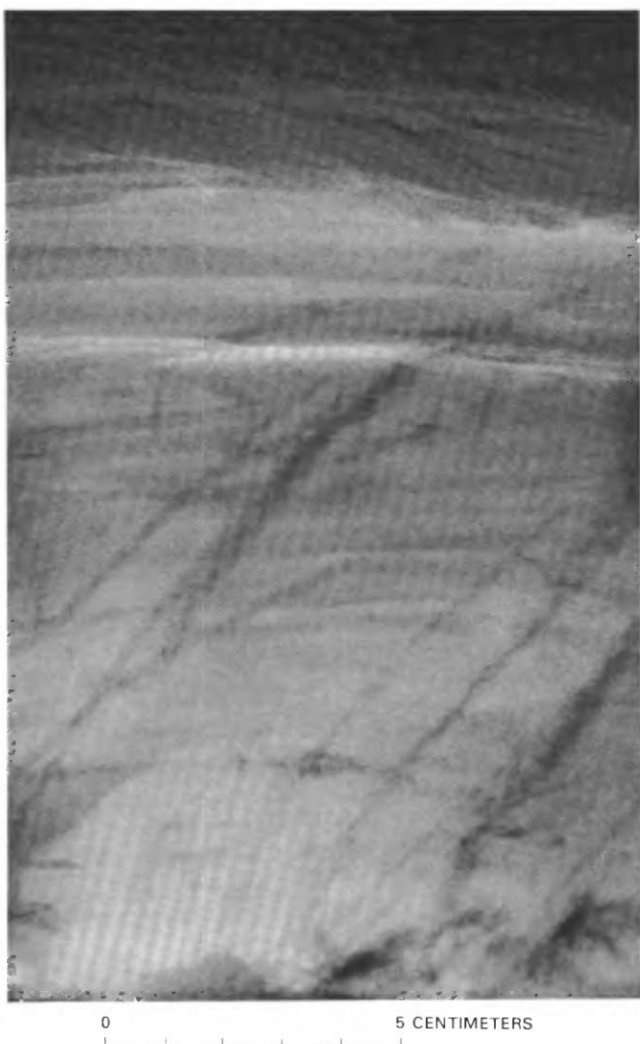


FIGURE 16.9.—X-ray radiograph of core 14 taken along stream margin of Lagunitas Creek, showing blades of saltgrass (*Salicornia*) crossing bedding planes.

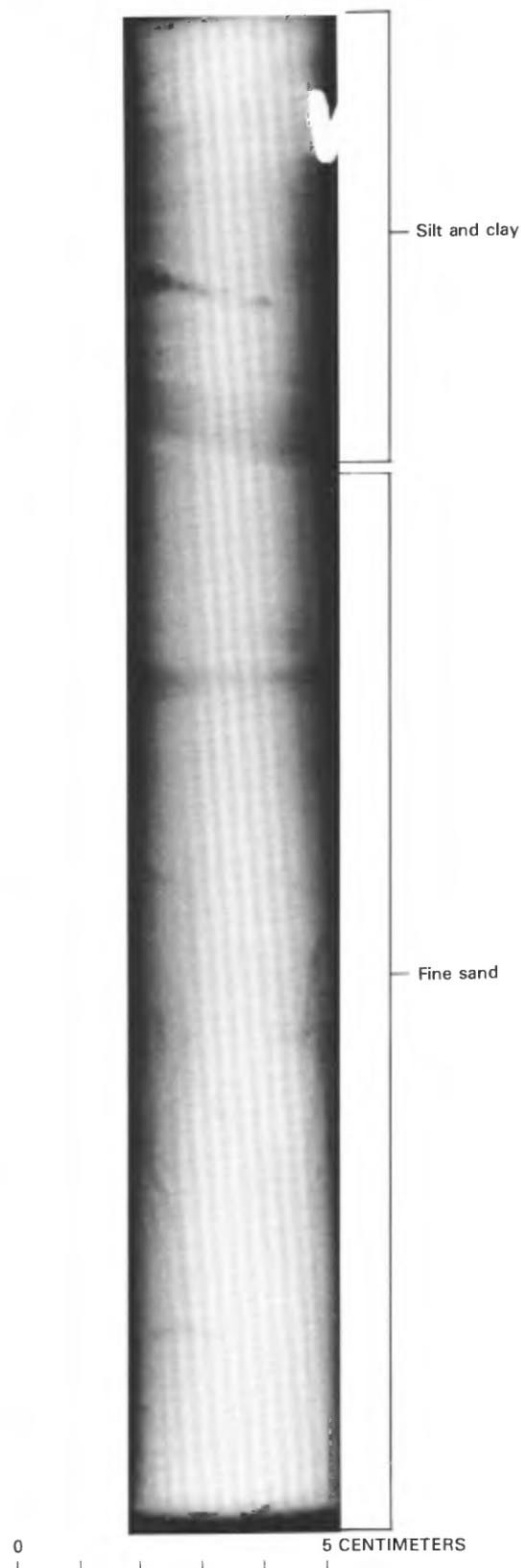


FIGURE 16.10.—X-ray radiograph of core 1 taken near Walker Creek delta, showing textural grading of flood layer.

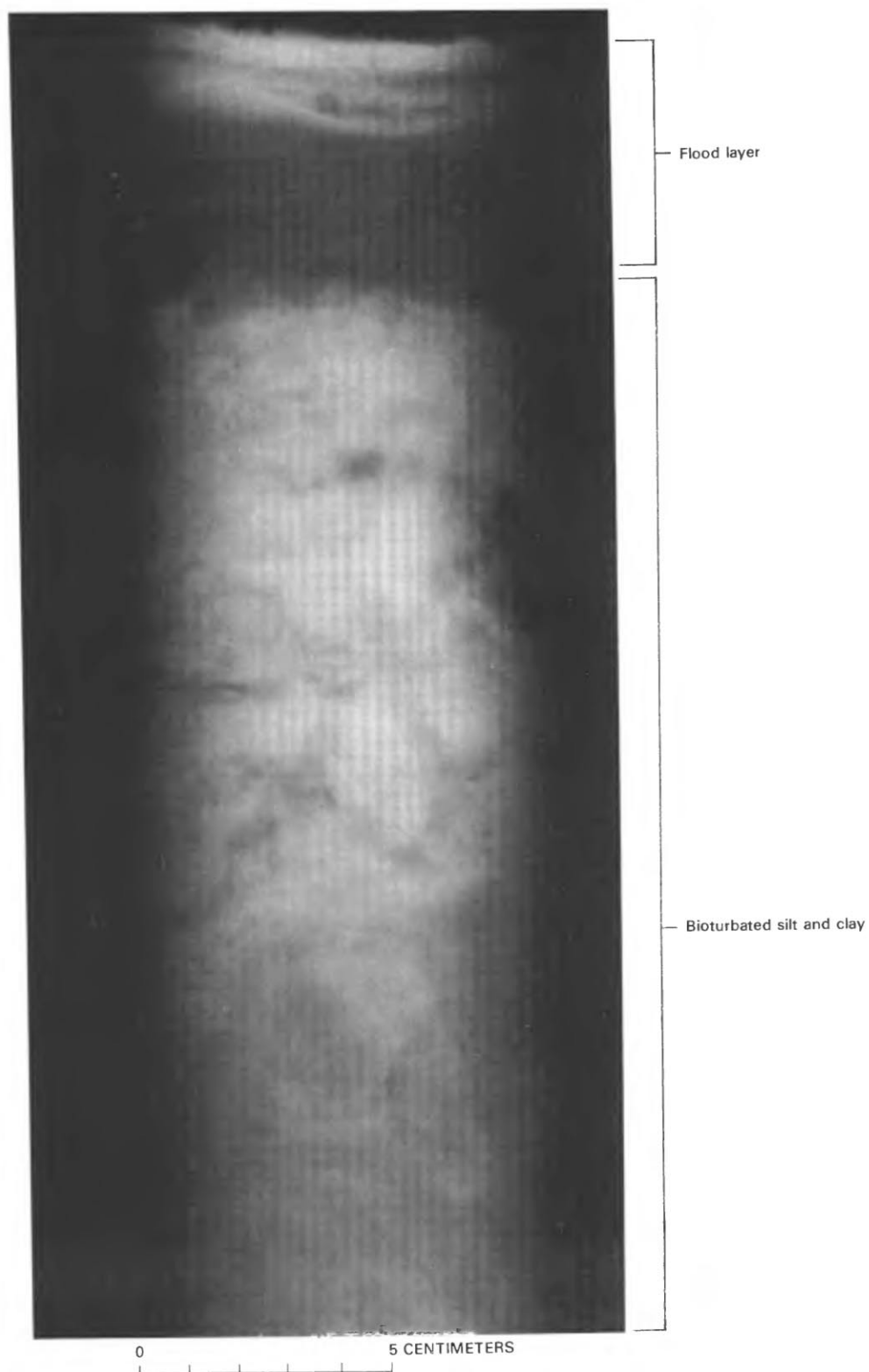


FIGURE 16.11.—X-ray radiograph of core 19 taken near Lagunitas Creek, showing internal lamination of flood layer.



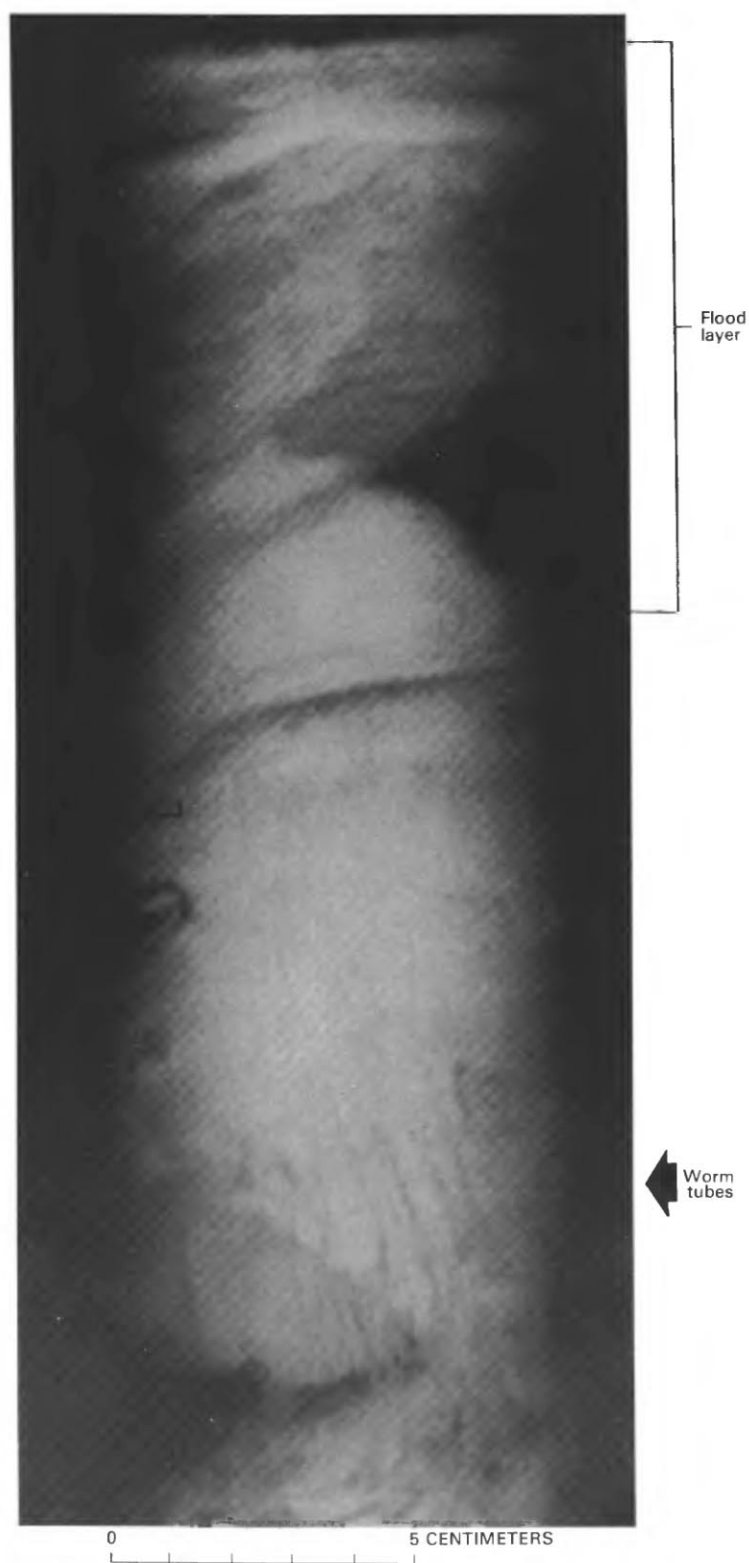


FIGURE 16.12.—X-ray radiograph of core 1 taken near Walker Creek delta, showing truncation of worm tubes by flood layer.

Cores taken 7 months after the flood in the area of Lagunitas Creek also contain remnants of the flood layer. Figure 16.22 shows two cores from the Lagunitas Creek delta. The surface layer is colonized by U-shaped burrowers and has no visible lamination, whereas 4 to 6 cm below this surface layer is a finely laminated layer underlain by intensely bioturbated sediment throughout the rest of the core. This finely laminated layer is inferred to be the remnant flood layer.

#### DISCUSSION AND CONCLUSION

The January 1982 storm caused a major depositional event in Tomales Bay. Most of the sediment introduced

into the bay was derived from Walker and Lagunitas Creeks; the smaller streams that empty into the bay contributed only minor amounts of sediment. The landslides on the west side of the bay, though devastating to property in that area, were only very minor immediate sources of sediment to the bay.

The deposits resulting from the flooding of Walker and Lagunitas Creeks were evident in cores taken shortly after the storm. The texture and thickness of these flood deposits vary. Coarsest on the deltas (or in streambeds leading into the deltas), the flood layers fine progressively bayward from the delta front. Recognizable flood deposits were found only in the vicinity of the deltas, within about a kilometer of the delta fronts. Cores taken in the central part of the bay showed no visible effects of the floods,

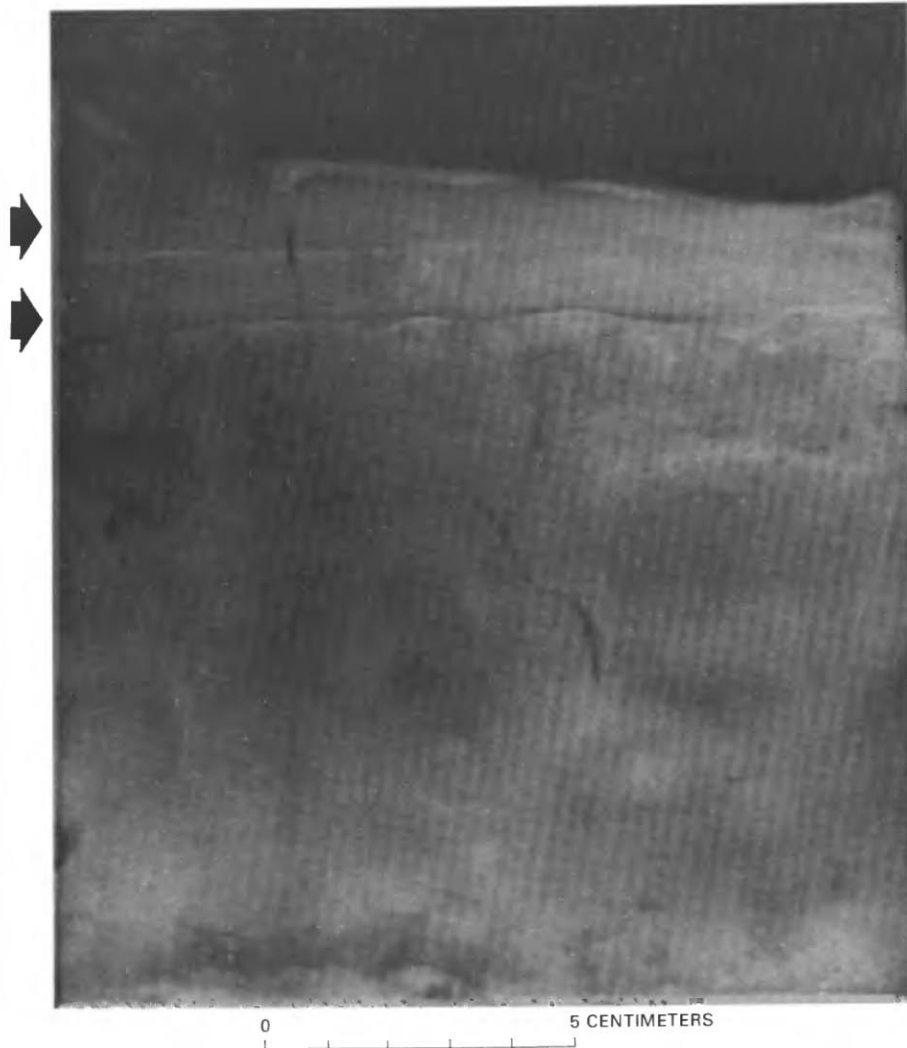


FIGURE 16.13.—X-ray radiograph of core 4 taken off Walker Creek delta, showing double layer (arrows).

and any sediment deposited there was only millimeters or less thick.

Cores taken on the south side of the Walker Creek delta suggest that the flood deposition there may have been somewhat more complex than elsewhere. The double layer shown in figures 16.13 and 16.14 implies either deposition in two phases (bedload followed by suspended load) or interruption of deposition by an interval of erosion, possibly by unusually high waves associated with the storm. A slight concentration of fine sand at the contact between the two layers supports an erosional hypothesis.

The flood layers still remain discernible in cores taken 6 to 9 months after the storm, although these layers underwent varying degrees of bioturbation. Layering attributable to prior floods was absent within the cores. Although floods may contribute the bulk of the sediment that accumulates near the deltas, the stratification associated with these deposits appears to be lost during the intervals between floods.

The only place in the bay where flood layers are likely to be preserved is in the salt marshes at the south end of the bay. Cores taken through the cutbanks of streams crossing these marshes contain alternating layers of

sand and mud (figs. 16.23-16.24). The sandy layers probably represent flood accumulations that resemble those left on the present marsh surface by the January 1982 flood.

Some of the cores taken bayward from the Walker Creek delta demonstrate how the flood deposits and tidally generated deposits merge in the bay. Figure 16.25 shows a core taken in this area in June 1982 that contains a homogeneous layer of clay—presumably the result of the January 1982 flood—overlain by a thin layer of fine sand. This sand was clearly introduced during the interval following the storm, probably by tidal currents.

The infauna in the area apparently mixes fines derived from floods with sand brought in by the everyday tidal activity. On the delta fronts, however, the sand likely also accrues during floods.

Thus, deposition in Tomales Bay appears to result from three different mechanisms (fig. 16.26). (1) On and near the deltas of Walker and Lagunitas Creeks (and, to a lesser extent, at the mouths of the smaller ephemeral streams), sedimentation is predominantly episodic, the result of floods like that of January 1982. (2) On the west side of the bay between Toms Point and Pelican

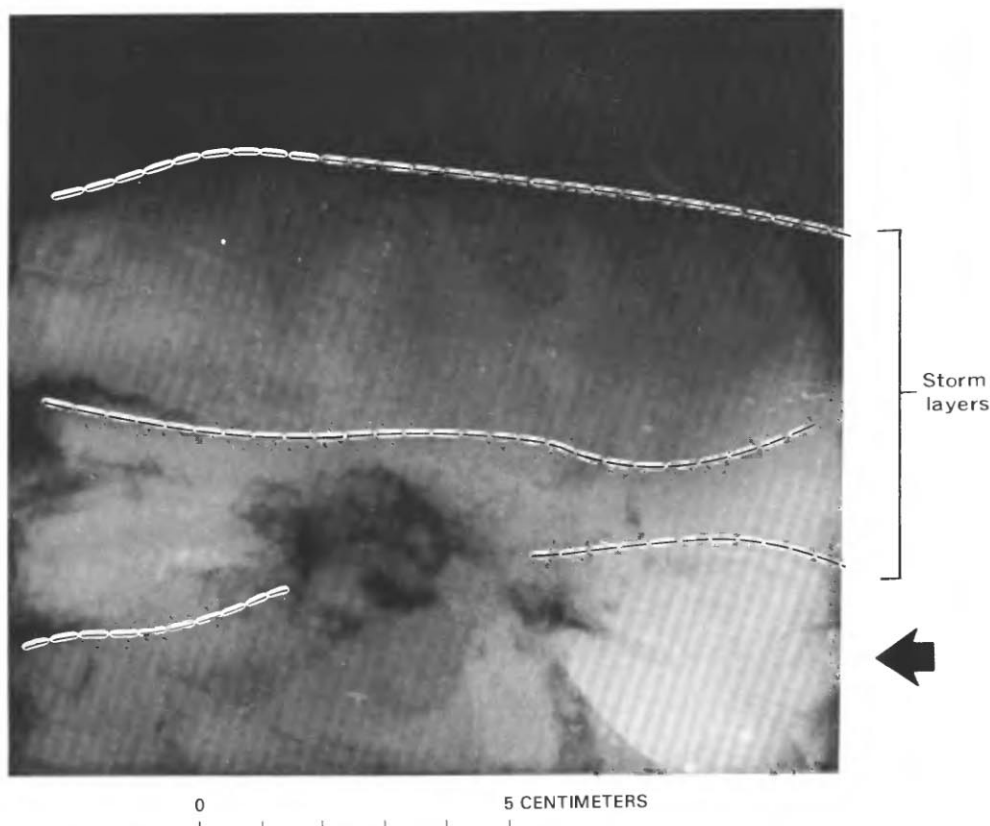


FIGURE 16.14.—X-ray radiograph of core 2 taken from edge of Walker Creek delta, showing probable double storm layer. Lower prestorm layer contains an articulated open clam (arrow).

Point, and northward to the mouth of the bay, sediment accumulation is largely by tidal processes and is essentially nonepisodic (other than the episodicity induced by fluctuations within the tidal range). (3) In the central part of the bay, sedimentation is very slow, and the accumulation of silt and clay probably results from both the episodic addition of small amounts of sediment during floods and the daily fixation of terrigenous fines by filter-feeding benthic organisms.

The limited number of cores taken in the bay after the January 1982 flood and the locally irregular accumulation on the deltas preclude an accurate estimate of the volume of sediment contributed to the bay by this event. The volume of sediment probably exceeded  $0.25 \times 10^6 \text{ m}^3$ , on the basis of the thickness of the flood layers in the

fronts of the Walker and Lagunitas Creek deltas. Daetwyler (1965) used bathymetric changes to infer that  $2.6 \times 10^6 \text{ m}^3$  of solid sediment accumulated at the mouth of Walker Creek between 1861 and 1931; most of this deposition probably occurred episodically, as the result of floods.

The January 1982 flood was especially devastating to the shellfishing industry in Tomales Bay. The area of the Walker Creek delta, the site of much of this industry in the bay, was particularly affected. Oyster growers there estimate a complete loss of juvenile stock and a heavy loss of selling stock. Such losses are due to the episodic discharge of large volumes of sediment from the creek and can be anticipated to occur again in this area as the result of future floods.

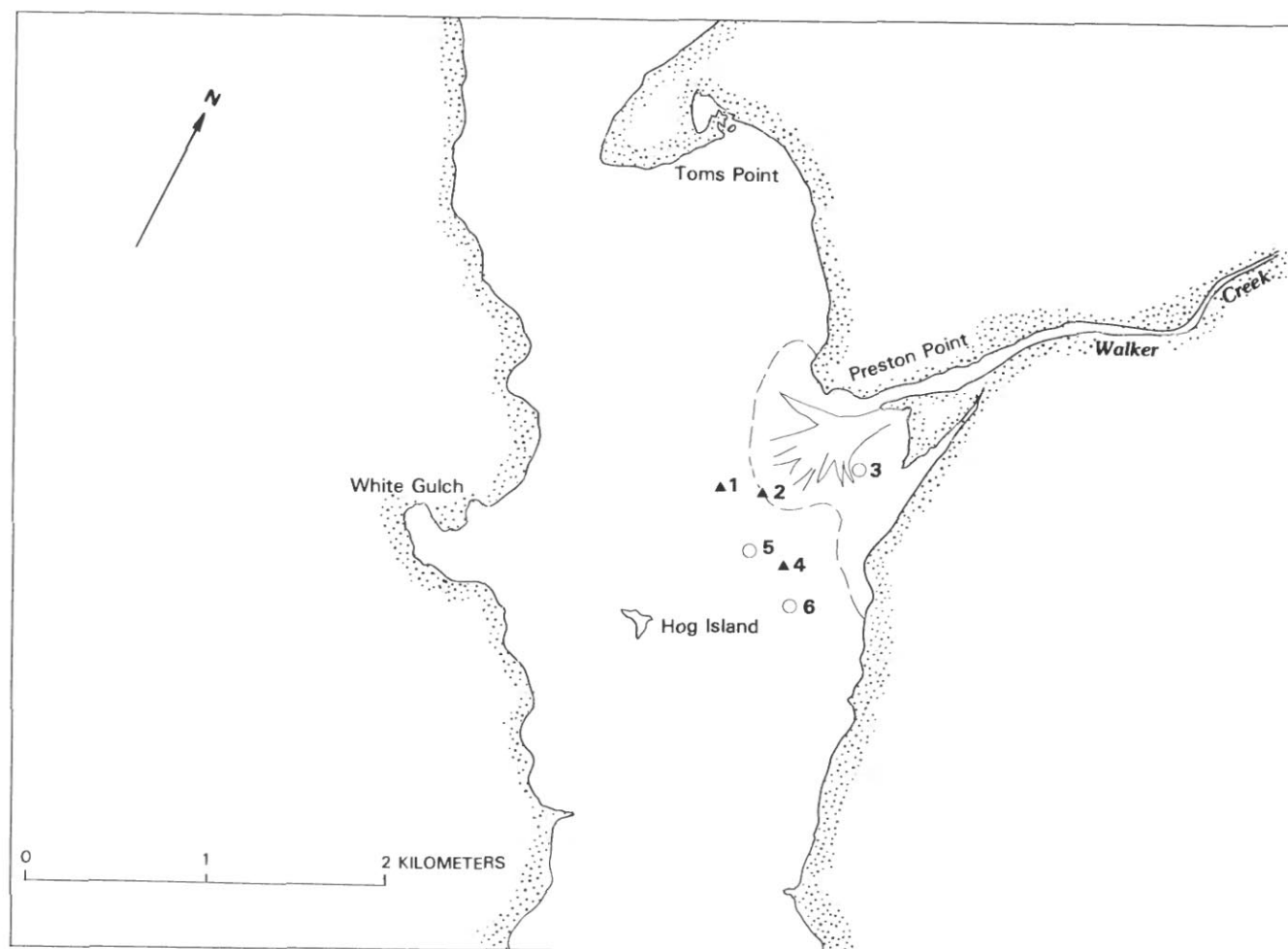


FIGURE 16.15.—Area of Walker Creek delta, showing locations of selected cores taken in February and March 1982 (triangles) and in June–September 1982 (circles). Dashed line, low-tide level.



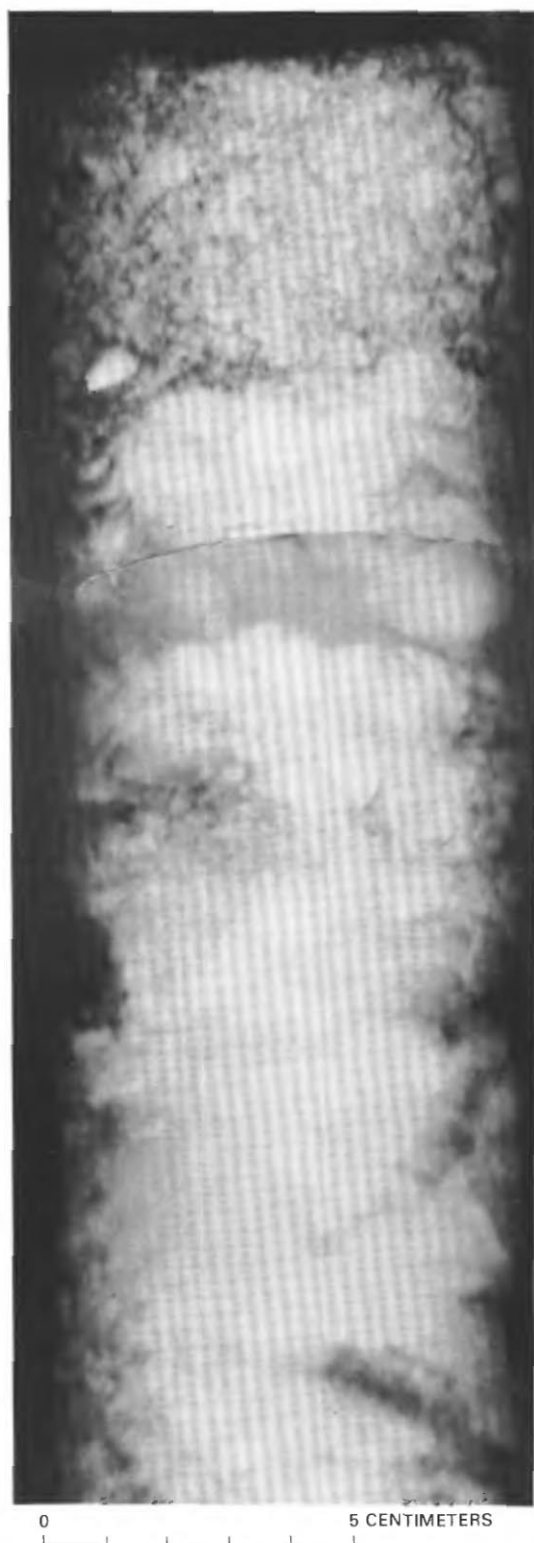


FIGURE 16.16.—X-ray radiograph of core 15 taken through gravel exposed at stream margin of Lagunitas Creek.

#### REFERENCES CITED

- Daetwyler, C.C., 1965, Marine geology of Tomales Bay, central California: San Diego, University of California, Ph.D. thesis, 219 p.
- 1966, Marine geology of Tomales Bay, central California: La Jolla, Calif., Scripps Institution of Oceanography and Pacific Marine Station Research Report 6, 169 p.
- Hein, J.R., Scholl, D.W., Gutmacher, C.E., 1975, Neogene clay minerals of the far Northwest Pacific and Southern Bering Sea: Sedimentation and diagenesis: International Clay Conference, Mexico City, 1975, Proceedings, p. 71-80.
- Johnson, R.G., Bryant, W.R., and Hedgpeth, J.W., 1961, Ecological survey of Tomales Bay: Stockton, Calif., University of the Pacific, Pacific Marine Station Research Report, 19 p.
- Jordan, C.F., Fryer, G.E., and Hemmen, E.H., 1971, Size analysis of silt and clay by hydrophotometer: *Journal of Sedimentary Petrology*, v. 41, no. 2, p. 489-496.
- National Climatic Center, 1982, Climatological data: California: January 1982: Asheville, N.C., U.S. National Oceanic and Atmospheric Administration, Environmental Data and Information Service, v. 86, no. 1.
- Thiede, Jorn, Chriss, T.M., Clauson, M., and Swift, S.A., 1976, Settling tubes for size analysis of fine and coarse fractions of ocean sediments: U.S. Office of Naval Research report under Contract N00014-67-A-0369-0007, Project NR083-102, 45 p.
- U.S. Army Corps of Engineers, 1973, Shore protection manual: Fort Belvoir, Va., U.S. Army Coastal Engineering Research Center, 2 v.
- U.S. Geological Survey, 1959-82, Water resources data for California: Walker Creek: U.S. Geological Survey Water-Data Reports.
- 1954-82, Water resources data for California: Lagunitas Creek: U.S. Geological Survey Water-Data Reports.

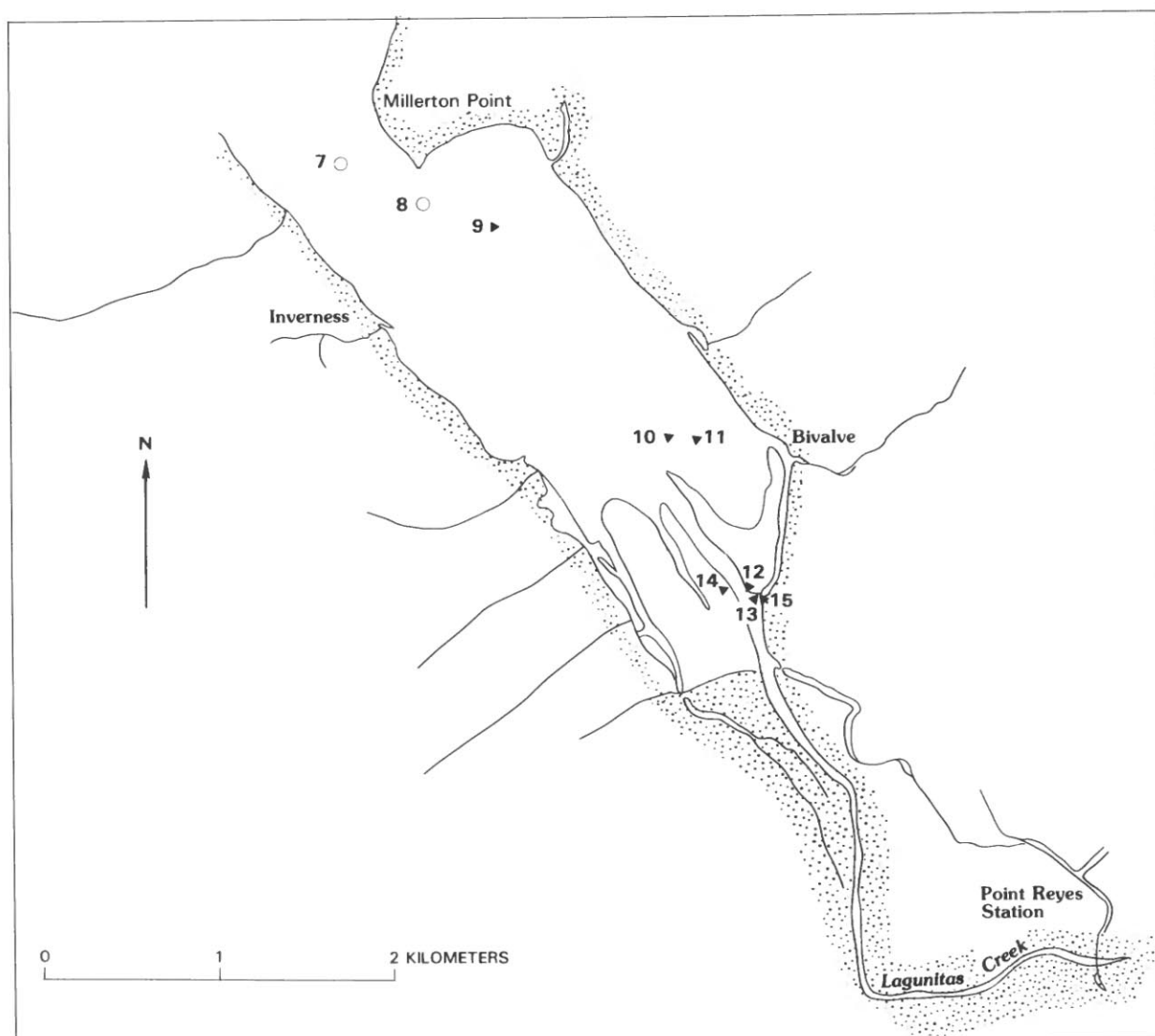


FIGURE 16.17.—Area of Lagunitas Creek, showing locations of selected cores taken in February and March 1982 (triangles) and in June-September 1982 (circles).

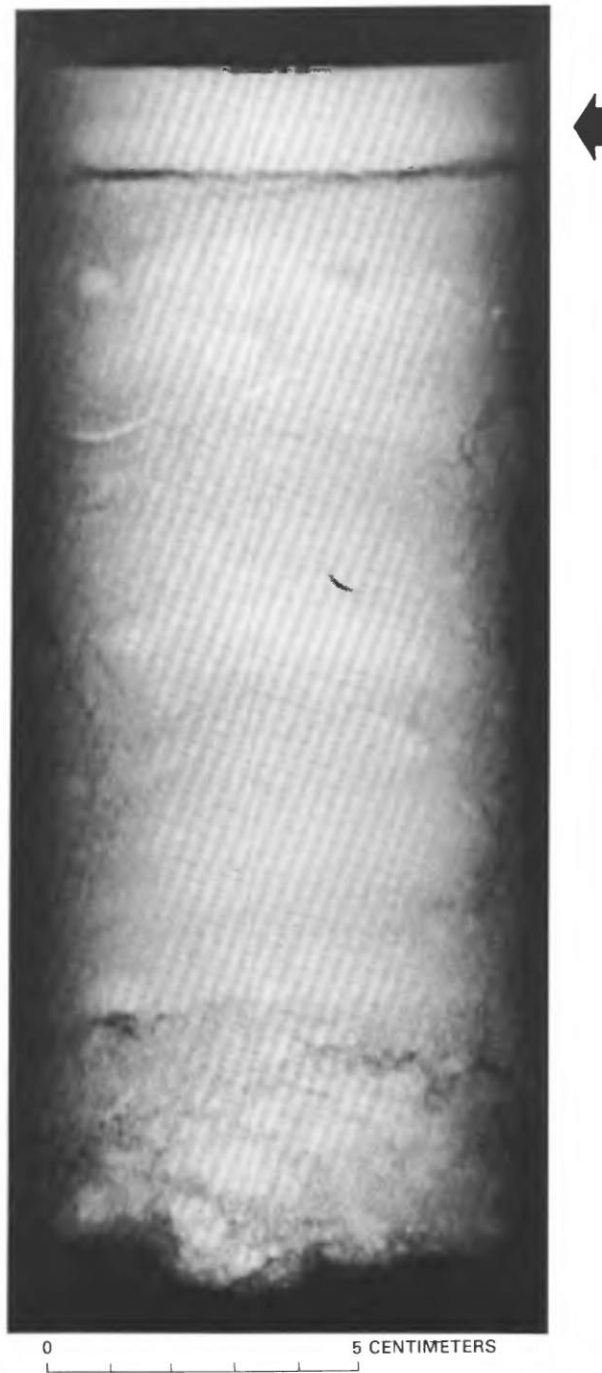


FIGURE 16.18.—X-ray radiograph of core 11 taken at front of Lagunitas Creek delta, showing finer sediment at surface (arrow).

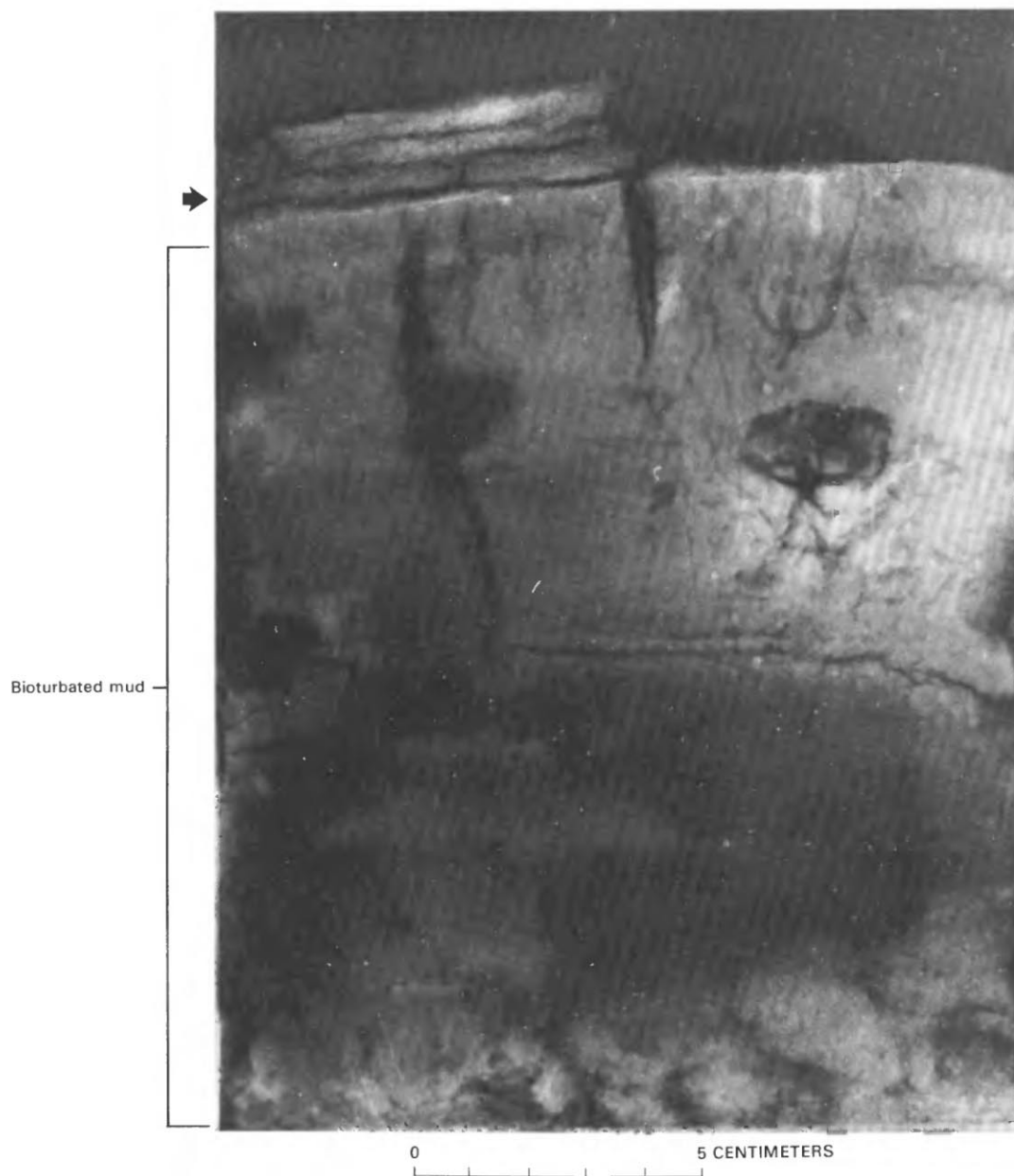


FIGURE 16.19.—X-ray radiograph of core 10 taken on intertidal flats of Lagunitas Creek, showing sand (arrow) at sediment surface.



FIGURE 16.20.—X-ray radiograph of core 3 taken on Walker Creek delta along channel margin in September 1982, showing U-shaped burrows in flood layer. Arrow denotes current direction.



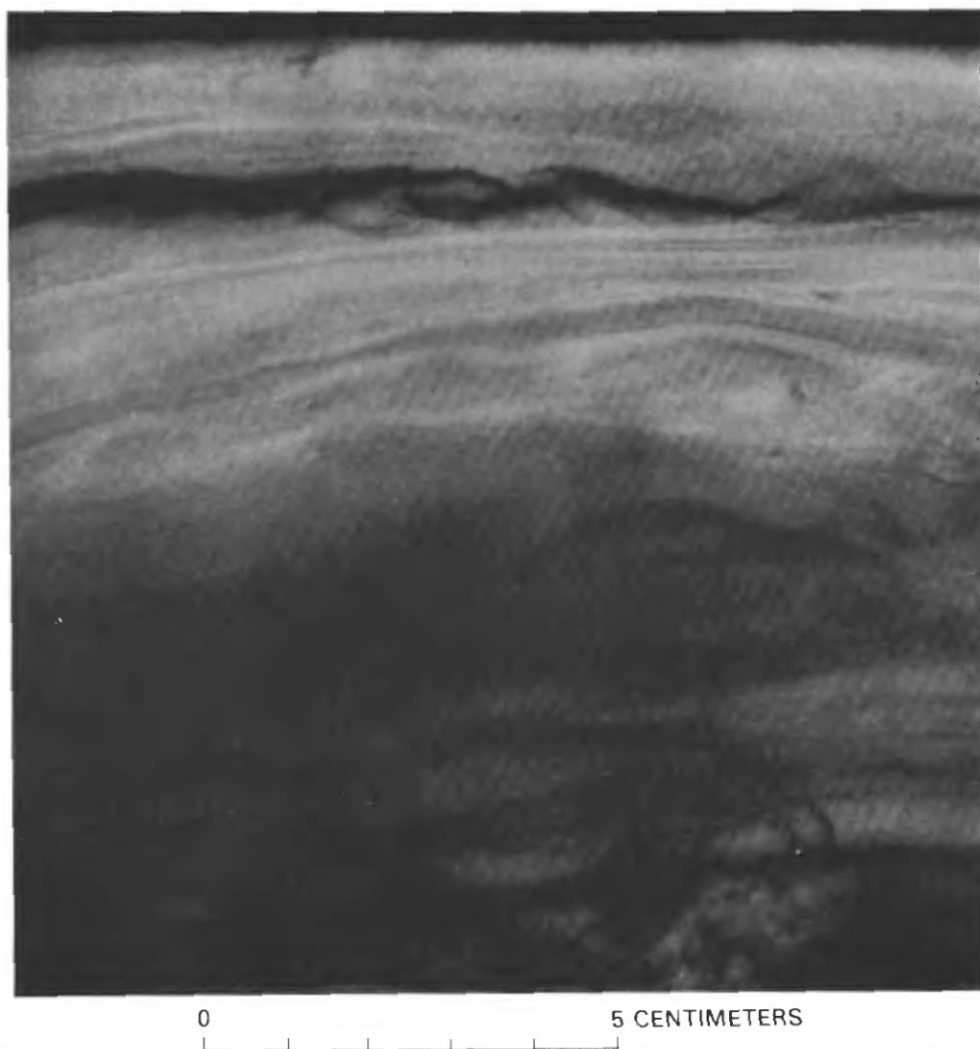


FIGURE 16.21.—X-ray radiograph of core 6 taken near Walker Creek delta in June 1982, showing very little bioturbation.

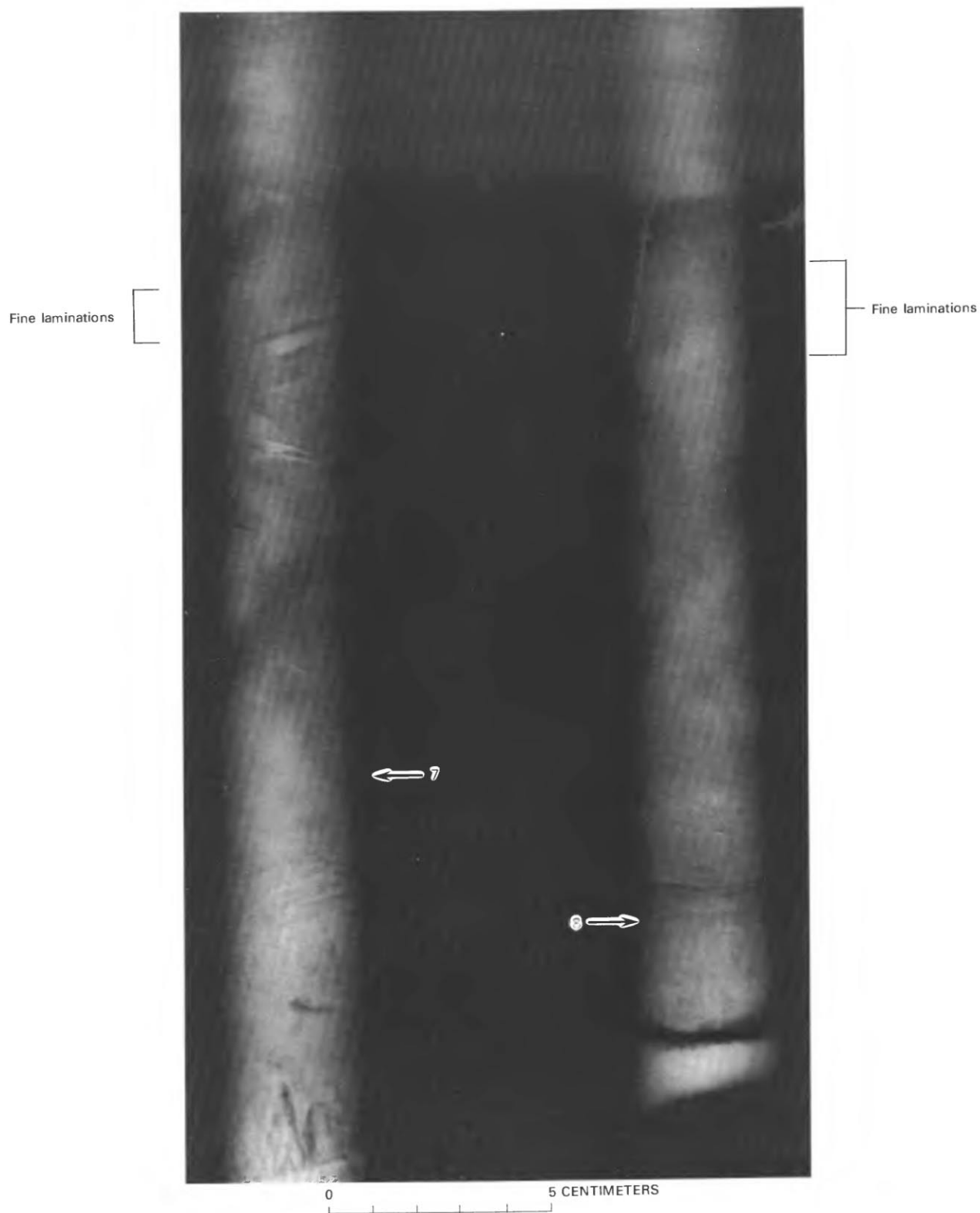


FIGURE 16.22.—X-ray radiographs of cores 7 and 8 taken off Lagunitas Creek in July 1982, showing intense bioturbation in lower sections and a finely laminated layer 4 and 6 cm, respectively, below surface. Surface layer is being colonized by U-shaped burrowers.

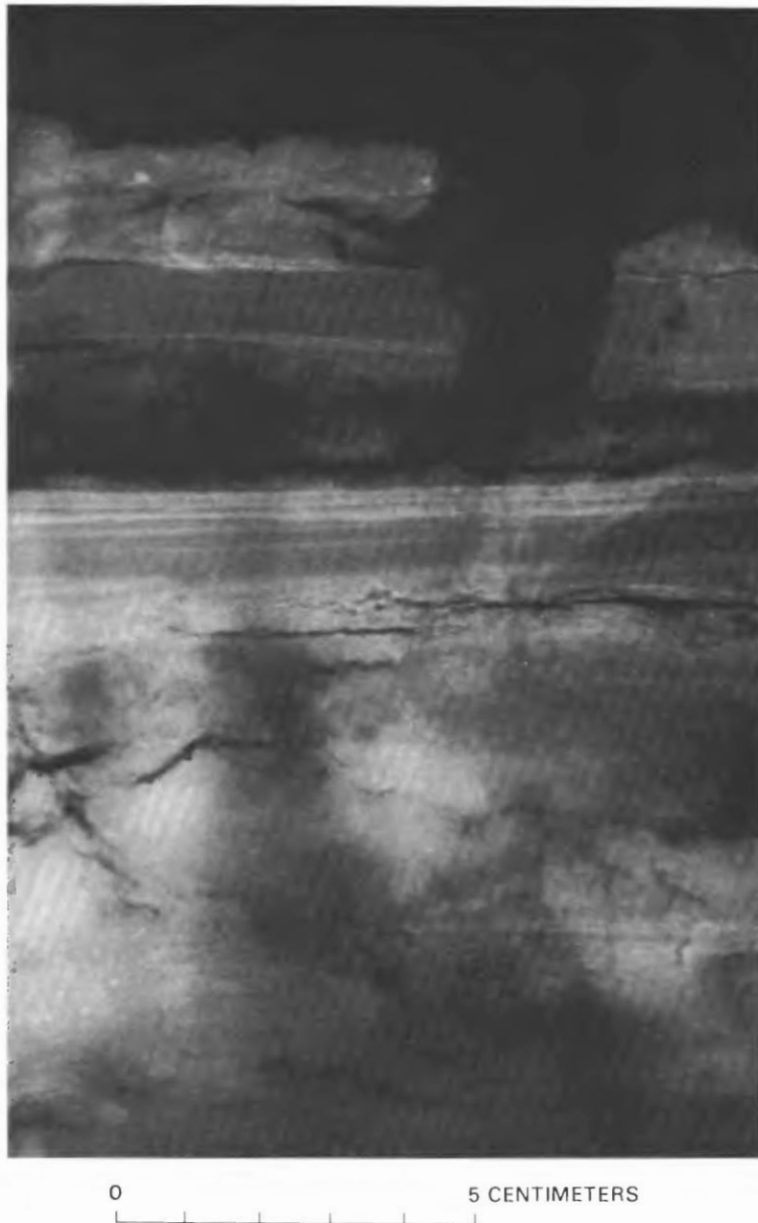


FIGURE 16.23.—X-ray radiograph of core 12 taken through cutbanks of marshes, showing alternating layers of sand (light) and mud (dark). These layers were probably formed by past flood accumulations similar to those left by the January 1982 flood.

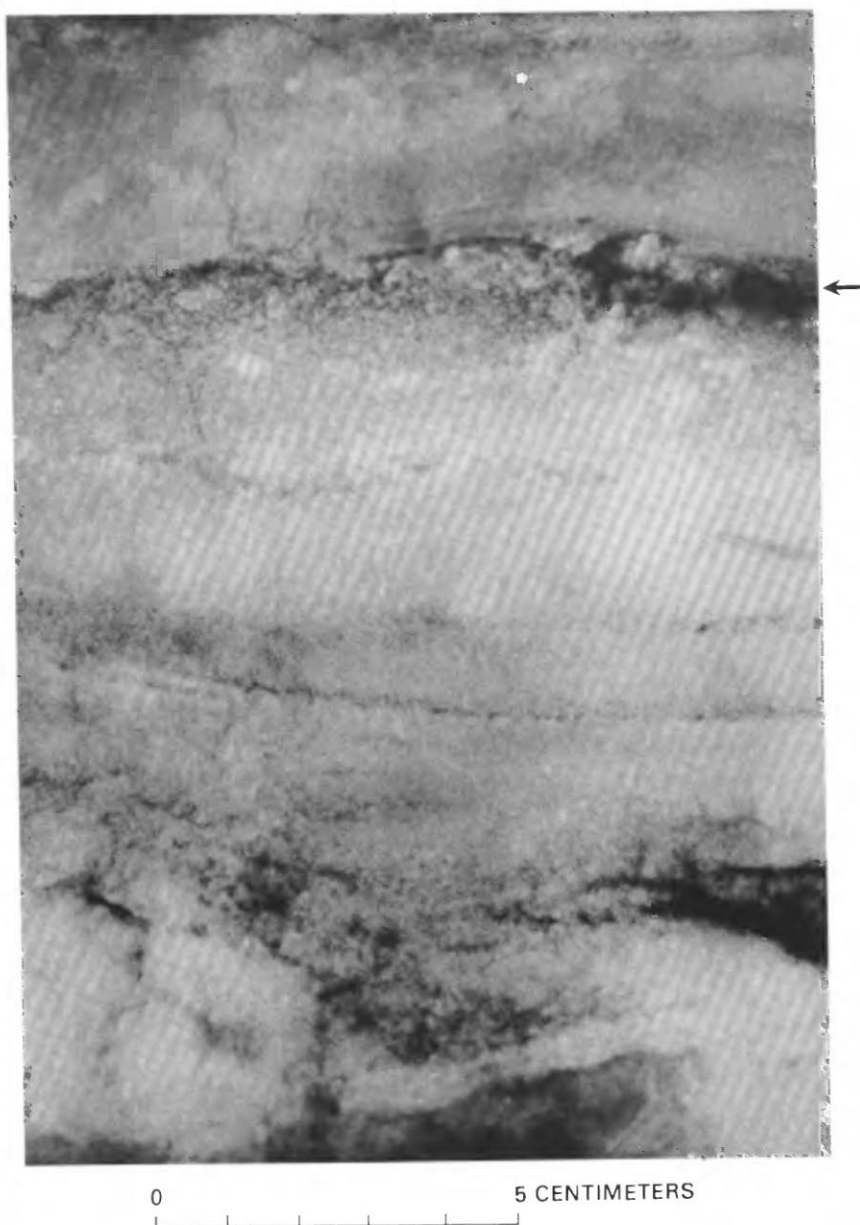


FIGURE 16.24.—X-ray radiograph of core 13 taken below core 12 on salt marsh, showing coarser sediment (arrow).

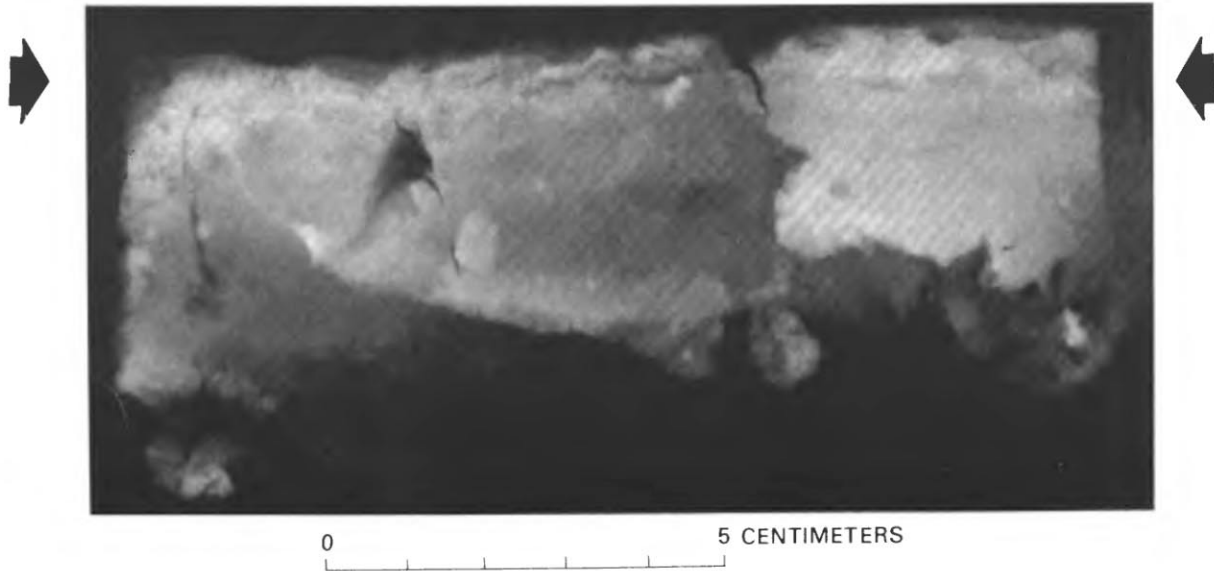


FIGURE 16.25.—X-ray radiograph of core 5 taken in area of Walker Creek in June 1982, showing a homogeneous layer of clay (flood layer) overlain by a thin mixed layer of fine sand (arrows) introduced by tidal currents.



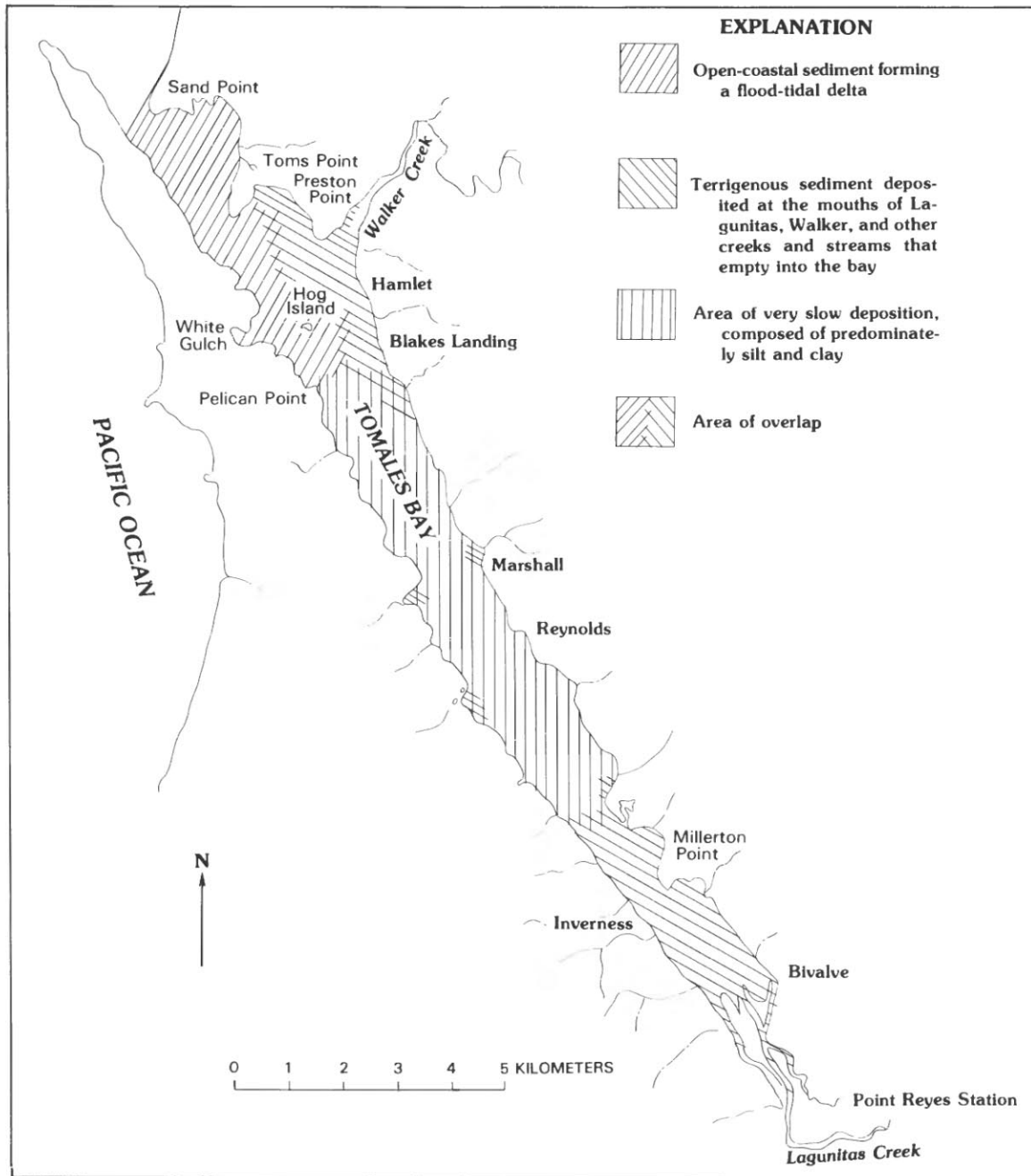


FIGURE 16.26.—Tomales Bay, showing areal distribution of sediment-depositional types.

---

## SELECTED SERIES OF U.S. GEOLOGICAL SURVEY PUBLICATIONS

---

### Periodicals

**Earthquakes & Volcanoes** (issued bimonthly).

**Preliminary Determination of Epicenters** (issued monthly).

### Technical Books and Reports

**Professional Papers** are mainly comprehensive scientific reports of wide and lasting interest and importance to professional scientists and engineers. Included are reports on the results of resource studies and of topographic, hydrologic, and geologic investigations. They also include collections of related papers addressing different aspects of a single scientific topic.

**Bulletins** contain significant data and interpretations that are of lasting scientific interest but are generally more limited in scope or geographic coverage than Professional Papers. They include the results of resource studies and of geologic and topographic investigations; as well as collections of short papers related to a specific topic.

**Water-Supply Papers** are comprehensive reports that present significant interpretive results of hydrologic investigations of wide interest to professional geologists, hydrologists, and engineers. The series covers investigations in all phases of hydrology, including hydrogeology, availability of water, quality of water, and use of water.

**Circulars** present administrative information or important scientific information of wide popular interest in a format designed for distribution at no cost to the public. Information is usually of short-term interest.

**Water-Resources Investigations Reports** are papers of an interpretive nature made available to the public outside the formal USGS publications series. Copies are reproduced on request unlike formal USGS publications, and they are also available for public inspection at depositories indicated in USGS catalogs.

**Open-File Reports** include unpublished manuscript reports, maps, and other material that are made available for public consultation at depositories. They are a nonpermanent form of publication that may be cited in other publications as sources of information.

### Maps

**Geologic Quadrangle Maps** are multicolor geologic maps on topographic bases in 7 1/2- or 15-minute quadrangle formats (scales mainly 1:24,000 or 1:62,500) showing bedrock, surficial, or engineering geology. Maps generally include brief texts; some maps include structure and columnar sections only.

**Geophysical Investigations Maps** are on topographic or planimetric bases at various scales; they show results of surveys using geophysical techniques, such as gravity, magnetic, seismic, or radioactivity, which reflect subsurface structures that are of economic or geologic significance. Many maps include correlations with the geology.

**Miscellaneous Investigations Series Maps** are on planimetric or topographic bases of regular and irregular areas at various scales; they present a wide variety of format and subject matter. The series also includes 7 1/2-minute quadrangle photogeologic maps on planimetric bases which show geology as interpreted from aerial photographs. Series also includes maps of Mars and the Moon.

**Coal Investigations Maps** are geologic maps on topographic or planimetric bases at various scales showing bedrock or surficial geology, stratigraphy, and structural relations in certain coal-resource areas.

**Oil and Gas Investigations Charts** show stratigraphic information for certain oil and gas fields and other areas having petroleum potential.

**Miscellaneous Field Studies Maps** are multicolor or black-and-white maps on topographic or planimetric bases on quadrangle or irregular areas at various scales. Pre-1971 maps show bedrock geology in relation to specific mining or mineral-deposit problems; post-1971 maps are primarily black-and-white maps on various subjects such as environmental studies or wilderness mineral investigations.

**Hydrologic Investigations Atlases** are multicolored or black-and-white maps on topographic or planimetric bases presenting a wide range of geohydrologic data of both regular and irregular areas; principal scale is 1:24,000 and regional studies are at 1:250,000 scale or smaller.

### Catalogs

Permanent catalogs, as well as some others, giving comprehensive listings of U.S. Geological Survey publications are available under the conditions indicated below from the U.S. Geological Survey, Books and Open-File Reports Section, Federal Center, Box 25425, Denver, CO 80225. (See latest Price and Availability List.)

"**Publications of the Geological Survey, 1879- 1961**" may be purchased by mail and over the counter in paperback book form and as a set of microfiche.

"**Publications of the Geological Survey, 1962- 1970**" may be purchased by mail and over the counter in paperback book form and as a set of microfiche.

"**Publications of the U.S. Geological Survey, 1971- 1981**" may be purchased by mail and over the counter in paperback book form (two volumes, publications listing and index) and as a set of microfiche.

**Supplements** for 1982, 1983, 1984, 1985, 1986, and for subsequent years since the last permanent catalog may be purchased by mail and over the counter in paperback book form.

**State catalogs**, "List of U.S. Geological Survey Geologic and Water-Supply Reports and Maps For (State)," may be purchased by mail and over the counter in paperback booklet form only.

"**Price and Availability List of U.S. Geological Survey Publications**," issued annually, is available free of charge in paperback booklet form only.

**Selected copies of a monthly catalog** "New Publications of the U.S. Geological Survey" available free of charge by mail or may be obtained over the counter in paperback booklet form only. Those wishing a free subscription to the monthly catalog "New Publications of the U.S. Geological Survey" should write to the U.S. Geological Survey, 582 National Center, Reston, VA 22092.

**Note.**--Prices of Government publications listed in older catalogs, announcements, and publications may be incorrect. Therefore, the prices charged may differ from the prices in catalogs, announcements, and publications.